New Folder Name LIGO STUDY SUMMARY REPORT
VOLUME II (Appendix)

FILE : T880080

LIGO STUDY

JPL SUMMARY REPORT

January 18, 1988

(VOLUME II)

APPENDIX

LIGO STUDY - APPENDIX TO JPL SUMMARY REPORT

TABLE OF CONTENTS

I. INTRODUCTION

II. SITE DATA REPORTS - CALIFORNIA

III. SITE DATA REPORTS - MAINE

IV. VACUUM PUMPING STUDIES

V. OUTGASSING AND CLEANING TECHNIQUES REFERENCE DATA

VI. ALTERNATE CONFIGURATION COSTING AND SCHEDULING DATA

LIGO STUDY - APPENDIX TO JPL SUMMARY REPORT

INTRODUCTION

Volume II is an Appendix which incorporates materials and reports relevant to Volume I of the JPL Summary Report.

In addition to these two volumes see also JPL documents:

Site Selection Evaluation, Gravity Wave Detector Facility

October 3, 1984

Site Selection Evaluation, Gravity Wave Detector Facility

Addendum; Orientation and Expansion

October 15, 1984

Preliminary Concept Design and Cost Estimate Progress Report

December 12, 1984

Additional background information covering materials, design and associated cost estimates bearing on alternate LIGO configurations are maintained in JPL files.

BATCH START

STAPLE
OR
DIVIDER

SITE DATA REPORTS

CALIFORNIA

ENVIRONMENTAL SETTING FOR EDWARDS AFB

Source: Environmental study by Engineering-Science approx 1984

Note: This article speaks to the Muroc fault (see last page)

CHAPTER 2

ENVIRONMENTAL SETTING

GENERAL GEOLOGIC REGIME

Antelope Valley and the area surrounding Rogers Dry Lake have been the subject of geohydrological investigations since as early as 1911, when Harry R. Johnson authored "Water Resources of Antelope Valley" in U.S. Geological Survey (U.S.G.S.) Water-Supply Paper 278 (Johnson, 1911). Around the turn of the century it was discovered that the valley contained large quantities of groundwater that, when extracted through wells, could be used for irrigation, transforming the valley into productive agricultural land.

Hundreds of wells have been installed to tap valuable water resources, which in the early days were thought to be practically inexhaustible. Some people, however, recognized the fact that even though "water keeps spouting out from wells developed in areas of artesian groundwater conditions," the resource was indeed limited. In the 1911 report, Mr. Johnson cautioned that "even though the groundwater appears to be inexhaustible, it is indeed finite," and the continued unmanaged use of the resource could lower the level of the water table and eventually dry out the groundwater reservoir.

The same view was presented in the later U.S.G.S. Water-Supply Paper 578 (Thompson, 1929). That paper advocated conservation of the water supply if maximum use is to be obtained. However, during the past 70 years extraction of groundwater has continued at a rapid pace with resulting declines in water tables and decreases in the areal extent of artesian conditions. The results, at least on the surface, have been to transform the nonirrigated lands from a semiarid grassland to a desert-like environment.

The overdrafting of the groundwater within Antelope Valley and specifically around Rogers Dry Lake near the aquifer boundaries has created unique hydrological conditions, with fluctuating water levels and continuously changing regimes of confinement, semiconfinement, and nonconfinement of the groundwater.

Groundwater in the major part of Antelope Valley, including the southern part of Rogers Dry Lake, occurs under confined conditions, even though in some cases the confinement is no longer effective to produce artesian flow due to overdraft. Along the "shores" of Rogers Dry Lake and north of the lake bed, groundwater occurs mainly under unconfined conditions.

The location and extent of water-bearing material is mainly dependent on the geologic history of an area. Antelope Valley is a triangular closed basin bordered by the active Garlock Fault to the north-northwest and the active San Andreas Fault to the south. Movement along these two faults, emplacement of granitic rocks, and regional uplift created the closed basin that exists today. During and following the uplift of the mountains, erosional processes were intensified. Precipitation resulted in runoff; the greater the surface gradient, the higher the velocities of the runoff, and therefore the higher the erosion potential. Eroded material from the mountains surrounding Antelope Valley was brought to the basin floor, including the Rogers Dry Lake area, by local streams. During times of heavy precipitation the eroded material consisted of mixed gravel and sand; the gravel and sand layers that are encountered today in the subsurface material have a relatively high porosity and excellent water-bearing capabilities. These layers constitute the main aquifers. Overlying and interfingering the sand and gravel are silt and clay lenses and layers which were deposited during times of little precipitation within the ancient lake that once covered the major part of Antelope Valley. These finer-grained materials have low porosity (45 to 50 percent) and permeability (0.0001 to 0.1 gallons/day/square foot). In many places, the clay and silt act as confining layers, preventing water within the lower-lying sand and gravel layers from rising to its potentiometric level. Figure 2.1 depicts a conceptual drawing of the transition zone between lake deposits and bedrock/ alluvium material; as

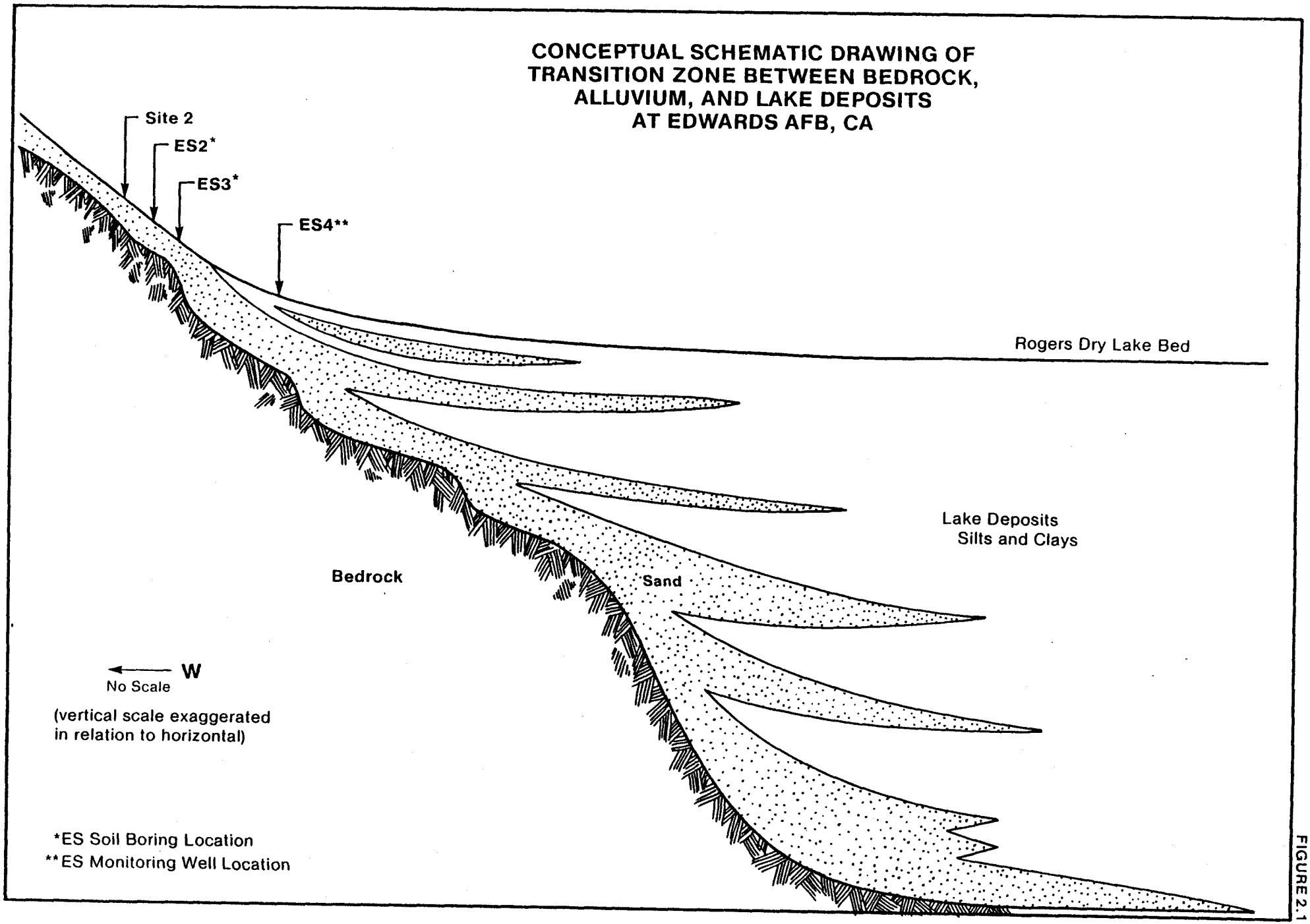
CONCEPTUAL SCHEMATIC DRAWING OF
TRANSITION ZONE BETWEEN BEDROCK,
ALLUVIUM, AND LAKE DEPOSITS
AT EDWARDS AFB, CA
Site 2
ES2*
ES3*
ES4**
Rogers Dry Lake Bed
Lake Deposits
Silts and Clays
Sand
Bedrock
W
No Scale
(vertical scale exaggerated
in relation to horizontal)
*ES Soil Boring Location
**ES Monitoring Well Location

FIGURE 2.1

illustrated, recharge to the shallower water-bearing sands could occur through the "daylighting" layers (U.S.G.S., 1980).

GENERAL HYDROLOGIC REGIME

Water within the groundwater basin is derived from several sources. Some water is connate water, i.e., water trapped within the sediments from the time of deposition. Other water is provided through recharge into the water-bearing materials along the basin boundaries where sand and gravel layers "daylight"; still another source is from percolation through the valley floor. Figure 2.2 shows the surface geology at Edwards Air Force Base and in the vicinity of Rogers Dry Lake; as can be seen, the lake is bordered by a variety of sand, gravel, and silt deposits consisting of younger alluvium (yielding water to wells when saturated), younger fan deposits (primarily located above the water table, yielding little water to wells), lakeshore deposits (above the water table), old windblown sand, and dune sand (yielding water locally to wells from perched water tables).

Groundwater recharge from the valley floor (Rogers Dry Lake) is quite limited. The lake bed surface consists of playa deposits, silt, and clay which have low permeabilities, retarding downward migration of water. Water ponding on the lake surface during the rainy season primarily evaporates; limited seepage may occur through cracks developed during the summer, but the contribution of rainwater to the aquifer system should be limited.

Groundwater flow and direction in the main water-producing aquifers near Edwards AFB are largely dominated by pumping wells, resulting in changes in the regional gradient from north to south. Figure 2.3 shows the groundwater table contours as of 1979 (U.S.G.S., 1980). A groundwater trough was located immediately south of the Main Base as a result of groundwater pumping; the groundwater table elevation at that time was estimated to be about 2,200 feet above mean sea level, or 100 to 120 feet below the ground surface. Groundwater in the vicinity of the trough is moving toward this depression from the north, south, and west; to the east is the boundary of the valley aquifer systems. It should be noted, however, that these groundwater contours are based on water level

FIGURE 2.2

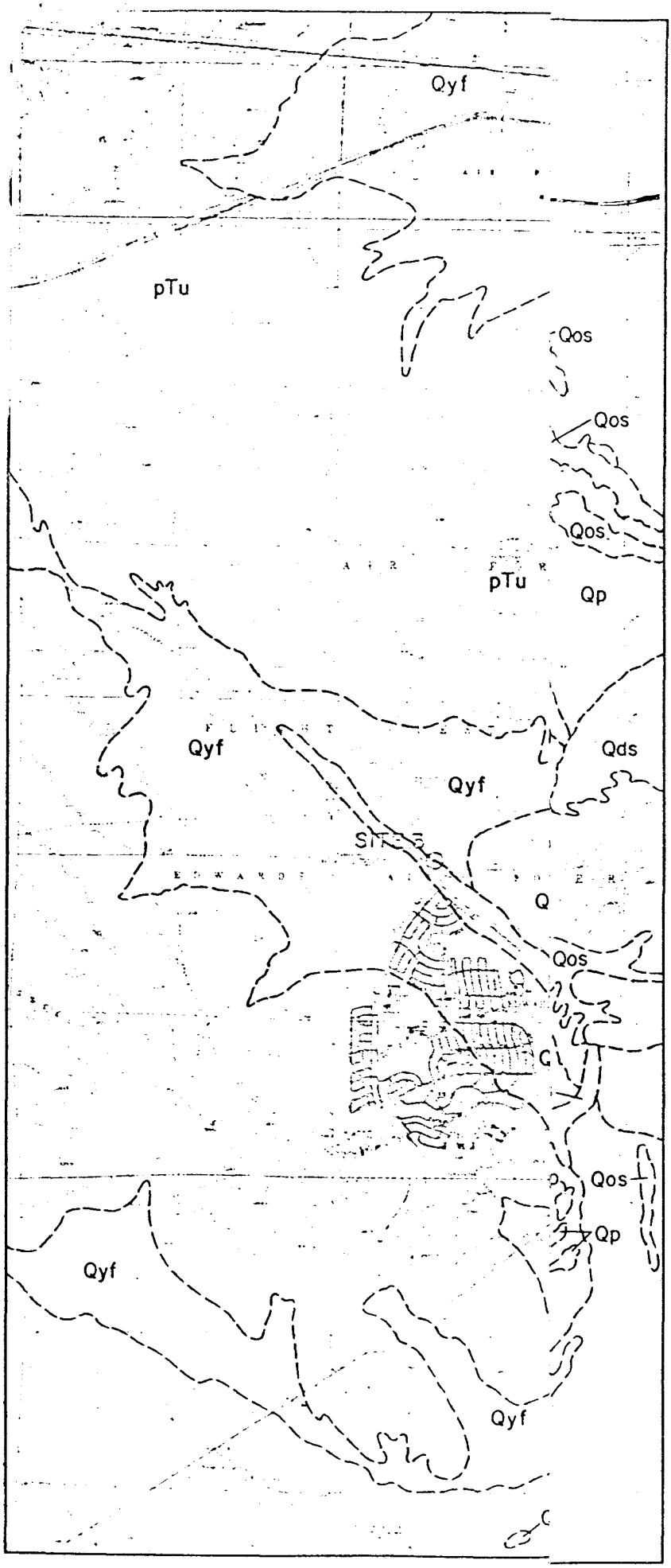

INSTALLATION
RESTORATION
PROGRAM
PHASE II
FIELD EVALUATION

EDWARDS AFB

LEGEND

- Qya — Younger Alluvium
- Qyf — Younger Fan Deposits
- Qp — Playa Deposits
- Qds — Dune Sand
- Qos — Old Windblown Sand
- Qls — Lakeshore Deposits
- pTu — Bedrock
- A' A — Location of Geologic Cross-Section

Source: U.S. Geol. Survey Bulletin No. 91-6, 1962.

1/2 0 1
MILE

GEOLOGY IN THE VICINITY OF EDWARDS AIR FORCE BASE

GROUNDWATER TABLE CONTOURS OF AQUIFERS 200 TO 500-FOOT DEPTH BELOW GROUND SURFACE

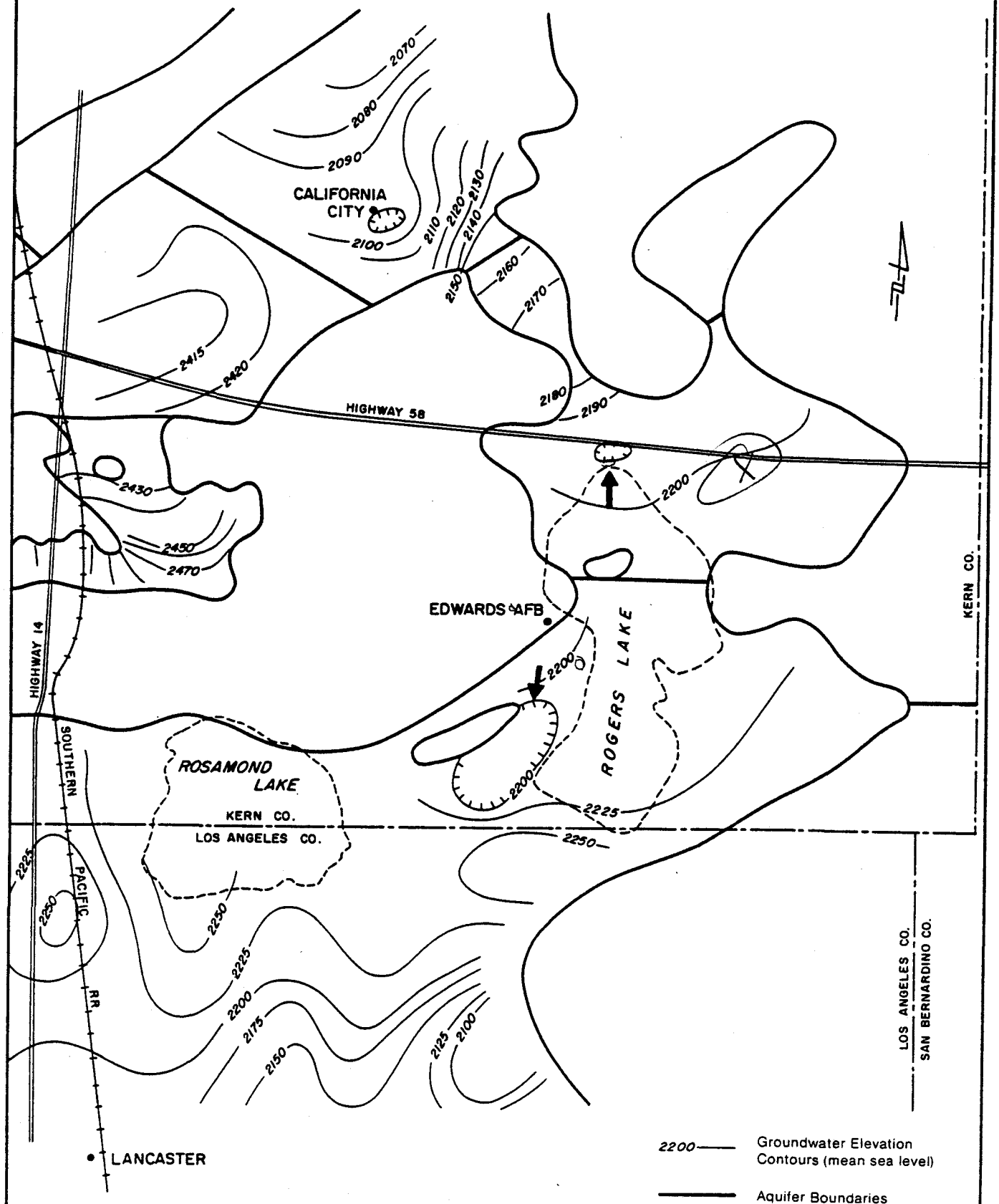

Source: U.S. Geol. Survey, 1980.

EDWARDS AFB

measurements from wells penetrating to depths of 200 feet to 500 feet, and are therefore not indicative of shallow groundwater conditions (Moyle, 1982).

Along the northern shores of Rogers Dry Lake by the North Base, the groundwater movement is in a south-to-north direction; a trough exists immediately around this part of the Base due to local groundwater extraction. A groundwater barrier exists just north of the Main Base across the dry lake bed, consisting of a zone of material with low permeability; this barrier is possibly the extension of the Muroc Fault trending in a northwest-southeast direction. The elevation of the groundwater in the North Base area was about 2,190 feet in 1979. Groundwater level contours for this area are included on Figure 2.3.

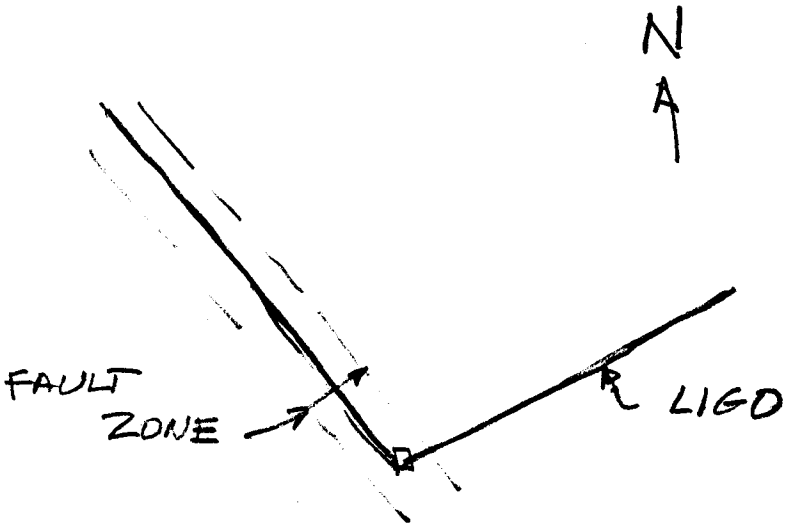

SEE FOLLOWING MAP & DISSCUSSION.

FROM: ENVIORMENTAL STUDY BY ENGINEERING SCIENCE ~1984

DMS
1-29-86

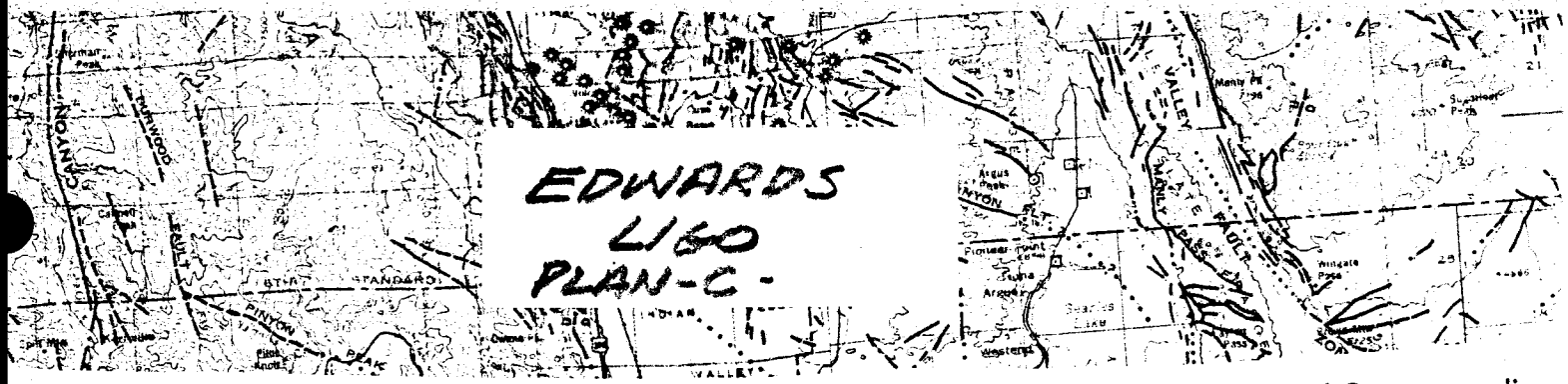

Pre-Quaternary fault (older than 2 million years) or fault without *recognized* Quaternary displacement. (Some faults shown bounding Quaternary rocks and older rocks are included in the pre-Quaternary category because the source of mapping used was of a reconnaissance nature, or the mapping was not done with the object of dating fault displacements.)

Faults shown in this category should not necessarily be considered "dead". Evidence for recency of movement may not have been observed, or it may be lacking because the fault may not be in contact with Quaternary deposits. In many cases, the evidence may have been destroyed by erosion, covered by vegetation, or by works of man.

BMS-9
OCT-14-87

Main Base and South Base

Geohydrology

The Main Base is located along the west shore of Rogers Dry Lake at the terminus of a large deposit of alluvium extending southwesterly toward Rosamond Dry Lake. It is within this alluvium that most of the water wells at the Main Base are located. The alluvium (younger) extends northward from the South Base to the Main Base and pinches out north of the Main Base to a width of about one-quarter mile toward the North Base. The alluvium consists of gravel, sand, silt, and clay beneath the alluvial plains. This alluvium is largely above the water table, but where saturated, the alluvium yields water to wells. Bordering the alluvium to the west is a narrow band of lakeshore deposits northward from the Main Base. These deposits consist of gravel and sand and some silts and clays, and are located above the water table. Further westward are younger fan deposits, made up of poorly sorted gravel, sand, silt, and mudflow debris that is locally derived. These deposits are largely above the water table and yield little water to wells immediately west of the Main Base. The gently sloping hill where Site 2 is located consists of basement rock of granitic origin (quartz monzonite). The material is deeply weathered locally resulting in soil mantle development. The granite-type rocks are fractured and yield some water from cracks and fissures (see Figure 2.2 for delineation of geologic units).

Perhaps as many as 200 wells have been completed in the past in the Main Base and South Base areas to provide drinking and irrigation water for the now abandoned town of Muroc. Most of these wells have been sealed off or abandoned as new water supply wells were installed in other areas. Well logs exist for a limited number of the old wells;

inspection of the logs allows a general interpretation of the areal and vertical relationship of the geologic subsurface conditions in the South Base area. Pertinent existing logs for wells near the Base disposal sites are included in Appendix B. Figures 3.3 and 3.4 show schematic geologic cross-sections based on old well logs, as well as on the logs prepared during the recent installation of monitoring wells. The sections show the subsurface geology in a north-south direction from the Main Base to the South Base. The granite hills northwest of the Main Base continue southward overlain by about 70 feet of lake shore and alluvial deposits. A sudden drop occurs south of the South Base, where the granite bedrock is found at a depth of more than 240 feet. The sediments overlying the granitic basement rock consist of variable thicknesses of lenticular, interfingering clay, silt, and sand.

In order to define the hydrological regime, geological logs as well as historical water level data are necessary. Within the Main Base and South Base areas, this information was available for only two wells. One well, 9N/9W-6E1, is located on the South Base, and another well, 9N/10W-12R1 (Main Base Well 6), is south of Old Hospital Road (see Figure 3.5 for location). The geological logs for both wells are part of the cross-section A-A', presented in Figure 3.3. The original well log for 9N/10W-12R1 is presented in Figure 3.6. This figure shows a total drilling depth of 252 feet, with apparent water-bearing sands at 169 to 178 feet and at 223 to 248 feet. Perforations in the well casing were located at these intervals. Sands at shallower depths did not appear to show water at the time of well installation in 1944. In 1951 the depth of the well was recorded as 186.6 feet, a difference of 65.6 feet from the original depth; this could be due to siltation of the well. There are no data on the water level immediately following well completion, but in 1948 the water level was recorded at 11.1 feet below ground surface. At this depth, the well log shows that the subsurface material consists of clay (non-water-bearing) extending to a depth of 131 feet; thus the water in the well must have risen from the water-bearing sands at 169 feet to its recorded depth. This would indicate that the water was under confined conditions at the time of installation and that the more than 100 feet of clay acted as a confining layer.

CROSS-SECTION A-A'
MAIN BASE AND SOUTH BASE
EDWARDS AIR FORCE BASE, CA
(for location, see Figure 2.2)

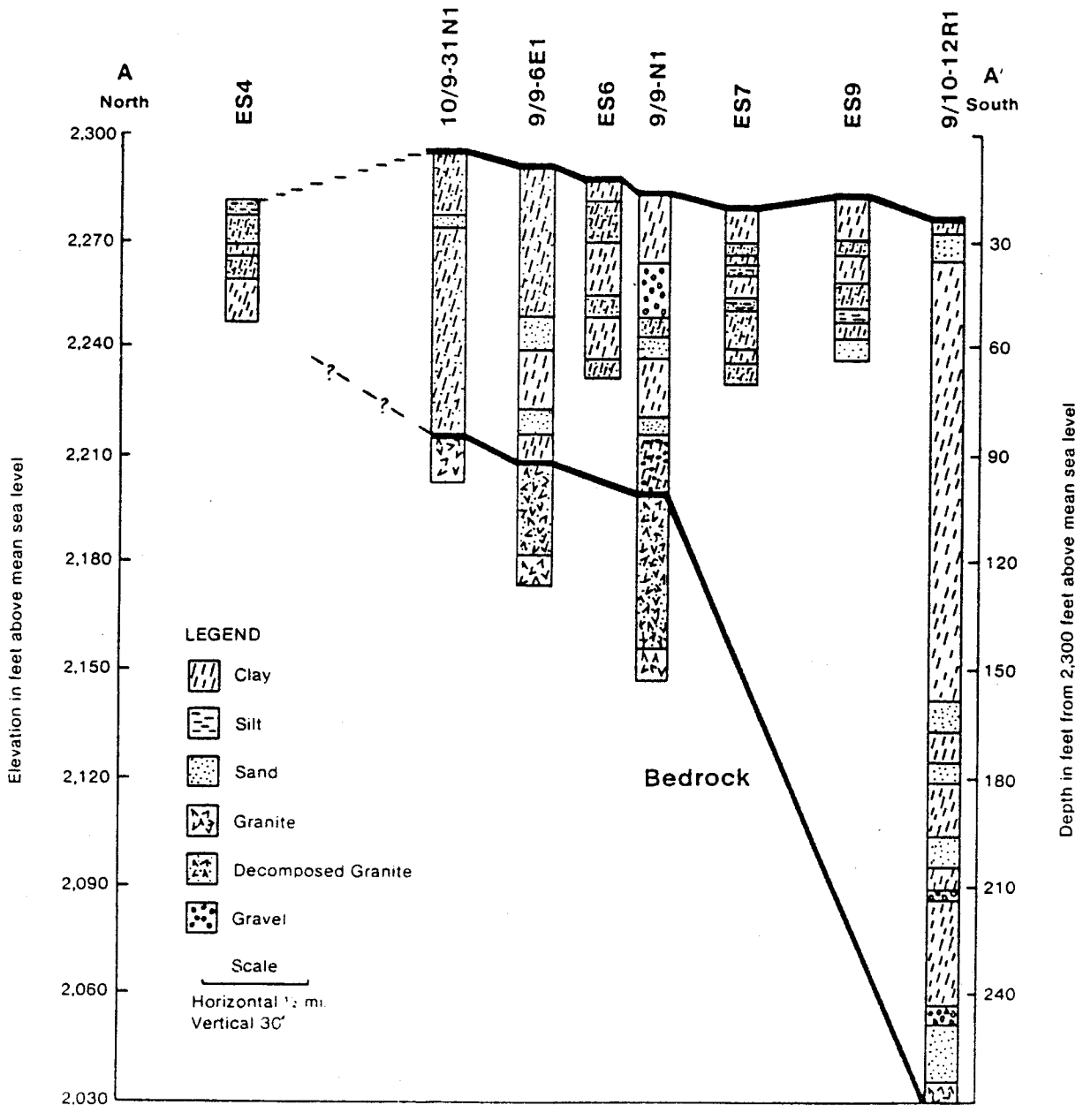

CROSS-SECTION B-B'
MAIN BASE AND SOUTH BASE
EDWARDS AIR FORCE BASE, CA
(for location, see Figure 2.2)

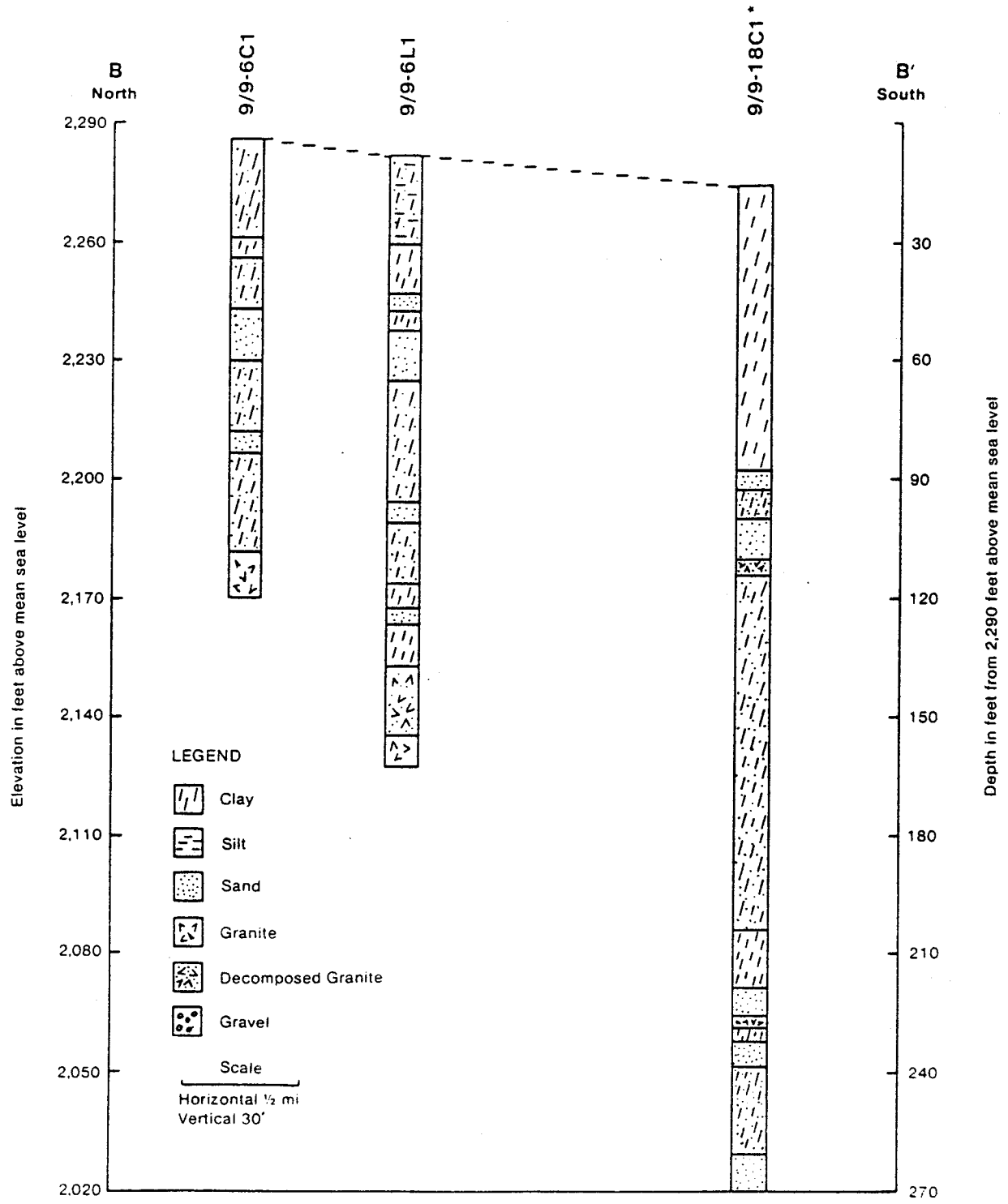

* When this well was drilled in 1944 water was encountered at 75 feet, but rose to 10 feet, indicating confined conditions at that time.

FIGURE 3.5

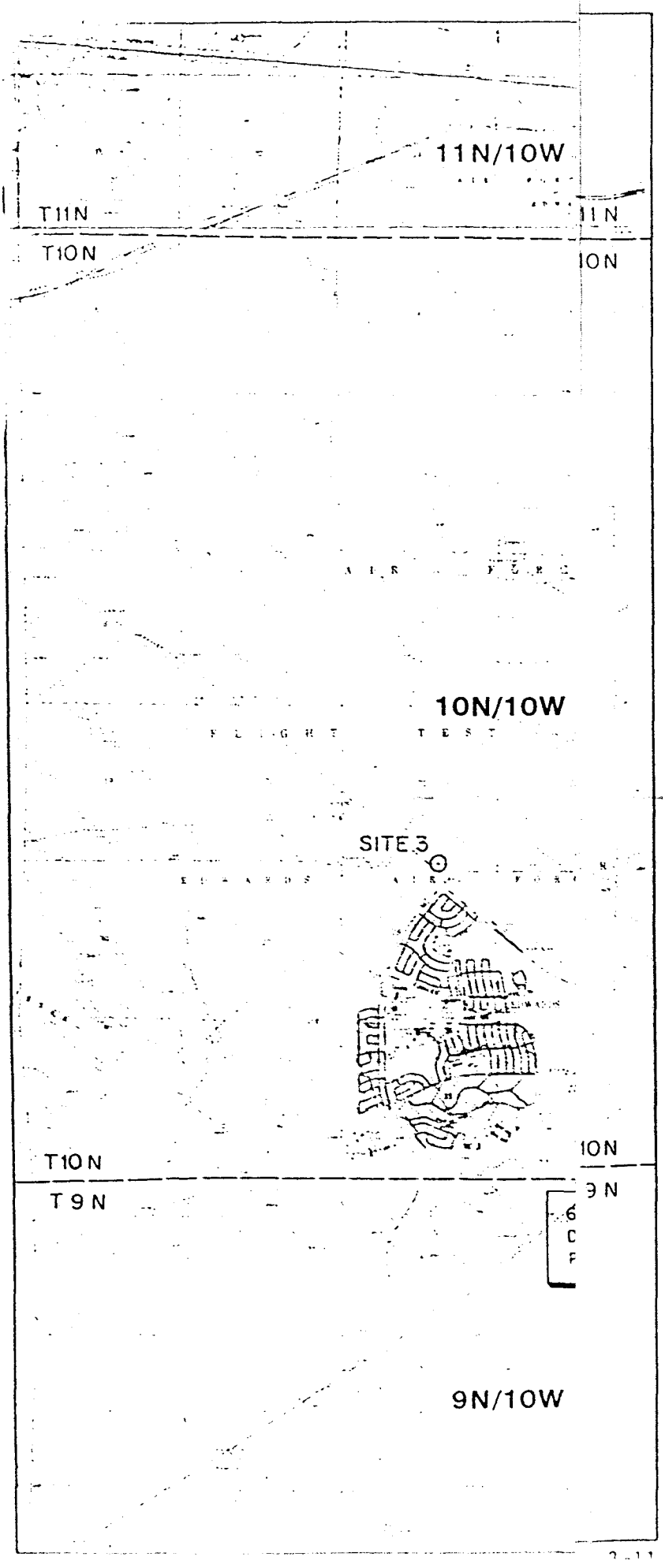

EDWARDS AFB

INSTALLATION
RESTORATION
PROGRAM
PHASE II
FIELD EVALUATION

LEGEND

- ● Active Production Wells
- △ Abandoned Wells

USGS Number
Base Well Number

12R1 (MB-6)
D : 252' — Depth of Well
P : 169'-178' — Perforated Intervals in Casing

(See Appendix B for standard California well numbering system)

1/2 0 1
MILE

LOCATION OF BASE WELLS WITH WELL LOGS AVAILABLE

ORIGINAL WELL LOG FROM SOUTH BASE
WELL 9N/10W-12 R1

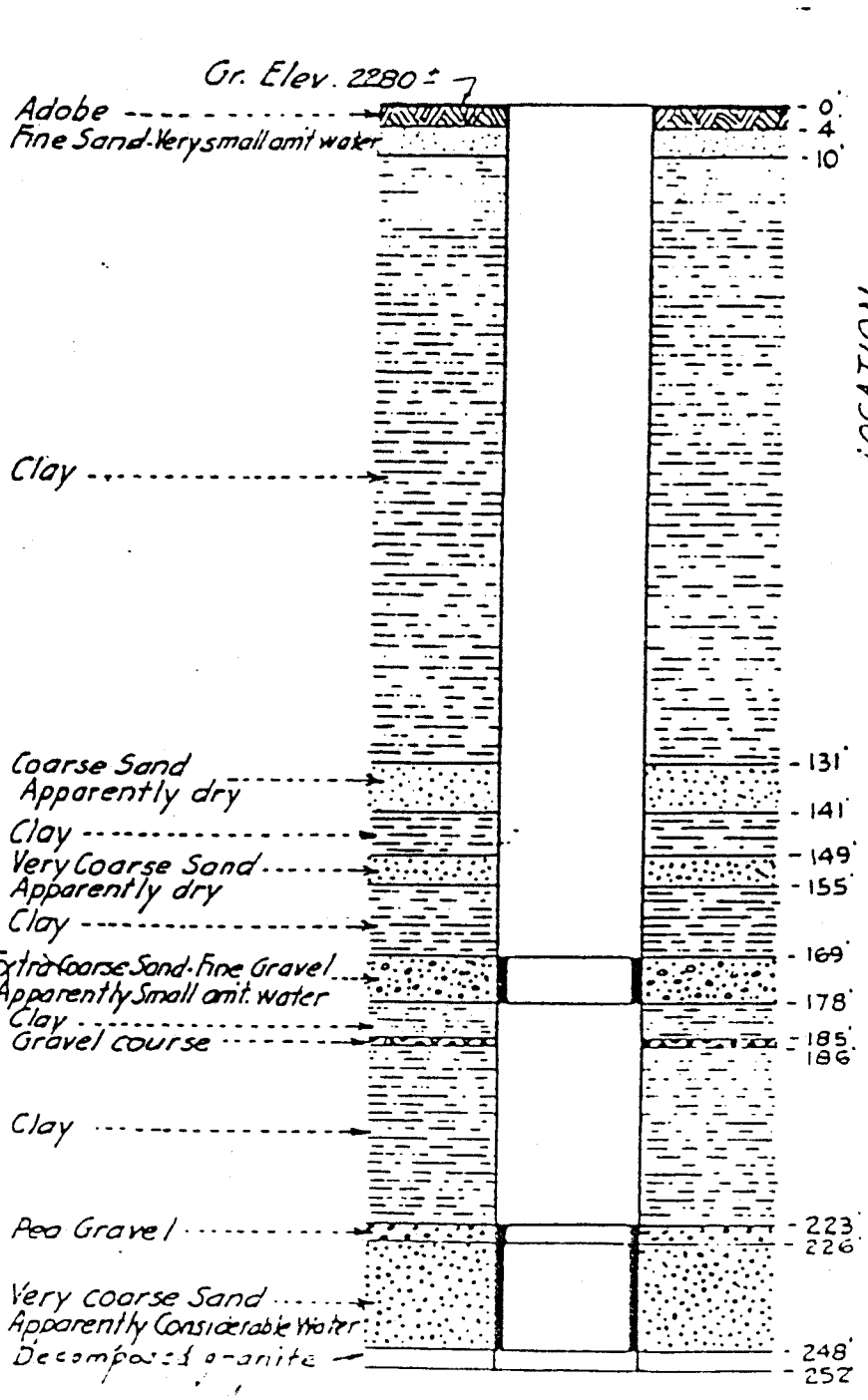

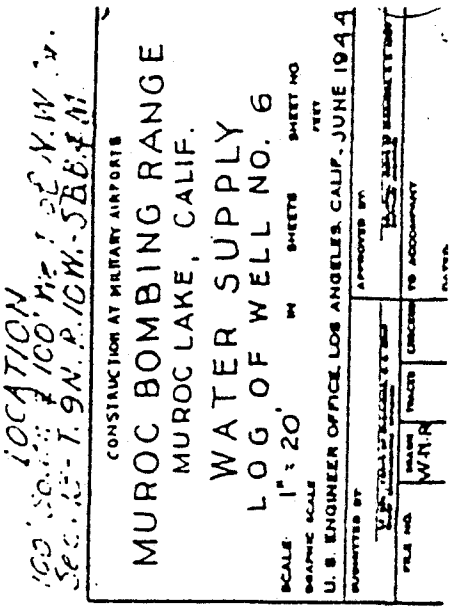

Contractor: E.W. Brockman
Driller - Jim Cahall.
Work begun: 16 Mar. 1944.
Work completed 27 Mar '44.
Pump Tested 5 Apr. 1944
Well abandoned.

The water levels in the 9N/10W-12R1 well from 1948 to 1981 have been presented graphically on Figure 3.7. The data show a steadily declining water level from 11.1 feet in 1948 to 89.65 feet in 1981. Although monthly readings were discontinued in 1966, monthly records from the 1960's show an annual seasonal variation in the water levels of about 7 feet, and an overall yearly decline of about 3 feet. This indicates that following the yearly low water level of August and September, the water level never recovered to its previous shallower depth. The 1981 water level reading of 89.65 feet appears to indicate that the water in the well is still under confined conditions since the first perforations are at a depth of 169 feet, and the massive clay layer reaches down to a depth of 131 feet.

South Base Well 9N/9W-6E1 was drilled in 1942 to a depth of about 107 feet into bedrock. In 1951, the depth of the well was recorded as 103.7 feet, or 3.3 feet shallower than when completed in 1942; this could be due to siltation of the well. The original well log presented on Figure 3.8 indicates that sands should be located at various intervals below 37 feet. The log does not indicate which of these sands were water bearing at the time of installation. The perforations extend from 35 feet to 96 feet, with the static water level recorded as 36 feet on the original well log. Available data do not indicate whether the water was confined or unconfined; however, when a pump test was performed in 1942, 67 feet of drawdown resulted while pumping 254 gallons per minute, which could be indicative of nonconfining conditions.

Water level data for 9N/9W-6E1 are available from 1942 to date. The water levels show a continuous downward trend from the initial 36 feet to 51.17 feet in April 1981, a total drop of 15.17 feet in 39 years, or less than 0.5 foot per year. Seasonal water levels generally appear to vary less than 0.25 foot.

The wells described above are indicative of the geohydrologic environment existing along the shores of Rogers Dry Lake. The Main Base and South Base are located in a hydrological transition zone where the groundwater can be under confined and/or nonconfined conditions. In this transition zone, the thickness of sediments overlying bedrock vary dramatically over short distances; the thicknesses of water-bearing

WATER LEVEL DATA FROM 1948 TO 1981
WELLS 9N/9W-6E1 and 9N/10W-12R1
EDWARDS AFB, CA

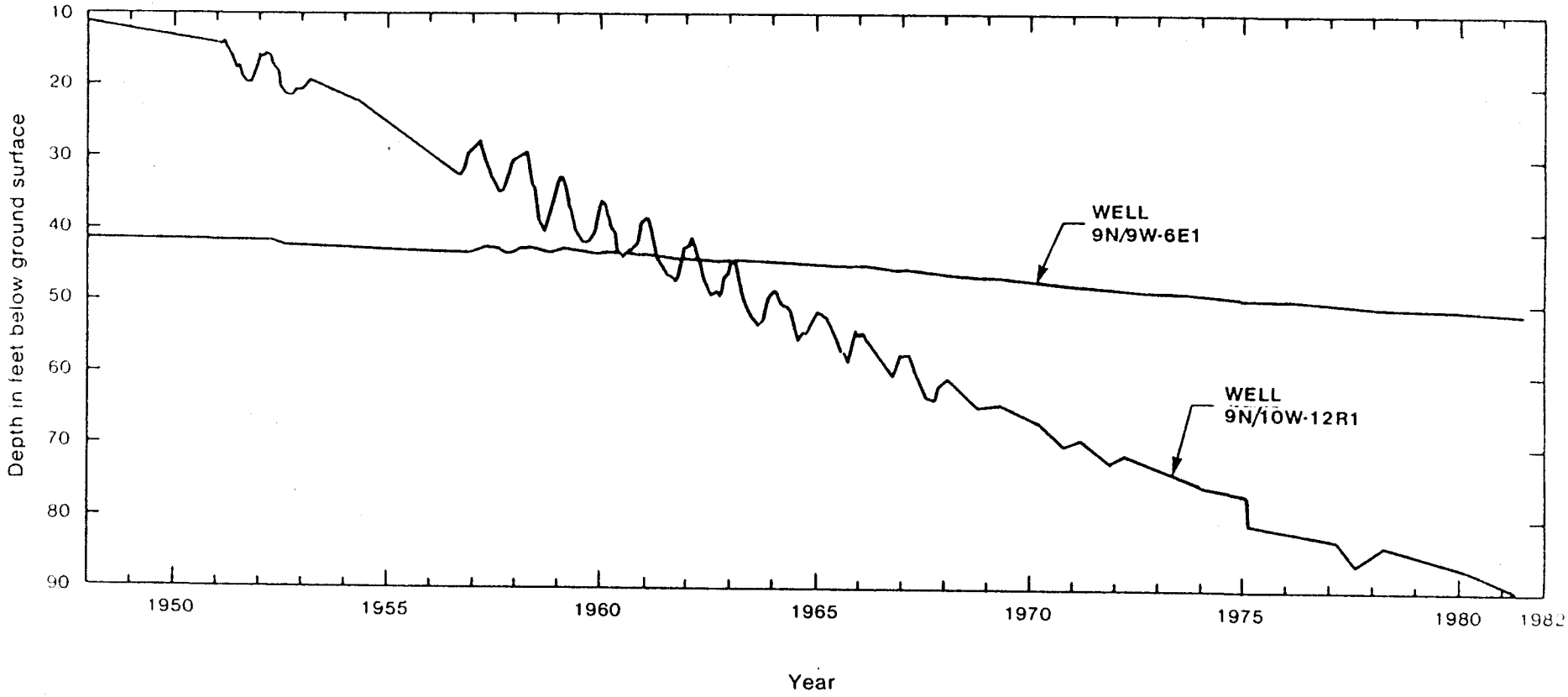

ORIGINAL WELL LOG FROM SOUTH BASE
WELL 9N/9W-6E1

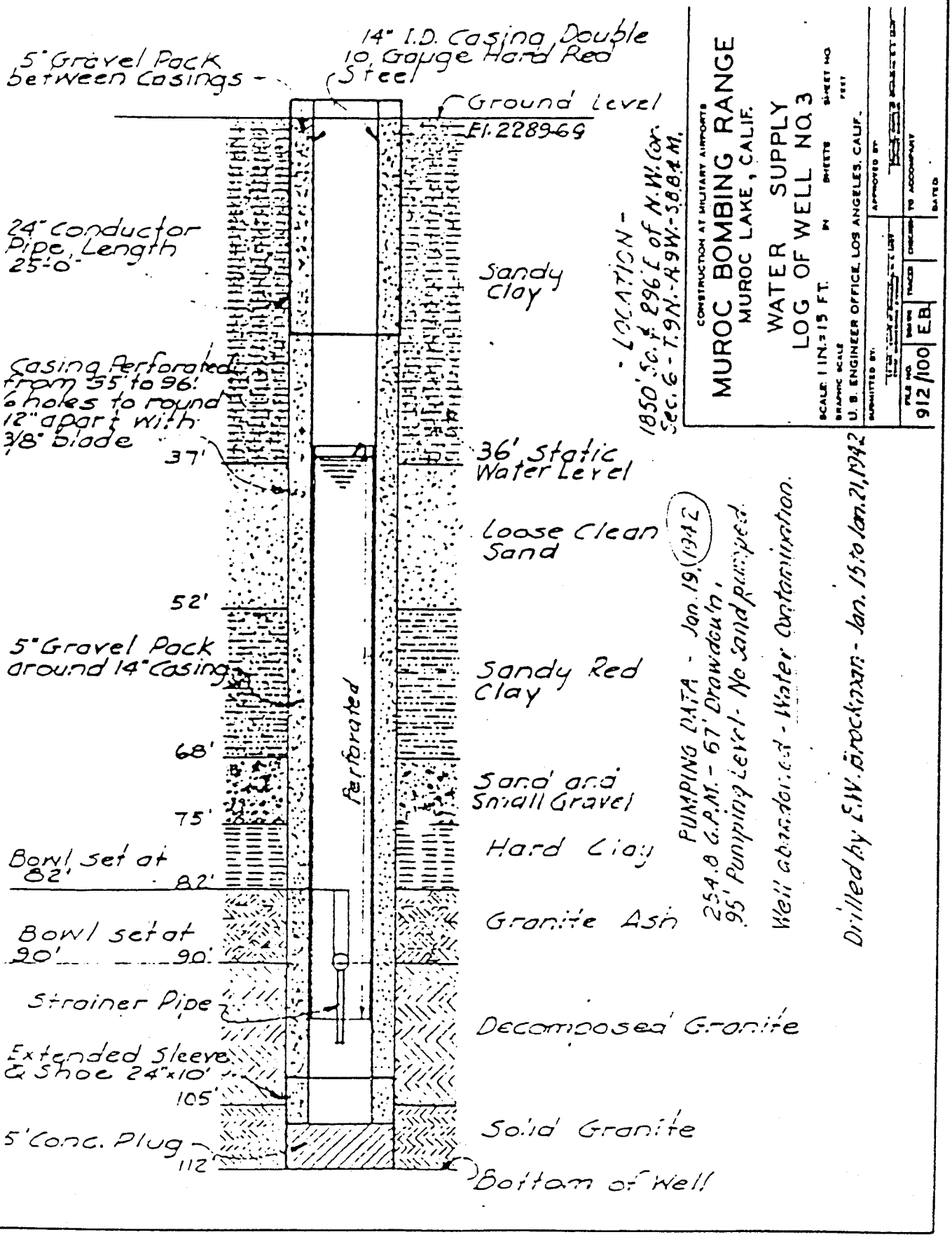

sands and gravels are lenticular and interfingering with clays and silts, and perched water conditions are distinct possibilities. Here, different groundwater zones experience different seasonal variations, and the decline in the water table over time depends on the aquifer location and characteristics.

BIOLOGICAL SURVEY AND IMPACT ASSESSMENT OF GRAVITY WAVE OBSERVATORY, EDWARDS AIR FORCE BASE

By:

Michael J. O'Farrell, Ph.D.
Jack C. Fisher
Stephen B. Lacy

Prepared by:

WESTEC Services, Inc.
5510 Morehouse Drive
San Diego, CA 92121
Project No. 36018001

Prepared for:

Jet Propulsion Laboratory
California Institute of Technology
4800 Oak Grove Drive
Pasadena, CA 91109
Contract No. IC-798439

August 1985

TABLE OF CONTENTS

Title	Page
INTRODUCTION	1
METHODS	1
EXISTING CONDITIONS	1
Vegetation	1
Wildlife	4
SENSITIVE SPECIES	4
Vegetation	4
Wildlife	11
SENSITIVE HABITATS	12
IMPACTS	12
Vegetation	12
Wildlife	12
CONCLUSIONS	13
LITERATURE CITED	14

LIST OF FIGURES

Number	Title	Page
1	Vicinity Map Showing Location of Project Site	2
2	Vicinity Map Showing Project Location, Vegetative Habitats, and Sensitive Plant and Animal Species	3

LIST OF TABLES

Number	Title	Page
1	Checklist of Plant Species Observed on the Proposed Caltech Gravity Wave Facility	5

TABLE OF CONTENTS (Continued)

LIST OF TABLES (Continued)

Number	Title	Page
2	Checklist of Reptiles, Birds, and Mammals Observed on the Proposed Caltech Gravity Wave Facility	8
3	Sensitive Plant Species Searched for at the Proposed Facility Site	10

INTRODUCTION

The California Institute of Technology Jet Propulsion Laboratory is proposing to construct an L-shaped horizontal facility approximately 3962 m by 30 m on each side. The proposed facility site is located at Edwards Air Force Base in the Mojave Desert on the northeast end of Rogers Dry Lake (Figure 1). The purpose of the present study is to provide a biological reconnaissance with emphasis on the presence of rare or sensitive species and provide any necessary mitigation measures as needed to reduce or avoid adverse impacts.

METHODS

The proposed project site was subjected to a 100 percent walkover survey to delineate plant communities, obtain a point-in-time inventory of the biota present, and identify the presence or potential for recognized sensitive species. The project was originally proposed at 5 km on a side. The field surveys reviewed the 5 km project and this is reflected in the mapping of vegetative habitat and sensitive plants and animals (Figure 2).

The field survey was conducted on 13 and 14 May 1985 after perusal of the pertinent literature and occurrence maps. Plant communities were delineated on USGS 15 minute topographic maps. A record was made of all species observed and sensitive species observed were accurately located on the topographic maps.

The proposed project area was not flagged and was sufficiently vague on the maps provided to require a greater swath to be surveyed than the stated 30 m. This was particularly true for the two ends of the L-shaped site because a minor change in orientation at the right angle axis would cause a significant divergence at the end of the site 5 km away. An attempt was made to identify the extent or potential of occurrence of sensitive species at least 100 m on either side of the project site. In this manner a more informed judgement can be made with respect to the effects of the final placement of the proposed facility.

EXISTING CONDITIONS

Vegetation

The proposed alignment crossed parts of seven sections in R8W and R9W T10N. The elevation ranged from 695m to 701m (2280 to 2300 feet). It crossed two recognizable plant communities (Figure 2), the Shadscale Scrub and the Alkali Sink Scrub (Thorne, 1976). The Shadscale Scrub community was dominated by Shadscale (Atriplex confertifolia), Burro-bush (Ambrosia dumosa) and Goldenhead (Acamptopappus sphaerocephalus). The 56 plant species found on the site in this community are listed in

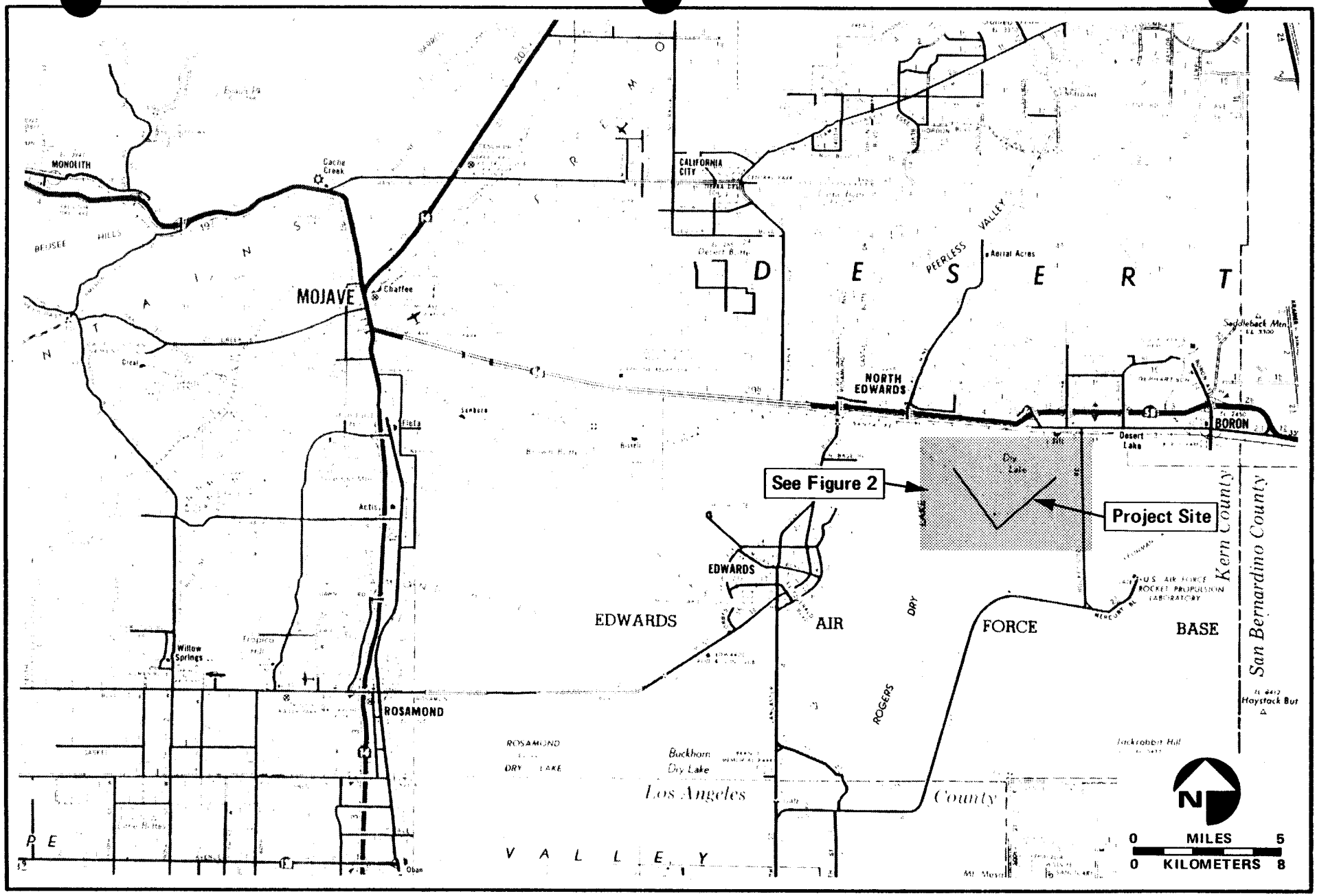

Vicinity Map Showing Location of Project Site

FIGURE 1

WESTEC Services, Inc.

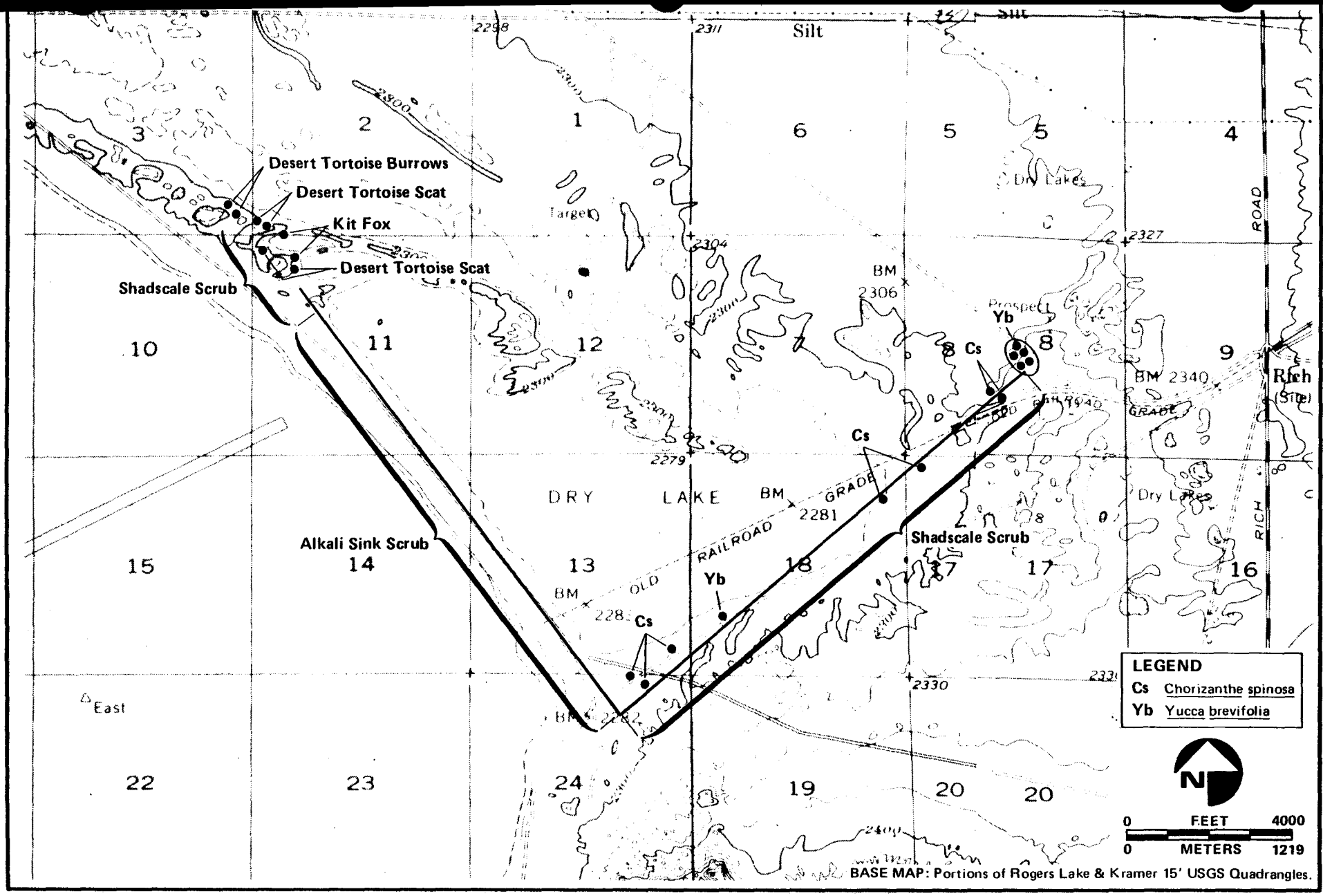

Vicinity Map Showing Project Location, Vegetative Habitats, and Sensitive Plant and Animal Data

FIGURE 2

WESTEC Services, Inc.

Table 1. This community was characteristically rather sparse and occupied the upland parts of the study site, notably the stabilized dunes at the border of Rogers Dry Lake.

The Alkali Sink Scrub community was found at the lowest portion of the proposed development where it crossed a narrow arm of ground between Rogers Dry Lake and another small dry lake to the northeast. This community was very sparse and was dominated by Torrey Inkweed (Suaeda torreyana) and Shadscale (Atriplex confertifolia). A total of 13 species were found in this community (Table 1).

Wildlife

The inventory generated during the present survey (Table 2) for terrestrial vertebrates, although not exhaustive, was consistent with the fauna expected in Mohave Desert alkali scrub and shadscale habitats. Moe and Lawrence (1981) provide a more detailed inventory, although a four season examination would be necessary to approach a complete list, particularly with respect to birds.

Predators were conspicuously low in abundance although one area just northwesterly of the western leg of the project contained a number of Kit Fox (Vulpes macrotis) dens (Figure 1). One large natal den was also located, but all the evident sign indicated last year's occupancy with no recent sign. All scat observed was from last year also. The larger stabilized dunes along the border of the dry lake northwest of the project area appear to be a preferred area for predator activity.

Raptors were absent from the area during the present survey which is probably related to the timing of the walkover. There is a lack of suitable roost and nesting sites in the immediate area. Fall and winter foraging activity probably represents the major raptor activity on the proposed facility site.

SENSITIVE SPECIES

Vegetation

Four sensitive plant species were searched for on the basis of their known occurrence on Edwards Air Force Base (Table 3; Moe and Lawrence, 1980, 1981; Smithsonian Institute, 1978). None of these species are currently listed as threatened or endangered by State or Federal agencies (California Department Fish and Game, 1984; U.S. Fish and Wildlife Service, 1983a). Following is a brief description of each species, its distribution, California Native Plant Society (CNPS) status, habitat and presence in the study area.

Chorizanthe spinosa in the Polygonaceae is known from dry sandy and gravelly places from Rabbit Springs to Red Rock Canyon in the Mojave Desert. It has been found in Los Angeles, Kern and San Bernardino Counties. It has been placed on the

Table 1

CHECKLIST OF PLANT SPECIES OBSERVED
ON THE PROPOSED CALTECH GRAVITY WAVE FACILITY
MAY 1985

Family/Species[1]	Common Name[2]	Community[3] SH	AS
Agavaceae			
Yucca brevifolia	Joshua Tree	X	
Asteraceae			
Acamptopappus sphaerocephalus	Goldenhead	X	
Ambrosia dumosa	Burro-bush	X	
Anisocoma acaulis	Scale Bud	X	
Artemisia spinescens	Bud Artemisia	X	X
Chaenactis fremontii	Pincushion Flower	X	
Chrysothamnus paniculatus	Punctate Rabbitbrush	X	
Coreopsis bigelovii	Bigelow Coreopsis	X	
Haplopappus laricifolius	Goldenbush	X	
Hymenoclea salsola	Cheesebush	X	
Machaeranthera tortifolia	Desert Aster	X	
Malacothrix glabrata	Desert Dandelion	X	
Monoptilon bellioides	Mojave Desert Star	X	
Rafinesquia neomexicana	New Mexico Chicory	X	
Stephanomeria pauciflora	Desert Straw	X	
Tetradymia glabrata	Horsebrush	X	
Tetradymia stenolepis	Mojave Horsebrush	X	
Boraginaceae			
Cryptantha circumscissa	Western Forget-me-not	X	
Cryptantha sp.	Cryptantha	X	
Brassicaceae			
Lepidium flavum	Yellow Pepper Grass	X	X
Lepidium fremontii	Desert Alyssum	X	
Lepidium perfoliatum	Perfoliate Peppergrass	X	X
Stanleya pinnata	Princes Plume	X	
Cactaceae			
Opuntia basilaris	Beavertail	X	
Campanulaceae			
Nemacladus glanduliferus	Thread Plant	X	
Capparaceae			
Cleomella obtusifolia	Stinkweed	X	X
Chenopodiaceae			
Atriplex confertifolia	Shadscale	X	X
Atriplex phyllostegia	Arrow Scale		X
Eurotia lanata	Winterfat	X	

Table 1

CHECKLIST OF PLANT SPECIES OBSERVED
ON THE PROPOSED CALTECH GRAVITY WAVE FACILITY
MAY 1985 (Continued)

Family/Species[1]	Common Name[2]	Community[3] SH	AS
Suaeda torreyana	Torrey Inkweed	X	X
Convolvulaceae			
Cuscuta sp.	Dodder	X	
Geraniaceae			
Erodium cicutarium	Filaree	X	
Hydrophyllaceae			
Nama demissum	Purple Nama	X	
Phacelia crenulata	Notch-leaved Phacelia	X	
Phacelia distans	Wild Heliotrope	X	
Phacelia fremontii	Fremont Phacelia	X	X
Loasaceae			
Mentzelia albicaulis	Small Blazing Star	X	
Nyctaginaceae			
Mirabilis bigelovii	Wishbone Bush	X	
Onagraceae			
Camissonia boothii	Bottlebrush	X	X
Camissonia claviformis	Clavate Camissonia	X	
Papaveraceae			
Eschscholzia minutiflora	Little Golden Poppy	X	
Poaceae			
Bromus rubens	Foxtail Chess	X	
Hordeum glaucum	Foxtail	X	
Oryzopsis hymenoides	Ricegrass	X	
Schismus arabicus	Arabian Grass	X	X
Polemoniaceae			
Eriastrum diffusum	Spreading Eriastrum	X	
Langlosia mathewsii	Desert Calico	X	
Polygonaceae			
Chorizanthe brevicornu	Brittle Spineflower	X	
Chorizanthe rigida	Rigid Spiny Herb	X	
Chorizanthe spinosa	Mojave Chorizanthe	X	X
Eriogonum maculatum	Spotted Buckwheat	X	
Eriogonum nidularium	Whisk Broom	X	

Table 1

CHECKLIST OF PLANT SPECIES OBSERVED
ON THE PROPOSED CALTECH GRAVITY WAVE FACILITY
MAY 1985 (Continued)

Family/Species[1]	Common Name[2]	Community[3] SH	AS
Polygonaceae (Continued)			
Eriogonum reniforme	Kidney-leaved Buckwheat	X	
Oxytheca luteola	Yellow Spiny Cape	X	X
Oxytheca perfoliata	Punctured Bract	X	
Solanaceae			
Lycium andersonii	Anderson Thornbush	X	X
Lycium cooperi	Peach Thorn	X	

1 Scientific nomenclature follows Munz (1974).

2 Common names follow Jaeger (1968) or DeDecker (1984)

3 Plant community designations follow Thorne (1976).

SH Shadscale Scrub
AS Alkali Sink Scrub

Table 2

CHECKLIST OF REPTILES, BIRDS, AND MAMMALS OBSERVED
ON THE PROPOSED CALTECH GRAVITY WAVE FACILITY
MAY 1985

Family/Species[1]	Common Name
REPTILES	
Testudinidae	
Scaptochelys (= *Gopherus*) *agassizi*	Desert Tortoise
Iguanidae	
Callisaurus draconoides	Zebra-tailed Lizard
Phrynosoma platyrhinos	Desert Horned Lizard
Uta stansburiana	Side-blotched Lizard
Teiidae	
Cnemidophorus tigris	Western Whiptail
BIRDS	
Alaudidae	
Eremophila alpestris	Horned Lark
Corvidae	
Corvus corax	Common Raven
Mimidae	
Toxostoma lecontei	Le Conte's Thrasher
Emberizidae	
Amphispiza belli	Sage Sparrow
Xanthocephalus xanthocephalus	Yellow-headed Blackbird
MAMMALS	
Leporidae	
Sylvilagus audubonii	Desert Cottontail
Lepus californicus	Black-tailed Jack Rabbit
Sciuridae	
Ammospermophilus leucurus	White-tailed Antelope Squirrel
Heteromyidae	
Dipodomys merriami	Merriam's Kangaroo Rat
Dipodomys microps	Chisel-toothed Kangaroo Rat

Table 2

CHECKLIST OF REPTILES, BIRDS, AND MAMMALS OBSERVED
ON THE PROPOSED CALTECH GRAVITY WAVE FACILITY
MAY 1985 (Continued)

Family/Species[1]	Common Name
Canidae	
Canis latrans	Coyote
Vulpes macrotis	Kit Fox
Mustelidae	
Taxidea taxus	Badger

1 Nomenclature follows Jennings (1983) for reptiles, A.O.U. (1983) for birds, and Jones et al. (1982) for mammals.

Table 3

SENSITIVE PLANT SPECIES SEARCHED
FOR AT THE PROPOSED FACILITY SITE

Family/Species	Common Name	CNPS Status[1]
Apiaceae		
Cymopterus deserticola	Desert Cymopterus	List 1B, FED 2
Polygonaceae		
Chorizanthe spinosa	Mojave Chorizanthe	List 4
Amaryllidaceae		
Muilla coronata	Pigmy Muilla	Appendix 1
Liliaceae		
Calochortus striatus	Alkali Mariposa	List 1B, FED C3

[1] Smith and York (1984)

List 1: Plants of Highest Priority
- 1A: Plants Presumed Extinct in California
- 1B: Plants Rare or Endangered in California and Elsewhere

List 2: Plants Rare or Endangered in California, but Common Elsewhere
List 3: Plants About Which We Need More Information
List 4: Plants of Limited Distribution (A Watch List)
Appendix 1: Plants Considered, But Not Included

Federal Status:
- FED C1: Plants About Which Enough is Know to List
- FED C2: Plants About Which More Information is Needed
- FED C3: Plants Which Have Been Shown to be too Common for Listing

watch list of plants with limited distribution (List 4), but it is not considered in immediate threat (Smith and York, 1984). This species was found in the study area which crosses a known population (Figure 2; Moe and Heckard, 1977). It was not, however, found throughout the entire known population zone. This species was found within or adjacent to the east arm of the alignment within the Shadscale Scrub community in Sec 13 and Sec 24 T1ON R9W and Sec 8, Sec 17 and Sec 18 T1ON R8W.

Calochortus striatus in the Liliaceae is known to occur between 760m and 945m elevation (2500 and 3100 feet) often in mesic places about playas and in washes from San Bernardino County to Las Vegas, Nevada and Los Angeles to Kern and Tulare Counties. It is listed by the CNPS as being rare and endangered in California; however, Federally it is considered as too widespread to be threatened (Smith and York, 1984). This species was not found on the study site.

Cymopterus deserticola in the Apiaceae is known to occur in Creosote Bush Scrub and Joshua Tree Woodland (Thorne, 1976) between 760m and 945m elevation (2500 and 3100 feet) in Inyo, Kern, Los Angeles, and San Bernardino Counties. It is considered endangered in California by the CNPS (Smith and York, 1984), and sufficient evidence exists for listing Federally (U.S. Fish and Wildlife Service, 1983a). This species is known to occur near to the study area; however, it was not found on the proposed development site and probably does not exist there.

Muilla coronata in the Liliaceae is known to occur in heavy soils from Lone Pine to the Antelope Valley. It is found in the Shadscale Scrub plant community. This species has been considered too common for Federal listing and was considered by the CNPS but not listed (Smith and York, 1984). It was not found during the present survey.

Wildlife

No Federal or State-listed animal species were found during the present survey (California Department Fish and Game, 1980; U.S. Fish and Wildlife Service, 1983b). A slight potential exists for the patchy ocurrence of the State-listed Mohave Ground Squirrel (Spermophilus mohavensis) along the project alignment. Potentially suitable habitat exists, but no individuals were observed or heard vocalizing.

Desert Tortoise (Scaptochelys agassizi), currently being considered for Federal listing, is known from the vicinity of the project site. Desert Tortoise scat, a single shell, and burrows were found off the northwestern end of the facility site (Figure 2). Most of the sign was at least one year old. Abundance on the proposed site is apparently low.

A variety of raptors would be expected to use the general area for foraging purposes, but no potential nesting or roost sites occur within the proposed alignment.

SENSITIVE HABITATS

Moe and Lawrence (1980, 1981) discussed the sensitivity of the stabilized sand dune habitat on the edges of Rogers Dry Lake. They considered it sensitive since this type of habitat is not commonly found in the desert. Along the study alignment this is the habitat type covered by the Shadscale Scrub plant community and in which Chorizanthe spinosa was found.

Joshua Trees (Yucca brevifolia) are designated as sensitive by Kern County and require a permit to remove (Moe and Lawrence, 1980, 1981). Several Joshua Trees were located near the alignment (Figure 2).

IMPACTS

Vegetation

The proposed development will impact a large known population of Chorizanthe spinosa along most of its entire length. This species was not found throughout much of the adjacent known area during this field study, but this is not unusual since it is an annual and responds to the variable effects of rainfall. It has been collected at other locations in the study area by Moe and Lawrence (1980, 1981). This species is not officially listed by wildlife agencies or by the CNPS as rare and endangered. If the alignment can be developed within the existing road which it parallels or placed on the playa where no vegetation is found, impacts will be negligible. Impact will otherwise be considered minimal since this species has a low sensitivity status and is known to occur elsewhere on the Edwards Air Force Base and in the Mojave Desert.

Several Joshua Trees were observed along the alignment near the end of the proposed east arm of the project. The alignment was not marked in the field and its exact placement may miss these specimens. Kern County has an ordinance to protect the indiscriminant taking of specimens from other than private property and the State via the California Food and Agriculture Code regulates the harvesting of native species for sale. Neither of these regulations directly applies to the Federal lands where the project is proposed but should be taken into consideration.

Wildlife

Construction activities will necessarily remove all species within the 30 m corridor for the entire length of the alignment. The number of individuals affected will be small due to the restricted width of the corridor. All the species in question excepting those discussed under Sensitive Species are widespread throughout the Mohave Desert. Consequently, direct impacts to the existing habitats are judged negligible. With regard to the State-listed Mohave Ground Squirrel, the effect of the proposed project is

expected to be nonsignificant due to the lack of sightings. With regard to the Desert Tortoise, the potential effect is expected to be negligible due to the lack of evidence of recent use of the area by the species.

Portions of the eastern leg of the proposed facility will be situated atop a large berm or will lie within an excavated trench. If vegetation is allowed to establish on the side slopes of these manmade features, the wildlife will take up residence. Therefore, the long term effects may be somewhat positive in nature.

CONCLUSIONS

Since the field review of the site, the final project alignment has been shortened by over 1000 m thereby eliminating potential direct effects to existing resource elements such as Kit Fox dens, Desert Tortoise burrows, and Joshua Trees. The effect of the project on the extant resources is thus considered negligible and no additional measures are recommended.

LITERATURE CITED

A.O.U. 1983. Check-list of North American birds. American Ornithologists' Union, Allen Press, Lawrence, Kansas. 877 pp.

California Department of Fish and Game. 1980. Endangered rare and threatened animals of California, The Resources Agency, September 15.

California Department of Fish and Game. 1984. Designated endangered or rare plants, The Resources Agency, July 1.

DeDecker, M. 1984. Flora of the northern Mojave Desert, California, California Native Plant Society, Special Publication No. 7.

Jennings, M.R. 1983. An annotated checklist of the amphibians and reptiles of California. California Fish and Game 69:151-171.

Jones, J.K., Jr., D.C. Carter, H.H. Genoways, R.S. Hoffman, and D.W. Rice. 1982. Revised checklist of North American mammals north of Mexico. Occas. Papers Mus., Texas Tech Univ. 80:1-22.

Moe, L.M. and L. Heckard. 1977. Rare plant survey (map). Data from files of Environmental Engineering Office, Edwards Air Force Base.

Moe, L.M. and G.E. Lawrence. 1980. Preliminary ecological assessment report for proposed NUWAX activity on Edwards Air Force Base. Prepared for U.S. Air Force.

Moe, L.M. an G.E. Lawrence. 1981. Biological survey and impact assessment for proposed LANTIRN testing activity Edwards Air Force Base, California. Prepared for U.S. Air Force.

Munz, P.A. 1974. A flora of southern California. Univ. California Press, Berkeley. 1086 pp.

Smith, J.P., Jr. and R. York. 1984. Inventory of rare and endangered vascular plants of California. California Native Plant Society, Special Publication No. 1 (3rd Edition).

Smithsonian Institution. 1978. Interim technical report on endangered and threatened plants of Edwards Air Force Base. Prepared for U.S. Air Force.

Thorne, R.F. 1976. The vascular plant communities of California. Pp. 1-31, in Proc. Symp. on plant communities of southern California. California Native Plant Society, Special Publ. No. 2.

United States Fish and Wildlife Service. 1983a. Endangered and threatened wildlife and plants: Supplement to review of plant taxa for listing as endangered or threatened species, Federal Register 48(229):53670-53670, November 28.

United States Fish and Wildlife Service. 1983b. Republication of the lists of endangered and threatened species, Department of Interior, July 27, 25 pp.

Jaeger, E.C. 1968. Desert wildflowers. Stanford University Press, Stanford, California. 322 pp.

WIND ROSE EDWARDS AFB

1942-1965 Annual

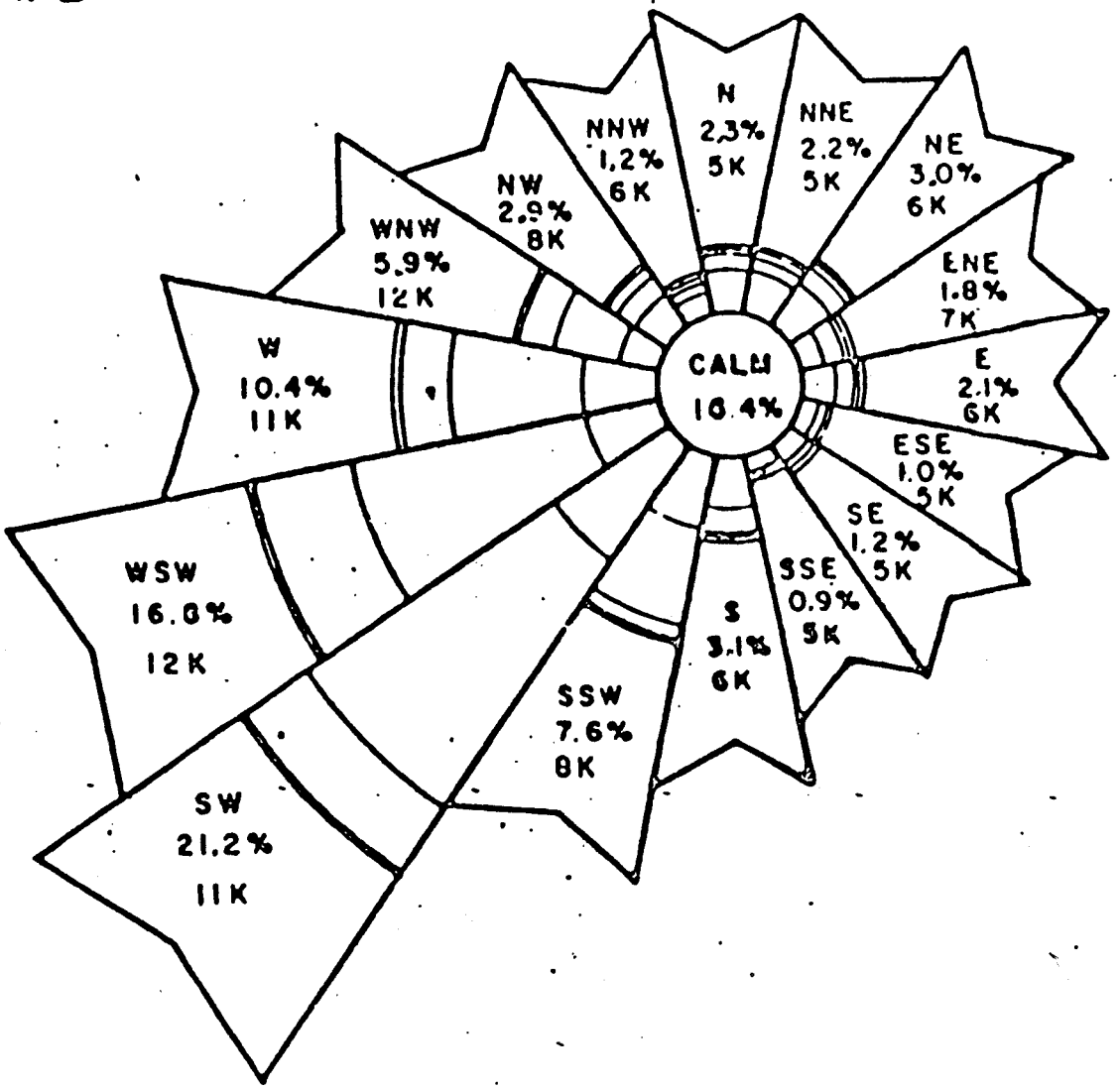

EXTREME PEAK GUST W65K 1957 WNW 65K 1954

LEGEND

% = PERCENTAGE FREQUENCY OF OCCURRENCE

K = KNOTS

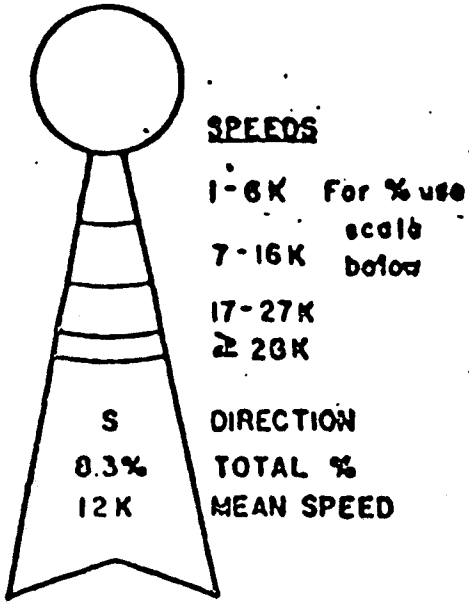

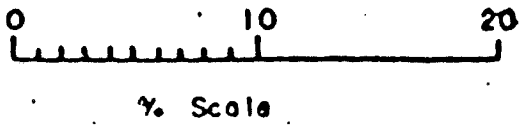

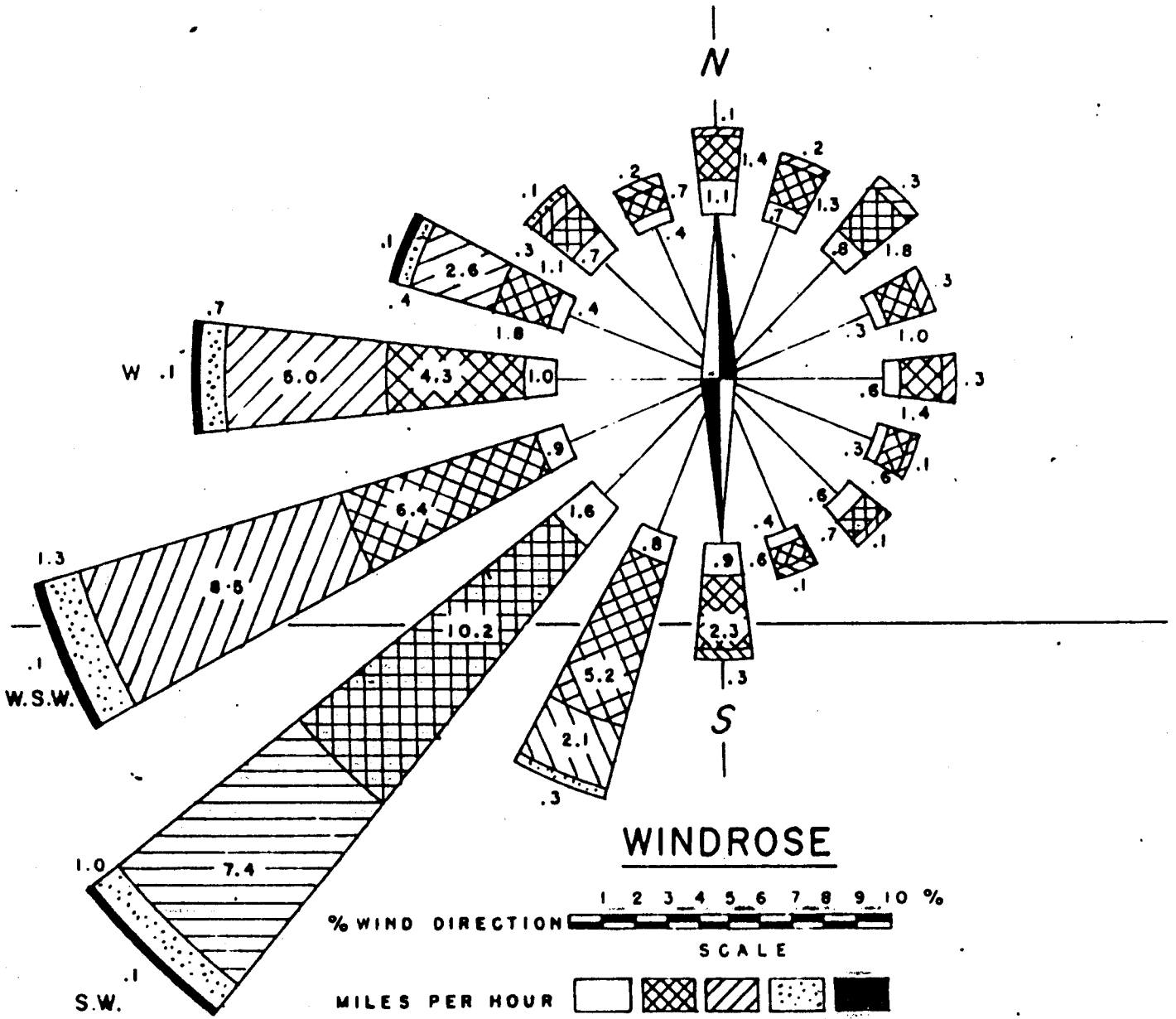
N
.1
1.4
1.1
.2
.7
1.3
.3
.8
1.8
.3
.3
1.0
.3
.6
1.4
.3
.6
.1
.6
.7
.1
.4
.6
.1
.9
2.3
.3
S
.8
5.2
2.1
.3
1.6
10.2
.9
6.4
1.3
8.6
.1
W.S.W.
1.0
7.4
.1
S.W.
.1
2.6
.4
1.8
.2
.7
.4
.1
.3
1.1
.7
.4
.7
W .1
6.0
4.3
1.0
WINDROSE
1 2 3 4 5 6 7 8 9 10 %
% WIND DIRECTION
SCALE
MILES PER HOUR
1-3 3-11 12-21 22-27 28-40
LEGEND

WIND ROSE - EDWARDS AFB, CA

ANNUAL

PERIOD OF RECORD - 1941-1972

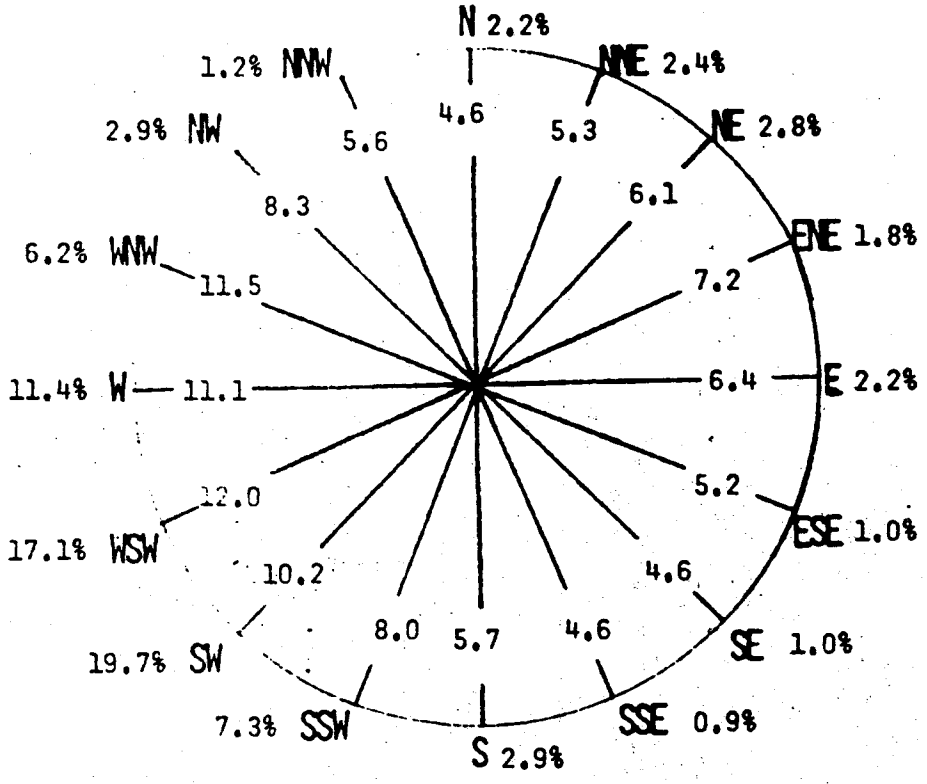

CALM = 17.1%

NOTE: PERCENTAGES SHOWN INDICATE FREQUENCY, BY DIRECTION OF SURFACE WINDS. FIGURES INSIDE CIRCLE INDICATE MEAN WIND SPEED FROM CORRESPONDING DIRECTION (SPEED IN KNOTS).

BATCH START

STAPLE
OR
DIVIDER

SITE DATA REPORTS

MAINE

Weston Geophysical
CORPORATION

September 25, 1986
WGC - R834

CALIFORNIA INSTITUTE OF TECHNOLOGY
4800 Oak Grove Drive
Pasadena, CA 91109

ATTN: Mr. Bert M. Sweetser, P.E.

Gentlemen:

In accordance with your authorization, Weston Geophysical Corporation has conducted a seismic refraction survey at your site in Columbia, Maine.

This work was performed to determine the depth to bedrock, the rippability of materials above the bedrock and to establish groundwater conditions.

Coverage took place between Stations 45+00 and 65+00 of the north westerly "L" leg, on a 400-foot cross line at Station 55+00, and on a line approximately 200-feet west and parallel to the north westerly "L" leg Stations 53+00 to 57+00.

This report presents the results and findings of the refraction survey.

Very truly yours,

WESTON GEOPHYSICAL CORPORATION

Paul S Fisk

Paul S. Fisk

PSF:pj-0662J

SEISMIC REFRACTION SURVEY
LASER INTERFEROMETER GRAVITY WAVE OBSERVATION SITE
COLUMBIA, MAINE

Prepared for

CALIFORNIA INSTITUTE OF TECHNOLOGY

SEPTEMBER 1986

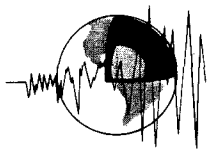

Weston Geophysical
CORPORATION

TABLE OF CONTENTS

		Page
LIST OF FIGURES		ii
1.0	INTRODUCTION & PURPOSE	1
2.0	LOCATIONING & SURVEY CONTROL	1
3.0	METHODS OF INVESTIGATION	1
4.0	MATERIAL IDENTIFICATION BASED ON SEISMIC VELOCITY VALUES	2
5.0	DISCUSSION OF FINDINGS	2
6.0	RECOMMENDATIONS	4
FIGURES		
APPENDICES		
A	SEISMIC REFRACTION SURVEY METHOD OF INVESTIGATION	

LIST OF FIGURES

FIGURE 1 AREA OF INVESTIGATION

FIGURE 2 PLAN MAP

FIGURE 3 SEISMIC REFRACTION PROFILES

FIGURE 4 RIPPER PERFORMANCE AS RELATED TO SEISMIC WAVE VELOCITIES

1.0 INTRODUCTION & PURPOSE

A seismic refraction survey was conducted on September 3 and 4, 1986 for the California Institute of Technology for the Laser Interferometer Gravity Wave Observation [LIGO] site in Columbia, Maine. A total of 2,800 feet of seismic data were obtained along 3 survey lines to determine the depth to bedrock and the seismic velocity of the soil strata and bedrock. The results of this study are to be used to classify the bedrock, determine the rippability of the materials and to establish groundwater conditions.

2.0 LOCATION & SURVEY CONTROL

The location of the area of investigation is shown on Figure 1, a segment of the Eastport, Maine [1 to 250,000] United States Geological Survey Quadrangle map. The specific location of the refraction survey lines are shown on Figure 2. Survey control for the northwesterly "L" line was provided to Weston Geophysical by the California Institute of Technology. The cross line at Station 55+00 and the Parallel Line 53+0 to 57+0 were located using compass bearings and tape measurements. Vertical control for the cross and parallel lines was determined from topographic maps provided to Weston Geophysical by the California Institute of Technology.

3.0 METHODS OF INVESTIGATION

Seismic refraction data were acquired with a 24-trace refraction system, utilizing 400-foot spread lengths with 10- and 20-foot geophone spacings. A discussion of the seismic refraction profiling techniques is included as Appendix A.

4.0 MATERIAL IDENTIFICATION BASED ON SEISMIC VELOCITY VALUES

Using seismic data alone, materials are placed into broad classifications based on the velocity of the seismic wave transmitted through them. Each velocity value does not have a unique material correlation, but most bedrock as well as overburden types fall within particular velocity ranges.

The following table of velocity values and material identifications is based on numerous measurements and correlations for similar geologic sequences as those occurring at this site.

Seismic Velocities [ft/sec.]	Material Identification
2,000 - 3,000	Most likely an unsaturated glacial till that may contain large boulders. May require localized drilling and blasting for excavation [in larger/wide excavations, boulders may be removed; in smaller/narrow excavations, boulders may have to be blasted to be removed].
4,500 - 5,500	Water saturated glacial till [probably with large boulders] and/or clays. May require localized drilling and blasting for excavation where boulders are encountered.
12,000 - 13,000	Bedrock, slightly weathered to unweathered.

5.0 DISCUSSION OF FINDINGS

The results of this survey are presented in profile form on Figure 3. Material classifications associated with the various seismic velocity ranges detected by this survey are listed in Section 4.0 of this report.

The width of the excavation may influence the method to be used for removal of boulders. In larger/wide excavations boulders may be removed, but in narrow excavations boulders may require drilling and blasting to be removed. In larger wide excavations, the glacial till [4,500 - 5,500 ft/sec.] may require some ripping; the clays [if such exist] can probably be excavated with heavy equipment. In smaller narrow excavations, boulders may require systematic drilling and blasting for removal. To assist in evaluating which seismic velocity ranges may be excavated by ripping, see Figure 4 - a manufacturers chart of ripper performance as related to seismic wave velocities. This figure indicates approximate seismic velocity ranges that can be loosened by various ripping equipment.

The bedrock surface along the 2,000-foot section of the northwesterly "L" leg investigated is generally flat with its highest elevation [approximately elevation 259] occurring between Stations 57+00 and 58+00. The currently planned excavation alignment will most likely require removal of approximately 5- to 7-feet of bedrock between Stations 52+75 to 59+00 and Stations 60+50 to 62+00. Bedrock along the rest of the northwesterly "L" leg investigated [Stations 45+00 to 65+00] appears to be up to 7-feet below the proposed bottom of the excavation.

The crossline @ 55+00 and the parallel line refraction results indicate that bedrock is deeper to the west. Bedrock between Stations 53+00 and 57+00, 200-feet west of the northwesterly "L" leg, is below the 250-foot elevation. These results indicate that if the alignment is moved to this location possibly no bedrock materials would have to be removed.

The higher velocity overburden [4,500 - 5,500 ft/sec. velocity material] overlying the bedrock is most likely water saturated [water saturated materials generally have a unique seismic velocity range of 4,800 to 5,200 ft/sec.]. These materials were consistently close to the 5,000 ± ft/sec. value indicating water saturation.

The 2,000 to 3,000 ft/sec. velocity material is associated with unsaturated overburden materials, probably ground marine type glacial till. These materials are from 5- to 10-feet thick throughout the area investigated.

6.0 RECOMMENDATIONS

Boring data should be acquired at Station 57+00 of the northwesterly "L" leg and at 55+00 of the parallel line. These borings would provide valuable data for correlation with the seismic results.

This investigation indicates that bedrock is generally 2- to 7-feet deeper then the planned bottom of the LIGO "Tunnel". However, this survey also determined two locations where bedrock will have to be removed for excavation of this alignment.

It is Weston Geophysical's experience that the most cost effective method for evaluating such alignments is to acquire seismic refraction data along the entire alignment with short X-lines at critical locations [shallow areas] and then drill selected locations to obtain confirmatory data. The seismic refraction data provides continuous information between the borings; the borings provide correlation data and confirmation of seismic results, especially with regard to the method of excavation and water table conditions.

FIGURES

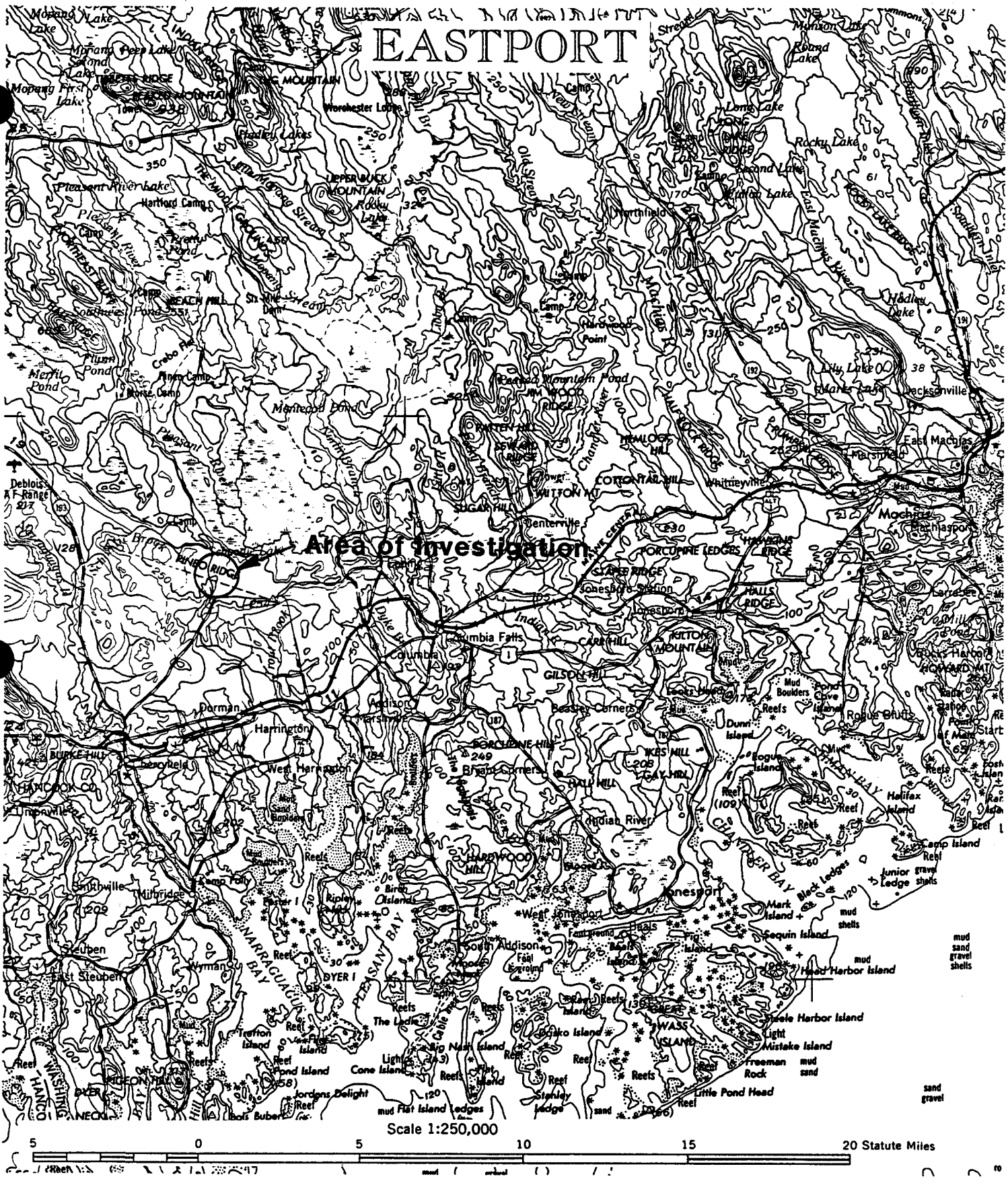

SEISMIC REFRACTION SURVEY LASER INTERFEROMETER GRAVITY WAVE OBSERVATION SITE COLUMBIA, MAINE prepared for CALIFORNIA INSTITUTE OF TECHNOLOGY	AREA OF INVESTIGATION
	WESTON GEOPHYSICAL CORPORATION September 1986 Figure 1

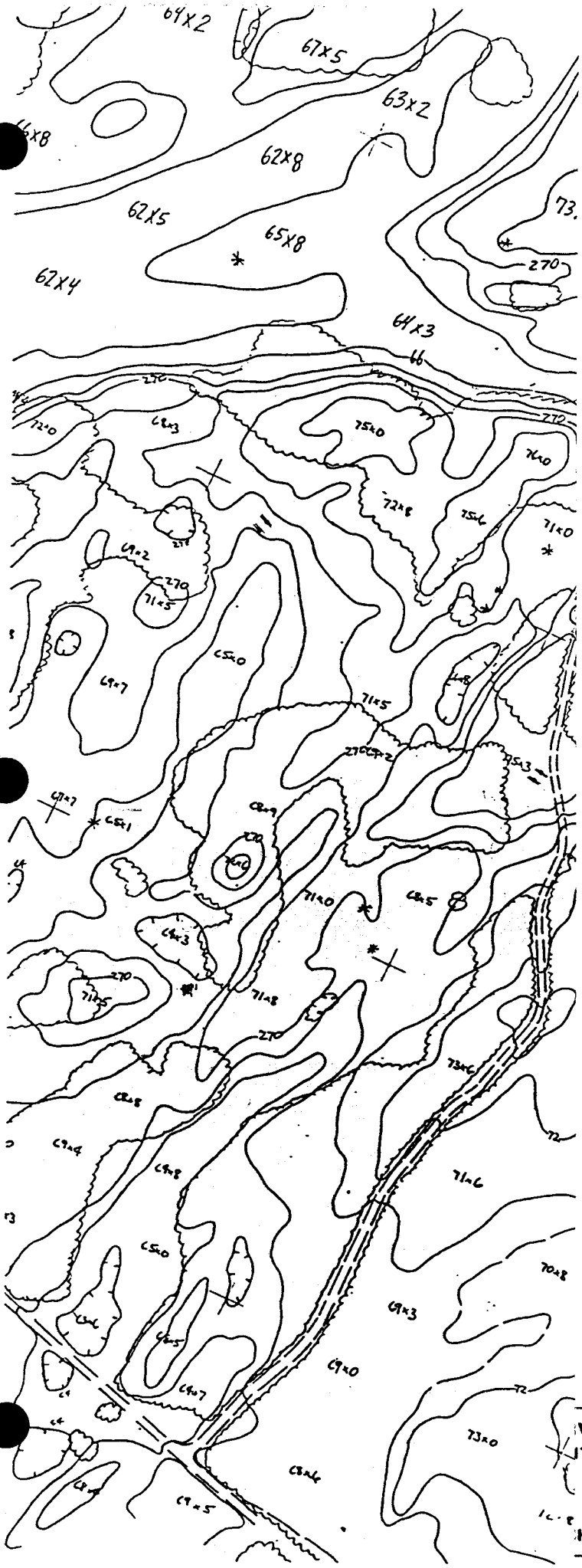

VEY TY WAVE	PLAN MAP
HNOLOGY	WESTON GEOPHYSICAL CORPORATION September 1986 Figure 2

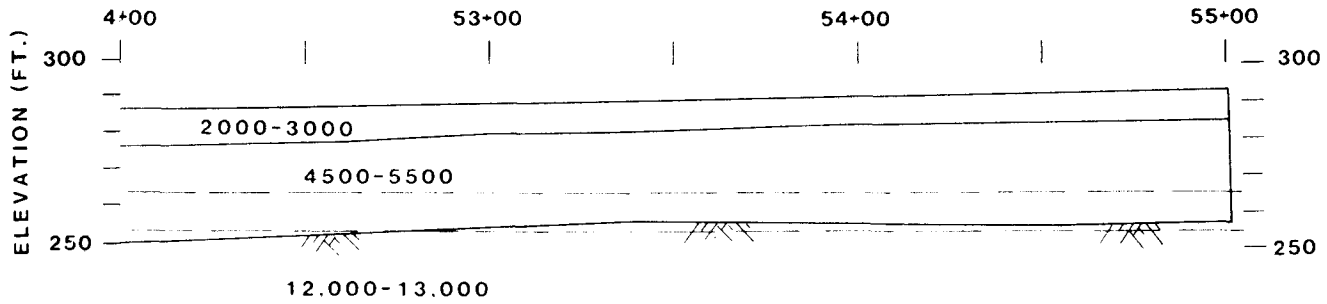

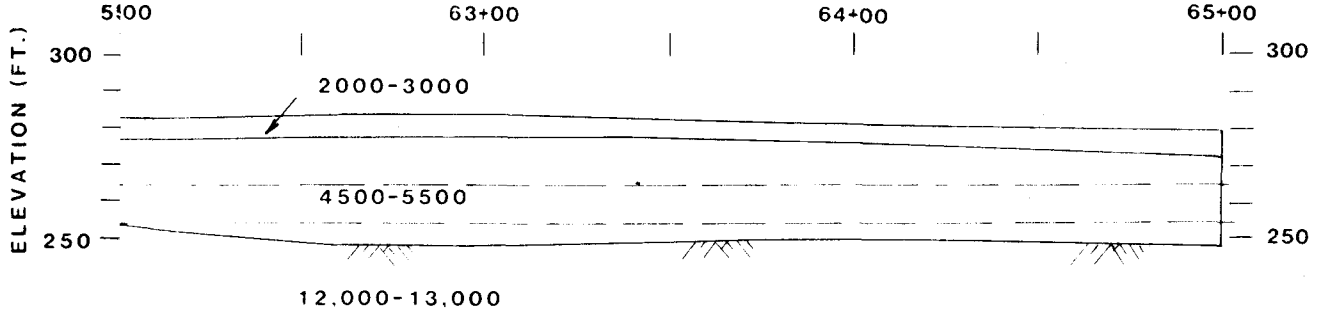

/EST

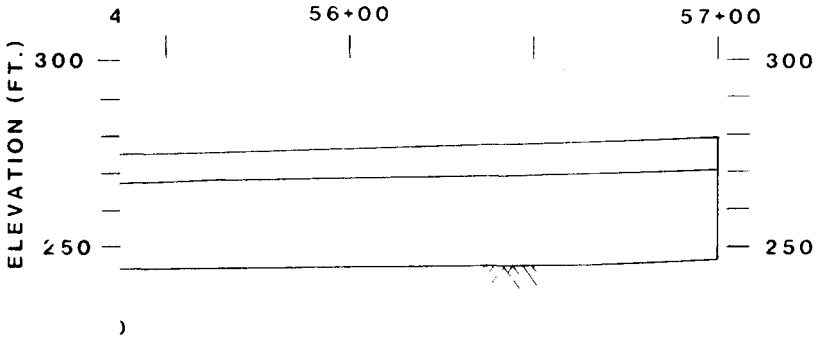

)

SEISMIC REFRACTION SURVEY LASER INTERFEROMETER GRAVITY WAVE OBSERVATION SITE COLUMBIA, MAINE prepared for CALIFORNIA INSTITUTE OF TECHNOLOGY	SEISMIC REFRACTION PROFILES WESTON GEOPHYSICAL CORPORATION September 1986 Figure 3

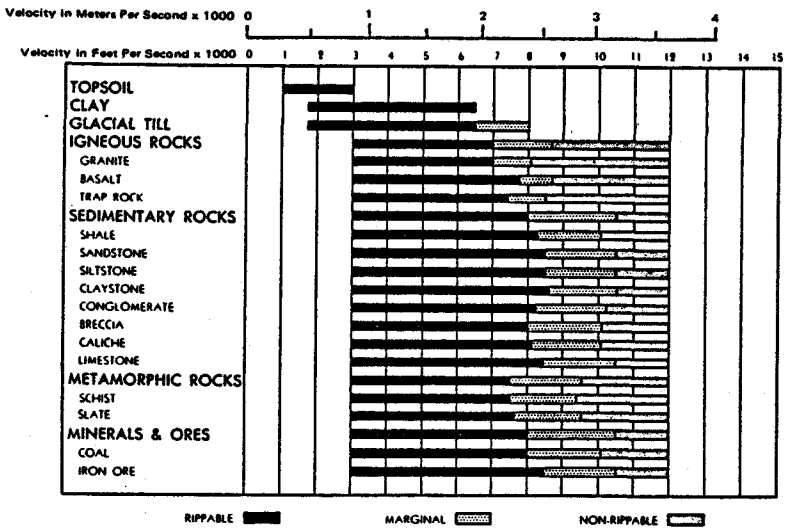

D9G — No. 9 Series D RIPPER

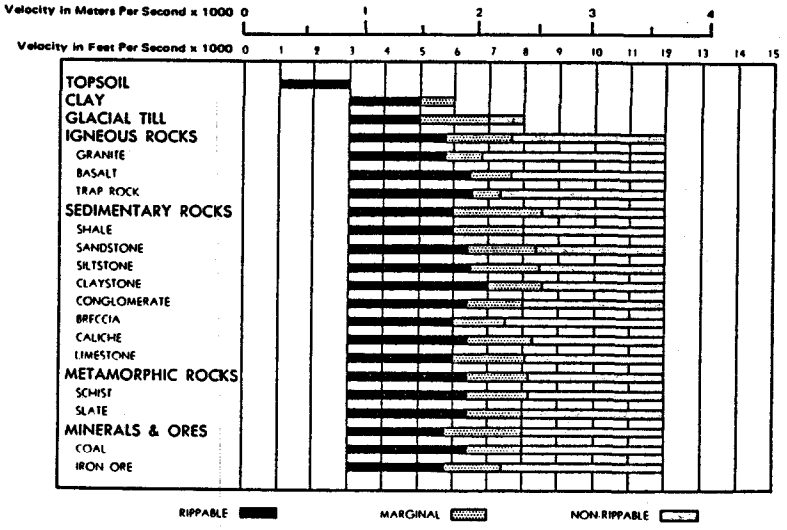

D8H — No. 8 Series D RIPPER

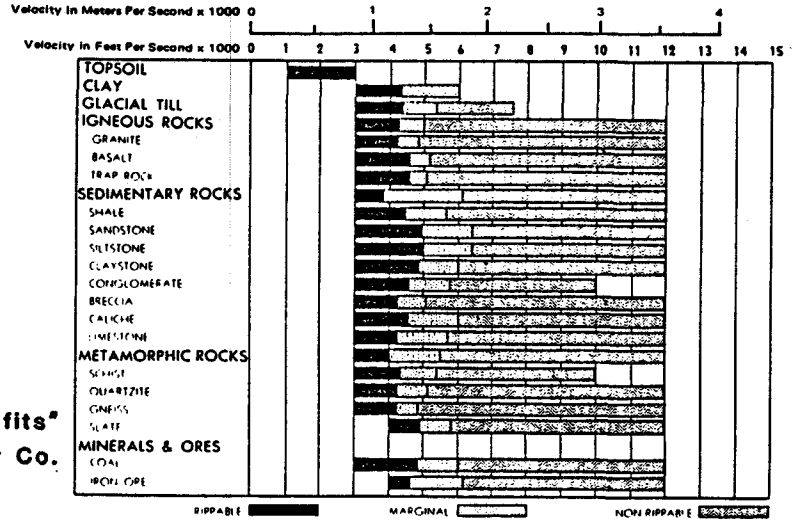

D7F — No. 7 RIPPER

From "Handbook of Ripping, a guide to greater profits" by Caterpillar Tractor Co.

SEISMIC REFRACTION SURVEY LASER INTERFEROMETER GRAVITY WAVE OBSERVATION SITE COLUMBIA, MAINE prepared for CALIFORNIA INSTITUTE OF TECHNOLOGY	RIPPER PERFORMANCE AS RELATED TO SEISMIC WAVE VELOCITIES WESTON GEOPHYSICAL CORPORATION September 1986 Figure 4

APPENDIX A

SEISMIC REFRACTION SURVEY
METHOD OF INVESTIGATION

GENERAL CONSIDERATIONS

The seismic refraction survey method is a means of determining the depths to a refracting horizon and the thickness of major seismic discontinuities overlying the high-velocity refracting horizon. The seismic velocities measured by this technique can be used to calculate the mechanical properties of subsurface materials [moduli values], as well as for material identification and stratigraphic correlation.

Interpretations are made from travel time curves showing the measurement of the time required for a compressional seismic wave to travel from the source ["shot"] point to each of a group of vibration sensitive devices [seismometers or geophones]. The geophones are located at known intervals along the ground surface, as shown in Diagram A. Various seismic sources may be used, including a drop weight, an air gun, and small explosive charges.

FIELD PROCEDURE FOR DATA ACQUISITION

Weston Geophysical Corporation uses a seismic recording technique of continuous profiling and overlapping spreads for engineering and ground water investigations. The seismic refraction equipment consists of a Weston Geophysical trace amplifier, Model USA780, with either a WesComp II™ [a field computer system developed by Weston], or a recording oscillograph.

Continuous profiling is accomplished by having the end shot-point of one spread coincident with the end or intermediate position shot-point of the succeeding spread. The spread length used in a refraction survey is determined by the required depth of penetration to the refracting horizon. It is generally possible to obtain adequate penetration when the depth to the refracting horizon is approximately one-third to one-quarter of the spread length.

In general, "shots" are located at each end and at the center of the seismic spread, Diagram B. The configuration of the geophone array and the shot point positions are dependent upon the objectives of the seismic array.

As mentioned above, seismic energy can be generated by one or more of several sources.

The seismometer or geophone is in direct contact with the earth and converts the earth motion resulting from the shot energy into electric signals; a moving coil electromagnetic geophone is generally used. This type of detector consists of a magnet permanently attached to a spiked base which can be rigidly fixed to the earth's surface. Suspended within the magnet is a coil wrapped mass. Relative motion between the magnet and coil produces an electric current, with a voltage proportional to the particle velocity of the ground motion.

The electric current is carried by cable to the recording device which provides simultaneous monitoring of each of the individual geophones. The operator can amplify and filter the seismic signals to minimize background interference. For each shot the seismic signals detected by a series of geophones are recorded on either photographic paper or magnetic tape, depending on job requirements. Included on each shot record is a "time break" representing the instant at which the shot was detonated.

INTERPRETATION THEORY

The elastic wave measured in the seismic refraction method, the "P" or compressional wave, is the first arrival of energy from the source at the detector. This elastic wave travels from the energy source in a path causing adjacent solid particles to oscillate in the direction of wave propagation. Diagram A shows a hypothetical subsurface consisting of a lower velocity material above a higher velocity material. At smaller distances between source and detector the first arriving waves will be direct waves that travel near the ground surface through the lower velocity material. At greater distance, the first arrival at the detector will be a refracted wave that has taken an indirect path through the two layers. The refracted wave will arrive before the direct wave at a greater distance along the spread because the time gained in travel through the higher-speed material compensates for the longer path. Depth computations are

based on the ratio of the layer velocities and the horizontal distance from the energy source to the point at which the refracted wave overtakes the direct wave.

Generally the interpretation is by one or more of several methods [W.M. Telford, et al, 1976] ray-tracing, wave front methods, delay times, critical distances, etc. In addition, either a forward or inverse interpretation can be performed using Weston's computer. Since successful refraction interpretation is based on experience, all interpretation of refraction data is performed or thoroughly reviewed by a senior staff geophysicist.

Reference

Telford, W.M.; Geldart, L.P.; Sheriff, R.E. and Keys, D.A., 1976, Applied Geophysics: Cambridge University Press.

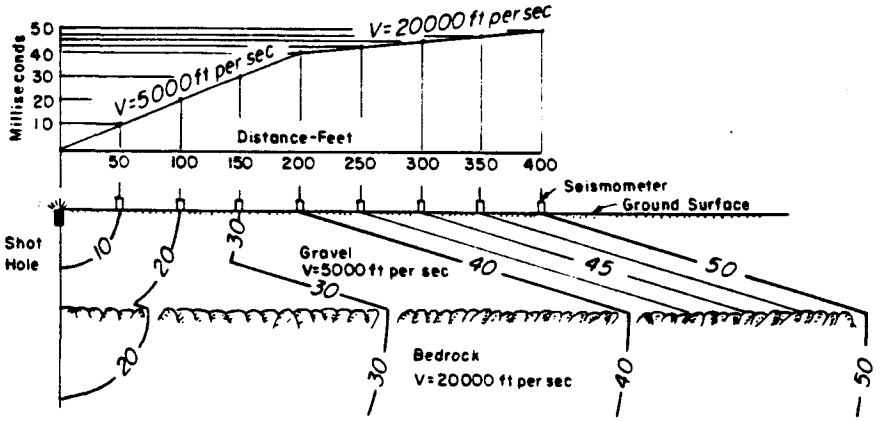

Plot of Wave Front Advance in Two Layered Problem

Linehan, Daniel, Seismology Applied to Shallow Zone Research, Symposium on Surface and Subsurface Reconnaissance, Special Technical Publication No. 122, American Society for Testing Materials, 1951.

Diagram A

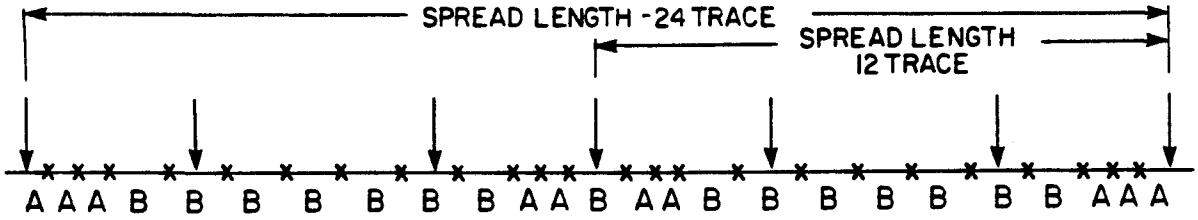

SPREAD LENGTH	GEOPHONE LOCATION A	B
400' - 24 TRACE or 200' - 12 TRACE	10	20
600' - 24 TRACE or 300' - 12 TRACE	15	30
1000 - 24 TRACE or 500' - 12 TRACE	25	50

LEGEND

↓ = GENERAL LOCATION OF "SHOT" POINT

x = GEOPHONE LOCATION

Geophone Interval-Spread Length Relationship

Diagram B

LASER INTERFEROMETER GRAVITY WAVE OBSERVATORY
DEPTH TO GROUND WATER AND BEDROCK
PRELIMINARY GEOTECHNICAL REPORT

INTRODUCTION

Robert G. Gerber, Inc. (RGGI) recently performed a preliminary subsurface exploration for the proposed gravity wave observatory tunnel in Columbia, Maine. Authorization and on-site supervision of this work were provided by representatives of the California Institute of Technology (Cal Tech).

The purpose of this exploration was to collect subsurface information in areas of the proposed alignment where ground water and bedrock were suspected to be above the planned depth of construction excavation. The subsurface exploration include drilling test holes to identify subsurface materials, and installing test wells at selected locations for measurement and sampling of ground water.

The exploration focused on a segment of the northwestern alignment, between Stations 18+00 and 69+00 where surface topography and geophysical profiles indicated ground water and bedrock to be above the planned tunnel invert. Borings where made at other locations on the northwest and northeast alignments to identify subsurface conditions where topography and geology were believed to be more typical of the general project area. Following the completion of field work, test hole data were reviewed and combined with other surface and subsurface information to develop our understanding of local geologic conditions and their potential effect on the construction of the facility.

This report summarizes the data obtained at the site and presents a discussion of geologic and hydrologic conditions of those portions of the alignment that were explored.

BACKGROUND

The proposed observatory tunnel will be located on a regionally high plain known as the blueberry barrens of Pineo Ridge. This broad and open area is characterized by relatively dry and sandy soil which supports the commercial growth of blueberries. The blueberry barrens form an arc-shaped landform which extends in an east-west orientation and covers approximately 10 square miles. The elevation of the barrens ranges from about 260 feet above mean sea level (MSL) at the southern margins to about 329 feet MSL at a hilltop near the center of the feature. Except for the local topographic variations associated with the central hill and several small drainage channels, elevations generally range from 260 feet to 275 feet MSL.

The surficial geology of Pineo Ridge and the surrounding area has been mapped by Borns (1982) and recently re-mapped by Miller (1986). Gilman (1961) mapped the bedrock geology of the area. These geologic maps and reports have been published by the Maine Geological Survey and are listed in the Reference

LASER INTERFEROMETER GRAVITY WAVE OBSERVATORY
DEPTH TO GROUND WATER AND BEDROCK
PRELIMINARY GEOTECHNICAL REPORT

INTRODUCTION

Robert G. Gerber, Inc. (RGGI) recently performed a preliminary subsurface exploration for the proposed gravity wave observatory tunnel in Columbia, Maine. Authorization and on-site supervision of this work were provided by representatives of the California Institute of Technology (Cal Tech).

The purpose of this exploration was to collect subsurface information in areas of the proposed alignment where ground water and bedrock were suspected to be above the planned depth of construction excavation. The subsurface exploration include drilling test holes to identify subsurface materials, and installing test wells at selected locations for measurement and sampling of ground water.

The exploration focused on a segment of the northwestern alignment, between Stations 18+00 and 69+00 where surface topography and geophysical profiles indicated ground water and bedrock to be above the planned tunnel invert. Borings where made at other locations on the northwest and northeast alignments to identify subsurface conditions where topography and geology were believed to be more typical of the general project area. Following the completion of field work, test hole data were reviewed and combined with other surface and subsurface information to develop our understanding of local geologic conditions and their potential effect on the construction of the facility.

This report summarizes the data obtained at the site and presents a discussion of geologic and hydrologic conditions of those portions of the alignment that were explored.

BACKGROUND

The proposed observatory tunnel will be located on a regionally high plain known as the blueberry barrens of Pineo Ridge. This broad and open area is characterized by relatively dry and sandy soil which supports the commercial growth of blueberries. The blueberry barrens form an arc-shaped landform which extends in an east-west orientation and covers approximately 10 square miles. The elevation of the barrens ranges from about 260 feet above mean sea level (MSL) at the southern margins to about 329 feet MSL at a hilltop near the center of the feature. Except for the local topographic variations associated with the central hill and several small drainage channels, elevations generally range from 260 feet to 275 feet MSL.

The surficial geology of Pineo Ridge and the surrounding area has been mapped by Borns (1982) and recently re-mapped by Miller (1986). Gilman (1961) mapped the bedrock geology of the area. These geologic maps and reports have been published by the Maine Geological Survey and are listed in the Reference

section of this report.

A site-specific geophysical survey was performed over a portion of the proposed project alignment in September by Weston Geophysical Corporation. Weston conducted a seismic refraction survey along 2000 feet of the northwest tunnel alignment between stations 45+00 and 55+00, and a 700 foot refraction survey line, west of the alignment at station 55+00. The report prepared by Weston dated September, 1986 presents seismic refraction profiles and a discussion of the survey findings.

GEOLOGIC SETTING

Surficial Geology

The glacial landforms of the area are described by Borns as a complex of a terminal moraine of the Pineo Ridge glacial readvance, and an associated glacial outwash delta. A terminal moraine may be described as a distinct accumulation of unsorted, unstratified soil deposited along the leading edge of an advancing glacier. Landforms commonly associated with terminal moraines include ridges, knolls and hummocks, often surrounding closed depressions. Soil materials range from clay to large boulders and are commonly heterogeneous.

Cobbles and boulders are common in moraines (owing to the capacity of glacial ice to transport tremendous loads). Although these materials are typically oriented randomly throughout the moraine, localized concentrations, and boulder trains may be present. Generally speaking, boulders less than two feet in mean diameter are most common in terminal moraines. However, boulders of several cubic yards in size may also be present. Such large boulders are evident on the surface of the barrens.

Terrain relationships of the area suggest that as the glacial advance stagnated, the ice was in contact with the sea, and as the retreat began, melt water from the glacier and sea water reworked the moraine. Poorly sorted outwash materials and reworked till may have been deposited at the margins of the terminal moraine in a beach or submarine environment. This transition zone deposit, or diamicton, may contain all of the constituent materials of a moraine, but may be somewhat stratified as a result of a marine depositional environment.

Outwash deltas are relatively flat-lying deposits, composed predominantly of sand and gravel carried by meltwaters to a low-energy environment at the edge of the glacier. Although granular materials comprise the majority of these land forms, silt and clay layers may fill channels in the deposit. Similarly, cobbles and some boulders are present in the delta topset beds. Boulder and cobble content usually decreases with distance from the terminal moraine.

Since outwash deltas aggrade in both horizontal and vertical directions, a characteristic sequence of layers typically develops. Finer grained soils are deposited in sloping layers at the face of the delta (foreset beds) building a soil formation that eventually extends from the ocean floor up to sea level. These deposits, in turn, are overlain by coarser soils (topset beds) deposited by outwash streams in shallow water or beach environments. The result is a sequence with decreasing grain size with depth.

Outwash deltas may be interlayered with diamicton deposits in the proximal (near source) portions of the feature. They may also include materials, such as boulders, that are ice rafted to more distal (away from source) areas, and dropped into the aggrading sediments of the delta.

Bedrock Geology

The bedrock geology of the Cherryfield area, as mapped by Gilman, consists of two Formations. Intrusive granites of Devonian age were mapped in the north portion of the area while volcanic rocks of the Columbia Falls Formation, Ordovician-Precambrian age, are mapped in the south portion. In the area of Pineo Ridge, bedrock is overlain by surficial deposits and the contact of the two rock formations is obscured from view. Gilman's mapping indicates that bedrock located below the project site is of granitic composition. No faults were mapped in the project area.

Three areas of shallow bedrock were mapped by Borns in the surficial deposits of Pineo Ridge. These mapped areas of shallow bedrock are oblong in shape, having widths ranging from 2,500 feet to 4,000 feet. The locations of these areas mark the front of the terminal moraine, the furthest extent of the Pineo Ridge glacial readvance, and may have caused the stagnation of that advance.

The largest of the three areas of shallow bedrock is located immediately east of the northwest tunnel alignment. The other two areas are situated well to the west of that alignment and are bounded on the north by Schoodic Lake. It was the location of the large area of shallow bedrock, situated in close proximity to the proposed alignment between stations 45+00 and 65+00, that required field exploration to improve definition.

FIELD EXPLORATION

Exploratory drilling began at the proposed tunnel alignment on November 17 and was completed on November 20, 1986. A geologist from RGGI was on site to direct the exploration and to gather geologic data as drilling progressed. Seven locations were drilled in this program of field work, six of which were situated on the northwest alignment. One drilling location, situated on the northeast alignment was near the mid-point of that tunnel limb. Drilling locations were approved by Engineers from Cal Tech who were on site to supervise the drilling program.

Drilling equipment was supplied and manned by Maine Test Borings, Inc., of Brewer, Maine. The drill used was a Mobile B-47 that was mounted on an

all-terrain "Bombadier" tracked-carrier. Continuous flight helical augers were used to advance the borings.

A total of nineteen borings were made at the seven sites. Depths of these borings ranged from 4.2 feet to 30.0 feet below the surface. Hollow-stem augers measuring 3-3/8 inches I.D. were used at each location allowing down-hole sampling of the soil with split spoon samplers. Auger holes were advanced without water or other drilling fluid. In general, split-spoon samples were taken at five foot intervals. Several times, in very dense and bouldery soil, drive sampling recovery was limited or entirely unsuccessful.

When obtaining drive samples, the sampling procedure was conducted in accordance with the ASTM standard penetration test (ASTM D 1586). A 140-pound hammer was raised and dropped a distance of 30 inches to advance a standard 1.4-inch I.D. split spoon sampler into the soil. Blows were counted at 6-inch intervals and recorded on the field log together with descriptions of the recovered soil, identified ground water, and behavior of the drilling equipment. Soil samples were placed in glass jars and made air-tight immediately after being described. Following the completion of the drilling program, the samples were transported to the RGGI office and soil laboratory for re-examination and storage.

Large and numerous boulders prevented hollow stem augers from reaching the planned depth of drilling in all but one of the five original borings. These were located to investigate the area identified as having bedrock within the proposed construction excavation. Boring B-1, located at station 17+37, was completed to a total depth of 24.5 feet using hollow-stem augers. Where hollow-stem augers were ineffective, solid stem augers were used in efforts to penetrate to the desired depth of drilling. As many as four additional attempts were made at some drilling locations. In all, twelve probe holes were made in addition to the seven borings made using hollow-stem augers.

Due to the unexpectedly difficult drilling conditions encountered in borings B-2 through B-5, RGGI's geologist recommended that two additional borings be made. This would permit reconnaissance of other portions of the alignments and correlation of terrain variations with subsurface conditions over the larger project area. Boring B-6 was drilled at station 9+35 and offset 70 feet west of centerline to place it in a wind-row of small pine trees, out of actively cultivated blueberry fields. This boring was advanced to a total depth of 29.5 feet using hollow-stem augers and allowed collection of soil samples and subsequent installation of a monitoring well. Boring B-7 was drilled at station 53+76 on the previously unexplored northeast alignment, approximately where the powerline crosses that limb of the proposed tunnel. Difficult drilling conditions, similar to those encountered in borings B-2 through B-5, were experienced at this location. Boring B-7 was advanced to only 4.5 feet in bouldery soil when the drill developed severe mechanical difficulties preventing further advancement of the boring. Drilling was then terminated.

INSTRUMENTATION

Ground water monitoring wells were installed in three of the borings: B-1 at station 17+37; B-2b at station 34+70; and B-6 at station 9+35. The locations of these borings were planned and field-adjusted so that the ground water monitoring wells would be placed in areas near access trails or roads but protected from truck or other agricultural equipment.

Each of these monitoring wells was constructed of 2-inch I.D. schedule 40 pvc pipe and included a five foot section of well screen with 0.020" slots. Clean uniform sand was used to backfill the screened portion of the monitoring well installed at boring B-2b to prevent silt from accumulating in the well bottom. Naturally clean and poorly graded sand was encountered in borings B-1 and B-6 so imported backfill was not used at those locations. Bentonite was used around the surface of each monitoring well to prevent surface water from migrating through the backfill of the boring to the ground water table.

Ground water depth measurements were made at each of the three monitoring wells during the drilling program as indicated on Table 1. Additional readings and ground water samples may be obtained at a future date.

EVALUATION

Soil conditions observed in the borings of this exploration program varied with location and terrain and correlated well with the distinctly different glacially derived soil deposits of the Pineo Ridge area. Similarly, ground water conditions were consistent with the terrain and with the permeability of the soil formations observed at the site. The exploration technique of drilling with medium weight drilling equipment using helical augers was not successful in confirming the depth to bedrock as intended in this program.

Both northeast and northwest trending tunnel alignments traverse the glacially derived terrain complex of the terminal moraine and outwash delta of Pineo Ridge as mapped by Borns of the University of Maine.

Exploration of the northwest alignment indicates that borings B-2 and all other borings located on that limb north of that location are situated on the terminal moraine deposits. These deposits were found to be dense to very dense materials containing a heterogeneous mixture of soil, cobbles, and boulders. The moraine soils that were observed were moderate to poorly drained in a ground water sense.

Surficial soils information from this exploration and Quaternary Geology maps indicate that a drainage channel trending northeast to southwest across the barrens and intersecting the the northwest tunnel alignment at approximately station 34+50, marks the transition zone of terminal moraine to outwash plain. Boring B-2 was placed at this intersection. Ground water was observed at a depth of 5 feet in the monitoring well installed at boring B-2, the only well installed in the moraine deposit.

Subsurface conditions observed at locations south of the transition zone, in borings B-1 and B-6, were characteristic of the outwash delta mapped in that area. Both borings encountered stratified granular soils with cobbles and boulders near the surface and decreasing grain size with depth. Piezometers were installed in B-1 and B-6. Ground water was measured at depths of 17.1 and 25.0 feet, respectively.

Exploration of the northeast alignment was outside the original scope of this program. However, we drilled an initial boring (B-7) at station 53+76. Subsurface conditions, within the 4.5 feet of depth at that boring were characteristic of the terminal moraine deposits mapped in that area. Like boring B-2, boring B-7 appeared to be located in a transition zone of the two major landforms of the project area. Although no stream channel was evident to mark the transition, a decrease in the number and size of exposed boulders to the south and west indicated a gradual transition from the terminal moraine to outwash plain landform. Terrain mapping indicates the intersection of the northeast alignment and the landform transition zone to be between stations 50+00 and 70+00.

RECOMMENDATIONS

This early phase of site exploration has provided initial soil and ground water information that can be used to develop our understanding of general terrain types and relationships. However, the findings of shallow ground water and large boulders in the extensive terminal moraine deposits make additional geotechnical and hydrogeological information of immediate importance to the design of the observatory tunnels.

Additional exploration of the northwest tunnel alignment should be made using techniques other than hollow-stem augers. This phase of investigation should be part of a preliminary geotechnical investigation to study the subsurface conditions of both tunnel alignments. The program should include test pit excavations, borings with instrumentation, and seismic refraction surveys. Test pits should be made using equipment capable of excavating to 25 feet. Additional drilling should be done using casing that can be rotated to cut through boulders. Refraction surveys should be conducted over the entire alignment with cross-lines made at several locations.

Measurements of depth to ground water should be made at the three installed monitoring wells during spring recharge. Ground water samples should be obtained in May, 1987, and analyzed to develop baseline water quality levels for the site.

References

Borns, H.W. Jr., 1978, Emerged Glacial Marine Deltas in Maine. University of Maine, Orono, for Maine State Planning Office, Augusta, Maine. 32 pages.

Borns, H.W. Jr., and Anderson, B., 1982, Reconnaissance Surficial Geology of the Cherryfield Quadrangle, Maine, Open file map. Scale 1: 62,500, University of Maine, Orono, for the Maine Geological Survey, Augusta, Maine.

Gilman, R.A., 1961, Reconnaissance Bedrock Geology of the Cherryfield Quadrangle, Maine. Scale 1:62,500, Maine Geological Survey, Augusta, Maine.

Flint, R.F., 1964, Glacial and Quaternary Geology. Yale University, John Wiley & Sons, Inc., New York, New York. 892 pages.

Weston Geophysical Corporation, 1986, Seismic Refraction Survey, Laser Interferometer Gravity Wave Observatory Site, Columbia, Maine. Westboro, Mass.

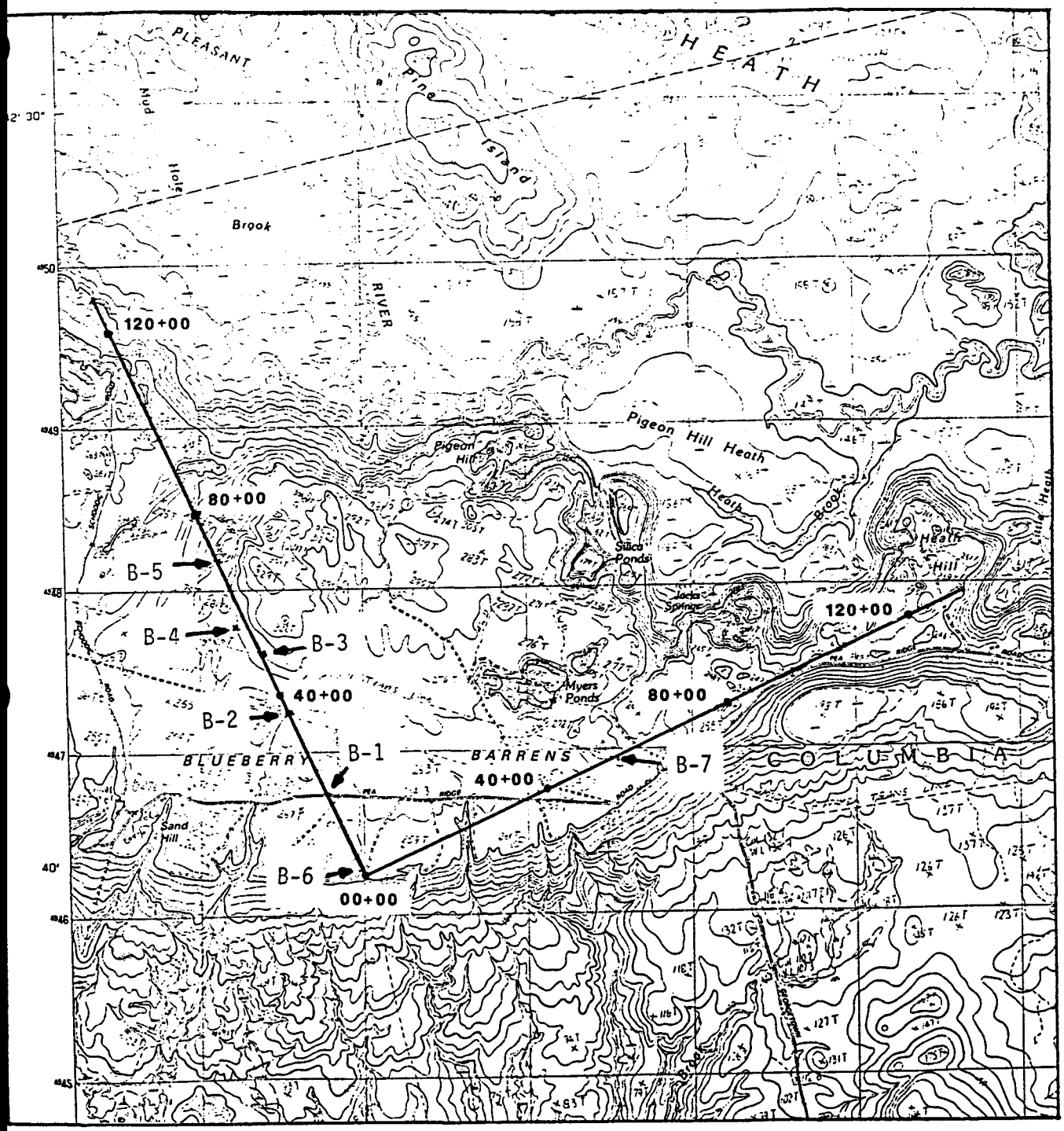

PLAN OF BORING LOCATIONS

SCALE

1-inch = 3,000-feet

LEGEND

00+00 Station points

B-1 Boring numbers

GRAVITY WAVE OBSERVATORY

COLUMBIA, MAINE

ROBERT G. GERBER, INC.

17 WEST STREET

FREEPORT, MAINE

FIGURE 1

AINE TEST BORINGS, INC.
REWER, MAINE 04412

CLIENT
Robert Gerber

SHEET 1 OF 1
HOLE NO. B-1

ER
Tom Schaefer

PROJECT NAME
Gravity wave

LINE & STATION
NW 17 + 37

JOB NUMBER
86-245

LOCATION
Columbia, Maine

OFFSET
0

GROUND WATER OBSERVATIONS
____ FT. AFTER ____ HOURS
____ FT. AFTER ____ HOURS

	CASING	SAMPLER	CORE BARREL
TYPE	HS	SS	
SIZE I.D.	3 3/8"	1 3/8"	
HAMMER WT.	300	140	
HAMMER FALL	16"	30"	

DATE START 11/18/86 DATE FIN. 11/18/86
SURFACE ELEV. APPROX. 265'
GROUND WATER ELEV. APPROX 248'

CASING BLOWS PER FOOT	SAMPLE NO.	O.D.	PEN.	REC.	DEPTH @ BOT.	BLOWS PER 6" ON SAMPLER 0-6	6-12	12-18	VANE READING	DEPTH	STRATUM DESCRIPTION
										0.5	Topsoil.
	1D	2"	18"	5%	1.5	2	2	3		2.0	Brown silty fine to med. sand. (SM)
										4.0	Brown silty med. to fine sand w/little gravel. (SM) MEDIUM DENSE; DRY.
	2D	2"	18"	90%	6.5	11	20	30		8.3	Brown med. to coarse sand w/some fine sand & coarse gravel. (SW) DENSE; DRY. SAND is subangular to ANGULAR IN SHAPE.
	3D	2"	18"	80%	11.5	19	24	23		13.0	Brown med. to coarse sand w/some fine sand & gravel trace of cobbles. (SW) DENSE; DRY.
	4D	2"	18"	60%	16.5	9	15	14			Brown fine to med. sand w/little silt. (SP) SOIL TEXTURE VARIES W/ DEPTH IN this INTERVAL, BECOMING FINER W/ DEPTH SATURATED AT APPROX. 17 feet.
	5D	2"	18"	0%	21.5	6	22	53			SAND is subANGULAR to subROUNDED POSSIBLE RUNNING SAND IN UNCONFINED CONDITIONS.
	6D	2"	18"	100%	25.0	30	62	94		25.0	
											Bottom of boring @ 25.0' Installed well to 23 feet. SCREEN from 18' to 23'. Water @ 17.1'

SAMPLES
D = Splite Spoon
C = 2" Shelby Tube
U = 3½" Shelby Tube

SOIL CLASSIFIED BY:
[x] Driller - Visually
[X] Soil Technican - Visually
[ ] Laboratory Tests

REMARKS
USCS SOIL DESCRIPTIONS MADE by visual inspection.
BORING LOG ANNOTATED BY RGGI GEOLOGIST J. HILLIER

HOLE NO. B-1

AINE TEST BORINGS, INC. REWER, MAINE 04412	CLIENT Robert Gerber	SHEET 1 OF 1 HOLE NO. B-2
ER Tom Schaefer	PROJECT NAME Gravity wave	LINE & STATION NW 34+40
B. JOB NUMBER 86-245	LOCATION Columbia, Maine	OFFSET CENTERLINE

GROUND WATER OBSERVATIONS

_____ FT. AFTER _____ HOURS

_____ FT. AFTER _____ HOURS

	CASING	SAMPLER	CORE BARREL
TYPE	HS	SS	
SIZE I.D.	3 3/8"	1 3/8"	
HAMMER WT.		140	
HAMMER FALL		30"	

DATE START 11/17/86 DATE FIN. 11/17/86

SURFACE ELEV. Approx. 268'

GROUND WATER ELEV. Approx. 263'

CASING BLOWS PER FOOT	SAMPLE NO.	O.D.	PEN.	REC.	DEPTH @ BOT.	BLOWS PER 6" ON SAMPLER 0-6	6-12	12-18	VANE READING	DEPTH	STRATUM DESCRIPTION
										0.4	Topsoil. (OL)
	1D	2"	18"	10%	1.5	3	3	6		2.0	Gray brown silty fine sand w/little coarse sand.
											Brown silty fine sand w/some coarse gravel & cobbles
										5.0	
	2D	2"	12"	60%	6.0	48	88				Gray, brown gravelly sand, trace of cobbles.
										7.7	VERY DENSE; WET below 5ft. (SP) Numerous boulders
											Refusal @ 7.7'

SAMPLES
D = Splite Spoon
C = 2" Shelby Tube
U = 3½" Shelby Tube

SOIL CLASSIFIED BY:
[X] Driller - Visually
[X] Soil Technican - Visually
[ ] Laboratory Tests

REMARKS:
USCS SOIL DESCRIPTIONS MADE by visual inspection
BORING LOG ANNOTATED by R.G.G.I. GEOLOGIST J. HILLIER
THE PRESENCE of COBBLES AND
BOULDERS is INFERRED by DRILLING ACTION.

HOLE NO. B-2

AINE TEST BORINGS, INC.
REWER, MAINE 04412

CLIENT
Robert Gerber

SHEET 1 OF 1
HOLE NO. B-2A

ER
Tom Schaefer

PROJECT NAME
Gravity wave

LINE & STATION
NW 34+40

JOB NUMBER
86-245

LOCATION
Columbia, Maine

OFFSET
CENTERLINE

GROUND WATER OBSERVATIONS
____ FT. AFTER ____ HOURS
____ FT. AFTER ____ HOURS

	CASING	SAMPLER	CORE BARREL
TYPE	probe		
SIZE I.D.	auger		
HAMMER WT.			
HAMMER FALL			

DATE START 11/17/86 DATE FIN. 11/17/86
SURFACE ELEV.
GROUND WATER ELEV.

CASING BLOWS PER FOOT	SAMPLE NO.	SAMPLE O.D.	SAMPLE PEN.	SAMPLE REC.	SAMPLE DEPTH @ BOT.	BLOWS PER 6" ON SAMPLER 0-6	6-12	12-18	VANE READING	DEPTH	STRATUM DESCRIPTION
											Brown gravelly sand w/cobbles & boulders.
										9.2	Refusal @ 9.2'

SAMPLES
D = Splite Spoon
C = 2" Shelby Tube
U = 3½" Shelby Tube

SOIL CLASSIFIED BY:
[X] Driller - Visually
[ ] Soil Technican - Visually
[ ] Laboratory Tests

REMARKS:

HOLE NO. B-2A

AINE TEST BORINGS, INC.
REWER, MAINE 04412

CLIENT
Robert Gerber

SHEET 1 OF 1
HOLE NO. B-2B

ER
Tom Schaefer

PROJECT NAME
Gravity wave

LINE & STATION
NW 3+70

JOB NUMBER
86-245

LOCATION
Columbia, Maine

OFFSET
CENTERLINE

GROUND WATER OBSERVATIONS
____ FT. AFTER ____ HOURS
____ FT. AFTER ____ HOURS

	CASING	SAMPLER	CORE BARREL
TYPE	HS	SS	
SIZE I.D.	3 3/8"	1 3/8"	
HAMMER WT.		140	
HAMMER FALL		30"	

DATE START 11/17/86 DATE FIN. 11/17/86
SURFACE ELEV. APPROX. 268'
GROUND WATER ELEV. APPROX. 263'

CASING BLOWS PER FOOT	SAMPLE NO.	SAMPLE O.D.	SAMPLE PEN.	SAMPLE REC.	SAMPLE DEPTH @ BOT	BLOWS PER 6" ON SAMPLER 0-6	6-12	12-18	VANE READING	DEPTH	STRATUM DESCRIPTION
										0.5	Topsoil.
										1.5	ORGANIC Silt w/ some SAND (OL)
										5.0	Brown silty fine sand w/some coarse sand, gravel, & cobbles.
	1D	2"	18"		6.5	21	32	42		8.2	Brown med. to coarse sand w/some gravel & silt. DENSE to VERY DENSE; WET. (SW) MANY Cobbles AND BOULDERS.

Refusal @ 8.2

Installed well to 8.2'. SCREEN from 3.2' to 8.2'.
Water @ 6.1'
WATER MEASURED at 5.45' in WELL 11/20/86.

SAMPLES
D = Splite Spoon
C = 2" Shelby Tube
U = 3½" Shelby Tube

SOIL CLASSIFIED BY:
[X] Driller - Visually
[X] Soil Technican - Visually
[ ] Laboratory Tests

REMARKS
USCS SOIL DESCRIPTIONS MADE by visual INSPECTION.
BORING LOG ANNOTATED BY RGGI GEOLOGIST J. HILLIER.
THE PRESENCE of COBBLES AND BOULDERS is INFERRED from DRILLING ACTION.

HOLE NO. B-2B

AINE TEST BORINGS, INC.
REWER, MAINE 04412

CLIENT
Robert Gerber

SHEET 1 OF 1
HOLE NO. B-2C

ER
Tom Schaefer

PROJECT NAME
Gravity wave

LINE & STATION
NW 34+70

JOB NUMBER
86-245

LOCATION
Columbia, Maine

OFFSET
CENTERLINE

GROUND WATER OBSERVATIONS
____ FT. AFTER ____ HOURS
____ FT. AFTER ____ HOURS

	CASING	SAMPLER	CORE BARREL
TYPE	probe		
SIZE I.D.	auger		
HAMMER WT.			
HAMMER FALL	"		

DATE START 11/18/86 DATE FIN. 11/86/86
SURFACE ELEV.
GROUND WATER ELEV.

CASING BLOWS PER FOOT	SAMPLE NO.	SAMPLE O.D.	SAMPLE PEN.	SAMPLE REC.	SAMPLE DEPTH @ BOT.	BLOWS PER 6" ON SAMPLER 0-6	6-12	12-18	VANE READING	DEPTH	STRATUM DESCRIPTION
											Brown silty fine to med. sand w/coarse gravel, some cobbles, and boulders.
										8.3	
											Refusal @ 8.3'
											Caved @ 4.4'
											Water @ 4.3'

SAMPLES
D = Splite Spoon
C = 2" Shelby Tube
U = 3½" Shelby Tube

SOIL CLASSIFIED BY:
[x] Driller - Visually
[ ] Soil Technican - Visually
[ ] Laboratory Tests

REMARKS:

HOLE NO. B-2C

AINE TEST BORINGS, INC. REWER, MAINE 04412	CLIENT Robert Gerber	SHEET 1 OF 1 HOLE NO. B-2D
ER Tom Schaefer	PROJECT NAME Gravity wave	LINE & STATION NW 34+80
JOB NUMBER 86-245	LOCATION Columbia, Maine	OFFSET 30 ft. EAST

GROUND WATER OBSERVATIONS

_____ FT. AFTER _____ HOURS

_____ FT. AFTER _____ HOURS

	CASING	SAMPLER	CORE BARREL
TYPE	probe		
SIZE I.D.	auger "		
HAMMER WT.			
HAMMER FALL	'		

DATE START 11/18/86 DATE FIN. 11/18/86

SURFACE ELEV. APPROX. 266'

GROUND WATER ELEV. APPROX 263'

CASING BLOWS PER FOOT	SAMPLE NO.	O.D.	PEN.	REC.	DEPTH @ BOT.	BLOWS PER 6" ON SAMPLER 0-6	6-12	12-18	VANE READING	DEPTH	STRATUM DESCRIPTION
											Brown silty fine to med. sand w/some coarse gravel, & cobbles.
										6.0	
										7.9	Brown med. to coarse sand w/cobbles & boulders, some silt.
											Refusal @ 7.9'
											Caved @ 3.8'
											Water @ 3.4'

AMPLES
D = Splite Spoon
C = 2" Shelby Tube
U = 3½" Shelby Tube

SOIL CLASSIFIED BY:
[X] Driller - Visually
[ ] Soil Technican - Visually
[ ] Laboratory Tests

REMARKS:

HOLE NO. B-2D

AINE TEST BORINGS, INC. REWER, MAINE 04412	CLIENT Robert Gerber	SHEET 1 OF 1 HOLE NO. B-3
LER Tom Schaefer	PROJECT NAME Gravity wave	LINE & STATION NW 49 + 16
JOB NUMBER 86-245	LOCATION Columbia, Maine	OFFSET CENTERLINE
GROUND WATER OBSERVATIONS ____ FT. AFTER ____ HOURS ____ FT. AFTER ____ HOURS	CASING / SAMPLER / CORE BARREL TYPE: HS / SS / — SIZE I.D.: 3 3/8" / 1 3/8" / — HAMMER WT.: — / 140 / — HAMMER FALL: — / 30" / —	DATE START 11/18/86 DATE FIN. 11/86/86 SURFACE ELEV. APPROX. GROUND WATER ELEV. NOT OBSERVED

CASING BLOWS PER FOOT	SAMPLE NO.	O.D.	PEN.	REC.	DEPTH @ BOT	BLOWS PER 6" ON SAMPLER 0-6	6-12	12-18	VANE READING	DEPTH	STRATUM DESCRIPTION
										0.5	Topsoil.
	1D	2"	18"	5%	1.5	2	7	5		3.8	Brown silty fine sand w/trace of coarse sand. (SM)
	2D	2"	10"	75%	5.8	41	75				(SM) Brown, silty fine sand w/little coarse sand, trace to some GRAVEL; MANY cobbles; some boulders. SAMPLER MAY BE obstructed by cobbles: soil is DENSE to VERY DENSE; DAMP.
	3D	2"	6"	75%	10.5	88					
	4D	2"	5"	0%	14.9	100				14.9	Refusal at 14.2' Bottom of boring @ 14.9' Caved dry @ 12.4'

SAMPLES
D = Splite Spoon
C = 2" Shelby Tube
U = 3½" Shelby Tube

SOIL CLASSIFIED BY:
[X] Driller - Visually
[ ] Soil Technican - Visually
[ ] Laboratory Tests

REMARKS
BORING LOG ANNOTATED BY RGGI GEOLOGIST J. HILLIER.
THE PRESENCE of cobbles AND boulders is INFERRED from DRILLING action.

HOLE NO. B-3

INE TEST BORINGS, INC. EWER, MAINE 04412	CLIENT Robert Gerber	SHEET 1 OF 1 HOLE NO. B-3A
Tom Schaefer	PROJECT NAME Gravity wave	LINE & STATION NW 49+41
JOB NUMBER 86-245	LOCATION Columbia, Maine	OFFSET CENTERLINE

GROUND WATER OBSERVATIONS

____ FT. AFTER ____ HOURS

____ FT. AFTER ____ HOURS

	CASING	SAMPLER	CORE BARREL
TYPE	probe		
SIZE I.D.	auger"		
HAMMER WT.			
HAMMER FALL			

DATE START 11/19/86 DATE FIN. 11/19/86

SURFACE ELEV. ____

GROUND WATER ELEV. ____

CASING BLOWS PER FOOT	SAMPLE NO.	SAMPLE O.D.	SAMPLE PEN.	SAMPLE REC.	SAMPLE DEPTH @ BOT.	BLOWS PER 6" ON SAMPLER 0-6	BLOWS PER 6" ON SAMPLER 6-12	BLOWS PER 6" ON SAMPLER 12-18	VANE READING	DEPTH	STRATUM DESCRIPTION
											Brown silty fine sand w/some gravel & cobbles. Some boulders
										12.7	
											Refusal @ 12.7' Caved dry @ 11.5'

SAMPLES
D = Splite Spoon
C = 2" Shelby Tube
U = 3½" Shelby Tube

SOIL CLASSIFIED BY:
[X] Driller - Visually
[ ] Soil Technican - Visually
[ ] Laboratory Tests

REMARKS

HOLE NO. B-3A

MAINE TEST BORINGS, INC.
BREWER, MAINE 04412

"BORING LOG"

PROJ. Gravity wave, Columbia, Maine

CLIENT Robert Gerber

BORING NO. B-3B
LINE & STA. 49 + 54
OFFSET CENTERLINE
GR. ELEV. APPROX. 284'
DATE: 11/19/86

A	STRATUM DESCRIPTION	BLOWS PER____	B
	Brown silty fine sand w/some gravel & cobbles.		
~~11.2~~			
	Refusal @ 11.2'		
	Caved dry @ 9.4'		
	Driller: Tom Schaefer		
	JOb # 86-245		

BORING NO. B-3C
LINE & STA. 49 + 88
OFFSET CENTERLINE
GR. ELEV. APPROX. 281'
DATE: 11/19/86

A	STRATUM DESCRIPTION	BLOWS PER____	B
	Brown silty fine sand w/some gravel & cobbles, trace of boulders.		
~~21.3~~			
	Refusal @ 21.3'		

1. COL. A depth in feet
2. COL. B
3. HAMMER = 140#; FALL 30"
4. SAMPLER = ____ O.D. SPLIT SPOON
5. GWT = GROUND WATER

AND - 40 to 50%
SOME - 10 to 40%
TRACE - 0 to 10%

MAINE TEST BORINGS, INC.
BREWER, MAINE 04412

CLIENT
Robert Gerber

SHEET 1 OF 1
HOLE NO. B-4

ER
Tom Schaefer

PROJECT NAME
Gravity wave

LINE & STATION
NW 55 + 00

B. JOB NUMBER
86-245

LOCATION
Columbia, Maine

OFFSET
200' WEST

GROUND WATER OBSERVATIONS
T ____ FT. AFTER ____ HOURS
T ____ FT. AFTER ____ HOURS

	CASING	SAMPLER	CORE BARREL
TYPE	HS	SS	
SIZE I.D.	3 3/8"	1 3/8"	
HAMMER WT.		140	
HAMMER FALL		30"	

DATE START 11/19/86 DATE FIN. 11/19/86
SURFACE ELEV. ____
GROUND WATER ELEV. ____

CASING BLOWS PER FOOT	SAMPLE NO.	O.D.	PEN.	REC.	DEPTH @ BOT	BLOWS PER 6" ON SAMPLER 0-6	6-12	12-18	VANE READING	DEPTH	STRATUM DESCRIPTION
										1.0	Topsoil. (OL)
	1D	2"	18"	10%	1.5	1	2	6		2.0	Brown fine sandy silt w/trace of coarse sand & grave
										4.2	Brown silty fine to med. sand w/coarse gravel & cobbles.
											Bottom of boring @ 4.2'
											REFUSAL IN boulders

SAMPLES
D = Splite Spoon
C = 2" Shelby Tube
U = 3½" Shelby Tube

SOIL CLASSIFIED BY:
[x] Driller - Visually
[ ] Soil Technican - Visually
[ ] Laboratory Tests

REMARKS:

HOLE NO. B-4

MAINE TEST BORINGS, INC.
BREWER, MAINE 04412

"BORING LOG"

PROJ. Gravity wave, Columbia, Maine
CLIENT Robert Gerber

BORING NO. B-4A
LINE & STA. 55 + 00
OFFSET 200' WEST
GR. ELEV. Approx. 272'
DATE: 11/19/86

A	STRATUM DESCRIPTION	BLOWS PER____	B
1.0	Topsoil.		
3.0	Brown fine sandy silt w/trace of coarse sand & gravel.		
	Brown silty fine to med. sand w/fine to coarse gravel, some cobbles.		
	SATURATED at 11.5 ft.		
15.5			
	Brown silty fine to med. sand w/little coarse sand & gravel.		
30.0			
	Bottom of boring @ 30.0' Water @ 11.5'		
	Driller: Tom Schefer Job # 86-245		

BORING NO. B-5
LINE & STA. 69 + 00
OFFSET CENTERLINE
GR. ELEV. Approx. 272'
DATE: 11/19/86

A	STRATUM DESCRIPTION	BLOWS PER____	B
0.5	Topsoil.		
3.9	Brown silty fine sand w/coarse gravel, cobbles & boulders.		
	Bottom of boring @ 3.9' Dry		

1. COL. A depth in feet
2. COL. B
3. HAMMER = 140#; FALL 30"
4. SAMPLER = O.D. SPLIT SPOON
5. GWT = GROUND WATER

AND - 40 to 50%
SOME - 10 to 40%
TRACE - 0 to 10%

MTB-13

AINE TEST BORINGS, INC.
REWER, MAINE 04412

CLIENT
Robert Gerber

SHEET 1 OF 1
HOLE NO. B-5A

R
Tom Schaefer

PROJECT NAME
Gravity wave

LINE & STATION
69 + 00

JOB NUMBER
86-245

LOCATION
Columbia, Maine

OFFSET
CENTERLINE

GROUND WATER OBSERVATIONS
____ FT AFTER ____ HOURS
____ FT. AFTER ____ HOURS

	CASING	SAMPLER	CORE BARREL
TYPE	HS		
SIZE I.D.	3 3/8"		
HAMMER WT.			
HAMMER FALL			

DATE START 11/19/86 DATE FIN. 11/19/86
SURFACE ELEV.
GROUND WATER ELEV.

CASING BLOWS PER FOOT	SAMPLE NO.	SAMPLE O.D.	SAMPLE PEN.	SAMPLE REC.	SAMPLE DEPTH @ BOT	BLOWS PER 6" ON SAMPLER 0-6	6-12	12-18	VANE READING	DEPTH	STRATUM DESCRIPTION
										0.5	Topsoil.
										4.1	Brown silty fine sand w/coarse gravel, cobbles, boulders.
											Bottom of boring @ 4.1' Dry

SAMPLES
D = Splite Spoon
C = 2" Shelby Tube
U = 3½" Shelby Tube

SOIL CLASSIFIED BY:
[X] Driller - Visually
[ ] Soil Technican - Visually
[ ] Laboratory Tests

REMARKS:

HOLE NO. B-5A

MAINE TEST BORINGS, INC.
BREWER, MAINE 04412

"BORING LOG"

PROJ. Gravity wave, Columbia, Maine
CLIENT Robert Gerber

BORING NO. B-5C
LINE & STA. 68+65
OFFSET CENTERLINE
GR. ELEV. APPROX. 272'
DATE: 11/19/86

A	STRATUM DESCRIPTION	BLOWS PER____	B
	Brown sandy gravel w/cobbles & boulders.		
6.2			
	REFUSAL ON boulder		
	Bottom of boring @ 6.2' Dry.		
	Driller: Tom Schefer Job # 86-245		

BORING NO. B-5D
LINE & STA. NW 68+60
OFFSET 30' WEST
GR. ELEV. APPROX. 272'
DATE: 11/19/86

A	STRATUM DESCRIPTION	BLOWS PER____	B
	Brown silty fine sand w/fine to coarse gravel, some cobbles & boulders.		
15.7			
	Refusal @ 15.7' Dry		

1. COL. A depth in feet
2. COL. B
3. HAMMER = 140#; FALL 30"
4. SAMPLER = ____ O.D. SPLIT SPOON
5. GWT = GROUND WATER

AND - 40 to 50%
SOME - 10 to 40%
TRACE - 0 to 10%

MTB-13

MAINE TEST BORINGS, INC.
BREWER, MAINE 04412

"BORING LOG"

PROJ. Gravity wave, Columbia, Maine

CLIENT Robert Gerber

BORING NO. B-5B
LINE & STA. NW 68+50
OFFSET CENTERLINE
GR. ELEV. Approx. 272'
DATE: 11/19/86

BORING NO. _____
LINE & STA. _____
OFFSET _____
GR. ELEV. _____
DATE:

A	STRATUM DESCRIPTION	BLOWS PER____	B
4.7	Brown sandy gravel w/cobbles & boulders.		
	REFusal on boulder Bottom of boring @ 4.7' Dry		
	Driller: Tom Schaefer Job # 86-245		

A	STRATUM DESCRIPTION	BLOWS PER____	B

1. COL. A depth in feet
2. COL. B _____
3. HAMMER = 140#; FALL 30"
4. SAMPLER = _____ O.D. SPLIT SPOON
5. GWT = GROUND WATER

AND - 40 to 50%
SOME - 10 to 40%
TRACE - 0 to 10%

AINE TEST BORINGS, INC. REWER, MAINE 04412	CLIENT Robert Gerber	SHEET 1 OF 1 HOLE NO. B-6
ER Tom Schaefer	PROJECT NAME Gravity wave	LINE & STATION NW 9+35
JOB NUMBER 86-245	LOCATION Columbia, Maine	OFFSET 70' WEST

GROUND WATER OBSERVATIONS

25.0 FT. AFTER 3 HOURS

____ FT. AFTER ____ HOURS

	CASING	SAMPLER	CORE BARREL
TYPE	HS	SS	
SIZE I.D.	3 3/8"	1 3/8"	
HAMMER WT.		140	
HAMMER FALL		30"	

DATE START 11/20/86 DATE FIN. 11/20/86

SURFACE ELEV. Approx. 260'

GROUND WATER ELEV. Approx 235'

CASING BLOWS PER FOOT	SAMPLE NO.	O.D.	PEN.	REC.	DEPTH @ BOT	BLOWS PER 6" ON SAMPLER 0-6	6-12	12-18	VANE READING	DEPTH	STRATUM DESCRIPTION
											Brown gravelly sand w/cobbles. (SP) SOIL GRAINS ARE ANGULAR to SUB ANGULAR DRY to DAMP; DENSE.
										5.0	
	1D	2"	18"	50%	6.5	47	56	65		7.0	Brown fine to coarse sand w/gravel. SAMPLER obstructed by boulder
	2D	2"	18"	90%	11.5	19	25	27			(SP) Brown ~~fine to~~ coarse sand w/~~little~~ SOME gravel POORLY GRADED; SUB ANGULAR SAND AND SUB ROUNDED to SUB ANGULAR GRAVEL; DENSE; DAMP. - becoming finer w/ depth
	3D	2"	18"	100%	16.5	20	45	78			
	4D	2"	18"	90%	21.5	27	52	56		25.5	
	5D	2"	18"	90%	26.5	20	52	68			(SP) Brown fine to med. sand w/trace of coarse sand. VERY DENSE; WET.
	6D	2"	18"	100%	29.5	19	52	78		29.5	
											Bottom of boring @ 29.5' Installed well

SAMPLES
D = Splite Spoon
C = 2" Shelby Tube
U = 3½" Shelby Tube

SOIL CLASSIFIED BY:
[X] Driller - Visually
[ ] Soil Technican - Visually
[ ] Laboratory Tests

REMARKS:
USCS SOIL DESCRIPTIONS MADE by visual inspection.
BORING LOG ANNOTATED by RGGI GEOLOGIST J. HILLIER.
THE PRESENCE of cobbles AND boulders INFERRED from DRILLING ACTION.

HOLE NO. B-6

AINE TEST BORINGS, INC.
REWER, MAINE 04412

CLIENT
Robert Gerber

SHEET 1 OF 1
HOLE NO. B 7

LER
Tom Schaefer

PROJECT NAME
Gravity wave

LINE & STATION
NE 53+76

JOB NUMBER
86 245

LOCATION
Columbia, Maine

OFFSET
CENTERLINE

GROUND WATER OBSERVATIONS
____ FT. AFTER ____ HOURS
____ FT. AFTER ____ HOURS

	CASING	SAMPLER	CORE BARREL
TYPE	HS		
SIZE I.D	3 3/8"		
HAMMER WT.			
HAMMER FALL			

DATE START 11/20/86 DATE FIN. 11/20/86
SURFACE ELEV. ____
GROUND WATER ELEV. ____

CASING BLOWS PER FOOT	SAMPLE NO.	SAMPLE O.D.	SAMPLE PEN.	SAMPLE REC.	SAMPLE DEPTH @ BOT.	BLOWS PER 6" ON SAMPLER 0-6	BLOWS PER 6" ON SAMPLER 6-12	BLOWS PER 6" ON SAMPLER 12-18	VANE READING	DEPTH	STRATUM DESCRIPTION
										4.5	Brown gravelly sand w/cobbles & boulders.
											Refusal on boulders Bottom of boring @ 4.5' Dry

SAMPLES
D = Splite Spoon
C = 2" Shelby Tube
U = 3½" Shelby Tube

SOIL CLASSIFIED BY:
[X] Driller - Visually
[ ] Soil Technican - Visually
[ ] Laboratory Tests

REMARKS
Boring terminated after mechanical failure caused by drilling dense, bouldery soil.

HOLE NO. B-7

CALIFORNIA INSTITUTE OF TECHNOLOGY

04/25/86 PASADENA, CALIFORNIA 91125

LASER INTERFEROMETER GRAVITY-WAVE OBSERVATORY PROJECT

TO: Kip, Rai and Ron REFERENCE: IOM04252

FROM: Frank

SUBJECT: Application for a State of Maine Project Approval/Permit

I have attached a copy of the application referenced above for your information. It appears that we will have to make some decisions quite quickly about how we are going to implement the system at Columbia. I have a copy of the instructions (77 pages) that go with the application in my office and I have sent copies to Greg Van Der Werff and Phil Trusell. It is my intention to select a contractor, possibly E. C. Jordan Co. of Portland, Me to complete the application and do some of the planning for us. This appears to be the least expensive manner to approach the issue since organizations such as Jordan have completed numerous applications like this one. I was cautioned by Hollis McGauflin, Director of Land Quality for Department of Environmental Protection, that generally people that are inexperienced in preparing the application read too much into it and get themselves into trouble. I have given a copy of the application and application instructions to Bert Sweetser and he is preparing a Statement of Work for the Contractor.

It also appears that we will not have to do a biotic survey at Columbia. I will notify Chris Campbell at University of Maine at Orono that we will not require the services of his people this summer.

The archaeological work will be accomplished by Jim Petersen and Dave Putnam of the University of Maine at Augusta. They gave me a signed proposal (also attached) for $15,150.30; the cost is about 50 per cent more than I had anticipated or budgeted, but they indicated that because the site was so large, they would require this amount to meet the State requirements. Apparently they had already discussed the estimate with Arthur Spiess and some reductions were made. Implicit in the discussions between Petersen and Spiess is the understanding that the work that they do at Columbia meets the State of Maine requirements. In any event I am going to send Spiess a copy of the proposal and ask him to indicate to me in writing that he concurs with it.

Bert Sweetser and I met with Petersen and Putnam in the office of Howard

G. Sachs, Provost and Vice President of Academic Affairs. Provost Sachs indicated his support for the Project and would like to have someone give a talk at the University in the near future. I, of course, volunteered that Rai would be delighted to do this and gave them his phone number.

Department of Environmental Protection
Bureau of Land Quality Control
State House Station 17
Augusta, Maine 04333
Tele: (207) 289-2111

L-_____
(For office use only)

APPLICATION FOR PROJECT APPROVAL UNDER THE SITE LOCATION OF DEVELOPMENT LAW (38 M.R.S.A., Sections 481-488)

PLEASE TYPE OR PRINT:

This application is for: _____ New Site _____ Existing Modification

Name of Applicant: _____

Name of Project: _____

Address: _____ Tel. No.: _____

Local Contact or Agent (Name & Tel. No.): _____

LOCATION OF ACTIVITY:

Road, Street, or Nearest Route Number: _____

City/Town/Plantation: _____ County: _____

By signing below, the applicant (or authorized agent) certifies that he/she has

1. Published a public notice once in a newspaper circulated in the area where the proposed project site is located;

2. Sent a copy of the notice form to the owners of the property abutting the land upon which the proposed project site is located;

3. Sent a copy of the notice form to the chief municipal officer and chairman of the municipal planning board of the municipality in which the proposed project site is located; and

4. Filed a duplicate of this application at the municipal office, or if the proposed site is located in an unorganized township, at the office of the County Commissioners.

DATE: _____ _____
SIGNATURE OF APPLICANT

(IF SIGNATURE IS OTHER THAN APPLICANT, ATTACH LETTER OF AGENT AUTHORIZATION) _____
PRINT NAME & TITLE

The qualified professional person responsible for preparing this application and/or attaching pertinent site and design information hereto, by signing below, certifies that the application for project approval is complete and accurate to the best of his/her knowledge:

Date: _____ Name: _____ Re/Cert/Lic No.: _____

Engineer ____
Geologist ____
Soil Scientist ____

INSTRUCTIONS
SITE LOCATION APPLICATION

These instructions are provided to assist you in filing a Site Location application. Check the completed items:

____ 1. Publish the public NOTICE once in a newspaper circulated in the area where the project is located. (A form is provided for this and is attached to the application.) The notice should appear in the paper during the week the application is filed with this Department.

____ 2. Send a copy of the NOTICE form attached to this application to the owners of property abutting the project. Their names and addresses can be obtained from town tax maps or local public officials. Abutters should receive notice during the week the application is filed with this Department.

____ 3. Send a copy of the NOTICE form attached to this application and a DUPLICATE OF THE APPLICATION to the Municipal Office, or if the project is located in an unorganized area, send the duplicate to the Office of the County Commissioners.

____ 4. Attach a complete copy of deed, lease, purchase option, or other evidence of your title, right or interest in the property.

____ 5. If any site plans, drawings, soils maps, or other data are on sheets larger than 8 1/2 by 11", twelve (12) copies must be submitted. If information is on 8 1/2 by 11" sheets or smaller, only one copy is needed providing it is of reproducible quality. **ALL PLANS SHALL BE FOLDED TO SIZE 8 1/2 BY 11" OR THE APPLICATION WILL BE RETURNED.** This allows for convenient mailing to review agencies.

____ 6. Obtain the appropriate USGS topographic map (available at most sporting goods, book, hardware, stationery stores, etc.). Indicate the location of your project on the map, and attach it to the application.

____ 7. **FILL OUT THE APPLICATION COMPLETELY. INCOMPLETE APPLICATIONS WILL BE RETURNED.**

____ 8. Send the application along with all attachments to the: Department of Environmental Protection, Bureau of Land Quality Control, State House Station 17, Augusta, Maine 04333.

NOTE

A. Be sure to send your application in well in advance of the date on which you plan to start the project. The statute allows up to 105 working days to process the application, however, we will do our best to process the application as soon as legally possible.

B. The Department does not require that the application or plan be prepared by professionals except as required by law. However, past experience indicates that professional assistance is helpful and in many instances this advice can be used to overcome site limitations through proper design.

C. If the application is signed by someone other than the property owner, or an agent, submit a statement explaining that they are filing the application for you.

D. If the applicant is a corporation, attach a certificate of good standing from the Secretary of State of Maine. (Telephone 207-289-3676)

E. Keep a copy of the completed application form for your files. This copy will be helpful in speeding up communications with the DEP staff if any questions arise during the review of a project.

F. Upon the approval of a project by the Board of Environmental Protection, a permit will be issued and sent to the applicant. The applicant should read through the permit issued in order to become familiar with any conditions placed on the project approved. Failure to comply with conditions of approval may lead to the revocation of a permit.

G. Applicants should contact the DEP staff if questions arise at any point during the application and review process. (Telephone 207-289-2111)

1. State below the general objectives of the project as proposed, including, as appropriate, number of lots, size of buildings, parking lots, etc.

_____

_____

_____

_____

2. ATTACH AN OPERATIONAL PLAN AS EXHIBIT #A setting forth the anticipated sequence of construction for the major aspects of the proposed project (e.g. roads, retention basins, sewer lines, seeding or other erosion control measures, pollution abatement measures, etc.). The plan shall include the approximate dates for start and completion of construction.

_____

_____

3 a. State below the estimated total cost of the proposed project and itemize the estimated major expenses, including the projected cost of measures taken to minimize or prevent adverse effects on the environment during the construction and operation of this project:

Roads	_____	Erosion Control	_____
Sewers	_____	Pollution Abatement	_____
Structures	_____	Landscaping	_____
Water Supply	_____	Other	_____
		TOTAL:	_____

b. ATTACH EVIDENCE AS EXHIBIT #B of the applicant's financial capacity to undertake the proposed project. Submit one of the following: (PLEASE CHECK ONE)

____ 1. A letter from a financial institution, governmental agency, or other funding agency indicating a commitment to provide a specified amount of funds and the uses for which the funds may be utilized.

____ 2. In cases where funding is required but there can be no commitment of money until approvals are received, a letter of "intent to fund" from the appropriate funding institution indicating the amount of funds and their specified uses.

____ 3. The most recent corporate annual report indicating availability of sufficient funds to finance the development together with explanatory material interpreting the report.

____ 4. Copies of bank statements or other evidence indicating availability of funds if the developer will personally finance the development.

____ 5. In cases where funding is required but a final commitment of all necessary money cannot be made until all approvals are received and other reasonable conditions are met, an applicant shall be deemed to have demonstrated sufficient financial capacity to gain conditional approval if it has:

a. Secured a cash equity commitment to the project sufficient to demonstrate the applicant's ability to go forward. The Board will consider 20 percent equity of the total cost of a project as the normal equity commitment but reserves the right to lower or raise this amount if special circumstances of an individual project warrant it, and

b. Submitted a financial plan for the remaining financing, and

c. Received a letter from an appropriate financial institution expressing its intention to provide that financing subject to reasonable conditions of acceptance.

(Ref. Chapter 373, Section 1 & B.E.P. Policy #18)

4. ATTACH A NARRATIVE AS EXHIBIT #C describing the applicant's technical ability to undertake the proposed development. Include the following information:

a. A statement of the developer's prior experience and appropriate training relating to the nature of the proposed development.

b. A description of the types of personnel who will be employed to design, install, and operate pollution control measures.

(Ref. Chapter 373, Section 2)

5. ATTACH EVIDENCE AS EXHIBIT #D that shows the applicant has made adequate provision for solid waste disposal. Submit the following information:

a. A list of the types and estimated amounts of solid waste to be generated by the development. Indicate the method of collection and the location of the solid waste disposal facility for each waste listed.

b. A copy of Form D, or a letter containing the same information, for each solid waste disposal facility. NOTE: Form D is to be filled out by the owner of the solid waste disposal facility or by the Mayor, Town Manager, or Selectmen if the facility is run by the municipality.

(Ref. Chapter 373, Section 3)

6. ATTACH A NARRATIVE AS EXHIBIT #E identifying the nature and potential sources of odors from the development. Provide an estimate of areas affected, and methods of control. (Ref. Chapter 373, Section 4)

7. Check how water is to be supplied to the site (Ref. Chapter 373, Section 5):

a. _____ Individual wells. Provide a letter from a geologist or a well driller knowledgeable about the area that indicates a sufficient and healthful water supply is likely to be available. (Ref. Chapter 373, Section 5B2.)

b. _____ Central wells. Provide evidence that there will be sufficient water; that well construction will be in conformance with Maine Drinking Water Regulations 22 M.R.S.A., Section 601; and evidence to ensure proper operation and maintenance of the system. (Ref. Chapter 373, Section 5B4.)

c. _____ Off-site utility company or public agency. Attach a letter from the supplier that demonstrates that a sufficient and healthful water supply exists and may be utilized by the development. (Ref. Chapter 373, Section 5B1.)

d. _____ Other.

8. If other than a residential subdivision, indicate the total water usage anticipated (gallons per day): _____.

9. State below the present condition of the public access routes to the proposed project.

a. Road Name_____ e. Width of Road Shoulder_____

b. Type (gravel/asphalt)_____ f. Number of Lanes_____

c. Condition (good, fair, poor)_____

d. Width of Travel Surface (excluding road shoulders)_____

(Ref. Chapter 374, Section 1)

10. State below the nature of the interior roads and parking system within the proposed project. The plans must include a typical cross-section of roads proposed (see page 9 for minimum standards). (Ref. Chapter 374, Section 1)

a. Name of Road_____ f. Parking Lot Size_____

b. Type_____ g. Number of Spaces_____

c. Width of Travel Surface (excluding road shoulders)_____ h. Width of Right-of-Way_____

d. Width of Road Shoulders_____ i. Sight distance at any proposed intersection_____

e. Length of Roads _____ j. Speed limit at any proposed intersection_____

k. Anticipated Completion Date_____

11. a. ATTACH STATEMENT AS EXHIBIT #F indicating the maintenance responsibility for roads of any commonly owned facilities. If the road(s) are to be dedicated as a town road(s), indicate who will maintain the road(s) until the town accepts the responsiblity.

    b. Developments generating excessive amounts of traffic will be required to submit a traffic study and/or marketing study to verify certain road and traffic control improvements.

    (Ref. Chapter 374, Section 1)

12. ATTACH A NARRATIVE AS EXHIBIT #G identifying all point source and non-point source air emissions deriving from the project, including but not limited to stacks, unpaved roads or areas, vehicular traffic, etc. Include a summary of emission components to show types and amounts of particulate matter (particles) and all gaseous components. (Ref. Chapter 375, Section 1)

    *NOTE: AN AIR EMISSIONS LICENSE FROM THE AIR BUREAU MAY BE REQUIRED. FOR FURTHER INFORMATION CONTACT THE BUREAU OF AIR QUALITY CONTROL AT 289-2437.

13. ATTACH A NARRATIVE AS EXHIBIT #H identifying any potential large scale water vapor emission from the project (e.g. processing plants, power generating facilities, etc.) which may effect a change in local climate. Identify all sources and amounts of such emissions associated with the project. (Ref. Chapter 375, Section 2)

14. ATTACH PLANS AND STATEMENTS AS EXHIBIT #I indicating those aspects of the development which may cause any alterations in natural drainage ways. (Ref. Chapter 375, Section 3) These should include, but not be limited to the following:

    a. A description showing how the development will or will not cause any alteration of natural drainage ways;

    b. A description of how the changes in surface drainage might effect other properties;

    c. A description of the general topography of the site. (Flat, steep, hilly, etc.) Include and show on plans any portion of the site subject to flooding or ponding;

    d. The name and location of any body of water on or abutting the site. Also indicate how close the site is to the nearest body of water.

15. ATTACH PLANS AND STATEMENTS AS EXHIBIT #J indicating measures which will be taken to control surface water runoff:

a. Submit calculations for predevelopment and post-development stormwater runoff for the site for a 25-year 24-hour frequency storm. If post-development peak discharge is greater than predevelopment peak discharge, submit calculations, plans, and specifications for a stormwater retention structure. This requirement may be waived depending on the individual project. However, in order for this requirement to be waived, the applicant must demonstrate that the increase in the peak discharge will be minimal. (Ref. Chapter 375, Section 4) (NOTE: ALL WORK PERFORMED BY A PROFESSIONAL ENGINEER MUST BE STAMPED AND SIGNED.)

b. List all rights-of-way or easements which will be designated as components of the stormwater management system lying within and outside the development site (show on plans).

_____

_____

_____

c. List the party(ies), their address and telephone number responsible for the maintenance of the stormwater management system._____

_____

_____

(Ref. Chapter 375, Section 4)

16. ATTACH A NARRATIVE AND PLANS AS EXHIBIT #K indicating the measures which will be followed to control erosion and sedimentation during the construction phase and after the completion of the project. These should include, but not be limited to the following: (Ref. Chapter 375, Section 5)

a. Drainage and slope data to include location and size of culverts, areas to be riprapped, location and typical cross-section of drainage ditches.

b. For areas to be seeded, indicate seed mixture by percent; type of fertilizer; application rates of seed, fertilizer and lime (lb./100 square feet).

c. Areas to be mulched and type of mulch.

d. Sedimentation pond locations and appropriate engineering data where applicable.

e. Indicate the timing and sequence of the above proposed erosion and sedimentation control measures.

f. Describe the proposed maintenance of all erosion and sedimentation control facilities which will remain after the project is completed including a designation of responsible parties. (Ref. Chapter 375, Section 5)

17. a. Will sewage disposal be by individual subsurface systems?

Yes ___ No ___

b. If sewage disposal is to be a central on site system with collection lines, state the name, address and telephone number of the person or agency responsible for the maintenance of such system and the installation schedule. Provide a letter assuring that proper service is, or will be, available.

c. If municipal or quasi-municipal sewage treatment is planned or is suspected to be necessary, provide the estimated total gallons per day of waste water to be generated. Also, the appropriate sewage treatment plant must submit a letter, including the above estimate, that states that the collection pipes and wastewater treatment plant both have the capacity to manage the increase in wastewater flow. (Ref. Chapter 375, Section 6)

18. a. If the proposed project will discharge any liquid waste from any commercial or industrial processing, or any sewage, into any stream, river, pond, lake or other body of water, including tidal waters, provide the following information:

BODY OF WATER	TYPE OF DISCHARGE	QUANTITY (Gal/Day)

b. Has a waste discharge license been applied for from the Department of Environmental Protection, Bureau of Water Quality Control?
Check One: YES ___ NO ___

(Ref. Chapter 375, Section 6)

19. ATTACH AS EXHIBIT #L the results of an on-site soil investigation done by a qualified evaluator. This may require that a soils map be submitted which is to the same scale as the site plan. The soils designations, lines or demarcation and test pit locations are to be shown directly on the site plan. If the application is for a subdivision, test pits must be made and reported on each proposed lot. All other applications must have test pits made in areas of proposed subsurface sewage disposal and/or construction location. (Ref. Chapter 375.7 and 376)

20. a. Will the proposed project be located on a mapped sand and gravel aquifer as determined by the Maine Geological Survey? YES ___ NO ___

b. ATTACH A NARRATIVE AS EXHIBIT #M describing what measures will be taken to prevent the degradation of existing ground water quality. (Ref. Chapter 375, Section 7)

21. a. Estimate the quantity of groundwater to be used by the proposed development. _____ (gal/day)

b. In areas where salt water intrusion, the lowering of the groundwater level, or land subsidence have been or can reasonably be expected to be a problem, submit a report by a duly qualified person addressing the potential effects of groundwater use by the proposed development.

(Ref. Chapter 375, Section 8)

22. ATTACH A NARRATIVE AND A PLAN VIEW AS EXHIBIT #N which shows all proposed buffer strips, their dimensions, type of buffer being employed, and maintenance responsibility. (Ref. Chapter 375.9 and 375.15)

23. ATTACH A NARRATIVE AS EXHIBIT #O identifying the source and nature of significant noise and explain methods to be utilized to reduce its impact, specifically any noise that will exceed 10 dbA over background levels. (Ref. Chapter 375, Section 10)

24. ATTACH A NARRATIVE AS EXHIBIT #P describing proposed protection of any historic sites, structures, archaeological sites that have been designated on the project site or in the immediate vicinity. (Contact the Maine Historic Preservation Commission for assistance at 289-2132) (Ref. Chapter 375, Section 11)

25. ATTACH A NARRATIVE AS EXHIBIT #Q which describes any "unusual natural areas" located on or near the project site. Describe the methods that will be used to protect them. (Ref. Chapter 375, Section 12)

26. ATTACH A NARRATIVE AS EXHIBIT #R describing the aspects of the proposed project which might block the sun's rays on neighboring structures or on adjacent properties. (Ref. Chapter 375.13)

27. a. ATTACH A NARRATIVE AS EXHIBIT #S which describes what provisions will be made in designing the project to minimize its visual impact to the surrounding area.

b. Include a description of what efforts will be made to preserve any existing elements of the site which contribute to the maintenance of scenic character (Ref. Chapter 375, Section 12).

28. a. ATTACH A NARRATIVE AS EXHIBIT #T which describes what provisions will be made to minimize impact on wildlife and fisheries habitat located on, and surrounding the project site.

b. Include any provisions which will be made to mitigate adverse effects on wildlife and fisheries caused by the project.

29. Submit 12 copies of site plans, drawn to a scale sufficient to show all details and be entirely ledgible:
(Recommended Scale: 1"=100') (ALL PLANS SHALL BE FOLDED 8 1/2" x 11")

a. Location, function and ground area of all structures and facilities.
b. Location, ground area of parking lots and all roads, length and typical cross-section of roads.
c. The nature and extent of any site work such as filling, grading, drainage, dredging, etc.
d. The nature and extent of any proposed construction or facilities related to the project.
e. The topography of the project site using 5 foot contours.
f. Streams and drainage ways.

(Ref. Chapter 375, Section 15)

FORM D

TO: DEPARTMENT OF ENVIRONMENTAL PROTECTION: Site Permits Division

FROM: _____
(Owner/Operator of the Solid Waste Disposal Facility to be used)

I am aware of _____ proposal to dispose of _____ cubic yards of _____
(The Applicant's) (Volume)

per year at the _____ solid waste disposal facility. According to the attached calculations, I project the current life expectancy of the waste disposal facility to be _____ years. The increase of _____ cubic yards of _____ from the applicant's development will shorten the life expectancy of the waste disposal facility by _____ years.

I agree to accept the volume and types of waste listed above. The _____
(solid waste disposal facility)

currently operates under the following outstanding permits:

A. _____

_____

B. _____

_____

C. _____

_____

etc.

The conditions on the outstanding permits are:

1. _____

_____

2. _____

_____

3. _____

_____

4. _____

_____

etc.

These permits and conditions are being complied with in the following manner:

A. _____

_____

B. _____

_____

C. _____

_____

D. _____

_____

etc.

D.E.P. MINIMUM ROADWAY SPECIFICATIONS

for all Town & Private Roadways

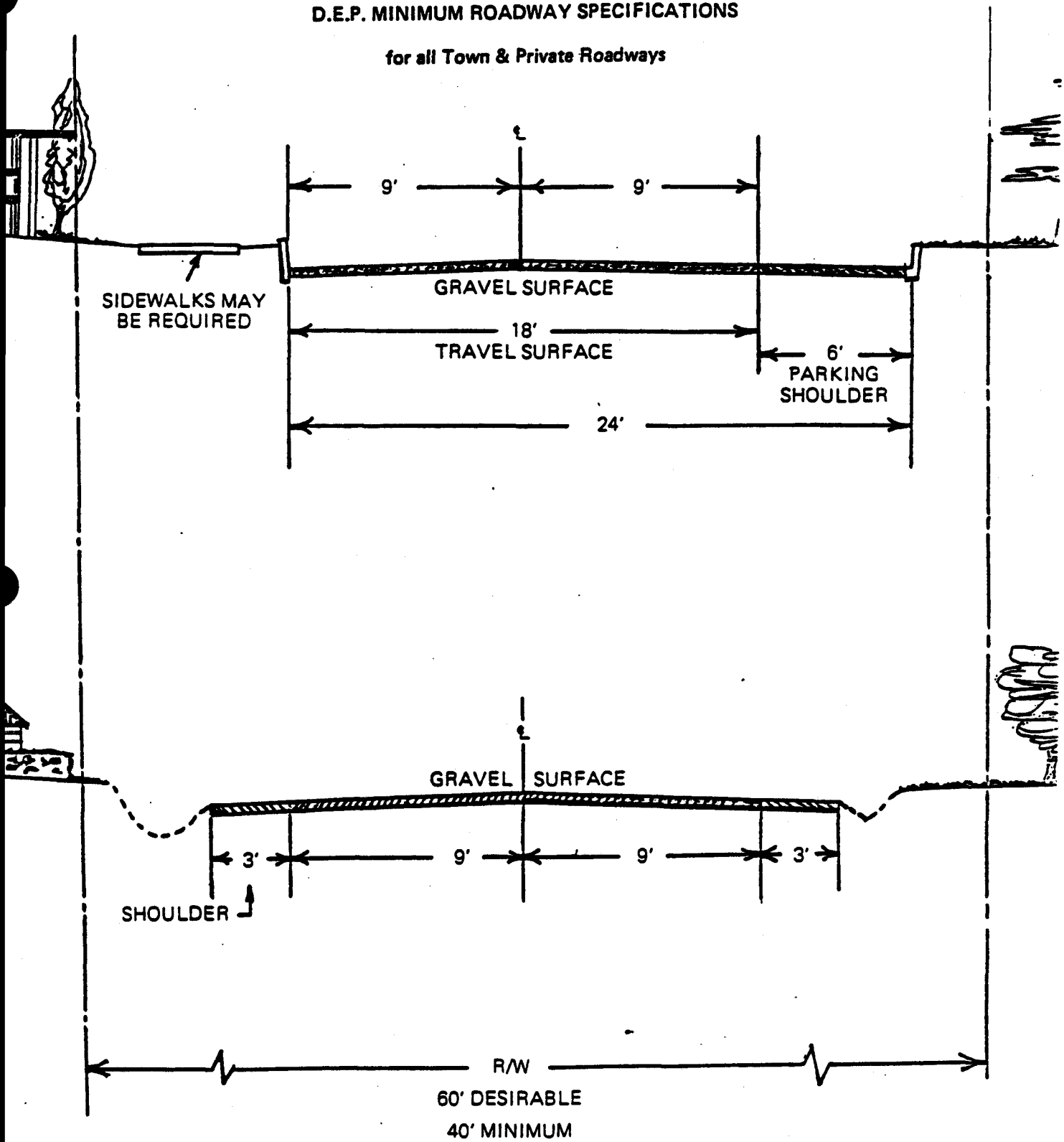

In order to save time when reviewing projects, D.E.P. is requesting that soils information be presented in a log format.

Lot No.	T.P. No.	Soil Name (Soil Scientists Only)	Plumbing Code Designation (As per table 6-1)	Textural Classifications	Depth of Pit	Depth to Seasonal Water	Depth to Impervious Layer	Depth to Bedrock	Area of Suitable Soil

A suggested set of requirements for the establishment of an association for road maintenance is as follows.

- The association shall be established by deed covenants or lease agreements.
- The developer shall specify the common facilities or properties in the development, the extent and time of their transfer to the association, and the arrangements for transfer of association control to the property owners, lessees, or other person or body.
- The covenants shall give each lot owner or lessee rights in and responsibilities for the common facilities or properties.
- The association shall be incorporated and named in the deed covenants or lease agreements.
- The covenants or lease agreements shall give each lot owner or lessee automatic membership and voting rights in the association.
- The assessment collection shall be strengthened by a covenant or lease provision making an unpaid assessment a lien against a delinquent owner's or lessee's property.
- The covenant or lease agreement shall be automatically renewable at the end of its basic term.

NOTE: The applicant shall use this form or one containing identical information to notify abutters, municipal officials, and local newspapers.

NOTICE

Please take notice that _____
Name of Applicant

_____
Address of Applicant

is filing for a Site Location permit with the Maine Department of Environmental Protection pursuant to the provisions of 38, M.R.S.A., Sections 481 to 489 to

_____
(State specifically what is to be done)

_____

_____

_____

_____

_____

_____

in the Town of _____

The application will be filed for public inspection at the Department's Office in Augusta and at the municipal offices on _____
Date

Written comments from an interested person must be sent to the Department of Environmental Protection, State House Station #17, Augusta, Maine 04333, within 14 days of filing of the application to receive consideration.

Request for a public hearing must also be sent to the Department of Environmental Protection within 14 days of the filing of the application.

Columbia Gravity Wave Project

Archaeological Phase I Survey

Scope-of-Work

by

Dr. James B. Petersen

and

David E. Putnam

Archaeology Program

Dept. of Social Sciences & Business

University of Maine at Farmington

Roger Spear

Signature of Approving Official, UMF

4/24/86

Date

Roger Spear, Executive Director of General Administration

Name Title

James B. Petersen

James B. Petersen, Principal Investigator

4/24/86

Date

I. Introduction

A. State Historic Preservation Officer Requirements

This work must be designed to locate and assess archaeological sites of significance to the National Register of Historic Places, or to show that such sites are extremely unlikely to be encountered in the impact area.

The impact area is to be defined as all areas that will be affected by the proposed construction of a Laser Interferometer Gravity-wave Observatory (LIGO) system in Columbia Township, Washington County, Maine. This proposed scientific facility will entail construction of two gravity wave antenna, each of which will be confined to a corridor roughly 61 m (200 ft) in width and some 3,962 m (13,000 ft) in length. More extensive localized disturbance will result from the construction of support facilities at the near right angle intersection of the two corridors. The actual construction site lies on Pineo Ridge, a well known late Pleistocene moraine and delta complex, to the south of the Pleasant River and the Great Heath, the largest raised bog in Maine. The Pineo Ridge locality includes a variety of topographic features, such as parallel ridges, wave cut cliffs, dry stream beds and kettle hole ponds, which may preserve evidence of past human occupation or utilization. It seems possible, if not quite likely, that some evidence of Maine's earliest human populations, the Paleo-Indians who were present by 8,500 B.C., may be preserved on the ancient landforms at Pineo Ridge.

The Phase I archaeological survey will be designed to test all likely areas within the confines of the proposed project

impact area as itemized above. In particular, archaeological testing will be concentrated on portions of the Pineo Ridge locality where cultural remains might be expected, such as terrace margins along ancient drainages or those which command broad vistas over the surrounding landscape. Results of the survey must be judged satisfactory by Mr. Earle G. Shettleworth, Jr., State Historic Preservation Officer, Maine Historic Preservation Commission (M.H.P.C.).

The following criteria for National Register significance should be followed as outlined by the M.H.P.C.:

1) With few exceptions, prehistoric sites that have not been disturbed by erosion or human activity so greatly as to lack data of scientific (research) interest are of National Register significance. (In practice, a site must be virtually destroyed to lack research interest.) Such relatively undisturbed sites can be expected in buried alluvial contexts, or other fortuitiously preserved settings across the landscape. It will be only the latter generalized circumstance that accounts for the presence of any possible sites in the project area since alluvial deposition of sediments largely ceased there in the late Pleistocene epoch. Erosion, rather than deposition, has affected Pineo Ridge since then.

2) All European domestic and industrial sites of the seventeenth-century without extensive disturbance are of National Register significance. Eighteenth-century sites must be judged on the merits of the context and

preservation. Nineteenth-century sites and later are not of significance unless of unusual character.

This cope-of-work covers Phase I survey with limited or no Phase II testing and site characterization to determine National Register eligibility. Phase II and any Phase III work which may be determined necessary by the present research are beyond its scope and must be treated separately and subsequently.

B. Problem Statement

The area to be affected by the proposed LIGO system has never been the subject of a systematic archaeological survey, but it lies near several localities where coastal sites have been studied. These include research in the Frenchman's Bay (Hadlock 1939, 1941; Rowe 1940; Smith 1929), Rogue Island (Sanger and Chase 1983), and Passamaquoddy Bay (e.g., Sanger 1979, 1985) areas, as well as other intermediate coastal localities (Steve Cox and Dave Sanger, personal communication). These projects have demonstrated the relative richness of archaeological sites in coastal settings, but with few exceptions (e.g., Kopec 1985), comparable research has not been undertaken away from the immediate coast. Thus, this survey takes on added significance, particularly if intact ancient landforms preserve cultural remains.

In light of these and other projects in the wide region, we can expect the following general site types in the project area:

1) Euroamerican habitations and industrial sites of post-Revolutionary War settlement. Most of these should

lie on bluff tops, or near modern dam locations and therefore may not be present in the project area.

2) Prehistoric (Indian) sites of the Ceramic period (1,000 B.C. - A.D. 1,550) are generally located on low-slope areas near "strategic" settings, such as falls, trubutary streams and springs.

3) Sites of greater antiquity (Archaic age, 7,000 B.C. - 1,000 B.C., or Paleo-Indian age, ? - 7,000 B.C.) are more rare in correlation with their age. These again are generally located in "strategic" spots of various sorts and for the Paleo-Indian period included relatively high, open areas in accord with environmental conditions (tundra parkland) and human subsistence patterns of that period. It is this latter setting that can be expected in the project area.

Because of the lack of previous survey work, the present work plan is limited to Phase I research. No allowance is made for Phases II or III. Should a site or sites of potential National Register significance be discovered, additional work beyond the present proposal will be required. It is impossible to assess the probability or scope of such without completion of the Phase I research.

II. Work Plan

A. Field Work

Archaeological field work will be conducted using a systematic methodology well outlined elsewhere (e.g., Petersen et.al. 1986).

Shovel test pits, 0.50 x 0.50 m, will be excavated at varied intervals (5 or 10 m) and all sediment will be screened through 6.0 mm (1/4 in) hardware cloth after areas of "high probability" for sites have been identified through a walk over of the entire project area and on the basis of an aerial photograph terrain analysis. David Putnam has conducted this preliminary analysis using a standardized methodology (Way 1973).

The field work will be stratified by probability among the following considerations:

1) particular emphasis will be given to ancient terrances and other prominent landforms identified through the aerial photographic analysis which lie adjacent to drainages and which offer commanding views of the surrounding area. The generally treeless project area, due in large part to maintenance of modern commercial blueberry tracts, should offer many such possible testing localities. At least 12 localities of this sort have been identified through the aerial photo analysis; of course, others may be identified during the field work. These are considered first priority testing localities.

2) Second order priority is accorded to localities which exhibit either adjacent drainage, or a commanding view, of which there are many more in the project area than in the first category.

3) Third order priority localities include a variety of other less distinguished settings. A small sample of such spots along the two corridors will be tested to

guard against sampling bias, but such areas are not likely to yield significant cultural remains.

The total field work will include 12 days, during which time a field supervisor and assistant supervisor will direct a crew of three research assistants. The principal investigator will be engaged on a half time basis (six days) during the field work in the conduct of project-related matters, such as field inspection and consultation with personnel, as needed.

B. Lab Work

Two research assistants will expend two weeks (10 days) in the processing, correlation and brief analysis of all recovered materials. These employees will also product written site descriptions, maps, artifact illustrations and assist the principal investigator in the preparation of a Phase I report. The principal investigator will be responsible for the report, however, and as author and editor will expend four weeks (20 days) in report preparation.

A detailed letter outlining the major results of the Phase I survey can be expected within 3-4 weeks following completion of the field work. This letter will initially satisfy FERC compliance for this level of investigation and permit further planning and negotiation should any additional Phase II or Phase III field work be necessary. The detailed final report may not be prepared immediately, however, depending on the contractor's schedule of other work. It can be expected within two to six months and will not in any way hold up the compliance process.

References Cited

Hadlock, Wendell S.

1939 The Taft's Point Shell Mound at West Gouldsboro, Maine. Robert Abbe Museum Bulletin 5.

1941 Three Shell Heaps on Frenchman's Bay. Robert Abbe Museum Bulletin 6.

Kopec, Diane

1985 The Eddie Brown Collection of the West Grand Lake Area, Maine. Maine Archaeological Society Bulletin 25(2): 3-37.

Petersen, James, B. and David E. Putnam (with contributions from Julie Johnson, Gary Laverdiere and Jeff Parker)

1986 Archaeological Phase II Testing in the Williams Hydro-electric Dam Increased Pool Area, Somerset County, Maine. Report prepared for Central Maine Power Company, Augusta. Archaeology Program, Dept. of Social Sciences and Business, University of Maine, Farmington.

Rowe, John H.

1940 Excavations in the Waterside Shell Heap, Frenchman's Bay, Maine. Papers of the Excavators' Club 1(3).

Sanger, David

1979 The Ceramic Period in Maine. In: Discovering Maine's Archaeological Heritage, edited by D. Sanger, pp. 99-115. Maine Historic Preservation Commission, Augusta.

1985 Cultural Ecology in Passamaquoddy Bay, New Brunswick. Maine Archaeological Society Bulletin 25(1): 10-16.

Sanger, David and Thomas Chase

1983 An Introduction to the Archaeology of the Rogue Island Group, Maine. Paper presented at the annual meeting of the Canadian Archaeological Association, Halifax.

Smith, Walter B.

1929 The Jones Cove Shell-heap at West Gouldsboro, Maine. Lafayette National Park Museum Bulletin 1.

Project Budget

Field Work (12 days)

1.	Salaries	
	Field Supervisor @ $75/day	$ 900.00
	Asst. Supervisor @ $60/day	720.00
	Crew (3) @ $50/day	1,800.00
	P.I. @ $100/day	600.00
		$4,020.00
2.	24% Fringe on Salaries	$ 964.80
3.	Per Diem @ $20/day for 66 days	$1,320.00
4.	Mileage @ 22¢/mile	$ 440.00
5.	Equipment & Supplies	$ 300.00
6.	Overhead @ 27% off-campus	$1,902.10
		$8,946.90

Lab Work (10-20 days)

1.	Salaries	
	Principal Investigator @ $100/day	$2,000.00
	Research Assistants (2) @ $50/day	1,000.00
		$3,000.00
2.	24% Fringe on Salaries	$ 720.00
3.	Report Costs (drafting, copying, etc.)	$ 500.00
4.	Overhead @ 47% on-campus	$1,983.40
		$6,203.40

PROJECT TOTAL $15,150.30

04/28/86

CALIFORNIA INSTITUTE OF TECHNOLOGY

GRAVITY WAVE PROJECT TEAM MASTER DISTRIBUTION LIST

DATE 4-28-86

CALTECH - NAME	OFFICE PHONE	MAIL STATION
AKUTAGAWA, CINDY	356-4098	130-33
BOSTICK, ALAN	356-4017	130-33
BRANIGAN, TOM	356-6225	1-71
✓BURK, JERRY	356-3913	103-33
CHEN, Y-T	356-4018	130-33
CLARK, STEVE	356-4610	130-33
✓DREVER, RON	356-4291	130-33
MELTON, BILLIE	356-2190	130-33
✓SCHUTZ, FRANK	356-4438	130-33
SMITH, SHERI	356-4017	130-33
SPERO, BOB	356-4437	130-33
STONE, ED	356-4241	103-33
✓THORNE, KIP	356-4598	130-33
✓VAN DER WERFF, GREG	356-6266	115-6
VASS, STEPHEN	356-4610	130-33
ZUCKER, MIKE	356-4017	130-33

MIT - NAME	OFFICE PHONE	MAIL STATION
✓BINSACK, JOE	617-253-7501	37-241
BURKA, MICHAEL	617-253-4824	20-F-001
JEFFRIES, ANDREW	617-253-6410	20-F-001
LINSAY, PAUL	617-253-4824	20-F-001
PETTINGILL, GORDON	617-253-7501	37-241
SAULSON, PETER	617-253-4824	20-F-001
✓TRUSELL, PHIL		12-192
✓WEISS, RAINER	617-253-3527,-4824	20-F-001

JPL - NAME	OFFICE PHONE	MAIL STATION
BRUNDIGE, M.L.	577-5712	180-305
CHAHINE, MOUSTAFA	354-6077	180-904
ELDER, BOB	577-9886	511-204U
FRAZER, ROBERT	354-4613	183-104
GIN, WINSTON	354-5488	198-102
JOHNSON, J.K.		157-205
✓LOBB, VERL	577-9791	511-201A
LYMAN, PETE	354-4500	511-201A
MATHISON, DICK	354-3924	238-540
MCCLURE, DON	354-6207	264-800
✓MENNINGER, FRED	577-9860	511-204U
PARKS, BOB	354-3400	180-904
PORTER, BILL	354-5470	180-503
REUKAUF, PAUL	805-277-7010	JPL-EF
STOLLER, FLOYD	577-9785	511-201A
✓SWEETSER, BERT	577-9865	511-201A
WIGGINS, CECIL	354-2076	238-540

DRAFT

GRAVITY WAVE OBSERVATORY

APPLICATION FOR PROJECT APPROVAL

PRELIMINARY, FOR INFORMATION ONLY

1. General Objectives and Project Description

1.1 General Objectives

The California Institute of Technology (CIT) and the Massachusetts Institute of Technology (MIT) plan to construct a facility to detect gravitational waves emanating from outer space over a period of 20 years or more. As part of this program continuing research will be conducted to enhance the performance of the detection system.

1.2 General Description

1.2.1 Land Requirements

The facility shown on the Plot Plan M-1 consists of two tunnels, one running northeasterly and the other northwesterly. Each tunnel will be approximately 13,000 feet in length. The facility will be constructed within a 200 foot right-of-way except for the north most 1300 feet of the northwesterly leg will be 400 feet wide due to the area required for earth fill placement.

The project will cross parcels owned by twelve different owners as shown on the Property Map Index, Town of Columbia, Dwg M-2. The parcels are as follows: Tax Map 5 Parcel 9, Tax Map 9 Parcels 1 and 2, Tax Map 10 Parcels 1, 4, 5, 9, 11, 15, 20, 24, and Tax Map 11 Parcel 20.

The right-of-way intersects Schoodic County road at two locations as shown on Dwg M-1. The Columbia Town Council has agreed in principle to grant an easement to pass under this road.

1.2.2 Tunnel Installation

A major structural feature of the project is the 10-12 ft. diameter corrugated metal pipe (CMP) tunnel to be installed full length on each arm. The pipe will be buried under 3 feet minimum of earth in both the cut and fill areas. A preliminary profile of the CMP tunnel is shown on Dwgs M-3 and M-4.

Limited soil borings have been placed on a 3000 foot length of the north westerly arm which indicate the groundwater is above the CMP tunnel invert in this area. A drainage system will be installed below the invert elevation consisting of perforated pipes embedded in a graded filter sand. This drainage system will carry the groundwater to an area which is lower, or to daylight in an existing drainage course.

Additional soil investigations are planned over the entire project area including seismic refraction surveys and test pits to determine the soil properties required for final design. Tests will be made of the groundwaters to determine quality and establish if treatment is required.

1.2.3 Other Construction Features by Area

1.2.3.1 Area A (See Plot Plan M-1)

Apex building, 6000 sq. ft.

Chain link fenced area, 40,000 sq. ft.

Parking for six cars

Well, domestic water and fire protection system

Sewer lines, septic tank and leach field

1.2.3.2 Areas B, C, D, E

Mid and End Buildings, ~~2700~~ 1100 sq. ft.

Chain link fenced area, 10,000 sq. ft.

Parking for 3 cars

Domestic water system, well, treatment and pressure tank

Sewer line, septic tank leach field

A typical building is shown on Dwg M-5.

1.2.3.3 Area F

This is the support area which will incorporate the following facilities:

A single story 6000 square foot support building housing offices, shops storage and a two car garage.

Chain link fenced area, 40,000 sq. ft.

Well, domestic water, and fire protection system.

Sewers, septic tank and leach field.

Parking for 10 cars

Closed circuit cooling tower to be piped underground to area A.

Electrical substation 34.5 KV/4160 V, 2000 KVA.

1.2.4 Tunnel Access

Every 400 to 800 feet along the tunnel, structures will be constructed to provide access to sections of the tunnel containing vacuum pumps. These structures will be fenced and will be approximately 100 square feet in plan. An alternate scheme being studied may utilize manholes to provide this access.

A conceptual cross-section of the access structures is shown on Dwg M-6.

1.2.5 Interior Access Road - New

A 12 ft. minimum wide access road will be constructed along the alignment. This road will be similar in construction to the existing unpaved public roads on site consisting of a gravel base.

1.2.6 Power Distribution

Commercial power will be extended from Harrington to the site at 34.5 KV by the Bangor Hydro-Electric Company.

Power at 4160 volts will be distributed along the tunnel alignment using direct burial cables at 3 ft depth with substations at 400 ft. intervals.

1.2.7 Experimental Apparatus

The experimental apparatus will utilize large vacuum chambers in the five buildings at the end and mid points of the two arms of the installation and at the apex. Connecting these vacuum chambers will be a 4-foot diameter vacuum pipe which is contained in the tunnel. It is the receiver system contained in the Apex building that is used to perform the actual experiments. A laser beam entering at the apex is split and travels along both tubes simultaneously, bouncing between mirrors mounted on suspended inertial test masses. These masses move relative to each other as a gravity wave passes, causing a differential in the travel time of the laser beams which is then measured and analyzed. The sensitive nature of the experiments

require that the site be as free as possible from both acoustic and seismic noise.

2. Operational Plan (Exhibit A)

A preliminary schedule is furnished which shows a construction period of 5 1/2 years duration as shown in Exhibit A.

3. Estimated costs (1986)

Roads	$ 300,000
Sewers	60,000
Structures & Tunnel	6,700,000
Water Supply	120,000
Erosion Control	300,000
Pollution Abatement	0
Landscaping	20,000
Other - Mech. Elect., Research equip.	30,500,000
Total Cost	$38,000,000

Financial Capacity (Exhibit B)

This project will be funded by the National Science Foundation, a U.S. Government Agency.

4. Technical Ability (Exhibit C)

This project will be managed by CIT/MIT. Detailed design will be by qualified architect-engineer firms and construction will be by qualified general contractors.

5. Solid Waste Disposal (Exhibit D)

Solid waste will be handled by a contract with a local existing solid waste disposal service.

6. Potential Sources of Odors (Exhibit E)

The installation is a passive system that does not generate any effluent gases of an odorous nature.

7-8. Water Supply

This facility will be serviced by wells located at each construction area (A, B, C, D, E, F). These wells will be used to supply water for sanitary purposes for an average of 8 people per day. The estimated daily usage is 1500 gallons.

9. Public Access Roads

The public access roads to the site are adequate. The primary road used will be Schoodic Road, a gravel road which is in fair to good condition.

There are no shoulders and the road width is approximately 12 feet. It is wide enough for cars to pass each other, but would generally be considered a wide, single lane road.

10. Interior Road, Parking

An access road will be constructed paralleling the tunnel alignment of the observatory. The road will be 12 feet in width with a gravel surface with 2 ft shoulders. Parking will be provided at each of the areas as follows: Area A - 6 cars; Areas B, C, D, E - 3 cars; Area F - 10 cars. Parking areas will be gravel surfaced.

There is no visual obstruction at any intersection of the interior access roads with schoodic road. Stop signs will be posted at all intersections between the interior access roads and the existing roads. The speed limit along the interior access roads will be 35 miles per hour.

11. Road Maintenance (Exhibit F)

The maintenance of the interior access roads constructed as a part of the facility will be the responsibility of CIT/MIT.

Very little additional traffic will be generated on Schoodic Road as a result of the construction of this facility. The additional traffic will be due to a normal crew of five people working at the site on a regular basis. In addition to these personnel, traffic will be generated by 5 to 8 people from Caltech and MIT that will work at the facility on an intermittent basis.

12. Air Emissions (Exhibit G)

The principal air emissions that will emanate from this installation are due to vehicular traffic. A maximum of 5 to 10 trips along each leg per day would be anticipated. The only other emission is due to periodic release of dry nitrogen gas mixed with dry air. This latter release is not expected to occur more often than once a week. The volume expected to be released at any one time will not exceed 75,000 cubic feet. Since air ~~normally~~ contains 80 percent nitrogen, this does not pose a problem.

13. Water Vapor Emissions (Exhibit H)

There will be releases of water vapor emissions from this facility.

14. Alterations in Natural Drainage Ways (Exhibit I)

(This work to follow as part of the detailed design)

15. Measures to Control Surface Runoff (Exhibit J)

(This work to follow as part of the detailed design)

16. Measures to Control Erosion and Sedimentation (Exhibit K)

(This work will follow as part of the detailed design)

17. Sewage Disposal

Sewage Disposal will be by individual subsurface systems consisting of septic and leaching fields.

18. Liquid Wastes

There will be no discharge of liquid wastes from the project. All cooling systems are closed loop.

19. On-Site Soil Investigation (Exhibit L)

Soil investigations have been completed on a small portion of the alignment and are submitted as Exhibit L. Additional work will follow.

20. Sand and Gravel Aquifers (Exhibit M)

The proposed facility will be located on a mapped sand and gravel aquifer.

There will be no degradation to the groundwater quality since the appropriate sewage treatment will be installed and no discharge of any material which would degrade the groundwater quality is planned.

21. The daily use of ground water will be about 1500 gallons per day. Salt water intrusion is not a problem because the amount of ground water used is quite small and the ocean is sufficiently far from the site so as not to pose a problem.

22. Buffer Strips (Exhibit N)

A minimum easement of 200 ft wide is planned. The actual construction will occupy only a fraction of this area and the major portion of the construction is buried either in cut or fill. Most of the area will be planted with ground cover.

23. Source and Nature of Noise (Exhibit O)

The facility is passive and will not generate any significant acoustic noise during normal operation. The exacting nature of the measurements to be made require minimum ambient noise levels. All motors will be mechanically isolated to reduce the generation of noise and to prevent vibrations of a mechanical or acoustical nature from being coupled into the system. Any coupling in excess of _____ db above the normal background would impair measurements of gravitational waves.

24. Historic or Archaeological Site (Exhibit P)

Exhibit P attached provides an archaeological survey of the site by the University of Maine indicating no archaeological findings in the area of construction.

25. Unusual Natural Area (Exhibit Q)

Since a major portion of the project is buried there will be a minimum impact on the existing use of the land.

BATCH START

STAPLE
OR
DIVIDER

VACUUM PUMPING STUDIES

ANTARES-High Energy Gas Laser Facility

Reprinted From

Inertial Fusion Program

Progress Report

January-December 1981

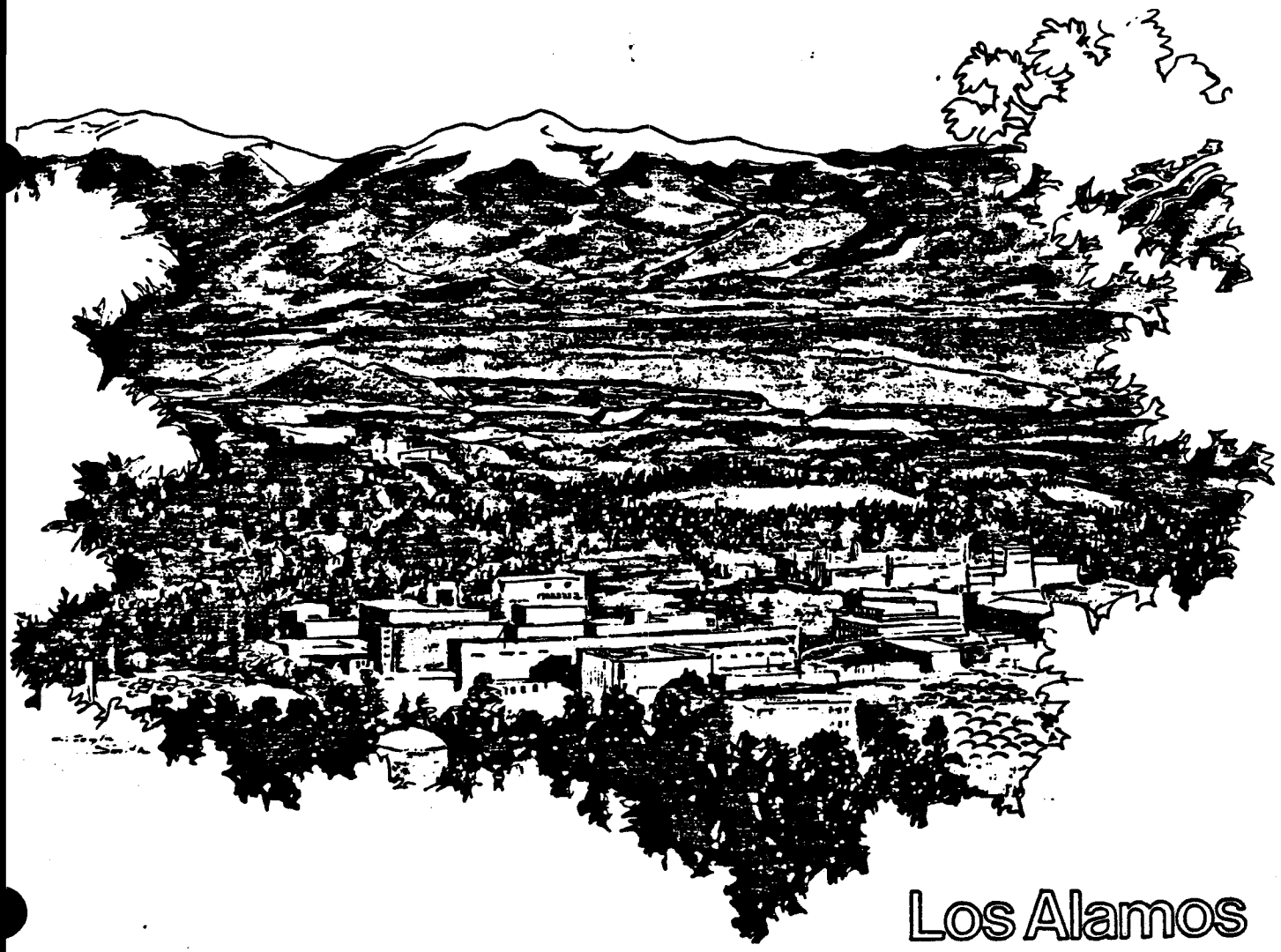

Los Alamos

Los Alamos National Laboratory
Los Alamos, New Mexico 87545

TABLE OF CONTENTS

Acronyms.....7

ANTARES-High Energy Gas Laser Facility.....8

Overview and Status.....8

Front End System.....8

Electron-Beam Gun.....11

Target System.....14

Optical Beam Management.....17

Diagnostics.....22

Controls.....27

Retropulse Isolation.....30

Conclusion.....30

ACRONYMS

ACN	Antares control system computer network
AGP	alignment gimbal positioner
DVS	detector and visible source
EMI	electromagnetic interference
HELGF	High Energy Gas Laser Facility
MI	machine interface
OEL	Optical Evaluation Laboratory
OTB	optical test bed
PAM	power amplifier module
PDM	Pittsburgh-Des Moines Steel Company
RSS	root sum of squares
SCC	subsystem-control computer

ANTARES—HIGH ENERGY GAS LASER FACILITY
(H. Jansen)

The Antares CO_2 laser system represents the next generation of CO_2 lasers needed to investigate the feasibility of laser-driven ICF. The Antares project was redirected in 1979 from a six-beam, 100-kJ system to the present Antares configuration of two 20-kJ power amplifiers that will deliver 40 TW on target in late 1983, 1 year earlier than the full design.

OVERVIEW AND STATUS (H. Jansen)

The Antares short-pulse CO_2 laser system was originally designed to deliver 100 kJ in a 1-ns pulse to a target using six large amplifiers. In 1979 we decided to reduce the initial system configuration from six to two amplifiers. The two-amplifier configuration, delivering 35-40 kJ to a target, would be completed in 1983 under present anticipated funding, 1 year earlier than the original date for the full system.

All building facilities have been completed (Fig. II-1). The complex consists of a main Laser Hall, a Target Building that houses the TVS, and an Office Support Facility. Hardware for the two amplifiers is in place (Fig. II-2). The first amplifier is used as an electrical checkout system, without the complexity of the optical train to check out the operation of the energy storage and associated control system, as well as for small-signal gain measurements. The second amplifier is used as an OTB to check out the optical alignment and controls system without the complexity of the electrical system. We expect to complete construction in late 1983.

FRONT-END SYSTEM (R. Gibson)

Introduction

The front end of the Antares system (Fig. II-3) will deliver 90 J in a 1-ns pulse to each of the two power

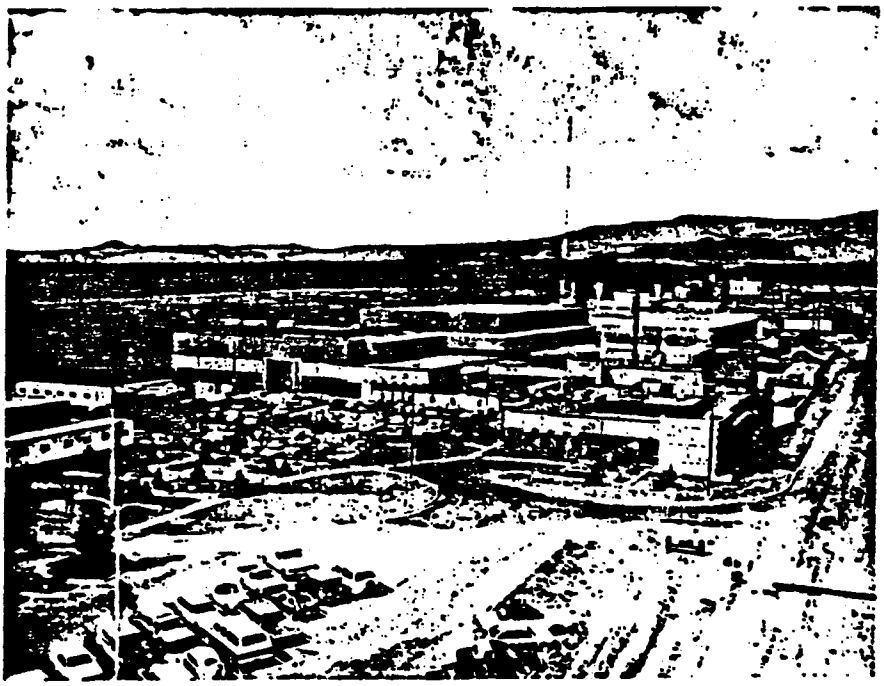

Fig. II-1. Antares main Laser Hall at left, Target Building in right background, and Office Support Facility foreground.

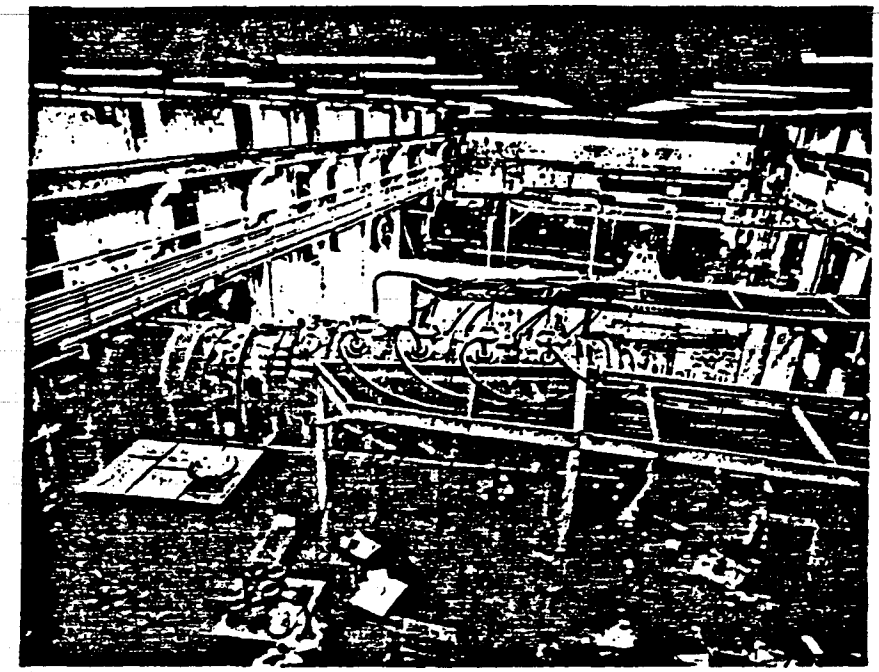

Fig. II-2. Antares Laser Hall with two amplifiers in place. The green amplifier is being used as a test bed for electrical checkout. The brown is used as a test bed for optical checkout.

amplifiers. (90 J is the required input to the power amplifiers for optimum energy extraction.) The short front-end pulse is generated in a single oscillator; the beam is then split into two and each is amplified to 90 J in separate driver amplifiers. The output to the amplifiers is an annular pulse of ~15-cm o.d. The front end has been prototyped in a final configuration and subsequently moved to its Antares location.

Description

We installed the prototype front-end beamline at its permanent location in the basement of the Laser Hall. The system is operational and will be used in initial energy-extraction experiments. An advanced multiline oscillator will be completed in later stages of the Antares project.

The front end is a three-stage assembly consisting of a tunable multiline oscillator, a preamplifier (triple-pass Lumonics 602), and two driver amplifiers (triple-pass 15- by 15- by 200-cm electron-beam-controlled discharge amplifier), one for each beamline.

Tests on the prototype beamline revealed a major problem that required the reconfiguration of some parts—diffraction coupling occurred between passes through the optics of the Cassegrain telescopes that are used in both the preamplifier and driver amplifiers. This coupling generated postpulses of considerable magnitude in both amplifiers. The postpulses may not reduce the initial energy delivered to the target, but they do complicate the interpretation of experimental results: physical processes occur that are difficult to separate from those caused by the first pulse.

We changed the preamplifier optics to a simple nonexpanding triple-pass configuration that eliminates the coupling problem and still provides adequate drive for two beamlines. Diffraction coupling in the driver was suppressed by masking unused portions of the telescope mirrors and optimizing the gain and saturable-absorber pressure.

Results

With only one pulse from the driver amplifier, we can produce the required 90 J of energy in a 1-ns pulse with the driver Marx bank charged to only 55 kVdc, which is two-thirds of the maximum design voltage. Thus, we demonstrated that the front-end amplifiers can easily

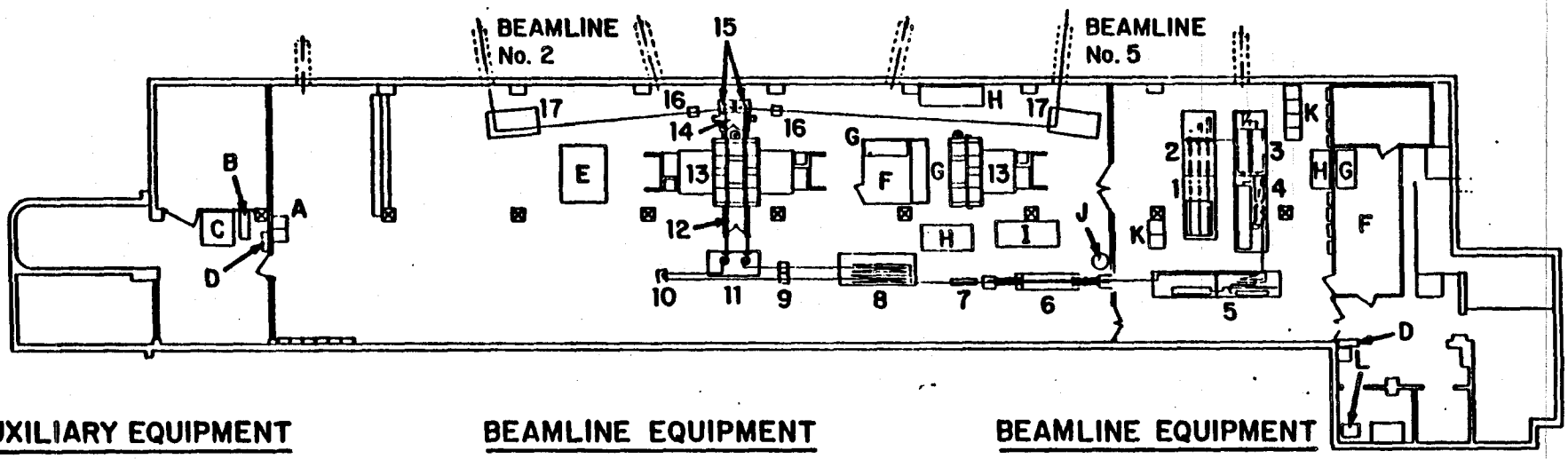

AUXILIARY EQUIPMENT

A. GAS-MIXING STATION
B. VACUUM PUMP (SF_6 SERVICE)
C. VACUUM PUMP (DRIVER SERVICE)
D. CLEAN ROOM CLOTHING SHELF
E. ELECTRON-GUN PULSER
F. SCREEN ROOM (DIAGNOSTICS)
G. DIAGNOSTICS TABLES
H. DIAGNOSTICS INPUT OPTICS TABLES
I. SMALL-SIGNAL GAIN PROBE LASER
J. PREAMPLIFIER POWER SUPPLY
K. INSTRUMENTION RACKS
L. VACUUM PUMP (OSCILLATOR SERVICE)

BEAMLINE EQUIPMENT

1. STABLE OSCILLATORS
2. ATTENUATORS
   POCKET CELLS
   PATH LENGTH ADJUSTERS
   BEAM COMBINERS
3. FOUR-PASS PREAMPLIFIER
   (LUMONICS 922)
   ONE-PASS PREAMPLIFIER
   (LUMONICS 922)
4. GEMINI OSCILLATOR
   SPATIAL FILTER No. 1
   SWITCH OUT
5. SPATIAL FILTER No. 2
   ALIGNMENT BEAM INJECTION STATION
6. TRIPLE-PASS PREAMPLIFIER
   (LUMONICS 602)

BEAMLINE EQUIPMENT

7. SATURABLE-ABSORBER CHAMBER
8. BEAM SPLITTER
   SPATIAL FILTER No. 3
9. ALIGNMENT TELESCOPE
10. PATH LENGTH ADJUSTER
11. DRIVER INPUT OPTICS TABLE
    BEAM STEERING MIRRORS
    PRIMARY CASSEGRAIN OPTIC
12. PARASITICS SUPPRESSION CHAMBER
13. DRIVER AMPLIFIER
14. SECONDARY CASSEGRAIN OPTIC
    DIAGNOSTIC PICK-OFF STATION
15. DRIVER OUTPUT TURN MIRRORS
16. BEAM BLOCK AND CALORIMETER
17. POWER AMPLIFIER
    ALIGNMENT STATION

Fig. II-3. Antares [illegible]-end layout.

deliver a single 1 ns 90 J pulse to each of the two power amplifiers.

ELECTRON BEAM GUN (C. Mansfield, G. Allen)

Assembly and Testing

To control the discharge in the 48 chambers of the power amplifier, we need 48 large-area electron beams with an electron energy of ~500 keV and an intensity of ~50 mA cm^2. These beams are produced by a broad-area coaxial electron gun. The electron gun for the first power amplifier has been assembled (Fig. II-4) and electrically tested in a dedicated test facility.

The facility consists of a main room with appropriate x-ray shielding, a control room, and an EMI-shielded data-acquisition room. All data links to a DEC 11/60 computer comprise electro-optical transmitters, fiber-optic cables, opto-electrical receivers, and transient digitizers. During testing of the gun, we gathered considerable experience that will be applied to the final Antares data-collection system.

We routinely monitored the major variables: cathode voltage, cathode current, grid voltage, grid current, total return current, Marx charge voltage, and return current via the electron-gun shell. Variables that were monitored occasionally were total Marx voltage and cathode to grid differential voltage.

Preliminary Test Results (C. Mansfield)

Operating Parameters. Major operational parameters of the electron gun with a grid resistance of 180 Ω are

- peak cathode voltage (kV) 450
- vacuum load impedance (Ω) ~15
- length of time cathode remains above 350 kV (μs) ~2
- output current density (mA/cm^2) ~ 60
- variation of current density (%)
  - window-to-window <±20
  - shot-to-shot <±20.

High-Voltage Limitation. During the test program, it became rapidly apparent that the gun in its original configuration and assembly did not reliably reach the required operating voltage of ~500 keV. We believe electron energies of 500 keV or more are required to prevent streamer formation at the anode of the gas

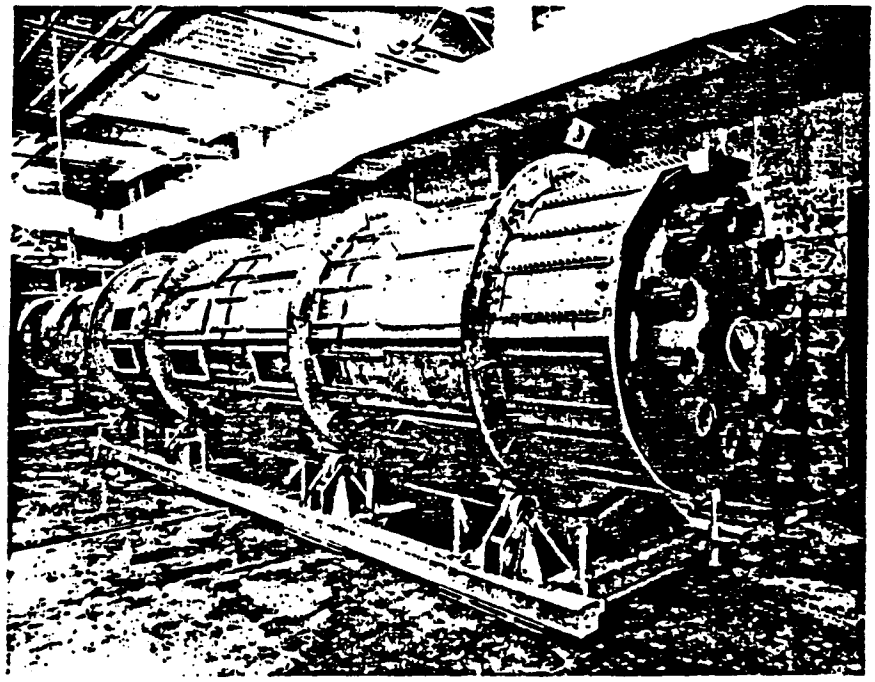

Fig. II 4. Antares electron gun on fixture in test facility. The copper-colored sections are the foil apertures for the electron gun.

discharge (the electrons enter the discharge volume through the cathode foil window).

Vacuum arcs begin to form during the electron-gun high-voltage pulse. Their onset depends on voltage amplitude. These arcs are of no operational consequence if they occur after the maximum laser gain has been reached in the discharge, which is typically the case. The problem arises from the amount of destructive energy that the arcs can deposit in the electron foil window. The higher the number of arc shots, the shorter the mean time between failures of the gun.

Considering the design value of the average electric field (~30 kV/cm) between gun grid and anode or cathode and minimal field enhancement in areas other than the emitter blades, the reasons for arc formation include surface contamination, choice of materials, inductive arcing at strategically important points, local vacuum leaks, or the traveling-wave nature of the applied voltage.

We achieved dramatic improvements in preventing arc formation through cleanliness during assembly, especially by avoiding the formation of any hydrocarbon-based surface films. The fact that arcs tend to strike the bottom of the electron-gun shell is the primary indicator that cleanliness is critically important. We also found that dc conditioning is an important method to significantly increase the voltage.

In addition to cleaning and dc conditioning, we introduced a diverter spark gap in the Marx generator. This gap does not prevent arc formation, but it shunts the Marx energy, thus reducing the arc energy and increasing the mean time between failures of the gun. We are completing a detailed analysis of gun operation from an electrical circuit point of view. This analysis, coupled with future improved diagnostics, will help us decide whether the relatively complex transmission line of the gun may be at the heart of the problem.

Reliable gun operation at 450 kV is now possible (600 shots in one test sequence) and gives some indication that self-conditioning during operation may have moved this point closer to 500 kV.

Diagnostic Improvements. Initial diagnostics consisted only of current and voltage measurements in the Marx tank. Because a number of questions relating to gun operation imply that at least some gun problems are electrodynamic, that set of existing diagnostics was inadequate. Several new diagnostic tools have been developed to gain a more complete understanding of electron-gun operation.

Cerenkov Current Density Measurements. The intensity of the Cerenkov radiation emitted by electrons in the design energy range is nearly linear with current density. By placing 6-mm-thick lucite plates over the windows and photographing the light emitted when the beam of electrons hits the plate, we obtained a time-integrated high-spatial-resolution recording of current density.

Faraday Current Density Probes. Faraday cup current-density probes were developed to measure the time structure of the current density through the gun windows. Because these probes had to intercept a considerable (100-cm^2) area of beam to develop a usable signal, they provide only a limited measure of spatial resolution.

The probe design is very simple. A collecting plate is mounted perpendicularly to the electron-beam flux on ceramic standoffs from an aluminum base plate. The base plate, in turn, is mounted both electrically and mechanically to the outside of the electron-gun shell. A standard current-monitor transformer (dB/dt probe) measures the current. The output of the current transformer is connected directly to the transient digitizers in the screen room. Extreme caution in grounding the coaxial cables and avoiding ground loops prevented the pickup of unwanted noise by the data-acquisition system.

Through the use of collector probes and the Cerenkov detectors, we found that the current density along the opening in the gun was nearly constant. Current probes, in addition to the Faraday technique, were used successfully to characterize the gun.

Gun Pressure Measurements. An ionization vacuum gauge that senses pressure variations in the gun after a shot is one of the most important indicators of shot-to-shot gun performance. During a shot, electron and ion bombardment of interior gun walls results in a pressure pulse within the gun. A standard ionization vacuum gauge will not respond fast enough to follow the initial pressure surge; however, the response is proportional to the pressure surge. We use the pressure gauge mainly to indicate impending major arcing in the gun. When a major arc occurs, the pressure may surge by three orders of magnitude over those seen in normal operation.

The pressure recordings also explain why the gun may not be fired faster at a given rate. A finite time (several minutes) is required for the vacuum pumps to return the gun pressure to a level at which it can be fired without a gaseous arc developing.

Photometric Recording. A considerable amount of light is generated inside the electron gun during operation. We installed windows at the ends of the gun, each window located so that the emission blades can be seen through a hole in the grid. Photographs taken through these windows gave an early indication of the arc location. Later, mirrors were placed to provide a wide-angle view of the region between the grid and the shell.

A photomultiplier placed at the end windows provided information about the timing of major arcing occurrences. We found a definite correlation between visible arcs and the Marx current and voltage traces. By proper grounding and shielding, such a high-impedance device offers considerable promise for future use of high-speed spectroscopy as a diagnostic tool for understanding electron-gun behavior.

Vacuum Diagnostic Port. We built a vacuum diagnostic port that can be attached to the electron gun in place of an electron-beam window. This port has a 15.24-cm (6-in.) gate valve through which we can sample a relatively large area of the electron beam. Although we have only used this port to photograph emission sites on the emission blades, in the future we will also measure electron energy distributions and soft x-ray spectra.

Direct Current Conditioning. High-voltage conditioning is an important factor in obtaining proper operation of high-voltage equipment. Conditioning combines at least two phenomena: burning off potential emission sites and outgassing surfaces by heating. Our initial conditioning efforts in pulsed mode involved shorting the grid to the cathode and pulsing the gun at high voltage. Later, we found that better results can be obtained by connecting a dc (250-kV) supply to the cathode with a series-limiting resistor. After 1 to 2 h of operation with currents of 1-3 mA, this treatment resulted in drastically lowered gun pressures and increased hold-off voltages.

Diverter Gap (G. Allen). Gun arcing usually occurs at late times, 5-6 μs after the pulse begins and energy is deposited in the laser gas. Such arcs do not affect the laser operation: however, they ultimately (*after several* arcs in the same location) destroy electron-gun foil windows. The obvious protection against this damage is to divert the remaining energy stored in the Marx generator from the gun.

The two approaches we investigated were a nontriggered water gap and a triggered gas gap. The former had the advantage of being automatic. As soon as the Marx generator is erected, streamer formation begins in the water; gap closure is timed by the spacing of the gap. However, shock waves will eventually destroy the water gap, and residual arc resistance competes with the impedance of the arc in the gun. A triggered, pressurized gas gap does not exhibit these problems, but triggering such devices in the high-EMI environment of the Marx generator presents well-known difficulties. Fiber-optic decoupling overcame EMI-induced difficulties so that this approach was successful.

Vacuum Pump Studies (C. Winkelman)

The initial design of the electron-gun vacuum system incorporated a turbomolecular pump as the principal vacuum pump. This system was functionally tested and installed on the first electron gun for performance tests. The performance of this pumping system was considered satisfactory until the turbomolecular pump disintegrated during electron-gun testing. Other problems and less dramatic failures also occurred, and a tightened program schedule necessitated an alternative pumping system. As a result, we redesigned the electron-gun vacuum system and incorporated cryogenic pumps.

Hardware. The turbomolecular pumping system incorporated the TMP-3500 as the principal vacuum pump. The TMP-3500 is a 50-cm (20-in.)-diam throughput pump with a pumping speed for air (at 293 K) of 3500 L/s.

The cryogenic pumping system, on the other hand, incorporates the Cryo Torr 400 as the principal vacuum pump, which, at 40-cm (16-in.) throughput, has a pumping speed for air (at 293 K) of 5000 L/s and is a capture pump. A WS150 roots blower pumps the system from the 10^{-3}-torr roughing vacuum to the 10^{-5}-torr crossover at which the Cryo Torr pump is turned on. The D60A backs the blower, which is also used to regenerate the Cryo pump when it reaches its gas load limits.

Test Results. The electron gun is 1.52 m in diameter by 9.14 m long (~5 ft by 30 ft). The pumped volume is ~20 000 L and the required pressure is $<2 \times 10^{-6}$ torr after 24 h of pumping from ambient.

Tests to date have covered a wide variety of electron-gun operational conditions. The Cryo Torr-based system's ultimate pressure was $\sim 4.0 \times 10^{-7}$ torr, compared to the $\sim 5.0 \times 10^{-6}$ of the turbopump vacuum system.

Two electron-gun foil window failures during cryopump testing did not damage the Cryo Torr 400 pump. The TMP-3500 pump could have failed as a result of the large inrush of 3-atm laser gas into the vacuum chamber through the punctured foil window.

A typical pumpdown of the electron gun with the turbomolecular pumping system is plotted in Fig. II-5; a similar curve for the Cryo pumping system is shown in Fig. II-6. The passive, safe, and satisfactory operation of the cryogenic pumps recommend their use in the electron gun.

TARGET SYSTEM (P. Wolfe)

Overview

The target system includes

- a mechanism for inserting and precisely holding a fusion target,
- 72 optical mirrors for directing and focusing the 12 laser beamlets from each of the two Antares power amplifiers onto the target,

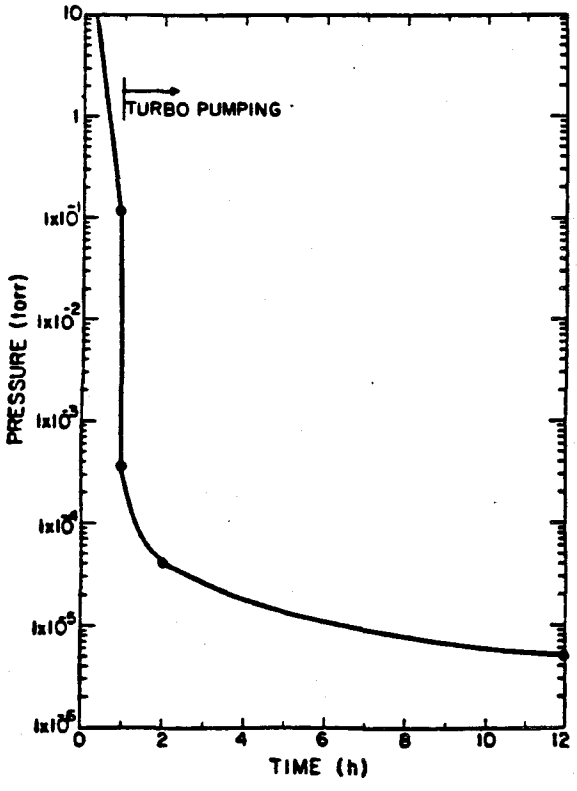

Fig II-5. Electron-gun pumpdown time with turbomolecular pump.

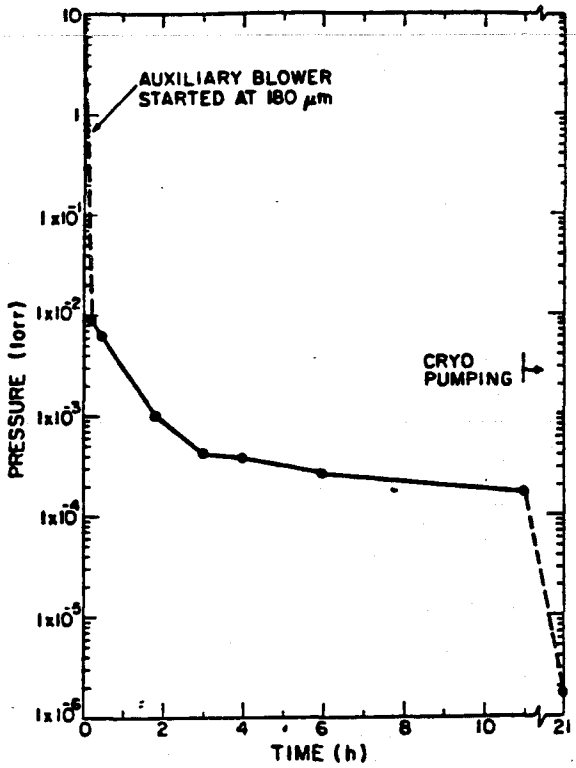

Fig. II-6. Electron-gun pumpdown time with cryogenic pump.

- a vacuum enclosure and pumps to provide the 2×10^{-6}-torr environment required by the charged-particle diagnostics, and
- a building housing the system.

The system also requires massive, rigid support stands for the mirrors, the target positioner, and the orthogonal pair of telemicroscopes to aid in positioning targets and auxiliary optical alignment devices.

In 1981, we completed the vacuum system and the Target Building that houses it. In addition, the target-chamber space frame was erected and installed, and all other support stands were received. Mirrors and positioners are being fabricated within the Antares large-optics system and are scheduled for installation with their support structures in spring 1982. We held a final design review of the target-insertion mechanism late in 1981. The mechanism will be completed and installed with the mirrors in time for end-to-end tests of the laser system that are scheduled for summer 1983. Because of funding limitations, the telemicroscopes will not be fabricated until 1983. Our subcontractor, Questar Corporation, completed the optical design of this system,

and we are proceeding with the mechanical design. The physical arrangement of the 7-m-diam Antares target chamber will make these the world's largest microscopes.

Target Vacuum System (TVS)

To minimize costs and optical aberrations, there is only a single salt window in each beamlet path between the Antares power amplifier gain regions and the target. Thus, the vacuum system extends all the way from the Target Building to the power amplifier output windows in the Laser Hall, through a beam tube, which is 1.5 to 1.8 m in diameter and ~50 m in total length. Additionally, the vacuum enclosure must be large enough to house the reflective optics that illuminate the target. This consideration, rather than the space required for the experiments themselves, dictates the size of the target chamber, a cylindrical vessel, about 7 m in diameter and 7 m long. It is designed to accommodate the 72 plane folding and 72 f/6 parabolic focusing mirrors for the original 6-beam Antares. (Each Antares beam is actually an annular array of 12 beamlets, each of which has an independent set of optics.) In addition to the large target chamber, each beam tube has a 3-m-diam, 3-m-tall turning-mirror chamber that houses an array of 12 plane turning mirrors. These chambers are arranged in two groups in the Target Hall, at the two ends of the target chamber. They direct the Antares beams from their parallel configuration as they leave the Laser Hall to the two-ended arrangement required by the target-chamber optical layout.

Late in 1978, a contract was awarded to Pittsburgh-Des Moines Steel Company (PDM) to design, fabricate, erect, and start up the entire vacuum system. By the end of 1979, the six beam tubes connecting the power amplifiers in the Laser Hall with the turning chambers in the Target Building had been installed, and three of the six turning chambers were in place.

At that time, the Antares project plan changed to permit early target experiments with only two power amplifiers. This redirection simplified the TVS because only one beam tube and one turning chamber were needed at each end of the target chamber. However, most potential savings were offset by the need to redesign the target-chamber heads and relocate some of the pumps from unused beam tubes. In addition, almost all parts for the original six-beam arrangement had already been made, and some unneeded parts had been installed.

We completed construction of the system by the end of 1980, and vacuum tests began with good results. By mid-1981, almost all contracted tasks were completed, including (1) comprehensive leak testing; (2) finalizing plans; (3) carrying out the acceptance test program; (4) adding a port to the target chamber for one of the telemicroscopes; (5) extensive cleaning and painting of the system exterior and the Target Building interior; (6) installing additional lighting, power outlets, and signal conduits at the target chamber; and (7) training Antares personnel in system operation and handling. The completed system is shown in Fig. II-7.

Vacuum performance of the TVS is noteworthy, in view of its ~1000-m^2 interior surface of stainless steel and its 600-m^3 volume. The roughing-pump package, a 2400-L/s blower with two mechanical backers, takes the system from atmospheric pressure to 10^{-3} torr in less than 2 h. Six cryogenic pumps, each with a speed of ~15 000 L/s for room-air constituents, reduce pressure to the specified operating level, 2×10^{-6} torr, in less than 3 additional hours. Base pressures of 10^{-7} torr can be held in the empty system with only two of the cryogenic pumps operating. When the target-chamber space frame was first installed (in not particularly clean condition), a pressure of 5×10^{-7} torr was achieved in 8 h, starting from atmospheric pressure. This performance is well within system specification.

Target-Chamber Space Frame

This complex stainless steel structure (Fig. II-8) mounts the target-insertion system and all its precisely located optical components and experimental apparatus. The general design for the six-beam version of Antares was completed early in 1979 and was well on its way to implementation when we shifted to the two-beam version. Accordingly, our redesign of the two-beam system changed the space frame as little as possible.

Final design and fabrication of the space frame were done by PDM, who held the contract for TVS. Extensive cross checking of the Antares and PDM designs was required before beginning fabrication at PDM's plant in Provo, Utah, in mid-1980. The Antares optical-tooling team monitored the correct placement of critical mounting surfaces.

Final assembly of the space frame in the Target Hall was completed in June 1981. Airpads and a runout table will move the 11-ton space frame out of the target

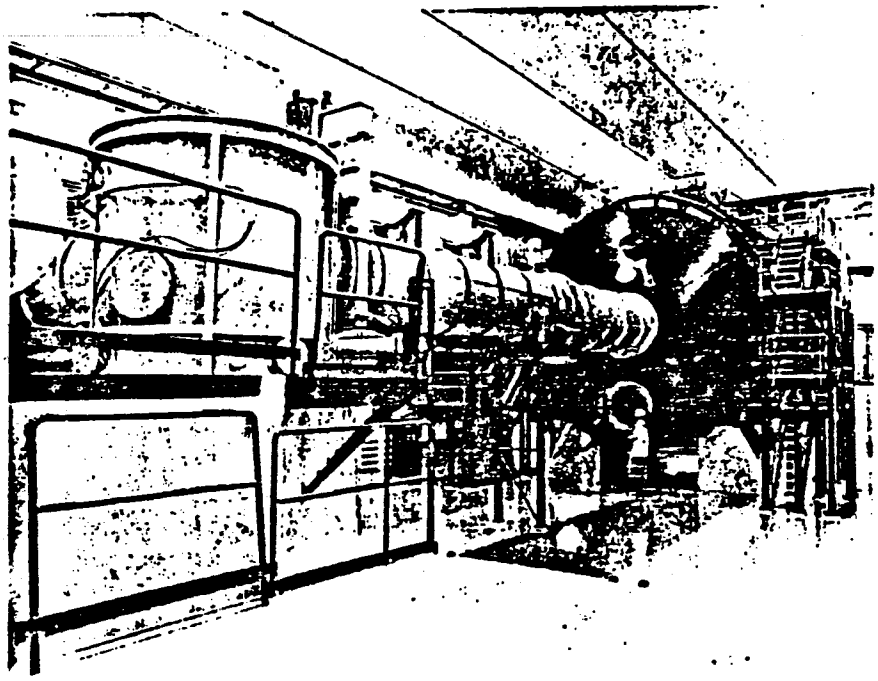

Fig. II-7. Antares Target Hall with the target chamber, connecting tube, and turning chamber. The turning-mirror chamber and the beam-transport tubes shown in beige conduct the beam to the target chamber.

Fig. II-8. Antares target chamber and space frame.

chamber for component installation and service. We will install the major support structure and mirror in 1982.

OPTICAL BEAM MANAGEMENT (Q. Appert)

Beam Alignment

Most of the Antares automatic alignment system hardware and concepts were tested successfully on the prototype beamline in the OEL and the OTB. The prototype beamline has been in operation for more than a year and was fully instrumented for the tests. The OTB, in Power Amplifier 5, consisted of one sector of optics that was installed early in the fiscal year, and of the assembled and aligned alignment station.

Alignment System Description

Antares requires beam centering on mirrors with accuracies equivalent to ±0.1 mm at a distance of 22 m (4.5×10^{-6} rad) and beam pointing at the target position within 45 μm (25×10^{-6} rad).

A single alignment station performs automatic alignment for each beamline. Intense, visible-point light sources are positioned at the desired beam centers along the beamline and are viewed by a telescope/TV camera from the alignment station (Fig. II-9). A video tracker determines the centroids of the light spots and generates error signals, which cause the computer control system to move appropriate mirrors in a closed-loop system. The video tracker overcomes diffraction limits when viewing down the beamline by resolving the diffraction spots to about 1 part in 10. We have achieved an accuracy of 0.03 mm at 22 m (1.5×10^{-6} rad) in 100 video frame samples (with a 3-s average). Averaging removes errors caused by scintillation and vibration.

Final alignment at the ultimate target position is accomplished with a CO_2 laser located at the alignment station and an aperture/detector combination. The detector aperture (or, equivalently, the pointing mirrors) is (are) moved under computer control to maximize the energy through the aperture. This final alignment removes error that results from dispersion in salt windows between visible and 10.6-μm light.

Prototype Beamline and Alignment System

The system (Fig. II-10) provided the first test of the overall alignment concept in the OEL. The prototype beamline substitutes a 17.8-cm (7-in.) -diam Questar telescope for the actual telescope that is being fabricated. An LSI-11 computer was used for control, and prototype stepper motor drives were used to drive the mirror positioner and telescope focus. Antares 1-mm fiber optics and light-source boxes were used for the point-light source.

Because the entire beamline was installed in ambient air, scintillation effects were pronounced, resulting in large excursions (5 to 10 TV lines) of the diffraction-limited light-source spots on the TV camera. This effect was overcome by taking large (100 to 1000) TV frame centroid samples and calculating the mean. Using this technique, the system automatically focused the telescope on each light source and corrected by a calculated amount each mirror that had been previously displaced.

Accuracies for beam centering and alignment were well within requirements. We determined the beam position at the target and tested algorithms to align coupled mirror sets on the OTB.

Beam Pointing at Target Position. We analyzed, prototyped, and tested a concept for beam alignment at the target position. The device, a detector and visible source (DVS), can be mounted on the alignment gimbal positioner (AGP), which points the DVS at each sector. The AGP also accepts a point diffraction interferometer for beam focus quality determination and analysis.

The DVS, as originally configured, consisted of a ZnSe imaging lens, germanium beam splitter, pyroelectric (CO_2) detector, and peak sense and hold circuitry (Fig. II-11). These elements were mounted in a package designed to replace a segment of the Smartt interferometer relay optics that are located in the aft portion of the AGP. All our testing has been accomplished in this configuration to date.

The ZnSe lens images on a 100-μm pinhole through the germanium beam splitter onto the pyroelectric detector. The germanium beam splitter also folds a visible fiber-optic light source into the optical path. The ZnSe lens then images this fiber-optic source onto the 100-μm pinhole. When the light source is illuminating the pinhole, the alignment telescope and video tracker may be used to locate the position of the DVS.

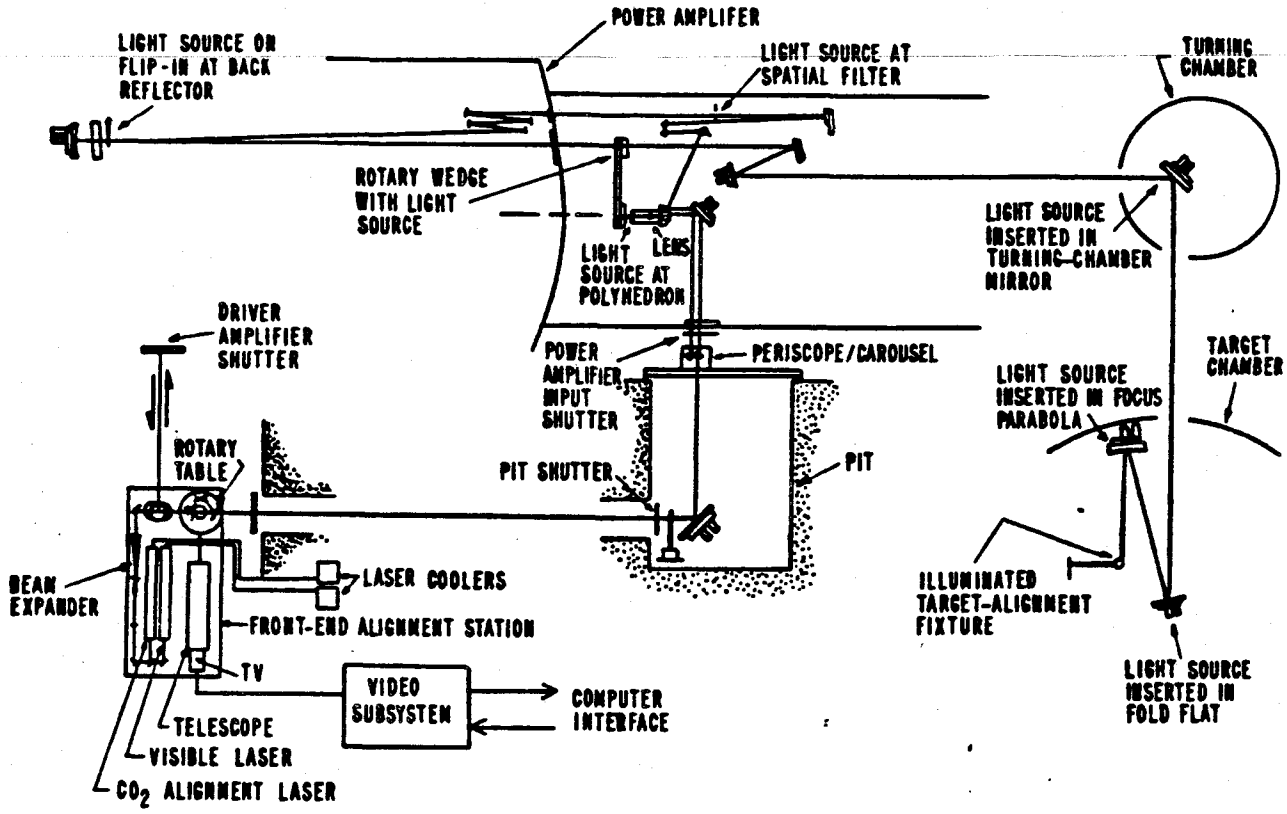

Fig. II-9. Antares automatic alignment schematic. The optical alignment path extends from the front-end room through the power amplifier and TVS onto the target position.

We have developed a simpler DVS design that eliminates the ZnSe lens. The new configuration retains the same concept but is smaller, requires no optics, and will be mounted on the AGP gimbal. The detector, pinhole, and germanium beam splitter are all mounted in a unit. Because the detector is only 5 mm from the pinhole, we eliminated the need for imaging optics. The design is 90% complete; fabrication will begin in January 1982.

When we examined the DVS in the OEL, we took into account two distinct considerations: the fundamental sensitivity of the device and the suitability of the software for beam alignment.

We plotted the laser beam profile as it swept across the DVS/pinhole system. The amplitude of the laser energy was attenuated to approximate the level anticipated in the operational system. These tests showed that the detector, electronics, and pinhole combination had sufficient sensitivity to locate the peak of the laser to the required accuracy of ±15 μm.

Alignment software was written for and exercised on the interim LSI-11 computer. With the aid of the video tracker, we evaluated the ability of the software and DVS system to align the laser to the required accuracy. We compared the DVS position as determined by the tracker before system alignment was disturbed and after the software had realigned the system. Results indicated that the system was aligned to within ±12 μm.

Alignment Gimbal Positioner (AGP). The AGP positions and points either the DVS or an interferometer, depending upon the type of alignment information needed. We will have the capability to focus each laser beam independently anywhere within a 1-cm^3 space surrounding the target center. To align the beams, the AGP will (1) hold a variety of detectors; (2) point a detector at each laser beam to within ±0.5 mm from a reference location in the x, y, and z axes; and (3) know the detector position relative to the reference throughout the travel of each motion to within a maximum root sum of squares (RSS) error of 15 μm.

Fig. II-10. The Antares prototype beamline in the OEL simulates the actual beamline configuration from the front-end alignment station to the target.

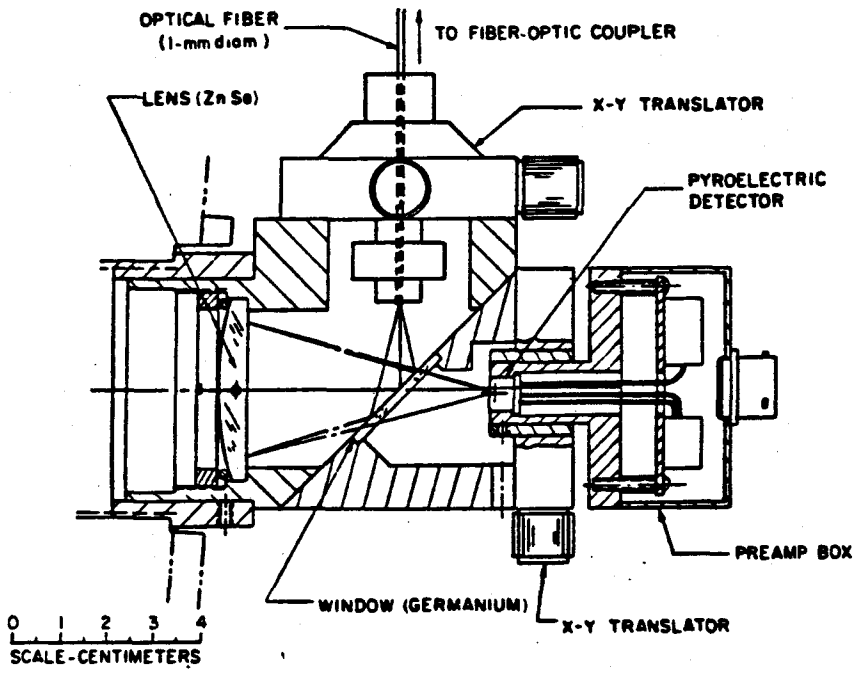

Fig. II-11. The DVS projects visible light from the target position to the alignment station telescope and detects CO_2 laser light from the alignment station.

The AGP consists of a gimbal mounted to an x, y, z micropositioner and a set of optics or electrical connections that relay the detector information outside the target chamber. The detector center is located precisely at the intersection of the two gimbal axes. This arrangement allows us to point the detector toward any position in space and translate it to within the limits of the micropositioner. Figure II-12 shows the AGP with the interferometer (detector).

Until recently, it was difficult to reliably position a detector with an accuracy of better than 20 μm by using a linear bearing system. Experience with an earlier instrument revealed that most of the difficulty could be attributed to Abbe offset error. This error is associated with measuring the position of a point offset from the measurement of the axis, as illustrated in Fig. II-13. This figure also dramatizes the effect of linear bearing straightness on Abbe offset error. The linear bearings used on the earlier instrument were crossed roller bearings that were lubricated with vacuum-compatible grease and had an a:b ratio (Fig. II-14) of ~6:1. For the AGP, the a:b ratio should be reduced as much as possible to obtain the linear bearing system that will give the best predictability for the detector position.

Six configurations were tested; data for each are given in Table II-1. Those with solid circular rails were superior to the others whether we used wet or dry lubricant. Configuration 5 had the lowest error for a polynomial fit of less than 1.5 μm (at 99% confidence) for all dial settings, significantly less than the 4.0-μm Abbe offset error budget.

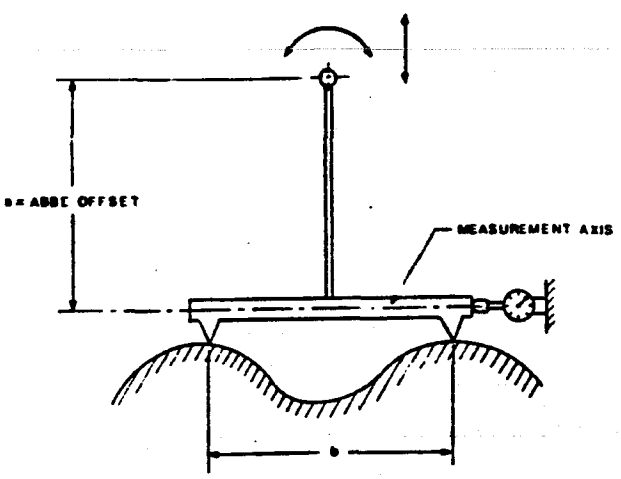

Fig. II-13. Abbe offset error description.

Although more severe tests are likely to result in poorer fits to the data, the precision we have obtained thus far makes us confident that we can meet the allotted error budget.

Tests of Optical Test Bed (OTB). We used the OTB to verify alignment algorithms, demonstrate alignment performance under system design pressures, and help develop component control software.

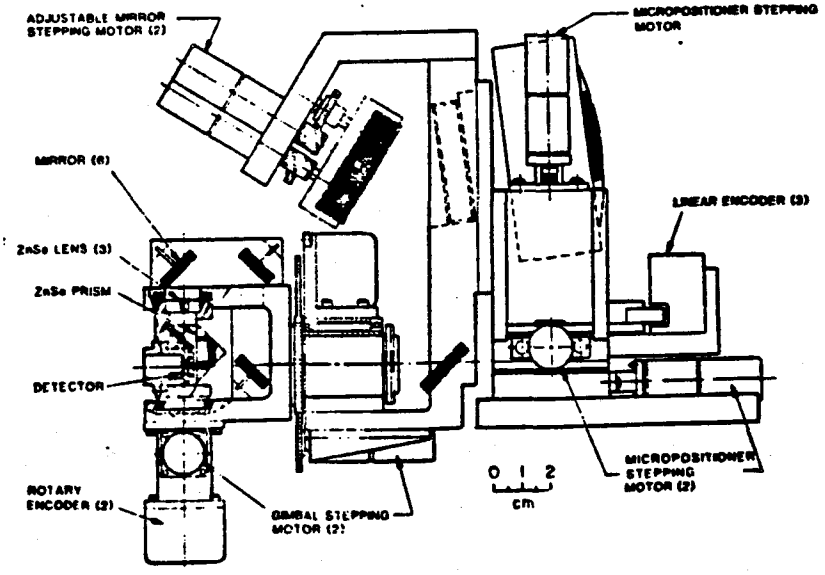

Fig. II-12. The AGP positions the DVS for each beam sector at the target position.

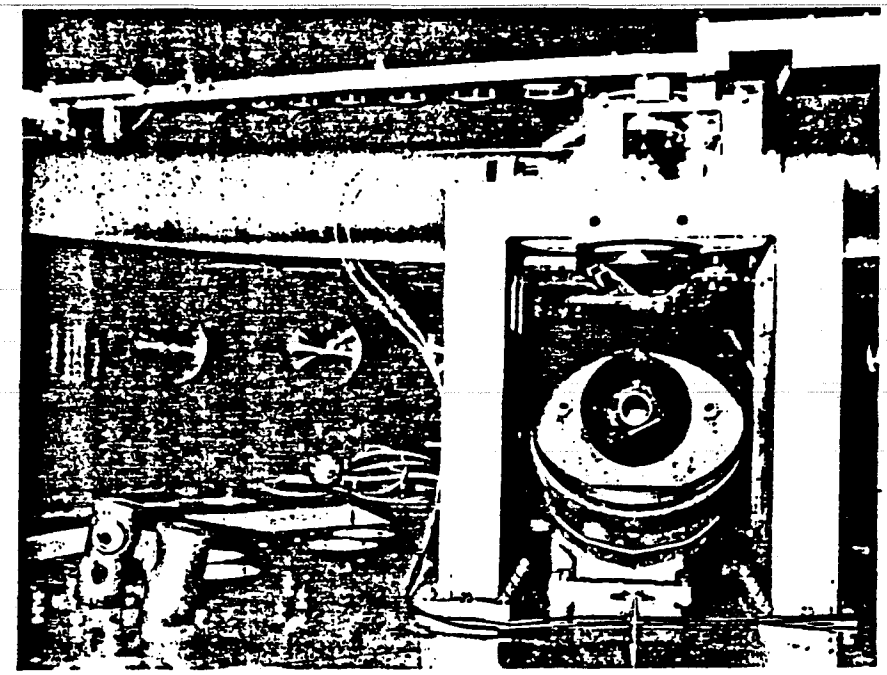

Fig. II 14. Rotating wedge assembly and polyhedron beam splitter mounted in power amplifier. The wedge rotates to each sector being aligned; it compensates for the wedged exit salt window and provides a light source for beam alignment to the periscope mirror. The image of the polyhedron beam splitter reflected from the micromachined copper mirror surface indicates the high optical quality.

TABLE II-1. Configuration Data For Prospective AGP Linear Bearings

Configuration Number	Roundness or Lubrication and Configuration Description	Parallelism of Rail or Roller (μm)	Surface Finish[a] (μm)
1	Dry, crossed roller bearings	1.25	<0.2
2	Fomblin-lubricated bearing ways and square cross-section rails	1.0	0.05
3	Nedox-coated bearing ways and circular cross-section rails	1.25	<0.2
5	Fomblin-lubricated bearing ways and circular cross-section rails	1.25	<0.2
6	Fomblin-lubricated rollers	1.25	<0.2

[a]RSS.

We checked out procedures for the installation of optics and automatic alignment equipment. Figure II-14 shows the installed rotating wedge (for visible alignment compensation), the polyhedron, and the first turning mirror viewed from the beam input port. The back-reflector light-source flip-in is in front of the absorber-gas salt window in the assembled Power Amplifier 5 (Fig. II-15). Figure II-16 shows the assembled alignment station for Beamline 5.

Verifying alignment algorithms on the OTB was an extension of work begun in the OEL, where central obscuration of the telescope prevented evaluation of coupled-mirror alignment. The telescope in the OTB was a refractor with no obscuration; it permitted alignment of the polyhedron and back reflector. Both procedures employ a coupled-mirror alignment algorithm. Test results show that all sources examined could easily be aligned within the designated error budget.

Because the calibration data required to align the system are extensive, we need a single set of data for alignment regardless of system pressure or vacuum. We conducted tests to determine whether the system under pressure could be aligned with calibration data generated at ambient pressure. By using atmospheric data, we could align the pressurized system without difficulty. All light sources remained within the video tracker gate when we brought the system up to pressure.

The alignment algorithms as well as the pressure testing were verified with an interim LSI-11 computer. This experience helped us develop a software specification for the Antares computer. Now component control and the associated man/machine interface (MI) are operational on the OTB.

DIAGNOSTICS (J. Solid)

Calorimeters

The diagnostic system measures the laser parameters on the large-aperture portion of the Antares laser system from the power amplifier input to the target. The

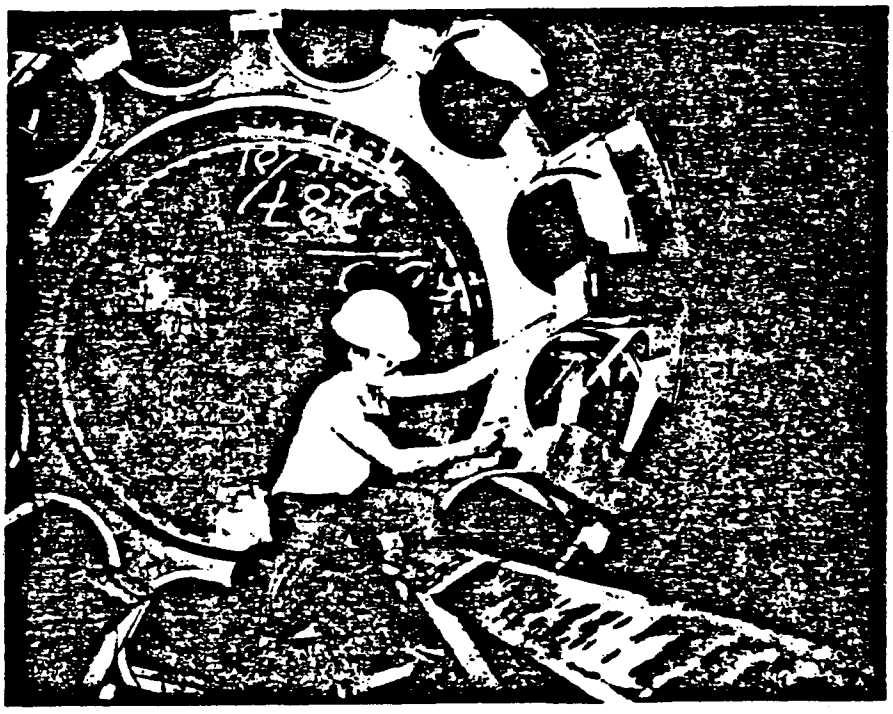

Fig. II-15. Flip-in light source mounted in place in power amplifier. An 18-in.-diam salt window is installed with a flip-in light source for beam alignment to the back reflector. We will mount 11 additional salt windows in the final configuration.

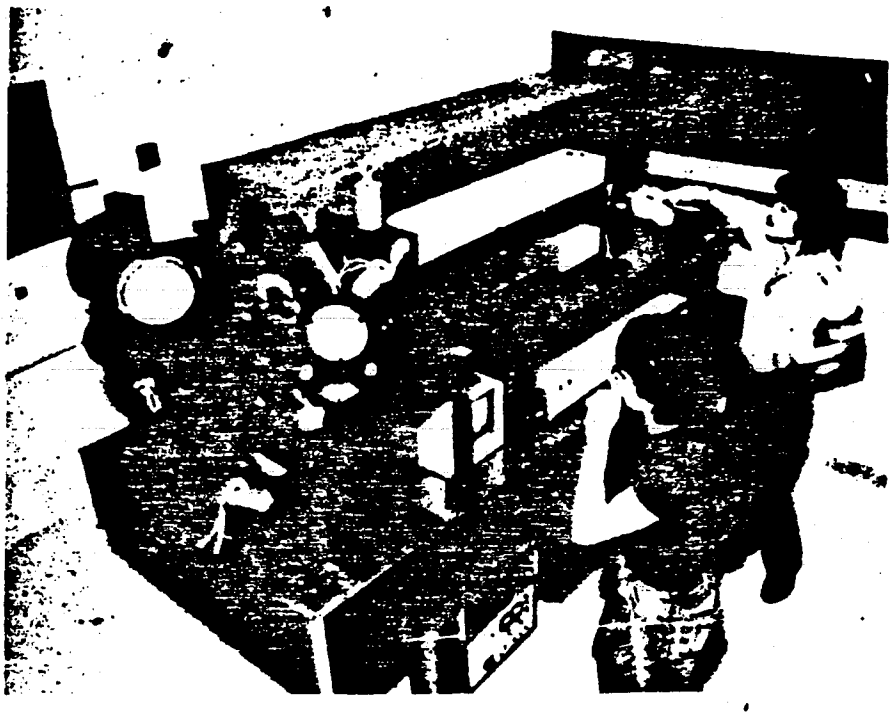

Fig. II-16. The alignment station in the front-end room contains a visible and CO_2 alignment laser and large-aperture variable focus telescope. It will be used to align the beamline from the power amplifier to the target position.

diagnostics for the front end and the driver amplifier are all available commercially, but nearly all other devices from the power amplifier to the target are custom made.

Energy and temporal pulse shape are the primary parameters to be measured. Energy is measured at five positions along the beamline: (1) at the input of the power amplifier by the input calorimeter; (2) at the input to each sector in the power amplifier by the input-sector calorimeters; (3) at the output of the power amplifier by the power amplifier full-power calorimeter; (4) at the turning chamber by the turning-chamber calorimeter; and (5) in the target chamber by the target-chamber full-power calorimeter. Neither full-power calorimeter is used during operation. Figures II-17 and II-18 point out the locations of the calorimeters in the system.

The calorimeter diameters range from 2.0 to 150.0 cm. We have developed both a Kapton/copper volume-absorbing isoperibol calorimeter and a beryllium oxide twinned calorimeter.

Beryllium Oxide. Using BeO as the radiation-absorbing element in isoperibol calorimeters has two advantages. First, we can use hybrid circuit-fabrication techniques to apply solder pads for the desired number of thermocouples. This eliminates the need for thermally conducting epoxies that are expensive, require 4 to 8 h of curing time, and contribute nonlinear thermal properties. Second, using the same techniques, we can sinter calibration resistors directly onto the BeO substrate to allow electrical heating with known energy. Inked thermocouple materials can also be used; however, metallic thermocouples (chromel/constantan) were chosen for their high responsivity (60.2 μV/K).

These calorimeters may be used for any radiation that deposits energy in the BeO. They have been used for protons as well as for 10.6-μm radiation. At 10.6 μm their sensitivity is ~1 mV/J. Their sensitivity to electrically deposited heat is about twice as high, showing that the effective absorptivity of the BeO for 10.6-μm radiation is ~50%. The absorbing BeO wafer was 32 mm square and 0.25 mm thick. The cooling mechanism for these pulse-measuring calorimeters is primarily radiative. To within 2%, they behave as ideal isoperibol (constant environment) calorimeters. The maximum radiance before we detect surface flashing is ~1 GW/cm^2.

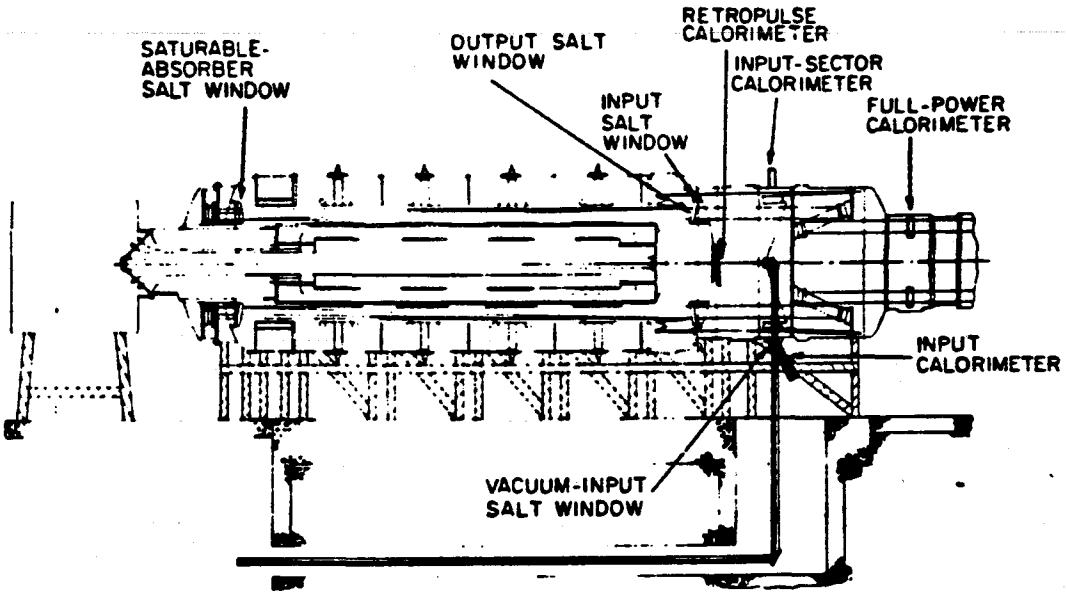

Fig. II-17. Calorimeter locations in the power amplifier. The input calorimeter measures the energy into the amplifier; the input-sector calorimeter measures the energy into each of the 12 sectors.

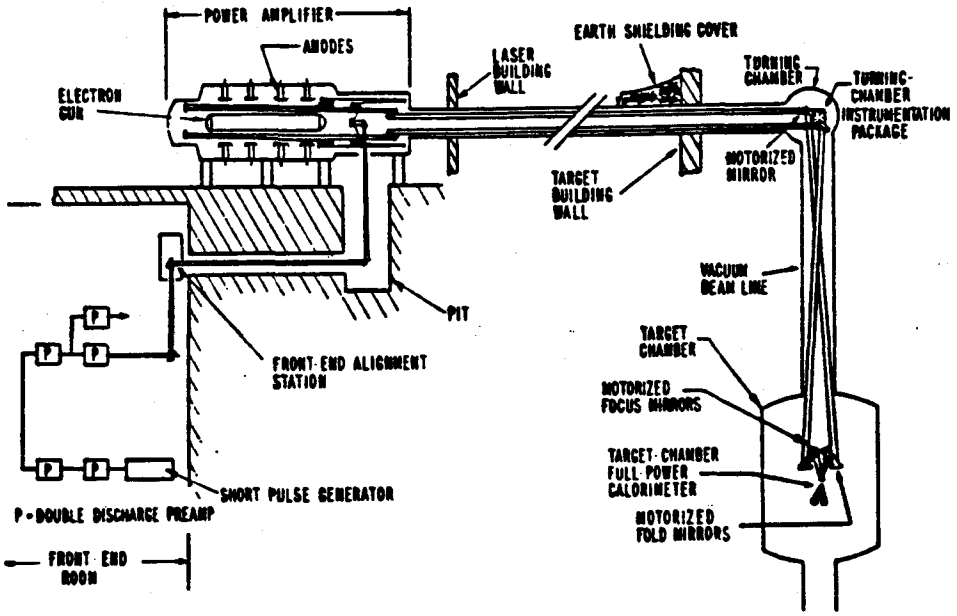

Fig. II-18. Beam-diagnostic location in the target-system beamline. The turning-chamber instrumentation package contains both calorimeter and temporal measuring devices.

Kapton Copper. Because BeO is expensive, BeO calorimeters are limited to small sizes. For large-aperture use (150 mm and larger, for example), we have developed a Kapton/copper calorimeter.

For pulsed-energy measurements in apertures up to 1.5 m, Kapton/copper laminate foils will be used as isoperibol calorimeters. These are volume-absorbing calorimeters in which the radiation is absorbed in a layer tens of wavelengths thick. The volume absorption reduces the surface temperature and increases the damage threshold as compared to surface-absorbing calorimeters. Kapton was chosen for its high absorption coefficient [330 cm^{-1} at the P(20) line of the 10-μm band of CO_2] and its useful short-pulse damage threshold (2.8 J/cm^2 or ~2.8 GW/cm^2). The copper backing integrates the absorbed heat pulse, and the resultant temperature pulse is sensed by Type-E thermocouples (chromel/constantan) soldered to the copper. We can then analyze time-vs-voltage traces of the thermocouples to obtain the energy absorbed. Using photolithographic techniques, calorimeters are fabricated to virtually any size or shape. We further expand the versatility of this technique by using single elements or several units in a thermocouple. Table II-II lists typical results for both the BeO and Kapton/copper calorimeters.

Fast Oscilloscopes

To faithfully record laser output pulses, a 3- to 5-GHz bandwidth is required. We use a 3.5- to 4.0-GHz instrument built by Los Alamos with a Tektronix, Inc. custom tube, the Model-1776 Microchannel Plate Oscilloscope. The trace is read by a silicon-intensified TV camera; it gives a 512-bit serial string composed of a 4-digit numerator and a 4-digit denominator that locate the centroid of the trace. The video digitizer is also designed and built by Los Alamos. The 10.6-μm power amplifier radiation detectors built at Los Alamos are two-segmented devices. Their signal is so strong that no amplifiers are required to drive the oscilloscope. A typical problem with ultra-high-speed recording devices is low sensitivity; however, by constructing the pyroelectric detectors with two segments, we achieved a high responsivity that obviates the use of amplifiers.

Testing. To test the temporal measurement method and hardware, we installed on Helios a prototype system or demonstration channel, A schematic of the system is shown in Fig. II-19. The system was constructed and its bandwidth was replaced. By removing the detector from the system and driving the system with a 20-ps step

TABLE II-II. Antares Large Beam-Diagnostic Calorimeters

	Input Characteristics		Signal Levels	
Calorimeter Type	Energy (E)	Flux (ϕ)	Output Voltage (V_o)	Output Resistance (Ω)
Input calorimeter Kapton/copper	0.4 J < E < 8 J	3.5 mJ/cm² < ϕ < 70 mJ/cm²	2.0 mV < V_o < 40 mV	432 Ω
Input sector Calorimeter BeO	0.050 J < E < 0.200 J	10 mJ/cm² < ϕ < 40 mJ/cm²	80 μV < ϕ < 320 μV	288 Ω
Full-power calorimeter[a] Kapton/copper	32 J < E < 1600 J per sector	40 mJ/cm² < ϕ < 2000 mJ/cm²	0.5 mV < V < 26 mV per element	120 Ω/ element
Turning-chamber calorimeter Kapton/copper	0.26 J < E < 31 J	0.39 mJ/cm² < ϕ < 47 mJ/cm²	1.7 mV < V < 510 mV	1.8 kΩ

[a]There are 12 sectors, each of which is divided into a 5 x 5 array of elements (300 elements totally).

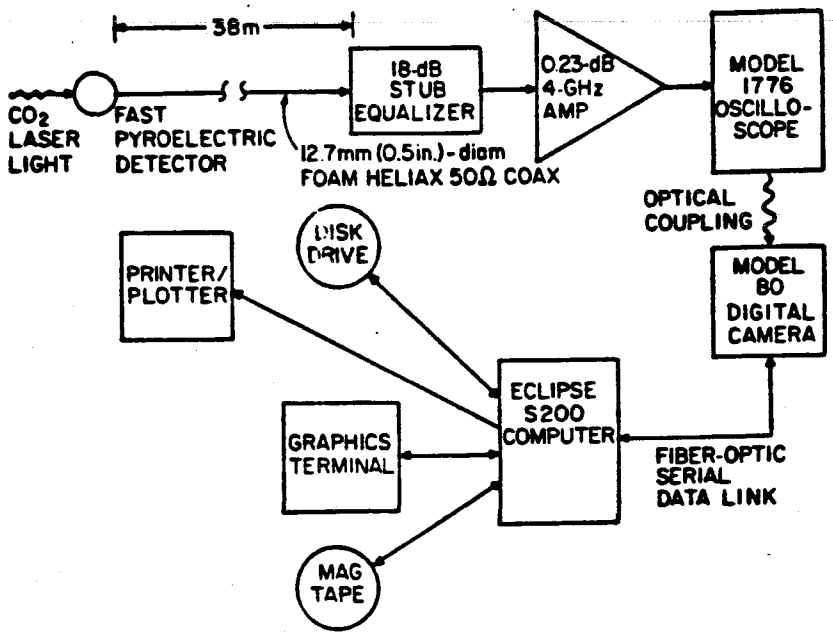

Fig. II-19. Schematic for testing fast oscilloscopes.

function, we attained an ~3-GHz bandwidth, as predicted. Figure II-20 shows the transformed time-domain data; the gain of the system was ~5dB.

We then applied the signal from the detector to a matched power divider. One output fed a close-in diagnostic recorder ~4.5 m from the detector, and the other fed the system being tested ~38 m away. The bandwidth of the close-in system was known to be ~1.5 GHz. Figure II-21 shows the results of a laser shot as

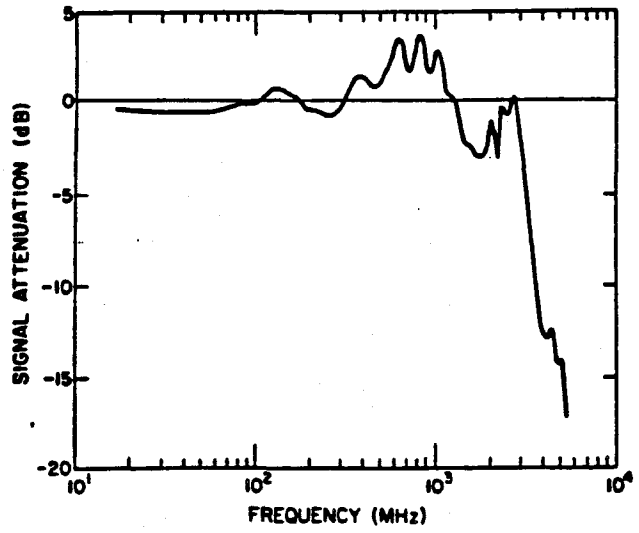

Fig. II-20. Model-1776 oscilloscope system response.

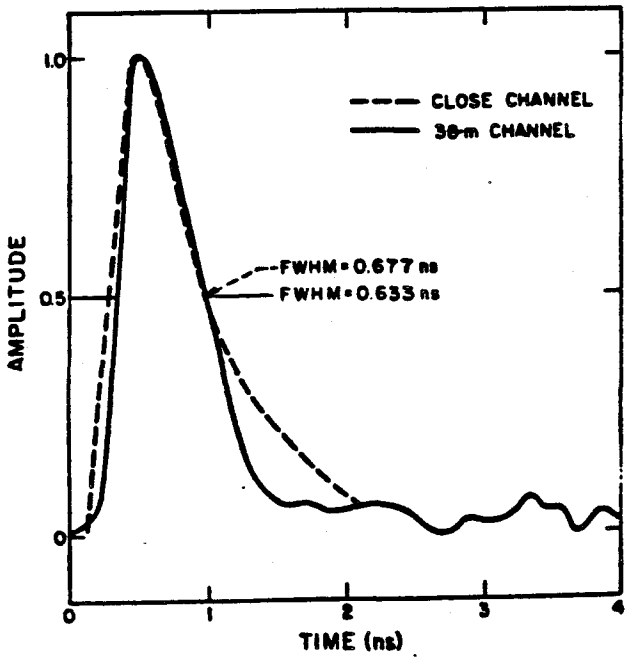

Fig. II-21. Laser pulse shapes, one produced by a close detector (dashed line), the other from a similar detector with a 38-m length of heliax (solid line).

seen on both channels viewing the same detector. Although the measured laser pulse was not severely band limited by either recording system, some differences can be seen in the overlay. The major feature is the long tail on the pulse shape of the close-in channel that is attributed to the reduced bandwidth of the close-in channel. This reduction was caused by the ~4.5 m of ~1-cm (3/8-in.) -diam foam dielectric coaxial cable used to connect the oscilloscope to the detector. We attributed additional minor differences in the two recorded pulse shapes to differences in the film-digitization methods employed. The close-in channel was digitized from Polaroid film on a digitizing pad to allow for a gross undersampling of the recorded trace. The remote channel was recorded on transparent film and then read on a 30X magnification film reader. Because of this difference, the close-in channel seemed to wash out some of the detail seen in the remote-channel trace. However, for the parameters of risetime, FWHM, and peak amplitude, the similarity is remarkable.

Results. Our work on Helios demonstrated a system capable of recording multigigahertz electrical signals from diagnostic detectors at a distance of ~38 m. This type of system provides a radiation- and noise-free environment to record fast, transient events produced by laser fusion. The system also encourages future expansion of diagnostic capabilities by not limiting diagnostic instrumentation to the immediate target-chamber area.

CONTROLS (M. Thuot)

Computer Control of Energy System and Power Amplifier on Beamline 2

The Antares control system computer network (ACN) provides three levels of laser control. The lowest, the MI, is composed of 38 LSI-11 microprocessors and a set of standardized interface hardware that serve as data multiplexers; these directly control valves, relays, and data-collection devices. Four subsystem-control computers (SCCs), PDP-1160s, control the major subsystems: optics and target, front end, Beamline 2, and Beamline 5. Most of the closed-loop control resides at this level. These computers also support a man/MI, so that each subsystem can be operated separately and concurrently. A PDP-11/70 computer will provide overall system control by coordinating the operation of the four SCCs and will provide the operator/MI for the entire system (Fig. II-22). The system design accommodates over 4000 control and data channels, as well as control of nearly 150 interacting processes. The control system has been designed and tested to operate without errors in the severe EMI environment generated by the laser.

The locally developed network communication software, TENnet, supports communication between computers in the network. This software also provides the required error-detection and recovery functions for link errors, loss of link, loss of a network processor, and loss of power.

Control Hardware. Hardware implementation of the Beamline 2 system control includes 10 computers operating in a hierarchical network. A PDP-11/60 minicomputer functions as the beamline controller, actively supervising nine MI computers that are distributed through functionally and physically independent parts of the beamline. Two MIs control the high-voltage power supplies. One MI computer-control and data-acquistion package is attached to each of the five pulsers. Each has a high-quality EMI-shielded enclosure that allows error-free operation in the high electromagnetic fields that surround the pulsers. Further, all data and control connections to these MIs are made with fiber-optic cables to eliminate conducted electrical noise. Another MI-controlled data-acquisition subsystem is located in the shielded room adjacent to the laser power amplifier (Fig. II-23). This subsystem has more than 100 fiber-optic data channels that record voltage and current waveforms as well as timing information from the power amplifier during operation. The ninth MI is the central timing controller that provides fiber optically transmitted triggers to the pulsers and data-acquisition systems.

This control system has been in operation for over 1200 shots since the electron gun was installed in the power amplifier. Relatively minor changes in the hardware, software, and timing system let us make extensive modifications to the electron gun, including the addition of a diverter gap and another trigger system. These late modifications did not change the basic system design, and the new software modules were integrated into system operation in a few weeks.

Control Software. The software system design now supporting Beamline 2 operation is the first version of the kernel software. The kernel software modules provide a

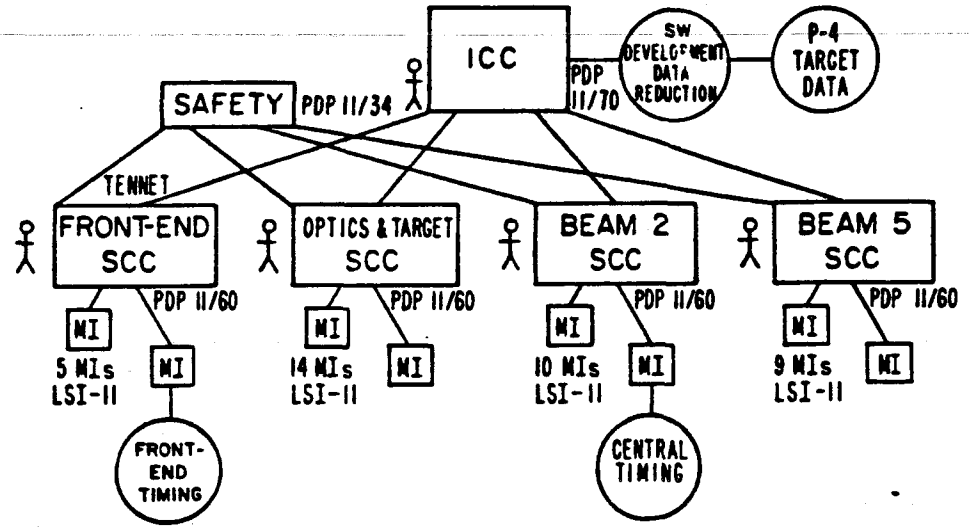

Fig. II-22. Antares control system computer network (ACN).

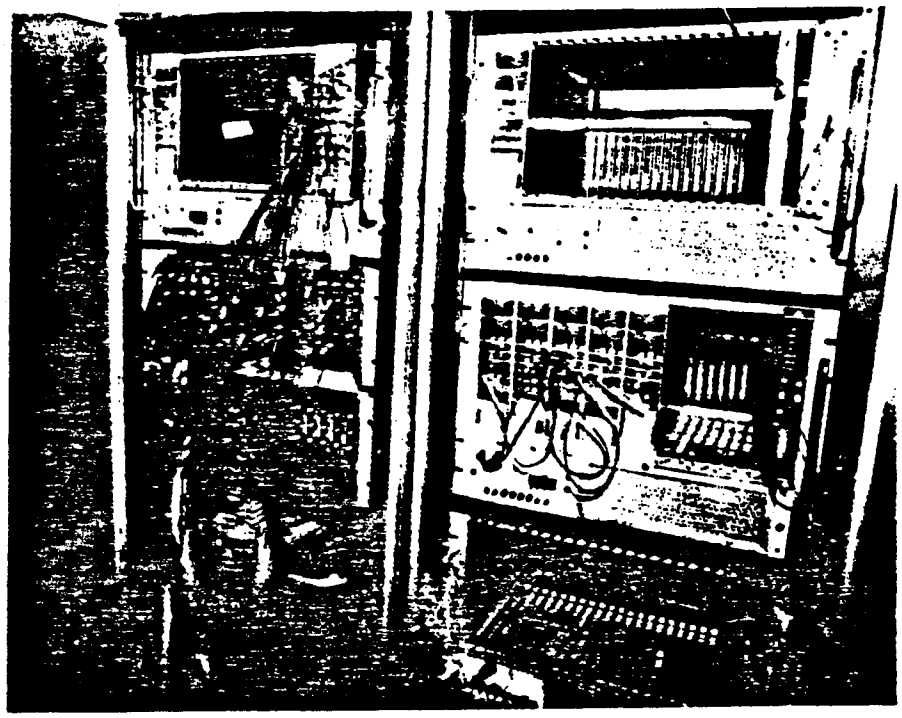

Fig. II-23. Power amplifier data system.

standard interface between the application control programs and the laser or operator. Two levels of applications programs have been written for Beamline 2 control. The first is called component control; it allows a low-level interface to each component (for example, relay, valve, or switch) in any controlled device. Using predefined kernel software modules now allows the computer to generate this application software almost entirely from the signal name list in the software specification. The low-level control access is used extensively to install, check out, and maintain the hardware.

Second-level control is provided by an application program called "charge and fire" that creates integrated operation of a beamline. The operator selects one of the five pulsers to operate, the level of charge voltage, the pressure settings, the fire timing, and other parameters. The operator also sets up data-acquisition channels in the power amplifier current-density measurement system. The computer then runs a test on the laser interfaces and control equipment and begins charging the pulsers. The charge process is represented graphically in real time on the operator's console. The operator is notified when the charge is complete and the energy system is fired. After the shot, the voltage and current waveforms, current-density waveforms, and timing data are displayed to the operator and transferred to a data base. The data base stores the raw data and makes the information readily available for analysis. A data analysis program that allows many mathematical functions to be applied to the data provides a processed graphical output.

Operation. The process of integrating the control and operation of Beamline 2 produced several changes in the implementation of the control system. These changes were in the area of operator interface, calibration, and data analysis. The major improvements in the operator interface will be addressed by the Version 2 man/MI described in the following section. Some changes were incorporated in the Version 1 programs used by the laser operators to increase their involvement in the control process. The system now provides more real-time data to the operators.

Calibration of the data system was revised in several areas. Hardware testing methods were devised to decrease data channel variability. Data-acquisition hardware was modified by the CAMAC vendor to improve interchangeability of modules. The calibration programs were revised to give the operator more data while calibration was in progress.

Data recall from the data base and analysis of the data produced several operational problems. The system had been designed for a batch-mode process, but the operators wanted to analyze data after each shot. The normal time for file transfer through the network delayed some operations. We will address this problem in the Version 2 beamline-control software to be available in spring 1982. We treated the immediate problem by training the operators to use the system more efficiently.

Automatic Alignment Controls

Introduction. A fully automatic computer-controlled system will align the laser beam. The alignment computers are an integral part of the ACN. There will be alignment control stations at the front end, the power amplifiers, the turning chambers, and the target chamber. Operators will be located in the central control room where color graphics terminals and television monitors are located.

Alignment is accomplished by establishing a known reference with respect to the front-end output beam at the alignment station in the front end. Everything in the rest of the beam path is aligned to that known reference by working mirror by mirror through the system. Light sources along the beam path are inserted in sequence. At each mirror a video processor at the front-end station looks through the downstream optics to the associated light source and determines the beam location. Error signals are sent to the control system, which then moves the mirrors so that the light source is positioned correctly. When this process is completed for all mirrors on a beam path, alignment is complete.

There are control functions to (1) turn on the light source, (2) search for the source when necessary, (3) read the tracker error signals, (4) calculate mirror movements, (5) execute mirror movements through stepping motors, and (6) verify that the process is complete. These steps are done sequentially along the beam path from front end to target.

Alignment Control Hardware. The ACN optics SCC is a PDP-11/60 minicomputer that controls the automatic alignment process. Seven LSI/11 microcomputers and their interface hardware, MIs, are located at the alignment stations and are connected to the SCC. The

MIs control and monitor stepping motors, light sources, TV trackers, and other miscellaneous components. A typical alignment MI includes an LSI/11 microcomputer, a stepping motor controller, binary control and monitor equipment, fiber-optic interfaces, power supplies, and EMI-shielding equipment. All components are from standard parts inventory for Antares.

The motor controller is a special system designed at Los Alamos and standardized for all Antares stepping motors. Each motor controller is linked to the MI. Motors are connected to a motor controller through a variable-sized matrix. The largest matrix possible in each motor controller is 8 × 32, for a maximum of 256 motors. We chose this design instead of commercially available motor controllers to reduce the number of motor controllers, reduce the amount of wiring to motors in power amplifiers, and reduce the number and cost of vacuum feedthrough connectors on the power amplifier and TVS. The design, installation, and testing are complete for one beamline's front-end and power amplifier alignment MIs. The computer can control and monitor 140 stepping motors, set and read tracker error data, and control 39 light sources required for front-end and power amplifier alignment.

Alignment Control Software. Alignment component control software was initially written with Version 1 kernel software to support hardware installation and testing. We use the Version 2 kernel software to implement the automatic alignment system.

The Version 2 kernel software expanded the capabilities of Version 1 in several key areas. It provides the necessary error-detection and alarm functions for closed-loop mirror-positioning control. It provides a true data base function to store and retrieve the nearly 15 000 constants, settings, and parameters in the alignment process. And it provides support for the high-performance Version 2 man/MI. This interface improves the interaction between the operators and the control system by providing immediate response and control verification to the operator, improving the control input function with a full-screen touch panel, and providing context changing, full-color display replacement, in less than 2 s.

The automatic alignment applications software now provides several Version 2 displays (Fig. II-24). We have implemented and tested the alignment calibration function of constants, parameter entry, and editing. We have also tested the basic control functions such as reading the tracker or moving a motor. In addition, we are testing the design and coding of the automatic alignment software for the power amplifier. We expect full automatic alignment through the power amplifier by March 1982.

RETROPULSE ISOLATION (T. Sheheen)

In all high-energy laser fusion systems, we must protect front-end oscillators and optical components from damage by laser pulses that are reflected into the laser systems from fusion targets. Any apparatus used in isolating the retropulse should be efficient, should have a high forward transmission and low backward transmission, be of minimum complexity for reliable operation, and (for Antares) should function in vacuum.

We have demonstrated that a CO_2 (10.6-μm) laser-initiated plasma may be formed at the aperture of a LiF spatial filter in a 10^{-6}-torr vacuum of sufficient density and lifetime to block the retropulse from re-entering the laser system. Plasma initiation is controlled by the fluence incident on the aperture edge of the spatial filter.

Our experiments use a CO_2 laser with a 1.1-ns pulse width and pulse energies up to 3 J. A chopped cw CO_2 probe laser at 9.6 μm was used to determine the blocking time of the laser-initiated plasma. Figure II-25 shows the paths and experimental configuration schematically.

With a 1.1-ns pulsed 10.6-μm CO_2 laser incident on the LiF aperture, at a 63-J/cm^2 fluence level on the edge of the 0.7847-mm-diam aperture, we have found that within the 1.1-ns pulse a plasma is initiated that produces a small-signal transmission of 64%. Within 40 ns, the plasma reaches a critical density of 10^{19} cm^{-3}—sufficient to block the 9.6-μm probe laser. The plasma persists at or above the critical density for 680 ns, which exceeds the retropulse return time for the Antares laser fusion system.

These experimental results indicate that an effective, passive retropulse-isolation system can be simply implemented in the Antares system.

CONCLUSION (H. Jansen)

In 1981 we have seen a significant change in the Antares project—from procurement and installation to testing of the hardware in laboratories or on the real machine. The culmination of all these efforts was a recently performed test on Power Amplifier 2. The entire power amplifier system with the energy-storage devices for the electron gun and the 48 laser discharges worked

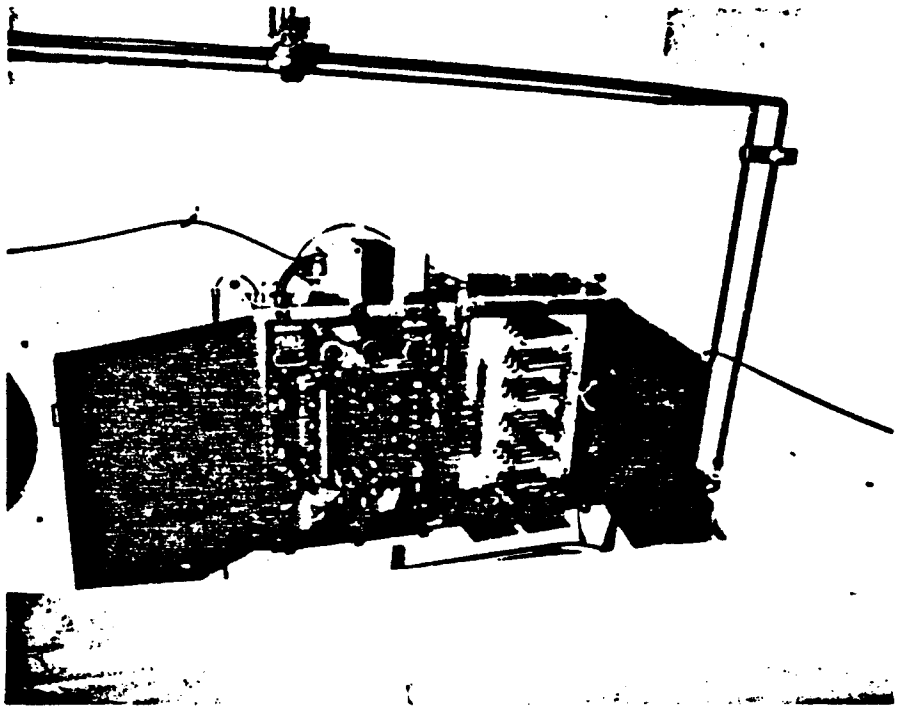

Fig. II-24. Front-end alignment motor driver.

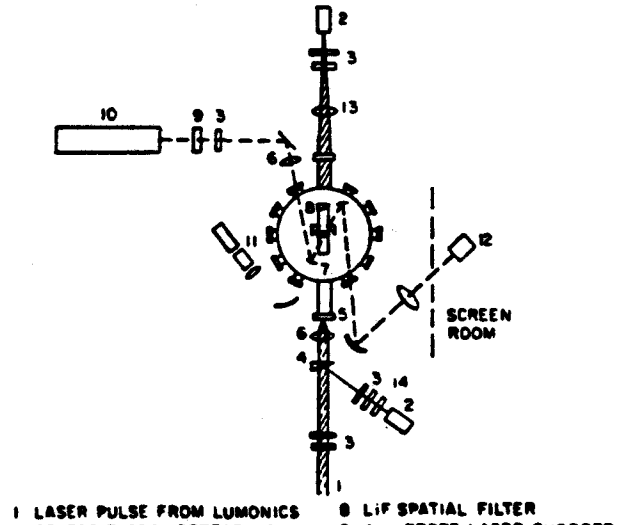

Fig. II-25. Experimental setup to investigate plasma formation.

in harmony under computer control from the control room. A small probe laser was sent through all four axial sections of the power amplifier and was amplified to design criteria. Next year, we will see energy extraction on three beams, and we plan to place one beam on target.

VACUUM SYSTEM AND TARGET CHAMBER FOR ANTARES HIGH-ENERY GAS LASER FACILITY

N. G. Wilson[+]
R. H. Swinderman[++]
J. M. Allen[+]
C. R. Winkelman[+++]

The Antares Laser of the Los Alamos National Laboratory High Energy Gas Laser Facility, a 200 kilojoule, carbon dioxide gas laser system, utilizes a high vacuum target chamber with integrally evacuated beam transport tubes from each of the Antares Power Amplifiers. The planned configuration of the Antares system utilizes six power amplifiers and beam transport tubes arranged so as to illuminate a target at the center of the target chamber through three ports in each end of the target chamber (Fig. 1). Mounted inside the target chamber is the mirror support space frame, required turning and focusing mirrors, beam alignment instruments, target insertion and positioning apparatus and target reaction diagnostics instrumentation. The initial installation of two of the planned six beam lines is now in operation. The two beam configuration is shown schematically in Fig. 2.

Primary design criteria for the Target Vacuum System (TVS) requires the achievement of a maximum operating vacuum level of 2×10^{-5} torr, 16 hours after start of evacuation of the TVS from atmospheric pressures with an experimental and government furnished equipment gas load of 4×10^{-2} torr liters per second. Additional functional design requirements included (a) mechanical pumps to be low vibration, direct drive type, (b)

[+]Los Alamos National Laboratory, Los Alamos, NM
[++]Pittsburgh Des Moines Steel Company, Pittsburgh, PA
[+++]Nelson and Johnson, Denver, CO

high vacuum pumps to be oil free to the maximum degree practical, low vibration, nonconsumable cryogen, minimum maintenance no adjustment machines for normal operations, (c) TVS envelope exposed to high vacuum of polish stainless steel, and (d) all systems monitored and operable from an integrated control console located remotely from all TVS operating systems. The maximum leak rate for any discrete leak in all vacuum components is 2×10^{-7} atm cc/sec (helium). A summary of the design characters of the TVS is shown in Table 1. Because of the extreme stability required of all internal mirrors and other apparatus, target chamber pumps which could cause thermal instability are not permitted.

Analysis of the possible approaches to constructing the target vacuum system resulted in a decision to place a single competitively determined contract with a qualified engineer, fabrication, erection and activation contractor. Pittsburgh Des Moines Steel Company was awarded this contract. In addition to the actual Target Vacuum System, the contractor was also assigned certain civil construction responsibilities necessary to integrate the TVS into the Antares-High Energy Gas Laser Facility. The TVS, in full operating condition with all equipment and controls has been sucessfully tested, meeting all design requirements and accepted by the Department of Energy and the Los Alamos National Laboratory.

A cooperative engineering design phase of the project during which "Los Alamos" and Pittsburgh Des Moines Steel Company personnel participated, resulted in a vacuum system arrangement shown previously in Fig. 1.

In the system configuration developed, six (6), 10,000 liter per second (air) helium refrigerator, cryogenic vacuum pumps, are used to provide high vacuum pumping of the TVS. A 2400 liter per second turbomolecular vacuum pump is included in the target chamber pump installation to provide non-condensable gas pumping. This pump is also used for intermediate "roughing" of the system during pump down to permit lowest practical vacuum level at cross-over from rough pumping of the TVS to high vacuum operation. A rough pumping package composed of a direct drive 5000 ft^3 per minute ROOTS blower and two direct drive, single stage, 500 ft^3 per minute trochoidal mechanical pumps is provided for pump down from atmospheric pressure to intermediate "roughing" pressure of the TVS, and evacuation of the helium refrigerator cryogenic pumps during regeneration.

Each major section of the TVS and each major pump is provided with isolation valves to minimize pump down time of the integrated system or repair/regeneration of all major pumps. The beam isolation valves are notable in that they are full diameter (65" i.d.) motor driven gate valves. The isolation gate valves for the two cryogenic pumps on the target chamber are provided with modulating controls to permit "throttling" of these pumps during cross-over to high vacuum operation.

Monitoring and control of all TVS systems function is provided in a remote control console located in a TVS control room adjacent to the Antares Target Building. Included in the console are Bayard Alpert ionization gauge control for gauge sensors located at principal pumps, each beam line, and the target chamber. Measurement of vacuum levels from intermediate vacuum to atmospheric pressure is accomplished by capacitance manometers. Operation of these sensors by the remote controls is accomplished by hard wire cables at distances of up to 200 feet.

Throughout the fabrication of the many sections of the beam lines and chamber, vacuum-helium-leak-testing was performed on the smallest sections practical. This procedure permitted the testing of a minimum number of welds or joints at each stage of fabrication/assembly. Leak testing procedures by the contractor, during section fabrication, made use of an oil diffusion pump backed by a ROOTS blower/mechanical pump package in which the helium mass spectrometer leak detector was installed in the diffusion pump foreline. In this arrangement a standard leak of a size typical of the maximum acceptabe leak, was installed in the component to be tested such that the standard leak could be valved into the component, followed by carefully monitoring of the leak detector indication. When the leak detector response reached an indication sufficiently above the background noise level (at least 20 divisions on the appropriate scale) the time was noted: all leak test procedures were then standardized to this measured indication - time interval.

Leak detection operations now in progress (subsequent to formal acceptance of the TVS) are now being performed in a classical vacuum leak testing procedure which, while requiring somewhat longer test times, produce the commonly used test characteristics of Minimum Detectable Leak (MDL), response time, and system sensitivity. Typical leak test system characteristics being realized are 2×10^{-11} atm cc per second per scale division sensitivity and 4×10^{-11} atm cc per second minimum detectable leak. Response times determined experimentally by allowing the standard leak signal to come to equilibrium are compared to the calculated value as described in Ref. 1:

$$RT_{63\%} = \frac{\text{System Volume}}{\text{Leak detector pumping speed}}$$

These procedures are currently being utilized with sufficient efficiency to permit the common practice of repair all detected leaks, thus resulting in a higher integrity vacuum envelope than was required by the contractor (2×20^{-7} atm cc per second) because of the MDL of 4×10^{-11} atm cc per second. Leaks being identified are primarily those in seals and otner component interfaces as a result of assembly contamination.

Operation of the TVS to date is demonstrating achievement of vacuum levels lower than that required by the design criteria i.e., typically a vacuum level of 5×10^{-7} torr is achieved after 12 hours pumping from atmosphere. Operation of the TVS is easily performed from the control console and reliability of the equipment, operated according a preplanned schedule, is excellent. A rigorous operation and maintenance plan is now being implemented which is expected to assure continued high performance, reliably operation.

(1) Handbook of Vacuum Leak Detection, N. G. Wilson and L. C. Beavis, American Vacuum Society Monograph Series, American Institute of Physics, 2nd Printing 1979.

DESIGN OF VACUUM SYSTEM

The specification for the target vacuum system and subsequent contract to PDM Corporation were on a performance basis. The basic components of target vacuum system were the target vacuum chamber, beam tubes two and five between the target chamber, the turning mirror chamber, rough vacuum system, high vacuum system, backfill air system and related control and instrumentation systems. Beam tubes two and five then extend from the turning mirror chamber, mainly under ground, to the laser building. Beam tubes one, three, four and six were also included from the laser building into the target building. Only vacuum roughing and repressurization capabilities were provided to beam tubes one and three and associated turning mirror chambers. Throughout the balance of this presentation we will not address beam tubes one, three, four and six since they are not an integral part of the total system. The system defined above is illustrated on the sketch showing the graphic display panel on Page 2.

A mirror space frame was also included in this project. The mirror space frame is contained inside the target vacuum chamber.

There were several specific requirements that effected the components mentioned above. The most critical requirements were:

- Both end heads of the target vacuum chamber were to be removable.
- The mirror space frame was to be removable from the target vacuum chamber.
- Beam tubes two and five were to have the capability of being isolated from the target chamber.

The target vacuum system was required to reach a pressure of 2×10^{-6} Torr in the target chamber within (16) sixteen hours. The repressurization system was to be accomplished utilizing a backfill air system from a bottle gas supply.

GRAPHIC DISPLAY PANEL

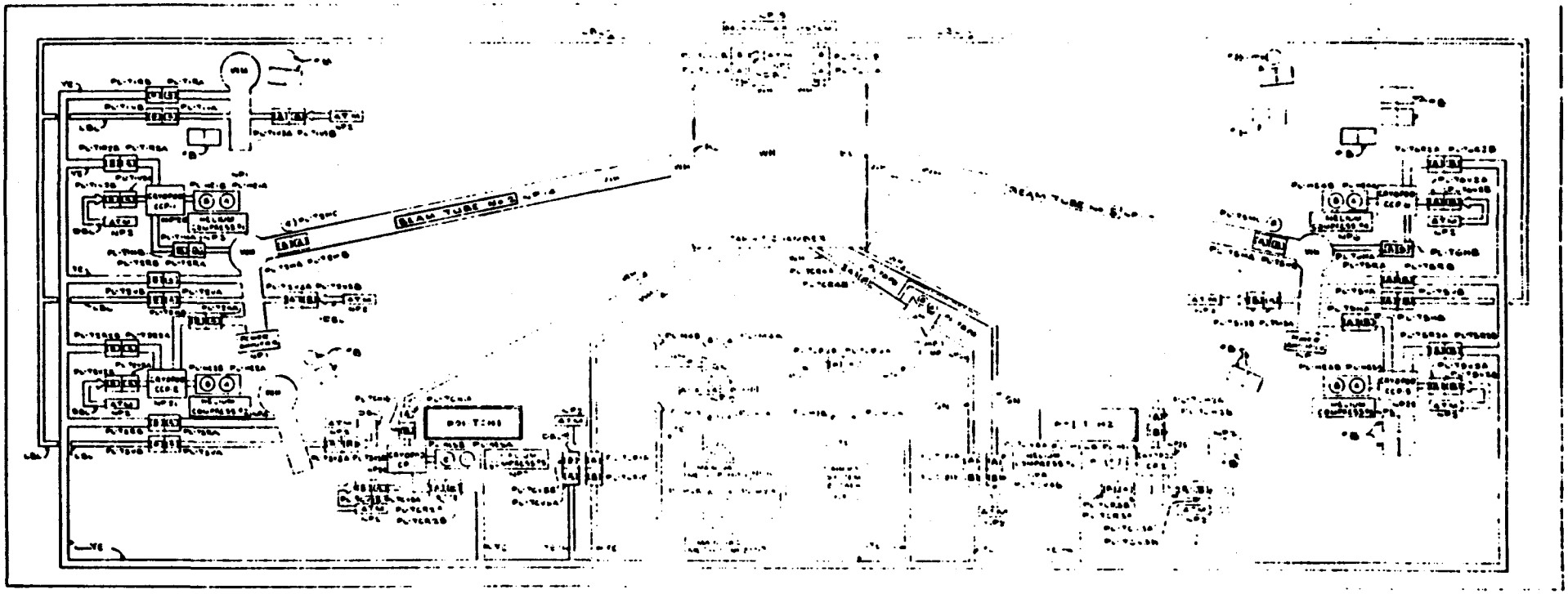

DESIGN OF VACUUM SYSTEM

The vacuum system was to consist of a roughing system, cryopumping system and turbomolecular pumping system.

Prior to the design evaluation of the vacuum system several factors had to be considered and evaluated.

The operating gas loads specified for the vacuum system were small compared to outgassing loads.

The laboratory operating personnel did not want to consider nitrogen as an additional utility therefore cryogenic vacuum pumping at liquid nitrogen temperatures could not be applied.

The target vacuum system was to be operable continuously for a period of 60 days.

The design pumping load for the vacuum system consisted of the system volume, an operating gas load, plus the outgassing of the stainless steel surface of the vacuum chamber and associated beam tubes. The published outgassing curves for stainless vary by a great degree. Based on actual data previously developed by PDM in comparison to the wide spectrum of published data an outgassing curve was developed for this project.

The design criteria for the target vacuum chamber and associated turning mirror chambers and beam tubes was as follows:

- ASME Section VIII Division 1 was to be used as a guide.
- Welding was to be in accordance with ASME Section IX.
- All surfaces exposed to vacuum will have a finish equivalent to #4.
- Seismic loading for all structures in accordance with UBC seismic risk zone 2.

The target chamber shell, turning mirror shell, interior of beam tubes, and all surfaces exposed to vacuum were constructed of 304 stainless compatible with the high vacuum environment. External stiffeners required for the vacuum and structural attachments were fabricated from carbon steel. The stainless steel interior of the chambers and beam tubes exposed to the vacuum were polished to a number 4 finish.

The target vacuum chamber was designed as a 24 foot diameter by 16 foot 6 inch long cylindrical shell with the axis being horizontal. The heads on each end of the vessel were designed to be removable. PDM's patented flexible seal (Patent No. 3158281) was utilized to provide the vacuum seal. This seal has been utilized for openings as large as 35 foot in diameter and is theoretically capable of sealing openings of any dimension. The flexseal concept is shown on Page 5.

The principle of this seal is to separate the sealing function from the structural flanges of the chamber and head. This is accomplished by utilizing structural flanges designed to carry appropriate pressure loads. The much smaller sealing flanges are attached to the structural flanges through thin flex plates designed to allow the sealing flanges to conform to a plane under vacuum load. Another feature of this seal which was specifically adaptable to this project was the elimination of a field machining requirement. Due to limited work space and target building access field machining of large segments was impractical. Therefore the use of the flex seal which is fabricated from shop machined segments eliminated the need for machining a large component.

PDM FLEXIBLE SEAL

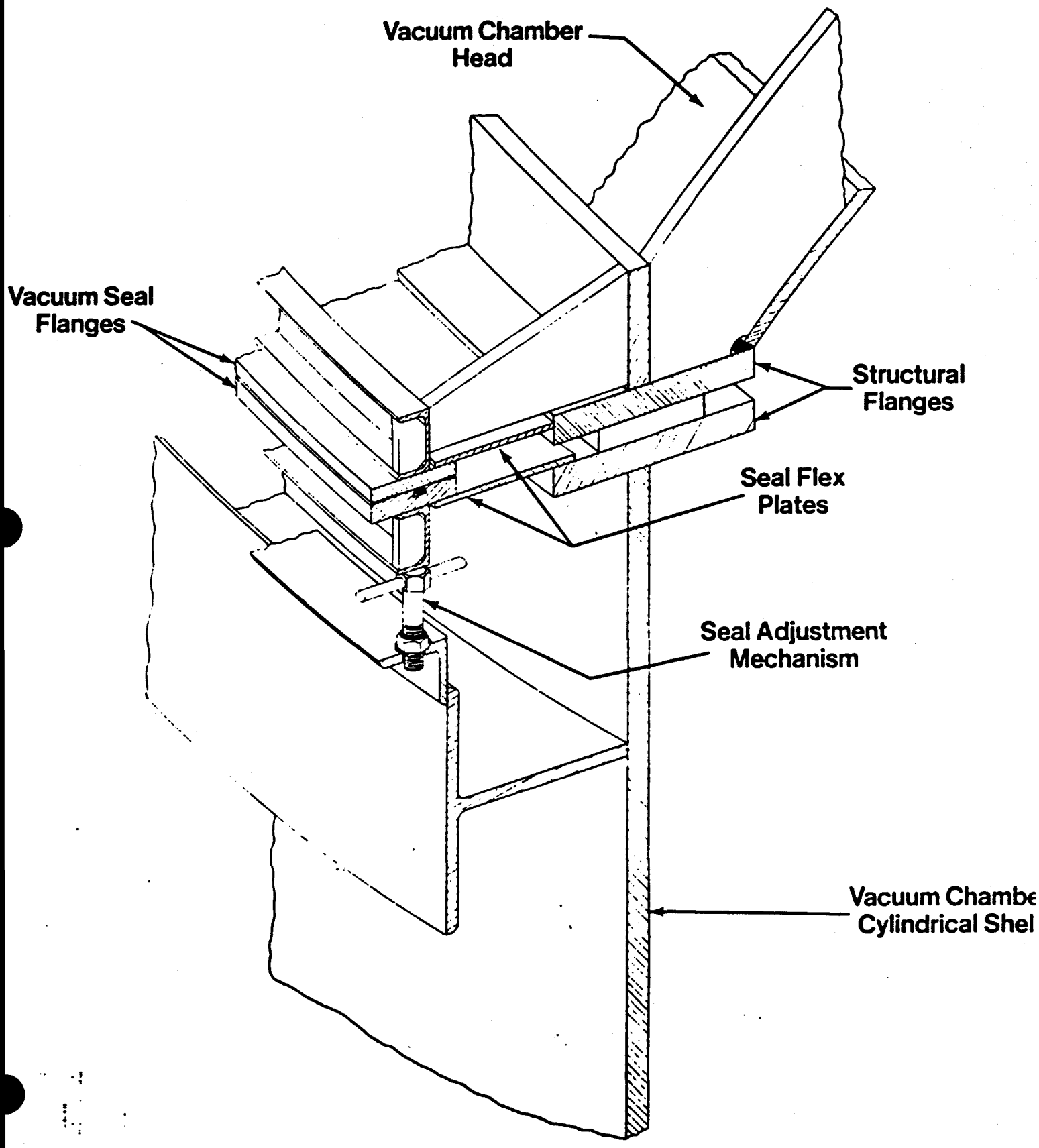

DESIGN OF VACUUM SYSTEM
PAGE 6

The beam tubes between the target vacuum chamber and the turning mirror chambers were 65 inches in diameter. Due to the chamber heads being removable sections of the beam tubes had to be also designed as removable in order to allow space for chamber head removal and removal of the mirror space frame from either side of the chamber.

The turning mirror chambers were designed as a vertical cylinder 10 foot inside diameter by 10 feet high. The top head of the chamber is removable with a conventional machined seal and an "O" Ring. A flat stainless steel weldment was imbedded in the concrete foundation to which the chamber shell was welded providing the chamber bottom.

The beam tubes between the turning mirror chambers and the laser building were designed as 74 inch diameter. These beam tubes between the target building and laser building were installed underground and contained in corrugated metal culverts.

The mirror space frame was dimensionally configured by the Los Alamos Scientific Laboratory. PDM designed the space frame and connections to allow the frame to meet the stringent tolerances and deflections required for the intended use. Stainless steel rectangular and square shapes were utilized for frame members. The mirror space frame was designed to be removed and inserted in the target vacuum chamber by utilizing an roll-air bearing system.

The design of the vacuum system incorporated the PDM developed outgassing rates and the operating gas loads specified by the laboratory. The performance requirement of evacuation of the target vacuum system in 1c hours to a pressure of 2×10^{-6} Torr led to the conclusion that a four hour roughing time be allotted.

DESIGN OF VACUUM SYSTEM

As previously mentioned the total gas load for the high vacuum pumping system consisted of the specified operating gas load plus the outgassing load of the stainless steel structure. The outgassing contributed the major portion of the total gas load. The composition of this outgassing load was assumed to be 99 percent H_2O, 0.9% air and 0.1% H_2.

The two beam vacuum system provided a total volume and surface area of approximately 22,000 cubic feet and 11,000 square feet of area.

The calculations for the two beam vacuum system, assuming a 10 hour outgassing rate, produced a total gas load summary for the high vacuum system of:

H_2O - 1.08×10^{-1} Torr Liters per Second $\frac{.108}{11000 \times 929} \Rightarrow 1.06 \times 10^{-8}$ TL/sec @ 10 hrs ✓

Air - 1.95×10^{-3} Torr Liters per Second

Plus additional gas loads from H_2, CO, CH_4 and CO_2.

The vacuum gauging system consisted of MKS Barratron Sensing Heads Type 222 and Type 220 with type PDR Digital remote indicators for the low and high vacuum ranges. The MKS gauge systems are located in the target vacuum chamber and in each isolatable section of the beam tube. High vacuum gauging was provided with AVEC ion gauges located in the target vacuum chamber and in the cryopods on the chamber and beam tubes.

DESIGN OF VACUUM SYSTEM

The vacuum roughing system proposed for this facility consisted of the following:

- Two Leybold Heraus TR630 Trochoid Mechanical Pumps
- Roots Type Blower RA 7001/2

The pumping speed for this roughing system ranged from 975 cfm for the 560 to 100 Torr range, to 4275 cfm for the 1×10^{-2} to 1×10^{-3} Torr range.

The application of equipment for the high vacuum pumping system was confined by the fact that the laboratory did not want to include the requirement of another utility such as liquid nitrogen. Another parameter that had to be considered was the requirement that the mirror space frame in the vacuum chamber and mirror support frame in the turning mirror chambers could not be exposed to the view angle of cryopumping surfaces. Taking into consideration the above parameters and the system gas loads, external cryopumps with refrigerators and remote gaseous helium compressors were selected for the high vacuum system, as listed below:

Six = CTI 20 inch diameter cryopumps

Each provided with a CTI Model 1020/F remote gaseous helium compressor.

The published pumping speeds for these cryopumps are:

25,000 liters per second H_2O

10,000 Liters per second Air

4,000 Liters per second H_2

The project specification also required that a turbomolecular pumping system be provided to pump the non-condensable gases. The selection was a Welch Model 3117S 2400 liter per second turbopump.

The above described vacuum pumping system was actually chosen to meet the performance requirements of the six beam tube configuration. The installed two beam tube configuration provided volumes and surface areas that were approximately 50 percent of the six beam tube system.

Two of the cryopumps were mounted on the TVS chamber and four of the cryopumps were to be mounted on the beam tubes. The cryopumps in the beam tubes were located between the 65ϕ beam tube isolation valve and the laser building. The project specification required that vacuum pumps be isolated from the vacuum system. The cryopod configuration for the cryopumps included a 24"ϕ vacuum gate valve allowing the cryopump to be isolated from the system. The 24"ϕ isolating gate valves for the two cryopumps on the target vacuum chamber were provided with specially designed modulating valves. This permitted the cryopumps to be brought on line at a higher system pressure by limiting the exposure of the cryopumping surface to the vacuum system.

The vacuum calculations for the TVS system produced the following results:

The roughing calculations for the two beam vacuum system produced a roughing time to base system pressure of 111 minutes.

The combined cryopumping speeds were calculated to be as follows for the two cryopumps on the TVS chamber:

H_2O - 39720 liters per second
Air - 15720 liters per second

For the four cryopods on the beam tubes the combined pumping speed was:

H_2O - 96120 liters per second
Air - 34740 liters per second

Utilizing the above pumping speeds and the 10 hour gas loads previously mentioned, the summation of partial pressures indicated that an ultimate pressure of 9.47×10^{-7} was achievable within the specified 16 hour vacuum pumping cycle.

The interlock logic system was designed to prevent operator error from affecting high vacuum during facility operation. The cryopump isolation valves are interlocked to close on increase in temperature of the cryopumping surface. All isolation vacuum valves are provided with differential pressure interlocks to prevent opening of a valve when a differential pressure exists across the valve. The vacuum control schematic is shown on Page 11.

Fabrication

The vacuum chamber was fabricated in large subassemblies to minimize field construction. Penetrations were machined and welded into subassemblies where practical.

VACUUM CONTROL SCHEMATIC

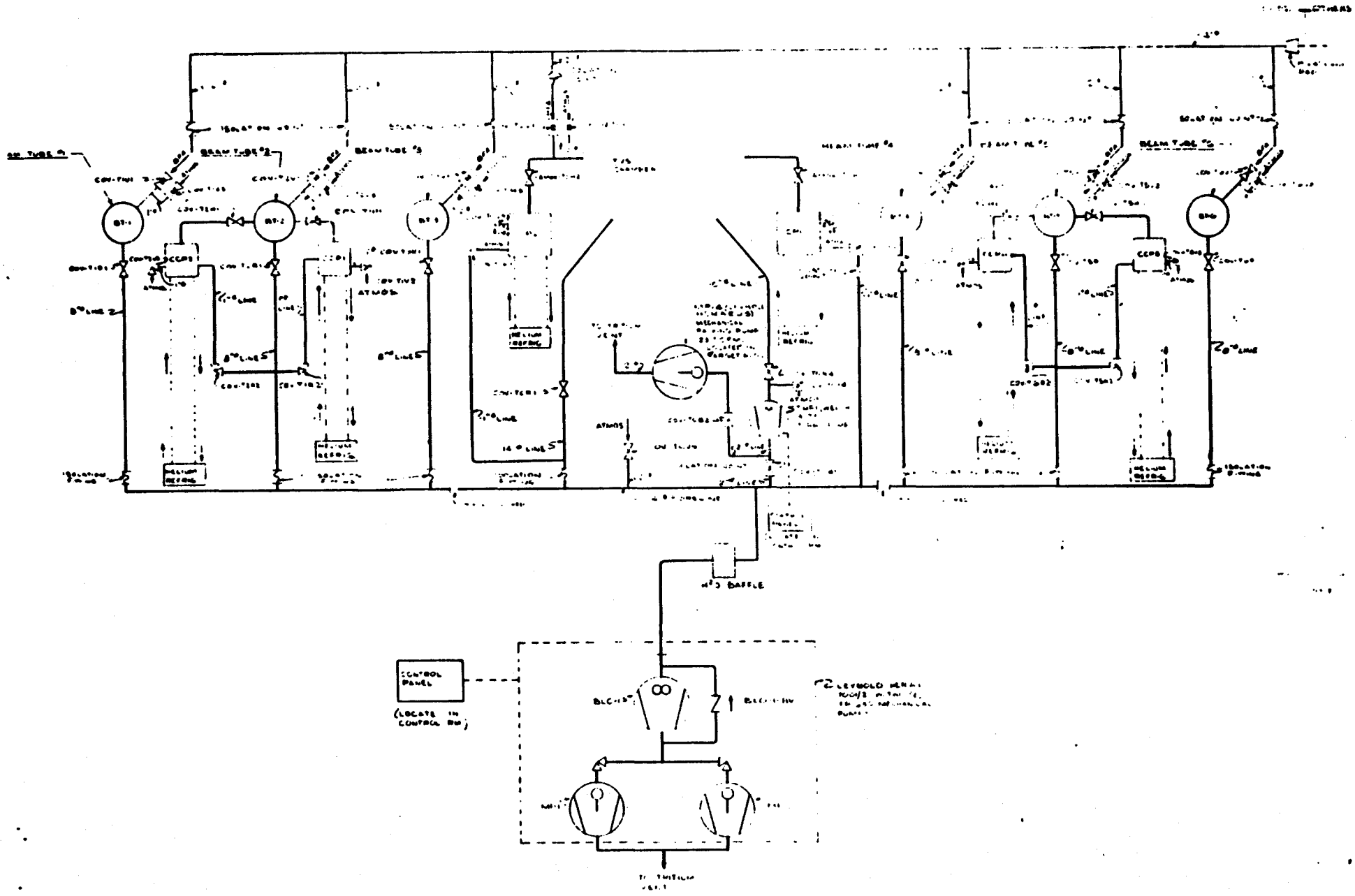

The removable head flex seal was subassembled and the seal bars machined prior to shipment. The polished surfaces that would ultimately be exposed to vacuum were covered with cloth tape for protection during shipment and erection.

Beam tubes were fabricated into large segments that would allow leak testing prior to their installation. The turning mirror chambers were fabricated as a unit in the shop. Penetrations were welded in place and the machining completed prior to shipment.

Construction

The construction sequence for the target vacuum chamber and beam tubes began with the installation of the beam tubes between the laser building and the target chamber building.

The turning mirror chambers were then installed to allow the final leak checking of the underground beam tubes to be completed prior to the closure of the corrugated conduit and earth backfill.

Concurrent with the above work erection was started on the target vacuum chamber beginning with the cylindrical portion of the chamber. The removable head assembly began during chamber erection so that upon completion of the chamber and removable heads the fit-up and installation procedure for the PDM flex vacuum seal could be performed. The vacuum facility erection sequence was then completed with the installation of the beam tubes between the target chamber and turning mirror chambers.

The mechanical installation for target vacuum system included the following:

- Installation of roughing system and associated piping.
- Installation of turbomolecular pump system.
- Installation of the cryopumps and compressors.
- Installation of backfill air system.
- Installation of the tritium vent system.
- Associated utilities such as pneumatic and cooling water systems.

The electrical portion of the project included the installation of motor control centers, power and control wiring for the complete target vacuum system. The control panel designed by PDM was located in the control room adjacent the target vacuum building. The control panel provides remote monitoring of the total system and control of equipment and valves.

System Activation and Acceptance Testing

The leak checking procedure applied to the target vacuum system included the following:

- Preliminary Leak Check
- High Vacuum Leak Test
- System Overall Leak Rate Test

The leak detection method utilized on the vacuum system was the helium mass spectrometer outside-in procedure. The helium mass spectrometer was utilized as the sensing element. A pressurized helium bottle with a spray probe was used as a tracer gas. The tracer gas when sprayed on the external suspected leak area.

When a leak was found the mass spectrometer meter indicated an increase above normal background reading.

The preliminary leak test was performed utilizing the roughing system to obtain a system base pressure of approximately 5 microns. Leaks when found were recorded and repaired after repressurization of the system.

The high vacuum leak test was performed with the vessel at high vacuum. The performance for the test required that the total vacuum system attain a helium gas leak rate of less than 1×10^{-4} scc/sec. with no single leak greater than 1×10^{-7} scc/sec.

With the system at high vacuum and the turbomolecular pump operating, the cryopumps were isolated from the system. The helium mass spectrometer leak checking method previously mentioned was then applied. After determining system sensitivity leak checking proceeded. When leak checking was completed the system was repressurized the leaks repaired and the procedure repeated until the system was in a no detectable leak condition.

The following procedure was then utilized to certify the vacuum system overall leak rate. The chamber and beam tube penetrations were bagged. All chamber and beam tube vacuum weld seams were bagged. With the system at high vacuum and the helium mass spectrometer system sensitivity at 1×10^{-7} scc/sec./division each bagged seam or penetration was incrementally flooded with helium and held for 3 minutes. The mass spectrometer meter readings were individually recorded. Upon completion of bag test a summation was performed to determine the overall leak rate was within specification limits.

DESIGN OF VACUUM SYSTEM

The acceptance testing of the TVS system included demonstration of system operation following the vacuum system logic for the various modes of operation. The target vacuum chamber and beam tubes between the beam tube isolation valve (including turning mirror chamber) and the gas laser can be rough vacuum pumped or high vacuum pumped either simultaneously or individually. The cryopumps can be isolated and regenerated with the system at high vacuum by closing the isolation valve on the cryoped. The target vacuum chamber or the beam tube sections beyond the beam tube isolation valve can be repressurized with the backfill air system either simultaneously or individually.

During the demonstration of the TVS facility the operating parameters, and associated pressures for the initiation of the various subsystems were verified. The mechanical roughing system is to be in operation between atmospheric pressure of 590 Torr and 1.5×10^{-2} (15 microns) Torr at which time cryopumping is initiated with the two target vacuum chamber cryopumps. The roots blower is brought on line during the roughing cycle at 100 Torr. The four cryopumps in the beam tubes are brought on line when the system pressure reached 1×10^{-3} Torr (1 micron). The turbomolecular pumping is initiated at 2×10^{-4} Torr system pressure.

The above parameters were suggested to provide smooth trouble free operation and obviously have been somewhat conservatively established. During the testing of the facility for instance the TVS chamber cryopumps were initiated with the system pressure as high as 50 microns by only partially opening the cryopump 24"ø isolation valves.

The curve shown on the following sketch on Page 16 is the acceptance test pump down curve for TVS system performance. This pump down however was performed prior to system leak checking which demonstrates the quality of high vacuum practice applied in system design and construction.

PUMP DOWN CURVE
HEGLF

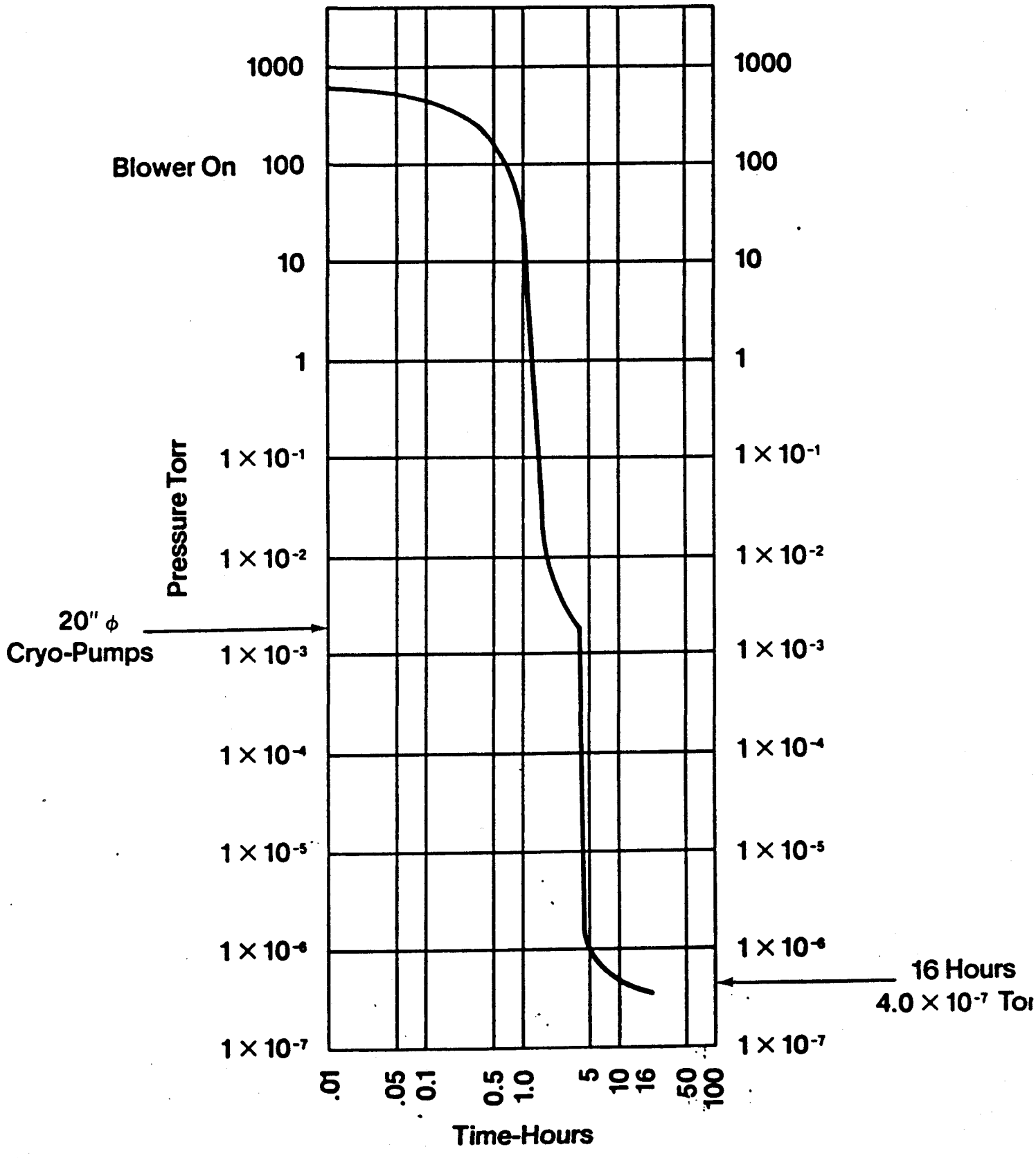

The ultimate pressure established by this pump down was 4×10^{-7} Torr in 16 hours. The performance pressure required by the project specification was 2×10^{-6} Torr in 16 hours.

This pump down curve does not represent the true capability of the TVS system. The roughing cycle for this curve was extended to attempt to obtain a low micron base pressure in the system for initiation of cryopumps. The cryopumps during this pump down were brought on line at 1×10^{-3} Torr when they could have been initiated at 15 microns or higher. When reviewing the pump down curve and associated times vs. pressure and comparing this data to the vacuum calculations it was apparent that the vacuum calculations were conservative. However, one must consider the effect of excellent performance of the vacuum pumping equipment utilized and fact that this equipment exceeded its published capabilities.

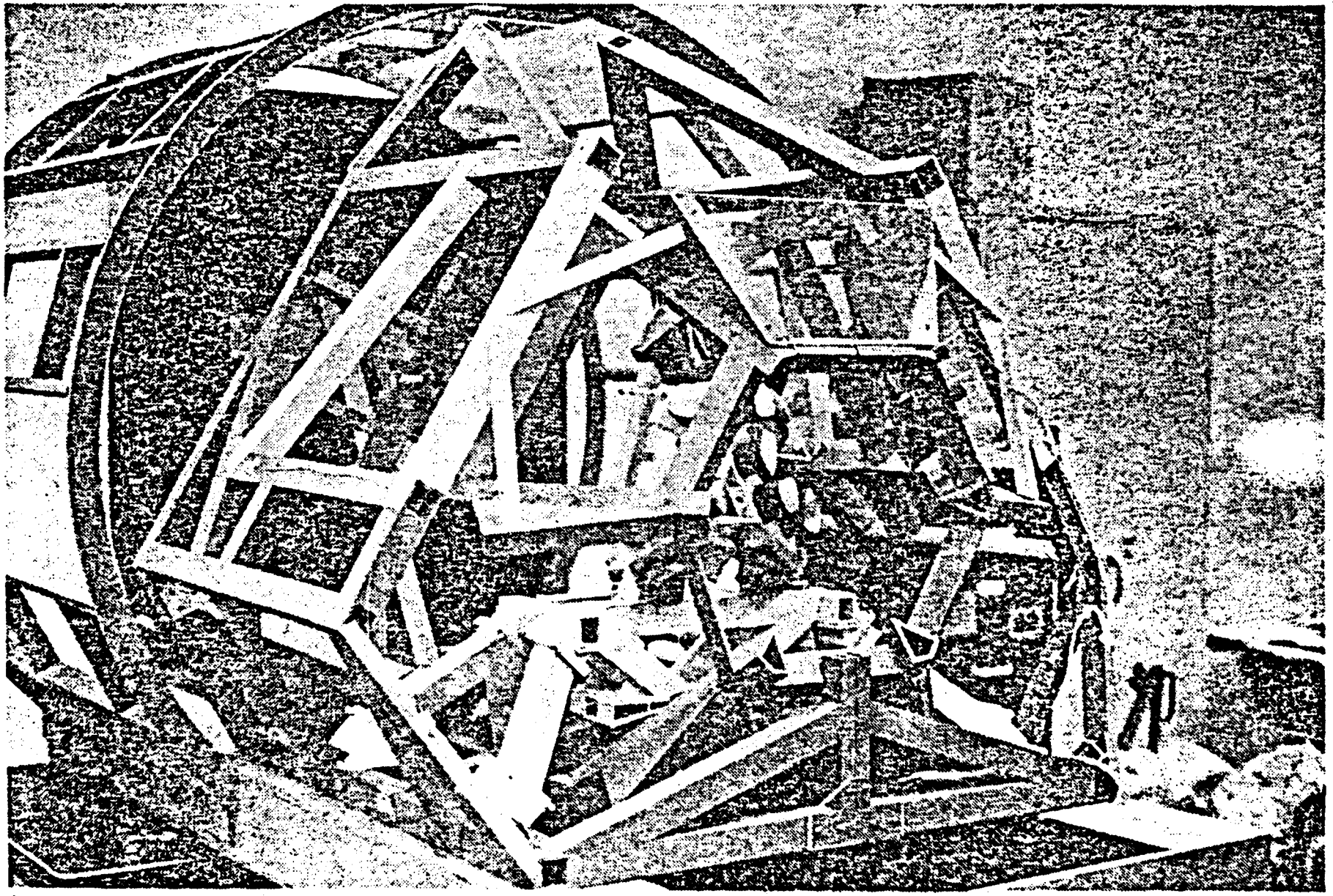

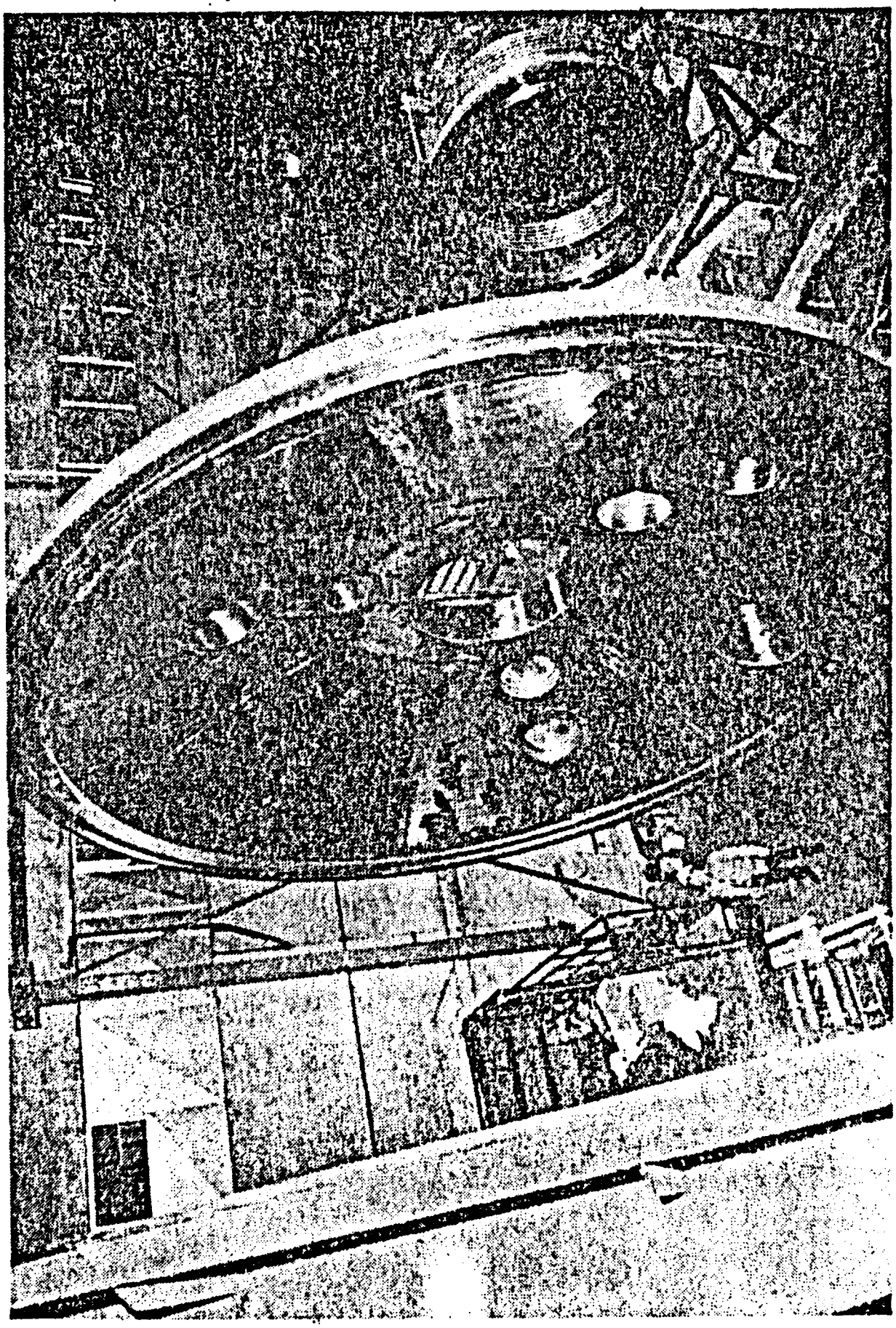

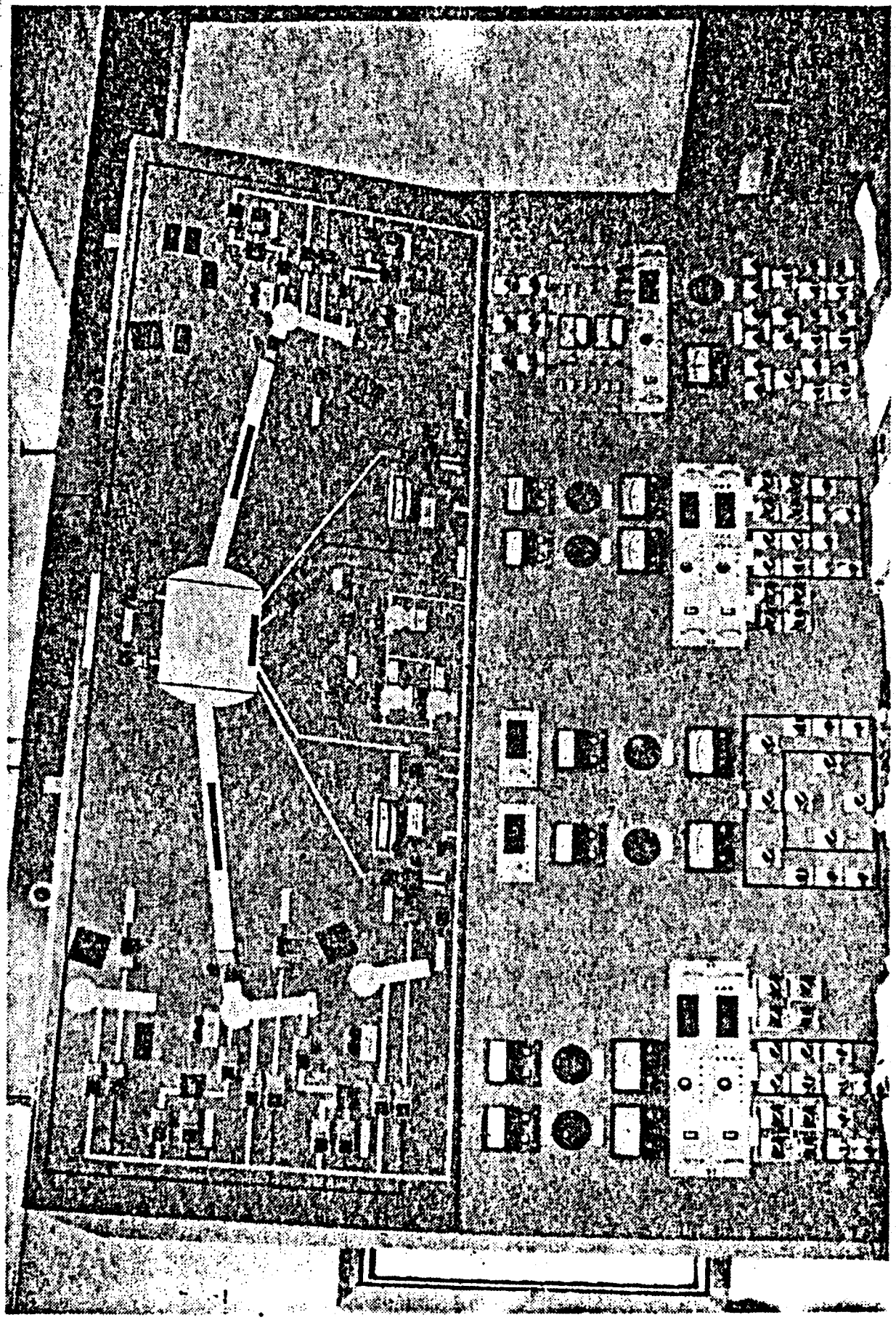

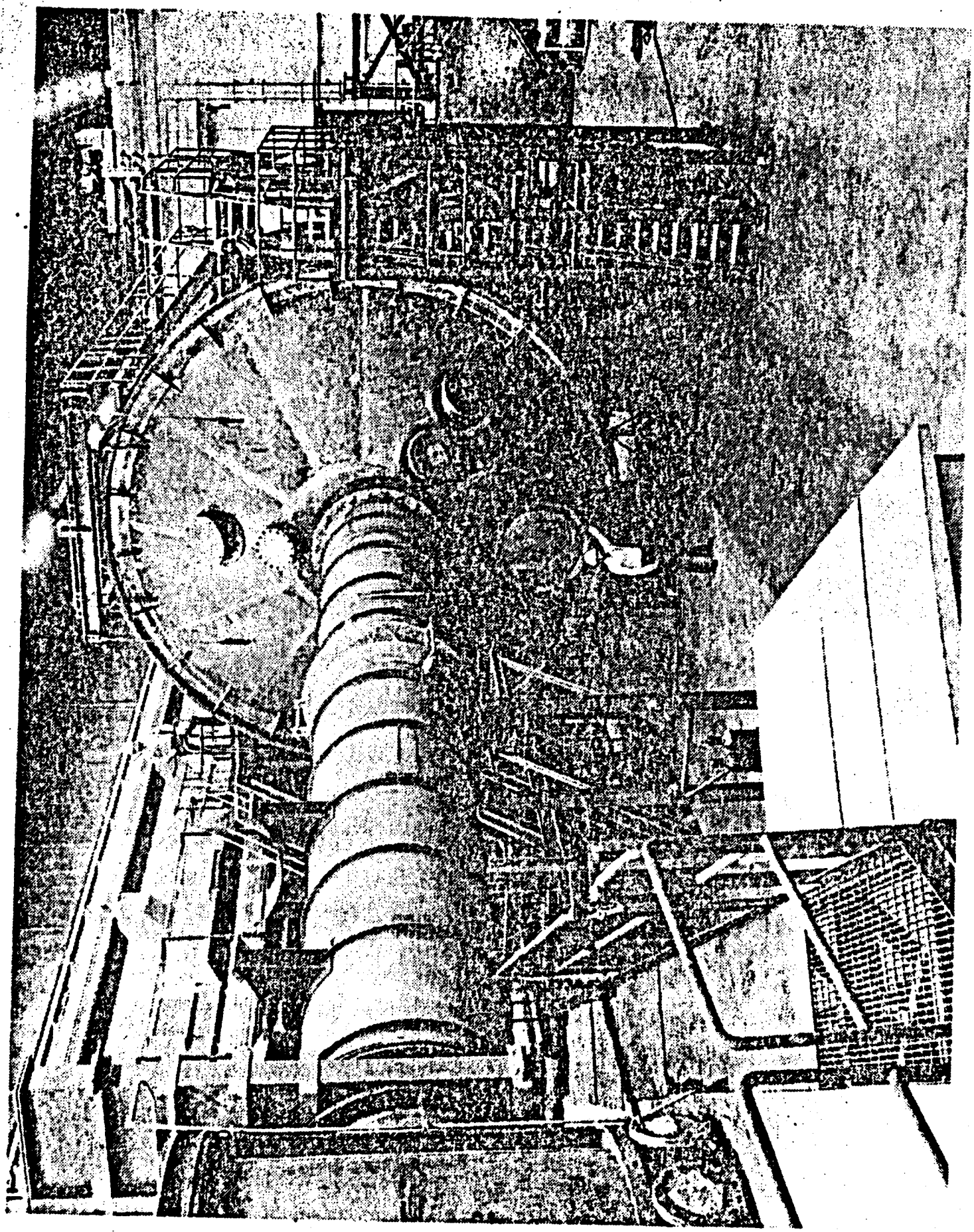

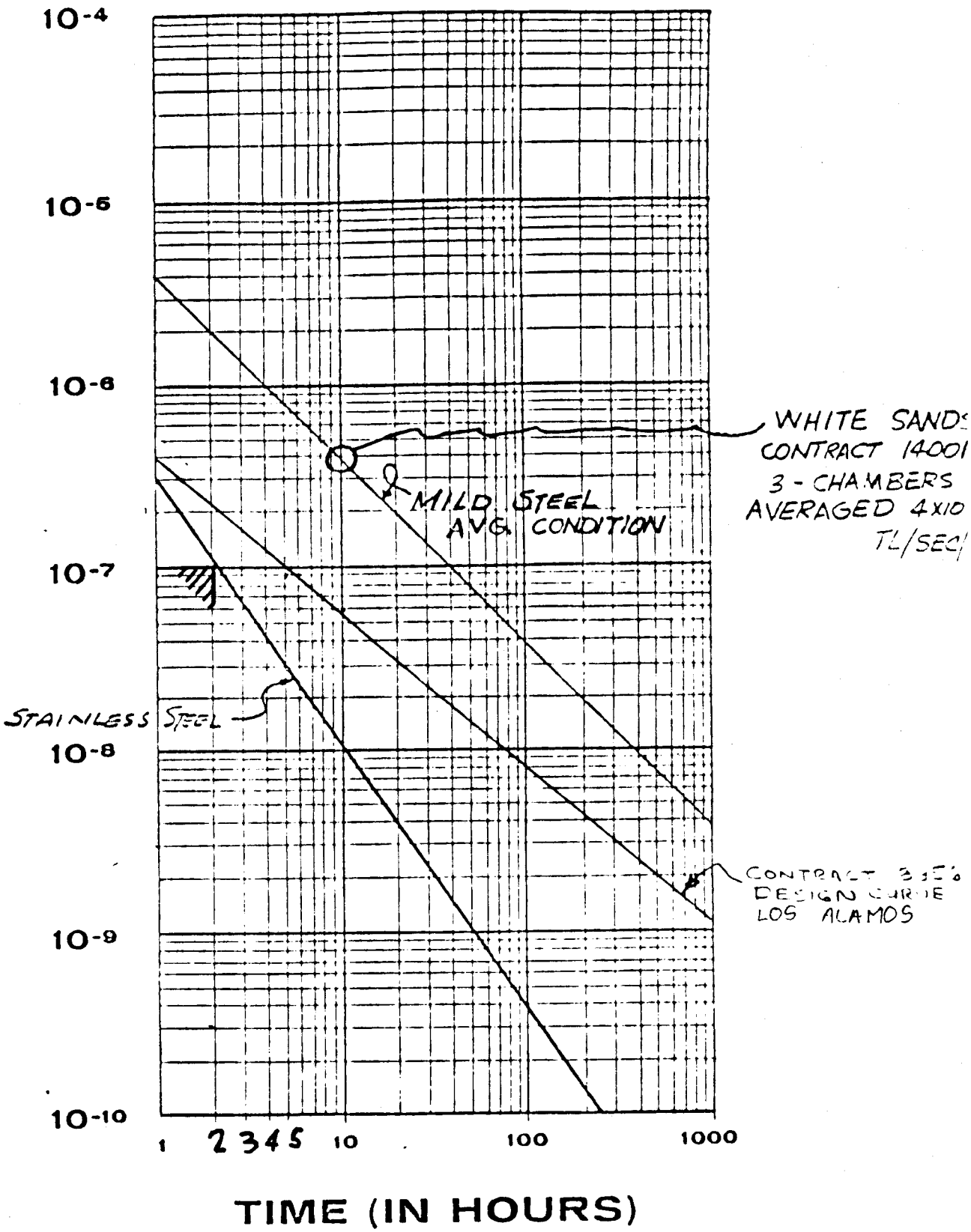

OUTGASSING RATE FOR NON-BAKEABLE SYSTEMS

TABLE 1

SUMMARY OF TVS DESIGN REQUIREMENTS

• System Volume	6 beam configuration	65,200 Ft^3 (1.8×10^6 liters)
	2 beam configuration	21,200 Ft^3 (6×10^5 liters)
• System Surface Area	6 beam configuration	25,700 Ft^2 (2.4×10^7 cm^2)
	2 beam configuration	10,700 Ft^2 (1×10^7 cm^2)
• Maximum Operating Pressure 16 hours After pump down from atmosphere.	6 beam configuration	2×10^{-6} torr (in target chamber)
	2 beam configuration	1×10^{-6} torr (in target chamber)

- All vacuum exposed surfaces - mechanically polished stainless steel
- Maximum discrete leak rate for all vacuum components - 8×10^{-7} atm cc per second (helium)
- No consumable cryogens
- Remote monitoring and operating console manually operated with rigorous safety an operating system interlocks.
- All operating equipment to be of lowest practical vibration level
- No target chamber pump permitted to cause thermal instability.

	Q - 10 hrs	
Copper - OFHC - CLEAN	6.3×10^{-10}	Torr-l/sec-cm²
Copper - UHAC-R1	2.4×10^{-10}	"
Copper - ELECTROPOLISHED	4.8×10^{-10}	"
SS - DEGREASED	2.7×10^{-10}	"
SS - ELECTROPOLISHED	8.0×10^{-11}	"
CS - CLEANED (GLASS BEADS)	3×10^{-7}	"
CS - NICKEL PLATED	1×10^{-9}	"
AL - CLEANED	1.1×10^{-8}	"
EPOXY - LIBA	7×10^{-7}	"
EPON 828	4×10^{-6}	"
EPON DEGASSED	5×10^{-9}	"
LUCITE	1×10^{-6}	"
TEFLON - OUTGASSED	2×10^{-7}	"
KEL-F	1×10^{-8}	"
NYLON	4×10^{-6}	"
MYLAR	7×10^{-8}	"
POLY CARBONATE	2×10^{-7}	"
POLY PROPYLENE	2×10^{-9}	"
VITON O-RING	2×10^{-7}	"
BUNA O-RING	3×10^{-7}	"
SILICON O-RING	2.2×10^{-7}	"
CONNECTOR - DEUTSCH - HERM	1.1×10^{-6}	"
CANNON - HERM	1×10^{-4}	"
GULTON - HERM	5.2×10^{-6}	"
KAPTON WIRE	1.3×10^{-7}	"
KAPTON WIRE COATED	3.4×10^{-9}	"
PHENOLIC MICROSWITCH	1.1×10^{-5}	"
STEPPER MOTOR	1.6×10^{-3}	"
POLY URETHANE PAINT	5.1×10^{-9}	"

MELINEX POLYESTHERIMIDE

BALZERS
HIGH VACUUM SYSTEMS AND COMPONENTS
8 SAGAMORE PARK ROAD
HUDSON, NEW HAMPSHIRE 03051
(603) 889-6888 TWX 7102287431

2 November 1984

KENTRON, INC.
4800 Oak Grove Drive
Pasadena, California 91109

Attn: Mr. Dave Killian M/S 511-204U

Dear Mr. Killian:

Thank you for your interest in Balzers' cryogenic pumps and systems. Enclosed are calculations for your system using two different pumps: a 20" pump, for comparison, and a 32" pump. We recommend the 32" pump as the most economical option. The pumping speeds for the RCP 501Z (20" pump) are given on the attached data sheet, UC 800 005 NE. The RCP 801 is still in development and will be marketed early next year. It uses a UCC 104 compressor, per data sheet UC 800 006 NE, and a larger cold head, not shown. The pumping speeds are very similar to our RKP 800, per data sheet BP 800 135 PE, except that the RCP 801 does not use LN_2.

We have also enclosed information on our B Series roughing pumps. We suggest using the DUO 016B for regeneration of the cryopump.

If we can be of any further service, please feel free to call either our sales engineer, Mr. Dennis Buckley, at 714-547-7767, or me at 603-889-6888.

Sincerely,

BALZERS

Glenn Connell

Glenn Connell
Product Manager
Cryogenic Products

GC/jmj

cc: D. Buckley

Enclosures:
Calculations
UC 800 004 NE
UC 800 005 NE
UC 800 006 NE
BP 800 135 PE
PK 800 063 PE

JPL/KENTRON: CALCULATIONS

MAIN TUBES:

$\phi = 1.22$ m $r = .609$ m.

$L = 10^4$ m. (10 km.)

AREA: $A = 2\pi rL + 2\pi r^2$ MAIN TUBES.

$= 38302\ m^2 + 2.34 m^2$

$= 38304\ m^2$

$\boxed{A_T = 3.83 \times 10^8\ cm^2}$ 3.8304714×10^8.

VOLUME: $V = \pi r^2 L$

$= 11675\ m^3. =$

$= 1.1675 \times 10^4\ m^3$

$\boxed{V_T = 1.1675 \times 10^7\ \ell.}$

END STATION:

PROPOSAL 1: 3 END STATIONS

PROPOSAL 2: 15 END STATIONS.

$\phi = 3.66$ m.

$L = 3.66$ m.

AREA: $A_S = 2\pi rL + 2\pi r^2$

$= 42.1\ m^2 + 21.0\ m^2$

$= 63.1\ m^2$

$= 6.31 \times 10^5\ cm^2$

A_S = PROPOSAL 1: $1.083 \times 10^6\ cm^2$. PROPOSAL 2: $9.465 \times 10^6\ cm^2$.

VOLUME: $V = \pi r^2 L$

$= 3.85 \times 10^1\ m^3$

$V = 3.85 \times 10^4\ \ell$

V_S = PROPOSAL 1: $1.155 \times 10^5\ \ell$ PROPOSAL 2: $5.775 \times 10^5\ \ell$.

VACUUM LEVEL 1: 1×10^{-6} T ~ 1×10^{-6} mbar

VACUUM LEVEL 2: 1×10^{-8} T ~ 1×10^{-9} mbar.

CONSIDER 4 CASES:

1. PROPOSAL 1, VACUUM 1
2. PROPOSAL 1, VACUUM 2
3. PROPOSAL 2, VACUUM 1
4. PROPOSAL 2, VACUUM 2.

PROPOSAL 1:

AREA: 3.84×10^8 cm^2.
VOLUME: 1.18×10^7 ℓ. ≅ 1.2×10^4 m^3
MATERIAL: S.S.

PROPOSAL 2:

AREA: 3.93×10^8 cm^2
VOLUME: 1.23×10^7 ℓ.
MATERIAL: S.S.

LET t_f = 1 WK = 604,800 S. t_o = 10 HRS. = 36,000 S.

$$S_{eff} = \frac{A \cdot \Phi \cdot t_o}{(P - P_o - D)\, t_f}$$

$\Phi = 2.7 \times 10^{-8}$ mbar-ℓ/s-cm^2

$P_o = 5 \times 10^{-9}$ mbar.

D = GAS IN.

$P \cong 1 \times 10^{-6}$ mbar

$P - P_0 = .995 \times 10^{-6}$ mbar

$\sim 1 \times 10^{-6}$ mbar

So, $S_{eff} = \dfrac{3.84 \times 10^{8}\ cm^2 \cdot 2.7 \times 10^{-8}\ mbar\,\ell/s\text{-}cm^2 \cdot 3.6 \times 10^{4}\ s}{1 \times 10^{-6}\ mbar \cdot 6.048 \times 10^{5}\ s.}$

$= 617000\ \ell/s.$

$S_{PUMP} \times \text{Loss} \sim 14{,}500\ \ell/s. \sim 25000 \times .6$ { AIR SPEED x COND. LOSS GATE VALVE, ET

OF PUMPS = 42.56

= 44 PUMPS. RCP 800

→ X SAFETY FACTOR 1.5

66 PUMPS RCP 800 TO REACH 1×10^{-6} mbar in 1 WK.

*

WHAT IS DESORPTION RATE OVER TIME

$\dot{R} = \varphi_i \cdot A$

$\dot{R}$ = DESORPTION mbar - ℓ/s.

R = GAS LOAD OVER TIME = $\int \dot{R}\, dt$.

R = CONSTANT.

$\therefore$ R = 893.5 BAR-LITER (AIR) / DAY.

CAPACITY OF PUMP RCP 800 = 4,000 B-L.

TOTAL CAPACITY = 264,000 B-L

$$\text{REGENERATION TIME} = \frac{\text{TOTAL CAPACITY}}{R}$$

= 295 DAYS.

NOW LET t = 30 DAYS
= 2.592×10^6 s.

USING SAME FIGURES AS ABOVE, FOR RCP 800 VERSION PUMP →

$$S_{eff} = \frac{(3.84 \times 10^8 \text{ cm}^2)(2.7 \times 10^{-8} \text{ mbar } \ell/\text{s-cm}^2)(3.6 \times 10^4 \text{ s})}{(1 \times 10^{-6} \text{ mbar})(2.592 \times 10^6 \text{ s})}$$

S_{eff} = 144,000 ℓ/s. TO REACH 1×10^{-6} mbar (7.6×10^{-7} T) IN 30 DAYS.

~ 10 PUMPS (@ 14,500 ℓ/s EFFECTIVE)

x SAFETY FACTOR 1.5

= 15 → 16 PUMPS. (RCP 800 SIZE)

REGENERATION TIME ~ 74 DAYS/PUMP.

NOW TO REACH 1×10^{-8} TORR (1.33×10^{-8} mbar) IN 30 DAYS,

$$S_{eff_{1\times10^{-8}}} = S_{eff_{1\times10^{-6}}} \left(\frac{1\times10^{-6}}{1\times10^{-8}} \right)$$

$$\equiv 100\, S_{eff_{1\times10^{-6}}}$$

$\sim$ 1,500 PUMPS. (RCP 800 VERSION)

SUMMARY: RCP 800 ~ 32" PUMP / RCP 501Z ~ 20" PUMP.

VACUUM	TIME	PUMP	EFFECTIVE AIR SPEED	SAFETY FACTOR	# of PUMPS	REGEN TIME
1×10^{-6} TORR	1 WK	RCP 800	~14,500 ℓ/s	~1.5	66	295 d.
	1 MO.	" "	" "	~1.5	16	74 d.
	1 WK.	RCP 501Z	~6,000 ℓ/s	~1.5	160	
	1 MO.	" "	" "	~1.5	40	
1×10^{-8} TORR	1 WK.	RCP 800	~14,500 ℓ/s	~1.5	~6,000	
	1 MO.	" "	" "	~1.5	~1,500	
	1 WK.	RCP 501Z	~6,000 ℓ/s	~1.5	~14,500	
	1 MO.	" "	" "	~1.5	~3,625	

BALZERS
HIGH VACUUM SYSTEMS AND COMPONENTS
46249 WARM SPRINGS BOULEVARD
FREMONT, CALIFORNIA 94539
(415) 651-3303

September 7, 1984

Mr. David Killian, MS/511-204U
KENTRON, Inc.
A Subsidiary of the Jet Propulsion Laboratory
4800 Oak Grove Drive
Pasadena, CA 91109

Dear Mr. Killian:

Thank you for your recent inquiry regarding Balzers' line of Roots Vacuum Pumps. We are pleased to respond with quotation Q-14894, which present the WOD 410B Roots Pump mounted on a frame.

If you would like to discuss the enclosed information, please contact Mr. Dennis Buckley, Balzers' sales engineer for your area, or myself.

Thank you again for your interest in Balzers' Roots Vacuum Pumps.

Sincerely,

BALZERS

Susan J. Lancia
Sales Secretary
Western Region

cc: D. Buckley
Enclosures

BALZERS
HIGH VACUUM SYSTEMS AND COMPONENTS
46249 WARM SPRINGS BOULEVARD
FREMONT, CALIFORNIA 94539
(415) 651-3303

Quotation No. Q-14894

PLEASE REFER TO THIS NUMBER WHEN ORDERING.

TO:

Mr. David Killian, MS/511-204U
KENTRON
A subsidiary of Jet Propulsion Labs
4800 Oak Grove Drive
Pasadena, CA 91109

DATE: September 7, 1984

TERMS: ½ % 10, Net 30

REF.: Verbal

ITEM	QTY.	CATALOG #	DESCRIPTION	UNIT PRICE	TOTAL PRICE
1.0	15	PPS32001	WOD 410B Roots pump unit with WKP 500 DUO 060A, mounted on a common frame with vacuum interconnections and safety valve, and ON/OFF switches.	11,546.00	173,190.00

DELIVERY AFTER ORDER ACKNOWLEDGEMENT: 8 to 10 Weeks

F.O.B. SHIPPING POINT: Hudson, New Hampshire

This quotation includes all of the terms and conditions on both the face and attached documents hereof. The attached detail terms and conditions of sale (Balzers document number UA 800003 PE/8107) are incorporated by reference as fully as if set forth on the face of this form. This offer may be accepted only on the exact terms set forth herein, and no other agreement in any way modifying any of said terms and conditions shall be accepted or be binding on Balzers unless accepted by it in writing.

Direct inquiries to:
Mr. Dennis Buckley
Sales Engineer
1420C South Village Way
Santa Ana, CA 92705
714-547-7767

TERMS AND CONDITIONS OF SALE

Products furnished and services rendered by Balzers are sold only on the terms and conditions stated herein. Notwithstanding any terms or conditions on Buyer's order, Balzers' performance of any contract is expressly made conditional on Buyer's agreement to Balzers' Terms and Conditions of Sale unless otherwise specifically agreed to in writing by Balzers. In the absence of such agreement, commencement of performance and/or delivery shall be for Buyer's convenience only and not be deemed or construed to be acceptance of Buyer's terms and conditions. If a contract is not earlier formed by mutual agreement in writing, acceptance of any Product or service shall be deemed acceptance of the terms and conditions stated herein.

Orders

All orders are subject to acceptance by Balzers, by receipt by the Buyer of Balzers' written Order Acknowledgement.

Quotations and Prices

All quotations are subject to the terms and conditions stated herein as well as any additional terms and conditions that may appear on the face of Balzers' quotation or proposal form. In the case of a conflict between the terms and conditions stated herein and those appearing on the face of Balzers' quotation or proposal form, the terms and conditions on the face of Balzers' quotation or proposal form shall control.

Balzers' prices and quotations are subject to the following:

(a) All published prices are subject to change without notice.

(b) Unless otherwise specified in writing, all quotations are firm for, and expire thirty (30) days after the date thereof or until earlier revoked or revised and constitute offers; provided that, budgetary quotations and estimates, indicated as such on the quotation, are for preliminary information only and shall neither constitute offers, nor impose any responsibility or liability upon Balzers.

(c) All shipments will be billed at prices in effect on the date of acceptance of Buyer's order.

(d) Unless otherwise stated in writing by Balzers, all prices quoted shall be exclusive of transportation, insurance, taxes (including without limitation, any use tax, sales tax or similar tax), license fees, customs fees, duties, and other charges related thereto, and Buyer shall report and pay any and all such shipping charges, premiums, taxes, fees, and other charges related thereto, and shall hold Balzers harmless therefrom.

(e) Stenographical, typographical and/or clerical errors are subject to correction.

(f) Prices quoted are for Products only and do not include technical data, proprietary rights of any kind, patent rights, qualification, environmental or other than Balzers' standard tests and other than normal domestic commercial packaging unless expressly agreed to in writing by Balzers.

(g) Published weights and dimensions are approximate only. Certified dimension drawings can be obtained upon request. Manuals, programs, listings, drawings or other documentation required must be referenced specifically, and will be the latest applicable version.

(h) The start date of the delivery term is the date of Balzers' order acceptance as indicated in the written order acknowledgement.

(i) Quoted delivery dates are those in effect on the date of quotation and are subject to change without notice.

Terms of Payment

Unless credit is granted, payment is due upon delivery. All payments for Products released and shipped on approved credit accounts shall be due in full thirty (30) days from date of invoice therefor. Absent written agreement to the contrary, payment shall be in U.S. dollars. A ½% discount will be given for payments made within ten (10) days from date of invoice. Past due balances shall be subject to a service charge of 2% per month (24% per annum), but not more than the amounts allowed by law. Partial shipments will be billed as made and payments therefor are subject to the above terms. Payment shall not be withheld for delay in delivery of required documentation unless a separate price is stated therefor, and then only to the extent of the price stated for such undelivered documentation. Balzers may cancel or delay delivery of Products in the event Buyer fails to make prompt payment therefor. Balzers reserves a purchase money security interest in all of the materials referenced herein in the amount of the purchase price. These interests will be satisfied by payment in full. A copy of this document together with any form of written acceptance may be filed on Balzers behalf with appropriate state authorities at any time as a financing statement in order to protect Balzers' security interest.

Transportation and Risk of Loss

Unless otherwise agreed to in writing by Balzers, all transportation shall be at the expense of Buyer. Balzers reserves the right to ship Products freight collect and to select the means of transportation and routing. Unless otherwise advised, Balzers may, but is not obligated to, insure to full value of the Products or declare full value thereof to the transportation company at the time of delivery and all such freight and insurance costs shall be for Buyer's account. Risk of loss or damage shall pass to Buyer upon delivery of the Products to the transportation company at the FOB point, whether or not installation is provided by or under supervision of Balzers. Confiscation or destruction of, or damage to Products shall not release, reduce or in any way affect the liability of Buyer therefor. Notwithstanding any defect or nonconformity, or any other matter, such risk of loss shall remain in Buyer until the Products are returned at Buyer's expense to such place as Balzers may designate in writing. Buyer, at its expense, shall fully insure Products against all loss or damage until Balzers has been paid in full therefor, or the Products have been returned, for whatever reason, to Balzers. All Products must be inspected upon receipt and claims should be filed with the transportation company when there is evidence of damage, either concealed or external. As used in the clauses appearing herein or attached hereto, "delivery" shall occur when Products are delivered at the FOB point, which shall be the point of manufacture or such other place as Balzers shall specify in writing, notwithstanding installation by or under supervision of Balzers.

Performance

Balzers shall not be liable in any way because of any delay in performance hereunder due to unforeseen circumstances or to causes beyond its control, including, without limitation, strike, lockout, riot, war, fire, act of God, accident, failure or breakdown of components necessary to order completion, subcontractor, supplier or Buyer caused delays, inability to obtain labor, materials or manufacturing facilities, or compliance with any law, regulation or order, whether valid or invalid, of any cognizant governmental body or any instrumentality thereof whether now existing or hereafter created. Performance shall be deemed suspended during and extended for such time as any such circumstances or causes delay its execution. Whenever such circumstances or causes have been remedied, Balzers will make and Buyer shall accept performance hereunder. In addition, Balzers' inventories and current production must be allocated so as to comply with applicable Government regulations. In the absence of such regulations, Balzers reserves the right, in its sole discretion, to allocate inventories and current production and substitute suitable materials when, in its opinion, such allocation or substitution is necessary due to any such circumstances or causes. No penalty clause of any kind shall be effective. As used herein, "performance" shall include, without limitation, fabrication, shipment, delivery, assembly, installation, testing and warranty repair or replacement, as applicable.

Acceptance

Each Product furnished by Balzers shall be deemed accepted by Buyer unless notice of defect or nonconformity is received within thirty (30) days of delivery thereof; provided that Products for which Balzers agreed in writing to provide installation by its personnel, shall be deemed accepted by Buyer upon completion

(over)

by Balzers of its applicable acceptance tests or execution of Balzers' acceptance form by Buyer. Notwithstanding the foregoing, use of any such Product by Buyer, its agents, employees, or licensees, for any purpose after delivery thereof, shall constitute acceptance of the Product by Buyer.

Initial qualification of the Products to meet the applicable performance data is performed at Balzers factory prior to shipment. The Buyer is entitled to witness this factory testing which is based on functional performance of the individual subassemblies and components and the integrated equipment. Measured parameters are defined by the performance specification for each subassembly or component. These procedures will also be performed at the Buyer's installation site for final acceptance, if agreed upon in writing by Balzers.

Terminations

Any order for a catalog listed Product accepted by Balzers and terminated by Buyer prior to delivery, shall be subject to a termination charge of not less than fifteen percent (15%) of the order value to cover costs of processing and order handling; termination thereof within thirty (30) days after delivery shall be subject to a termination charge of not less than twenty-five percent (25%) of the order value; thereafter no such order may be terminated except by mutual agreement in writing. Before any Products are returned to Balzers due to such termination, written authorization from Balzers or its authorized representative for the return and instructions as to how and where these products should be returned must be obtained. Any Product returned to Balzers shall be sent prepaid via the means of transportation indicated as acceptable by Balzers. No order for non-catalog or non-standard products may be terminated by Buyer except by mutual agreement in writing. Terminations by mutual agreement are subject to the following conditions: (1) Buyer will pay, at applicable contract prices, for all Products which are completely manufactured and allocable to Buyer at the time of Balzers' receipt of notice of termination; (2) Buyer will pay all costs, direct and indirect, which have been incurred by Balzers with regard to Products which have not been completely manufactured at the time of Balzers' receipt of notice of termination plus a pro rata portion of normal profit on the contract; (3) Buyer will pay a termination charge on all other Products affected by the termination. Balzers' normal accounting practices shall be used to determine costs and other charges. To reduce termination charges, Balzers will divert completed parts, material or work-in-process from terminated contracts to other customers whenever, in Balzers sole discretion, it is practicable to do so.

Confidential and Proprietary Information

The Buyer agrees to not disclose to any person outside of its employ any confidential and/or proprietary information of Balzers relating in any way to the Products which may be disclosed to it. Upon termination of any order or relations between the parties, Buyer shall return to Balzers, upon Balzers request, all drawings, descriptions, or other material received from Balzers and all other materials containing confidential materials relating to the Products. Buyer shall not allow persons outside of its employ to inspect such portions or components of the Products identified by Balzers to be confidential or proprietary without the written consent of Balzers.

Warranty

Any warranty contained herein shall be to the original Buyer only. Products manufactured by Balzers are warranted against defects in materials and workmanship for twelve (12) months from date of shipment thereof to Buyer, and Balzers' liability under valid warranty claims is limited, at the option of Balzers, to repair, replacement, or refund of an equitable portion of the purchase price of the Product. Balzers shall have no liability for any defect in material or workmanship unless notice of such defect is received by Balzers within twelve (12) months from the date of shipment. Items expendable in normal use are not covered by this warranty. All warranty replacement or repair of parts shall be limited to equipment malfunctions which, in the sole opinion of Balzers, are due or traceable to defects in original materials or workmanship. All obligations of Balzers under this warranty shall cease in the event of abuse, accident, alteration, misuse or neglect of the equipment. In-warranty repaired or replacement parts are warranted only for the remaining unexpired portion of the original warranty period applicable to the repaired or replaced parts. After expiration of the applicable warranty period, Buyer shall be charged at the then current prices for parts, labor, and transportation.

The Buyer understands and acknowledges that the Products may require installation in carefully controlled and monitored operating environments and that properly trained or skilled personnel will be required in order to achieve proper performance from the Products. Balzers expressly disclaims any responsibility for loss or damage caused by the installation or use of its Products by the Buyer other than in proper operating environments and in accordance with proper operating procedures.

Warranties given by suppliers of equipment or proprietary components not manufactured by Balzers but incorporated by Balzers into its Products shall be passed on to Buyer; provided that in no event shall Balzers have any liability for failure of any such supplier to perform on its warranty.

THE FOREGOING WARRANTIES ARE IN LIEU OF ALL OTHER WARRANTIES EXPRESS OR IMPLIED, INCLUDING, BUT NOT LIMITED TO, THE IMPLIED WARRANTIES OF MERCHANTABILITY AND FITNESS FOR A PARTICULAR PURPOSE.

Warranty Replacement and Adjustment

All claims under warranty should include the Product serial number, the date of shipment, and a full description of the circumstances giving rise to the claim. Before any Products are returned for repair and/or adjustment, written authorization from Balzers or its authorized representative for the return and instructions as to how and where these Products should be returned must be obtained. Any Product returned to Balzers for examination shall be sent prepaid via the means of transportation indicated as acceptable by Balzers. Balzers reserves the right to reject any warranty claim not promptly reported and any warranty claim on any item that has been altered or has been returned by non-acceptable means of transportation. When a Product is returned for examination and inspection, or for any other reason, Buyer shall be responsible for all damage resulting from improper packing or handling, and for loss in transit, notwithstanding any defect or non-conformity in the Product. In all cases, Balzers has sole responsibility for determining the cause and nature of failure, and Balzers' determination with regard thereto shall be final. Any Products returned to Balzers, for whatever reason, will be free from hazardous substances, including, but not limited to, corrosive, radioactive, or toxic substances.

If it is found that Balzers' Product has been returned without cause and is still serviceable, Buyer will be notified and the Product returned at its expense; in addition, a charge for testing and examination may be made on Products so returned.

Limitation of Remedies

Balzers' entire liability and the Buyer's exclusive remedy for any defects in materials or workmanship or non-performance of the Products shall be as set forth above under "Warranty". For any other claim related in any way to the subject matter of the sale of Balzers' Products, Balzers' liability, regardless of the form of action, whether in contract or tort, including negligence, shall be limited to the dollar amount Balzers actually receives for the Products furnished, or to be furnished, or services rendered, or to be rendered, as the case may be, which is the subject of claim or dispute. The foregoing limitation of liability may not apply to the payment of damage awards relating to personal injuries caused solely by Balzers' negligence.

In no event will Balzers be liable for any damages caused by the Buyer's failure to perform the Buyer's responsibilities, or for lost profits or other consequential damages, even if Balzers has been advised of the possibility of such damages, or for any claim against the Buyer by any other party.

General

If any provision or provisions of these terms and conditions are held to be invalid, illegal, or unenforceable; the validity, legality and enforceability of the remaining provisions shall not in any way be affected or impaired thereby.

No action, regardless of form, arising out of, or in any way connected with, the Products furnished or services rendered by Balzers, may be brought by Buyer more than one (1) year after the cause of action has accrued.

All contracts between Balzers and the Buyer shall be construed under and governed by the laws of the State of New Hampshire.

VAT INCORPORATED, Vacuum Valves Technology
Suite 3100, 600 West Cummings Park,
Woburn, Massachusetts 01801,USA,
Phone: (617) 935-1446 and 935-1825
~~Mailing-Adress:~~ ~~P.O. Box 2877~~
~~Woburn, Massachusetts 01888 (1577)~~

VAT
INCORPORATED

September 14, 1984

Mr. David A. Killian
Kentron International, Inc.
JPL Mail Stop 511-204R
4800 Oak Grove Drive
Pasadena, CA 91109

Dear Dave:

I greatly enjoyed visiting with you and Fred during your last visit East, and am very sorry for not responding to you earlier with Ball Park Prices on the valves that we discussed.

There were two types of valves that we discussed. One was an Elastomer Sealed Gate Valve with a Bellows Seal on the Actuator. The Price of this Valve would be approximately $71,000.00 per valve, with a Viton Bonnet Seal. If the Bonnet Seal has to be a Metal Gasket, the price would be $8,400.00 more per valve.

The second valve we discussed would be our All Metal Valve with an All Metal Seal. The price of this Valve would be about $225,000.00 per valve. We have considerable experience in designing and building the All Metal Valve in a smaller size, but there would be considerable engineering involved in making the 48" diameter Valve. As a matter of fact, for your reference, we feel it would take about $500,000.00 to build the first prototype.

I hope that these Ball Park Figures will provide you with some help in stabilizing your design.

Cordially,

VAT INCORPORATED

Solomon P. Cole
General Manager

SC/bee

QUOTATION

GNB Corporation
29393 Pacific St. • Hayward, CA 94544
(415) 537-4722

NO. Q-1608
DATE September 24, 1984
Page 1 OF 1 PAGES

TO JET PROPULSION LABORATORY
4800 Oak Grove Dr.
Pasadina, CA 91109
Attn: Dave Killian
MS-511, Rm - 204

F.O.B. Hayward, CA

YOUR REFERENCE	RE. YOUR	OUR REFERENCE	DELIVERY
Gate Valve	☒ CALL ☐ LETTER ☐ WIRE	Q-1608	Delivery: 12-14 weeks ARO Terms: Net 30 days

ITEM NO.	QUANTITY	DESCRIPTION	UNIT PRICE	AMOUNT
1	1ea	HIGH VACUUM GATE VALVE GNB Corporation Model #G48ESO. This valve has the following features: A.) 48 inch diameter bore B.) Electric motor with brake - Ballscrew drive. C.) Type 304 stainless steel construction. D.) Viton O-ring seals. E.) 56 inch ASA bolt circle. Holes tapped 1½ - 6 NC in 22 places. F.) Valve will normally close on power failure. G.) Solenoid is "continuous duty" rated. H.) Electrical requirement is 110v - 60HZ I.) Electrical connection is ½" FPT J.) Air input connection is ¼" FPT K.) Estimated weight of valve is 5700 lbs. Drawing #41483 BASE PRICE	$34,954.00ea	

UNLESS OTHERWISE STATED, ALL OUR QUOTATIONS ARE FOR PROMPT ACCEPTANCE AND ARE SUBJECT TO CHANGE WITHOUT NOTICE. WE APPRECIATE THIS OPPORTUNITY TO QUOTE AND HOPE WE MAY BE FAVORED WITH YOUR ORDER.

THIS QUOTATION SUBMITTED BY:

Gary N. Burnett
President
TITLE

RCD 8-27-84
Oak

Chicago Bridge & Iron Company

301 East Colorado Boulevard
Pasadena, California 91101
213 684 0840

August 22, 1984

Jet Propulsion Laboratory
2555 East Colorado Blvd.
Pasadena, California

Attention: David A. Killian
Project Engineer

Reference: Gravity Wave Detector Facility
Vacuum Chamber Budget Pricing
CBI Reference No. LA 6878

Gentlemen:

On July 17, 1984 you met with CBI Engineering and Marketing people at our Oak Brook, Illinois Headquarters and discussed vacuum vessel requirements in connection with the Gravity Wave Detector Facility. CBI agreed to provide JPL with budget pricing based upon the Chamber sizes and configurations described in your Drawing No. 9486800 (Rev. A).

Attached is a summary of budget pricing for the 4 alternate configurations in the 5 diameters requested. You may interpolate for different diameters.

Our pricing assumes the following conditions for design and supply:

1. All vessels have been assumed to be shop built-up including final cleaning and helium leak testing. We have not included shipment or site installation.

2. The stainless steel inside surfaces shall be polished to a #4 finish and all welds TIG washed.

3. Openings and chamber door flanges shall utilize single "O"-Ring gaskets.

4. All full opening doors include latching mechanisms.

5. We have not included any provisions for seismic loading.

6. ASME does not require any radiographic examination (RT) of butt welded joints in vacuum vessels, however, we have included spot RT as this is generally specified.

7. The vessels have been priced assuming materials acceptable for a temperature range from -20°F to +100°F. (A240-TP304 S.S.).

8. Budget pricing assumes current day costs. Any state or local sales or use taxes have not been included.

We would again like to emphasize that as the project proceeds CBI is interested in participating in all aspects of design, shop fabrication, and field installation of all structures, foundations, systems and controls on a turnkey single responsibility basis. As you develop the project scope please keep in mind CBI's far greater capabilities. I've enclosed a qualification book and other brochures that describe our capabilities in greater detail.

If we can be of further assistance, please give us a call.

Very truly yours,

Paul Moses

Paul A. Moses
Contracting Engineer
PAM/jm

VACUUM CHAMBER BUDGET PRICING

Chamber Configuration	Size (inches)	Weight (lbs)	Price $
Alt. A	168	16,800	96,600
	144	14,300	82,800
	120	13,100	70,900
	96	10,900	64,600
	72	8,700	51,700
Alt. B	168	17,100	169,700
	144	14,500	145,000
	120	12,400	124,800
	96	10,900	109,900
	72	9,800	99,600
Alt. C	168	17,700	170,500
	144	15,100	146,400
	120	12,700	124,300
	96	11,400	111,600
	72	10,000	98,700
13' high Alt. D $\pi d L + 2\frac{\pi}{4} d^2$ $\pi d \left(L + \frac{d}{2}\right)$	168 14'	880 Ft²	16,200 $/Ft² 193.	169,800
	144 12	715	13,500 198	142,000
	120 10		11,700	123,400
	96 8		10,600	112,900
	72 6		9,600	102,300

Pittsburgh-Des Moines Corporation

Company Correspondence

Pittsburgh, PA

RECEIVED

AUG 27 1984

PDM SAN MATEO

RECEIVED AUG 21 1984 PDM LOS ANGELES

Date August 20, 1984

Subject JPL - GRAVITY WAVE ANTENNA

To M. E. Miles - SMT

From S. M. Jantsch

Copies

R. R. Lentz
D. W. McGuigan - FUL
J. Rouse - CVI
J. C. Murphy
F. A. Kuhs
L. E. Anderson

We have completed our budget pricing effort with the following results:

A. END STATION VESSELS

Three types of vessels, ranging in diameter from 6' to 14' are being considered. JPL's request was for a per chamber price. Of course this is affected by the total quantity of one type purchased; we assumed at least two or three of each type and diameter would be procured. Notice Types B and C are grouped together; there was so little difference between the prices as to be be insignificant.

$\Delta = 12{,}000$

	ft^2	Type B & C	Type D	$\$/ft^2$
14' ϕ	880	$193,000	$205,000	233.
12' ϕ	715	$178,000	$190,000	266.
10' ϕ		$158,000	$170,000	
8' ϕ		$148,000	$160,000	
6' ϕ		$128,000	$140,000	

Seam/Seam = 8'

Flange { 30" high, 5" wall - strong

4 - 4" dia flanges

B. FABRICATION AND ERECTION OF 4' ϕ TUBE

Based upon my knowledge of the X-ray test facility at Marshall Space Flight Center in Alabama, I assumed using 1/4" SS spiral wound pipe stiffened with carbon steel. Also included are expansion bellows, cryopump ports and isolation valves at each end station terminal point. Pipe support are not included. I assumed they would be made of concrete and installed by others. Our present day budget price is $31 million. FOR 20KM

C. CRYOPUMPING ANALYSIS

CVI calculated the gas load requirements using the outgassing data from HEGLF. Their initial calculation for pumping just the tubes was 8600 20" ϕ cryopumps to make the JPL desired 1×10^{-8} torr. PDM Engineering confirmed

SUBJECT: JPL - GRAVITY WAVE ANTENNA

C. CRYOPUMPING ANALYSIS (Continued)

the validity of CVI's calculation. In addition, each end station will require from 15 to 20 or more 20" ϕ cryopumps. This is approximately $250 million of cryopumps, not counting valves, backing pumps and other support equipment plus installation.

CVI, Jim Rouse, then suggested a possible viable alternate.

a) Run a 2" to 4" diameter pipe filled with LN_2 down the inside of the tube. This will pump the water vapor which is a vast majority of the wall outgassing.

b) To pump the remaining gasses only a few cryopumps per tube segment, between end stations, would be necessary.

c) Instead of having enough cryopumps on each end station capable of 10^{-8} torr, just have enough to get to about 10^{-6} or 10^{-5}; then when the tube valves are opened, the LN_2 filled pipe in the tubes will do the rest of the pumping. Without going through a great deal of analysis, it is felt that each end station might only need two cryopumps.

This alternative requires a great deal of LN_2. For one test facility, approximately 43,000 gallons of LN_2 are vaporized each day. In addition, it takes about 15,000 to 20,000 gallons of LN_2 to charge the lines. It is envisioned that to conserve nitrogen, because of the remote location of the facility, a nitrogen reliquefier would be appropriate.

An ROM price for this alternate system, installed, is $18 million.

A second viable alternate would be for JPL to relax the required 10^{-8} torr vacuum level.

D. ATTACHMENTS

Back-up calculations for the above prices are attached along with J. Rouse's memo concerning his results.

Steve

:pm

subject JPL Gravity Wave Antenna, First Cut at Sizing High Vacuum System P 18450

date August 17, 1984

TO T. Hickey

from J. Rouse

in reply to

copies to T. Driscoll, C. Hood, F. Kuhs(PDM), R. Lentz(PDM), S. Jantsch(PDM)

Following up on the August 3rd meeting with PDM and the two JPL representatives, I've taken a preliminary look into the number of cryopumps required to provide the potential facility's characteristics. These results indicate the pressure they're asking for (1 x 10-8 torr) is a much greater driving force than the scale of the facility.

In the following analyses, I have assumed the total gas load on a practical facility would be like that experienced by PDM, at HEGLF. I have looked at two cases:

CASE 1

All of the high vacuum pumping is accomplished with 20 inch cryopumps, distributed as required to achieve a uniform pressure of 1 x 10-8 torr.

For one complete system (consisting of 10.1 km of tubes, plus 13 cylindrical chambers) reaching the desired pressure would require approximately 8600 cryopumps.

Since this would not constitute an acceptable concept, I've looked at an alternative.

CASE 2

Since 99% of the outgassing is water and JPL is presently thinking of isolation valves at each of the cylindrical chambers, I would propose a full length LN2 cooled tube to provide significant water pumping speed in the long tubes. This tube would also provide great longitudinal stabilization to the pressure. It would be jumpered around the chambers.

With a four inch tube, only 4 to 8 cryopumps would be distributed along the 1.2 m tubes of the facility. These pumps would be the only source of Nitrogen and Hydrogen

pumping speed. The pressure inside the long tubes would be maintained well below the required 1 x 10-8 torr. Total LN2 consumption would be about 25 to 30 gpm! this could be provided thru a small nitrogen reliquefier system.

The results are not as comforting when the chambers are considered. If only cryopumps are used to maintain the pressure there, each one will require 15 to 20 (20 in.) cryopumps (depending on the chamber size).

CONCLUSIONS

The primary force driving these results is the very high vacuum being requested. The HEGLF pressure (5 x 10-7 torr) is 50 times higher than this, therefore it takes about 50 times as many pumps to do the job!

I would suggest that our potential customer reevaluate the pressure requirements, in light of these rough results. What would be the risks of conducting the experiment at 1 x 10-7 torr?

If the use of nitrogen cooled surfaces can be accepted, some larger LN2 surfaces could be attached, inside the 1.2 m tubes, but just outside the chambers. These would provide significant augmentation to the water pumping speed of the cryopumps in the chambers and probably reduce their required numbers to a manageable level.

Jim Rouse

MILL LANE ENGINEERING CO., INC.
VACUUM Equipment
12 GARFIELD CIRCLE – BURLINGTON, MASS. 01803
Area Code (617) Telephone 272-2310

September 18, 1984

Mr. David A. Killian
J. P. L. Mail Stop 511-204R
4800 Oak Grove Drive
Pasadena, Ca. 91109

Dear Mr. Killian:

My appologies for the delay in getting this cost estimate for End Station-GWA, Pressure Vessel to you. The following are prices, based on 6 and 26 units and optional alternates B, C & D as requested.

Assembly	Options	6 Units	26 Units
-6	B or C	$92,250. ea.	$83,860. ea.
-7	B or C	$77,110. ea.	$70,090. ea.
-8	B or C	$69,175. ea.	$62,885. ea.
-9	B or C	$58,945. ea.	$53,585. ea.
-10	B or C	$53,790. ea.	$48,900. ea.
-11	D	$98,850. ea.	$89,860. ea.
-12	D	$84,540. ea.	$76,850. ea.
-13	D	$75,980. ea.	$69,070. ea.
-14	D	$65,315. ea.	$59,375. ea.
-15	D	$60,010. ea.	$54,550. ea.

$/ft² 112.

(.91 × $102.

You had also expressed an interest in our model 5042 Gate Valve and 5052R Angle Valve, fabricated in T-304 stainless steel and modify for electric motor actuation.

The price for a 48" Gate Valve is Forty Three Thousand Eight Hundred Ten Dollars ($43,810.00) and for the 48" Angle Valve is Twenty One Thousand Four Hundred Fifteen Dollars ($21,415.00).

MILL LANE ENGINEERING CO., INC.

II

The quantity discount for both models is 10% on 4 to 9 units and 15% for 10 to 25 units.

Hope this information is sufficient for your project evaluation at this time.

Please do not hesitate to call me should you have any questions.

Sincerely,

Mill Lane Engineering Co., Inc.

Lawrence F. Doo
President

Enc: 5042 & 5052R Cat. Sheets.

MILL LANE ENGINEERING CO., INC.

VACUUM Equipment

Vacuum
GATE VALVES
Model 5042
Sizes 4 in. to 60 in.

GATE VALVES

Model 5042

Sizes 4 in. to 60 in.

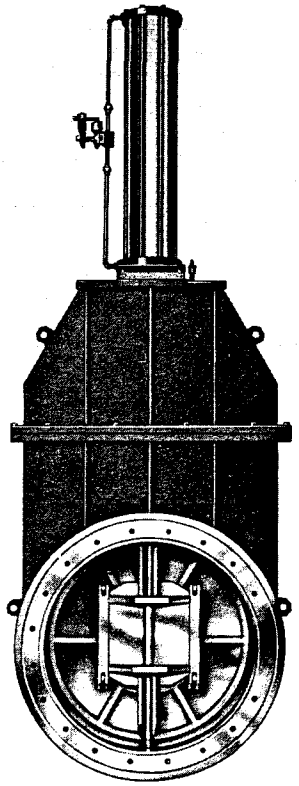

DESCRIPTION:

The Mill Lane model 5042 vacuum gate valves are fabricated construction and available in carbon steel, stainless steel and carbon steel/nickel plated. These valves are designed for vacuum locks on in-line system, isolation valves in space simulators, vacuum furnaces and high vacuum diffusion pumps.

Mill Lane's model 5042 gate valves are field proven since 1960 and accepted as the highest quality engineered and constructed vacuum valve available in the market. Internal tracks assure parallel movement of valve disc and linkage action for perpendicular seating so there is no scuffing of O-Ring seal.

Sizes are available in 4" to 60".

Rectangular or square gate valves are available on request.

FEATURES

- Highest conductance
- Seal against atmosphere in both directions (OPTICAL)
- Removable gate and actuator without breaking from vacuum line
- Mass spectrometer leak tested
- Speed control of gate open & close

OPTIONS

- Open and Close limit switches
- Special flanges & drilling
- Water cooled flanges/gate
- Heat shield for gate
- Viton O-Rings
- Roughing port

MILL LANE ENGINEERING CO., INC.

12 GARFIELD CIRCLE
BURLINGTON, MASS. 01803

Area Code 617
Telephone 272-2310

SPECIFICATION DIMENSIONS

Sizes 4 in. to 60 in.

Model 5042

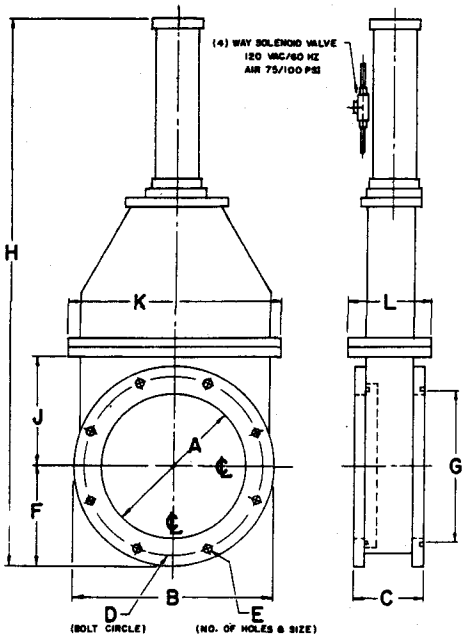

Note:
All bolt holes straddle center lines. "O" ring groove as shown unless otherwise stated.
All dimensions in inches.

VALVE SIZE NOM.	A	B	C	D	E	F	G	H	J	K	L	REMARKS
4"	4	9	4	7 1/2	(8) 5/8-11NC	4 1/2	5	26	7 3/4	5 1/8	4 1/2	
	5 1/4	9	4	7 1/2	(8) 5/8-11NC	4 1/2	5 1/4	29	11	5 7/8	4 1/2	
	5 3/4	9	4	7 1/2	(8) 5/8-11NC	4 1/2	5 1/4	29	11	5 7/8	4 1/2	
6"	6	11	4 5/8	9 1/2	(8) 3/4-10NC	5 1/2	7 1/2	33 1/4	11 5/8	10	4 7/8	
	7	11	4 5/8	9 1/2	(8) 3/4-10NC	5 1/2	7 1/2	33 3/4	11 7/8	11 3/4	4 7/8	
	7 3/4	11	4 5/8	9 1/2	(8) 3/4-10NC	5 1/2	8	33 3/4	11 7/8	11 3/4	4 7/8	
8"	8	13 1/2	5 3/8	11 3/4	(8) 3/4-10NC	6 3/4	9 1/2	41 3/4	14	13 1/2	5 3/8	
	8 3/4	13 1/2	5 3/8	11 3/4	(8) 3/4-10NC	6 3/4	9 1/2	41 3/4	14	13 1/2	5 3/8	
10"	10	16	5 3/4	14 1/4	(12) 7/8-9NC	8	11	48 1/2	9 3/8	15 3/4	6 3/8	
	11 1/2	16	5 3/4	14 1/4	(12) 7/8-9NC	8	12	48 1/2	9 3/8	17 3/8	6 3/8	
12"	12	19	6	17	(12) 7/8-9NC	9 1/2	13	54 7/8	11 7/8	18	6 3/8	
	13	19	6	17	(12) 7/8-9NC	9 1/2	14	54 7/8	11 7/8	19	6 3/8	
14"	14	21	6 3/8	18 3/8	(12) 1-8NC	10 1/2	15	58 3/8	13 1/8	20 1/2	7 3/8	
16"	16	23 1/2	7 1/2	21 1/4	(16) 1-8NC	11 3/4	17 1/2	68	14 1/8	23	8 1/8	
	17 3/4	23 1/2	7 1/2	21 1/4	(16) 1-8NC	11 3/4	19	68 3/8	14 1/8	25 1/8	8 1/8	
	18	23 1/2	7 1/2	21 1/4	(16) 1-8NC	11 3/4	19	68 3/8	14 1/8	25 1/8	8 1/8	
18"	18	25	8	22 3/4	(16) 1 1/8-7NC	12 1/2	20	70 3/8	15 1/8	25 1/8	8 1/8	
20"	20	27 1/2	8	25	(20) 1 1/8-7NC	13 3/4	21	81 1/2	16 1/8	27 1/8	8 3/8	
	21	27 1/2	8	25	(20) 1 1/8-7NC	13 3/4	22	81 1/2	16 1/8	29 1/8	8 3/8	
24"	24	32	9	29 1/2	(20) 1 1/8-7NC	16	25	94	19 7/8	32	9 3/8	
30"	30	38 3/8	9 3/8	36	(28) 1 1/8-7NC	19 3/8	31	108 1/2	24 3/8	38	9 3/8	
32"	32 1/8	38	10	36 1/4	(16) 3/4-10NC	19	32 3/8	88 3/8	29 3/8	38 1/2	10 1/2	
38"	38	41 3/8	10	38 1/2	(14) 1 1/2-6NC	20 7/8	38 3/8	128 1/2	30 1/8	44 1/2	11	
	39	41 3/8	10	38 1/2	(28) 3/4-10NC	20 7/8	38	128 1/2	30 1/8	44 1/2	11	
36"	36	46	10	42 3/8	(32) 1 1/2-6NC	23	38	129 1/2	31 3/8	48 1/2	11	
40"	40	50	10	46 1/2	(30) 1 1/8-7NC	25	42	144 1/2	33 3/8	48 1/8	11	
42"	42	53	10	48 1/2	(30) 1 1/2-6NC	26 1/2	44	147	35 3/8	51	11	
48"	48	59 1/2	12	56	(44) 1 1/2-6NC	29 3/4	50	169	40 3/8	58	12 3/8	
	52	59 1/2	12	56	(44) 1 1/2-6NC	29 3/4	52 3/8	170	40 3/8	62	12 3/8	
60"	60	73	14	68 1/8	(52) 1 1/2-6NC	36 1/2	62	204	50 1/2	72	14	

GATE VALVES

MILL LANE ENGINEERING CO., INC.

VACUUM Equipment

OTHER VACUUM PRODUCTS

CUSTOMIZED VACUUM EQUIPMENT
BELL JAR SYSTEM
PRODUCTION COATER

BOX COATER
WEB OR ROLL COATER
CONTINUOUS IN-LINE SYSTEM

CUSTOMIZED GLASS WORK
IONIZATION VACUUM GAUGE
GLASS TO METAL SEAL

ANGLE VALVE
GATE VALVE
VALVE/TRAP

MILL LANE ENGINEERING CO., INC.

VACUUM Equipment

MODEL 5052R
VACUUM ANGLE VALVES

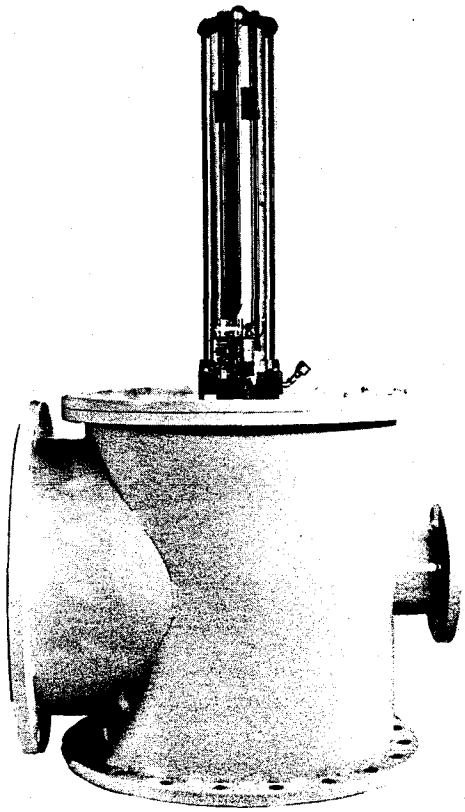

DESCRIPTION

The Mill Lane model 5052R vacuum angle valves are fabricated in carbon steel, stainless steel and carbon steel/nickel plated.

Although these valves are basically designed for high vacuum isolation of main chamber to diffusion vacuum pumps, they are also used as large vacuum manifold valves. Oversized porting assures maximum valve conductance to mate with standard high speed diffusion pumps.

Mill Lane's model 5052R angle valves are serviceable from the top removable bonnet flange which eliminated the need to disconnect the valve from the high vacuum pump and chamber.

Sizes are available in 4" to 60".

FEATURES

- Maximum Conductance
- Oversized Ports
- Fail-Safe Feature in Electrical Power Failure
- Mass Spectrometer Leak Tested
- Speed Control Valve Disc Open and Close

OPTIONS

- Open and Close Limit Switches
- Special Flanges and Drilling
- Water Cooled Flange/Body
- Viton O-Rings
- Roughing Port

MILL LANE ENGINEERING CO., INC.
12 GARFIELD CIRCLE
BURLINGTON, MASS. 01803
Area Code 617
Telephone 272-2310

SPECIFICATION DIMENSIONS

VALVE SIZE INCH	A	B	C	D	E	F	G	H	J	K	L	M
4"	5 1/4	9	(8) 3/4 DIA.	7 1/2	(8) 5/8-11NC	5 1/2	6	24 3/4	5 1/2	11 1/4	5/8	5/8
*	5 3/4	9	(8) 3/4 DIA.	7 1/2	(8) 5/8-11NC	5 1/2	6	24 3/4	5 1/2	11 1/4	5/8	1
6"	7	11	(8) 7/8 DIA	9 1/2	(8) 3/4-10NC	6 1/2	7 1/2	27 1/4	6 1/4	12 1/2	5/8	5/8
*	7 3/4	11	(8) 7/8 DIA	9 1/2	(8) 3/4-10NC	6 1/2	8	27 1/4	6 3/4	13	5/8	11/8
8"	8 3/4	13 1/2	(8) 7/8 DIA.	11 3/4	(8) 3/4-10NC	8 1/4	9 1/2	29	7 5/8	14 3/8	3/4	3/4
10"	11 1/2	16	(12) 1" DIA.	14 1/4	(12) 7/8-9NC	9 1/2	12 1/4	36 1/2	9	17 3/4	3/4	3/4
*	12	16	(12) 1" DIA.	14 1/4	(12) 7/8-9NC	9 1/2	12 1/2	35 1/2	9	17 7/8	3/4	1 1/4
12"	13	19	(12) 1" DIA.	17	(12) 7/8-9NC	10 1/2	14	40	9 3/4	19 1/2	3/4	3/4
14"	14	21	(12) 1 1/8 DIA.	18 3/4	(12) 1-8NC	13	15	42 1/2	11	21	7/8	7/8
16"	18	23 1/2	(16) 1 1/8 DIA	21 1/4	(16) 1-8 NC	14	19	48	12 5/8	24 1/2	7/8	1
18"	18	25	(16) 1 1/4 DIA.	22 3/4	(16) 1 1/8-7NC	15 1/2	19	50 1/4	13 1/2	25 7/8	7/8	1
20"	21	27 1/2	(20) 1 1/4 DIA.	25	(20) 1 1/8-7NC	16	22	54	14	28 1/4	1	1
24"	24	32	(20) 1 3/8 DIA.	29 1/2	(20) 1 1/4-7NC	17 1/2	25	65	17 1/2	34 1/2	1 1/8	1 1/8
30"	30	38 3/4	(28) 1 3/8 DIA.	36	(28) 1 1/4-7NC	22	31	78 1/2	20	42	1 1/8	1 1/8
* 32"	32 1/8	38	(16) 7/8 DIA.	36 1/4	(16) 3/4-10NC	24	33 1/2	76 1/4	19 1/4	39 1/8	1 1/8	1 3/8
* 35"	35	41 3/4	(28) 7/8 DIA.	38 1/2	(28) 3/4-10NC	25	36	78 3/8	22	47 3/8	1 1/8	1 1/2
* 35"	35	41 3/4	(14) 1 5/8 DIA	38 1/2	(14) 1 1/2-6NC	25	35 3/4	80	23	46 7/8	1 1/8	2
36"	36	46	(32) 1 5/8 DIA.	42 3/4	(32) 1 1/2-6NC	26	38	86 1/2	24	50	1 3/8	1 3/8
42"	42	53	(36) 1 5/8 DIA.	49 1/2	(36) 1 1/2-6NC	30	44	97 1/2	28	58	1 3/8	1 3/8
* 48"	52	59 1/2	(44) 1 5/8 DIA.	56	(44) 1 1/2-6NC	33	53	120	32	70 5/8	1 1/2	2
												2
60"	60	73	(52) 1 5/8 DIA.	69 1/4	(52) 1 1/2-6NC	40	62	128	38	76	1 5/8	

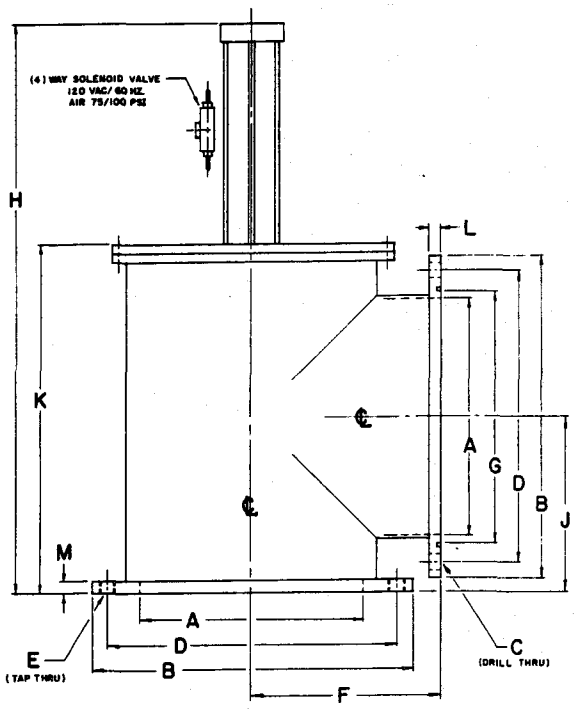

NOTES:

1. ALL DIMENSIONS IN INCHES.
2. SPECIAL DRILLING UPON REQUEST.
3. ALL BOLT HOLES STRADDLE CENTERLINES.
4. O-RING GROOVE AS SHOWN UNLESS OTHERWISE STATED.
5. PLEASE CONSULT MANUFACTURER FOR FINAL REVISION.
6. * - OVERPORT BLIND TAP HOLES ON BOTTOM FLANGE.

MILL LANE ENGINEERING CO., INC.

VACUUM Equipment

OTHER VACUUM PRODUCTS

CUSTOMIZED VACUUM EQUIPMENT
BELL JAR SYSTEM
PRODUCTION COATER

BOX COATER
WEB OR ROLL COATER
CONTINUOUS IN-LINE SYSTEM

CUSTOMIZED GLASS WORK
IONIZATION VACUUM GAUGE
GLASS TO METAL SEAL

ANGLE VALVE
GATE VALVE
VALVE/TRAP

HIGH VACUUM
EQUIPMENT CORP.
110 INDUSTRIAL PARK ROAD • HINGHAM, MA 02043 • TEL: 617/749-9000 • TWX: 710-348-0160

September 14, 1984

JPL
4800 Oak Grove Drive
Pasadena, CA 91109

Attention: David A. Killian, Project Engineer
JPL Mail Stop 511-204R

Reference: Gravity Wave Detector Facility
HVEC Proposal No. CCA9-2210

Gentlemen:

In response to your verbal request for a budgetary price for the vacuum chambers listed below we are pleased to offer the following ROM quotation:

Reference your Drawing J-9A86800, Rev. A:

Assembly No.	Quantity	Unit Price
-6	2	$220,000
-7	2	190,000
-8	2	170,000
-9	2	155,000
-10	2	140,000
-11	1	240,000
-12	1	215,000
-13	1	195,000
-14	1	160,000
-15	1	145,000

4/ft² 250.

Please note that prices quoted are based on the quantity of each assembly stated on JPL Drawing J-9486800, Rev. A. If combinations of assemblies are ordered in significant quantities, HVEC would be more than happy to discuss quantity discounts.

Please also note we have not considered assemblies #1-5 of the above referenced JPL drawing per your instructions. Should you require pricing information on assemblies 1-5 please advise and we would be happy to respond.

The above pricing does not consider any applicable taxes and f.o.b. point is Hingham, MA. Since the above quoted price is for preliminary use by JPL only, shipment of the equipment is not offered due to the fact that lead time will vary depending on time and placement of order. If you would advise when an order date is scheduled we would then offer an approximate delivery date.

We would like to thank you for the opportunity to review your vacuum related needs and we look forward to working together on this project in the near future. Should you have any questions or require additional information please feel free to contact me.

Very truly yours,

HIGH VACUUM EQUIPMENT CORP.

Joseph J. Sgambato
Sales Manager

JJS/jm

cc: Frederick J. Menninger, Jr.
Technical Group Supervisor
Ground Antennas and Facilities Engineering Section

P AVE (T)	OUTGASS RATE (T-L/S-CM**2)	PUMP SPEED(L/S)	NUMBER:	DISTANCE(M)
1.00E -6	1.00E -10	10000.00	14	708.
1.00E -7	1.00E -10	10000.00	61	162.
1.00E -8	1.00E -10	10000.00	417	24.
1.00E -6	2.00E -10	10000.00	21	469.
1.00E -7	2.00E -10	10000.00	104	96.
1.00E -8	2.00E -10	10000.00	802	12.
1.00E -6	3.00E -10	10000.00	27	365.
1.00E -7	3.00E -10	10000.00	144	69.
1.00E -8	3.00E -10	10000.00	1185	8.
1.00E -6	4.00E -10	10000.00	32	303.
1.00E -7	4.00E -10	10000.00	184	54.
1.00E -8	4.00E -10	10000.00	1569	6.
1.00E -6	5.00E -10	10000.00	38	262.
1.00E -7	5.00E -10	10000.00	223	45.
1.00E -8	5.00E -10	10000.00	1952	5.
1.00E -6	6.00E -10	10000.00	43	232.
1.00E -7	6.00E -10	10000.00	262	38.
1.00E -8	6.00E -10	10000.00	2335	4.
1.00E -6	7.00E -10	10000.00	48	208.
1.00E -7	7.00E -10	10000.00	301	33.
1.00E -8	7.00E -10	10000.00	2718	4.
1.00E -6	8.00E -10	10000.00	52	190.
1.00E -7	8.00E -10	10000.00	340	29.
1.00E -8	8.00E -10	10000.00	3101	3.
1.00E -6	9.00E -10	10000.00	57	175.
1.00E -7	9.00E -10	10000.00	379	26.
1.00E -8	9.00E -10	10000.00	3484	3.
1.00E -6	1.00E -9	10000.00	61	162.
1.00E -7	1.00E -9	10000.00	417	24.
1.00E -8	1.00E -9	10000.00	3867	3.

P AVE (T)	OUTGASS RATE (T-L/S-CM**2)	PUMP SPEED(L/S)	NUMBER:	DISTANCE(M)
1.00E -6	1.00E -11	10000.00	4	2495.
1.00E -7	1.00E -11	10000.00	14	708.
1.00E -8	1.00E -11	10000.00	61	162.
1.00E -6	2.00E -11	10000.00	5	1728.
1.00E -7	2.00E -11	10000.00	21	469.
1.00E -8	2.00E -11	10000.00	104	96.
1.00E -6	3.00E -11	10000.00	7	1389.
1.00E -7	3.00E -11	10000.00	27	365.
1.00E -8	3.00E -11	10000.00	144	69.
1.00E -6	4.00E -11	10000.00	8	1186.
1.00E -7	4.00E -11	10000.00	32	303.
1.00E -8	4.00E -11	10000.00	184	54.
1.00E -6	5.00E -11	10000.00	9	1049.
1.00E -7	5.00E -11	10000.00	38	262.
1.00E -8	5.00E -11	10000.00	223	45.
1.00E -6	6.00E -11	10000.00	10	947.
1.00E -7	6.00E -11	10000.00	43	232.
1.00E -8	6.00E -11	10000.00	262	38.
1.00E -6	7.00E -11	10000.00	11	868.
1.00E -7	7.00E -11	10000.00	48	208.
1.00E -8	7.00E -11	10000.00	301	33.
1.00E -6	8.00E -11	10000.00	12	805.
1.00E -7	8.00E -11	10000.00	52	190.
1.00E -8	8.00E -11	10000.00	340	29.
1.00E -6	9.00E -11	10000.00	13	753.
1.00E -7	9.00E -11	10000.00	57	175.
1.00E -8	9.00E -11	10000.00	379	26.
1.00E -6	1.00E -10	10000.00	14	708.
1.00E -7	1.00E -10	10000.00	61	162.
1.00E -8	1.00E -10	10000.00	417	24.

P AVE (T)	OUTGASS RATE (T-L/S-CM**2)	PUMP SPEED(L/S)	NUMBER:	DISTANCE(M)
1.00E -6	1.00E -11	10000.00	4	2495.
1.00E -7	1.00E -11	10000.00	14	708.
1.00E -8	1.00E -11	10000.00	61	162.
1.00E -6	1.10E -11	10000.00	4	2373.
1.00E -7	1.10E -11	10000.00	14	670.
1.00E -8	1.10E -11	10000.00	66	151.
1.00E -6	1.20E -11	10000.00	4	2267.
1.00E -7	1.20E -11	10000.00	15	637.
1.00E -8	1.20E -11	10000.00	70	142.
1.00E -6	1.30E -11	10000.00	4	2173.
1.00E -7	1.30E -11	10000.00	16	608.
1.00E -8	1.30E -11	10000.00	74	133.
1.00E -6	1.40E -11	10000.00	4	2089.
1.00E -7	1.40E -11	10000.00	17	582.
1.00E -8	1.40E -11	10000.00	79	126.
1.00E -6	1.50E -11	10000.00	4	2014.
1.00E -7	1.50E -11	10000.00	17	558.
1.00E -8	1.50E -11	10000.00	83	120.
1.00E -6	1.60E -11	10000.00	5	1946.
1.00E -7	1.60E -11	10000.00	18	537.
1.00E -8	1.60E -11	10000.00	87	114.
1.00E -6	1.70E -11	10000.00	5	1885.
1.00E -7	1.70E -11	10000.00	19	518.
1.00E -8	1.70E -11	10000.00	91	109.
1.00E -6	1.80E -11	10000.00	5	1828.
1.00E -7	1.80E -11	10000.00	19	500.
1.00E -8	1.80E -11	10000.00	96	104.
1.00E -6	1.90E -11	10000.00	5	1776.
1.00E -7	1.90E -11	10000.00	20	484.
1.00E -8	1.90E -11	10000.00	100	100.

P AVE (T)	OUTGASS RATE (T-L/S-CM**2)	PUMP SPEED(L/S)	NUMBER:	DISTANCE(M)
1.00E -6	1.00E -12	10000.00	1	8165.
1.00E -7	1.00E -12	10000.00	4	2495.
1.00E -8	1.00E -12	10000.00	14	708.
1.00E -6	2.00E -12	10000.00	1	5736.
1.00E -7	2.00E -12	10000.00	5	1728.
1.00E -8	2.00E -12	10000.00	21	469.
1.00E -6	3.00E -12	10000.00	2	4660.
1.00E -7	3.00E -12	10000.00	7	1389.
1.00E -8	3.00E -12	10000.00	27	365.
1.00E -6	4.00E -12	10000.00	2	4018.
1.00E -7	4.00E -12	10000.00	8	1186.
1.00E -8	4.00E -12	10000.00	32	303.
1.00E -6	5.00E -12	10000.00	2	3580.
1.00E -7	5.00E -12	10000.00	9	1049.
1.00E -8	5.00E -12	10000.00	38	262.
1.00E -6	6.00E -12	10000.00	3	3257.
1.00E -7	6.00E -12	10000.00	10	947.
1.00E -8	6.00E -12	10000.00	43	232.
1.00E -6	7.00E -12	10000.00	3	3006.
1.00E -7	7.00E -12	10000.00	11	868.
1.00E -8	7.00E -12	10000.00	48	208.
1.00E -6	8.00E -12	10000.00	3	2804.
1.00E -7	8.00E -12	10000.00	12	805.
1.00E -8	8.00E -12	10000.00	52	190.
1.00E -6	9.00E -12	10000.00	3	2637.
1.00E -7	9.00E -12	10000.00	13	753.
1.00E -8	9.00E -12	10000.00	57	175.
1.00E -6	1.00E -11	10000.00	4	2495.
1.00E -7	1.00E -11	10000.00	14	708.
1.00E -8	1.00E -11	10000.00	61	162.

P AVE (T)	OUTGASS RATE (T-L/S-CM**2)	PUMP SPEED(L/S)	NUMBER:	DISTANCE(M)
1.00E -6	1.00E -10	1000.00	41	239.
1.00E -7	1.00E -10	1000.00	386	26.
1.00E -8	1.00E -10	1000.00	3833	3.
1.00E -6	2.00E -10	1000.00	80	125.
1.00E -7	2.00E -10	1000.00	769	13.
1.00E -8	2.00E -10	1000.00	7664	1.
1.00E -6	3.00E -10	1000.00	118	84.
1.00E -7	3.00E -10	1000.00	1152	9.
1.00E -8	3.00E -10	1000.00	11493	1.
1.00E -6	4.00E -10	1000.00	156	64.
1.00E -7	4.00E -10	1000.00	1535	7.
1.00E -8	4.00E -10	1000.00	15326	1.
1.00E -6	5.00E -10	1000.00	195	51.
1.00E -7	5.00E -10	1000.00	1918	5.
1.00E -8	5.00E -10	1000.00	19154	1.
1.00E -6	6.00E -10	1000.00	233	43.
1.00E -7	6.00E -10	1000.00	2301	4.
1.00E -8	6.00E -10	1000.00	22978	0.
1.00E -6	7.00E -10	1000.00	271	37.
1.00E -7	7.00E -10	1000.00	2684	4.
1.00E -8	7.00E -10	1000.00	26811	0.
1.00E -6	8.00E -10	1000.00	310	32.
1.00E -7	8.00E -10	1000.00	3067	3.
1.00E -8	8.00E -10	1000.00	30645	0.
1.00E -6	9.00E -10	1000.00	348	29.
1.00E -7	9.00E -10	1000.00	3450	3.
1.00E -8	9.00E -10	1000.00	32767	0.
1.00E -6	1.00E -9	1000.00	386	26.
1.00E -7	1.00E -9	1000.00	3833	3.
1.00E -8	1.00E -9	1000.00	32767	0.

P AVE (T)	OUTGASS RATE (T-L/S-CM**2)	PUMP SPEED(L/S)	NUMBER:	DISTANCE(M)
1.00E -6	1.00E -11	1000.00	6	1618.
1.00E -7	1.00E -11	1000.00	41	239.
1.00E -8	1.00E -11	1000.00	386	26.
1.00E -6	2.00E -11	1000.00	10	958.
1.00E -7	2.00E -11	1000.00	80	125.
1.00E -8	2.00E -11	1000.00	769	13.
1.00E -6	3.00E -11	1000.00	14	690.
1.00E -7	3.00E -11	1000.00	118	84.
1.00E -8	3.00E -11	1000.00	1152	9.
1.00E -6	4.00E -11	1000.00	18	541.
1.00E -7	4.00E -11	1000.00	156	64.
1.00E -8	4.00E -11	1000.00	1535	7.
1.00E -6	5.00E -11	1000.00	22	447.
1.00E -7	5.00E -11	1000.00	195	51.
1.00E -8	5.00E -11	1000.00	1918	5.
1.00E -6	6.00E -11	1000.00	26	380.
1.00E -7	6.00E -11	1000.00	233	43.
1.00E -8	6.00E -11	1000.00	2301	4.
1.00E -6	7.00E -11	1000.00	30	331.
1.00E -7	7.00E -11	1000.00	271	37.
1.00E -8	7.00E -11	1000.00	2684	4.
1.00E -6	8.00E -11	1000.00	34	294.
1.00E -7	8.00E -11	1000.00	310	32.
1.00E -8	8.00E -11	1000.00	3067	3.
1.00E -6	9.00E -11	1000.00	37	264.
1.00E -7	9.00E -11	1000.00	348	29.
1.00E -8	9.00E -11	1000.00	3450	3.
1.00E -6	1.00E -10	1000.00	41	239.
1.00E -7	1.00E -10	1000.00	386	26.
1.00E -8	1.00E -10	1000.00	3833	3.

P AVE (T)	OUTGASS RATE (T-L/S-CM**2)	PUMP SPEED(L/S)	NUMBER:	DISTANCE(M)
1.00E -6	1.00E -11	1000.00	6	1618.
1.00E -7	1.00E -11	1000.00	41	239.
1.00E -8	1.00E -11	1000.00	386	26.
1.00E -6	1.10E -11	1000.00	6	1509.
1.00E -7	1.10E -11	1000.00	45	219.
1.00E -8	1.10E -11	1000.00	425	24.
1.00E -6	1.20E -11	1000.00	7	1416.
1.00E -7	1.20E -11	1000.00	49	202.
1.00E -8	1.20E -11	1000.00	463	22.
1.00E -6	1.30E -11	1000.00	7	1334.
1.00E -7	1.30E -11	1000.00	53	187.
1.00E -8	1.30E -11	1000.00	501	20.
1.00E -6	1.40E -11	1000.00	7	1261.
1.00E -7	1.40E -11	1000.00	57	175.
1.00E -8	1.40E -11	1000.00	539	19.
1.00E -6	1.50E -11	1000.00	8	1197.
1.00E -7	1.50E -11	1000.00	61	164.
1.00E -8	1.50E -11	1000.00	578	17.
1.00E -6	1.60E -11	1000.00	8	1139.
1.00E -7	1.60E -11	1000.00	64	154.
1.00E -8	1.60E -11	1000.00	616	16.
1.00E -6	1.70E -11	1000.00	9	1087.
1.00E -7	1.70E -11	1000.00	68	146.
1.00E -8	1.70E -11	1000.00	654	15.
1.00E -6	1.80E -11	1000.00	9	1040.
1.00E -7	1.80E -11	1000.00	72	138.
1.00E -8	1.80E -11	1000.00	693	14.
1.00E -6	1.90E -11	1000.00	10	997.
1.00E -7	1.90E -11	1000.00	76	131.
1.00E -8	1.90E -11	1000.00	731	14.

P AVE (T)	OUTGASS RATE (T-L/S-CM**2)	PUMP SPEED(L/S)	NUMBER:	DISTANCE(M)
1.00E -6	1.00E -12	1000.00	1	7082.
1.00E -7	1.00E -12	1000.00	6	1618.
1.00E -8	1.00E -12	1000.00	41	239.
1.00E -6	2.00E -12	1000.00	2	4694.
1.00E -7	2.00E -12	1000.00	10	958.
1.00E -8	2.00E -12	1000.00	80	125.
1.00E -6	3.00E -12	1000.00	2	3650.
1.00E -7	3.00E -12	1000.00	14	690.
1.00E -8	3.00E -12	1000.00	118	84.
1.00E -6	4.00E -12	1000.00	3	3034.
1.00E -7	4.00E -12	1000.00	18	541.
1.00E -8	4.00E -12	1000.00	156	64.
1.00E -6	5.00E -12	1000.00	3	2619.
1.00E -7	5.00E -12	1000.00	22	447.
1.00E -8	5.00E -12	1000.00	195	51.
1.00E -6	6.00E -12	1000.00	4	2316.
1.00E -7	6.00E -12	1000.00	26	380.
1.00E -8	6.00E -12	1000.00	233	43.
1.00E -6	7.00E -12	1000.00	4	2083.
1.00E -7	7.00E -12	1000.00	30	331.
1.00E -8	7.00E -12	1000.00	271	37.
1.00E -6	8.00E -12	1000.00	5	1898.
1.00E -7	8.00E -12	1000.00	34	294.
1.00E -8	8.00E -12	1000.00	310	32.
1.00E -6	9.00E -12	1000.00	5	1745.
1.00E -7	9.00E -12	1000.00	37	264.
1.00E -8	9.00E -12	1000.00	348	29.
1.00E -6	1.00E -11	1000.00	6	1618.
1.00E -7	1.00E -11	1000.00	41	239.
1.00E -8	1.00E -11	1000.00	386	26.

48"

P AVE (T)	OUTGASS RATE (T-L/S-CM**2)	PUMP SPEED(L/S)	NUMBER:	DISTANCE(M)
1.000E-06	1.000E-12	1000.00	1	7081.
1.000E-07	1.000E-12	1000.00	6	1618.
1.000E-08	1.000E-12	1000.00	41	239.
1.000E-06	2.000E-12	1000.00	2	4694.
1.000E-07	2.000E-12	1000.00	10	958.
1.000E-08	2.000E-12	1000.00	80	125.
1.000E-06	3.000E-12	1000.00	2	3649.
1.000E-07	3.000E-12	1000.00	14	690.
1.000E-08	3.000E-12	1000.00	118	84.
1.000E-06	4.000E-12	1000.00	3	3034.
1.000E-07	4.000E-12	1000.00	18	542.
1.000E-08	4.000E-12	1000.00	156	64.
1.000E-06	5.000E-12	1000.00	3	2619.
1.000E-07	5.000E-12	1000.00	22	447.
1.000E-08	5.000E-12	1000.00	195	51.
1.000E-06	6.000E-12	1000.00	4	2316.
1.000E-07	6.000E-12	1000.00	26	380.
1.000E-08	6.000E-12	1000.00	233	43.
1.000E-06	7.000E-12	1000.00	4	2083.
1.000E-07	7.000E-12	1000.00	30	331.
1.000E-08	7.000E-12	1000.00	271	37.
1.000E-06	8.000E-12	1000.00	5	1897.
1.000E-07	8.000E-12	1000.00	34	294.
1.000E-08	8.000E-12	1000.00	310	32.
1.000E-06	9.000E-12	1000.00	5	1745.
1.000E-07	9.000E-12	1000.00	37	264.
1.000E-08	9.000E-12	1000.00	348	29.
1.000E-06	1.000E-11	1000.00	6	1618.
1.000E-07	1.000E-11	1000.00	41	239.
1.000E-08	1.000E-11	1000.00	386	26.

60"

P AVE (T)	OUTGASS RATE (T-L/S-CM**2)	PUMP SPEED(L/S)	NUMBER:	DISTANCE(M)
1.000E-06	1.000E-12	1000.00	1	8110.
1.000E-07	1.000E-12	1000.00	6	1595.
1.000E-08	1.000E-12	1000.00	49	201.
1.000E-06	2.000E-12	1000.00	1	5197.
1.000E-07	2.000E-12	1000.00	11	890.
1.000E-08	2.000E-12	1000.00	97	102.
1.000E-06	3.000E-12	1000.00	2	3943.
1.000E-07	3.000E-12	1000.00	16	621.
1.000E-08	3.000E-12	1000.00	145	69.
1.000E-06	4.000E-12	1000.00	3	3215.
1.000E-07	4.000E-12	1000.00	20	478.
1.000E-08	4.000E-12	1000.00	193	52.
1.000E-06	5.000E-12	1000.00	3	2730.
1.000E-07	5.000E-12	1000.00	25	388.
1.000E-08	5.000E-12	1000.00	241	41.
1.000E-06	6.000E-12	1000.00	4	2380.
1.000E-07	6.000E-12	1000.00	30	327.
1.000E-08	6.000E-12	1000.00	289	35.
1.000E-06	7.000E-12	1000.00	4	2115.
1.000E-07	7.000E-12	1000.00	35	283.
1.000E-08	7.000E-12	1000.00	337	30.
1.000E-06	8.000E-12	1000.00	5	1906.
1.000E-07	8.000E-12	1000.00	40	249.
1.000E-08	8.000E-12	1000.00	384	26.
1.000E-06	9.000E-12	1000.00	5	1736.
1.000E-07	9.000E-12	1000.00	44	222.
1.000E-08	9.000E-12	1000.00	432	23.
1.000E-06	1.000E-11	1000.00	6	1595.
1.000E-07	1.000E-11	1000.00	49	201.
1.000E-08	1.000E-11	1000.00	480	21.

72"

P AVE (T)	OUTGASS RATE (T-L/S-CM**2)	PUMP SPEED(L/S)	NUMBER:	DISTANCE(M)
1.000E-06	1.000E-12	1000.00	1	8767.
1.000E-07	1.000E-12	1000.00	6	1491.
1.000E-08	1.000E-12	1000.00	58	171.
1.000E-06	2.000E-12	1000.00	1	5411.
1.000E-07	2.000E-12	1000.00	12	799.
1.000E-08	2.000E-12	1000.00	116	86.
1.000E-06	3.000E-12	1000.00	2	4002.
1.000E-07	3.000E-12	1000.00	18	547.
1.000E-08	3.000E-12	1000.00	173	58.
1.000E-06	4.000E-12	1000.00	3	3200.
1.000E-07	4.000E-12	1000.00	24	416.
1.000E-08	4.000E-12	1000.00	230	43.
1.000E-06	5.000E-12	1000.00	3	2676.
1.000E-07	5.000E-12	1000.00	29	335.
1.000E-08	5.000E-12	1000.00	288	35.
1.000E-06	6.000E-12	1000.00	4	2304.
1.000E-07	6.000E-12	1000.00	35	281.
1.000E-08	6.000E-12	1000.00	345	29.
1.000E-06	7.000E-12	1000.00	4	2025.
1.000E-07	7.000E-12	1000.00	41	242.
1.000E-08	7.000E-12	1000.00	403	25.
1.000E-06	8.000E-12	1000.00	5	1808.
1.000E-07	8.000E-12	1000.00	47	212.
1.000E-08	8.000E-12	1000.00	460	22.
1.000E-06	9.000E-12	1000.00	6	1634.
1.000E-07	9.000E-12	1000.00	52	189.
1.000E-08	9.000E-12	1000.00	518	19.
1.000E-06	1.000E-11	1000.00	6	1491.
1.000E-07	1.000E-11	1000.00	58	171.
1.000E-08	1.000E-11	1000.00	575	17.

BATCH START

STAPLE
OR
DIVIDER

OUTGASSING AND CLEANING TECHNIQUES

REFERENCE DATA

vacuum division varian

VR-51

Killian

REVIEW OF OUTGASSING RESULTS

by

Yale Strausser

Varian Associates

Palo Alto, California

Please address inquiries to: VACUUM DIVISION, VARIAN ASSOCIATES
611 Hansen Way, Palo Alto, California, U.S.A.

European inquiries: Varian SpA, via Varian
10040 Leini, Torino, Italy

I. INTRODUCTION

This report covers state-of-the art information on outgassing rates of metals. The first section reviews work that has been accomplished in this area (published and unpublished). The second section will deal with the work that is presently in progress at Varian Associates.

Detailed information on outgassing rates is valuable in a number of ways. Primarily this information enables one to predict the pressure-versus-time characteristics of a given vacuum system or to design and construct a vacuum system in which a particular pressure-versus-time characteristic is required. Second, if the outgassing rates are known for each gas present, then the pressure of a particular gas can be controlled without concern for pressures of other gases. Third, a knowledge of outgassing rates and an understanding of the mechanisms involved will facilitate an intelligent selection of materials having minimum outgassing rates that is consistent with other material requirements for each component of a vacuum system. Finally, a knowledge of outgassing rates as a function of time and temperature may lead to an understanding of the mechanisms by which these gases are generated, and thereby lead to methods for substantially reducing outgassing rates.

II. REVIEW OF PREVIOUS WORK

A review of the published work on outgassing rates shows that there is a wide variance in the values reported for similar materials. To a certain extent this variance can be ascribed to the different techniques used by the different authors to obtain their values. For this reason it is necessary to describe and evaluate the various techniques used. This is the purpose of the next section. Another significant factor in this variation is the pre-treatment of the sample surfaces including mechanical, chemical, and vacuum pre-processing. Measurements have been reported on the first pumpdown of samples of as-received materials. This condition is seldom representative of the outgassing of that material which would be observed in typical vacuum applications. The most representative values are probably those obtained from samples which have had at least a degreasing and a vacuum pumpdown and bakeout. After an exposure to atmosphere, such a sample would then begin to exhibit characteristics typical of such a component in a vacuum system. In Section B, where the published results are summarized, information describing pre-treatment of the samples is included wherever possible.

A. REVIEW OF MEASUREMENT TECHNIQUES

With one exception all of the techniques that have been used to determine outgassing rates involve solving the differential equation for the variation of pressure with time in a vacuum system:

$$V \frac{dp}{dt} = Q - Sp \qquad (1)$$

where:

- V = volume of the system
- p = pressure in the system
- t = time
- Q = outgassing rate of all surfaces
- S = pumping speed of all pumps

In the case where V dp/dt << Sp, the solution for Q is trivial, because Q = Sp. This case is the basis for the technique most often used. A system using this technique is shown schematically in Figure 1. A chamber of volume V, which may either be the sample or which may contain the sample, is pumped through a known conductance, C. On either side of C, gauges monitor the pressure as a function of time during a pumpdown. When the condition of V dp/dt<<Cp is met, the outgassing rate is calculated from

$$Q = C(p_1 - p_2) \tag{2}$$

where p_1 = pressure in the chamber

p_2 = pressure in the pump

By using a pump whose speed is >> the conductance C for all gases, many workers have eliminated the measurement of p_2 since it would then be $< < p_1$.

Numerous difficulties may be encountered in the use of this technique:

1. The use of a gauge inside the sample chamber can be a source of error in two ways. First, the gauge pumping speed must be much smaller than the conductance C for each gas present in the system. At the same time C must be much less than S, the speed of the pump, again for each gas present. This provides a significant lower limit to the size of the pump. Second, the gauge may be a source of gas that is comparable to the outgassing rate of the sample. Gas may be released from the gauge in at least four different ways. These are:

   a. If the gauge is the hot-filament type, the hot parts of the gauge will give off gas over a long period of time unless, and sometimes even if, it can be outgassed at a temperature significantly above its

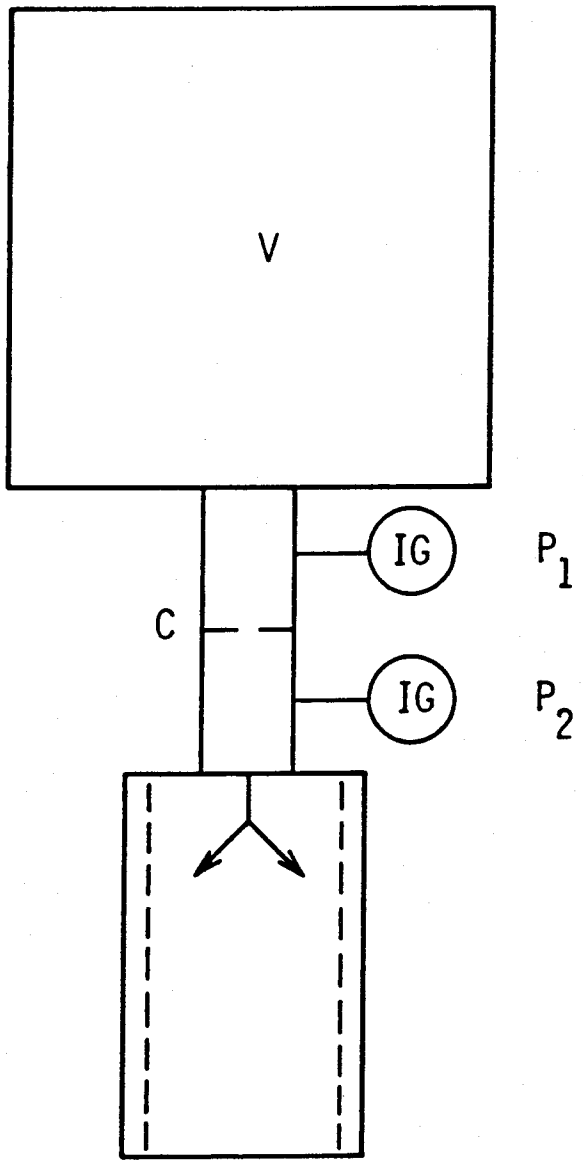

Figure 1. Schematic of System Using $Q = C\Delta p$ Method

operating temperature. The source of this gas is apparently related to the diffusion of impurities out of the bulk of these hot parts.

b. In gauges which use electron bombardment to produce ions, the surfaces on which the electrons are collected may release gases (both ions and neutrals) through electron bombardment-induced desorption.

c. The ion current collector of the gauge will contain a large number of gas atoms which have been buried there as a result of their high impact energies. These atoms will be released after some storage time as a result of the collection of other ions. This storage time will result in false measurements of gas composition vs time in a system in which the composition is changing.

d. Gases present in the system can be converted at these surfaces from one compound to another. As an example, oxygen may pick up a carbon atom to form carbon dioxide.

2. Another important problem area is the use of small samples enclosed in a larger chamber rather than having the chamber itself be the sample. Again, there are different ways in which this technique can cause problems. First, the enclosure walls can have an outgassing rate that is comparable to or greater than that of the sample. Most authors who use this technique make a blank run on the system without any sample and then subtract the outgassing rates thus obtained from the sample outgassing rates measured subsequently. However, with our limited knowledge of outgassing rates and their dependence on many important parameters, it is difficult to establish that the outgassing rates of the chamber varied in the same way, with time, on runs which included samples as they varied on the blank run. Also, this technique frequently results in the type of large errors which occur when two nearly equal

numbers are subtracted to obtain a small difference between them, in this case, the outgassing rate.

A second interaction between the sample and the enclosure is that the gas that is desorbed from the sample can re-adsorb on the enclosure walls, where it can have a significantly different adsorption lifetime. If this adsorption time on chamber walls is longer than the time of the experiment, then the enclosure acts as a pump and the sample appears to have released little or none of that particular gas. If the adsorption time on the walls is less than the time of the experiment then the sample simply appears to be outgassing more slowly than it actually is.

3. In using this measurement technique, care must be taken to ensure that the conductance of the aperture C is << the speed of the pump. If it is not, then the conductance C used in equation (2) will not be independent of the pumping speed S, and S must be known as a function of pressure p. As mentioned above, this conductance limitation results in a requirement for a large pump, since C must also be >> the pumping speed of the sum of any pumps or pseudo-pumps in the chamber (ion gauges, pumping of the enclosure walls, etc.).

A variation on the Q = Sp method is one called the Oatley method[1]. Actually Oatley devised a method for measuring pumping speed[2] and some workers[1,3] have used his method in conjunction with outgassing work to ensure that the S in the Q = Sp relationship was known at all times. The system used is the same as that in Figure 1 except that the conductance of the aperture is variable. If S_1 and S_2 are the pumping speeds available above and below the conductance C respectively, then:

$$Q = C (p_1 - p_2) \quad (3)$$

or rearranging, $$p_1 = Q/C + p_2 \quad (4)$$

and, $$Q = S_2 p_2 \quad (5)$$

By varying C, one can produce a plot of p_1 vs $\frac{1}{C}$. The intercept of this straight line with the $\frac{1}{C}$ axis will be $- p_2/Q$ or $-1/S_2$. Using this value for S_2 along with a measured value of p_2 will give a value for Q. The advantage claimed for this method is that at low outgassing rates it leads to smaller errors. This is because $Q = C (p_1 - p_2)$ involves determining a small difference between two large numbers. The disadvantages are that a gauge is still required in the sample chamber, the measurement of S_2 is probably not as accurate as the calculation of C, and each time a pressure figure is required one must make a series of measurements at varying values of C while assuming that during this time Q and p_2 remain constant.

Another approach to solving the differential equation is to eliminate the pumping term by setting S = 0. This is accomplished by removing all pumps from the system. The equation then reduces to $Q = Vdp/dt$. Graphically measuring the slope of a curve of pressure vs time and multiplying this by the volume of the system gives the value of Q. This is called the "rate-of-rise" method. While this is a popular technique, its users generally do not rigorously satisfy the condition that S = 0. First of all, the measurement of dp/dt requires a gauge in the system, and most gauges used have a non-zero pumping speed. A second problem introduced by the gauge is that of gauge outgassing which was described above. If an ion pump is used on the system it must be valved off, because simply turning it off does not stop its pumping action.

The most serious problem in the use of this method is that of re-adsorption of desorbed gases. This action can be observed qualitatively by considering a simple, Henry's-Law type of model. As the pressure rises in the system following the removal of all pumps, the equilibrium gas coverage on the surfaces will increase. In this model the surface coverage, σ, is equal to the residence time of the gas atom on the surface, τ, times the arrival rate at the surface from the gas phase, ν. The arrival rate is:

$$\nu = 3.5 \times 10^{22} \frac{p\gamma}{(MT)} \; 1/2 \text{ molecules/cm}^2 \cdot \text{sec} \qquad (6)$$

where:

M	=	molecular weight of the gas
T	=	temperature of the gas
γ	=	sticking coefficient of the gas molecule on the surface

Thus, as the pressure increases, ν increases. Since $\sigma = \nu\tau$, the coverage on the surface increases. This means that the surfaces are acting as a pump and, as a result, the measured value of dp/dt is too low. Experimental comparisons of the rate-of-rise method with other methods of measuring outgassing rates have shown this technique to give lower values[4].

A third method that has been used to measure outgassing rates involves the substitution of a known leak for the sample[5]. As shown in Figure 2, the sample is connected through a valve to a pumping system. On the pump side of the valve, a system is connected which can inject a leak of known flow rate into the system. There is also a pressure gauge on this same side of the valve. At any time during the pumpdown of the sample chamber, the valve can be closed after the pressure is noted,

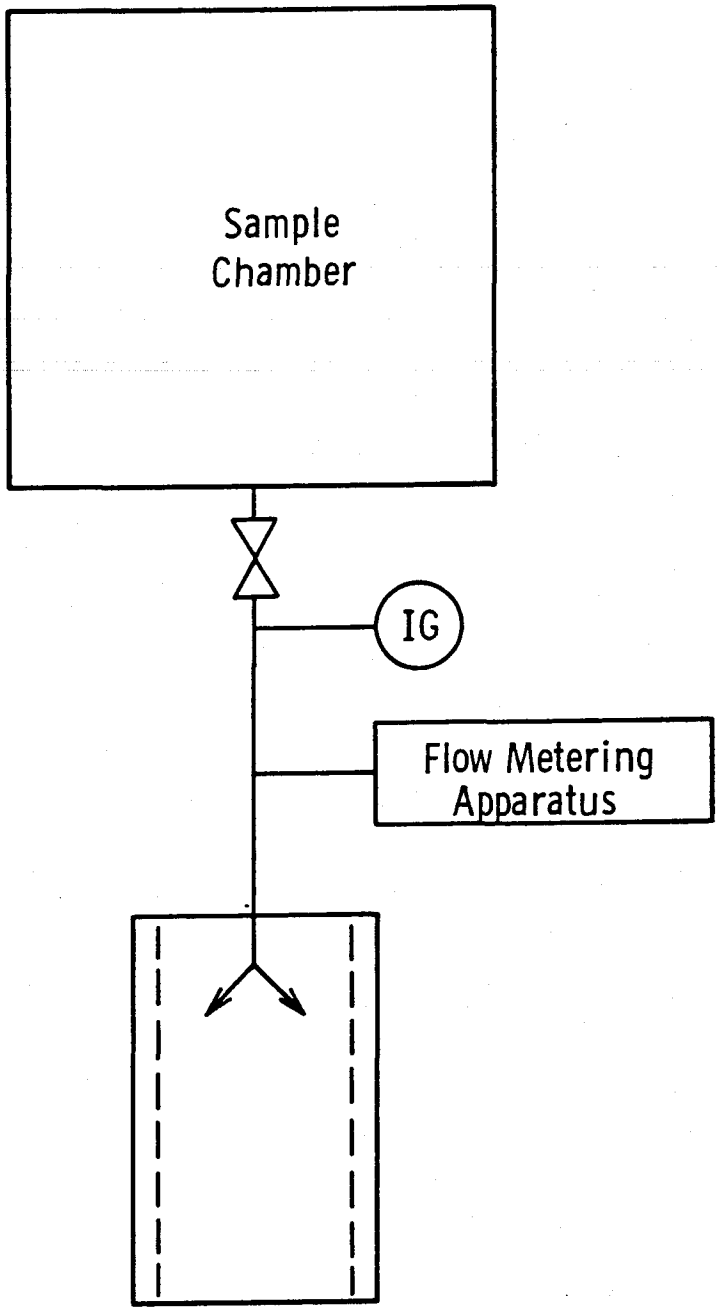

Figure 2. Schematic of System Using the Method of Substituting a Known Leak for the Sample

and the leak can be opened and adjusted so that the pressure is the same as it was with the valve open. When this pressure is matched, the flow rate is measured and this divided by the sample surface area gives the specific outgassing rate.

The difficulties encountered in this type of system are:

1. The accuracy of making flow rate measurements limits this method to measurement of relatively high outgassing rates.
2. To use this method properly would require that the composition of the leak gas be the same as that outgassing from the sample. During a pumpdown this composition is changing continuously. Therefore it would be extremely difficult to match.

B. REVIEW OF PUBLISHED RESULTS

The earliest published literature on measuring the outgassing rates of metals dates back only to 1956. However, since then extensive results on "total outgassing rates" have been published. By this, is meant rate measurements based on readings of total pressure gauges. Only since 1966 have results been presented on outgassing rates of the individual gas species present in a vacuum system. Papers have been presented and published by Kirkendall, et al[6], Calder and Lewin[7], Strausser[8,9], and Barton and Govier[10] concerning outgassing rates of each of the species of gas released from various types of stainless steel.

The reported values of total outgassing rates of copper, aluminum, and stainless steel will be given in this section along with a discussion of the results of Calder and Lewin and of Barton and Govier. The results reported by Strausser are included in the following section.

1. Copper

Five reports contained outgassing rates of copper. In all of these experiments the copper sample was enclosed in another container, thus allowing the problem of interactions with the enclosure walls.

In the paper of Kirkendall, et al, measurements were made on copper samples that were dropped into an oven which had been pre-heated to temperatures in the range of 500°C to 700°C. Outgassing rate measurements were then made for H_2, H_2O, $CO + N_2$, and CO_2 as a function of the pre-treatment of the copper sample. These pre-treatments included (1) degreasing and chemical polishing, (2) hydrogen firing, (3) vacuum firing, (4) oxidizing, (5) nickel plating, (6) gold plating, and (7) titanium coating. The most significant discovery of this investigation is that coating the copper with titanium reduces by a factor of 10 the total amount of gas released from a degreased and chemically polished sample. The amount of gas released from this titanium-coated sample was also significantly less than that from any other sample, except the vacuum-fired sample, which released about the same amount. Since these results were all taken at elevated temperatures, they are not included in the comparison of copper outgassing rates presented in Figure 3.

Basalaeva[5] obtained the results shown in Figure 3 using the method of replacing sample outgassing by a leak from a flow-measuring device. He has reported values for copper samples which were (1) untreated, (2) washed in benzol and acetone, and (3) scoured and washed in benzol and acetone. The data seem to have been taken only for the first five hours of the first pumpdown on each sample. The different pre-treatments result in a factor of about 100 difference in outgassing rates after five hours. These results are difficult to interpret and/or apply because:

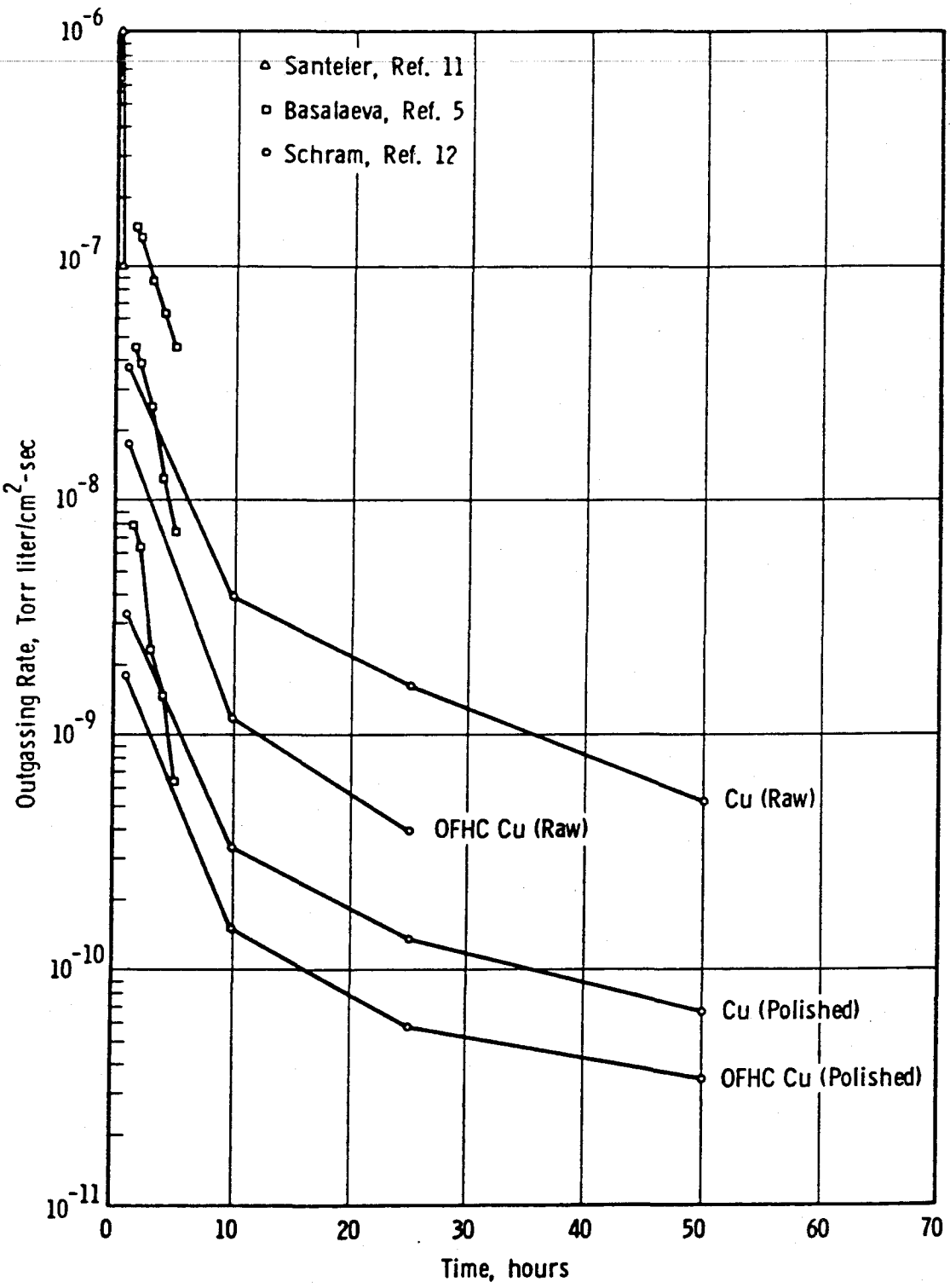

Figure 3. Compilation of Copper Outgassing Rates

1. Outgassing rates were measured only on the first pumpdown from air of each sample, and not after repeated pumpdowns and/or bakeouts.

2. Measurements were made only during the first five hours of a pumpdown.

3. Sufficient information is not given in the paper to place any limits on the accuracy of the measurement technique.

The results reported by Santeler[11] are of little practical importance because the duration of the measurements was limited to less than one hour and because he gives very little information about his experimental apparatus and technique.

The most useful results on outgassing rates of copper are those reported by Schram[12]. He used the system shown in Figure 4. By having two identical sample chambers on his system, one with a sample and the other one empty, he was able to make reasonable corrections for the outgassing of the enclosure wall and of the pressure-measuring devices. However, he still did not get around the problem of pumping of the gauging or the enclosure walls. Thus, he eliminated the sources of error which would tend to give him values that are too high, but not those that would lead to values that are too low.

He reported values of outgassing rates on the initial pumpdown of four samples. These consisted of (1) OFHC copper which was not pre-treated except for degreasing and wiping with ethyl alcohol (this was done to all four samples), (2) OFHC copper which was mechanically polished, (3) one of copper which was not OFHC and which was not pre-treated, and (4) one which was non-OFHC copper and was mechanically polished.

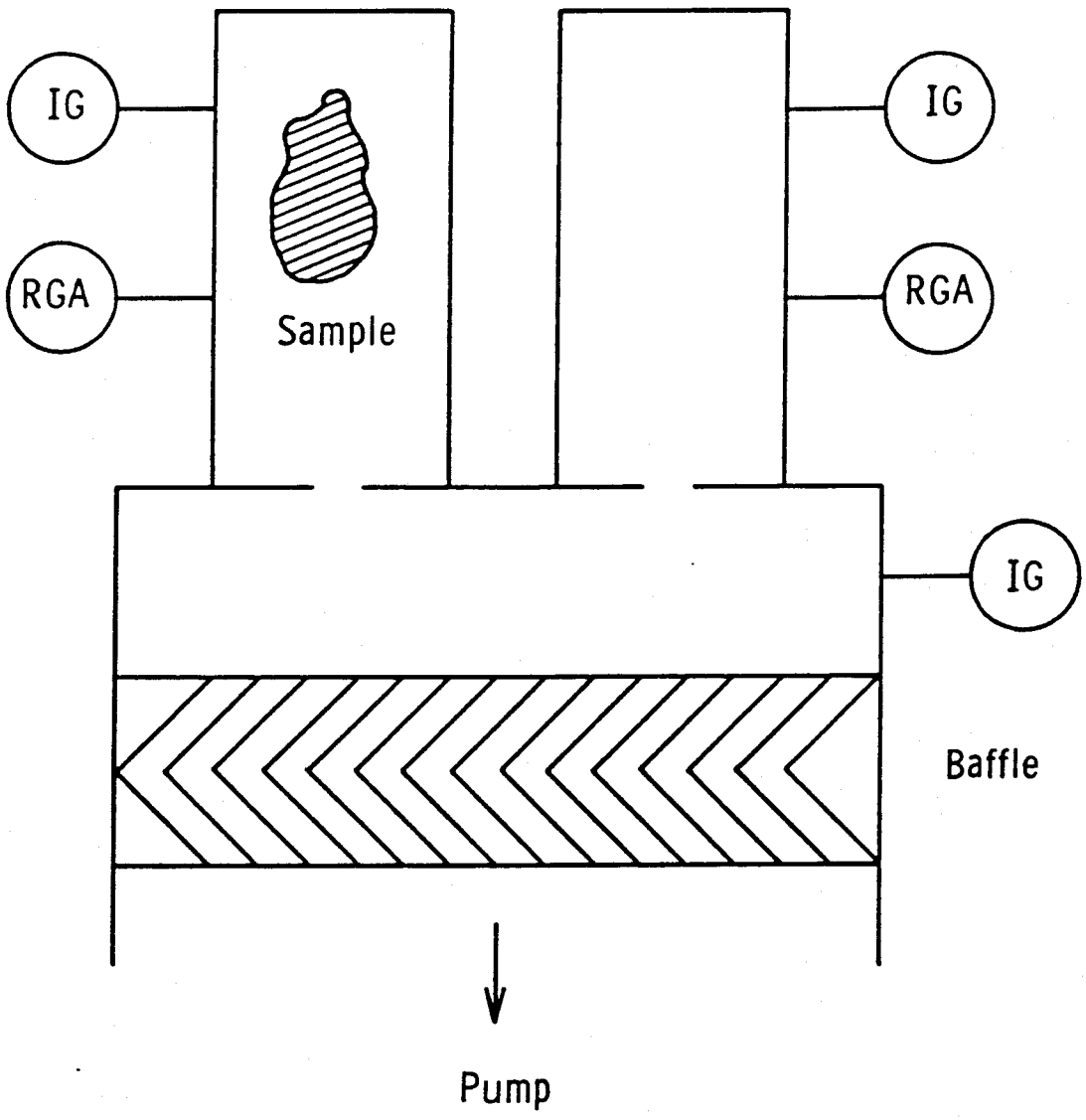

Figure 4. Schematic of System Used by Schram

These results are shown in Figure 3. Two influential factors are evident here. One is whether or not the copper is OFHC. The other is the effect of mechanical polishing. The OFHC copper has an outgassing rate 1/4 to 1/2 that of non-OFHC copper. Mechanical polishing results in improvement by a factor of 10. This effect of mechanical polishing is consistent with many other reports. It indicates that significant improvements in outgassing rates can be obtained by removing surface layers of the order of a few microns from many different materials as received.

2. Aluminum

Seven papers in the literature report results on aluminum. In three of these, the test sample is its own vacuum enclosure, while in the others a small sample is inserted into an enclosure of a different material. The results are shown in Figure 5.

The findings of Power and Robson[4] are the lowest values reported. This is, at first glance, somewhat inconsistent with the fact that they used a sample inside another enclosure. However, from the sketch of their experimental system, it appears likely that the gauge pumping in the sample enclosure is not insignificant compared to the conductance of the aperture to the pump. Furthermore, they state that outgassing rates based on rate-of-rise measurements (which they can take in addition to $Q = C\Delta p$ type measurements) are very much less than their reported values. This is a further indication that a significant amount of pumping takes place within the sample chamber. Power and Robson do not give enough information on their system to permit any evaluation of the results beyond these very qualitative observations.

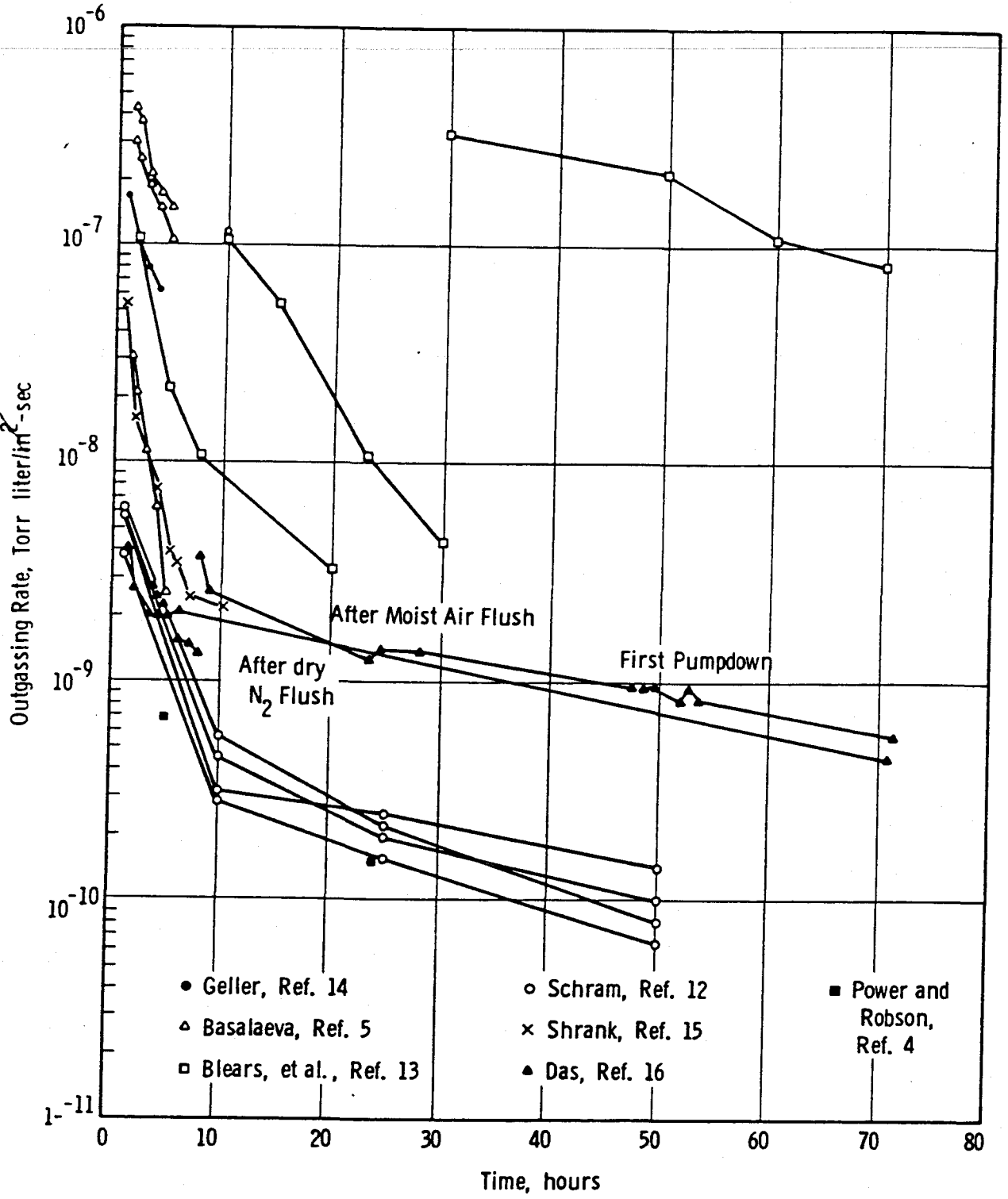

Figure 5. Compilation of Aluminum Outgassing Rates

The data of Blears, et al[13] is also difficult to evaluate because of the inadequate information on their system. Their measurements are made by "placing the sample in a pot which is pumped through a known conductance and measuring the pressure with a direct-insertion ion gauge." They used three samples of aluminum which were described only as "anodized and boiled", which gave the highest outgassing rates, "anodized", which was in the middle, and "bright rolled, cleaned in Stergene", which gave the lowest rates. The most interesting aspect of these results is the wide range of rates obtained with different pre-treatments.

Basalaeva, using the same system he used for his measurements on copper, also observed differences of orders of magnitude for different pre-treatments. The three samples he reported on were untreated Duralumin, which gave the highest values; Duralumin washed in benzol and acetone, which was in the middle; and Duralumin scoured and washed in benzol and acetone, which gave the lowest rates. The process of scouring, which is not described in any detail, was even more effective in reducing outgassing rates of aluminum than it was in the case of copper. The oxide layer, which is always present on aluminum unless it has been cleaned in high vacuum, has been reported to be very spongy and probably capable of holding large amounts of water vapor. The scouring reported by Basalaeva very likely removed this oxide layer from his samples. Although the layer would immediately begin to re-form on the surface, it was probably significantly thinner if he put the sample in a vacuum system soon after scouring.

Schram[12] also reported results on samples which had different pre-treatments. He used the same system that was described in the section on copper. His samples included one described as "fresh", one that

had been degassed for 24 hours, one that had apparently been degassed and then exposed to air for three hours, one that is described as "raw", and ten samples that had been anodically oxidized to different extents. The anodically oxidized samples all had considerably higher outgassing rates than any of the other four samples. At one hour the outgassing rates of the anodized samples ranged from 7 to 600 times those of the 24-hour degassed sample. At 10 hours the range was 3.3 to 400 times. He does not give rates for the anodized samples after 10 hours.

Figure 5 gives the data on the four samples that were not anodically oxidized and, for comparison, a point at 10 hours from the most severely anodized sample.

Schram's data on anodized aluminum are difficult to analyze in any depth, but some consistencies stand out. First, there is the thickness of the anodized layer. He used samples 2μ, 20μ, and 100μ thick. The rates for the 20μ anodized layers were about an order of magnitude higher than those of the 2μ anodized samples. The 100μ samples gave rates that are about a factor of 5 times those of the 20μ anodized samples. Thus, the outgassing rate is proportional to the thickness of the anodized layer.

A second correlation is with pore size. On samples with larger pore size, all other things apparently being the same, he obtained higher outgassing rates. A third comparison can be made on the basis of air exposure, although these results are not as consistent. On the samples with 2μ or 20μ thick oxide layers the outgassing rates were lower for those samples that were exposed to air for longer times than for those that were apparently inserted immediately into the experimental system. However, in the case of the samples with 100μ anodized layers, the long exposure to air resulted in higher outgassing rates.

The work of Geller[14] was done using the aluminum sample as the vacuum enclosure and doing a $Q = C\Delta p$ type measurement. He does not describe what pre-treatment, if any, his Duralumin sample had. His results are consistent with the other values reported, but due to the lack of information given on his samples and the short duration of his tests, one cannot draw any significant conclusions from them.

Shrank, et al[15] used a 5083-0 aluminum alloy chamber for their tests on a system using the rate-of-rise technique ($Q = V\ dp/dt$). They studied two samples. One was in an as-received condition. The other had been given a No. 4 finish by grinding the surface with 150-grit abrasive paper. They made only very short tests at room temperature because their main interest was in outgassing rates of chilled surfaces. Over a two-hour period the outgassing rate of the as-received surface was lower than that of the ground surface by a factor of about 5. Then a leak was found in the No. 4 finish tank and it was repaired as the test continued. The rates for the No. 4 finish tank then went below those of the as-received tank until they chilled the No. 4 finish tank at six hours. This was the only run they made on this chamber.

Das[16] measured the outgassing rates of a 6061-T6 aluminum alloy bell jar using the same system used by Shrank, et al. There is no discussion of the pre-treatment of the bell jar, except that he refers to it as a "rough-ground surface." He ran three pumpdown tests on the bell jar. The first was a pumpdown plus bakeout. The bell jar was then exposed to dry nitrogen; a second pumpdown and bakeout were run; the bell jar was then exposed to moist air; then the third pumpdown and bakeout were completed. The second run, after the dry nitrogen exposure, gave the lowest rates of the three, although there was not a significant difference among any of the three.

The main observation that can be made on these total outgassing rate measurements on aluminum, (aside from the large spread in values) is that the outgassing rate depends on the thickness of the oxide layer. In all cases, the outgassing rates are lowered by grinding or polishing away the naturally existing surface layers. They are increased by anodically oxidizing the samples. It is natural to assume, as some of these authors did, that oxidizing the aluminum would result in a more stable, passive surface on the aluminum and that this surface would then result in lower outgassing rates. And it is probably true that a slightly oxidized surface will give the lowest outgassing rates for aluminum. Certainly all the surfaces studied had some oxide coating on them. However, if the oxide layer is allowed or caused to grow, the porosity of this oxide film causes it to adsorb large quantities of gas, resulting in a marked increase in outgassing rates.

3. Stainless Steel

The outgassing rate data that have been obtained from stainless steel samples are summarized in Table 1 and plotted in Figure 6. Because of the variety of surface finishes and stainless steel types represented, it will be difficult to make meaningful comparisons with the stainless steel data even to the extent of observing trends as was done for copper and aluminum.

The data reported by Hoyt[17] while giving low absolute values, probably due to his use of the rate-of-rise technique and the pumping action of the gauge, allows intercomparisons of the various surface treatments. One important surface sample type that he did not include is a sample that is not treated or that is only degreased. On the basis of first pumpdown data, although he allowed the pumpdown to proceed only for

TABLE 1

Summary of Stainless Steel Outgassing Rate Measurements

Source	Material	Measuring Technique	Sample is Enclosure	Symbol on Figure 6
Hoyt Ref. 17	304 stainless steel - chemically cleaned electropolished hydrogen-fired chemically etched bead blasted	$Q = V\frac{dp}{dt}$ (rate of rise)	Yes	0
Schram Ref. 12	ICN 472 ICN 472 sand blasted NS 22S mechanically polished NS 22S electropolished NS 22S	$Q = C\Delta p$	No	ϕ
Reinath and Scalise Ref. 18	Stainless steel - cleaned by hot tricloroethylene bath, acetone rinse, and dried with cylinder nitrogen	$Q = Sp$	Yes	▲
Power and Robson Ref. 4	EN 58B electropolished	$Q = C\Delta p$	No	Θ
Das Ref. 16	rough ground 304 stainless steel	$Q = V\frac{dp}{dt}$	Yes	•
Schrank, et al. Ref. 15	304 ELC stainless steel - "as received" No. 4 finish	$Q = V\frac{dp}{dt}$	Yes	ϕ
Geller Ref. 14, 19	stainless steel - tricloroethylene cleaned and dried	$Q = C\Delta p$	Yes	▲

TABLE 1 (Contd)

Source	Material	Measuring Technique	Sample is Enclosure	Symbol on Figure 6
Basalaeva Ref. 5	untreated stainless steel	Substitution of calibrated leak	No	□
Blears, et.al. Ref. 13	steel, nickel-plated steel, rusty steel, shot blasted stainless steel	Q = Sp	No	 x
Power and Crawley Ref. 20	Ni plated steel Cr plated steel polished mild steel stainless steel	Q = CΔp	No	 +
de Csernatony Ref. 21	EN 58F stainless steel	Q = CΔp	Yes	■
Thibault, et al. Ref. 3	Z3CN 18-8	Oatley	Yes	Received too late to be included.

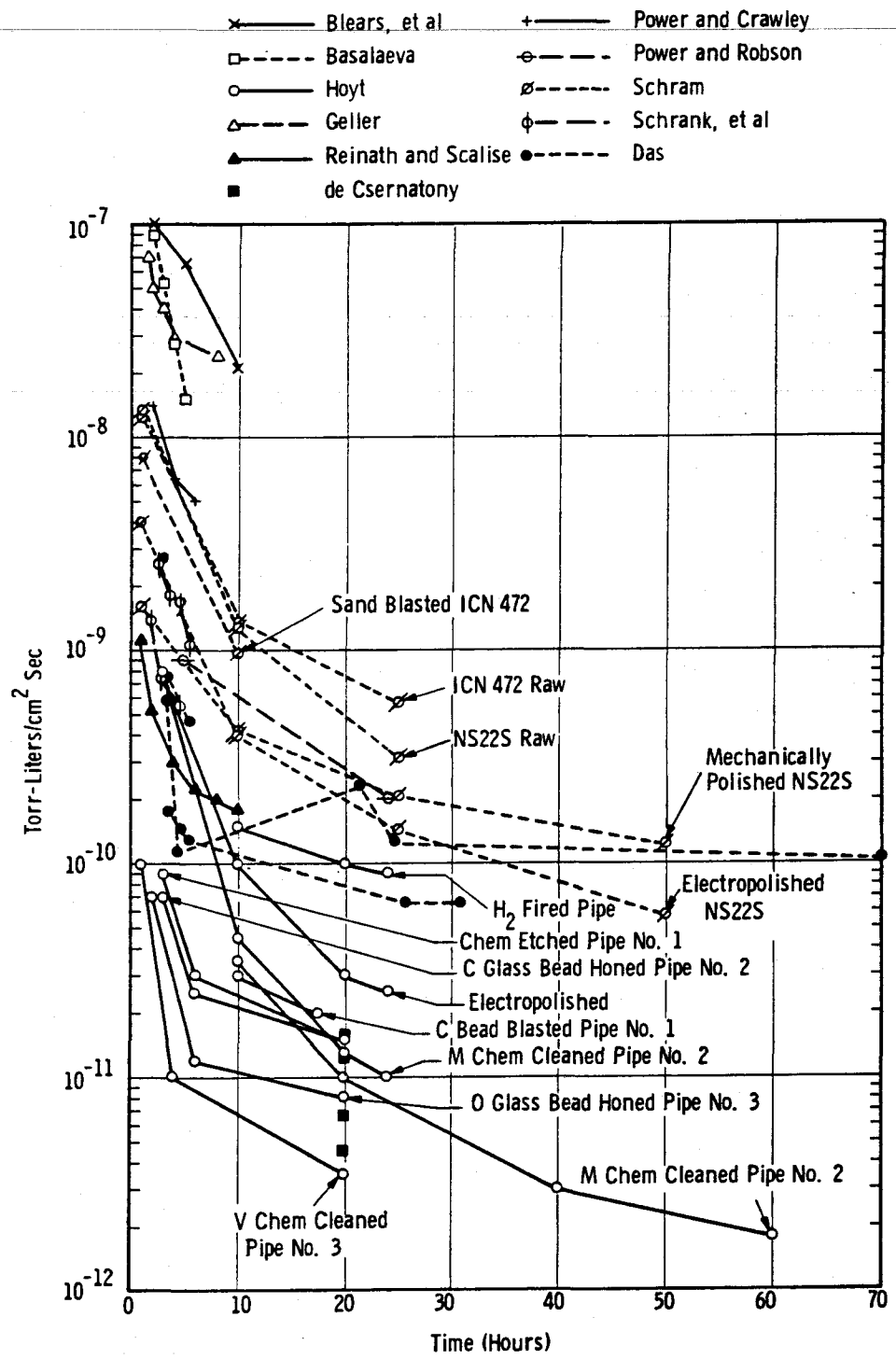

Figure 6. Compilation of Stainless Steel Outgassing Rates

24 hours in most cases, it appears that the samples cleaned by chemical cleaning only will show the lowest outgassing rates. The outgassing rates of the samples cleaned by chemical cleaning plus bead blasting start out quite low. But they do not decrease nearly as fast as those of samples that were only chemically cleaned. The chemically etched sample is in this same category. On the other hand, the electropolished sample and the hydrogen-fired sample always had higher rates than the chemically cleaned samples.

After the initial pumpdowns, Hoyt obtained data during and after 400°C bakeouts and subsequent air exposures. The results after bakeout and cooldown showed the hydrogen-fired and electropolished samples again the highest at 4×10^{-12} Torr-liters/cm^2 · sec. The chemically cleaned samples were at 1×10^{-12} and 5×10^{-13} Torr-liters/cm^2 · sec. The chemically etched sample and the bead-blasted samples were in the middle and low 10^{-13} Torr-liters/cm^2 · sec range.

After the initial pumpdown and bakeout, subsequent pumpdowns in all cases yielded lower outgassing rates whether the sample had been exposed to air or to nitrogen.* Hoyt even found that, after the initial pumpdown and 400°C bakeout, a subsequent pumpdown without bakeout brought the sample down to the same low outgassing rate after about four days. However, after the bakeout he found the outgassing rates extremely sensitive to temperature, with a temperature coefficient of outgassing of approximately 5×10^{-14} Torr-liters/cm^2 · sec · °C. This is, of course, to be expected from the thermal desorption rate (equation 18). The desorption rate is less sensitive to temperature for those gases with lower binding energies which represent the majority of the gas load prior to bakeout. However, after an effective bakeout

the only surface gases remaining would be those with somewhat higher binding energy. Their outgassing rates would be more strongly dependent on temperature.

Schram[12], using the system described above, measured rates for samples that were "raw", sand-blasted, mechanically polished, and electropolished. The data indicate again that treatments which remove a significantly thick surface layer result in lowered outgassing rates. The sand-blasted sample is better than a raw sample of the same type by about a factor of 2. The mechanically polished sample is better by a factor of 10 initially, although its rate of decrease in outgassing rate is not as large as that of the raw sample. The electropolished sample is only about a factor of 4 better initially, but its rate of decrease is comparable to that of the raw sample.

The results of Shrank, et al[15] also point to this effect. Their sample that was polished to a No. 4 finish gave results that are about a factor of 3 better than the as-received sample.

The remaining measurements that have been reported for stainless steel are included in Figure 6 but as they do not lead to any significant comparisons they will not be discussed further.

In terms of a model, the only obvious conclusion that can be drawn from the total outgassing rate measurements on stainless steel is that removing the naturally occurring surface layers from the material will reduce outgassing rates. This is, of course, the same conclusion that came from the copper and aluminum data. The only difference is that the effect seemed to be most pronounced with aluminum and least with stainless steel. The results on the anodically oxidized aluminum,

together with the fact that the naturally existing surfaces on all of these metals are oxide films, seem to indicate that this effect is related to adsorption on metal oxides.

Also, recent photographs of metal oxides and metal-oxide interfaces made with a scanning electron microscope[22] show that the surface area produced by the formation of oxides could easily increase, by an order of magnitude, the true surface area of these materials. A further indication of this relationship is that naturally occurring oxide films are thickest on aluminum and thinnest on stainless steel. This suggests the desirability of coating with a thin film of a metal whose oxide grows only a monolayer thick.

Schram has attempted measurements of the true surface area of metals using combinations of the point B, BET, and Kaganer methods[23]. His preliminary results gave values of f, (where f = true surface area/ apparent geometric surface area), which were ~2.5 for electropolished NS 225 stainless steel, ~200 for anodized aluminum (20μ oxide layer), and ~5 for untreated OFHC copper. These numbers are in the same order as the amount of improvement in outgassing rates that can be obtained by removing the as-received surface layers from these materials.

4. Results Which Give Rates on Each Species Present

R. Calder and G. Lewin at CERN conducted an investigation of the contribution of the diffusion process to the problem of hydrogen outgassing from stainless steel[7]. They first predicted, from the theory of diffusion in metals, the combinations of bakeout time and temperature that would be required to reduce to some desired value the room-temperature hydrogen outgassing rate of samples with a known initial

hydrogen concentration dissolved in the bulk. They then measured the outgassing rates from samples which had undergone a variety of bake-out treatments and essentially substantiated their predictions.

The system in which they made their measurements is shown in Figure 7. This is a $Q = C\Delta p$ type system in which the pressure gauge is an omegatron mass spectrometer. Rather than having two pressure-measuring devices, they used just one omegatron and valved it in alternately above and below the flow-measuring conductance. The sample is its own vacuum enclosure, although the outgassing rates that they are actually measuring include, in addition to the sample, two valves and some tubing.

Their samples were fabricated from "as-received" 2-mm-thick rolled U15C stainless steel which is a low-carbon 300-series stainless steel. Degreasing was the only cleaning treatment used.

A general result that they obtained is that, after what they term a normal bakeout (24 hours at 300°C), 99% or more of the desorbing gas is hydrogen which is outgassing at a rate of about 10^{-12} Torr-liters/cm^2 · sec It should be mentioned that they do not calibrate their omegatron but, rather, use the manufacturer's calibration figures.

A specific example of their results is shown in Table 2. This sample was baked for 25 hours at 300°C at four different times. Outgassing rates after each of these bakeouts are given for hydrogen, water vapor, carbon monoxide-nitrogen, oxygen, and carbon dioxide. Also, before each bakeout the sample was warmed up through a temperature ramp to determine the temperature dependence of the outgassing rates. The room temperature hydrogen outgassing rate can be seen to decrease after each successive bakeout. This agrees with the depletion of bulk

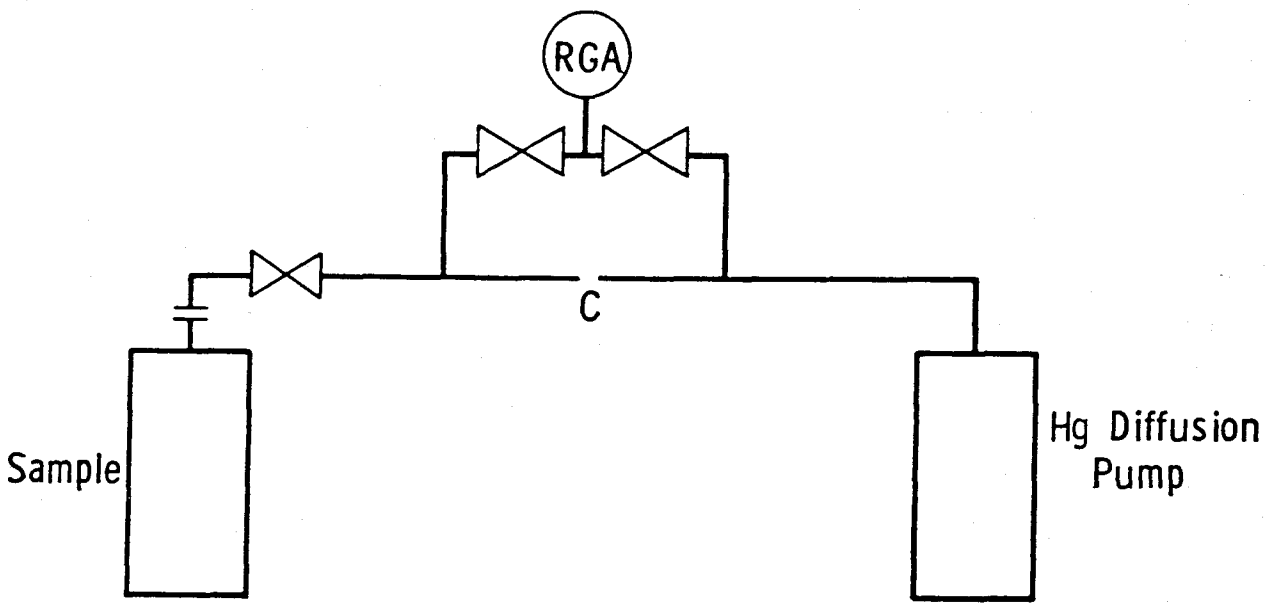

Figure 7. Outgassing Rate Measurement System Used by Calder and Lewin

TABLE 2

Outgassing Rates of 300 Series Stainless Steel According to Calder and Lewin

Specimen		Outgassing Rates, Torr-liters/cm^2 · sec				
Treatment	Temperature °C	H_2	H_2O	$CO-N_2$	O_2	CO_2
25 Hour Bake	300	---	---	---	---	---
	20	3.9×10^{-12}	---	1.7×10^{-14}	---	1.9×10^{-14}
Temperature Ramp	40	1.3×10^{-11}	---	---	---	---
	100	2.1×10^{-10}	1.3×10^{-13}	4.7×10^{-13}	1.8×10^{-12}	1.7×10^{-12}
25 Hour Bake	300	---	---	---	---	---
	20	3.0×10^{-12}	---	---	---	1.7×10^{-14}
Temperature Ramp	35	5.6×10^{-12}	---	---	---	2.5×10^{-14}
	53	1.6×10^{-11}	---	---	---	3.3×10^{-14}
	75	4.4×10^{-11}	4.6×10^{-14}	---	---	5.8×10^{-14}
25 Hour Bake	300	---	---	---	---	---
	20	1.5×10^{-12}	---	---	---	---
Temperature Ramp	47	5.3×10^{-12}	---	---	---	1.7×10^{-15}
	72	1.5×10^{-11}	---	2.8×10^{-14}	---	5.4×10^{-15}
	105	3.9×10^{-11}	---	6.3×10^{-14}	---	8.7×10^{-15}
	145	9.2×10^{-11}	3.1×10^{-13}	1.4×10^{-13}	---	1.0×10^{-14}
	200	2.5×10^{-10}	6.1×10^{-13}	2.6×10^{-13}	---	3.6×10^{-14}
25 Hour Bake	300	---	---	---	---	---
	20	1.2×10^{-12}	---	4.3×10^{-15}	---	---

hydrogen during the bakeout. Water vapor peaks appear only when the sample is heated. It is not clear why the mass 28 peak is present in the beginning of the tests, disappears in the middle, and reappears at the end. Oxygen is seen only during the first temperature ramp. Carbon dioxide disappears from the room-temperature rates very early in the testing and thereafter is present only during the temperature ramps and then in decreasing amounts. These gases are the only ones seen in the omegatron spectra.

The conclusions that can be drawn from this work are, first, that the relatively high hydrogen outgassing rate seen after bakeout comes from diffusion of hydrogen that is dissolved in the bulk of the stainless steel. Furthermore, it has been shown that by proper bakeout this source of hydrogen can be depleted to the point where its outgassing rate is less than 10^{-14} Torr-liters/cm^2 · sec. It also has been shown, as predicted by diffusion theory, that relatively thin samples of stainless steel can be thoroughly degassed by normal 300°C bakeout.

Barton and Govier[10] have studied the outgassing of small samples (4 cm^2 apparent geometric surface area) of 18/8/2 stainless steel. These were inserted into a small oven attached to the ion source of a mass spectrometer. The samples were pre-treated in various ways including (1) dry machining, (2) machining while using cutting fluid, (3) coarse machining while using cutting fluid, (4) electropolishing, (5) vapor blasting, and (6) baking in air at 450°C.

It is difficult to comment on their technique because their report does not describe the relationship between the ion current at the collector of the mass spectrometer and their reported outgassing rates. However, they must suffer from the problems involved in using a small sample inside a larger chamber.

The main value of these data is in the inter-comparisons that can be made between the different pre-treatments. The testing sequence used was to insert the sample into the oven, measure outgassing during a 450°C bakeout for 20 hours, remove the sample to atmosphere for 24 hours, re-insert the sample in the system, and measure outgassing rates during another 20-hour, 450°C bakeout. This allows a comparison on the basis of the total quantity of gas released from each sample during each of its two bakeouts. This is shown in Table 3. The total gas evolved is based on the ion source sensitivity for nitrogen. These data indicate that outgassing measurements made during first pumpdown and bakeout of samples can lead to numbers that are high by a factor of about 20. They also indicate that electropolishing is the most satisfactory cleaning treatment although machining using a lubricant is not much worse after the second pumpdown. Finally, these results again indicate a close connection between true surface area and outgassing rate.

TABLE 3

Outgassing Results from Barton and Govier[10]

Sample Pre-treatment	Surface Finish (μ inches)	Total Gas Evolved (Torr-Liters/cm^2) 1st Bake	2nd Bake
Electropolishing	14	247×10^{-5}	21×10^{-5}
Machining using cutting fluid	31	345×10^{-5}	32×10^{-5}
Vapor Blasting	36	290×10^{-5}	60×10^{-5}
Dry Machining	46	960×10^{-5}	68×10^{-5}
Baking in air at 450°C	78	310×10^{-5}	164×10^{-5}
Course machining using cutting fluid	160	1400×10^{-5}	80×10^{-5}

III. RESULTS OF WORK AT VARIAN

The above review of previous work lists a number of difficulties involved in the techniques that have been used in making outgassing rate measurements. In order to circumvent these problems a different method has been used in this study than in any of those previously described. The basic idea of this technique is to make a standard Q = cp measurement of the outgassing rate of a sample and then suddenly remove the sample from the system and measure the background pressures in the system which lead to most of the previously described errors. A schematic diagram of the system is shown in Figure 8. The procedure for measuring outgassing rates follows.

As the system is pumping down, the valve to sample Tank 1 is open and the valve to sample Tank 3 is closed. When an equilibrium pressure condition is reached between the sample and the gas sampling manifold (the section bounded by the three valves and containing the ionization gauge and the residual gas analyzer) a measurement is taken of the partial pressures of each of the gases present. The term equilibrium in this case means that the $V\frac{dp}{dt}$ term in equation (1) is negligible and that the pressure in the manifold is nearly equal to that in the sample. The valve to Tank 1 is then immediately closed and a second set of partial pressure measurements is made. The outgassing rate from the sample tank of each gas at that time is then equal to the partial pressure of that gas measured with the valve open minus the partial pressure of that gas that was measured with the valve closed, multiplied by the pumping speed for that particular gas. Thus, in essence we are making a standard Q = Sp measurement and applying a correction term to account for possible gauge outgassing, pump backstreaming, or other such effects.

As the system pumps down this same process can then be repeated for the other sample tank. As this is repeated throughout the pumpdown, the total pressure

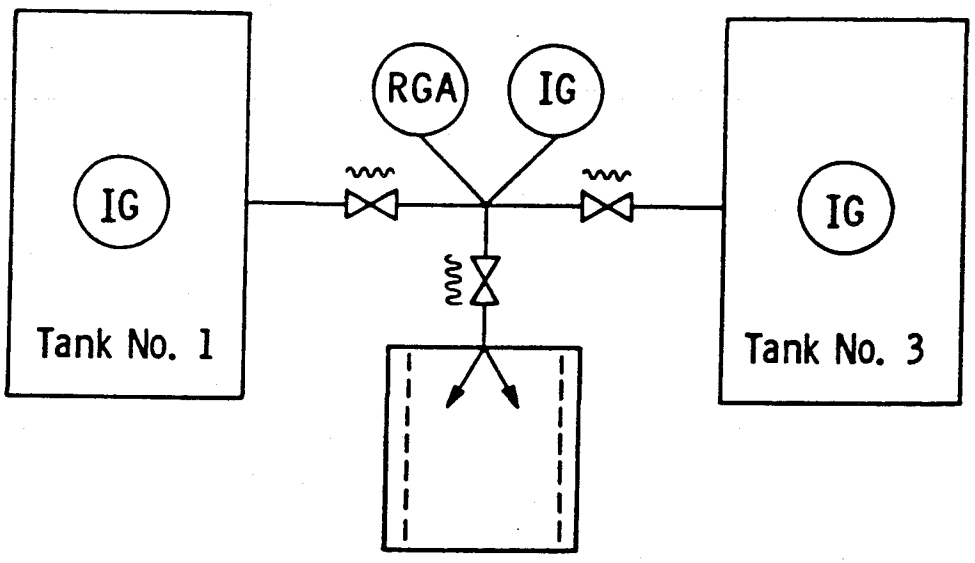

Figure 8. Schematic View of Experimental System

output from the manifold ionization gauge is of the form shown in Figure 9. Partial pressure measurements are made just before and just after each valve closure, resulting in one measurement of outgassing rate for each time a valve is closed.

There are certain aspects of this type of system that must be carefully considered when using this technique or the resulting data. These aspects include the pumping speed of the pump, calibration of the partial pressure measuring device, the method of data acquisition and analysis, and the preparation of the samples and the relation of their size to the available pumping speed.

A. PUMPING SPEED

The pump used in these measurements is a 500 liter/second diode-type sputter-ion pump. In order that the pumping speed would be known for all gases throughout the pressure range of the pumpdown, the pump was conductance-limited to 5.5 liters/second nitrogen speed at the gas sampling manifold. Thus, a constant speed could be used for each gas in the outgassing rate calculations throughout the pumpdown. In order to see that the speed at the gas sampling manifold is the proper one to use, instead of that at the sample tank, the following set of equations can be written. Letting the subscript 1 refer to quantities at the sample tank and 2 refer to quantities in the manifold, the outgassing rate in the tank at equilibrium with the valve open is,

$$Q_1 = S_1 p_1 \tag{7}$$

and that of the manifold is

$$Q_2 = S_2 p_2 - Q_1 \tag{8}$$

since the gas being released from the tank goes into the manifold. With the valve closed this becomes

$$Q_2 = S_2 p_2' \tag{9}$$

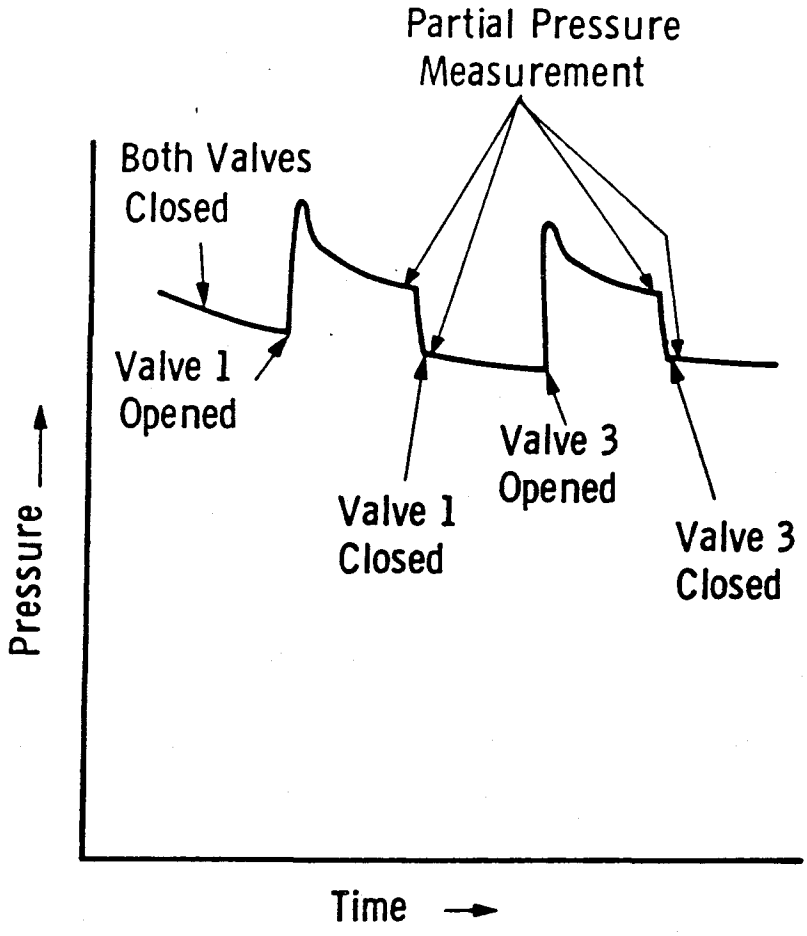

Figure 9. Form of the Pressure-vs-Time Curve

where the prime indicates the condition that the valve is closed. The outgassing rate of the sample tank is then found from

$$Q_2 = S_2 p_2' = S_2 p_2 - Q_1$$

$$Q_1 = S_2 (p_2 - p_2'). \qquad (10)$$

This equation must be solved for each gas present.

The pump is so strongly conductance-limited that this technique is a $Q = C\Delta p$ type measurement even though the pressure on the pump side of the conductance is not measured. Since this is of the order of a 1% correction for all but the rare gases, it is possible to neglect it.

Another possible source of error is the pumping or conversion speed of the hot filaments of the ion gauge and the quadrupole mass spectrometer, and of the hot surfaces around them. For some gases, particularly oxygen, this could be significant, possibly as high as 1 liter/second. However, since the system is calibrated in-situ for each gas of interest the calibration factors include a correction for this effect.

B. CALIBRATION

If accurate partial pressure measurements are to be made on the system, then accurate sensitivities must be available for each gas of interest. To obtain these values the Varian quadrupole mass spectrometer was calibrated, in place in the system, on each gas for which outgassing rates were calculated. These values include sensitivities in amps at the collector/Torr of pressure at the ion source for each peak of importance in the cracking pattern of each of the gases.

The calibration was done by attaching a flow measuring device onto the gas sampling manifold in place of one of the sample tanks. One-by-one each gas of interest was then leaked into the manifold which was pumped through a known

conductance. The true pressure of the gas in the manifold could be calculated by measuring its flow rate. The height of each of the peaks in the spectrum was then measured and divided by the calculated pressure in the system to give the quadrupole sensitivities. At the same time the output of the Bayard-Alpert Gauge was recorded and its sensitivities were calculated. This procedure was repeated several times for each gas. Table 4 lists the average values obtained for each of the gases studied. The pressures that were produced in the manifold were in the range from 10^{-5} to 10^{-8} Torr and were varied through this range on different runs on each gas. All of the measurements were made at a fixed resolution setting on the quadrupole which correspond to a resolution of 70 at mass 44.

These calibration runs were made with the bakeable valve between the pump and the manifold removed and replaced by an aperture whose conductance could be calculated. After the calibration of the quadrupole was completed the aperture was removed and the valve replaced. Another set of calibration runs was then made except that the quadrupole sensitivities were considered as known and the pumping speed at the manifold was solved. This was 5.5 ℓ/s (nitrogen).

C. DATA ACQUISITION AND ANALYSIS

The raw data that are produced by this system consist of mass spectra taken before and after each valve closure during the pumpdown. The difficulties encountered in acquisition are first of all the voluminous amount of information that is produced and therefore the time involved in reducing it and, secondly, the need for wide dynamic range in the measuring system. The initial set up was as follows: The quadrupole output was fed into a Keithley 416 electrometer. To obtain dynamic range, the electrometer range was switched manually whenever possible. The output signal from the electrometer was fed into three parallel strip-chart recorders, each operating at a different sensitivity. After the experiment each of the three stacks of recorder paper was scanned visually and the heights of the important peaks in the mass spectra

TABLE 4

Quadrupole Mass Spectrometer Sensitivity (Amps/Torr)

and Bayard-Alpert Gauge Factor F, where

$$F = \frac{P_{true}}{P_{indicated}}$$

Gas / m/e	H_2	He	CO	N_2	CH_4	H_2O	O_2	C_3H_8	A	CO_2
1	4.48×10^{-8}				1.76×10^{-7}	6.58×10^{-7}		1.13×10^{-7}		
2	6.40×10^{-6}	5.63×10^{-8}			2.66×10^{-7}	3.59×10^{-7}		3.54×10^{-7}		
4		4.66×10^{-6}								
12			8.00×10^{-7}		5.52×10^{-7}			1.30×10^{-7}		1.44×10^{-6}
14			2.04×10^{-7}	1.92×10^{-6}	2.72×10^{-6}			4.93×10^{-7}		1.72×10^{-7}
15					1.49×10^{-5}			1.18×10^{-6}		
16			3.38×10^{-7}		1.82×10^{-5}	6.69×10^{-7}	1.91×10^{-6}			2.42×10^{-6}
17						5.40×10^{-6}		9.27×10^{-8}		
18						2.21×10^{-5}				
20									6.61×10^{-6}	
22										6.99×10^{-7}
28			4.20×10^{-5}	3.97×10^{-5}						1.24×10^{-5}
32							2.73×10^{-5}			3.01×10^{-7}
39								6.41×10^{-6}		
40								1.45×10^{-6}	6.41×10^{-5}	
44								1.00×10^{-5}		6.64×10^{-5}
F	3.03	7.78	1.24	1.34	1.00	1.35	1.56	0.47	1.07	1.17

were recorded. These values were then punched onto IBM cards for analysis by a cracking pattern analysis program. This was obviously a very time-consuming procedure when many data points were attained during a pumpdown.

The data acquisition system has been improved to operate as follows: The quadrupole sweep voltage is obtained externally from a voltage divider network. A stepping switch drives a series of mercury-wetted relays which transmit the voltages produced in the voltage divider network into the quadrupole. Each of the voltages is set to correspond to the correct sweep voltage for one of the important peaks in the mass spectrum. Therefore, as the stepping switch moves from one relay to the next the sweep voltage in the quadrupole jumps the quadrupole from the top of one peak of interest in the mass spectrum to the next. In this way the unnecessary information in the mass spectrum is eliminated.

The output of the quadrupole at the top of each of these peaks is fed into an EG & G digital, autoranging picoammeter. This device measures currents from 10^{-14} amps to 10^{-2} amps while automatically changing its range and polarity as required. The output from the EG & G is BCD data which goes through a Varian coupler and into a teletype machine which prints the peak height values and simultaneously punches them on paper tape.

For analysis of the data the peak height values are inserted in a computer program which does a cracking pattern analysis on them and, using the calibrated sensitivities for the quadrupole, prints out true values of partial pressure of each gas of interest on either side of each valve closure. The partial pressures after each valve closure are then subtracted from the corresponding one before the closure and outgassing rates are calculated for each gas at that time.

D. SAMPLES

The samples that we have used are standard 18" o.d. x 30" long stainless steel bell jars. They are 304 or 304L stainless steel and are fabricated like those supplied on Varian vacuum systems except that end plates are welded onto both ends instead of just one. These bell jars have two 6" o.d. x 4" i.d. ports attached to ConFlat® Flanges. A 1-1/2" bakeable valve and a Varian nude ionization gauge are attached to one port. The other port is attached to the gas sampling manifold and the pump.

The apparent geometric surface area of a sample is 1.40×10^4 cm^2 (as opposed to the true surface area which would include the extra area which results from surface roughness). There is a small transition between the tank and the valve on the gas sampling manifold which goes from a 6" o.d. ConFlat Flange to a 4-1/2" o.d. ConFlat Flange. In cases where this part is not treated in accordance with the sample under investigation it represents about 329 cm^2 of untreated surface area or 2.3% of the total area.

One aspect of this system that is not comparable to a standard vacuum system is the ratio of the pumping speed to the surface area of the sample. In this system it is 5.5 liters/second/1.4×10^4 cm^2 or 3.9×10^{-4} liters/second $\cdot$ cm^2. In a more typical vacuum system it would be about 100 times this value. Thus, in comparing this system with a "standard" one the only significant difference is that at the same time from beginning of pumpdown this system will have a pressure that is about 100 times as high as the "standard" system. The effect that this would have on outgassing rates then would be to change the ratio, R, of the number of molecules arriving at the surface/cm^2 $\cdot$ sec to the number/cm^2 $\cdot$ sec leaving the surface due to outgassing. The arrival rate ν is,

$$\nu = 3.51 \times 10^{22} \frac{p}{(MT)} \, 1/2 \text{ molecules/cm}^2 \cdot \text{sec} \quad (11)$$

The outgassing rate is (from equation 10):

$$q = \frac{S}{A}(p_{open} - p_{closed}) \times 3.2 \times 10^{19} \text{ molecules/cm}^2\text{sec} \quad (12)$$

where S = pumping speed at the manifold for the gas of interest

A = surface area of sample in cm^2

p_{open} = partial pressure of gas of interest when valve to gas sampling manifold is open

p_{closed} = partial pressure of gas of interest when valve to gas sampling manifold is closed.

We then have

$$R = \frac{\nu}{q} = \frac{3.51 \times 10^{22}}{3.2 \times 10^{19}} \quad \frac{Ap}{S\ \Delta p(MT)^{1/2}} \quad (13)$$

where $\Delta p = p_{open} - p_{closed}.$ (14)

For nitrogen at room temperature,

$$R = 1.1 \times 10^{3} \left(\frac{\lambda}{S}\right)\left(\frac{p}{\Delta p}\right) \frac{1}{(28 \times 300)^{1/2}} \quad (15)$$

for this system,

$$\frac{A}{S} = 2.55 \times 10^{3} \quad (16)$$

and therefore,

$$R = 3.06 \times 10^{4} \left(\frac{p}{\Delta p}\right). \quad (17)$$

In a typical experiment $\left(\frac{p}{\Delta p}\right)$ varies from about 1.1 to 50 and thus R varies from 3.4×10^{4} to 1.5×10^{6}. The "standard" system would then exhibit a variation in R from 3.4×10^{2} to 1.5×10^{4}. Thus, in either case the arrival rate is >> the outgassing rate. For this reason it should then be safe to assume that this is not an important difference from a typical system.

E. EXPERIMENTAL DIFFICULTIES

In using this system in the measurement of outgassing rates four problems were encountered that are of particular interest.

The first of these is the outgassing from the gas sampling manifold. This is corrected by measuring pressures both before and after the sample tank is closed and then using the pressure difference in calculating outgassing rates. However, when the system is at very low pressures the outgassing of the hot filaments of the ionization gauge and the quadrupole mass spectrometer frequently represents 90% to 99% of the total pressure of some or all of the gases present. Thus, the pressure variation on closing the valve may be in the noise on the quadrupole output. This effect invariably occurs after a bakeout even when both gauges are degassed at the end of bakeout.

A second problem that occurs in the use of this system is a result of using two sample tanks simultaneously. In order to avoid exposing either tank to the outgassing from the other tank we do not open both of the sample valves at the same time. As a result each tank is open to the pump slightly less than half of the total time during pumpdown. This then causes difficulties when plotting outgassing rates vs time. The problem is whether the time used should be just that which the tank has been open to the pump or whether it should be the total time of the experiment. Since this problem has not been resolved the reference tank will not be used in most of the future work on this system.

The third problem area is the accuracy required in the quadrupole calibration data and in electron multiplier gain values. The electron multiplier gain value problem is particularly serious since the gain for each gas is continually changing and since it is quite inconvenient to measure multiplier gain values along with each outgassing rate measurement.

The accuracy required in the quadrupole sensitivities is not that desired in the final data. For example, if the hydrogen contribution to the mass 2 peak is 1% of the total peak height then the cracking pattern used for water vapor must be accurate to better than 99% or you may not see any hydrogen. The same is true for nitrogen and carbon monoxide which can be masked by the cracking patterns of CH_4, CO_2, or C_3H_8.

The fourth difficulty that was observed is a result of trying to measure total pressures in the sample tanks during the experiments. During some of the initial work with the system the partial pressures in the gas sampling manifold were measured while turning an ionization gauge on and off in the sample tank. In doing this, the gauge contributed significantly to the hydrocarbon peaks in the 39 to 44 range. Since that time the ionization gauge has not been used in the sample tank.

F. RESULTS

Results have been obtained thus far on samples which were cleaned by: (1) only degreasing, (2) the standard cleaning given to Varian vacuum systems, and (3) a sample tank cleaned by the Diversey DS-9 cleaning treatment. This section will discuss these results.

1. Standard Cleaning

The first effort in the experimental work was to establish the outgassing rates resulting from our standard cleaning treatment as the other treatments will then be compared with this system. The standard cleaning treatment for 304 stainless steel consists of:

1. Vapor degreasing in trichlorethylene,
2. Cleaning in Oakite,
3. Hot water rinse,

4. 33% HNO_3, 33% HF, 33% H_2O bath, by volume at room temperature,
5. H_2O rinsing, dry, and bag.

Figures 10 and 11 show results obtained with this cleaning, except that the acid bath had only 2% HF, which was the standard cleaning used until July 1967. These results are for a pumpdown plus a 12-hour bakeout to 300°C. The sample tank had thermocouples mounted on it and a temperature-vs-time curve obtained from one of them is shown in Figure 12. It can be seen that during the bakeout the large fluctuations in outgassing rates correlate with fluctuations in temperature.

This particular run is the first one that was made on this system and at that time the heating was done by strip heaters mounted on the side of the sample tanks. The tanks were then wrapped with aluminum-coated fiberglass. As a result of the problems encountered on this run with temperature variations, both over the sample at a given time and at a given point on the sample with time, we have since constructed an oven which encloses the gas sampling manifold and the samples.

The results obtained with the oven used for a 150°C bake for 24 hours are shown in Figures 13 and 14. This sample was given the presently used standard cleaning. The significant improvement in the quality of the data is attributable to two things. First, the improved temperature control afforded by the oven and, second, the better data acquisition system described previously.

A significant improvement can be seen in the outgassing rates of certain gases when comparing the results of the 2% HF cleaning with those produced by the 33% HF bath. Comparisons can only be made with the pre-bakeout data, but there are obvious differences even here.

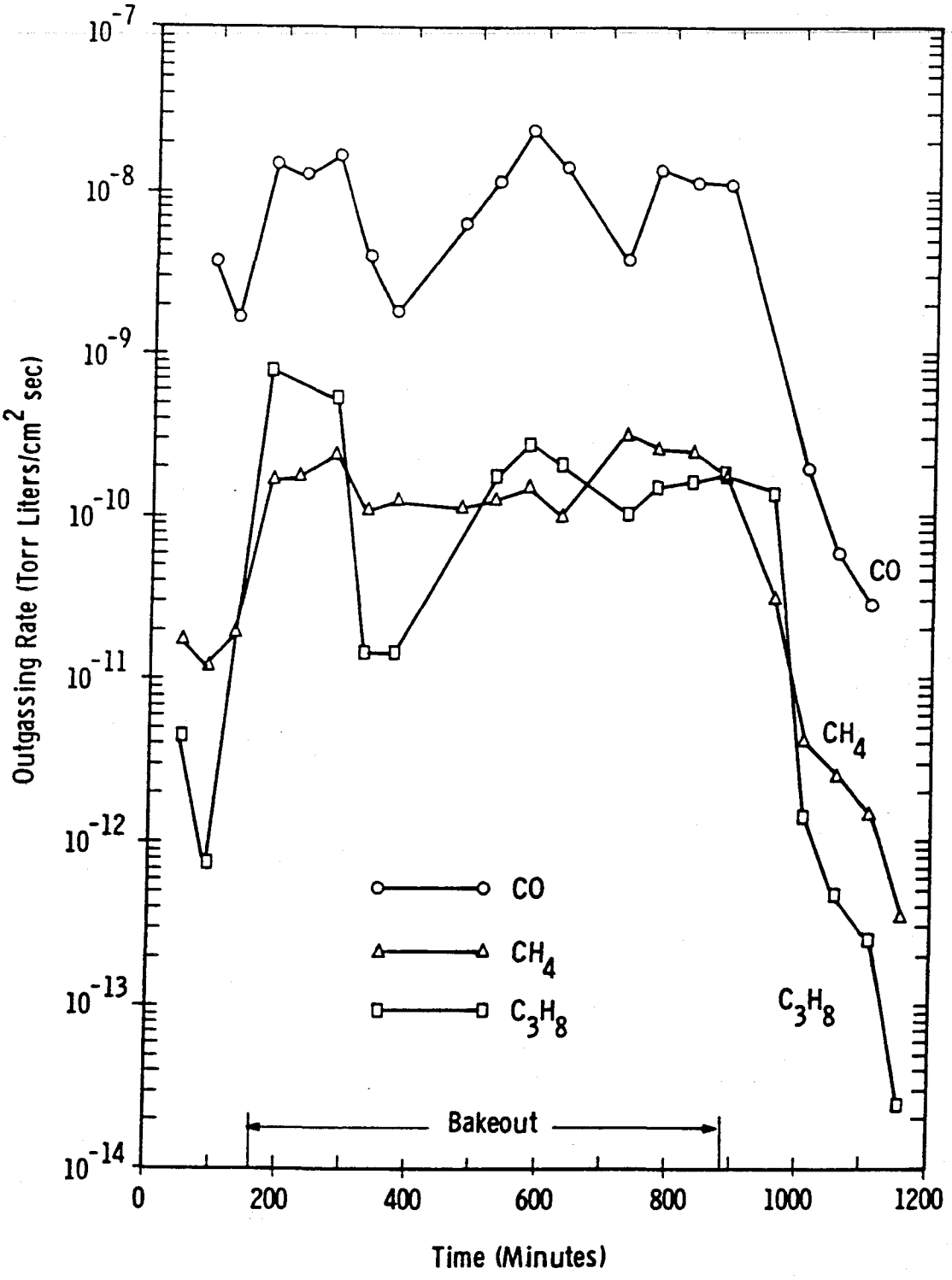

Figure 10. Outgassing Rates for CO, CH_4, C_3H_8 from Sample with 2% HF Cleaning

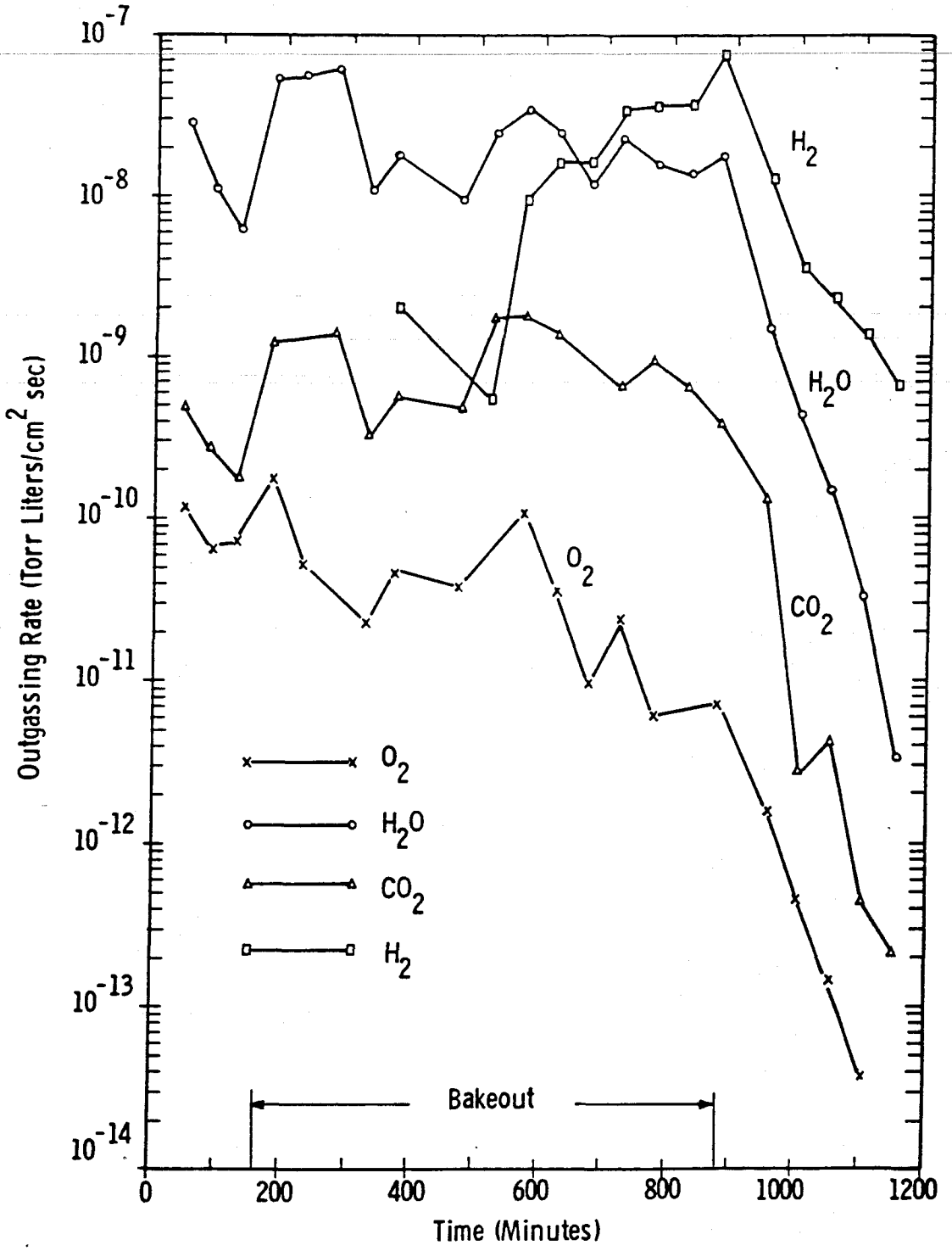

Figure 11. Outgassing Rates for H_2, H_2O, CO_2, O_2 from Sample with 2% HF Cleaning

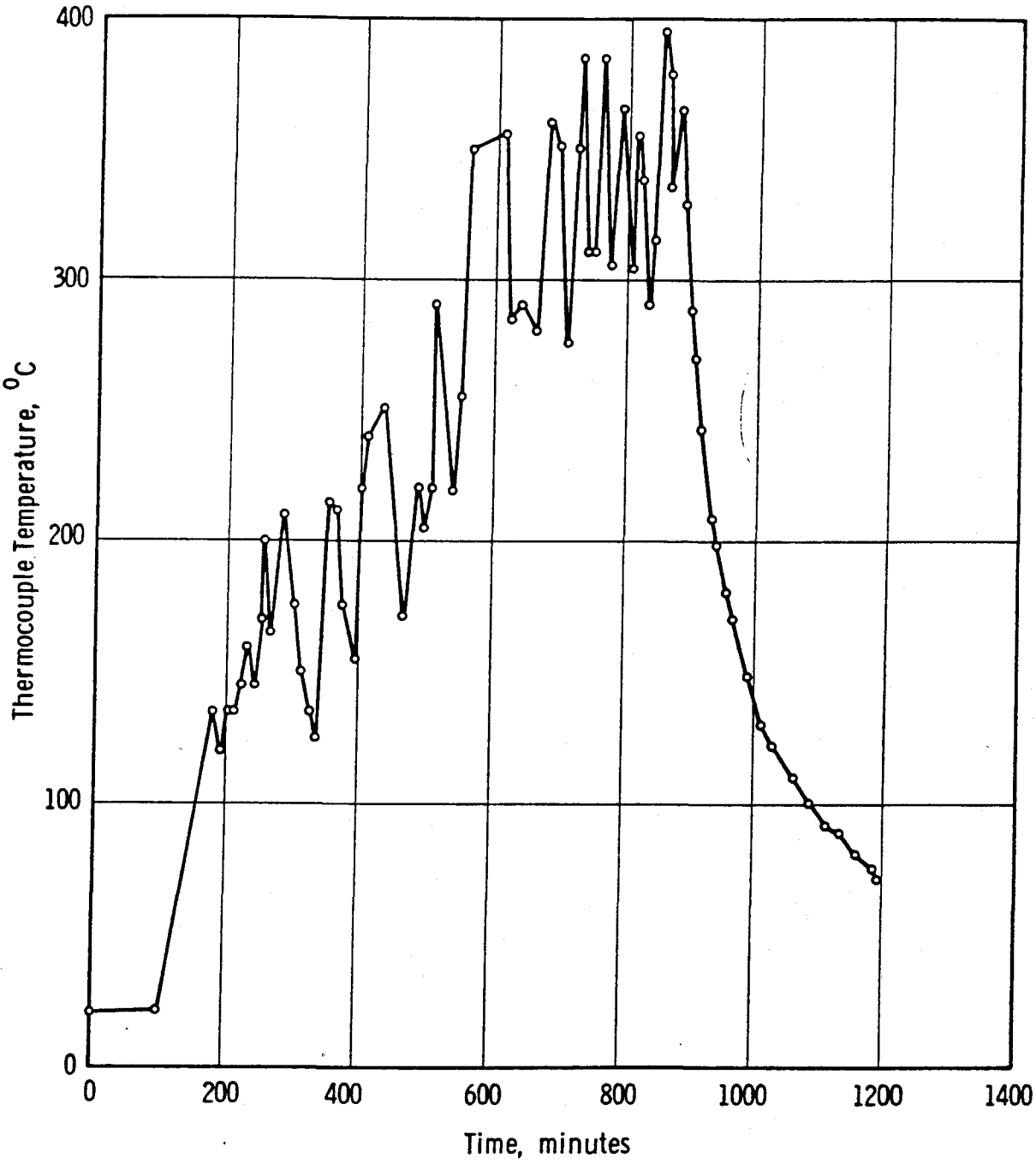

Figure 12. Temperature Variation During Bakeout of 2% HF Cleaned Sample

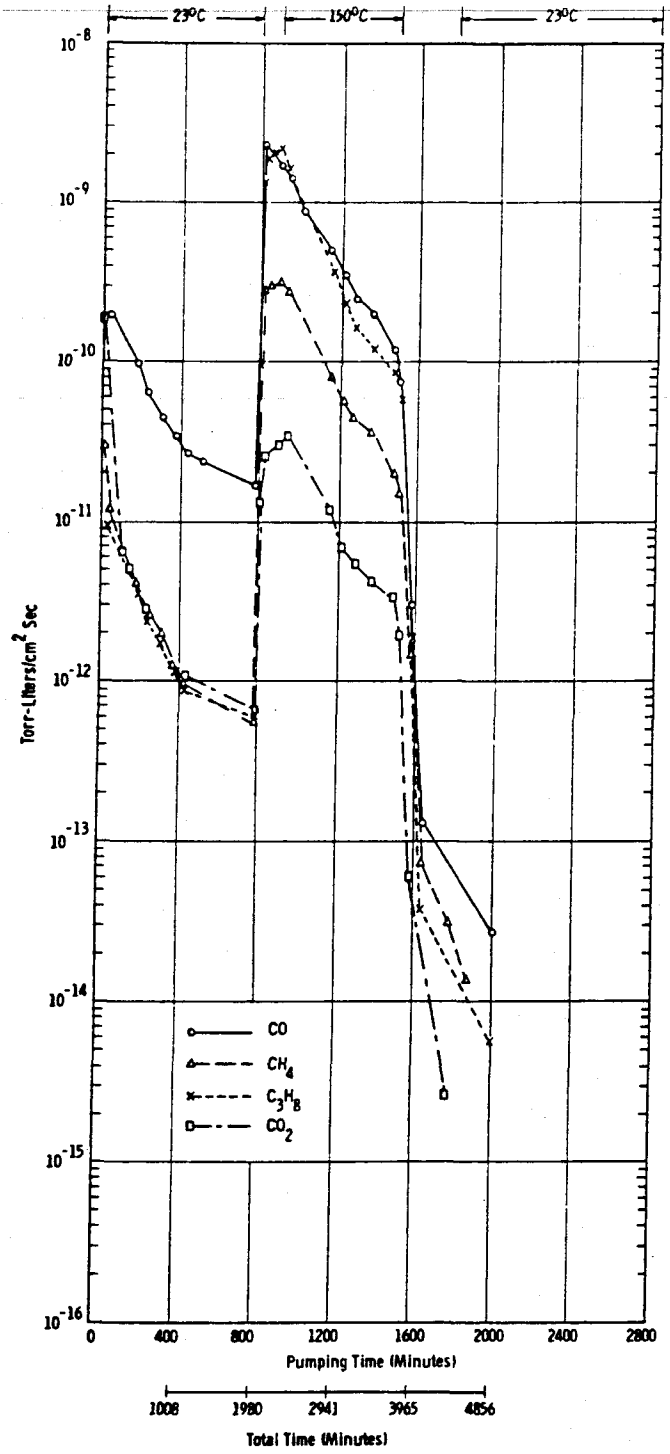

Figure 13. Outgassing Rates for CO, CH_4, C_3H_8, CO_2 from Sample with 33% HF Cleaning

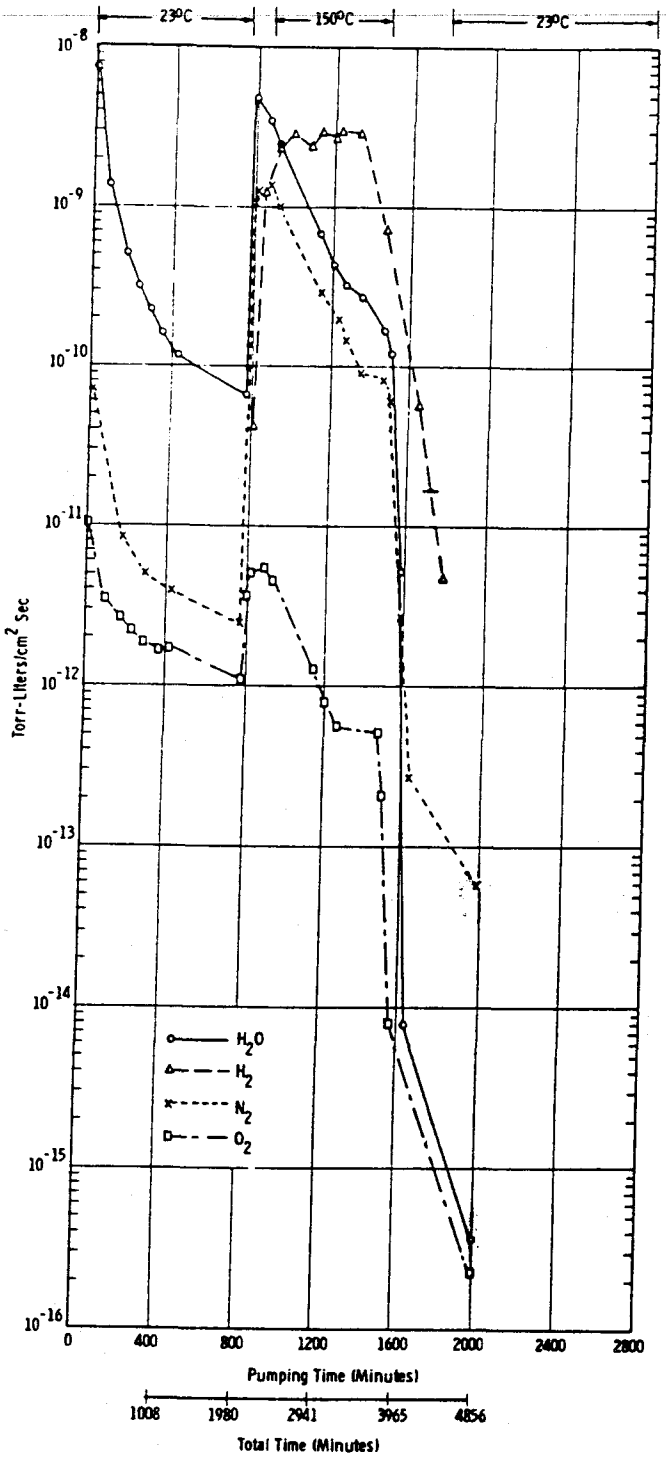

Figure 14. Outgassing Rates for H_2O, H_2, N_2, O_2 from Sample with 33% HF Cleaning

At ~100 minutes into the pumpdowns the following comparison can be made:

TABLE 5

Outgassing Rates

Gas	With 2% HF Cleaning	With 33% HF Cleaning
H_2O	9.8×10^{-9}	1.4×10^{-9}
CO	3.2×10^{-9}	1.8×10^{-10}
CO_2	2.5×10^{-10}	1.0×10^{-11}
O_2	6.7×10^{-11}	3.5×10^{-12}
CH_4	1.4×10^{-11}	1.1×10^{-11}
C_3H_8	7.4×10^{-13}	8.7×10^{-12}

Thus, except for the hydrocarbons, there is about a factor of ten improvement in using the newer cleaning solution prior to bakeout. In the pre-bakeout period all of the samples tested have shown water to be the most significant component in the desorbing gas, ranging from ~75% in the case of the 2% HF cleaning to ~95% in the case of DS-9 cleaning. Similarly, carbon monoxide has always been the second most significant component. It is interesting to note that even in the early stages of pumpdown the ratios of the various outgassing components are not what would be expected from the standard atmospheric composition. Obviously, what is important is the relative binding energies of the different molecules on the surface and not their relative concentrations. This can be seen from the desorption rate equation for thermal desorption,

$$\frac{d\sigma}{dt} = \nu_o, \sigma_o \; \Theta^n e^{-E_D/kT} \qquad (18)$$

where

σ = surface coverage in molecules/cm^2

ν_o, σ_o are constants

Θ = σ/σ_o

n = order of the desorption process

E_D = energy required for desorption

k = Boltzmann's constant

T = temperature of the surface.

Thus, the desorption rate is only proportional to the nth power at the relative surface concentration, where n is 1, 2, or at most 3, and is exponentially proportional to the surface binding energy.

Also of interest in the pre-bakeout period is the fact that no hydrogen outgassing is observed. As pointed out previously the minimum hydrogen outgassing rate that could be observed is determined by the accuracy of the cracking pattern sensitivity data for the quadrupole mass spectrometer. If the sensitivities that were used were accurate to within 10%, a hydrogen outgassing rate would be observed if it were greater than 0.56% of the water vapor rate at that time. This can then place an upper limit on what the hydrogen outgassing rate could be during this period.

During bakeout there is not much that can be said from the data on the 20% HF cleaned sample because of the quality of the data. The only observation that can be made is that a hydrogen outgassing rate appears as bakeout begins and is roughly proportional to temperature. From the work of Calder and Lewin[7] this is what would be expected. The data from the 33% HF cleaned tank are in agreement on this point in that the hydrogen rate appears as the sample is warmed and during the period where the temperature is held constant at 150°C the hydrogen outgassing rate is essentially constant.

It is also interesting to note in these data the shape of the outgassing rate curves as the sample is initially heated. In the case of H_2O and CO, the outgassing rates hit a peak as soon as the temperature starts to rise and fall from there as the sample continues to heat up. However, all of the other gases increase their outgassing rates as the sample is initially heated but do not reach their peak until the maximum bakeout temperature is reached. This could be explained by H_2O and CO having surface binding states with low binding energies and whose coverage can be depleted quickly so that all of the molecules in these states desorb soon after the initial temperature rise. The desorption rate then decreases with increasing temperature. During the part of the curve where the temperature is stable at 150°C all of the desorption rates except that of hydrogen decrease with time indicating a depletion of those molecules which are in the lower binding energy sites. Measurements can and have been made during the cooling down portion of the bakeout which indicate the range of binding energies that is depleted during the bakeout. The results of these measurements will be discussed later. The fact that the hydrogen desorption rate does not change with time is further evidence of the applicability of the bulk diffusion theory for the source of the hydrogen.

It is also interesting to note the different levels of outgassing rates assumed during bakeout by a variety of gases which were all outgassing at essentially the same rate before bakeout. Prior to bakeout CH_4, C_3H_8, CO_2, and O_2 were all outgassing at nearly the same rate. At 150°C, each of the rates is approximately an order of magnitude different from the others. Consideration of this in terms of the thermal desorption rate equation (equation 18) shows that the gas whose desorption rate changes by the greatest amount has the highest binding energy. Therefore, in order for that gas to also have the highest desorption rate at

the higher temperature it must have a significantly higher coverage. If you assume that all of these gases have a first order desorption (n = 1) (in equation 18) then an analysis shows the following relationships of their binding energies, E:

$$E_{C_3H_8} - E_{CH_4} = 3.82 \text{ kcal/mole}$$

$$E_{CH_4} - E_{CO_2} = 4.23 \text{ kcal/mole}$$

$$E_{CO_2} - E_{O_2} = 3.70 \text{ kcal/mole,}$$

and the following relationships between coverages at the time at which bakeout started:

$$\sigma_{C_3H_8} = 666\, \sigma_{CH_4}$$

$$\sigma_{CH_4} = 1370\, \sigma_{CO_2}$$

$$\sigma_{CO_2} = 520\, \sigma_{O_2}$$

This indicates that the oxygen that is desorbing at this time is coming from a state that has a low coverage and also a very low binding energy. At the other end of the spectrum, the propane that is desorbing has a binding energy that is 11.75 kcal/mole higher and it has a surface concentration that is $\sim 5 \times 10^8$ higher in terms of molecules/cm^2.

After bakeout, as the samples cool down, all of the outgassing rates fall rapidly. On the run with the 2% HF cleaned tank the measurements were discontinued when it had cooled to only ~100°C and so the room temperature outgassing rates are not known. However, the data in Figures 13 and 14 do show room temperature outgassing rates. At this

point hydrogen is outgassing at a rate which is two orders of magnitude above each of the other gases. It is likely that the room temperature equilibrium hydrogen outgassing rate after bakeout is the same as it was prior to bakeout. This is because a 150°C, 24-hour bakeout is not sufficient to significantly deplete the hydrogen that is dissolved in the bulk of the stainless steel[7].

The rates for all of the gases are in good agreement with the results of Calder and Lewin[7] which were presented earlier and which resulted from a 300°C, 25-hour bakeout. The additional temperature which they used did not significantly reduce the total outgassing rate. Future tests will attempt to establish the minimum bakeout that will still produce these values of outgassing rate.

It is of interest to calculate the total number of molecules of each gas that were removed from each cm^2 of surface during the pumpdown. This can be obtained by simply integrating the outgassing rate-vs-time curve. The result will be the number of molecules/cm^2 removed during the time that the data were being taken. It will not tell anything about the number remaining on the surface or about the number that were removed prior to the first data point. However, prior to the first data point most of the gas that was removed from the system was volume gas not gas from the walls of the sample. The results of the integration are shown in Table 6.

Thus, in the case of each gas listed the removal of the listed number of molecules/cm^2 caused the outgassing rate/cm^2 to change from that measured at the initial data point in the run to that of the final data point in the run. For water vapor this is a change of over seven orders of magnitude. For the other gases it is less, but in all cases it is more than three orders of magnitude.

TABLE 6

Total Quantity of Gas Removed From Sample with Standard Cleaning

Gas	Quantity Removed (mole/cm^2)	Final Outgassing Rate (Torr-liters/cm^2 · sec)
H_2O	2.4×10^{15}	3.5×10^{-16}
H_2	2.9×10^{15}	4.7×10^{-12}
CO	1.07×10^{15}	2.7×10^{-14}
N_2	7.25×10^{14}	5.9×10^{-14}
C_3H_8	1.05×10^{15}	5.5×10^{-15}
CH_4	1.95×10^{14}	1.4×10^{-14}
CO_2	4.41×10^{13}	2.6×10^{-15}
O_2	6.80×10^{12}	2.2×10^{-16}

It is interesting to compare the amounts of each gas that were removed. It might seem logical to expect that they would be removed in ratios that are approximately proportional to the atmospheric composition, except for hydrogen, since atmospheric exposure is the source of the other gases. This is obviously not the case.

One further piece of information that can be extracted from these data is an indication of the activation energy for desorption. It can be seen from the thermal desorption rate equation (equation 18), that a plot of log $(d\sigma/dt)$ vs $1/T$ should yield a straight line for each gas, whose slope is proportional to E_D, the desorption energy. To do this requires data for $d\sigma/dt$ over a range of temperatures and also requires that the gas coverage of the surface is not changed significantly while the temperature is

being varied. There are two times during these experiments when data are obtained over a temperature range. They are during the warming up part of the bakeout and during cooldown after bakeout. It is obvious from doing the integration of Qdt that during cooldown there is only a very small amount of gas removed from the surfaces so that these data can be used in such an analysis.

Figure 15 shows an example of such a plot from the data of Figures 13 and 14 for CH_4, CO, and H_2O. The activation energy for each gas can be calculated from the slopes of the straight lines that were fitted to the experimental points. This analysis cannot be applied to the hydrogen data because the rate-limiting process may very well be the hydrogen diffusion from the bulk rather than thermal desorption from the surface. The results of this analysis on the other seven gases are given in Table 7.

TABLE 7

Activation Energies for Desorption From Sample With Standard Cleaning After 150°C Bakeout

Gas	Desorption Activation Energy (Kcal/mole)
O_2	17.0
N_2	16.6
CO	17.7
CO_2	15.8
H_2O	22.4
CH_4	12.2
C_3H_8	17.4

These numbers represent the binding energies of these gases in the configuration (surface coverage, structure of the surface, etc.) in which they existed at the end of the pumpdown. It is not possible, from these

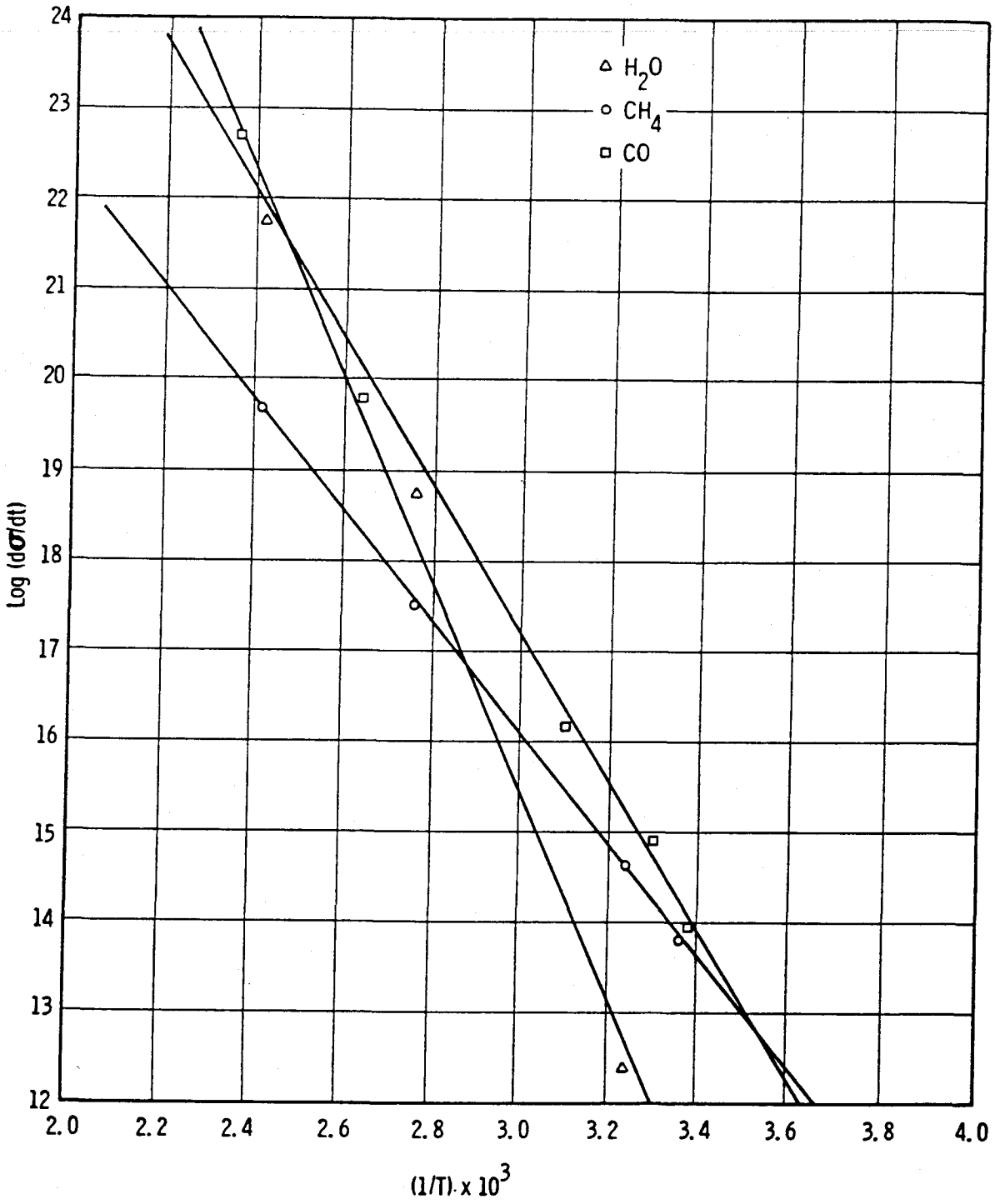

Figure 15. Derivation of Activation Energies for Desorption

data, to specify the coverage of any of the gases that existed at that point. It is interesting to note, however, the fairly narrow spread in binding energies. This suggests that the surface of a vacuum system contains a wide spectrum (in terms of binding energy) of adsorption sites for each gas, and that low desorption rates are obtained by removing all of the molecules from all of the sites whose binding energy is less than some value, either by just pumping and waiting for a long time or by bakeout. If this model is true then the spread in the measured binding energies and the degree to which the data fit a straight line would give an indication of how closely spaced (again in terms of binding energy) the sites are. If there were a nearly continuous spectrum of sites for each gas then it would be expected that a certain bakeout would result in removal of all of the gas below a certain binding energy for all of the gases and there would be very little spread in the energies measured in this way. Also if this were true the data would not fit a straight line very well because they would represent the superposition of a lot of straight lines resulting from the contribution from each of the binding states, each having a slightly different slope. O_2, N_2, CO, CO_3, and C_3H_8 could fit a model like this. However, H_2O and CH_4 do not. The low desorption energy measured for CH_4 could indicate that, as in the case of hydrogen, the source of the CH_4 is in the bulk of the stainless steel and the measured energy is some combination of the activation energies of diffusion and desorption. It is known[24] that hydrogen dissolved in steels reacts with the carbides in the steels forming methane which is then insoluble and must diffuse out of the steel or form pockets of methane gas which could leak into a vacuum system.

2. Only Degreasing

A sample tank was prepared that was standard in all aspects except that the only cleaning treatment that was applied was vapor degreasing in trichlorethylene after the tank had been assembled. The results obtained with this sample during a pumpdown with a 150°C bakeout are shown in Figures 16 and 17. These data were obtained on the same pumpdown as those shown in Figures 13 and 14 and so a direct comparison of the results of these two cleaning treatments is possible.

The first thing that is obvious from such a comparison is that initially the outgassing rates of most gases are higher for the standard cleaning than for the only-degreased sample. However, during the room temperature portion of the pumpdown the rates from the only degreased sample decrease more slowly and as a result when bakeout was started they were higher than those of the standard cleaning. During bakeout the outgassing rates of the only degreased sample are higher for all gases except hydrogen which would be expected to be the same for each tank as a result of the bulk diffusion source of the hydrogen and propane. Following bakeout both samples have essentially the same room temperature outgassing rates.

Another way of comparing the two samples is to compare the total amount of each gas that was released during the pumpdown. These values are listed in Table 8. These numbers were obtained, as was explained before, by numerical integration of the outgassing rate curves throughout the pumpdown.

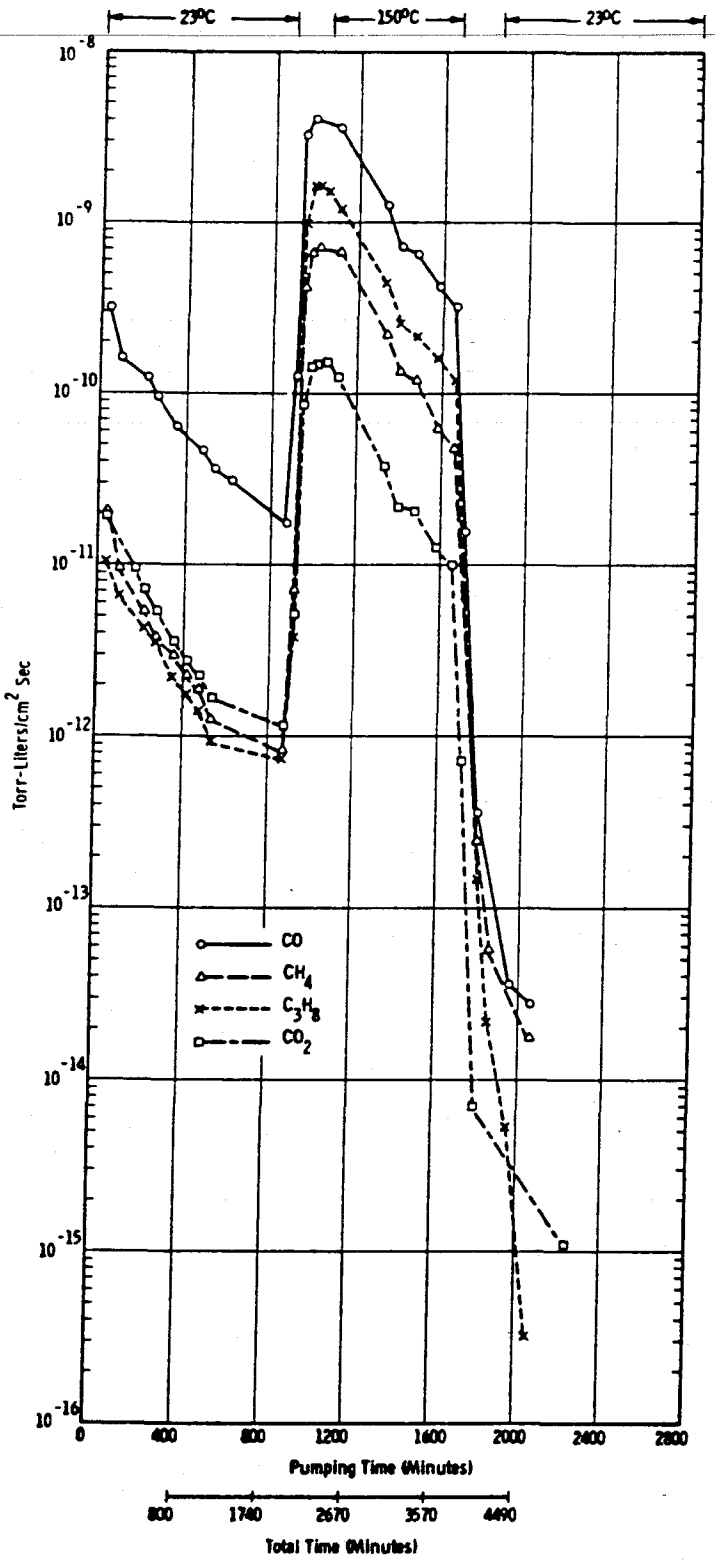

Figure 16. Outgassing Rates for CO, CH_4, C_3H_8, CO_2 from Sample with Only-Degreasing

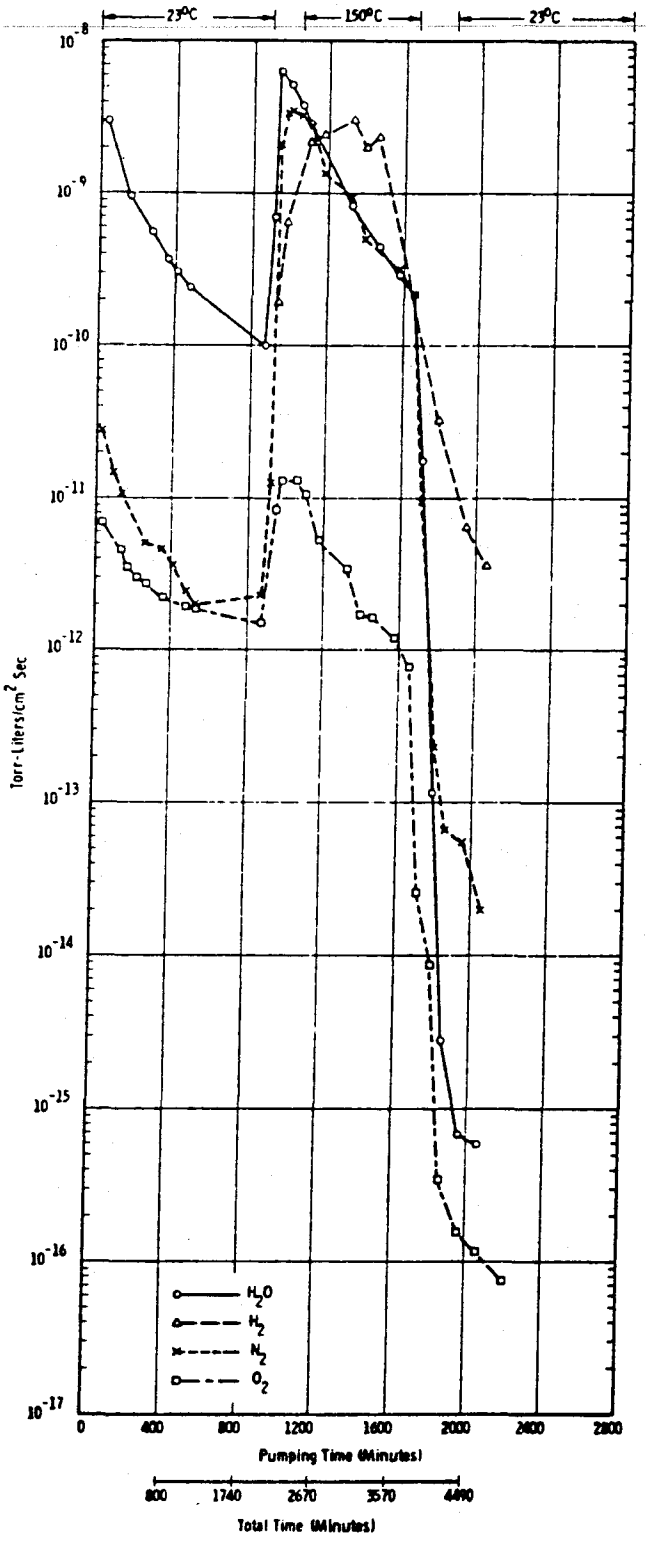

Figure 17. Outgassing Rates for H_2O, H_2, N_2, O_2 from Sample with Only-Degreasing

TABLE 8

Total Quantity of Gas Removed from Sample
Which was Only Degreased

Gas	Q_1, Quantity Removed from Standard Cleaned Sample	Q_2, Quantity Removed from Only-Degreased Sample	Q_2/Q_1
H_2	2.88×10^{15}	2.84×10^{15}	1
H_2O	2.4×10^{15}	3.64×10^{15}	1.5
CO	1.07×10^{15}	2.80×10^{15}	2.6
C_3H_8	1.05×10^{15}	9.91×10^{14}	0.94
N_2	7.25×10^{14}	1.94×10^{15}	2.7
CH_4	1.95×10^{14}	5.02×10^{14}	2.6
CO_2	4.4×10^{13}	1.00×10^{14}	2.3
O_2	6.8×10^{12}	1.17×10^{13}	1.7

The ratios of the quantities of gas released from one sample divided by the other are such that they could be explained by a difference in actual surface area produced by the different cleaning treatments. This subject has been investigated by Schram[12] and he has found ratios of apparent geometrical surface areas and actual surface areas which vary from 1.1 to 900 and, more important, variations on the same material, but with different surface treatments, of the order of a factor of three.

Another quantity that was calculated for this sample is the desorption activation energy, E_D, during cooldown after the bakeout. This was done in the same way as described in the previous section. Table 9 gives those values and those for the standard cleaned sample.

TABLE 9

Activation Energies for Desorption from Sample Only-Degreased after 150°C Bakeout

Gas	E_D - Only-Degreased (Kcal/mole)	E_D - Standard Cleaning (Kcal/mole)
H_2O	25.1	22.4
CO	16.0	17.7
C_3H_8	17.2	17.4
N_2	15.4	16.6
CH_4	13.3	12.2
CO_2	17.5	15.8
O_2	15.7	17.0

In this parameter the different gases bear approximately the same relationship to one another in each tank and the values are nearly the same. Apparently E_D is determined more by the bakeout time and temperature than by the specific character of the surface. This adds more weight to the argument that there is a nearly continuous spectrum of binding site energies available on the surfaces and that a particular bakeout will remove all of the adsorbed particles from all sites whose binding energy is below a certain value.

3. DS-9 Cleaning

It has been reported by Milleron[25] that treatment of 304 stainless steel with the Diversey DS-9 process will substantially reduce outgassing rates. His results indicated that it should even be possible to attain pressures in the ultrahigh vacuum range without bakeout in systems treated by this process. Therefore, it was decided to measure outgassing rates on a sample tank that was treated by this process. The Diversey Co. was

contacted about treating a sample. They felt that they could not treat a sample of the size we use. Subsequently a company was located that agreed to do the treatment.

The results obtained from this sample are shown in Figure 18. The measured outgassing rates are, in nearly all cases, higher than those obtained in comparable situations from samples cleaned by the standard cleaning treatment. The few gases which had a lower outgassing rate constitute only a small percent of the total outgassing rate and so the net result is a higher total outgassing rate for this sample than for the standard cleaning.

The Diversey Co. has been informed of these results and they have now agreed to treat a sample for us to assure that it has been given the optimum DS-9 cleaning.

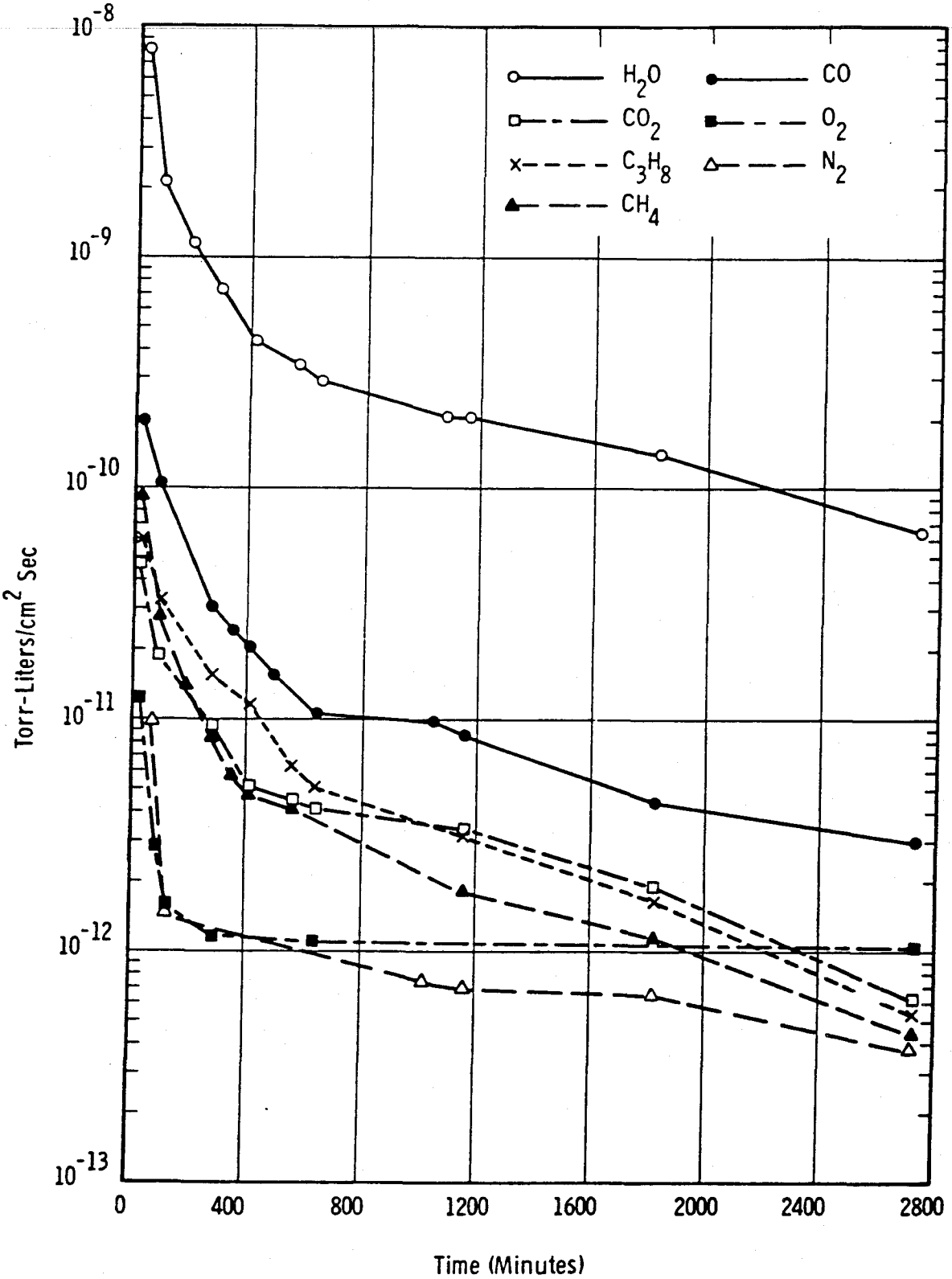

Figure 18. Outgassing Rates for Sample Cleaned by Diversey DS-9 Cleaning NO BAKEOUT

IV. SUMMARY AND CONCLUSIONS

Outgassing rate measurements on copper, aluminum, and stainless steel samples have been summarized and reviewed including a critical discussion of the experimental procedures used to make the measurements. Table 10 is a summary of values which are believed by the author to be representative of relatively good surfaces under typical conditions. In addition, the comparison of the many existing measurements of outgassing rates of these metals leads to the conclusion that variations in outgassing rate of a particular base material are due, to a significant degree, to variations in the extent of the oxide layer present on the surface. Furthermore, this effect is primarily a result of the ratio of the true surface area of the sample to the geometric area. The significance of the various cleaning treatments that have been used is simply to reduce this ratio. Thus, the most desirable treatment would be that which minimizes the true surface area by producing a smooth, flat surface.

Other properties which this optimum surface treatment should possess are that it should seriously impede or completely stop the diffusion of hydrogen from the bulk of the material and that the surface should be left free of carbon to inhibit the production of CO and CO_2 from adsorbed O_2.

TABLE 10

Recommended Values of Outgassing Rates
(Torr-Liters/cm^2 · sec)

Material	Outgassing Rates, Unbaked				Outgassing Rates After Bakeout	References	Remarks
	1 hour	4 hours	10 hours	40 hours			
Copper - OFHC - as-received surface removed	2×10^{-9}	8×10^{-10}	1.5×10^{-10}	4×10^{-11}		12	
Copper - OFHC - as-received surface not removed	2×10^{-8}	7×10^{-9}	1×10^{-9}	3×10^{-10}		12	
Copper - not OFHC - as-received, surface removed	4×10^{-9}	1.5×10^{-9}	3.5×10^{-10}	9×10^{-11}		12	
Copper - not OFHC - as-received, surface not removed	4×10^{-8}	1.5×10^{-8}	4×10^{-9}	8×10^{-10}		12	
Aluminum - anodized	2×10^{-6}	6×10^{-7}	1×10^{-7}	3×10^{-9}		12	
Aluminum - clean, but with some oxide	1×10^{-8}	3×10^{-9}	1×10^{-9}	3×10^{-10}		12	
Stainless steel - only degreased	2×10^{-9}	1×10^{-9}	2.5×10^{-10}	8×10^{-11}	4×10^{-12} 4×10^{-12}	7 9	150°C - 24 hr bake 300°C - 25 hr bake
Stainless steel - Varian standard cleaning	3×10^{-9}	5×10^{-10}	1.5×10^{-10}	4×10^{-11}	4×10^{-12}	9	150°C - 24 hr bake

REFERENCES

1. R. P. Henry, LeVide, No. 82, 226 (1959).
2. C. W. Oatley, Brit Journ Appl. Phys. 5, 358 (1954).
3. J. J. Thibault, J. Roussel, M. Jourdan, LeVide, No. 132, 309 (1967).
4. B. D. Power and F. C. Robson, Proc. of the Eighth National Vacuum Symposium of the AVS, 1175 (1961).
5. N. Ia. Basalaeva, Soviet Physics - Tech. Phys. 3, 1027 (1958).
6. T. D. Kirkendall, P. F. Varadi, and H. D. Doolittle, Jour. Vac. Sci. and Tech. 3, 214 (1966).
7. R. Calder and G. Lewin, Brit. Journ. of Appl. Phys. 18, 1459 (1967).
8. Y. E. Strausser, Presented at the 14th National Vacuum Symposium of the AVS, Kansas City, Mo. (1967).
9. Y. E. Strausser, Proc. of the 4th International Vacuum Congress, Manchester, England (1968). To be published.
10. R. S. Barton and R. P. Govier, Report No. CLM-R93, Culham Laboratory, Abingdon Berkshire, England (1968).
11. D. J. Santeler, Trans. of the Fifth National Symposium of Vacuum Technology, pp 1-8, Pergamon Press (1959).
12. A. Schram, LeVide, No. 103, 55 (1963).
13. J. Blears, E. J. Greer, and J. Nightingale, Advances in Vacuum Science and Technology II, 473, Pergamon Press, Oxford (1960).
14. R. Geller, LeVide, No. 74, 71 (1958).
15. M. P. Shrank, F. C. Benner, and D. K. Das, Report No. AEDC-TDR-64-53, Arnold Engineering and Development Center, Arnold Air Force Station, Tennessee (1964).
16. D. K. Das, Report No. AEDC-TDR-62-19, Arnold Engineering and Development Center, Arnold Air Force Station, Tennessee (1962).
17. E. Hoyt, Report No. SLAC-TN-64-5, Stanford Linear Accelerator Center, Stanford, California (1964).
18. F. S. Reinath and D. T. Scalise, Report No. UCRL-11808, Univ. of Calif. Lawrence Radiation Laboratory, Berkeley, Calif. (1965).
19. R. Geller, Le Vide, No. 69, 194 (1957).

REFERENCES (Contd)

20. B. D. Power and D. J. Crawley, Transactions First International Congress on Vacuum Techniques, 206, Pergamon Press, London (1960).

21. L. de Csernatony, Vacuum 16, 427 (1966).

22. V. R. Howes, Corrosion Science 8, 221 (1968).

23. A. Schram, Proceedings of the Ninth Annual Vacuum Symposium of the AVS, 301, Macmillan (1963).

24. H. C. Rogers, Science 159, 1057 (1968).

25. N. Milleron, IEEE Trans. on Nuclear Science, 794, June (1967).

Lansing

REDUCTION OF STAINLESS STEEL OUTGASSING

ON THE LARGE GRAVITY WAVE DETECTOR

SUPRIYA GHOSH

S.U.R.F PAPER

AUGUST 23,1985

ABSTRACT

This research paper discusses the outgassing phenomena in ultra-high vacuum systems. The Jet Propulsion Laboratory, under the management of the California Institute of Technology is presently examining the probability of building a large L-shaped gravity wave detector with each leg being 5-km long. The sensitivity of the detector should be higher than any other detector built so far. Hence, each 5-km long cavity is required to be at a vacuum of 10^{-8} torr. To achieve such a high level vacuum, the chamber surfaces need to be thoroughly outgassed. This paper discusses this outgassing problem and reviews past research work performed on the subject. A suggested cleaning procedure and test-model are also included at the end.

Table of Contents

Abstract

I. Introduction

II. Selection of Materials

III. Outgassing Characteristics

3.1. Pump-down time

3.2 Desorption Time

3.3 Diffusion

3.4 Permeability of Hydrogen

IV. Experiences learned from different surface treatment methods

4.1 Barton and Govier's work

4.2 Young's work

4.3 Strausser's work

4.4 Calder and Lewin's work

4.5 Nuvolone's work

V. Description of two, comparable, large systems

5.1 The Brookhaven System

5.2 The CERN System

VI. Conclusion

6.1 Summary on Outgassing

6.2 Proposal of a test-model

I. INTRODUCTION

The Jet Propulsion Laboratory under the management of the California Institute of Technology are collaborating with the Massachusetts of Technology to examine the feasibility of constructing a large, highly sensitive gravity wave detector. The detector will be in a giant L-shaped configuration with each leg being 5-kilometers long. These two legs will be cylindrical, made up in sections approximately 12 meters (40 feet)in length and with an inner diameter of 120 cm (4 ft). The cylindrical sections together with a number of end-chambers need to be maintained at an ultra-high vacuum pressure of 10^{-8} Torr.

The proposed gravity wave detector system (GWO) will be the largest in size, and the most sensitive device ever built to detect gravity waves. It works using the principle of laser interferometry, where four test-masses will be placed at the corners of the L-shape, 5-kilometers apart. Thus, if a transverse gravity wave ~~transverse~~ is traveling in a vertical direction, the two test-masses on one side of the L will move apart while the pair on the other side of the L will move closer together. The mass displacement,however,will be very minute, and this GWO system will use a multiple-laser interferometer setup to measure the effect. Gravitational waves, like visible light waves are transverse in nature and the maximum effect is obtained when the line joining the two masses is perpendicular to the direction of the propagation of the wave. Figure.1[40] illustrates the principle of operation. Curved mirrors are set up at each mass which will

reflect the light many times to increase many folds the phase difference. This phase difference will then be measured by photodiodes. The light may be provided by a powerful argon ion laser. However, in a 5-km long cavity the sensitivity of the light will be limited by air molecules bouncing in its path. Therefore,the pressure requirement inside is set initially to about 10^{-8}Torr.

This research paper concerns itself with the vacuum system and how to maintain the necessary pressure inside the chambers. A major problem faced when trying to lower the pressure to ultra-high vacuum levels is the rate of outgassing. At such low pressures a number of molecules free itself from the surrounding bulk and occupy the inner chamber area raising the vacuum level of the system. This paper will try to discuss ways to reduce this problem, and review past works on this subject.

II. SELECTION OF MATERIALS

In an ultra-high vacuum system, it is important to select the proper material for the fabrication of the chamber. It is essential that the material possesses good outgassing properties. The material should also be easy to handle and relatively inexpensive. Stainless Steel and Aluminum, both fulfill these qualifications well. However, the differences between these materials are considerable in what kind of conditioning is needed for each. Aluminum can be baked under vacuum to a maximum temperature of 200°C, and stainless steel to a temperature of 400°C, . Furthermore, aluminum cannot be annealed at 1000°C to eliminate hydrogen like stainless steel.

The first choice of material for the 5-km gravity wave vacuum chambers is stainless steel. The type of stainless steel chosen was 304L, an austenitic stainless steel that has been used frequently for vacuum systems. Its composition is : 18-20% Cr, 8-12% Ni, 0.03% C, 1.0% Si, 2.0% Mn, 0.045% P . The letter "L" stands for lower carbon content. Stainless steel 304 normally contains 0.08% C. Austenitic stainless steels are known to be highly ductile and have a very high resistance to corrosion. H.Eschbach[5] had performed several experiments with different types of stainless steel to find out which steel gave the lowest diffusion coefficients and permeabilities. He found that the austenitic 18-8 percent Cr-Ni steel to have the lowest permeability as shown in Figure 2.

It was found[5] that with the increase of alloy concentration

such as chromium and nickel both the diffusion coefficient and the permeability became smaller. The diffusion velocity decreases steadily as more chromium is added.

III. Outgassing Characteristics

3.1 Pumpdown Time. The 5-km long chambers need to be at a pressure in the ultra-high vacuum range. The term ultra-high vacuum generally refers to pressures below 10^{-7} Torr. The vacuum requirements of this system call for a pressure of approximately 10 Torr.? At this vacuum range, it is essential that the chamber material have the "best" outgassing properties possible,i.e. lowest outgassing rate. To fully understand the effect of outgassing on a vacuum vessel consider the case of a vessel under pumpdown. If a volume,V, is pumped by a pumping speed,S, then at time,t, the pressure-time relation is given by:

$$\frac{dp}{dt} = -\frac{S}{V}P \tag{1}$$

by integration from an initial pressure, p

$$\ln p = \ln p_o - \frac{S}{V}p$$

$$\text{or } P/p_o = e^{-S/V t} \tag{2}$$

3.2 Desorption Rate In a real system, when the pressure reaches 10^{-6} Torr, the pump-down curve in Figure.3 levels off, and becomes nearly constant with time. This phenomenon is due to material outgassing. At such low pressures, the gas molecules which had been adsorbed by the metal surface at atmospheric pressure, slowly desorb into the chamber. The rate of desorption will depend on the binding energies of the various gases "stuck" on the chamber surface, the surface temperature, and the total surface area. This can be seen from the desorption rate equation for thermal desorption:

$$\frac{d\sigma}{dt} = \nu_o \sigma_o \theta^n e^{-E_D/kT} \tag{3}$$

where σ = surface coverage in mol/cm , ν_o, σ_o = constants, $\theta = \sigma/\sigma_o$ n= order of the desorption process, E_D= energy required for

desorption, k= Boltzmann°s constant, and T= temperature of surface.

Equation.3 shows that the desorption rate is only proportional to the nth power of the molecule°s surface concentration, where n is usually 1 or 2, and it is exponentially proportional to the binding energy.

There are two principal ways that adsorption types can take place in a system: physisorption and chemisorption. The rate of desorption at constant temperature will increase linearly with the pressure of the gas.?, A quantity known as the adsorption isotherm (θ) relates these two measurements. The rate of desorption depends upon the equation of Polyani-Vigner :

$$\frac{dn_s}{dt} = \nu_o n_m f'(\theta) \exp(-E/RT) \qquad (4)$$

Where n_s is the number of molecules on the surface at time,t. ν is the frequency of vibration of sorbed molecules, normal to the surface, and n is the number of molecules in a monolayer. R.J. Elsey,[1] using equation (4), calculates the desorption of physisorbed molecules. The values are: ν_o at around 10^{13} Hz, and n about 10^{15} molecules/cm . Since $\nu_o = 1/\tau_o$, $\tau = \tau_o \exp(E/RT)$ (5) where is the residence time. The universal gas constant R is 2 cal/deg-mole. Equation (5) gives $\tau = 2\ \mu s.$ τ_o

Thus gases that are physisorbed desorb very quickly at room temperature. A complete equation which describes the entire process can be written as follows:[1]

$$V \frac{dn_v}{dt} = -\frac{\bar{c}}{4} n_v A_p + \frac{n_s A_s}{\tau} - \frac{\bar{c}}{4} n_v \alpha A_s \qquad (6)$$

where $(\bar{c}\ n_v A_p)/4$ is the gas removed by the pump, $n_s A_s/\tau$ is the

gas desorbed by the surface, and $(\bar{c}\, n_v \alpha A_s)/4$ is the gas adsorbed by the surface = $(\bar{c}\, n_v \alpha A_s)/4$

n_v is the molecular density of the gas phase

V is the volume of the vessel being pumped

A_p is the area of outgassing surface

$\bar{c}$ is the average velocity of the gas molecules

α is the sticking coefficient

Another equation dealing with surface phenomena needs to be considered.

$$A_s \frac{dn_s}{dt} = -\frac{n_s A_s}{\tau} + \frac{\bar{c}}{4} n_v \alpha A_s \qquad (7)$$

Equation (6) and (7) can be combined and differentiated to obtain:

$$\frac{d^2 n_v}{dt} + \left[\frac{\bar{c}}{4V}(\alpha A_s + A_p) + \frac{1}{\tau}\right]\frac{dn_v}{dt} + \frac{\bar{c}}{4V} \cdot \frac{A_p}{\tau} \cdot n_v = 0 \qquad (8)$$

Equation (8) can then be plotted to obtain pump-down curves.

When a vacuum system is in equilibrium, the outgassing rate has a direct relationship with the pumping speed, and the gas inside the system.

$$Q = (S) \times (P) \qquad (9)$$

where Q= total outgassing rate in torr-l/s

S= pumping speed in liter/sec

P= pressure in Torr

A typical outgassing plot against time is given by R.J.Elsey[1] in Figure.4. This is a log-outgassing rate vs. log-time graph. The curve in Fig.4 shows a negative linear relationship between these two parameters.

The pumping speed for most high-vacuum pumps are given in terms of dry air (M.W. 29) or nitrogen (M.W. 28). If any other

gas is being pumped then the speed will differ as a function of the molecular weight of the gas. For example to determine the pumping speed for Argon for a pump rated at 100 liter/sec for air:

Pumping Speed of Argon

$$= \text{Pumping Speed of Air} \times \sqrt{\frac{\text{Molecular Weight of air}}{\text{Molecular Weight of argon}}} \qquad (10)$$

$$= 1000\left(\sqrt{\frac{28}{40}}\right)$$

$$= 837 \text{ l/s for argon}$$

3.3 Diffusion

We will now determine what contribution diffusion plays on outgassing characteristics. Diffusion takes place from the bulk of the material into the vacuum chambers. The one-dimensional diffusion equation for the case of a slab of unit cross-section and thickness, d, is given by:

$$D\frac{\partial^2 c}{\partial x^2} = \frac{\partial c}{\partial t} \qquad (11)$$

with the given Boundary Conditions: $c=c$ for $0 \le x \le d$ at $t=0$ and $c=0$ for $x=0$ and $x=d$ at $t>0$

The solution is presented by G.Lewin[41] as

$$c(x,t) = 2c_0 \frac{4}{\pi}\sum_{n=0}^{\infty}(2n+1)^{-1}\sin\pi\frac{(2n+1)}{d}\left(x\exp\left\{-\left(\frac{\pi(2n+1)^2}{d}\right)Dt\right\}\right) \qquad (12)$$

The instantaneous gas flow is

$$\dot{Q} = D\left(\frac{\partial c}{\partial x}\right)_{x=0} = (4c_0D)/d \sum_{0}^{\infty}\exp\left\{-\left(\frac{\pi(2n+1)^2}{d}\right)Dt\right\} \qquad (13)$$

Calder and Lewin[2] makes the approximation $Dt/d > 0.025$

Then $$C = c_o \frac{4}{\pi} \sin \frac{\pi x}{d} \exp\left(-\pi^{-2} d^{-2} Dt\right) \quad (14)$$

$$Q = 4 c_o D_r d^{-1} \exp\left(-\pi^{-2} d^{-2} Dt\right) \quad (15)$$

If a slab has been degassed at temperature T , for t_1 seconds, the outgassing at room temperature would be:

$$\dot{Q} = 4 c_o D_r d^{-1} \exp\left(-\pi^2 d^{-2} D_1 t_1\right) \quad (16)$$

At room temperature, Eschbach finds the diffusion coefficient of hydrogen to be $D = 5 \times 10^{-14}$ cm /s, and Calder and Lewin used c_o = 0.3 torr-l/cm .

Equation (16) will now be applied for a 2-mm stainless steel sheet after a bakeout at 300 C ($D_{300} = 3.5 \times 10^{-8}$ cm^2/sec) for 24 hours.

$$Q = 3.0 \times 10^{-13} \exp(-0.75)$$

$$Q = 1.4 \times 10^{-13} \text{ torr-l/cm-s} \quad (17)$$

A second bakeout reduces Q by a further factor $e^{-0.75} = 0.47$. Hence, the effect of diffusion or outgassing is small after a prolonged bakeout.

Calder and Lewin has shown[2] that the product $\dot{Q}_r$ is independent of time. So looking back at equation (16), since $D_1 t_1$ appears in the exponent, this means an increase in bakeout temperature has the same effect as an increase in time of bakeout at a lower temperature. The diffusion coefficient also varies exponentially with temperature. So the theoretical result is that a one hour bake-out at 1000°C has the same effect as 2500 hours at 300°C.

3.4 Permeability of Hydrogen

Permeability is the process of active diffusion, which in the case of an ultra-high vacuum system it signifies diffusion of hydrogen from the atmospheric pressure to the inside chamber where the concentration of molecules is approximately zero.

Permeability Constant, $K = D \times S$ (18)

=(Diffusion Constant)(Solubility Constant)

$K = K_o \exp(-E_k/RT)$ where $E_k = E_D + H_S$, H_s= Heat of Solution

The one-dimensional diffusion equation with different boundary conditions. $c=0$ for $0 \leq x \leq d$ at $x=0$ (19)

$c=0$ for $x=0$ at $t=0$

$c=c$ for $x=d$ at $t>0$

The solution for the equation is gven by Lewin[41] again

$$c(x,t) = \frac{c_1 x}{d} + \frac{2c_1}{\pi} \sum_1^{\infty} \frac{(-1)^n}{n} \sin \frac{n\pi x}{d} \exp\left\{-\left(\frac{n\pi}{d}\right)^2 Dt\right\} \quad (20)$$

The instantaneous permeation rate at time,t is

$$\left(\dot{Q}_{P_1}\right) = D\left(\frac{\partial c}{\partial x}\right)_{x=0} = D\,c_1/d + \frac{2Dc_1}{d} \sum_1^{\infty} (-1)^n \exp\left\{-\left(\frac{n\pi}{d}\right)^2 Dt\right\} \quad (21)$$

By taking the limit and setting $t \to \infty$, the summation term goes to zero. So $\left(Q_{P_1}\right)_r = c_1/d$ (22)

Lewin also gave the concentration, C, of a diatomic gas dissolved in a metal at temperature, T, with external pressure P as: (23)

$$C_1 = \frac{K_T}{D_T} P_1^{1/2}$$ where K_T =permeability constant

D_T =diffusion constant

The permeability constant, K, of hydrogen in stainless steel at room temperature is $K = 1.2 \times 10^{-16}$ torr$^{1/2}$-l/cm-s. At atmospheric pressure, the partial pressure of hydrogen = 3.8×10^{-4} torr.

By using a stainless steel thickness of 2 mm, for the GWO system,

$$(Q_{P_1})_r = \frac{c_1 D_r}{d} = \frac{K_r P_1^{1/2}}{d} \qquad (24)$$

$$= 1.2 \times 10^{-17} \text{ torr-l/s-cm}$$

Eq.24 shows that at room temperature the effect of hydrogen permeation is negligible. This value will be modified, however, at higher temperatures since permeation rate of hydrogen varies exponentially with temperature. So, at 300°C, where $K = 2.3 \times 10^{-10}$ $\text{torr}^{1/2}\text{-l/cm-s}$, and $D_{300} = 3.5 \times 10^{-8} \text{ cm}^2/\text{s}$, the value for hydrogen permeation for a 2-mm thick stainless steel slab is:

$$(\dot{Q}_{P_1})_{300} = \frac{K_{300}}{d} P_1^{1/2} = 2.3 \times 10^{-11} \text{ torr-l/cm}^2\text{-s}$$

This number will also change with time, and a prolonged bakeout at this temperature will bring the value up considerably, but still negligible for the GWO requirements. Thus Calder and Lewin found that after their normal bakeout, 99% of the residual gas was hydrogen.

IV. Experiences learned from different surface pre-treatment methods

The requirement of an ultra-high vacuum ($< 10^{-6}$ Torr) cannot easily be achieved by conventional methods. This is evident from Figure.3 showing that the vacuum pressure levels out against time at 10^{-6} Torr. Thus to attain an ultra-high vacuum inside the chamber the outgassing rate of the stainless steel has to be lowered to the least possible level. Many different surface preparations have been tested. Baking is found to be the most common method. B.B. Dayton[4] found that at room temperature, the total amount of gas given off by a metal surface over a period of 10 to 50 hours of vacuum pumping, ranges from 20 to 100 monolayers of molecules. This means that untreated metal samples outgas at the rate of about 10^{-7} torr-liter/sec-cm after 1 hour of vacuum pumping at room temperature. At this temperature, water vapor is by far the most dominant outgassing substance. But as the temperature of the stainless steel is raised, other factors become important, like diffusion of hydrogen from the bulk of the material.

Literature data on outgassing rates produced by different authors, have a wide variance in the values reported for the same materials due to using different surface-treatment techniques. In this article we will review some of these rates and comment on each type of surface treatment. We will review the work of five researchers who dealt primarily with stainless steel. These are: 1) R.S.Barton and J.P.Govier[12] 2) J.R. Young[9] 3) Y.Strausser[6] 4) R.Calder and G.Lewin[2] 5) L.Nuvolone[15]. The articles are arranged so that we follow the three important methods 1)

unbaked steel after various cleaning mathods 2) effect of different treatments along with a medium temperature bake and 3) high temperature vacuum-baking.

The first topic covered will be unbaked stainless steel after various cleaning methods. The technique of baking the stainless steel between the temperature of 200- 500°C has been widely used to attain lower outgassing figures. But in the gravity wave detector, baking the stainless steel chambers to such high temperatures would result in difficult engineering problems and high costs. It is, therefore, advantageous to experiment on decreasing the outgassing rate to its lowest possible level without the use of a bakeout procedure.

4.1 Barton and Govier's work.

R.S.Barton and J.P.Govier of UKAEA Research group, Culham Laboratory, England[12] have done extensive tests on unbaked stainless steel. Their goal was to find out if the outgassing rate could be reduced to 10^{-12} torr-litre/sec-cm^2 without the use of a bakeout. They tested a cylindrical sample made of 18/9/1 stainless steel, 16 cm in diameter and 75 cm length. The sample was first honed and vapor degreased in trichloroethylene and then baked at 450°C. Sample A was then exposed to air for 24 hours and then repumped after 48 hours. This treatment was used as a control against the unbaked steel samples and the outgassing rate obtained (after 48 hrs was 1.7×10^{-11} torr-l/s-cm^2) was then compared with the following different methods, shown in Figures.5, 6 and 7. The vapor degreasing of sample B was done by using a tricholoroethylene vapor bath. The curve of sample B is seen to be identical in nature to sample A producing an outgassing rate of 1.5×10^{-11} torr-l/s-cm^2 at 48 hours but traces of tricholoroethylene were visible in the mass spectrometer scan. This scan showed that the major gases were H_2O, CO, and CO_2.

Sample C was deliberately contaminated with machine oil and then vapor-degreased and the outgassing rate obtained after 48 hrs was 1.3×10^{-11} torr-l/s-cm^2, Samples D an E tested the difference between honed and machined surfaces. Sample F was vapor-degreased and electropolished. The following materials were used in the process:

N.Butyl Alcohol : 90 parts by volume

Orthophosphoric Acid : s= 1.75, 350 parts by volume

Current used : Approx. .075 A/cm (Total 180 A)
Time : 50 minutes

Recommended temp.: 70°C (probably rose to 90 C)

and after the electropolishing the samples were washed in tap water and then in dimineralized water. The total outgassing per square of sample is shown in the curves of Fig.7.

The sample (i) was baked in air to see the advantages of this over electroploishing. It was baked for 1 hour in air at 500 °C and then repumped. The outgassing showed an improvement of a factor of 2 over the electropolished surface and this was entirely due to a reduction of water vapor. The cleaning treatment process, DS-9 from the Diversey Chemical Co. was tested and it showed an outgassing time worse than the air-bake. The most significant reduction was shown from the plasma-torch cleaning. The specimen was degreased and then cleaned with a plasma-jet using argon gas and a constricted arc between a non-consumable electrode. This method would do well in large vacuum systems if local cracks appear in the stainless steel chambers. Barton and Govier comments that since the outgassing improvements obtained from an air-bake and plasma-torch cleaning are marginal over trichloroethylene vapor degreasing it might be advisable to use the vapor bath since it is easier to apply and is less costly.

After 70 hours of pumping, the composition shown by the mass spectrometer for the vapor-degreased specimen is the following: 58% H_2O, 20% CO, 12% CO_2, 9% Hydrocarbons, and 1% Trichloroethylene. The authors explain that 50% of the CO and CO_2, can come

from the ionization gauge used to measure the total pressure.

Figure.8 shows that the use of dirty hands on the vapor degreased sample causes negligible amount of difference in the curve although the authors suggest that the use of bare hands should be reserved for cases of emergency.

4.2. Young's Work

J.R.Young at the General Electric Corporation in 1968, did a number of experiments to reduce outgassing rates by using different surface treatments and a medium temperature bake. The experimental apparatus consisted of ⅛-inch thick 304 stainless steel tanks. They were 6 inches in diameter and 18 inches long, resulting in a surface area of 400 in^2. A diagram of this setup is shown in Fig.9.

The sample chamber was attached to a S.S. 304 T-section and an ionization gauge. A thin S.S.304 aperture which had a conductance of 4.4 litre/sec of H_2 was placed between the sample gauge volume and pumping chambers. The system was pumped by a Hg-diffusion pump and a Ti-sublimination pump. Young mentions that pressures below 10^{-10} torr were frequently obtained in this system and outgassing rates could be measured down to 3×10^{-13} torr-litre/s-cm^2. The outgassing rate Q was measured by taking the difference in pressure between gauge.1 and 2, and then multiplied by the conductance of the aperture. To test the different surface pre-treatments on the samples, the system was pumped for 15-30

hours at 250°C. The outgassing rate prior to baking for most samples were 10^{-10} torr-l/s-cm^2. Then the apparatus was allowed to cool down for 24 hours and the outgassing rate for each case was measured. Figure-10 has tabulated each surface pre-treatment and the respective outgassing rates.

The lowest rate recorded was 3×10^{-13} torr-l/s-cm^2, and this was for the stainless steel sample cleaned by glass-bead shot blasting and then baked twice. The first one was an air-bake and then a vacuum-bake for 15 hours at 250°C. The glass-bead shot blasting left a mat-finish with a surface roughness of 32 μin. Two different electropolished surfaces were tested with identical baking procedures, the first one was prepared using ElectroGleam No.55 solution, 2 A/in at 6 V DC, and this resulted in a surface roughness of 22-25 μin. The second one used the same method but the electropolishing was done more carefully resulting in a surface roughness of 4-6 μin. But the outgassing rate was not decreased by a significant amount and the extra cost for better roughness may not be justified. Young tried to determine if a surface layer of oxide helped reduce outgassing rate by forming a barrier for H_2 permeation. So, Sample B was baked again and this produced Sample D and the outgassing rate was significantly lower. Young also proved that a high-temperature bake is much more effective for S.S.304 by taking Sample C, and baking it again at 450 °C for 17 hours and the outgassing rate lowered dramatically to 4×10^{-13} torr-l/s-cm^2.

4.3 Y.Strausser's work

Mr. Strausser performed his research at Varian Associates in Palo Alto, California in 1967.[6] The setup used the standard equation $Q = SP$, to calculate the outgassing rate and minimized the measurement errors by also measuring the background pressure. A schematic diagram of this setup is shown in Figure.11 at the back. The RGA stands for the Residual Gas Analyzer and IG for the Ionization gauge. The outgassing rate is measured by subtracting the partial pressure of the two tanks. The pump used in these measurements was a 500 liter/second diode-type sputter ion-pump. The samples used were standard 18 inch O.D. by 30 inch long stainless steel tubes. The geometric surface area for each sample was $1.40 \times 10^4 cm^2$.

During the experiment, Strausser lists four major difficulties that were faced in calculating the true outgassing rate. These were the following 1) outgassing rate from the gas sampling manifold, 2) using the two sample tanks simultaneously, 3) accuracy of the quadropole calibration data and electron multiplier gain values 4) trying to measure total pressure in the sample tanks during the experiments.

Outgassing rates were obtained with the sample cleaned by 1) only degreasing 2) Varian Standard cleaning and 3) Diversey DS-9 cleaning treatment.

The Varian Standard cleaning procedure for 304 stainless steel follows these certain steps:

1) Vapor degreasing in trichloroethylene 2) cleaning in Oakite

3) Hot water rinse 4) 33% HNO_3, 33% HF, 33% H_2O bath by volume at room temperature 5) H_2O rinsing, dry and bag.

The results obtained from the Varian Standard cleaning are shown in Figures 11, 12, 13 and 14. Two different percentages of HF, were used. Figures 11 and 12 were treated with 2% HF and Fig.13 and 14 were treated with 33% HF. These results were obtained after a pumpdown and a 12-hour bakeout at 300 °C using strip-heaters to heat the stainless steel sample. Figures 13 and 14 are obtained after a 150 °C bake for 24 hours using an oven instead of a strip-heater.

When we compare the results produced by 2% and 33% HF concentrations in cleaning, we notice a signbificant improvement. Since different bakeout methods were used, comparisons can only be made on pre-bakeout data. After about 100 minutes of pumpdown, Table.3 records data comparing the two different concentrations of HF. We see a factor of ten improvement in the outgassing. Strausser reported that in the pre-bakeout period, all the samples showed H_2O to have the highest outgassing rate and CO to have the second highest. Also, during the pre-bakeout period, no hydrogen outgassing was observed but as the bakeout continued, the rate of hydrogen outgassing increased linearly with temperature. This outcome agrees with the study done by Calder and Lewin[2]. According to the graphs presented by Strausser, H_2O and CO outgassing rates hit a peak as soon as the temperature starts to rise and then falls from there. But the other gases reach their highest outgassing rate when the peak bakeout temperature is reached. Strausser also calculates the total

number of molecules of gas that were removed from the surface during pumpdown, by integrating the outgassing vs time curve and the final outgassing rate of each gas in Table 4.

Only Degreasing: A stainless steel 304 sample was tested in the same way as before except that it was only vapor degreased in trichloroethylene. The results are shown in Figures 15 and 16 and can be compared directly to the earlier graphs (Figs. 13 and 14). The outgassing rates for the degreased samples were lower at room temperature but after the bakeout the sample with Varian standard cleaning produced lower rates for most molecules. Table 5 compares total quantity of gas removed off the vapor-degreased and the Varian cleaned sample.

DS-9 Cleaning: The third treatment, used identical S.S. 304 samples that went through the Diversey-9 cleaning treatment. The outgassing curves are shown in Figure 17. These curves were produced without any bakeout procedure. Hence we found no H outgassing curve, and the dominant components are H_2O and CO. But the outgassing rates produced by this treatment were lower than any pre-baked samples cleaned by Varian Standard cleaning and degreasing. But since Strausser did not follow the bakeout procedure with this sample the outcome cannot be compared to the results obtained from previous methods.

4.4. Calder and Lewin's Work

R.S. Calder and G.Lewin at CERN, Geneva, Switzerland,[2] have performed extensive studies on proper bakeout methods to reduce the outgassing rates to the lowest possible. A sample of U15C, a low-carbon 300-series stainless steel was used for the test material and was subjected to various bakeout temperatures and time-lengths. Bakeout at 300 °C proved to be optimal and the outgassing rate measured after 24 hours of bakeout at 300 °C was about 10^{-12} torr-l/s-cm^2 .The residual gas was composed of 99% hydrogen. This procedure was then referred as a "normal bakeout".

As mentioned earlier, the diffusion constant of H_2 from the bulk varies exponentially with temperature. Hence, if a material is baked at a high temperature, a large decrease in the outgassing rate should occur in a short period of time. A high-temperature bakeout of a vacuum vessel can in principle be executed in situ or prior to assemblage of the whole system, since the diffusion of hydrogen at room temperature, as shown earlier is negligible.

To test the effectiveness of high temperature baking, Calderand Lewin performed experiments on four Specimens A, B, C, D. Specimen A was a seam-welded 2 mm thick stainless steel container, that was 30 cm long and 10 cm in diameter and was attached to the system by a ConFlat type flange. After a 45 hour degassing at 360 °C, the hydrogen degassed from the sample at a rate of 2×10^{-12} torr-l/cm^2 -s, and formed 99% of the flow. The residual gas

analysis and the outgassing rates are available in Table 7.

Specimen B was identical to A, except for the surface preparation. The data presented on Table 7 is measured at 20 °C (room temperature) and was obtained after a bakeout of 300°C for 25 hours. The table alos includes data after successive bakeouts and at higher than room temperature. The multiple bakeouts give successively lower values of H_2outgassing.

Specimen C was like A and B except itcontained in additional coiled strip of 0.25 mm thick stainless steel 20cm in width and 25 m long which gave it a further outgassing rate of 10^4 cm^2 . The system was degassed at 1000°C for 3 hours in a vacuum furnace at approximately 2×10^{-6} torr, and a further in situ bake was done at 360 °C for 25 hours, and the data is recorded in Table 8. Experiments showed that since the strip was thinner in diameter than the sample thickness it degassed much faster. After a normal bakeout, the value obtained was twenty times less for the thinner material.

Specimen D used specimen C with a new coil of 0.25 mm-thick stainless steel. This coil, however, had had no degassing treatment. The results are shown in Table 9. The outgassing rates obtained after a normal bakeout were slightly higher than the previous sample. After an exposure to 1 torr of H for 12 days the degassing rate are restored to the original value after a normal bakeout. Thus, specimen C and D prove the advantage of thinner chamber materials for reducing outgassing rates.

4.5 R. Nuvolone°s Work

Mr. Nuvolone performed his research at the Service de Physique Atomique, in Saclay, France and published his article in 1977.[15] The experimental apparatus uses a sample made of 316L stainless steel with a chamber diameter of 100 mm and a length of 400 mm. The pressures were measured by Bayard-Alpert ionization manometers, and a quadripole residual gas analyzer checked the composition of gases leaving. Before the baking, the sample went through the following cleaning pre-treatment: 1) 2-hour degreasing with perchloroethylene vapor and 125°C 2) washing for one hour in Diversey 708 cleaner at 55°C (in an ultrasonic cell) and 3) rinsing with clean water and drying.

Table 9 shows the different outgassing rates obtained after the eight bakeout techniques. Nuvolone found that degassing the stainless steel in an ultrahigh vacuum furnace (5×10^{-9} torr (≃ 6.5×10^{-7} Pa)) gave consistently the lowest outgassing rate. Nuvolone mentioned that the results of oxidation during air-bake really become effective at 400°C. Since oxidation of this type are hard to control in the outside atmosphere, that pure oxygen should be used instead. The best results are obtained when the oxygen is at 20 torr. If the stainless steel is pre-degassed at 800°C in a vacuum furnace and then stored in air for five months the outgassing rate can still be lowered to similar levels by letting it degas in vacuum, in situ, for 20 hours at 150 °C and then air-bake for 2 hours at 400°C.

However, the uses for an ultra-high vacuum furnace are limited by the size of the apparatus and the huge costs that are involved. It will be expensive to provide a furnace so huge as to serve the purpose of the Gravity Wave Detector project, since the diameter of the furnace needs to be greater than 120 cm and 10-15 meters in length.

V. Description of Two Comparable Large Systems

This section is going to discuss the experiences learned from two large vacuum systems comparable in size to the GWO. The two systems are already in working operation and have maintained an ultra-high vacuum. The two systems are 1) Brookhaven National Laboratory in Upton, New York, and 2) CERN, Geneva, Switzerland. We are going to review each vacuum system in detail and discuss their surface treatment and vacuum procedures.

5.1. The Brookhaven System

The Brookhaven National Labs constructed an Intersecting Storage Accelerator (ISABELLE) consisting of two rings having a circumference of 3.8 km each.[24,26,28,33,34] The vacuum system uses a 8.8 cm diameter circular pipe made of 304LN nitrogen-hardened stainless steel. The entire system is being pumped by a combination of titanium sublimation pumps and 30 l/sec ion pumps. These pumps are placed in pumping stationsspaced 5-meters apart. The total length of the system is approximately 7500 meters and contains 1500 pumping stations. Total pressures below 1×10^{-11} torr $\sim (1 \times 10^{-9}$ Pa) have been attained in the 15-m sections of this system.

Engineering Considerations: A sketch of the pumping station module is illustrated in figure. 18.

The initial pumpdown to the high vacuum range ($< 10^{-6}$ torr) is done by the turbomolecular and sorption pumps in the system. The titanium-sublimation pumps then take over and bring the pressure down to the 10^{-11} Torr range. Two of these pumping stations had

been joined by aluminum tubes to create the ISABELLE half-cell proto-type. The Al tubes were baked at 200°C and the stainless steel at 300°C and then a titanium flash was used. The pressure was then measured by a Bayard-Alpert gauge. Figure. 19 presents the actual pressure-time curve of this half-cell system which reached an equilibrium pressure of 6×10^{-12} Torr in 14 days.

Surface Preparations: The beam went through the following treatment:[26] "(a) degeased in acetone and alcohol (b) chemically cleaned in a solution of one-third NO ,one-third HF, and one-third H O (c) rinsed in water (d) rinsed in alcohol (e) fired in a vacuum furnace in 950 C for 2 hours at a pressure of $< 1 \times 10^{-4}$ Torr (f) leak checked (sensitivity 3×10^{-10} Torr-l/s) (g) glow-discharged in a separate vacuum chamber using the following procedure: (1) with a tube in the chamber a pressure of $< 1 \times 10^{-4}$ Torr was reached in the system; (2) Bake-out for ~ 18 hours at 200 °C; (3) after 200°C bake-out the temperature was lowered and stabilized at 100°C; (4) at 100°C a bypass-valve was closed to decrease the pumping speed to 1 l/sec (5) At this time the chamber was brought to a pressure of 50 microns with a gas mixture of 90% Ar and 10% O_2; (6) A tungsten wire of .020-in diameter running down the center of the beam tube had 400V at 0.5 Amps applied to it. Glow discharge was achieved ; (7) The glow was maintained for 1 hour. After the system cooled to room temperature it was back-filled with N_2 . (8) The tube was then removed, the ends capped with aluminum foil and bagged in plastic.

Vacuum Behavior: After the cleaning procedure a pressure of 3

$\times 10^{-11}$ Torr was obtained in the full cell. A residual gas analyzer measured the peaks of each gas which had a significant outgassing rate. This is shown in figure.20.
Hydrogen, as expected, was the dominant gas. The trace of Ar is left over from the Ar-glow discharge surface cleaning.

Turbomolecular pumps was used for the initial pump-down and bake-out cycle. A pressure of 10^{-6} Torr was attained after an hour of pumping. The ovens were then turned on and the cell section was baked at 300 C for 24 hours (normal bakeout, C&L[2]). The B.A. electron gauges were turned on at this time, so that the filament is outgassed along with the vacuum chamber. It would also measure the pressure of the system during the bake-out cycle. The titanium filaments and ion pump electrodes also are outgassed for four hours. At the end of the 24 hour bake-out the turbopump is isolated from the rest of the system. The titanium of the titanium-sublimation pump is flashed for 7 minutes, and the pressure in the system lowers to the 10^{-11} range in 12 hours. This whole procedure can be summarized by the chart shown in figure.21.

5.2. The CERN System.

The two-kilometer CERN Intersecting Storage Rings (ISR) in Geneva, has a ultrahigh vacuum chamber is composed of tubular sections having a diameter of 164 mm and a thickness of 2mm.[21,22,36]

These sections are connected by ConFlat type all-metal flanges that can withstand an in situ bake at 300 °C.

The rough pumping is accomplished by 70 turbomolecular pumping stations, the main pumping being provided by 280 triode-sputter ion pumps each having a 350 litre/sec pumping speed. This means 35 l/sec per square meter of surface area. The advantage of a sputter-ion pump is that it pumps all types of gases and has an unlimited capacity, which helps in the strong initial outgassing. The total pressure inside the chamber is 10^{-9} Torr or better. So the entire apparatus is equipped with heating tapes and ovens to provide for in situ baking at 300 C, and the system is thermostatically controlled.

Vacuum Procedure: This following procedure taken from R.L.Samuel°s article[21] has been successful for ultra-high vacuum chambers up to 44 meters in length.

"1) Preheating the chamber at atmospheric pressure in air, at a temperature not exceeding 200°C for 2 hours, with venting valves open. 2) Closing venting valves, pumping turbomolecular pumps for some 30 minutes until a pressure of <= 5×10^{-5} Torr is attained. 3) Switching on sputter-ion pumps, closing roughing valves. Reducing temperature to not more than 150°C prior to degassing of gauges, this temperature being adequate for the purpose. 4) Degassing gauges for some 30 minutes when pressure

<= 3×10^{-7} Torr. 5) Switching off heating on completion of gauge degassing."

Fig.22 shows the steps taken for an air-bake in the chambers. We see that the desired pressure (1×10^{-9} Torr) is attained 2 hours after the end of the air-bake, which is 7 hours from the start of the operation.

R.L.Samuel[21] mentions that the above method is quite reproducible and that after the end of 12 bakes, the method has shown identical results. Table 10 summarizes the average pressures obtained for different lengths of UHV chambers and for different bakeout times.

VI. Conclusion

6.1 Summary on Outgassing

After reviewing outgassing data from several different researchers, it is evident that outgassing is a complex phenomenon. The complete mechanism of outgassing is not yet fully understood. Hence, experimental data is needed to support the theoretical figures. Contributions to outgassing come from surface adsorption and from the bulk. The amount of each depends upon the state of the surface. However, it is probable that the process is controlled more by impurities such as carbon and oxides than by the base material or the gases desorbed. Several analytical techniques such as AUGER and SIMS spectroscopy[29] are being used by researchers to verify the phenomena most affecting the outgassing rate. The results show that outgassing rate depends primarily upon two different criteria: the amount of oxide layer on the surface, and the ratio of the true surface area of the sample to the geometric area. The various cleaning methods used by the different laboratories reduce the above ratio and thereby lower the outgassing rate. Following this logic, the most desirable treatment would be one which minimizes the true surface area by producing a smooth, flat surface.

The accumulation of oxides on the surface provides a barrier for the diffusion of hydrogen. Using the numbers provided by Calder and Lewin[2], this diffusion becomes noticeable at high temperatures and especially to systems having a large surface area. Huffine and Williams[18] have shown that H permeation can be

reduced by more than a factor of 10 by oxidizing the surface. According to most researchers the surface also needs to be free of carbon, so that CO and CO_2 molecules do not form from the adsorbed O_2.

A high temperature bakeout seems to be the method proposed by most researchers. Baking the vacuum chamber for an extended period of time desorbs the sorbed material rapidly and also pumps the gas at a higher pressure. Therefore, the total throughput of desorbed gas is increased during this period by a large factor. Calder and Lewin[2] finds that a "normal" bakeout procedure (300°C for 24 hours) thoroughly degasses relatively thin stainless steel. However, if a stainless steel is baked at a very high temperature (> 400°C), then according to them, the surface of the stainless steel will not easily get recontaminated.

The range of heat treatments used by different researchers can be distinguished into three main categories:

a) In situ bakeout - The outer walls are exposed to atmospheric pressure while the inside is evacuated by vacuum pumps. The duration of the bakeouts vary from one laboratory to another, but the treatments generally give outgassing rates in the order of 10^{-12} torr-l/cm^2 -s for temperatures at 100- 400 °C and times ranging from 20-100 hours.

b) Predegassing in Vacuum - Chamber parts are baked inside an ultra-high vacuum furnace (10^{-8}- 10^{-9} torr) for several hours at very high temperatures (800 -1000°C). Outgassing rates after the treatment have been in the 10^{-13} torr range.

c) Baking in air- The chamber surfaces have been oxidized by baking in air at temperatures from 100°C - 400°C. this method has

also produced outgassing values in the 10^{-13} torr range.

These values are dependent upon measurement conditions, and type of specimen (stainless steel composition, geometry, dimensions, machining, and surface pre-treatments). Such conditions vary from one laboratory to another and in this case it is necessary to determine if the conditions can be transposable to the GWO system.

The two systems, at Brookhaven and CERN have shown that pressures below the 10^{-8} torr requirement needed by the GWO system can be maintained in ultra-high vacuum chambers. However, the dimensional requirement for the GWO is enormous. The diameter of the GWO system is many times larger than any experimental setup operating at this present time. This means that the surface area of the system and the total outgassing rate will also be many orders larger than any other vacuum system.

6.2. Proposal of a test-model

To tackle the conditions for the gravity wave vacuum system effectively, a smaller test-model should be built. The results obtained from other working vacuum systems should be tested at identical experimental conditions to find out if these conditions are reproducible. A proposal for a test-model attaining proper outgassing procedures will now be suggested in this paper.

It would be wise to construct a sample test-chamber having a diameter of 48 cm and a length of 12 meters, so that it would be identical to the proposed chambers of the GWO system. This chamber can then be connected to a system which will measure its

outgassing rate. This system can use the standard outgassing measurement Q= SP. According to this mathod a chamber of volume,V, is pumped through a known conductance,C. When the condition V dp/dt << Cp is met, the outgassing rate is calculated from $Q= C (P_1 - P_2)$. the outgassing rate can be measured by two methods to allow for cross-checks. This can be accomplished properly accomplished by using ionization gauges and a mass spectrometer for measurement.

Before making any measurements, the sample surface needs to be pre-treated. It is important for the sample to achieve a very smooth, clean and inert surface. Smoothness is characterized by the reduction in the total outgassing surface area. The dominant residue gases such as H_2O, CO, CO_2, and H_2 need to be pumped out of the surface.

The following pre-treatment can be used in this case: 1) degreased in acetone and alcohol 2) chemically cleaned in a solution of 33%HNO_3, 33% HF, and 33% H_2O 3) rinsed in water 4) rinsed in alcohol, 4) degassed in a vacuum furnace at 900°C for 3 hours at a pressure $< 1 \times 10^{-4}$ torr. The chemical cleaning above is a variation of the Varian standard cleaning technique. Both Varian and Diversey-9 cleaning are effective cleaning procedures for this purpose and have been used by many other large vacuum systems.

Because of its size a furnace with an ultra-high vacuum will be costly and difficult to construct. Hence, this vacuum furnace can be at a less demanding pressure. The furnace can be attached to sputter-ion pumps. The advantage of these pumps are that they pump all types of gases and they have an unlimited capacity.

The test-model should then be tested for outgassing. If the rate is not at acceptable levels then the sample should be baked for more number of hours.

This procedure can be used for the test-section of the full GWO system as well. A high-temperature bake of the stainless section would, according to researchers, prevent steel from being easily recontaminated. This is beneficial to the GWO system since after the pre-treatment of the sections, it will take a considerable amount of time to assemble the complete system, and this may result in increasing the outgassing rate.

It might also be helpful if the 5-kilometer long cavities are subjected to a low-temperature degassing treatment. This can be accomplished by flowing Argon gas through the 5-km long tubes. The gas can be kept at a pressure $\sim 2 \times 10^{-2}$ torr. the high molecular weight of the Argon will free some of the molecules which had stuck to the surface following the pre-treatment. The extra weight will also help in pumping the Argon out of the system.

Thus, this above method is a possible procedure for measuring the outgassing phenomena. But the real results will not be achieved unless experiments are performed to prove the results attained from research. This opinion is being held by researchers in other laboratories as well. The vacuum system of the Gravity wave detector has to be fully tested before it can assume full-scale operation.

Addendum

The following brochures from three companies are being attached to this report.

1) Deritend-Hot Foil Inc.- gives a brief narrative and a price listings on Heating tapes-Type G, a particular heating tape already in use on the vacuum systems at Brookhaven and CERN.

2) Diversey-Wyandoatte Chemical Corp.- three articles have been added discussing technical and operating data of the DS-9 cleaning solution. A meeting had been set up with a sales representative of the company and the feasibility of DS-9 cleaning for the GWO system was discussed. The represemntative will keep the GWO team further informed on the use of the particular cleaning treatment.

3) Western Pneumatic Tube Co.- articles containing vapor degreasing and pickle house procedures are being attached. These procedures were used for the vacuum system presently in operation at Brookhaven.

LIST OF TABLES AND FIGURES

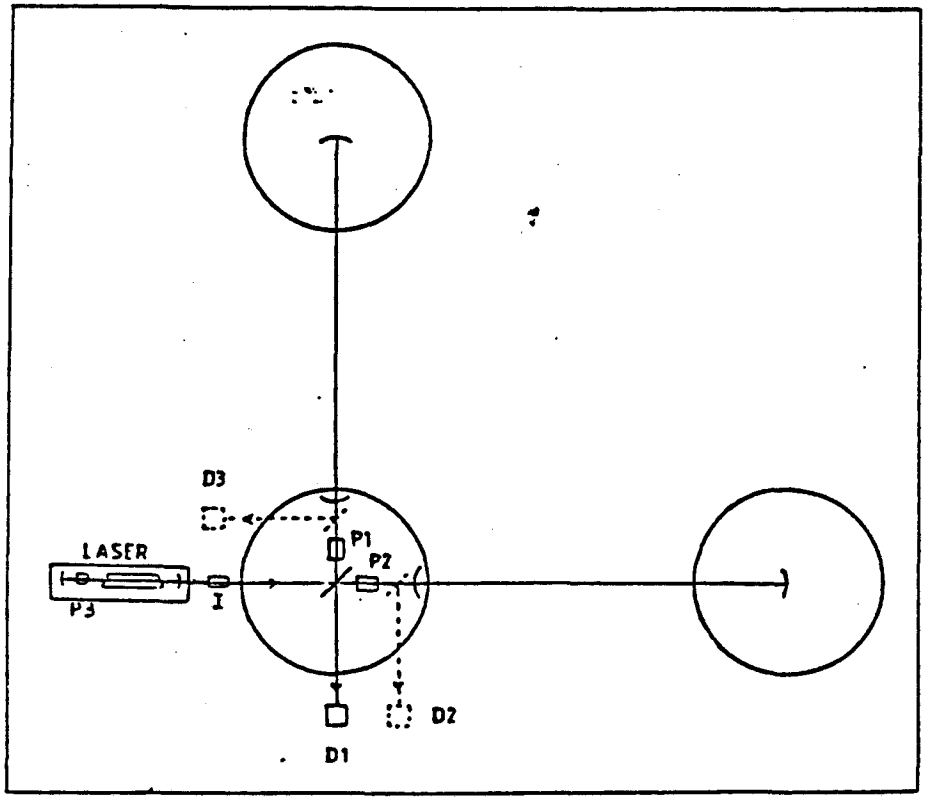

The simplified diagram above illustrates an optical cavity gravitational wave interferometer. Reflection of light many times between curved mirrors mounted on the test masses (indicated by circles) increases phase difference in the light coming back from each arm caused by motions of the masses. The phase difference is measured by photodiode D1, aided by electro-optical phase modulators P1 and P2 driven at a high radio frequency. Signals from auxiliary photodiodes D2 and D3 measure small deviations of laser wavelength from resonance with the cavities and may be used both to control average length of each cavity and reduce fast fluctuations in laser wavelength.

Fig. 1

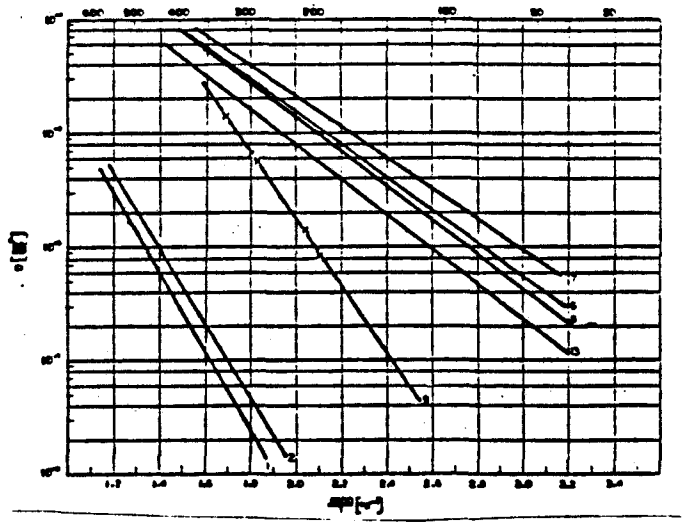

Fig. 2

Diffusion coefficients of hydrogen in various steels as a function of the reciprocal of the absolute temp.

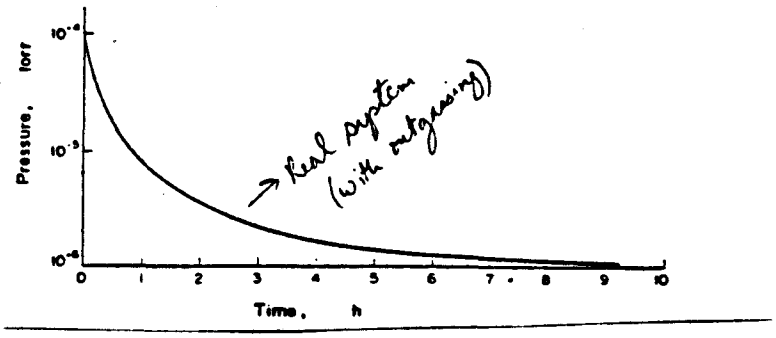

Fig.3. A typical pump-down curve.

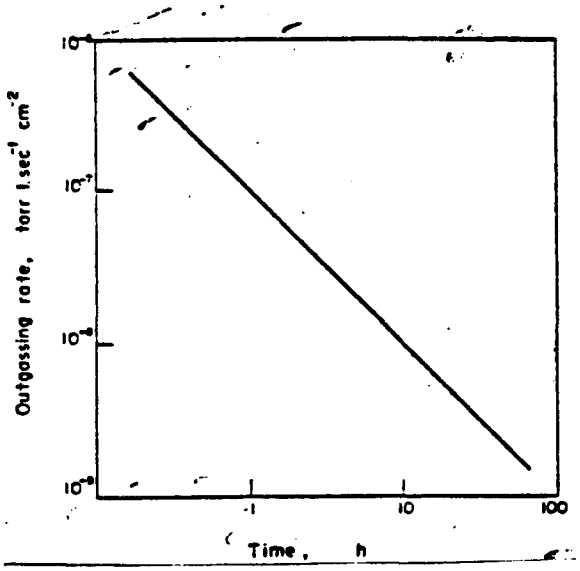

Fig.4. A typical outgassing rate plot

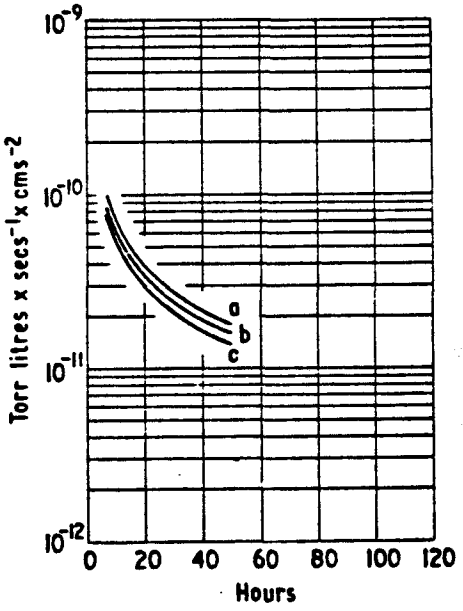

Fig.5. Total outgassing per cm^2 of sample as a function of pumping

a. Honed sample following bake in vacuo at 450°C & exposed to air. (Sample I Exp 2)
b. Sample exposed to air & vapour degreased. (Sample I Exp 3)
c. Sample following smearing with cutting oil & vapour degreasing. (Sample I Exp 4)

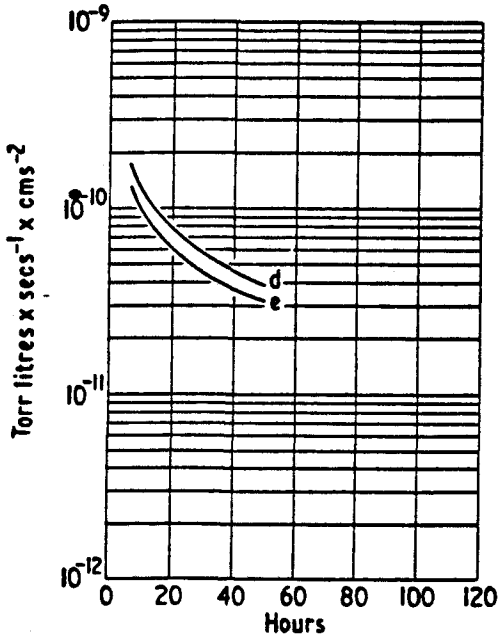

d. Sample honed & degreased (Sample 2, Exp. 5)
e. Sample machined & degreased (Sample 2, Exp. 9)

Fig 6. Total outgassing per cm^2 of sample as a function of pumping time.

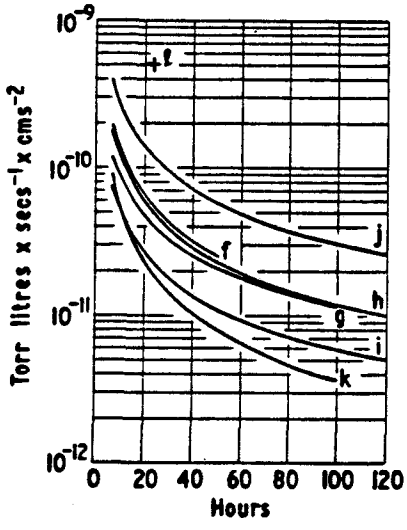

f. Sample electro polished only. (Sample 5 Exp 12)
g. Vapour degreased following Exp 12. (Sample 5 Exp 13)
h. Sample washed in demineralised water. (Sample 5 Exp 14)
i. Baked in air at 500°C following Exp 14. (Sample 5 Exp 15)
j. New sample cleaned by Diversey process. (Sample 6 Exp 17)
k. New sample machined degreased & contaminated with lard oil, then plasma cleaned. (Sample 8 Exp 23)
l. New sample contaminated with lard oil, no cleaning. (Sample 9 Exp 30)

Fig. 7. Total outgassing per cm^2 of sample as a function of pumping time.

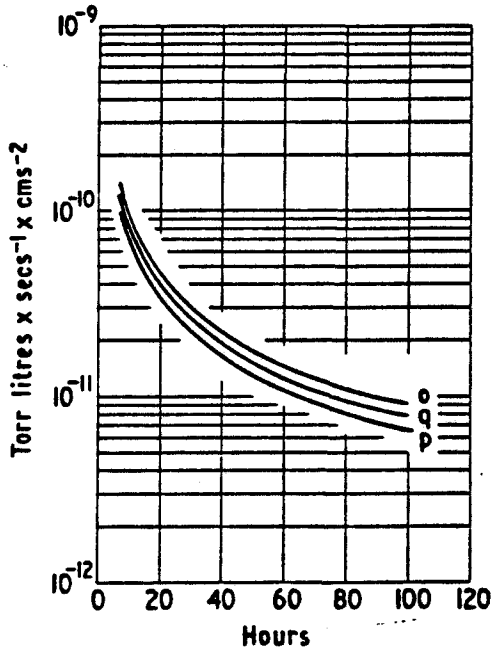

o. Sample vapour degreased only. (Sample 7 Exp 18)
p. Following exposure to air after bake at 400°C in vacuo. (Sample 7 Exp 20)
q. Sample smeared with sweat. (Sample 7 Exp 21)

Fig. 8. Total outgassing per cm^2 of sample as a function of pumping time.

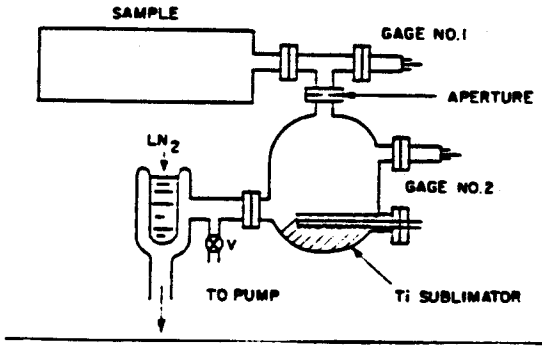

Fig.9. Schematic of experimental system of J.R. Young

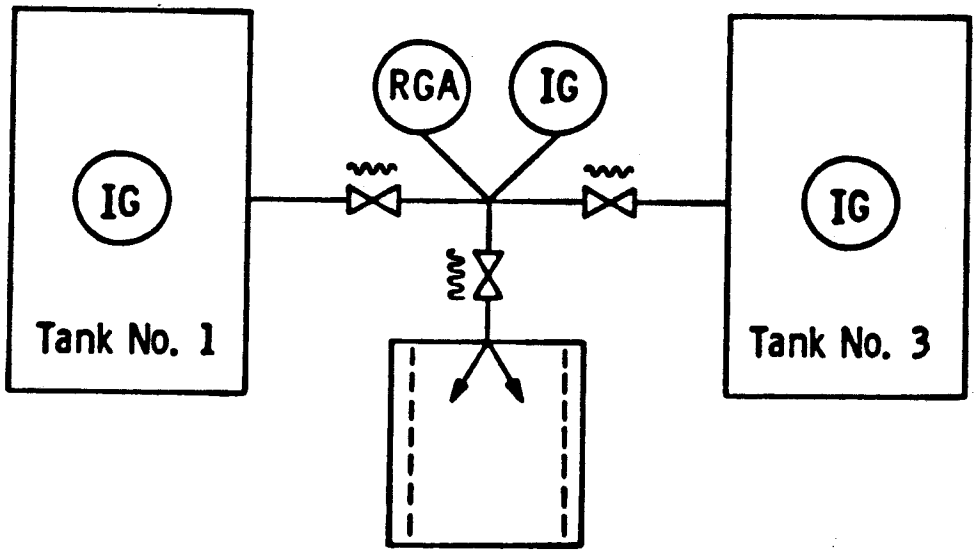

Fig.10. Schematic view of experimental system of Y. Strausser

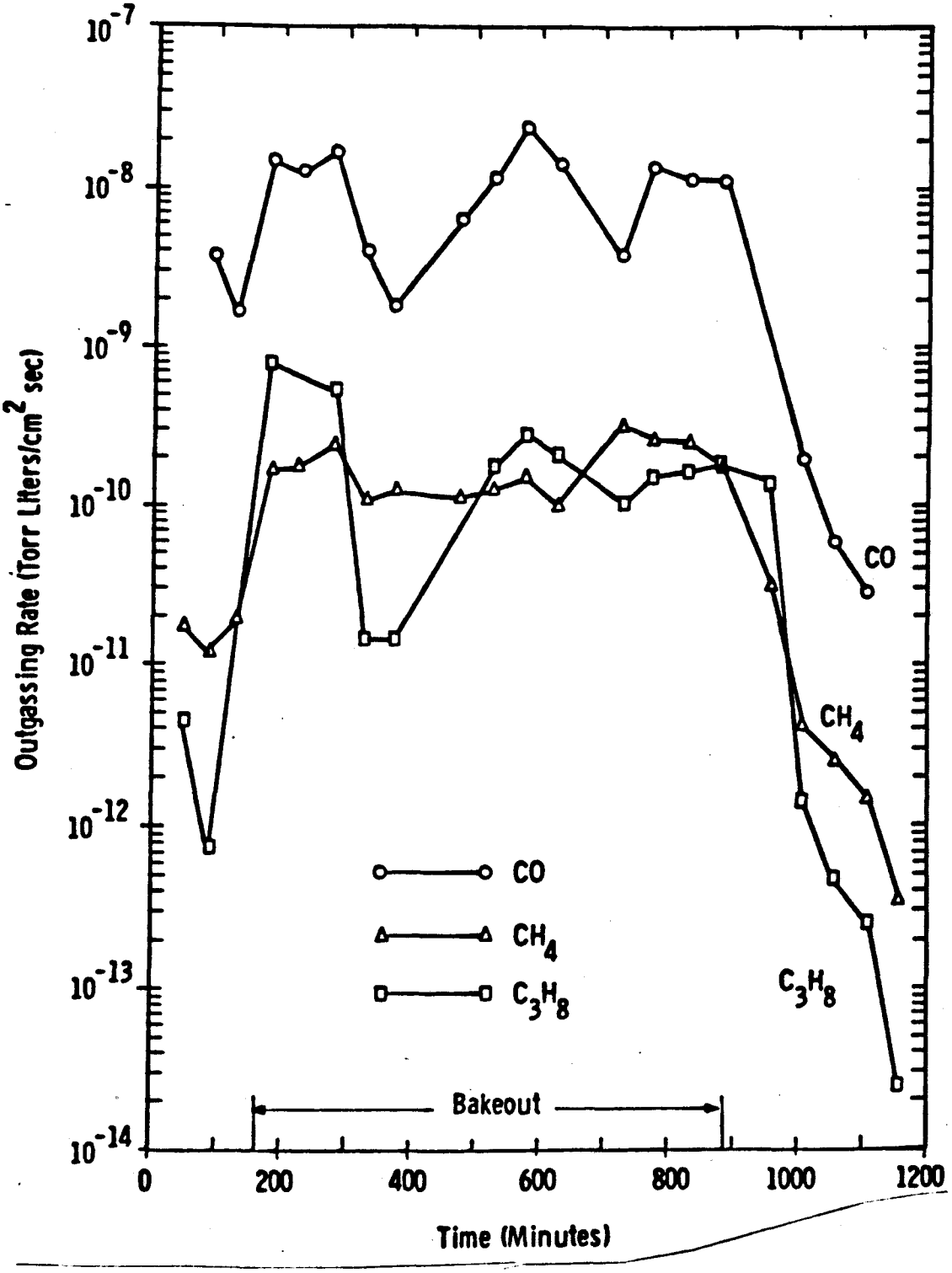

Fig.11. Outgassing Rates for CO, CH_4, C_3H_8 from samples with 2% HF Cleaning.

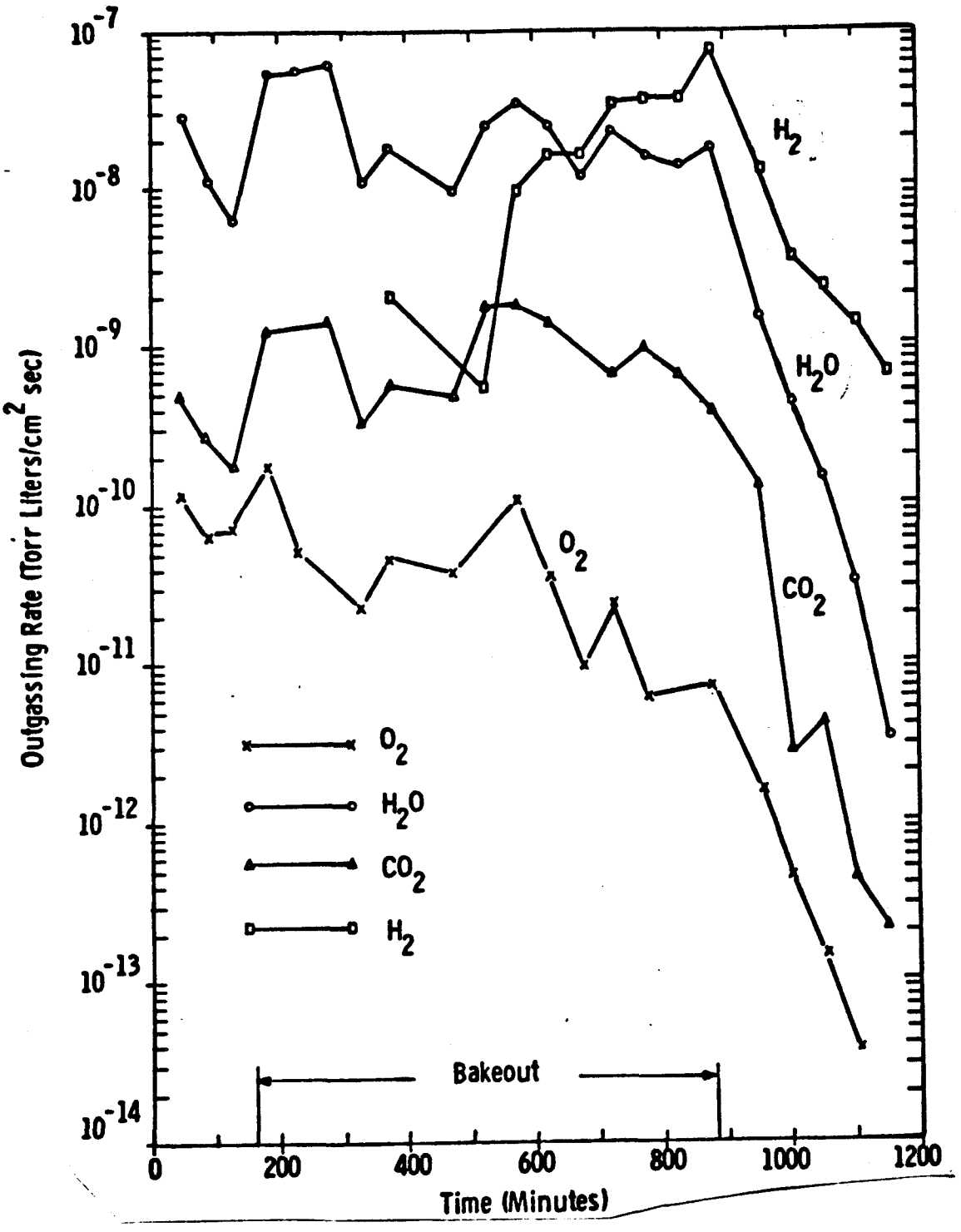

Fig. 12. Outgassing rates for H_2, H_2O, CO_2, and O_2 from Sample with 2% HF cleaning.

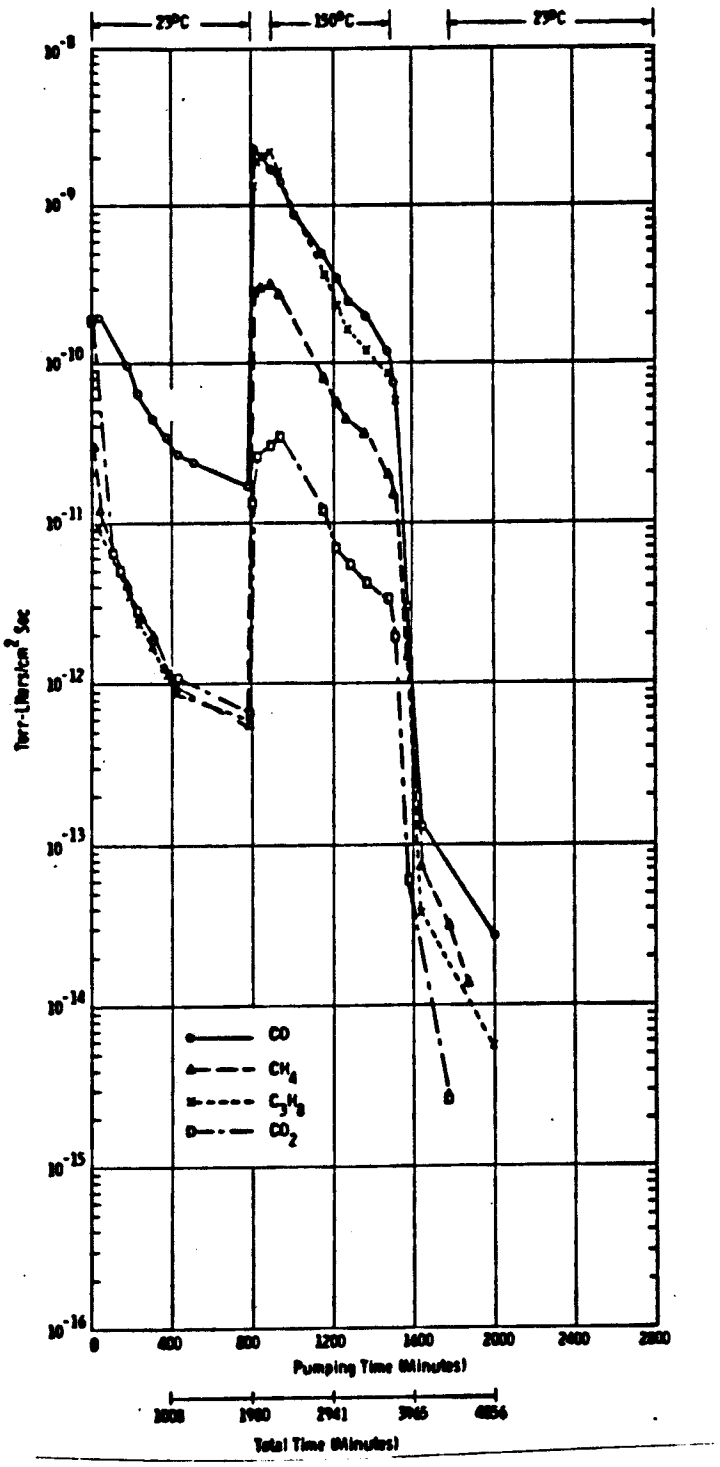

Fig.13. Outgassing Rates for CO, CH_4, C_3H_8, CO_2 from sample with 33% HF sample.

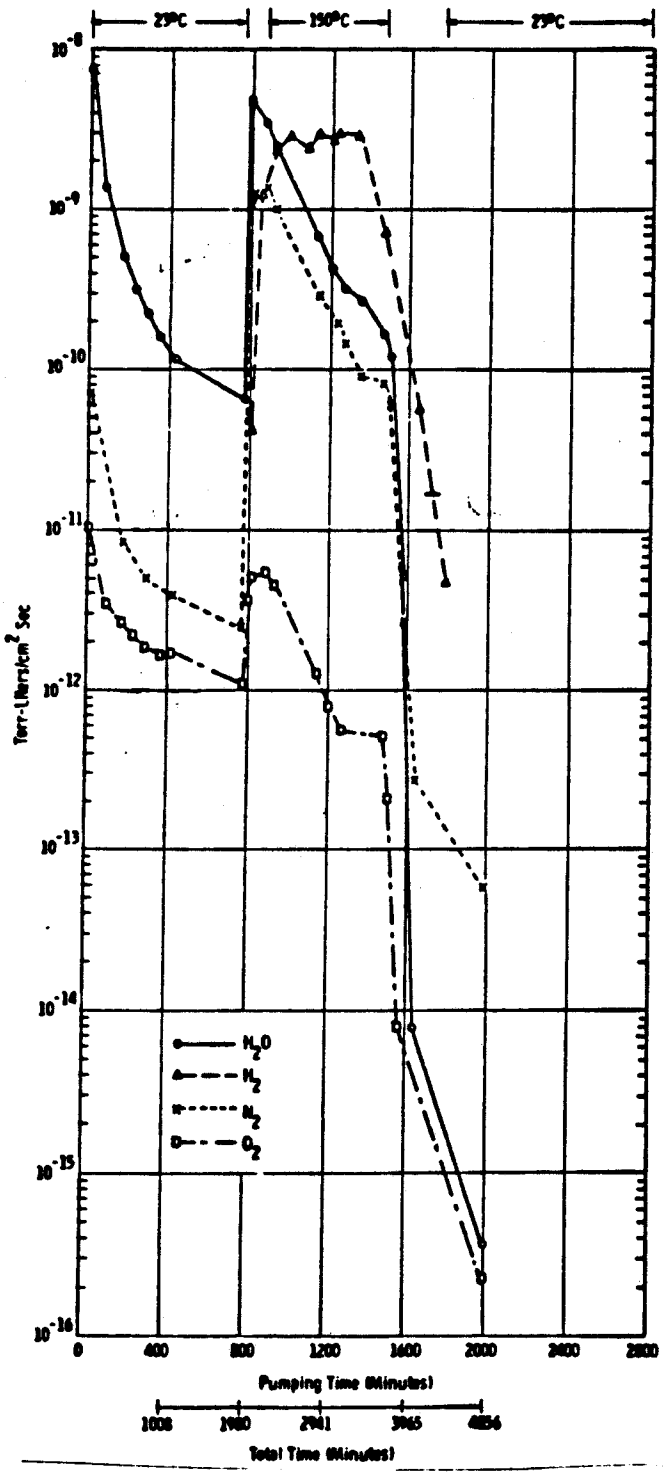

Fig.14. Outgassing Rates for H_2O, N_2, O_2 from sample with 33% HF cleaning.

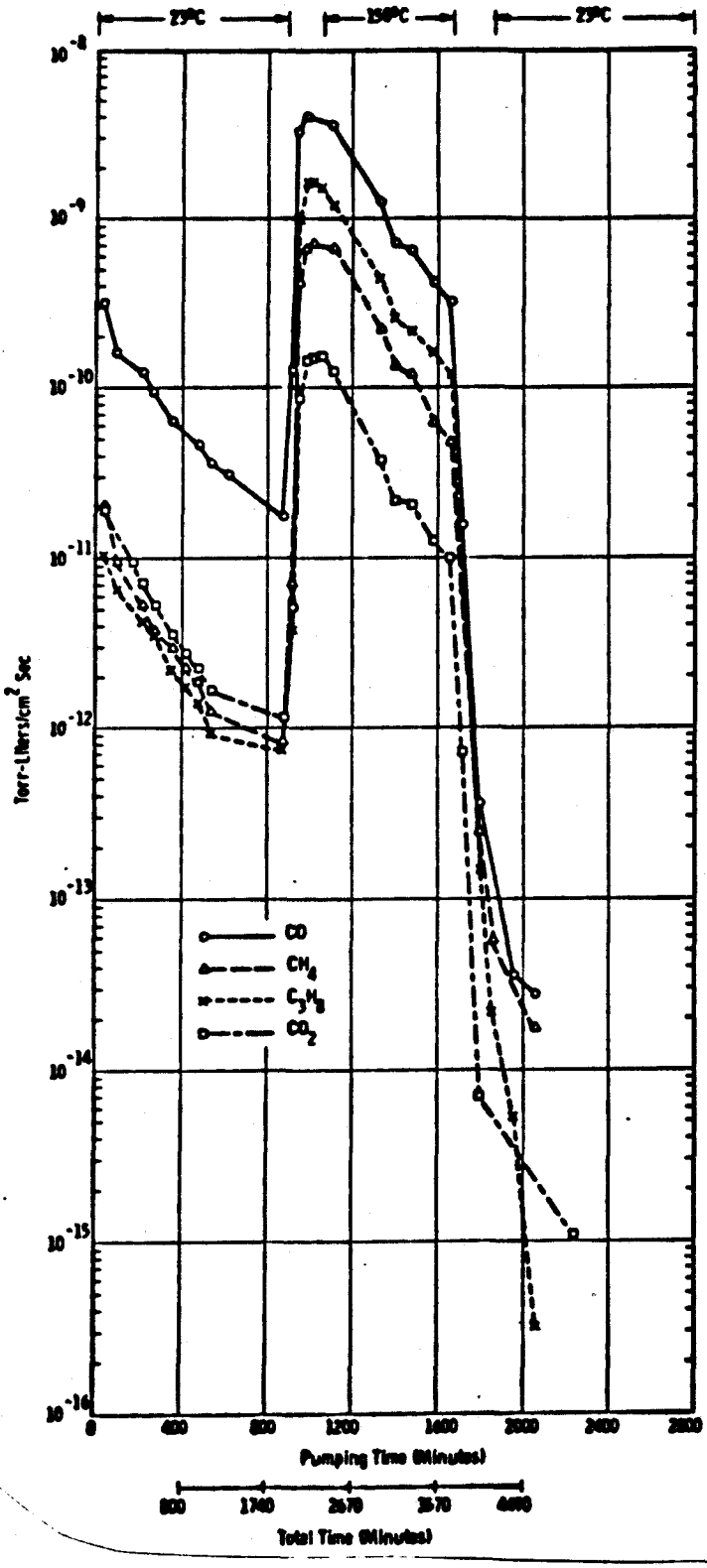

Fig. 15. Outgassing rates for CO, C_3H_8, CO_2 from sample with only-degreasing

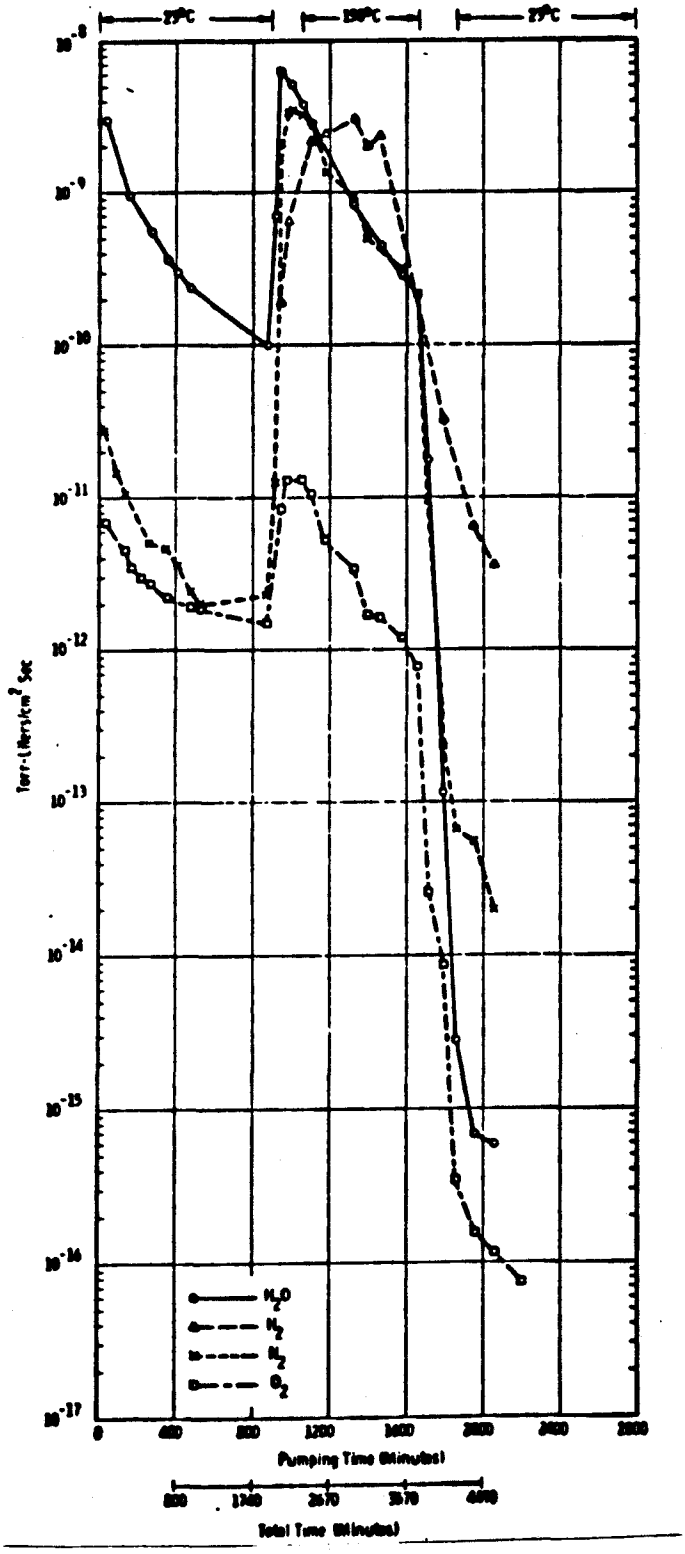

Fig. 16. Outgassing Rates for H_2, N_2, H_2O, O_2 from Sample with only-degreasing

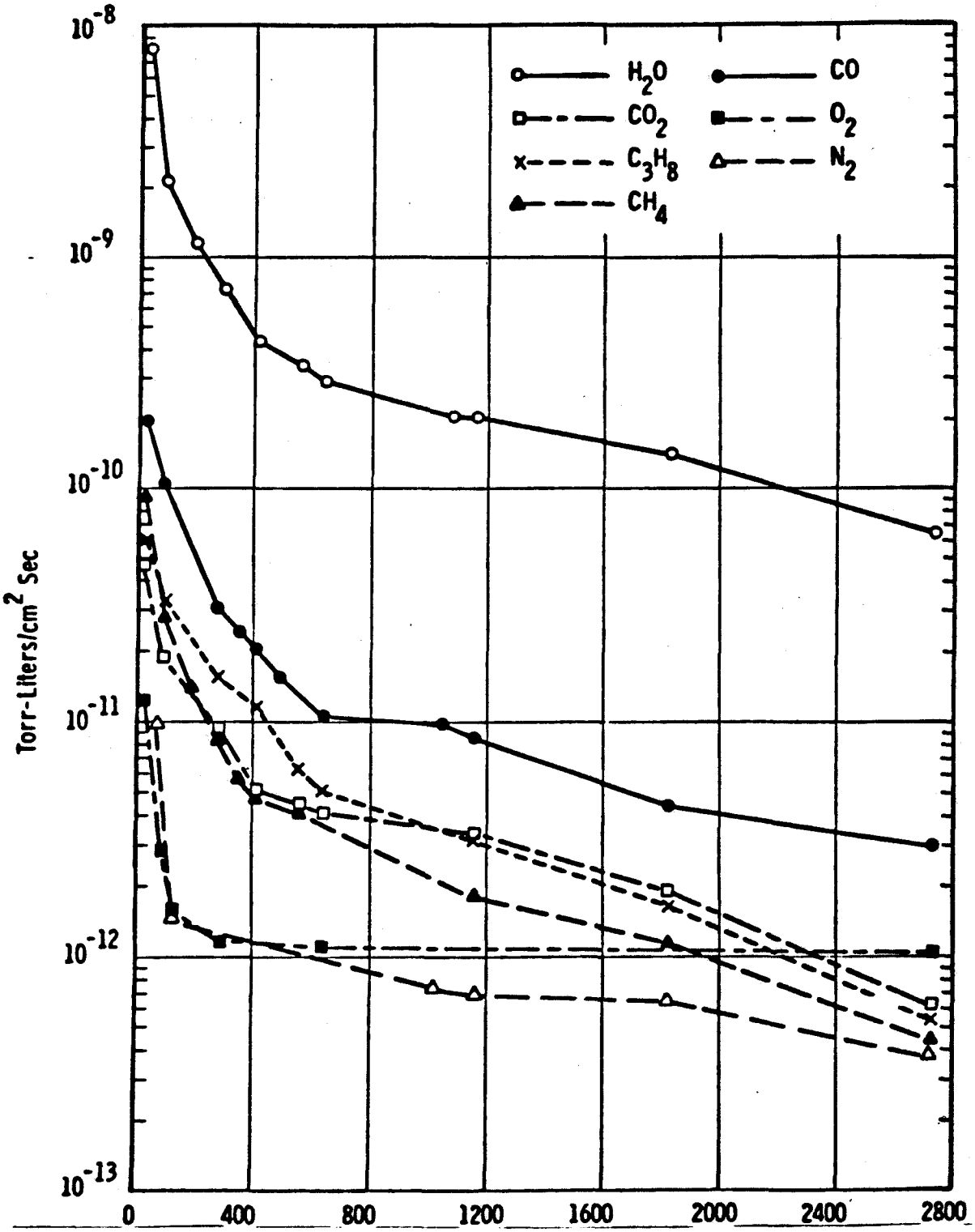

Fig. 17. Outgassing rates for sample cleaned by Diversey DS-9 Cleaning with no bakeout.

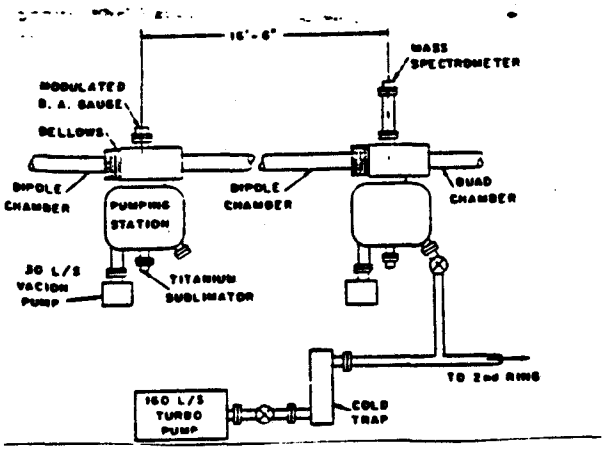

Fig. 18. Typical module of the ISABELLE system.

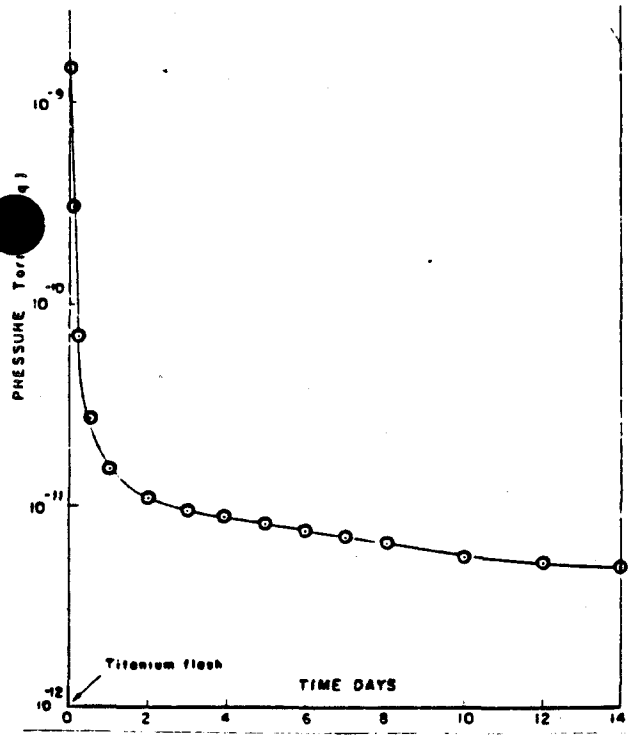

Fig. 19. Pump-down curve for the Half-Cell Vacuum envelope

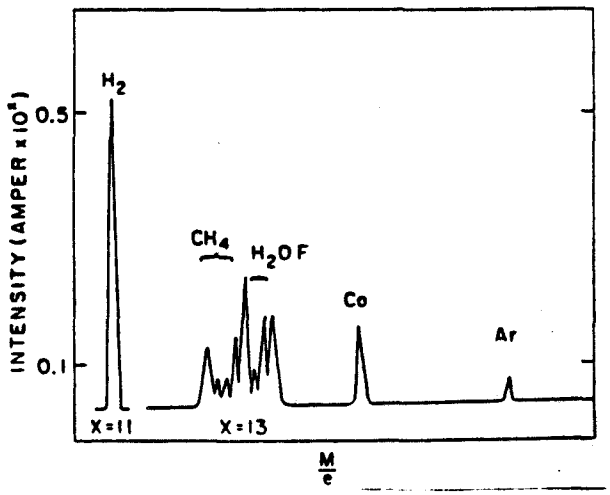

Fig. 20. Residual gas analyzer gases from normal operation of vacuum first-cell.

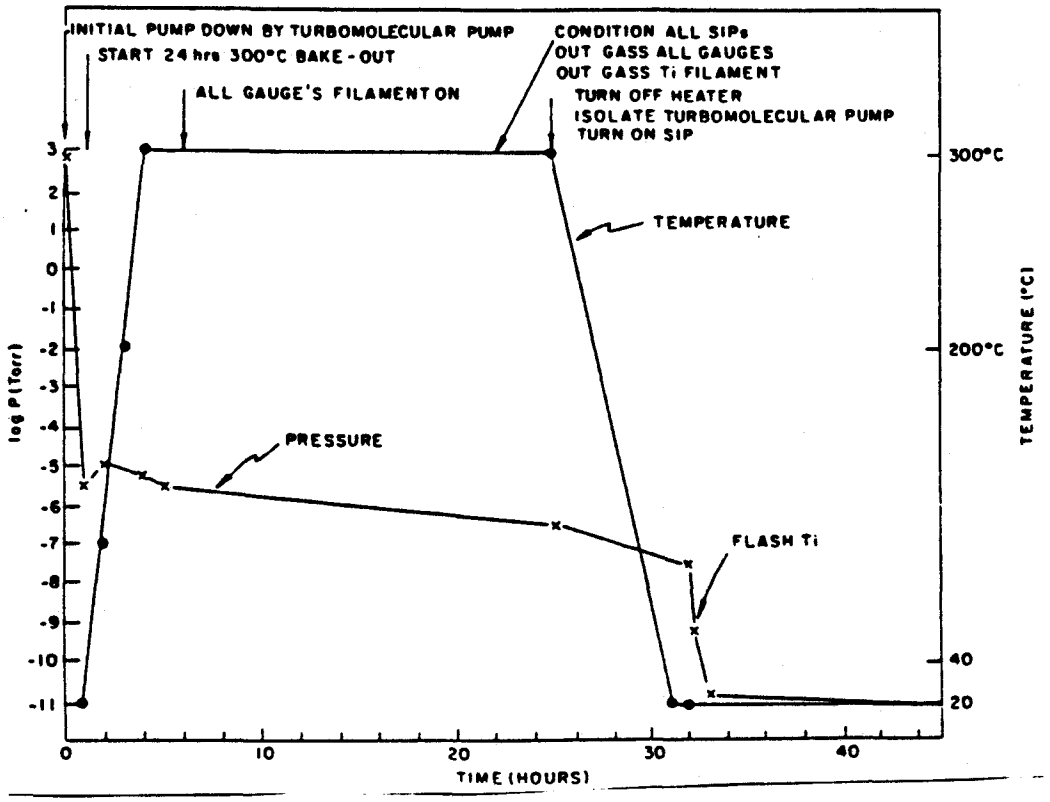

Fig. 21. General vacuum treatment and behavior of ISABELLE

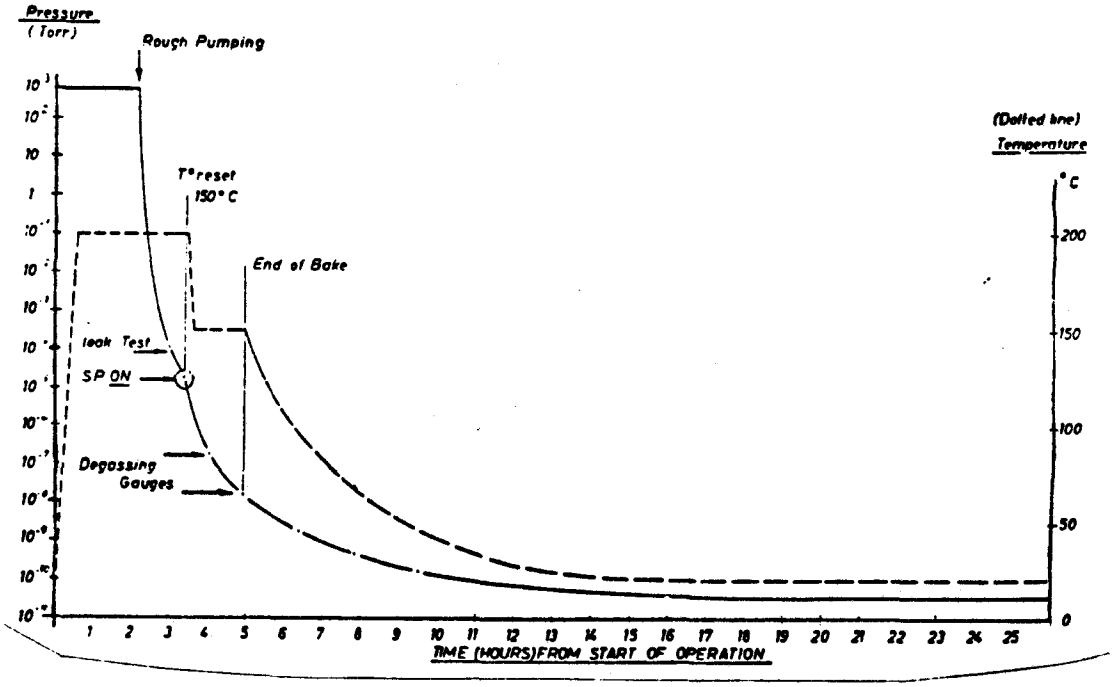

Fig. 22. Typical steps in air-bake of UHV chambers at the ISR.

Table 1. Barton & Govier, Outgassing rates after 48-hours.

SAMPLE	SURFACE TREATMENT	OUTGASSING RATE (Torr-l/sec-cm^2)
a	Honed sample following bake at 450°C and exposed to air.	2×10^{-11}
b	Sample exposed to air & vapor degreased.	2×10^{-11}
c	Sample smeared with oil and then vapor degreased.	2×10^{-11}
d	Sample honed & degreased	4×10^{-11}
e	Sample machined & degreased	3×10^{-11}
f	Sample electropolished only	2.5×10^{-11}
g	Sample vapor degreased following (f)	3×10^{-11}
h	Sample then washed in dimineralized water.	3×10^{-11}
i	Baked in air at 500°C after.	1×10^{-11}
j	Diversey process	6×10^{-11}
k	plasma cleaned	8×10^{-12}
l	lard oil, no cleaning	~
m	new sample machined + degreased	2×10^{-11}
n	Same sample, vapor blasted + degreased	1×10^{-11}
o	Sample vapor degreased only	1×10^{-11}
p	following exposure to air, then baked	8×10^{-12}
q	(p) Smeared with sweat	9×10^{-12}

Sample	Material and surface treatment	Outgassing rate after 24 h at room temperature Torr liter/sec cm^2
A	304 stainless steel (S. S.) cleaned by glass-bead shot blasting (32μ in. surface, baked 30 h at 250°C).	2×10^{-12}
B	304 S. S., 4–6μ in. electropolished surface (baked 30 h at 250°C).	3×10^{-12}
C	304 S. S., 20–25μ in. electropolished surface (baked 30 h at 250°C).	2×10^{-12}
D	Sample B (above) baked with inner and outer surface exposed to air 16 h at 250°C (plus an additional 15 h at 250°C under vacuum).	5×10^{-12}
E	304 S. S. cleaned by glass-bead shot blasting, then baked with inner and outer surface exposed to air 61 h at 450°C (additional 15 h at 250°C under vacuum).	3×10^{-12}
F	Sample E (above) after removal of inner and outer oxide by glass-bead shot blasting (additional 15 h at 250°C under vacuum).	3×10^{-12}
G	304 S. S., 20–25μ in. electropolished surface baked 30 h at 250°C plus 17 h at 450°C (continuation of sample C above).	4×10^{-12}
H	Aluminum, type 1100, cleaned with detergent, rinsed in acetone, baked 15 h at 250°C under vacuum.	4×10^{-12}

Table 2. Outgassing rates after 24 hrs at room temperature, from J.R. Young.

Gas	With 2% HF Cleaning	With 33% HF Cleaning
H_2O	9.8×10^{-9}	1.4×10^{-9}
CO	3.2×10^{-9}	1.8×10^{-10}
CO_2	2.5×10^{-10}	1.0×10^{-11}
O_2	6.7×10^{-11}	3.5×10^{-12}
CH_4	1.4×10^{-11}	1.1×10^{-11}
C_3H_8	7.4×10^{-13}	8.7×10^{-12}

Table 3. Outgassing rates after 100 min. of pumpdown.

Gas	Quantity Removed (mole/cm^2)	Final Outgassing Rate (Torr-liters/cm^2 · sec)
H_2O	2.4×10^{15}	3.5×10^{-16}
H_2	2.9×10^{15}	4.7×10^{-12}
CO	1.07×10^{15}	2.7×10^{-14}
N_2	7.25×10^{14}	5.9×10^{-14}
C_3H_8	1.05×10^{15}	5.5×10^{-15}
CH_4	1.95×10^{14}	1.4×10^{-14}
CO_2	4.41×10^{13}	2.6×10^{-15}
O_2	6.80×10^{12}	2.2×10^{-16}

Table 4. Total quantity of Gas removed from sample with standard cleaning.

Gas	Q_1, Quantity Removed from Standard Cleaned Sample	Q_2, Quantity Removed from Only-Degreased Sample	Q_2/Q_1
H_2	2.88×10^{15}	2.84×10^{15}	1
H_2O	2.4×10^{15}	3.64×10^{15}	1.5
CO	1.07×10^{15}	2.80×10^{15}	2.6
C_3H_8	1.05×10^{15}	9.91×10^{14}	0.94
N_2	7.25×10^{14}	1.94×10^{15}	2.7
CH_4	1.95×10^{14}	5.02×10^{14}	2.6
CO_2	4.4×10^{13}	1.00×10^{14}	2.3
O_2	6.8×10^{12}	1.17×10^{13}	1.7

Table 5. Total quantity of gas removed from sample which was only degreased.

Specimen preparation	Measurement temperature (°C)	H_2	H_2O	CO–N_2	O_2	CO_2
Degassed several times—total of 45 h at 360°C	24	1.3^{-12}†	—	—	—	—
		2.6^{-12}				
		2.3^{-12}				
	100	2.1^{-11}	—	[4.7^{-13}]	—	2.5^{-13}
	0	1.3^{-12}	—	—	—	—
Exposed to atmosphere for 3 h. Pumped under vacuum for 40 h	19	2.7^{-12}	6.4^{-12}	1.9^{-12}	2.2^{-12}	1.2^{-12}
Pumped under vacuum for further 4 days at room temperature	19	2.6^{-12}	1.0^{-12}	6.4^{-13}	8.4^{-14}	3.6^{-13}
Baked at 360°c for 24 h	19	9.9^{-13}	—	[2.6^{-15}]	—	—

† The superscripts denote the power of ten by which the numbers should be multiplied.

Table 6. Specimen A: outgassing rates (torr-ℓ/s-cm²)
(Calder & Lewin)

Specimen preparation	Measurement temperature (°C)	H_2	H_2O	$CO–N_2$	O_2	CO_2
Baked under vacuum for 25 h at 300°C	20	$3·9^{-12}$†	—	$1·7^{-14}$	—	$1·9^{-14}$
	20	$4·5^{-12}$	—	—	—	$2·0^{-14}$
	20	$[2·6^{-12}]$	—	$6·1^{-14}$	—	$1·5^{-14}$
Temperature of specimen raised	40	$1·3^{-11}$			—	
	100	$2·1^{-10}$	$1·0^{-13}$	$4·7^{-13}$	$1·8^{-12}$	$1·7^{-12}$
Baked under vacuum for 25 h at 300°C	20	$3·0^{-12}$	—		—	$1·7^{-14}$
	20	$3·0^{-12}$				
	20	$3·0^{-12}$				
	20	$2·8^{-12}$	—	$[8·6^{-15}]$	—	$1·1^{-14}$
Temperature of specimen raised	35	$5·6^{-12}$	$[7·8^{-15}]$	(- - -)	—	$2·5^{-14}$
	53	$1·6^{-11}$	$[6·4^{-15}]$	(- - -)	—	$3·3^{-14}$
	75	$4·4^{-11}$	$4·6^{-14}$	—	—	$5·8^{-14}$
Baked under vacuum for 25 h at 300°C	20	$1·5^{-12}$				
	20	$1·5^{-12}$	(- - -)	$[1·6^{-13}]$	—	(- - -)
	20	$1·4^{-12}$	—	—	—	—
Temperature of specimen raised	47	$5·3^{-12}$	—	$[5·2^{-15}]$	—	$[1·7^{-15}]$
	72	$1·5^{-11}$	—	$2·8^{-14}$	—	$[5·4^{-15}]$
	105	$3·9^{-11}$	—	$6·3^{-14}$	—	$[8·7^{-15}]$
	145	$9·2^{-11}$	$3·1^{-13}$	$1·4^{-13}$	—	$1·0^{-14}$
	200	$2·5^{-10}$	$6·1^{-13}$	$2·6^{-13}$	—	$3·6^{-14}$
Baked under vacuum for 25 h at 300°C	20	$1·1^{-12}$	—		—	—
	20	$1·2^{-12}$	—	$[4·3^{-15}]$	—	—

† The superscripts denote the power of ten by which the numbers should be multiplied.

Table 7: Specimen B, outgassing rates (Calder & Lewin)

Specimen preparation	Measurement temperature (°C)	H_2	H_2O	$CO–N_2$	O_2	CO_2
Degassed at 1000°C for 3 h in a vacuum furnace, then *in situ* bake at 360°C for 25 h	20	$1·3^{-14}$*‡	—	$1·0^{-14}$	—	$1·9^{-15}$
	20	$6·9^{-15}$*	—	$1·2^{-15}$	—	$1·9^{-15}$
	20	$1·3^{-14}$	—	(- - -)	—	$[4^{-16}]$
Raise temperature of specimen	100	$1·2^{-14}$	—	$2·1^{-14}$	—	$2·3^{-15}$
Baked for 72 h at 200°C under vacuum	20	$1·0^{-14}$	—	—	—	—
Raise temperature of specimen	100	$8·7^{-15}$	—	(- - -)	—	—
	200	$1·9^{-14}$	—	$3·1^{-14}$	—	—

* Not corrected for outgassing of untreated area.
‡ The superscripts denote the power of ten by which the numbers should be multiplied.

Table 8: Specimen C, outgassing rates (Calder & Lewin)

Specimen preparation	Measurement temperature (°c)	H_2	H_2O	$CO–N_2$	O_2	CO_2
Baked *in situ* at 360°c	20	$2{\cdot}7^{-14}$‡	—	[$1{\cdot}5^{-16}$]	—	(- - -)
for 24 h	20	$2{\cdot}5^{-14}$	—	(- - -)	—	(- - -)
	20	$2{\cdot}6^{-14}$				
Exposed to 1 torr of H_2 for	20	$6{\cdot}8^{-12}$				
12 days, then pumped	20	$5{\cdot}0^{-12}$				
under vacuum for 3 days at room temperature	20	$2{\cdot}6^{-12}$	$3{\cdot}3^{-13}$	(- - -)	—	$7{\cdot}9^{-15}$
Baked *in situ* at 360°c	20	$6{\cdot}0^{-14}$		$1{\cdot}9^{-14}$	—	[$3{\cdot}4^{-16}$]
for 24 h	20	$2{\cdot}7^{-14}$	—	$2{\cdot}0^{-15}$	—	[$1{\cdot}9^{-16}$]
	20	$3{\cdot}8^{-14}$	—	(- - -)	—	$1{\cdot}6^{-15}$

† Not corrected for outgassing of untreated area.
‡ Superscripts denote the power of ten by which the numbers should be multiplied.

Table.9. Specimen D, outgassing rates (Calder & Lewin)

Sample	Surface treatment	Outgassing rates in unit of 10^{-13} Torr l s^{-1} cm^{-2} H_2	H_2O	CO	A	CO_2
A	Pumped under vacuum for 75 h	670	430	65	...	10
	50-h vacuum bakeout at 150°C	290	13	4.5	...	0.3
B	40-h vacuum bakeout at 300°C	62	0.5	1.7	...	0.01
C	Degassed at 400°C for 20 h in a vacuum furnace [5.10^{-9} Torr (~6.5^{-7} Pa)]	14	0.2	0.33	0.12	0.08
	Degassed at 800°C for 2 h in a vacuum furnace [5.10^{-9} Torr (~6.5^{-7} Pa)]	2.7	...	0.05	...	0.04
D	Exposed to atmosphere for 5 months pumped under vacuum for 24 h.	...	55	50	...	10
	20-h vacuum bakeout at 150°C	2.5	...	0.06	...	0.03
	2 h. in air at atmospheric pressure at 400°C	13	...	0.84	...	0.3
E	Exposed to atmosphere for 5 months, pumped under vacuum for 24 h.	...	60	52	...	25
	20-h. vacuum baked at 150°C	13	0.56	0.28	...	0.13
F	2 h in oxygen at 200 Torr (~2.7×10^4 Pa) at 400°C	450	190	...	92	...
	20-h vacuum bakeout at 150°C	3.9	0.07	0.3	0.38	...
G	2 h in oxygen at 20 Torr (~2.7×10^3 Pa) at 400°C	...	15	10	6.5	...
	20-h vacuum bakeout at 150°C	...	0.67	0.48	0.34	...
H	2 h in oxygen at 2 Torr (~2.7×10^2 Pa) at 400°C	...	12	39	14	...
	20-h vacuum bakeout at 150°C	4.3	2.4	0.27	1.5	...

Table 10: Outgassing rates of 316L stainless steel after different processing as a function of the gases observed (Nuvolone)

A LIST OF SOURCES (REFERENCES)

① Outgassing of Vacuum Materials – R.J. Elsey
PART I - p. 299, Part II - p. 347
Vacuum/volume 25/number 7 -1975

② Reduction of stainless-steel outgassing in ultra-high vacuum.
- R. Calder & G. Lewin - Brit. Journal of Appl. Physics
Volume 18/1967 p. 459

③ Measurement of Gas Emission from Solid Surfaces
- F.J. Schittko Vacuum/Volume 13/1963 p. 525

④ Relations between size of Vacuum chamber, Outgassing Rate and Required Pumping Speed – B.B. Dayton
Trans. 6th AVS Symposium - 1959 p. 101.

⑤ Permeability Measurements with Gaseous Hydrogen for various Steels.
- H.L. Eschbach, F. Gross, and S. Schulien
Vacuum/Volume 13/1963 p. 543

⑥ Review of Outgassing Results
- Yale Strusser, Varian Assoc. Report No. Vr-51.

⑦ Outgassing Characteristics of Various Metals
- By D.J. Santeler Trans. 5th AVS Symp. 1958 p. 1.

⑧ The Influence of Adsorption and Desorption on Measurements of Low Pressures - G. Reich
Trans. 8th AVS Symposium - 1960 - p. 112

⑨ Outgassing Characteristics of Stainless Steel and Aluminum with Different Surface Treatments
- J. R. Young J. Vac. Sci. & Technol., 6, 1969, p. 398

⑩ Thermal Degassing of Materials
- Trans. 8th AVS Symp. - 1960 p. 149

⑪ Experiences with Demountable Ultra-high Vacuum System
- By B.D. Power and F.C. Robson
Trans. 9th AVS Symposium - Vol. 2. p. 1175

⑫ The Effect of Cleaning Techniques on the Outgassing Rate of 18/9/1 Stainless Steel
- R.S. Barton and R.P. Govier
Vacuum / Volume 20 / 1970 p. 1.

⑬ Gas Discharge Cleaning of Vacuum Surfaces
- R.P. Govier and G.M. McKracken
J. Vac. Sci. & Technol., No. 17, 5, p. 552

⑭ The Future of Vacuum Technology
- J.P. Hobson J. Vac. Sci. & Technol. A 2 (2), 1984, p. 144.

REFERENCES (CONTINUED)

* (15) TECHNOLOGY OF LOW-PRESSURE SYSTEMS – ESTABLISHMENT OF OPTIMUM CONDITIONS TO OBTAIN LOW DEGASSING RATES ON 316L STAINLESS STEEL BY HEAT TREATMENTS – R. NUVOLONE
J. VAC. SCI. TECHNOL., VOL. 14, No. 5, Sept/Oct. 1977 p. 1210.

(16) Interaction of Hydrogen with the Surface of Type 304 Stainless Steel - L.C. Beavis.
J. Vac. Sci. Technol., Vol. 10, No. 2, Mar/Apr. 1973. p. 386.

(17) Some Recent Developments in Vacuum Techniques for Accelerators and Storage Rings - Norman Melleron.
IEEE Transactions on Nuclear Science, June 1967. p. 794.

(18) Hydrogen Permeation Through Metals, Alloys and Oxides at Elevated Temperatures - C.L. Huffine and J.M. Williams.
Corrosion, Sept. 1960, p. 102.

(19) Sealing mechanisms in bakeable vacuum seals
- A. Roth., J. Vac. Sci. Technol. A 1(2), Apr-Jun 1983. p. 211.

GY * (20) A convenient electrical discharge method for eliminating hydrocarbon contamination from stainless steel UHV systems.
- R.M. Lambert and C.M. Comrie.
J. Vac. Sci. Technol., Vol. 11. No. 2. Mar/Apr. 1974 p. 530.

(21) Bake-out for UHV chambers in air at atmospheric pressure
R.L. Samuel – Vacuum, 20, number 7, p. 295.

(22) Ion induced gas desorption problems in the ISR.
R.S. Calder - Vacuum, vol. 24, number 10, p. 437.

(23) Ultrasensitive Leak Detection
- C.R. Winkelman, H.G. Davidson, Vacuum, vol. 29, number 10, p. 361.

(24) Performance of vacuum components operating at 1×10^{-11} torr.
- H.J. Halama.
J. Vac. Sci. Technol. 16(2), Mar/Apr. 1979 p. 717.

(25) Vacuum system for national synchotron light source.
- J.C. Schuchman, J.B. Godel, W. Jordan, and T. Overslulzen.
J. Vac. Sci. Technol. 16(2) Mar/Apr. 1979. p. 720.

(26) Ultrahigh vacuum system for ISABELLE full cell.
- R. Skelton, J. Briggs, T.S. Chou, C. Foerster, and P. Stattel.
J. Vac Sci. Technol., 17(1), Jan/Feb 1980 p. 342.

GY (27) Investigation by techniques of electron stimulated desorption of the merits of glow discharge cleaning of the surfaces of vacuum chambers at the CERN intersecting storage rings.
- A.W. Jones and E Jones and E.M. Williams.
Vacuum/vol 23/number 7 p. 227

GY X (28) Glow Discharge Cleaning of Stainless steel accelerator beam tubes — H.C. Hseuh, T.S. Chou and C.A. Christianson
J. Vac. Sci. & Technol. A 3(3), 1985 p. 518

(29) The Surface Cleanliness of 316L + N Stainless Steel Studied by SIMS and AES. — A.G. Mathewson
Vacuum / Volume 24 / 1974 p. 505.

(30) Electrostatic Getter-Ion Pump Performance
— Daniel G. Bills.
J. Vac. Sci. & Technol. No. 10, 1, 1973 p. 65

(31) Ultra-high Vacuum Technology for Storage Rings
— E. Fischer
IEEE Trans. Nuclear Science, Vol. NS-24, 3, 1977 p. 1227

(32) Permeation and Outgassing of Vacuum Materials
— W. G. Perkins
J. Vac. Sci. Technol. Vol. 10, No. 4, 1973 p. 543

(33) Characteristics of the ISABELLE Vacuum System.
— J.R. Aggus, D. Edwards, H.J. Halama, and J.C. Herrera
IEEE TRANS. N.S., Vol. NS-24, No. 3, June 1977., p. 1287.

(34) Evaluation of ISABELLE Full Cell Ultrahigh Vacuum
— C.L. Foerster, J. Briggs, T.S. Chou and P. Stattel
J. Vac. Sci. Technol., 18(3), April 1981 p. 1001.

(35) LLL 100-MeV Electron LINAC: Design Considerations and Performance of the Beam-Transport Vacuum System.
- M.C. Lara and H.E. Brooks
IEEE Trans. N.S., Vol. NS-22, No. 3, June 1975

(36) Two Kilometers at 10^{-10} Torr.
The CERN Intersecting Storage Rings for Protons
J. Vac. Sci. Technol., Vol. 9, 4, July-August 1972, p. 1203

(37) Review of sticking coefficients and sorption capacities of gases on titanium films.
- D.J. Harra.
J. Vac. Sci. Technol., Vol. 13, No. 1, Jan/Feb. 1976, p. 471

(38) A comparison of cryopump and diffusion pump performance on MMA 29x45 ft vacuum chamber.
J. Vac. Sci. Technol., 20(4), April 1982, p. 1005

(39) A cold-bore vacuum system design for POPAE.
Y. Cho, T.K. Khoe, J. Moenich, L.G. Ratner.
IEEE Trans. N.S., Vol. NS-24, No. 3, June 1977

(40) The Search for Gravitational Waves
- Ronald P. Drever
Engineering & Science - January, 1983

(41) The Search for Gravitational Waves
- S.L. Shapiro, R.F. Stark, S.A. Teukolsky.
American Scientist, Volume 73, p. 248.

(42) An Introduction to Stainless Steel
- J. G. Parr and A. Hanson.
American Society of Metals, Copyright. 1965.

(43) Fundamentals of Vacuum Science and Technology
- G. Lewin
McGrawhill Book Co, 1965, p. 32.

hotfoil®
Electric Heat Tracing

DERITEND-HOTFOIL INC.
623 MONTROSE AVENUE
SOUTH PLAINFIELD, N.J. 07080
TEL. (201) 668-4545
TELEX 350-782

July 30, 1985

Mr. Ghosh
Jet Propulsion Laboratories
4800 Oak Grove Drive
Pasadena, CA 91109

Subject: Heating Tapes - Type G

Dear Mr. Ghosh:

Very many thanks for calling me concerning the above.

I do confirm that for many years Brookhaven have used our heating tapes for bake-out purposes. They were used on Isabelle and are used on the light source. Also, Cern in Europe have virtually standardized on the G tapes, and success at Cern introduced us into Brookhaven.

Enclosed you will find a spec sheet on the type G tapes. The nichrome foils are crimped to corrugate them and sewn between layers of fiberglass tape. The foils are terminated at each end of the tape and leads attached at one end. Various lengths of the tape are available with respective wattages.

Please note that these are normal heating tapes. However, for Brookhaven there are two considerations and additions; the tapes are desized and anti-magnetic. "Desizing" is a process of baking the heating tapes to remove the size. The size is a binder used in the manufacture of glass fiber tape and gasses off at approximately 200°C. "Anti-magnetic" is to use all materials that are non-magnetic. With Brookhaven they must have non-magnetic materials due to the magnets in proximity to the bake out system. If you are not using magnets then you may not need to have the tapes non-magnetic. I would recommend desizing for your application as it will prevent excessive gassing-off on bake out.

Please note the desizing and anti-magnetic features adds 7½% for each process to the enclosed prices.

Delivery is 3-4 weeks on the tapes.

I am enclosing a small sample of the G tape and will, in the course of a week, send a longer piece for you to evaluate.

We will be more than happy to offer you any assistance and help you need at any time.

Yours sincerely,

Neville W. Richards
Sales Manager

NWR:rlc

type G 850°F (450°C)

For use up to 850°F (450°C) the type 'G' heating tape has foil elements insulated with three layers of woven glass cloth. Manufactured in widths of 1 inch (25 mm) and 1½ inches (38 mm), this tape is $\frac{1}{16}$ inch (1·5 mm) thick and has 2 ft (0·6 m) of glass insulated flexible cold lead.

When used in damp conditions, moisture-proof or water-proof thermal insulation should be fitted over the tapes.

Type 'G' tapes are designed to give very high loadings and are used in many research laboratories, atomic energy research installations, stress relieving, pre-heating prior to welding applications, baking out high vacuum plant and the heating of pipelines used in the transportation of low melting point metals.

1 in (25 mm) wide, 220 volt							1 in (25 mm) wide, 110 volt				
LENGTH		LOADING (Watt)					LOADING (Watt)				
Metre	Feet	G4-10	G10-20	G25-35	G50-100	G100-180	G4-10	G10-20	G25-35	G50-100	G100-180
1·8	6	—	—	—	580	1100	150	360	500	710	950
3·6	12	—	—	290	910	1650	180	320	290	880	1400
5·4	18	190	330	660	1250	2500	190	330	660	950	—
7·5	25	140	460	700	1650	2900	140	460	700	—	—
9	30	190	390	790	1550	2300	190	390	580	—	—
12	40	165	415	1150	1750	—	145	415	—	—	—
15	50	250	500	1400	—	—	240	350	—	—	—
18	60	290	750	1150	—	—	290	—	—	—	—
21	70	330	1000	—	—	—	250	—	—	—	—

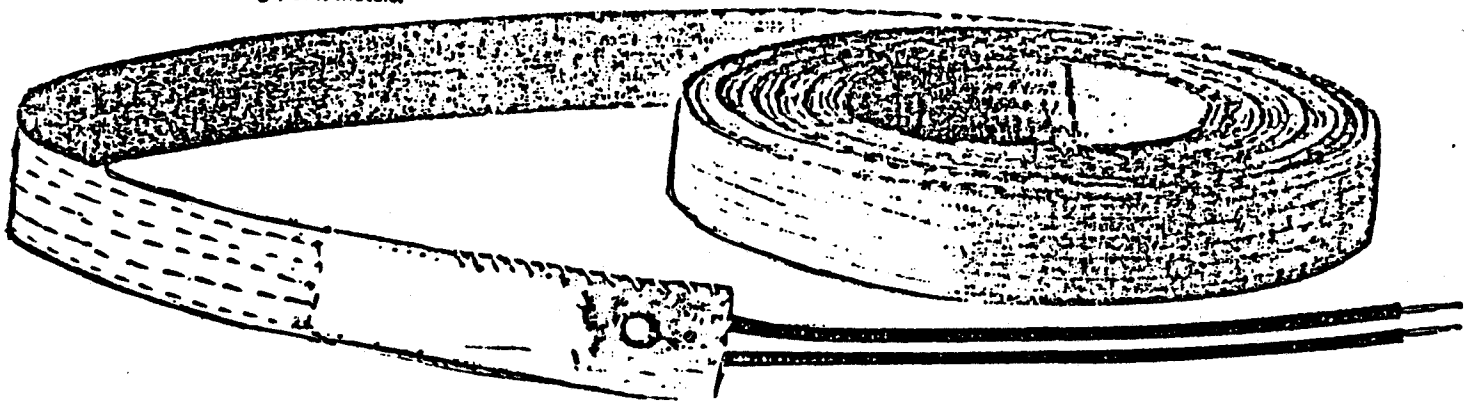

BRIT. J. APPL. PHYS., 1967, VOL. 18. PRINTED IN GREAT BRITAIN

Reduction of stainless-steel outgassing in ultra-high vacuum

R. CALDER and G. LEWIN†

CERN, Geneva, Switzerland

MS. received 16*th December* 1966, *in revised form* 22*nd May* 1967

Abstract. The outgassing rate of a 2 mm thick stainless-steel sheet was measured in ultra-high vacuum at constant pressure to avoid the readsorption occurring in a 'rate of pressure rise' determination. The rate was typically 10^{-12} torr l. cm^{-2} sec^{-1} and about 99% or more of the gas was hydrogen. Since stainless steel usually contains large amounts of hydrogen and the diffusion coefficient of hydrogen in stainless steel is high, it was suspected that the hydrogen diffuses to the surface from the interior of the metal and is released into the vacuum. Calculations show that the observed outgassing rate could be explained by such a process and should be reduced by several orders of magnitude by a high-temperature treatment. The effects of residual hydrogen in the treatment furnace and hydrogen permeation from the atmosphere are also considered in these calculations. The greater the thickness of the metal, the higher the temperature has to be. Measurements are in reasonable agreement with these calculations.

1. Introduction

It has been known for a long time that the outgassing rate of a material in vacuum can be reduced more rapidly by temporarily raising its temperature than by merely continuous pumping under vacuum at room temperature. Moreover, although the effectiveness of this 'bakeout' technique is known to depend on the temperature employed, the details of this dependence are not generally appreciated.

With regard to outgassing by surface desorption in ultra-high vacuum Hobson (1962) showed by calculation of a typical case that all gases which desorb only slowly at room temperature (i.e. those which constitute the gas load in a normal vacuum system) should be readily removed by a bakeout at 300°C. Only those gases which have a negligibly small desorption rate will remain at the surface. Experimental proof was given by Young and Hession (1964) who attained pressures below 10^{-10} torr in small laboratory systems baked for 15 hours at 250°C. It is also known that vacuum components operating at elevated temperatures must be degassed by temporarily raising the temperature sufficiently above the operating temperature. Todd (1955) showed theoretically and experimentally that the outgassing of a hot glass wall, treated as diffusion from a semi-infinite slab, could be reduced by such a treatment.

Type 300 stainless steel will constitute the vacuum wall of the intersecting storage rings now being built at CERN (Fischer 1965). Owing to the small cross section of the vacuum chamber the pumping speed will be quite limited and it is of paramount importance to reduce all sources of gas to a minimum. When measuring the outgassing rate of U15C stainless steel in ultra-high vacuum after a 300°C bakeout for 24 hours (hereafter referred to as a 'normal' bakeout) we found that about 99% or more of the gas was hydrogen which degassed at the rate of about 10^{-12} torr l. cm^{-2} sec^{-1}. U15C is a low-carbon 300 series type of stainless steel (see §4). Stainless steel often contains large amounts of hydrogen and the diffusion coefficient for hydrogen in type 300 stainless steels is quite high (Eschbach *et al.* 1963). This suggested an investigation to determine whether hydrogen dissolved in the bulk of the material was being continuously liberated at room temperature by a diffusion process.

† Now at Plasma Physics Laboratory, Princeton University, Princeton, New Jersey, U.S.A.

outgassing
1 surface desorption
2 bulk diffusion
1) is normal vac. load, all is out at 300°C
2) major portion at high temp.
300°C for 24 hr
Normal bakeout

2. Theory

2.1. *Effect of temperature on degassing*

The one-dimensional diffusion equation is

$$D\frac{\partial^2 c}{\partial x^2} = \frac{\partial c}{\partial t} \tag{1}$$

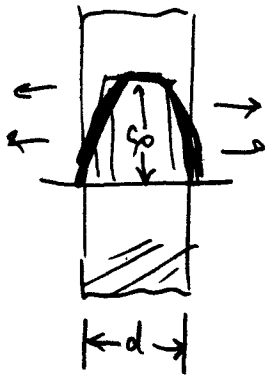

where D is the diffusion coefficient and c the concentration.

Equation (1) is solved for a slab of unit cross section and thickness d. Initially the concentration is c_0 and constant throughout. At time $t = 0$ vacuum is applied to both faces. The initial and boundary conditions are

$$c = c_0 \quad \text{for} \quad 0 \leqslant x \leqslant d \qquad \text{at} \quad t = 0$$

and

$$c = 0 \quad \text{for} \quad x = 0 \quad \text{and} \quad x = d \quad \text{at} \quad t > 0.$$

The solution is (Lewin 1965, p. 32)

$$c(x,t) = c_0 \frac{4}{\pi} \sum_0^\infty (2n+1)^{-1} \sin\frac{\pi(2n+1)x}{d} \exp\left\{-\left(\frac{\pi(2n+1)}{d}\right)^2 Dt\right\}. \tag{2}$$

The instantaneous gas flow from one face of the slab is

$$Q = D\left(\frac{\partial c}{\partial x}\right)_{x=0} = \frac{4c_0 D}{d} \sum_0^\infty \exp\left\{-\left(\frac{\pi(2n+1)}{d}\right)^2 Dt\right\}. \tag{3}$$

Values of

$$\sum_0^\infty \exp\left\{-\left(\frac{\pi(2n+1)}{d}\right)^2 Dt\right\}$$

as a function of Dt/d^2 are given in figure 1. For $Dt/d^2 > 0{\cdot}025$, as is the case in many practical situations, we can write, to a sufficient approximation,

$$c = c_0 \frac{4}{\pi} \sin\frac{\pi x}{d} \exp\left(-\pi^2 d^{-2} Dt\right) \tag{4}$$

and

$$Q = 4c_0 Dd^{-1} \exp\left(-\pi^2 d^{-2} Dt\right). \tag{5}$$

If a sheet has been degassed for t_1 seconds at a temperature T_1 the outgassing rate (immediately) afterwards at room temperature T_r is

$$Q_r = 4c_0 D_r d^{-1} \exp\left(-\pi^2 d^{-2} D_1 t_1\right). \tag{6}$$

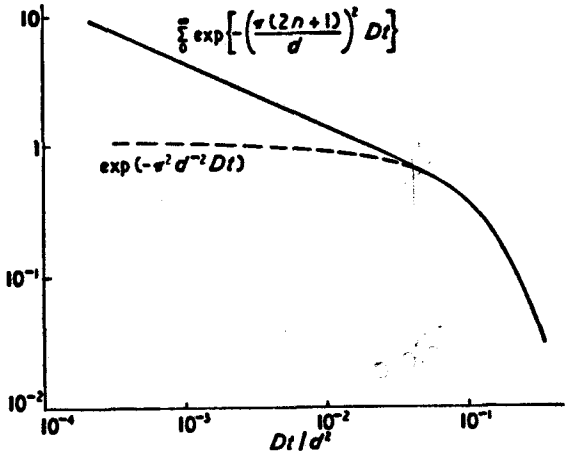

Figure 1. Plot of the infinite series of equation (3) and its first term.

It is shown in the Appendix that $\dot{Q}_r$ is, for all practical purposes, time independent. Since the product $D_1 t_1$ appears in the exponent, an increase of the bakeout temperature, which renders D_1 larger, has the same effect as an increase in the time of bakeout at a lower temperature. However, because of the exponential dependence of D on temperature (Eschbach *et al.* 1963) a large reduction in outgassing rate should be readily obtained by a high-temperature bakeout. For example, the diffusion constants for H_2 in stainless steel are (Eschbach *et al.* 1963) $D_{300} = 3{\cdot}5 \times 10^{-8}$ cm^2 sec^{-1} and $D_{1000} = 8{\cdot}7 \times 10^{-5}$ cm^2 sec^{-1}. Hence a one-hour bakeout at 1000°C is equivalent to 2500 hours at 300°C. Both are calculated by equation (6) to decrease the subsequent room-temperature outgassing rate, compared with that given after a normal bakeout, by more than a factor of 10^{30} for 2 mm thick material.

Clearly this enormous potential of high-temperature degassing cannot be utilized. It could be nullified by any small leak. Furthermore, other gases will desorb at much higher rates. The above calculation neglected permeation of atmospheric hydrogen and the influence of residual hydrogen pressure in the bakeout furnace. It is pertinent to examine the importance of these limiting effects to determine what degree of degassing is likely to be useful.

A high-temperature bakeout of vacuum-chamber components may, in principle, be executed either *in situ* or in a furnace prior to assembly, since diffusion at room temperature is negligible (see §§2.3 and 5.4). The latter case would necessitate a final, *in situ*, normal bakeout to remove surface contamination.

Hereafter we shall consider only 2 mm thick material unless it is explicitly stated otherwise. Stainless steel of 2 mm thickness is commonly employed in the fabrication of vacuum chambers. For material of other thicknesses the following calculations are easily modified.

2.2. *Outgassing after a normal bakeout*

Chemical analysis of hydrogen from the supplier (Compagnie des Atéliers et des Forges de la Loire, France) of our stainless steel gave 5 standard cm^3 per 100 g or, equivalently, $c_0 = 0{\cdot}3$ torr l. cm^{-3}. The diffusion coefficient for hydrogen in stainless steel at room temperature is (Eschbach *et al.* 1963) $D_r = 5{\cdot}0 \times 10^{-14}$ cm^2 sec^{-1}. The application of equation (6) for 2 mm sheet after a normal degas at 300°C for 24 hours gives

$$\dot{Q}_r = 3{\cdot}0 \times 10^{-13} \exp(-0{\cdot}75) = 1{\cdot}4 \times 10^{-13} \text{ torr l. cm}^{-2} \text{ sec}^{-1}. \quad (6a)$$

A second bakeout would reduce $\dot{Q}_r$ by a further factor $e^{-0{\cdot}75} = 0{\cdot}47$. The experimentally measured values were close to 10^{-12} torr l. cm^{-2} sec^{-1} and are not strongly dependent on further bakeout (see §5.2). There is some indication that c_0 may have been higher.

This calculation neglects the partial pressure of hydrogen at the outside wall. This pressure is supposed to be 4×10^{-4} torr (Gleuckauf 1951). We do not know how much it varies and what it was in our laboratory. At 300°C, the atmospheric hydrogen causes a surface concentration $c_a = 1{\cdot}4 \times 10^{-4}$ torr l. cm^{-3} (see equation (9)). After the bake, the maximum concentration in the centre is, from equation (4), $c_0(4/\pi)\,0{\cdot}47 = 0{\cdot}2$ torr l. cm^{-3}. Hence the effect of the atmospheric hydrogen is negligible in this case. The effect of permeation of a thoroughly degassed slab is treated in the next section.

2.3. *Permeation rate of atmospheric hydrogen*

It is assumed that the stainless steel has been completely degassed. Equation (1) is solved for a slab where c and P are initially zero. At time $t = 0$, one face is exposed to a constant pressure P_1 which produces a concentration c_1 at this surface while vacuum is maintained at the other face. Hence equation (1) must be solved with the following initial boundary conditions:

$$c = 0 \quad \text{for} \quad 0 \leqslant x \leqslant d \quad \text{at} \quad t = 0$$
$$c = 0 \quad \text{for} \quad x = 0 \quad \text{at} \quad t > 0$$
$$c = c_1 \quad \text{for} \quad x = d \quad \text{at} \quad t > 0.$$

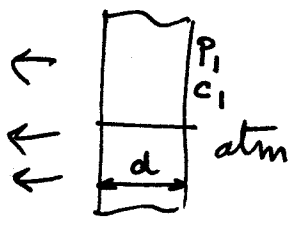

The solution is (Lewin 1965)

$$c(x,t) = \frac{c_1 x}{d} + \frac{2c_1}{\pi}\sum_1^\infty \frac{(-1)^n}{n}\sin\frac{n\pi x}{d}\exp\left\{-\left(\frac{n\pi}{d}\right)^2 Dt\right\}. \tag{7}$$

The instantaneous permeation rate at time t is

$$\dot{Q}_{P_1} = D\left(\frac{\partial c}{\partial x}\right)_{x=0} = \frac{Dc_1}{d} + \frac{2Dc_1}{d}\sum_1^\infty (-1)^n \exp\left\{-\left(\frac{n\pi}{d}\right)^2 Dt\right\}. \tag{8}$$

Values of

$$1 + 2\sum_1^\infty (-1)^n \exp\left\{-\left(\frac{n\pi}{d}\right)^2 Dt\right\}$$

as a function of Dtd^{-2} are given in figure 2.

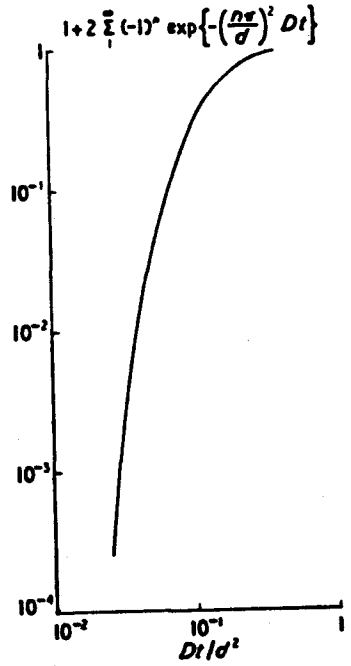

Figure 2. Plot of the infinite series of equation (8).

For $t \to \infty$, the equilibrium permeation flow rate at room temperature is

$$(\dot{Q}_{P_1})_T = D_T \frac{c_1}{d}.$$

For shorter times, such that $D_T t d^{-2} \leqslant 0{\cdot}02$, the permeation rate is

$$(\dot{Q}_{P_1})_T' < 10^{-4}(\dot{Q}_{P_1})_T.$$

(For 2 mm thick stainless steel this is true for $t \leqslant 10^{10}$ sec.)

The concentration c_1 of a diatomic gas dissolved in a metal at temperature T which is in equilibrium with an external gaseous pressure P_1 is (Lewin 1965)

$$c_1 = \frac{K_T}{D_T} P_1^{1/2} \tag{9}$$

where K_T is the permeability constant and D_T the corresponding diffusion constant. For

H_2 in stainless steel $K_r = 1{\cdot}2 \times 10^{-16}$ torr$^{1/2}$ l. cm^{-1} sec^{-1}. Thus for 2 mm stainless steel exposed to a partial pressure of 4×10^{-4} torr of hydrogen

$$(\dot{Q}_{P_1})_r = \frac{c_1 D_r}{d} = \frac{K_r P_1^{1/2}}{d} \simeq 1 \times 10^{-17} \text{ torr l. cm}^{-2} \text{ sec}^{-1} \tag{10}$$

and for practical times $(\dot{Q}_{P_1})_r' \ll 1 \times 10^{-21}$ torr l. cm^{-2} sec^{-1}. Hence concentration changes at room temperature are negligible.

However, the normal *in situ* bakeouts, by virtue of the greatly enhanced diffusion constant at the bakeout temperature, will modify the above conclusion to the extent of establishing near-equilibrium permeation rates. In fact, because K/D is a function increasing with temperature, the apparent permeation rate at room temperature after an *in situ* bakeout at temperature T will, in the limit, be increased above the value given by equation (10) to

$$(\dot{Q}_{P_1})_r^T = \left(\frac{K}{D}\right)_T \frac{D_r}{d} P_1^{1/2}. \tag{11}$$

Taking a temperature of 300°C where $K_{300} = 2{\cdot}3 \times 10^{-10}$ torr$^{1/2}$ l. cm^{-1} sec^{-1} and $D_{300} = 3{\cdot}5 \times 10^{-8}$ cm^2 sec^{-1}, equation (11) gives for the limiting value of hydrogen permeation

$$(\dot{Q}_{P_1})_r^{300} \simeq 3{\cdot}3 \times 10^{-17} \text{ torr l. cm}^{-2} \text{ sec}^{-1}.$$

The flow rate is 13% of this amount after 24 hours since $D_{300}\, t_{24}\, d^{-2} = 7{\cdot}5 \times 10^{-2}$ (see equation (8) and figure 2). It is worth noting that during a prolonged 300°C bakeout the hydrogen permeation rate would reach a limiting value of

$$(\dot{Q}_{P_1})_{300} = \frac{K_{300}}{d} P_1^{1/2} \simeq 2{\cdot}3 \times 10^{-11} \text{ torr l. cm}^{-2} \text{ sec}^{-1}.$$

Determination of hydrogen permeation through a suitable metal, for example palladium, at elevated temperatures may be a practical method to measure the partial pressure of hydrogen in the atmosphere.

2.4. *High-temperature bulk degassing in situ*

It is clear from the above considerations that any attempt to reduce the outgassing rate below about 10^{-16} torr l. cm^{-2} sec^{-1} is pointless. This, however, already represents a theoretical improvement factor of 10^3 on that obtained via a normal bakeout. We may calculate the bakeout requirements necessary to yield a $\dot{Q}_r = 10^{-16}$ torr l. cm^{-2} sec^{-1} for 2 mm stainless steel with an initial concentration of 0·3 torr l. cm^{-3} of hydrogen. It follows from equation (6) that

$$\dot{Q}_r = 10^{-16} = 3 \times 10^{-13} \exp(-\pi^2 d^{-2} Dt) \tag{12}$$

or $Dt = 3{\cdot}25 \times 10^{-2}$ cm^2. Table 1 is based on data from Eschbach *et al.* (1963).

Table 1. Bakeout times of 2 mm thick sheet at various temperatures for $\dot{Q}_r = 10^{-16}$ torr l. cm^{-2} sec^{-1}

t (sec)	D (cm^2 sec^{-1})	T (°C)
$1{\cdot}0 \times 10^6$ (11 days)	$3{\cdot}5 \times 10^{-8}$	300
$8{\cdot}6 \times 10^4$ (24 hours)	$3{\cdot}8 \times 10^{-7}$	420
$1{\cdot}1 \times 10^4$ (3 hours)	$3{\cdot}0 \times 10^{-6}$	570
$3{\cdot}6 \times 10^3$ (1 hour)	$9{\cdot}0 \times 10^{-6}$	635

In situ bakeouts up to temperatures of 420°C are feasible. Application of equation (11) at $T = 420$°C where $K_{420} = 3{\cdot}2 \times 10^{-9}$ torr$^{1/2}$ l. cm^{-1} sec^{-1} gives

$$(\dot{Q}_{P_1})_r^{420} = 4{\cdot}2 \times 10^{-17} \text{ torr l. cm}^{-2} \text{ sec}^{-1}$$

a value which is still quite acceptable.

2.5. *High-temperature bulk degassing in a furnace with residual hydrogen pressure*

If the degassing is performed at higher temperatures in a furnace, it is necessary to consider the partial pressure of hydrogen in the residual furnace atmosphere. A pressure of P_F torr will give rise to an equilibrium concentration in the material being degassed of

$$\left(\frac{K}{D}\right)_T P_F^{1/2} = c_F.$$

The result will be to modify equations (2) and (4) to give

$$c = c_F + (c_0 - c_F)\frac{4}{\pi}\sum_0^\infty (2n+1)^{-1} \sin\frac{\pi(2n+1)x}{d} \exp\left\{-\left(\frac{\pi(2n+1)}{d}\right)^2 Dt\right\} \quad (13)$$

$$\simeq c_F + (c_0 - c_F)\frac{4}{\pi}\sin\frac{\pi x}{d}\exp\left(\frac{-\pi^2 Dt}{d^2}\right). \quad (14)$$

Immediately after removal from the furnace the uniform concentration component would give a very high outgassing rate not controlled by diffusion and not easily calculated. However, the normal degassing operation, which would always be necessary to remove surface contamination received during assembly of the vacuum chamber, will reduce the outgassing component from c_F to a value again controlled by the diffusion mechanism. In practice, after a furnace treatment, the approximation (14) will always be valid and, using the same reasoning as in the Appendix, with subscripts f and n for the furnace and subsequent normal bakeouts, the net effect will be to give

$$c = \frac{4}{\pi}\sin\frac{\pi x}{d}\exp(-\pi^2 d^{-2} D_n t_n)\{c_F + (c_0 - c_F)\exp(-\pi^2 d^{-2} D_f t_f)\} \quad (15)$$

and

$$Q_r = 4 D_r d^{-1}\{c_F + (c_0 - c_F)\exp(-\pi^2 d^{-2} D_f t_f)\}\exp(-\pi^2 d^{-2} D_n t_n). \quad (16)$$

Even a rather moderate vacuum furnace ought to achieve a hydrogen partial pressure as low as 10^{-4} torr. At the highest furnace temperatures contemplated this would give

$$(c_F)_{700} = \left(\frac{K}{D}\right)_{700} P_F^{1/2}$$

$$= \frac{1{\cdot}26 \times 10^{-7}}{1{\cdot}16 \times 10^{-5}} 10^{-2} \simeq 1{\cdot}1 \times 10^{-4} \text{ torr l. cm}^{-3}.$$

It follows from equation (12) that $c_0 \exp(-\pi^2 d^{-2} D_f t_f) \simeq c_F$. Hence the furnace vacuum requirement is not critical.

It appears from the above considerations that outgassing rates of hydrogen from stainless steel down to approximately 10^{-16} torr l. cm^{-2} sec^{-1} ought to be obtainable. This represents an improvement factor of about 10^4 on rates normally measured. The improvement obtainable appears to be limited only by diffusion of atmospheric hydrogen or by the quality of the vacuum in the furnace. The generalization of the above considerations to material of various thicknesses is easy—thicker material must be degassed for a longer time, approximately proportional to the square of the thickness (or, alternatively, at a correspondingly higher temperature), to give the same outgassing rate and will exhibit a lower (inversely proportional to the thickness) permeation rate for atmospheric hydrogen. Thinner material may be more easily degassed but will suffer from an increased permeation rate.

3. Experimental details

The apparatus used to measure outgassing rates is shown schematically in figure 3. The primary consideration given to the designs was that of high sensitivity to enable small and easily prepared samples to be used. Moreover the specimen should remain at constant pressure to overcome the difficulties of readsorption which confuse the results obtained

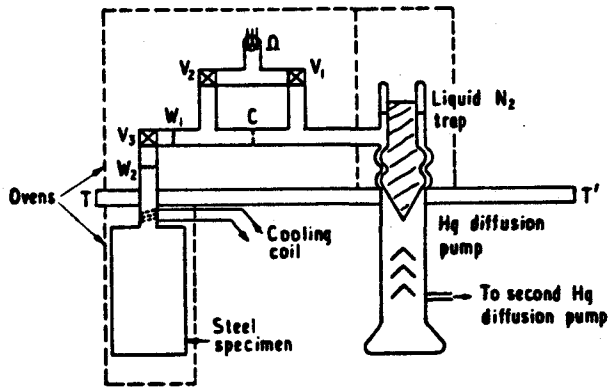

Figure 3. Apparatus used for the measurement of outgassing rates.

from methods involving the rate of pressure rise in a closed volume. A minimum specimen surface area of approximately 10^3 cm^2 was chosen as a compromise between giving measurable total gas flow, reasonable ease of fabrication and treatment and being large enough to have a realistic ratio of test surface to background area.

To detect and measure gas flow rates in the 10^{-12}–10^{-11} torr l. sec^{-1} range the measuring apparatus itself must be as small and as clean as possible. For this reason all the apparatus to the right of the metal-to-glass seal W_1 (see figure 3) was constructed in Pyrex 7740 glass. The measuring principle is to pass the gas flow $\dot{Q}_T(=\Sigma_t \dot{Q}_t)$ across a small conductance C to produce a pressure difference $\Delta P_T = \dot{Q}_T C^{-1}$ which is measured by the partial pressure analyser Ω. The basic restriction placed on the conductance C was that its value should be readily calculated from geometrical dimensions and not subject to variations due to contamination as can happen with some very low conductances made from porous materials. The result was a hole of approximately 1 mm diameter in a 0·2 mm thick glass diaphragm giving a conductance of about 0·1 l. sec^{-1} for nitrogen. The requirements on the two valves V_1 and V_2 are not stringent—they only need to provide a conductance in the closed position of value much less than C; simple all-glass ball and socket valves were used which were operated by an external magnet.

The partial-pressure gauge must satisfy three requirements: it must be sufficiently sensitive to detect a pressure difference of 10^{-11} torr (or a few times 10^{-12} torr in the case of hydrogen); it must have a pumping speed small compared with the conductance of C; and, preferably, it should be small and clean in accordance with the rest of the apparatus. An omegatron partial-pressure analyser was used to fulfil those conditions. With care the omegatron sensitivity is considerably higher than the minimum required here (it measures a partial pressure down to 10^{-11} torr and detects down to 3×10^{-12} torr), while its pumping speed is quoted (Peterman 1964, private communication) as being less than 10^{-5} l. sec^{-1}.

To make useful observations of $\Delta P \simeq 10^{-11}$ torr it is essential that the pressure is not more than one order higher than ΔP. A mercury diffusion pump designed at CERN (Opitz and Schneider 1960) and backed by a second mercury pump has been used. With a single liquid-nitrogen-cooled trap this pump will reach the 10^{-12} torr range; it was normally used in the 10^{-11} torr range. The trap is insensitive to coolant level since the upper part has a separate vacuum jacket. The whole glass system and the all-metal valve V_3 above the table top TT' may be degassed up to 400°c. During bakeout both valves V_1 and V_2 (and, depending on the experiment, V_3 also) are opened. In the final stage of the bakeout liquid N_2 is added to the trap. The valves and glass tubing have all approximately 3 cm bores and the overall length from the trap to V_3 is about 50 cm.

The specimen has a separate bakeout facility which may also be used when measuring the outgassing rate as a function of temperature. When doing this the cooling coil (see figure 3) serves to confine the heated region to the specimen alone.

Pressures were taken on either side of the conductance with the valve V_3 open and closed.

Let P_1 and P_2 denote pressures when V_3 is open on the specimen and pump sides of the conductance C respectively and P_1', P_2' the corresponding values when V_3 is closed. Then the total outgassing rate of the gas i is

$$Q_i = \{(P_1 - P_2)_i - (P_1' - P_2')_i\} C_i \qquad \text{torr l. cm}^{-2}\,\text{sec}^{-1}.$$

The determinations are subject to the usual inaccuracies of ultra-high vacuum measurements. The calibration used for the omegatron was as given by the manufacturer and experience has shown that in the ultra-high vacuum range this is good to within about 30%–40% when compared with a variety of ionization gauges. The calculation of the conductance is estimated to be within ±15%. Allowing for likely calibration errors of the ionization gauges the absolute values of the outgassing rates quoted are probably correct to within a factor of two. Relative values between two different gases or specimens will be more accurate—here the estimated reliability is ±30%.

4. Results and discussions

All specimens were fabricated from 'as received' 2 mm thick rolled U15C stainless-steel from Compagnie des Atéliers et Forges de La Loire, France. This is a low-carbon Cr–Ni stable austenitic stainless steel of the following nominal percentage composition: C = 0·02 max., Ni = 14–15·5, Cr = 16·5–18·0, Mn = 0·85–1·15, Si = 0·30–0·50, S = 0·015 max., P = 0·02 max., N = 0·04 max.

Evidence for a single-phase austenitic structure was obtained from extensive micrographical and magnetic permeability measurements. The former showed no signs of a second phase being present and the latter measurements gave the magnetic permeability not greater than 1·004. These observations were equally true for regions in a weld (Samuel 1966, private communication).

Values of Q_i for the several specimens are given in tables 2 to 5; multiple values under one heading are measurements on successive days and, in general, show the degree of reproducibility obtainable. Occasionally (e.g. table 5, row 2) there is a trend within such a group which may be significant. At other places (e.g. table 2, row 1) one entry seems to be much out of line and has been enclosed in curly brackets. The cause of this behaviour is not clear but is thought to have arisen because insufficient time was allowed for equilibrium to be established. These values have been omitted from graphs and subsequent discussions. A line indicates that the gas was below the detection limit (about 10^{-15} and 10^{-16} torr l. sec^{-1} cm^{-2} for tables 2 and 3 and tables 4 and 5 respectively where the specimen outgassing areas used were respectively 10^3 and 10^4 cm^2) and a value enclosed within square brackets is one within an order of magnitude above the detection limit but below the level of accurate measurement. Occasionally the sample appeared to act as a sink rather than a source for H_2O, CO–N_2 and CO_2, and a small negative flow was observed. These data, indicated by (- - -) in the tables, have not been satisfactorily explained.

4.1. *Specimen A*

Specimen A consisted of a seam-welded 2 mm thick stainless-steel container (30 cm long, 10 cm in diameter, with welded-on base plate) attached to the system by a ConFlat flange. The internal area of the specimen was $1{\cdot}1 \times 10^3$ cm^2, 80 cm^2 of which was the ConFlat flange. The background area consisted of 150 cm^2 of internal surface of connecting pipe and valve. Data from a series of outgassing measurements are presented in table 2. The main conclusions to be drawn are that after a fairly prolonged degassing at a moderate temperature (45 hours at 360°c) hydrogen was degassing at a rate of approximately 2×10^{-12} torr l. cm^{-2} sec^{-1} and formed more than 99% of the gas flow. This outgassing rate for hydrogen has a negative $1/T$ (T in °K) exponential dependence as expected (see curve A, figure 4). The slight flattening of the curve at 0°c could be accounted for by the pipe and valve surface above the specimen proper which remained at room temperature. The final data in table 2 give the results obtained after exposing the outgassed specimen to the atmosphere for 3 hours. This shows that, whereas the previously dominant hydrogen

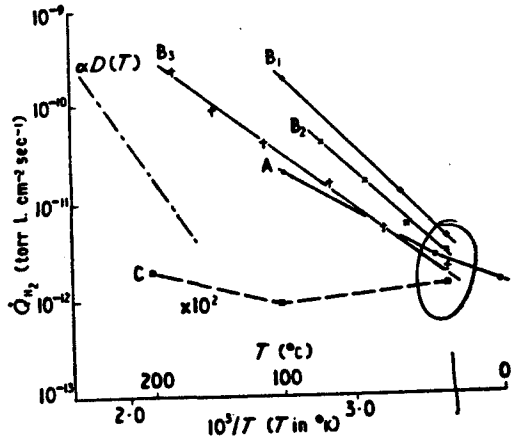

Figure 4. Dependence of outgassing rates on specimen temperatures (the data $D(T)$ showing the relative temperature dependence of the diffusion constant have been taken from Eschbach *et al.* (1963)).

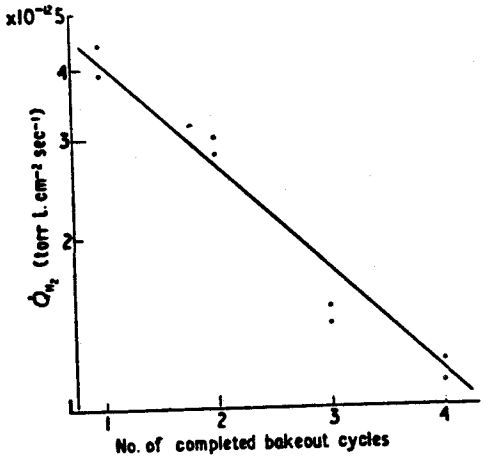

Figure 5. Dependence of outgassing rate of specimen B on bakeout time.

outgassing is unaffected, desorption rates of all other components commonly found in vacuum systems are increased considerably. These were observed to decay only slowly at room temperature but to be removed effectively by degassing for 24 hours at 360°C. It will be noticed that this latter degassing treatment further reduces the hydrogen outgassing rate to a moderate extent.

Table 2. Specimen A: outgassing rates (torr l. cm^{-2} sec^{-1})

Specimen preparation	Measurement temperature (°C)	H_2	H_2O	CO–N_2	O_2	CO_2
Degassed several times—total of 45 h at 360°C	24	{$1\cdot3^{-12}$†}	—	—	—	—
		$2\cdot6^{-12}$				
		$2\cdot3^{-12}$				
	100	$2\cdot1^{-11}$	—	[$4\cdot7^{-15}$]	—	$2\cdot5^{-13}$
	0	$1\cdot3^{-12}$	—	—	—	—
Exposed to atmosphere for 3 h. Pumped under vacuum for 40 h	19	$2\cdot7^{-12}$	$6\cdot4^{-12}$	$1\cdot9^{-12}$	$2\cdot2^{-12}$	$1\cdot2^{-12}$
Pumped under vacuum for further 4 days at room temperature	19	$2\cdot6^{-12}$	$1\cdot0^{-12}$	$6\cdot4^{-13}$	$8\cdot4^{-14}$	$3\cdot6^{-13}$
Baked at 360°C for 24 h	19	$9\cdot9^{-13}$	—	[$2\cdot6^{-15}$]	—	—

† The superscripts denote the power of ten by which the numbers should be multiplied.

4.2. *Specimen B*

Specimen B was identical in all respects to A and the results are presented in table 3. The four rows of data measured at about 20°C (room temperature) were each obtained after a bakeout at 300°C for 25 hours. Between these bakeouts the temperature dependence of the degassing rates was observed. The former data give the same general picture as those from specimen A—specifically that the dominant gas is always hydrogen at a few times 10^{-12} torr l. cm^{-2} sec^{-1}. It is of interest to note that the hydrogen outgassing rate decreased continuously during the course of the four bakeouts from about 4×10^{-12} to about

Table 3. Specimen B: outgassing rates (torr l. cm^{-2} sec^{-1})

Specimen preparation	Measurement temperature (°C)	H_2	H_2O	CO–N_2	O_2	CO_2
Baked under vacuum for 25 h at 300°C	20	$3\cdot9^{-12}$†	—	$1\cdot7^{-14}$	—	$1\cdot9^{-14}$
	20	$4\cdot5^{-12}$	—	—	—	$2\cdot0^{-14}$
	20	{$2\cdot6^{-12}$}	—	$6\cdot1^{-14}$	—	$1\cdot5^{-14}$
Temperature of specimen raised	40	$1\cdot3^{-11}$			—	
	100	$2\cdot1^{-10}$	$1\cdot0^{-13}$	$4\cdot7^{-13}$	$1\cdot8^{-12}$	$1\cdot7^{-12}$
Baked under vacuum for 25 h at 300°C	20	$3\cdot0^{-12}$	—		—	$1\cdot7^{-14}$
	20	$3\cdot0^{-12}$				
	20	$3\cdot0^{-12}$				
	20	$2\cdot8^{-12}$	—	[$8\cdot6^{-15}$]	—	$1\cdot1^{-14}$
Temperature of specimen raised	35	$5\cdot6^{-12}$	[$7\cdot8^{-15}$]	(- - -)	—	$2\cdot5^{-14}$
	53	$1\cdot6^{-11}$	[$6\cdot4^{-15}$]	(- - -)	—	$3\cdot3^{-14}$
	75	$4\cdot4^{-11}$	$4\cdot6^{-14}$	—	—	$5\cdot8^{-14}$
Baked under vacuum for 25 h at 300°C	20	$1\cdot5^{-12}$				
	20	$1\cdot5^{-12}$	(- - -)	{$1\cdot6^{-13}$}	—	(- - -)
	20	$1\cdot4^{-12}$	—	—	—	—
Temperature of specimen raised	47	$5\cdot3^{-12}$	—	[$5\cdot2^{-15}$]	—	[$1\cdot7^{-15}$]
	72	$1\cdot5^{-11}$	—	$2\cdot8^{-14}$	—	[$5\cdot4^{-15}$]
	105	$3\cdot9^{-11}$	—	$6\cdot3^{-14}$	—	[$8\cdot7^{-15}$]
	145	$9\cdot2^{-11}$	$3\cdot1^{-13}$	$1\cdot4^{-13}$	—	$1\cdot0^{-14}$
	200	$2\cdot5^{-10}$	$6\cdot1^{-13}$	$2\cdot6^{-13}$	—	$3\cdot6^{-14}$
Baked under vacuum for 25 h at 300°C	20	$1\cdot1^{-12}$	—		—	—
	20	$1\cdot2^{-12}$	—	[$4\cdot3^{-15}$]	—	—

† The superscripts denote the power of ten by which the numbers should be multiplied.

1×10^{-12} torr l. cm^{-2} sec^{-1} and that the components CO–N_2 and CO_2 decreased from about 1% of $\dot{Q}_{H_2}$ at the end of the first bakeout to very much less than 1% after three bakeouts. The data for $\dot{Q}_{H_2}$, plotted in figure 5, show a logarithmic decrease with successive bakeouts—behaviour to be expected from the analysis though the slope is somewhat smaller than expected (−0·43 instead of −0·75 from equation (6*a*)). This could be attributed to a slightly different diffusion coefficient.

The data taken between successive bakeouts and above room temperature are shown in figure 4, curves B_1, B_2 and B_3. The exponential dependence of $\dot{Q}_{H_2}$ on $1/T$ is maintained, although successive curves give not only lower absolute values of $\dot{Q}_{H_2}$ but also lower slopes. Further, the values of the activation energies involved may be calculated from these slopes on the assumption that $D_T = D_0 \exp(-E/kT)$ where E is the activation energy and $\dot{Q}(T) \propto D_T$. They are a factor between 1·5 and 2 times smaller than that found by Eschbach *et al.* (1963) for the diffusion of H_2 in stainless steel of somewhat different composition. The reasons for the progressive decrease in the slope of curves B_1, B_2 and B_3 corresponding to an apparent decrease in activation energy are not known.

4.3. *Specimen C*

Specimen C consisted of a cylinder like specimens A and B but connected to the system by welding without a flange joint. In addition it contained a coiled strip of 0·25 mm thick stainless steel 20 cm in width and 2·5 m long giving a further outgassing surface of 10^4 cm^2. The strip material was U15BM, almost identical to U15C. The spiral turns were spaced by small pieces of the same material to assure fair pumping speed everywhere. The ensemble was degassed at 1000°C for 3 hours in a vacuum furnace at approximately 2×10^{-6} torr before being welded on to the measuring equipment. There it was given a further 360°C bakeout for 25 hours to remove any surface contamination collected while exposed to the air. The outgassing data for this specimen are given in table 4. Most noticeable is the low value of $\dot{Q}_{H_2}$ ($\simeq 10^{-14}$ torr l. cm^{-2} sec^{-1}) which is now comparable with the initial

Table 4. Specimen C: outgassing rates (torr l. cm^{-2} sec^{-1})†

Specimen preparation	Measurement temperature (°C)	H_2	H_2O	CO–N_2	O_2	CO_2
Degassed at 1000°C for 3 h	20	$1{\cdot}3^{-14}$‡	—	$1{\cdot}0^{-14}$	—	$1{\cdot}9^{-15}$
in a vacuum furnace, then	20	{$6{\cdot}9^{-15}$}	—	$1{\cdot}2^{-15}$	—	$1{\cdot}9^{-15}$
in situ bake at 360°C for 25 h	20	$1{\cdot}3^{-14}$	—	(- - -)	—	[4^{-16}]
Raise temperature of specimen	100	$1{\cdot}2^{-14}$	—	$2{\cdot}1^{-14}$	—	$2{\cdot}3^{-15}$
Baked for 72 h at 200°C under vacuum	20	$1{\cdot}0^{-14}$	—	—	—	—
Raise temperature of specimen	100	$8{\cdot}7^{-15}$	—	(- - -)	—	—
	200	$1{\cdot}9^{-14}$	—	$3{\cdot}1^{-14}$	—	—

† Not corrected for outgassing of untreated area.
‡ The superscripts denote the power of ten by which the numbers should be multiplied.

outgassing rates of CO–N_2 and CO_2. After one day of pumping at room temperature the outgassing rates of both CO–N_2 and CO_2, the only gases detectable, had fallen to about 10% of that observed for H_2. Outgassing measurements made at elevated temperatures (see table 4 and figure 4) show that now Q_{H_2} has no temperature dependence up to 100°C and increases only by a factor of two on raising the temperature to 200°C. This is in distinct contrast with the previous measurements—Q_{H_2} for specimen B, for example, increased by more than two orders of magnitude over the same temperature range. This strongly suggests that the outgassing rates for specimen C measured at room temperature may be too high and in error owing to the outgassing of the untreated section between the specimen and the valve V_3. There is no reason to expect this surface to outgas at a rate other than that normally found for stainless steel, i.e. $Q_{H_2} \simeq 10^{-12}$ torr l. cm^{-2} sec^{-1}. Its area is about 1·4% of that of the specimen and it could, therefore, be responsible for all the hydrogen observed at room temperature and 100°C with the implication that the specimen outgassing rate was very much less than 10^{-14} torr l. cm^{-2} sec^{-1}. The latter is not unreasonable after a 1000°C bakeout for 3 hours (cf. §3).

Because the coiled strip of area 10^4 cm^2 was only 0·25 mm thick it would, according to equation (2), be degassed to a much greater extent than the 2 mm material. In fact even the normal bakeout of 300°C for 24 hours which yields a calculated outgassing rate of $1{\cdot}4 \times 10^{-13}$ torr l. cm^{-2} sec^{-1} for 2 mm material (see §2.1) gives, under the same conditions, a value more than twenty orders of magnitude lower for the thinner material. This point is pursued with the investigations on specimen D. Thus it may be concluded that all the increased outgassing at 200°C originates from the 2 mm material. The data must then be interpreted as indicating an outgassing rate of the order of 10^{-13} torr l. cm^{-2} sec^{-1} from the container at 200°C, arising from bulk degassing or permeation of atmospheric hydrogen.

Although the equilibrium permeation rate at 200°C ($K_{200} = 1{\cdot}0 \times 10^{-11}$ torr$^{1/2}$ l. cm^{-1} sec^{-1}) is about 10^{-12} torr l. cm^{-2} sec^{-1}, it is to be expected that the observed permeation rate following a 300°C bake for 24 hours would be

$$(Q_{P_1})_{300}\frac{D_{200}}{D_{300}} \times 0{\cdot}13 = 2{\cdot}3 \times 10^{-11} \times \frac{1{\cdot}8 \times 10^{-9}}{3{\cdot}5 \times 10^{-8}} \times 0{\cdot}13$$

$$= 1{\cdot}5 \times 10^{-13} \text{ torr l. cm}^{-2} \text{ sec}^{-1}.$$

The factor 0·13 allows for the non-equilibrium condition after 24 hours (cf. §2.3 and figure 2). Alternatively if the furnace atmosphere of 2×10^{-6} torr was entirely composed of hydrogen there would result an equilibrium concentration c_F in the specimen of $1{\cdot}7 \times 10^{-5}$ H_2 torr l. cm^{-3} (cf. §2.5). This would be expected to give outgassing rates of about 10^{-17}, 3×10^{-15} and 3×10^{-13} torr l. cm^{-2} sec^{-1} at the temperatures 20°C, 100°C and 200°C respectively, and could, therefore, account for the observed temperature dependence.

Although the above description based on a diffusion-controlled mechanism for the outgassing of H_2 is consistent with the data it is not conclusively the only description. For specimens A and B the temperature dependence of Q_{H_2} indicates convincingly that the controlling mechanism is one of bulk diffusion. For specimen C such data were not obtained—it would be necessary to go to higher temperatures or to an apparatus of improved sensitivity. Thus it can be argued that the high-temperature treatment did not reduce the dissolved hydrogen content but rather modified the surface in some way which blocked the release of H_2. The degassing rate would no longer be controlled by bulk diffusion and would no longer have the temperature dependence observed for specimens A and B. The high-temperature treatment could also have altered the microstructure of the material—this point was not checked. However, the only probable modification to the stable austenitic phase would be one of recrystallization. Because grain boundary diffusion of H_2 in austenite is only significant at very low temperatures (Lacombe 1957) such recrystallization would not be expected to affect the outgassing rate of H_2.

4.4. *Specimen D*

Specimen D was constructed by cutting open specimen C, replacing the coil of 0·25 mm thick stainless steel by a new piece, identical in all respects except that it had had no degassing treatment, and then rewelding the container. Outgassing rates (see table 5) obtained after 24 hours of baking at 300°C are only slightly higher than those obtained from specimen C. Following an exposure to 1 torr of H_2 for 12 days the degassing rates for H_2 after 3 days under vacuum are in the 10^{-12} torr l. cm^{-2} sec^{-1} range but are restored to the 10^{-14} torr l. cm^{-2} sec^{-1} range by a normal bakeout. Although the initial hydrogen concentration of the 0·25 mm thick material is not known, this behaviour suggests that it can be degassed effectively at 300°C and that neither the 2 mm thick nor the thin 0·25 mm material is sensitive to H_2 contamination at room temperature.

Table 5. Specimen D: outgassing rates (torr l. cm^{-2} sec^{-1})†

Specimen preparation	Measurement temperature (°C)	H_2	H_2O	CO–N_2	O_2	CO_2
Baked *in situ* at 360°C for 24 h	20	$2{\cdot}7^{-14}$‡	—	[$1{\cdot}5^{-16}$]	—	(- - -)
	20	$2{\cdot}5^{-14}$	—	(- - -)	—	(- - -)
	20	$2{\cdot}6^{-14}$				
Exposed to 1 torr of H_2 for 12 days, then pumped under vacuum for 3 days at room temperature	20	$6{\cdot}8^{-12}$				
	20	$5{\cdot}0^{-12}$				
	20	$2{\cdot}6^{-12}$	$3{\cdot}3^{-13}$	(- - -)	—	$7{\cdot}9^{-15}$
Baked *in situ* at 360°C for 24 h	20	$6{\cdot}0^{-14}$		$1{\cdot}9^{-14}$	—	[$3{\cdot}4^{-16}$]
	20	$2{\cdot}7^{-14}$	—	$2{\cdot}0^{-15}$	—	[$1{\cdot}9^{-16}$]
	20	$3{\cdot}8^{-14}$	—	(- - -)	—	$1{\cdot}6^{-15}$

† Not corrected for outgassing of untreated area.
‡ Superscripts denote the power of ten by which the numbers should be multiplied.

The ease with which thin material may be degassed *in situ* means that it is an interesting alternative to thicker material for the construction of vacuum chambers. The permeation rate from an external pressure of 4×10^{-4} torr of hydrogen should be only 1×10^{-16} torr l. cm^{-2} sec^{-1} at room temperature. In cases where structural weakness of such thin material is a big drawback it could still be used with advantage as a liner with some form of differential pumping for the intervening space. This could be particularly useful for a long tube pumped only at both ends where the extremely low outgassing rate of the liner could reduce considerably the mid-point pressure maximum.

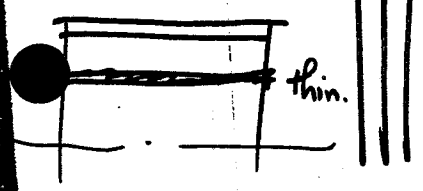

5. Summary and conclusions

After a normal bakeout hydrogen was observed to outgas at a rate of a few times 10^{-12} torr l. cm^{-2} sec^{-1} from a 2 mm thick stainless-steel wall and to constitute at least 99% of the desorbed gas. Calculations based on a diffusion model suggest that it should be possible to achieve outgassing rates for H_2 as low as 10^{-16} torr l. cm^{-2} sec^{-1} by using higher bakeout temperatures. The limiting factor is the absorption of atmospheric hydrogen during the bake. Experimentally it was found that after degassing 2 mm stainless-steel sheet for 3 hours at 1000°C the hydrogen outgassing rate was at least as low as 1×10^{-14} torr l. cm^{-2} sec^{-1} and, because of apparatus limitations, is estimated to be considerably lower.

As indicated by the diffusion-model theory, it has been found that relatively thin stainless steel is thoroughly degassed by normal bakeout procedures at 300°C. The value of such material in normal vacuum systems as liners, which may be degassed *in situ*, has been discussed.

Finally, it has been demonstrated that it is useful to raise the sample temperature when measuring extremely low outgassing rates. This not only produces a higher gas flow but also permits the separation of specimen outgassing from that of the measuring equipment.

The diffusion coefficients, permeability constants and hydrogen content of the atmosphere may differ from those values employed in our calculations. The treatment at 1000°C for 3 hours is probably rather drastic and adequate degassing could be obtained at considerably lower temperatures. Experiments are now in progress to determine the minimum temperature–time conditions necessary. It is hoped that, when these conditions are determined, it will be possible to include this treatment in the final stages of stainless-steel sheet or tube manufacture. This would be a convenient method because it has been shown that such material, after high-temperature degassing, is not readily recontaminated.

Acknowledgments

The authors wish to thank Mlle M. Hanney for computational assistance (figures 1 and 2) and P. Opitz for all the glass-blowing work during construction of the apparatus. It is a particular pleasure to thank F. Le Normand for his sustained and painstaking work during the collection of the experimental data.

Appendix

Equation (4),

$$c(x, t) = c_0 \frac{4}{\pi} \sin \frac{\pi x}{d} \exp\left(-\pi^2 d^{-2} Dt\right)$$

shows that the concentration distribution $c(x, t)$ approaches a simple sinusoidal form in space for large t such that $t > 0{\cdot}025\, d^2/D$. Thereafter the space form is constant and merely undergoes a continual decrease in amplitude through the exponential factor involving the time as long as vacuum is maintained on the surfaces. If a period of degassing at temperature T, long enough to establish the validity of equation (4), is followed by a further period in vacuum at room temperature, t_r, then the equation will become

$$c(x, t) = c_0 \frac{4}{\pi} \sin \frac{\pi x}{d} \exp\left(-\pi^2 d^{-2} D_T t_T\right) \exp\left(-\pi^2 d^{-2} D_r t_r\right). \qquad (17)$$

For stainless steel of $d = 2$ mm in which $D_r = 5 \times 10^{-14}$ cm^2 sec^{-1}, the second exponential factor in equation (4) is 0·99 only after about 30 years. For all practical purposes the outgassing rate at room temperature is time independent if equation (4) is valid and equal to that given by equation (6) immediately after the bakeout.

Alternatively we may consider equation (17) as describing the situation after two successive bakeouts—for example, one in a furnace at temperature T followed by a second at a temperature T'—by substituting $D_{T'}t_{T'}$ for $D_r t_r$.

References

ESCHBACH, H. L., GROSS, F., and SCHULIEN, S., 1963, *Vacuum*, **13**, 543–7.
FISCHER, E., 1965, *J. Vacuum Sci. Tech.*, **2**, 142–8.
GLEUCKAUF, E., 1951, *Compendium of Metrology*, Ed. T. F. Malone (Boston: American Meteorological Society), pp. 3–10.
HOBSON, J. H., 1962, *Trans. 8th Nat. Symp. Amer. Vac. Soc.*, 1961, Vol. 1 (New York: Macmillan), pp. 26–30.
LACOMBE, P., 1957, *La Diffusion dans les Metaux*, Eds J. D. Fast, H. G. van Buerin and J. Philibert (Eindhoven: Philips Technical Library).
LEWIN, G., 1965, *Fundamentals of Vacuum Science and Technology* (New York: McGraw-Hill).
OPITZ, P., and SCHNEIDER, F., 1960, *Vakuum-Tech.*, **9**, 104–5.
TODD, B. J., 1955, *J. Appl. Phys.*, **26**, 1283–43.
YOUNG, J. R., and HESSION, F. P., 1964, *J. Vacuum Sci. Tech.*, **1**, 65–6.

Outgassing of vacuum materials—I

R J Elsey, *The Rutherford Laboratory, Chilton, England*

A paper in our Education Series: The Theory and Practice of Vacuum Science and Technology in Schools and Colleges

In the absence of leaks, the outgassing of the chamber walls determines the lowest pressure obtainable in a vacuum system. Thus the selection of the materials of construction has a marked influence on the system's performance. Outgassing occurs by desorption from the surface and diffusion from the bulk material. Part I explores these processes and how they affect the pumpdown curve of the system.

1. Introduction

In general the technology of each vacuum region is different, i.e. the pumps, gauges, and materials are different. The lower the pressure the more difficult and more expensive it is to achieve. Also the lower the pressure the more important outgassing, i.e. the evolution of gases from the surfaces exposed to the vacuum becomes. Outgassing is relatively unimportant in the rough vacuum region and very important in the ultrahigh vacuum region.

When constructing a vacuum vessel or devices to be contained in a vacuum, the designer must use materials with low outgassing properties. However, other properties, e.g. strength, ease of fabrication, electrical and thermal conductivity, elasticity, optical properties, resistance to high temperature, and cost, will be more or less important according to the particular application. The choice of material is then often a compromise. Materials commonly used in vacuum systems include metals (e.g. stainless steel, aluminium, and copper), glasses and ceramics, and plastics and rubbers.

In high vacuum systems, vessels are usually constructed of steel or aluminium because these metals have reasonably good outgassing properties, are easy to fabricate, and are relatively inexpensive. Such systems have demountable flanges with 'O' ring seals made of rubbers such as Neoprene and Viton. They also frequently use copper tubing and since high vacuum systems are rarely baked, brass unions and valves. If the pumping speed is relatively high such systems can also tolerate a small quantity of plastic material but extreme care must be taken when choosing such materials since the outgassing properties vary considerably from one plastic to another.

With ultrahigh vacuum systems it is essential that they are constructed of materials with the best outgassing properties. Since such systems are usually baked the materials also have to withstand high temperatures. Stainless steel is therefore widely used for the vessel, connecting tubes, and valve bodies. All-metal seals are used, e.g. copper for gaskets and valve seats. Ceramic, in particular alumina, is used for electrical insulation. Rubbers and plastics are unacceptable for use in ultrahigh vacuum systems. Small systems can with advantage be constructed of Pyrex or Kodial glass which when baked has good outgassing properties. Glass systems are relatively inexpensive and can readily be fabricated by glass-blowing.

2. Effect of outgassing

Consider a perfect vacuum vessel, i.e. one that has zero leakage, gas permeability, and outgassing. Suppose that it is of volume V and is being pumped by a pump of volumetric pumping speed S. If at time t the pressure is p then the pressure–time relation is given by:

$$\frac{dp}{dt} = -\frac{S}{V} \cdot p$$

from whence

$$\ln p = \ln p_0 - \frac{S}{V} \cdot t$$

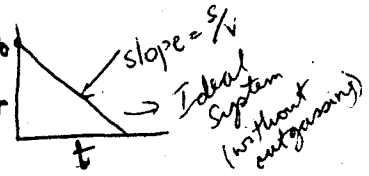

where p_0 is the pressure at time $t = 0$, i.e. at the commencement of pumping. A pump-down of such a system would therefore give a linear plot of ln p against time. Figure 1 is the pump-down curve of a typical real system and it can be seen that it is not linear. By the time the pressure has reached 10^{-6} torr it has become nearly constant. In the absence of leaks this is due to outgassing.

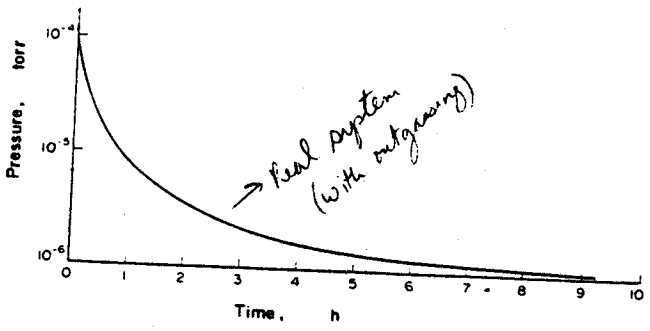

Figure 1. Typical pump-down curve.

Part of this gas is absorbed on the surfaces while they are at atmospheric pressure and then desorbed slowly when they are under vacuum. The rate of desorption will depend on the binding energies of the various gases to the surface, the surface temperature, and the surface coverage. Some gas is dissolved in the material during manufacture, then under vacuum slowly

diffuses out. The outgassing due to this mechanism will depend on the nature of the material, its temperature, the solubility of the gas, and its rate of diffusion. Finally, gas may be evolved after permeating through the walls of the vacuum chamber. This will depend again on the nature of the material and also on its thickness. Permeation is particularly noticeable in plastics and rubbers used for gaskets in high vacuum systems. It is also important in metals at high temperatures and in glass due to the permeability of this material to helium.

3. Adsorption

Adsorption of a gas onto a solid surface can take place by two principal methods. These are physical adsorption and chemical adsorption or chemisorption. In physical adsorption the gas molecules are attracted to the surface by Van der Waal's forces and the heat of adsorption is low (less than 10 kcal/mole). In chemisorption actual chemical combination occurs between the gas molecules and the molecules of the solid involving a sharing or exchange of electrons. Here the heat of adsorption is much higher (20–200 kcal/mole).

The quantity of gas adsorbed at constant temperature on a given surface increases with the pressure of gas in the gas phase. The relation between the quantity adsorbed and the pressure at constant temperature is called an *adsorption isotherm*. The three important isotherms are those attributed to Langmuir,[1] Freundlich,[2] and Temkin.[3]

3.1 Langmuir isotherm.

$$\theta = Ap/(1 + Ap)$$

where θ is the surface coverage.

$$A = \alpha/[n_m \nu \exp - E/RT . \sqrt{(2\pi mkT)}]$$

p is the pressure
α is the sticking coefficient
n_m is the number of molecules per cm² of surface $\sim 10^{15}$
ν is the vibration frequency of adsorbed molecules $\sim 10^{13}$ Hz
E is the adsorption energy
R is the universal gas constant
T is the absolute temperature
m is the molecular mass
k is Boltzmann's constant.

The Langmuir isotherm assumes that the adsorption energy is constant. It is applicable where the pressure and surface coverage are low i.e. $\theta < 0.3$.

3.2 Freundlich isotherm.

$$\theta = Bp^{1/n}$$

where n is ≥ 1,

and n and B are constants for a particular adsorbent.

The Freundlich isotherm is applicable at higher surface coverage than the Langmuir isotherm. It is semi-empirical, and assumes that the adsorption energy decreases exponentially with surface coverage.

3.3 Temkin isotherm.

$$\theta = \frac{RT}{\beta} \ln (cp).$$

The Temkin isotherm is derived from the Langmuir isotherm. It assumes that the adsorption energy decreases linearly with surface coverage.

i.e. $E = E_0(1 - \beta\theta)$ and $C = C_0 \exp E_0/RT$.

Figure 2 shows a comparison of the Langmuir, Freundlich, and Temkin isotherms[20]. Figure 3 shows a good fit of the Temkin isotherms for hydrogen on a molybdenum film at 78 K[4].

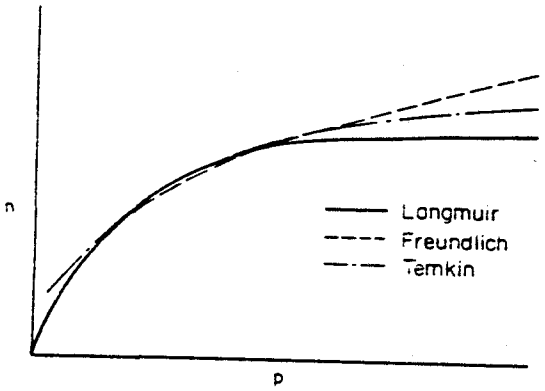

Figure 2. Comparison of Freundlich, Temkin and Langmuir isotherms. (Henry, 1969[20].)

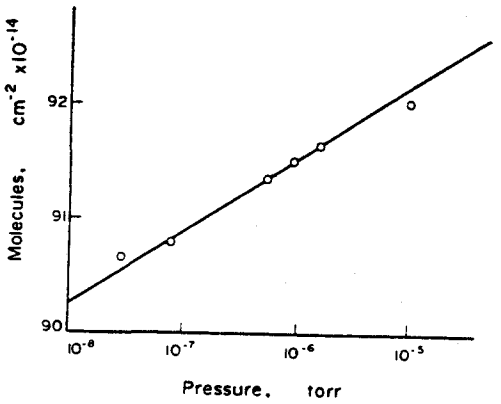

Figure 3. Test of Temkin isotherm for H_2 on Mo film at 78 K. (Hayward 1966[4].)

4. Desorption

If dn/dt is the rate of desorption of molecules

$$\frac{dn}{dt} = - Kf'(\theta) \exp(-E/RT)$$

where $f'(\theta)$ is a function of the surface coverage, K is a constant and E is the desorption activation energy.

By the equation of Polanyi-Vigner

$$\frac{dn_s}{dt} = \nu_0 n_m f'(\theta) \exp(-E/RT)$$

where ν is the frequency of vibration of sorbed molecules normal to the surface and n_m is the number of molecules in a monolayer.

n_s is the number of molecules on the surface at time t
ν_0 has a value about 10^{13} Hz
and n_m about 10^{15} molecules cm^{-2}

$$\nu_0 = \frac{1}{\tau_0}$$

where $\tau = \tau_0 \exp E/RT$ (where τ is the residence time).

If τ_0 is 10^{-13} s, E is 10 kcal/mole and T is 300 K
R is 2 cal deg^{-1} mole^{-1}.
This gives $\tau = 2$ μs.

Thus gases that are physisorbed are desorbed very quickly at room temperature.

An equation for the pump down of a system can be derived as follows:

If n_v is the molecular density of the gas phase
V is the volume of the vessel being pumped
A_p is the area of the pumping port
A_s is the area of outgassing surface
$\bar{c}$ is the average velocity of the gas molecules
α is the sticking coefficient.

Assuming τ is independent of surface coverage,

$$\text{Gas removed by the pump} = \frac{\bar{c}}{4} n_v A_p$$

$$\text{Gas desorbed by the surface} = \frac{n_s A_s}{\tau}$$

$$\text{Gas adsorbed by the surface} = \frac{\bar{c}}{4} n_v \alpha A_s$$

$$\therefore \frac{V dn_v}{dt} = -\frac{\bar{c}}{4} n_v A_p + \frac{n_s A_s}{\tau} - \frac{\bar{c}}{4} n_v \alpha A_s \qquad (1)$$

also for the surface.

$$A_s \frac{dn_s}{dt} = -\frac{n_s A_s}{\tau} + \frac{\bar{c}}{4} n_v \alpha A_s . \qquad (2)$$

Differentiating (1) and combining with (2)

$$\frac{d^2 n_v}{dt^2} + \left[\frac{\bar{c}}{4V}(\alpha A_s + A_p) + \frac{1}{\tau}\right]\frac{dn_v}{dt} + \frac{\bar{c}}{4V} \cdot \frac{A_p}{\tau} n_v = 0 . \qquad (3)$$

Hobson[5] has plotted solutions of equation (3) for various values of E (Figure 4).

This shows that at room temperature only adsorption energies between 15 and 45 K cal mole^{-1} give troublesome outgassing.

Also from equation (2) it can be seen that the net outgassing rate depends *inter alia* on the pressure.

Schram[6] has derived relations between dn/dt and pumping time t for several variations on the Polanyi-Vigner equation. The variations allow for the desorption energy to be constant or, as in the Temkin isotherm, to decrease linearly with surface coverage. They also allow for dissociation and readsorption of the gas molecules. Table 1 gives Schram's equations for six of the eight cases he has identified.

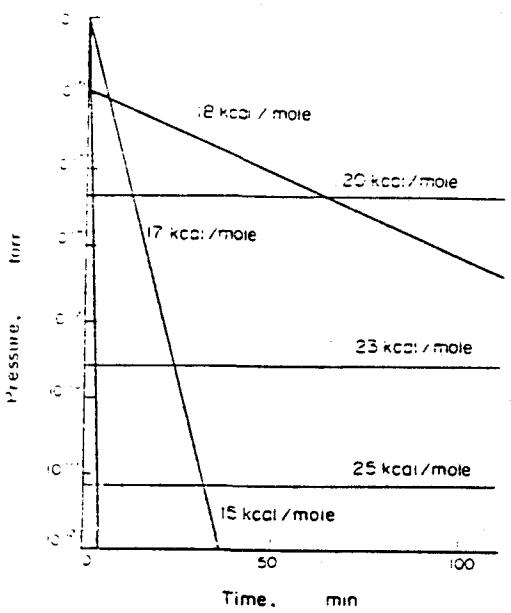

Figure 4. Pump-down curves for 100 cm^2 of material with one monolayer coverage for different heats of desorption. Pump speed 1 l. s^{-1}. (Hobson, 1961[5].)

Figure 5 shows $\log(-q)$ plotted againgt $\log(t)$ in three different cases and also for diffusion and permeation. The use of the Temkin isotherm derived for heterogeneous surfaces can successfully explain the slope of -1 often found for outgassing of unbaked metal systems.

However, when experimental outgassing curves are integrated, or when the formulae corresponding to experimental curves are integrated, it is found that for an unbaked metal surface the total quantity of gas desorbed can be as much as 100 times that

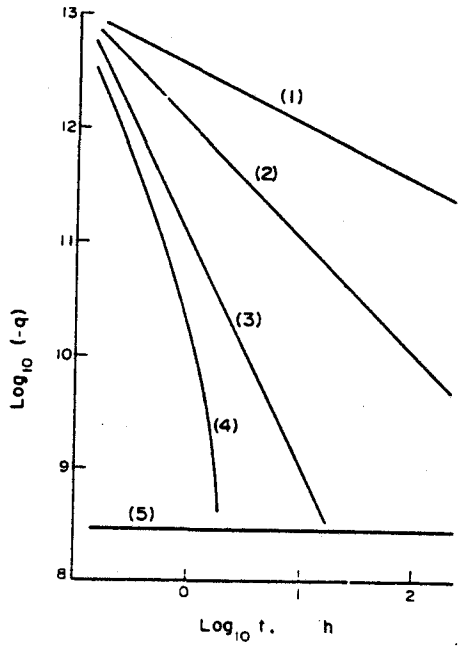

Figure 5. Time dependence of outgassing rate for different mechanisms (Schram, 1963[6]).
(1) $q \propto 1/t^{1/2}$ diffusion; (2) $q \propto 1/t$ Temkin; (3) $q \propto 1/t^2$ Langmuir —dissociation; (4) $q \propto e^{-\alpha t}$ Langmuir; (5) $q = q_0$ permeation.

Table 1 (Schram, 1963[6])

Case	Desorption energy			Variation of outgassing rate with time	
I	$E = E_0$			$\log(-q) = \log(-q_{01}) - \frac{1}{n_m} \cdot q_0 \cdot (t - t_0)$	
II	$E = E_0\left(1 - \beta\frac{n}{n_m}\right)$			$\log(-q) = -\log\left(\frac{\beta E_0}{n_m RT}\right) - \log(t - t_0)$	$\frac{1}{n} \ll \frac{\beta E_0}{n_m RT}$
				$\log(-q) = \log(-q_{01}) - \frac{1}{n_m} \cdot q_0 \cdot (t - t_0)$	$\frac{1}{n} \gg \frac{\beta E_0}{n_m RT}$
III	$E = E_0$	dissociation		$\log(-q) = \log\left(-\frac{n_m^2}{q_0}\right) - 2\log(t - t_0)$	
IV	$E = E_0\left(1 - \beta\frac{n}{n_m}\right)$	dissociation		$\log(-q) = -\log\left(\frac{\beta E_0}{n_m RT}\right) - \log(t - t_0)$	$\frac{2}{n} \ll \frac{\beta E_0}{n_m RT}$
				$\log(-q) = \log\left(-\frac{n_m^2}{q_0}\right) - 2\log(t - t_0)$	$\frac{2}{n} \gg \frac{\beta E_0}{d_m RT}$
V	$E = E_0$		readsorption	$\log(-q) = \log n_m(B - Cp) - (B - Cp)(t - t_0)$	B and C constants
VI	$E = E_0$	dissociation	readsorption	no satisfactory solution	
VII	$E = E_0\left(1 - \beta\frac{n}{n_m}\right)$		readsorption	$\log(-q) = -\log\left(\frac{\beta E_0}{n_m RT} - \frac{Cp}{q_0}\right) - \log(t - t_0)$	$\frac{1}{n} \ll \frac{\beta E_0}{n_m RT}$ p small t large
VIII	$E = E_0\left(1 - \beta\frac{n}{n_m}\right)$	dissociation	readsorption	no satisfactory solution	

corresponding to a monolayer. This gas is nearly all water vapour.[7] Schram after failing to find evidence for such a high specific surface roughness factor attributes his phenomena to an 'interior' surface composed of many small fissures in a surface oxide layer.

Dayton[8] has quoted evidence for such an oxide layer, e.g. Galbransen[9] has shown that oxide films on iron cannot be removed except by reduction in hydrogen at 500°C and that an oxide film 20 Å thick forms in 10 min in oxygen at room temperature. Evans[10] has shown that iron oxide films on iron will not be visible if less than 300 Å thick. 100 monolayers of water vapour are nearly 300 Å thick. Dayton has assumed the same type of surface and produced a hypothesis based on the diffusion of water vapour molecules through narrow capillaries of varying diameter. This hypothesis also leads to a curve on logarithmic co-ordinates of slope −1 and Dayton claims it is more consistent with experimental results for outgassing at various temperatures.

Mathewson[11] has carried out AES and SIMS on unbaked stainless steel samples which had been cleaned by various methods. The analysis failed to detect the base metal but detected 50–80% carbon in the first three monolayers. After bombarding with argon ions, no carbon or oxide was detected but iron and chromium in the proportion of the alloy was detected. Everett and Stone[12] have shown electron micrographs of Fe_3O_4 crystals with pores of 2×10^{-6} cm dia with a surface density of 2×10^{10} pores per cm^2 of surface which although not sufficient to account for the quantity of water vapour evolved does suggest that the micro-pore hypothesis of Schram and Dayton may be possible.

The more recent work of Mathewson and also of Park *et al*[13] and also of Beavis,[14] using surface analysis techniques suggest however that the surface layers of unbaked metals are more complicated than a metal oxide–water system, and contain much extraneous material such as carbon and alkali metals.

5. Diffusion

A contribution to the outgassing of the vessel walls and other components of a vacuum system is made by gas diffusing out of the bulk of the material. If, in fact, the gas diffuses right through the material from the outside the process is called permeation.

According to Fick's law of diffusion, gas flow in a solid is proportional to the concentration gradient of the gas in the solid.

Thus: $q = -D\frac{dc}{dx}$ First-order eq:

where q is the gas flow across unit cross-section in unit time in the direction x
D is the diffusion coefficient
and dc/dx is the concentration gradient.

The minus sign indicates that the gas flow is in the opposite direction to the concentration gradient. Diffusion is an activated process and the diffusion coefficient increases with temperature according to the equation

$$D = D_0 \exp(-E/RT)$$

where E is the activation energy for diffusion.

Diffusion is a slow process and in the condition before equilibrium is achieved Fick's second law of diffusion applies, namely:

$$D\frac{\partial^2 c}{\partial x^2} = \frac{\partial c}{\partial t}.$$ Second-Order eq:

This equation can be solved for geometries common in vacuum systems by inserting the appropriate boundary conditions. For example the boundary conditions for a vessel wall which is thick enough to be considered semi-infinite and which has an initial uniform gas concentration C_0 are:

$C = C_0$ for $x \geq 0$ when $t = 0$

$C = 0$ for $x = 0$ when $t > 0$.

The solution given by Lewin[15] is for unit area

$$c(x,t) = 2C_0(\pi)^{-1/2} \int_0^{x/2(Dt)^{1/2}} \exp(-y^2)\,dy$$

$$= C_0 \operatorname{erf} x/2(Dt)^{1/2} \quad \text{(error function)}.$$

The outgassing rate after a pumping time t is given by:

$$q_t = D\left(\frac{\partial c}{\partial x}\right)_{x=0}$$

$$= C_0 D^{1/2}(\pi t)^{-1/2},$$

i.e. the outgassing rate varies inversely with the square root of the pumping time.

The total amount of gas removed in time t

$$Q_t = \int_0^t D\left(\frac{\partial c}{\partial x}\right)_{x=0} dt$$

$$= 2\pi^{-1/2} C_0 (Dt)^{1/2}.$$

For a slab of material totally enclosed in a vacuum vessel such as a sample in an outgassing test the boundary conditions are different. This is the case of a finite slab.

The boundary conditions are:

$C = C_0$ for $0 \leq x \leq d$ when $t = 0$

$C = 0$ for $x = 0$ and $x = d$ when $t > 0$

where d is the thickness of the material.

The solution given by Lewin for unit area is

$$C = C_0 \frac{4}{\pi} \sum_{n=0}^{\infty} (2n+1)^{-1} \sin \pi \frac{(2n+1)}{d} . x .$$

$$\exp\left\{-\left[\frac{\pi(2n+1)}{d}\right]^2 . Dt\right\}.$$

From which the outgassing from both surfaces is

$$q_t = 2D\left(\frac{\partial c}{\partial x}\right)_{x=0} = 8\frac{C_0 D}{d} \sum_{n=0}^{\infty} \exp\left\{-\left[\frac{\pi(2n+1)}{d}\right]^2 . Dt\right\}.$$

The total amount of gas removed in time t is

$$Q_t = 2D\int_0^t \left(\frac{\partial c}{\partial x}\right)_{x=0} dt$$

$$= C_0 d\left\{1 - \frac{8}{\pi^2} \sum_{n=0}^{\infty} (2n+1)^{-2} \exp\left(-\left[\frac{\pi 2n+1)}{d}\right]^2 Dt\right)\right\}.$$

Calder and Lewin[16] have shown that for $Dt/d^2 > 0.025$ an approximation for q can be made

i.e. $$q_t = \frac{8C_0 D}{d} \exp -\{(\pi/d)^2 Dt\}.$$

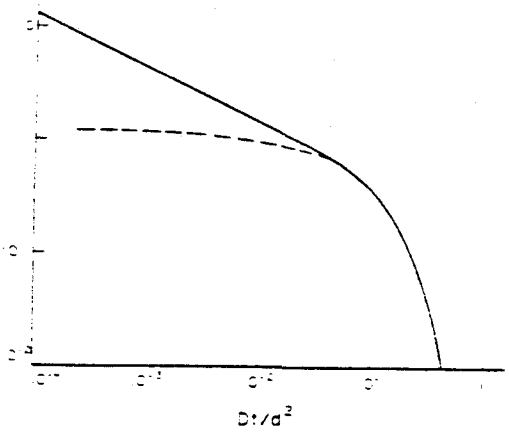

Figure 6. Plot of the infinite series of the diffusion equation for a slab of thickness d and of its first term. (Calder and Lewin, 1967[16].)

——— $\frac{8}{\pi^2} \exp\left\{-\left[\frac{\pi(2n+1)}{d}\right]^2 Dt\right\}$; ----- $\exp(-\pi^2 d^{-2} Dt)$.

The two exponential functions are plotted against Dt/d^2 in Figure 6. This shows that for $Dt/d^2 > 0.025$ the outgassing reduces rapidly and for $Dt/d^2 < 0.025$ it reduces with a slope of $-\frac{1}{2}$ on the logarithmic co-ordinates. Also according to Calder and Lewin if a finite slab of material is heated to a high temperature T_1 for a time t_1 seconds which is long enough for the condition $Dt/d^2 > 0.025$ to be satisfied and the sample is then cooled to room temperature T_r the resulting outgassing rate is given by

$$q_r = \frac{8C_0 D_r}{d} \exp -\{(\pi/d)^2 D_1 t_1\}$$

where D_1 is the diffusion coefficient of the material at temperature T_1, and D_r is the diffusion coefficient of the material at temperature T_r. This is a useful equation to determine the behaviour of a vacuum system during bake out. Arrhenius plots of the diffusion constants of various gas–metal combinations are shown in Figure 7.

The total quantity of water vapour outgassed by an unbaked metal surface during pump down corresponds to 100 monolayers on a smooth surface or alternatively to one monolayer and a surface with a roughness factor of 100. Dayton[8] has proposed a mechanism based on the diffusion of water vapour molecules out of capillaries in a thin oxide layer covering the metal surface. As has already been shown diffusion leads to outgassing rates which are proportional to $t^{-1/2}$ whereas outgassing rates of unbaked metals are known to be in general proportional to t^{-1}, t being the pumping time.

The Dayton theory assumes that the diameter and length of the capillaries will vary, giving rise to a range of diffusion coefficients. A time constant τ is introduced which is a function of the capillary diameter and length and the desorption energy of the water vapour molecules. When the pumping time t becomes greater than τ the outgassing rate should start to decay exponentially. It is assumed that for a given surface a distribution of values of τ will exist. It is also assumed that for a fraction $F(\tau)\,d\tau$ of the surface τ is constant where

$$\int_{\tau_0}^{\tau_m} F(\tau) d\tau = 1$$

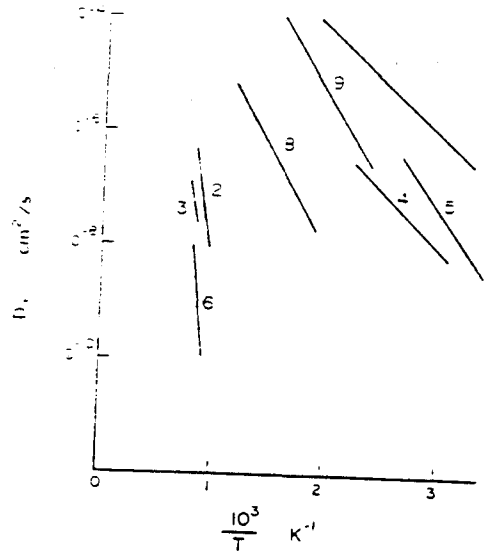

Figure 7. Diffusion constants. (1) H_2–Pd, Barrer; (2) N_2–Fe, Barrer; (3) CO–Ni, Nushman and Lafferty; (4) H_2–Ni, Barrer; (5) H_2–Fe, Barrer; (6) O_2–Ni, Dushman and Lafferty; (8) H_2–stainless steel (300), Eschbach; (9) H_2–stainless steel (400), Eschbach. (Lewin, 1965[15].)

and τ_0 and τ_m are the minimum and maximum values of τ. If τ and t are in hours the contribution to the outgassing rate by the fraction $F(\tau)d\tau$ is given by:

$$q_{tm} = \frac{C_0}{3600\tau^{1/2}(B/60 + t^a)}$$

where

$$t^a = t^{1/2} - \frac{\tau^{1/2}}{2}(1 - \exp\{-t/2\tau\})$$

and where B reduces to zero after a few seconds. This is an approximate solution to the equation derived from Fick's Law for the diffusion of gas through a solid of finite thickness.

The outgassing rate for the whole surface will be therefore

$$q_t = \int_{\tau_0}^{\tau_m} q_{tm} F(\tau)d\tau .$$

Dayton has illustrated the use of this equation by dividing the oxide layer into four regions such that $F(\tau_i)$ is constant over a range

$$\tau_i - \frac{\Delta\tau}{2} \text{ to } \tau_i + \frac{\Delta\tau}{2}$$

where i is an integer from 1 to 4. and

$$F(\tau_i)\Delta\tau = \frac{1}{4}.$$

Then the outgassing rate for the fraction

$F(\tau_i)\Delta\tau$

is given by:

$$q_i = \frac{1}{4} \cdot \frac{C_0}{3600} \cdot \frac{1}{t^{ai}\tau_i^{1/2}}$$

where

$$t^{ai} = t^{1/2} - \frac{\tau_i^{1/2}}{2}(1 - \exp\{-t/2\tau_i\}).$$

The total outgassing rate is given by:

$$q = \sum_{i=1}^{i=4} q_i .$$

Taking $C_0 = 8.6 \times 10^{-4}$ cm^3 H_2O vapour at STP cm^{-3} oxide for a thickness of 5×10^{-5} cm as a typical value. Dayton has plotted outgassing curves for the four regions on logarithmic coordinates. These curves are shown in Figure 8. The four curves are for values of τ of 0.25, 1, 4 and 16 h, respectively. The total outgassing rate is given by the broken line. It can be seen that while each individual curve is similar to Figure 6 for a constant diffusion coefficient, the broken line gives q_t more nearly proportional to t^{-1}. This condition will be more closely approached as $\Delta\tau \to d\tau$.

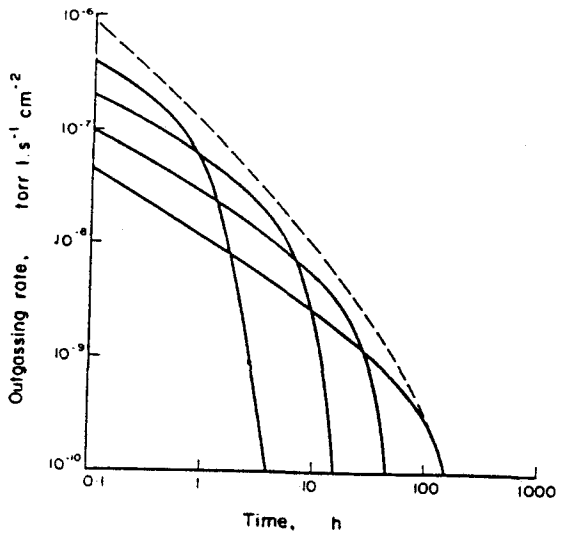

Figure 8. Total outgassing rate as a sum of curves for constant values of τ. (Dayton, 1961[8].)

6. Permeation

Permeation differs from gas flow through porous material or leaks in that it takes place by a process of active diffusion. First the gas dissolves in the solid on the side of highest gas concentration. It then diffuses through the solid and outgasses on the side of lowest concentration, i.e. the vacuum side. The permeability K of the material for a particular gas is given by

$$K = DS$$

where D is the diffusion coefficient and S is the solubility of the material for the gas. The permeability increases exponentially with temperature

i.e. $$K = K_0 \exp(-E_K/RT)$$

where $K_0 = D_0S_0$ and $E_K = E_D + H_s$.

where H_s is the heat of solution.

This rapid increase of permeability with temperature becomes important when vacuum systems are baked to high temperatures and may set an upper temperature limit for which a reduction in outgassing may be gained by baking.

The important cases where outgassing is increased by permeation are, hydrogen from the atmosphere permeating through the walls of a metal ultrahigh vacuum (uhv) system, helium from the atmosphere permeating through walls of a glass uhv system, and atmospheric gases permeating through plastic gaskets and windows in a high vacuum system.

6.1 Metals. The solution of the Fick's Law equation for permeation given by Lewin[15] is as follows. For a completely outgassed slab of metal that is suddenly exposed on one side to a pressure p_1 of gas, the other side being in vacuum the boundary conditions are:

$C = 0$ for $0 \leq x \leq d$ when $t = 0$

$C = 0$ for $x = 0$ when $t > 0$

$C = C_1$ for $x = d$ when $t > 0$.

The solution is

$$C(x,t) = \frac{C_1 x}{d} + \frac{2C_1}{\pi} \sum_{n=1}^{\infty} \left(\frac{-1}{n}\right)^n \sin \frac{n\pi x}{d} \cdot \exp\left\{-\left(\frac{n\pi}{d}\right)^2 Dt\right\}.$$

The permeation rate at time t is

$$q_{p_1} = \frac{DC_1}{d} + \frac{2DC_1}{d} \sum_{1}^{\infty} (-1)^n \exp\left\{-\left(\frac{n\pi}{d}\right)^2 Dt\right\}.$$

Calder and Lewin[16] have plotted

$$1 + 2 \sum_{n=1}^{\infty} (-1)^n \exp\left\{-\left(\frac{n\pi}{d}\right)^2 Dt\right\} \text{ against } \frac{Dt}{d^2}$$

and show that whereas for $t \to \infty$

$$(q_p)_{t=\infty} = D\frac{C_1}{d}.$$

For shorter times such that $Dt/d^2 \leq 0.02$ the permeation rate is 10,000 times less than the equilibrium rate. For 2-mm thick stainless steel at room temperature this is so if t is less than 300 years. Calder and Lewin show that the resulting outgassing for 2 mm thick stainless steel at room temperature due to the partial pressure of hydrogen in the atmosphere (4×10^{-4} torr) would be 10^{-17} torr l. cm^{-2} s^{-1} after equilibrium had been established, but for all practical times the rate would then not exceed 10^{-21} torr l. cm^{-2} s^{-1} which is negligible. However at the end of a prolonged 300°C bakeout the hydrogen permeation rate would be equivalent to an outgassing rate of 2.3×10^{-11} torr l. cm^{-2} s^{-1}. Subsequent cooling to room temperature would considerably reduce this outgassing rate to an insignificant level.

6.2 Glass. For $Dt/2 \geq 1$ Calder and Lewin show that outgassing due to helium permeation has become reasonably constant. D for He and Pyrex glass is 10^{-8} cm^2 s^{-1} at room temperature and for a glass wall 1.5 mm thick equilibrium would be reached in about 3½ weeks. In the case of a glass system therefore it is quite feasible for permeation to have reached equilibrium in practical times especially after a vacuum bake at 100 C has removed water vapour.

Rogers *et al* have measured the permeability of Pyrex glass for He and report it as 10^{-10} cm^2 s^{-1} i.e. the quantity of gas in cm^3 at STP flowing through 1 cm^2 of material 1 cm thick when the pressure difference is 1 atm. The partial pressure of helium in the atmosphere is $4 \cdot 10^{-3}$ torr[15] and K for He through glass is proportional to the pressure difference. For a small laboratory system containing a 1 l. glass sphere, pumped by a 1 l. s^{-1} pump this sets a low pressure limit of about 10^{-12} torr.

6.3 Plastics and polymers. Lebovits[19] has made a comprehensive review of the permeability of polymers to gases and vapours including tables of permeabilities of many of the popular gasket and thin film materials.

He has also outlined the factors influencing permeability in these materials. In the case of gases the permeability of a given material is inversely proportional to the molecular diameter of the gas molecule. Also the ratio of the permeabilities of two different gases in one material is the same as in another material within a factor of three even though the permeabilities of the materials to the same gas may differ by a factor of 1200. However, in the case of vapours, the permeability is highly dependent on the nature of the vapour and the material. In particular the permeability will be high where there is a chemical similarity between the vapour and the material. This is to be expected since the permeability is proportional to the solubility of the vapour and with organic materials, solubility is high where there is chemical similarity. Thus there is evidence of chemical interaction between the solid and the permeating vapour. The permeabilities of polyethylene and polyurethane to nitrogen are similar but polyurethane is thirty times more permeable than polyethylene to water vapour. Where the solubility of the vapour is very high, swelling of the solid occurs which also facilitates permeation due to the increased distance between the molecules of the solid. Thus the permeability of rubber gaskets to water vapour and air is increased if swelling has occurred due to the use of solvents for 'cleaning' or leak detection. In this respect the outgassing of elastomers is higher on the first pumpdown due to the release of chemicals used in manufacture than in subsequent pump-downs and a wide variation can occur between outgassing rates of the fresh material from different sources.

The permeability of polymers depends on the 'tightness' of the bonding, i.e. where a material possesses cross-links or a high degree of symmetry or crystallinity, the permeability will be lower. Also, where the material contains an impermeable filler such as particles of mica the diffusion paths will be long and the permeability will be lowered. Thus the permeability of polyethylene can be lowered by a factor of two by cross-linking and low density (non-crystalline) polyethylene is five times more permeable than high density polyethylene.

With permanent gases the permeation through polymers into vacuum is proportional to the partial pressure of the gas once equilibrium has occurred. With vapours, due to solubility the permeability will increase more rapidly than the vapour pressure when the vapour pressure rises. Hence in the case of vapours the permeability expressed as the rate of permeation through unit area and thickness for unit pressure difference is no longer a constant and is only valid for the conditions under which it is measured.

Other non-linear parameters include thickness. Normally permeation is inversely proportional to the thickness of the material. However due to the method of manufacture a thin film material may have a 'skin effect', i.e. if the surface layers are far less permeable than the bulk material the permeation may appear nearly independent of thickness.

The effect of temperature on the permeability of polymers is variable. It would be expected that the permeability would increase exponentially with temperature. However as it is common for structural changes and transitions to occur at moderate temperatures the effects of temperature are unpredictable.

7. Conclusion

The complex mechanisms of outgassing are not well understood. Contributions to outgassing come from surface desorption and from the bulk. Which predominates depends on the state of the surface. However the surface of common materials is an ill-defined mixture and it is probable that the process is controlled more by impurities such as carbon and oxides than by the base material or the gases desorbed. The earlier hypotheses of Dayton and Schram were largely based on outgassing data. After an interval of several years the development of sophisticated analytical techniques such as SIMS and Auger spectroscopy has allowed a start to be made on investigating the nature of the surfaces of common materials. This work may well clarify what is occurring during outgassing.

Acknowledgement

The author wishes to acknowledge the assistance given by the Rutherford Laboratory in the preparation of this article.

References

[1] I Langmuir. *J Am Chem Soc*, **40**, 1918, 1361.
[2] H Freundlich. *Colloid and Capillary Chemistry*, Methuen, London (1926).
[3] A Frumkin and A Slygin. *Acta Physiochim URSS*, 3, 1935, 791.
[4] D D Hayward, N Taylor and F C Tomkins *Disc Faraday Soc*, **41**, 1966, 75.
[5] J P Hobson. *Trans 8th AVS Vac Symp*, 1961, 26.
[6] A Schram. *Le Vide*, **103**, 1963, 55.
[7] C Hayashi. *Trans 4th AVS Vac Symp*, 1957, 13.
[8] B B Dayton. *Trans 8th AVS Vac Symp*, 1961, 42.
[9] E A Gulbransen. *Trans Electrochem Soc*, **82**, 1942, 375.
[10] J R Evans. *Metallic Corrosion Passivity and Protection*, 2nd Edn. Edward Arnold, London (1946).
[11] A G Mathewson. *Vacuum*, **24**, 1974, 505.
[12] D H Everett and F S Stone, *The Structure and Properties of Porous Materials*, p 91. Academic Press, New York.
[13] R L Park, J E Houston and D G Schreiner, *J Vac Sci Technol*, **9**, 1972, 1023.
[14] L C Beavis, *J Vac Sci Technol*, **10**, 1973, 390.
[15] G Lewin. *Fundamentals of Vacuum Science and Technology*, McGraw-Hill, New York (1965)
[16] R Calder and G Lewin, *Br J Appl Phys*, **18**, 1967, 1459.
[17] W A Rogers, R S Buritz and D Alpert, *J Appl Phys*, **25**, 1954, 868.
[18] R C Weast. *Handbook of Chemistry and Physics*, Chemical Rubber Co, Cleveland (1966).
[19] A Lebovits, *Modern Plastics*, March 1966, 139.
[20] R P Henry, *Le Vide*, **144**, 1969, 316.

Sorption – the taking-up of gas or vapour by a solid is known as sorption.

desorption - opp: i.e. the giving up of a gas or vapour by a solid.

Outgassing of vacuum materials—II

R J Elsey, *The Rutherford Laboratory, Chilton, England*

A paper in our Education Series: The Theory and Practice of Vacuum Science and Technology in Schools and Colleges.

Part II of this two part account examines the methods available for the measurement of outgassing rate. It recounts the results obtained for some selected materials and in particular examines methods for reducing the outgassing rates of materials for use in ultrahigh vacuum. Finally it presents outgassing rates for various materials in tabulated form.

1. Introduction

In any vacuum system that has reached equilibrium and in which leaks have been eliminated the pressure depends on the total outgassing of the system and the pumping speed of the pumps.

$$p = \frac{Q}{S} \text{torr}$$

where Q is the outgassing rate in torr litre per second (torr l. s^{-1}) and S is the pumping speed in l. s^{-1}. Strictly this formula is true only for a discrete part of the system where molecular flow prevails and where one can consider a volume into which gas is evolved from surfaces, and out of which gas flows due to pumping. It is not true for example where large differences of temperature exist, e.g. near cryo surfaces.

The rate of outgassing of a material is expressed in torr litre per second per square centimetre and the total outgassing of a system will be made up of the sum of the outgassing rate of each material present multiplied by its area. Frequently the pressure will depend on the outgassing of a large area of material with a low outgassing rate, e.g. the chamber wall, or a small area of material with a high outgassing rate, e.g. a rubber 'O' ring gasket or a component inside the system.

In general the pressure in a pumped vacuum system will slowly decrease with time due to the outgassing rate of the materials, reducing as gas is removed. This is because the rate depends on the surface coverage or on the concentration of gas dissolved in the material. Figure 1 shows a typical plot of log outgassing rate against log time.

The methods of measuring outgassing rates are described in detail later. There are two general methods. In one the sample is allowed to outgas in a sealed chamber and the rate of pressure rise measured. In the other the sample contained in a chamber is pumped at a constant and known pumping speed and the equilibrium pressure measured. In both methods allowance is made for the outgassing of the chamber by conducting blank runs.

2. Measurement of outgassing rate

Outgassing rate is defined by American Vacuum Society draft standard AVS 9.1–1964 Reporting of Outgassing Data as: '. . . the instantaneous net amount of gas leaving the material per unit of time'. 'Amount of gas' means effectively 'mass of gas'.

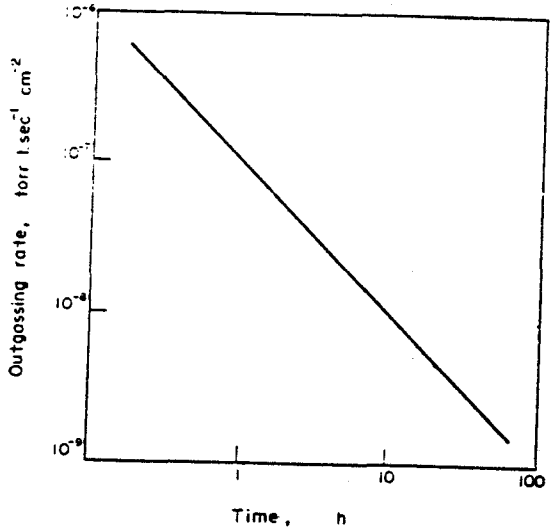

Figure 1. Typical outgassing rate plot.

This mass can be measured directly, but since it is more usual to measure the pressure and the volume rate of flow of the evolved gas, it is expressed in presure–volume terms namely torr litres, referred to a standard temperature. One torr litre at 23°C = 5.44×10^{-5} M grams where M is the molecular weight of the gas. The torr l. s^{-1} is the unit of throughput. Torr l. s^{-1} cm^{-2} is the unit of outgassing rate for materials used in a vacuum. Torr l. s^{-1} g^{-1} may also be used where the outgassing rate depends on the bulk properties of the material rather than its surface properties. Where the outgassing rate of a whole component composed of several materials is measured the rate is expressed in torr l. s^{-1} and is specific to that particular component.

As can be seen in Figure 1 the outgassing rate of a material at constant temperature reduces as the pumping time increases. The pumping time is usually expressed in hours. Outgassing rates may be presented in either graphical or tabular form. The plots of log outgassing rate against log time have negative slopes and are usually linear. The time starts at the commencement of pre-evacuation by a roughing pump and may extend to 100 h.

In tabular form, the outgassing rate after specified pumping times of say 4, 10 and 100 h is quoted together with the slope of the log–log plot for the same time. The outgassing rate is given the symbol K with a subscript indicating the pumping time. The

slope is given the symbol α and the negative sign is omitted. A typical statement is:

K_{10} stainless steel 5×10^{-10} torr l. s^{-1} cm^{-2}

α_{10} stainless steel 1.0.

Since the outgassing rates of unbaked materials are sensitive to temperature and since the tests take so long to perform thermostat control is necessary whatever method is used and a chart recorder is almost a necessity.

3. Methods of measurement

3.1 Throughput method. The throughput method attributed to Zabel[1] has attained considerable popularity. The results obtained by this method are the ones most relevant to continuously pumped vacuum systems. Essentially a sample of the material to be studied is placed in a vessel which is connected by a tube or orifice of known conductance to a high vacuum pump. A vacuum gauge, usually an ionization gauge but sometimes a residual gas analyser, is connected to the vessel containing the sample. The vessel is pre-evacuated, the time noted and the high vacuum pump started. When it is judged that the pressure is low enough the vacuum gauge is switched on and the chart recorder, if used, started. Alternatively to the use of a chart recorder, pressure readings are taken at intervals which are short at first but are longer as the rate of reduction of pressure becomes slower.

Figure 2 shows the apparatus used by Zabel to measure the outgassing rates of waxes and sealing compounds and Figure 3 the apparatus used at the Rutherford Laboratory to determine the outgassing rates of glass fibre expoxy laminates.[2,3] In the Zabel apparatus the sample chamber was connected to the pump by a small bore tube of conductance 0.042 l. s^{-1} for air calculated from the Knudsen formula for a long tube viz.:

$$C = \frac{1}{1000}\sqrt{\left(\frac{2\pi RT}{M}\right)} \cdot \frac{4r^3}{3l} \text{ l. s}^{-1}$$

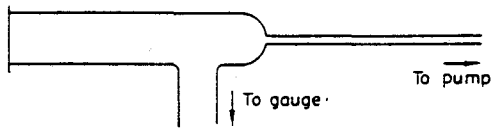

Figure 2. Zabel apparatus.

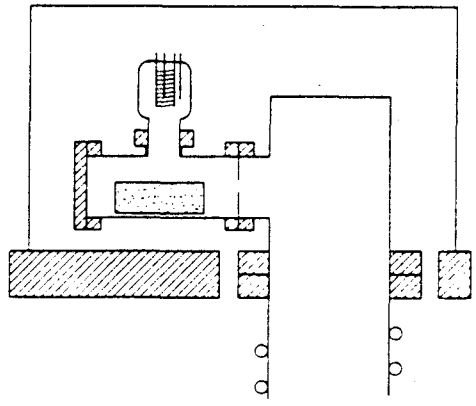

Figure 3. Modified Zabel apparatus used by Cross[2] and Grossart.[3]

where R is the universal gas constant; T is the absolute temperature; M is the molecular weight of the gas; r is the radius of the tube; l is the length of the tube in cgs units.

The Rutherford Laboratory apparatus uses an orifice plate having a circular hole (of approx. 3 mm dia) with chamfered edges. The plate was sealed between flanges with indium wire. The whole apparatus was constructed of stainless steel. The conductance was 1.0 l. s^{-1} calculated from the formula.

$$C = \frac{A}{1000}\sqrt{\left(\frac{RT}{2\pi M}\right)} \text{ l. s}^{-1}$$

where A is the area of the hole.

Since outgassing from the vessel walls contributes to the gas throughput it is necessary to conduct a blank run without the sample. The method of inserting the sample into the vessel has to be so controlled that blank runs are reproducible. For example, the time for which the interior of the vessel is exposed to the atmosphere between runs has to be kept reasonably constant.

Although the nature of the gases evolved from samples is not in general known, i.e., the gas will in general be a mixture of water vapour, hydrogen, carbon monoxide and other gases, in varying proportions, it is normal to calculate the conductance as though the gas were air or nitrogen. Likewise the sensitivity of ionization gauges is different for different gases and this will lead to a further error. If the gas is predominately water vapour as is the case for many unbaked materials, the value of conductance used will be in error by a factor equal to the ratio of the square roots of the molecular weights of air and water, i.e. 1.27. The sensitivity of ionization gauges for these two gases is about equal so the outgassing rate measured will be 21% too low. An extreme case is that of hydrogen. The ratio of the square roots of the molecular weight of hydrogen and air is 3.8 and the gauge sensitivity for hydrogen is about a factor of 2 lower than that for air so the combined effect is that the measured outgassing rate will be a factor of 7.6 too low.

Such errors can be avoided by the use of a residual gas analyser either instead of or in addition to the ionization gauges. However even if this instrument is not used the errors will not cause as much inconvenience as may be supposed especially if the results are expressed as air or nitrogen equivalents and the method of measurement stated. This is because the throughput method closely parallels the process that occurs when a vacuum system is pumped down from atmospheric pressure to high vacuum.

The outgassing rate is calculated from the pressure–time curve, i.e. the raw data as follows: the pressure readings obtained from the blank run are subtracted from the corresponding readings obtained from the sample run. Each difference is then multiplied by the conductance and divided by the surface area of the sample to obtain a series of outgassing rates corresponding to different pumping times. These are known as the 1 h ,10 h or 100 h outgassing rates etc.

Strictly the throughput is equal to the product of the conductance and the difference between the inlet and outlet pressures of the conductance.

$$Q = C(p_{in} - p_{out})$$

and both pressures are indeed measured by many workers.[4–12]

However in addition

$$Q = pS$$

where p is the pressure in the vessel; and S is the pumping speed out of the vessel

$$\text{also } \frac{1}{S} = \frac{1}{C} + \frac{1}{S_p}$$

where S_p is the speed of the pump

$$\text{hence } S = \frac{C}{1 + C/S_p}$$

$$\text{if } C \ll S_p \qquad \text{i.e. } S_p > 50C$$

$$S \simeq C$$

the error in ignoring p_{out} is negligible. This is the case when a 1 l. s^{-1} orifice is used in conjunction with a 2 in. diffusion pump. If the conductance is too small in relation to the surface area of the sample an error could be introduced due to readsorption of the gases evolved. Dayton[13] has examined this relationship and shows that readsorption becomes negligible when the area of the pumping orifice is greater than 100 times the product of the sample surface area and its sticking coefficient for the evolved gases. He states that in general this condition is met if the conductance is greater than a few tenths of 1 l. s^{-1} for several square centimetres of sample area. The apparatus he has used for measuring the outgassing rates of elastomers and vacuum waxes and greases is shown in Figure 4.

The sample area was about 100 cm^2 and the apparatus made of glass has a choice of two conductances selected by moving steel balls with a magnet. The conductances are 0.3 and 1.3 l. s^{-1}. These are sample to equivalent pumping areas of 4000:1 and 900:1. Dayton claims that for many materials there is no evidence of readsorption even with the smaller of these conductances.

Another source of error in outgassing measurements is the ionization gauge. The effect of gauge pumping and outgassing from the gauge has been investigated by Moraw.[14] A diagram of his apparatus is shown in Figure 5. The conductance could be switched between values of 0.09 and 1.5 l. s^{-1}. The sample vessel could be replaced with a needle valve so that pure gases H_2, CO, O_2 could be introduced and the effects on the two ionization gauges and the reisidual gas analyser noted. The difference of the peak heights obtained with the RGA before and after switching off the gauges was used to determine the true outgassing rate, by means of a computer programme. It was found that the ionization gauges (Balzers type IM 15) had a pumping speed for hydrogen of 0.12 l. s^{-1}, and zero for other gases when employing a thoriated iridium filament operated at 100 μA emission. With a tungsten filament operated at the same emission current, the pumping speed was 0.28 l. s^{-1}. It was also found that chemical reactions at these filaments considerably altered the residual gas composition.

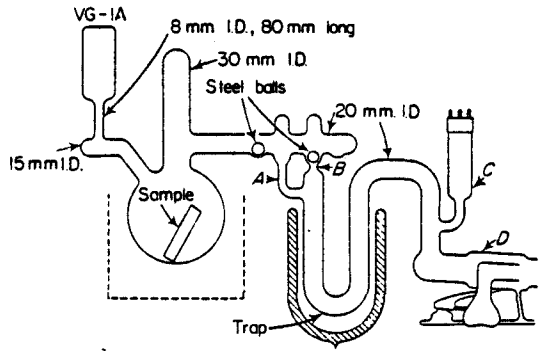

Figure 4. Apparatus used by Dayton.[13]

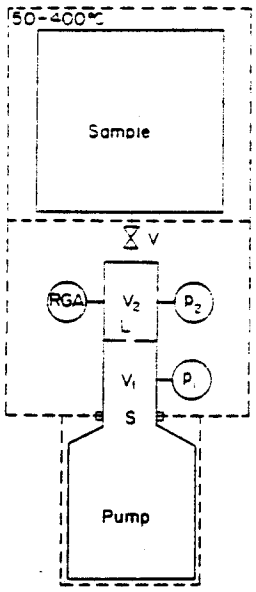

Figure 5. Apparatus used by Moraw.[14]

Using the gauge with thoriated iridium filament and measuring the outgassing rate of stainless steel after a 20 h bake at 100°C, with the 0.09 l. s^{-1} conductance, the measured outgassing rate was a factor of 2 low. For copper and aluminium the corresponding errors were 10 and 30%. Values of about 10^{-12} torr l. s^{-1} cm^{-2} were obtained for the 100°C baked stainless steel and copper and 4×10^{-14} torr l. s^{-1} cm^{-2} for aluminium. Using the 1.5 l. s^{-1} conductance the error was calculated to be less than 8% in all cases. It is noted that the corrected values using the small conductance agree well with those obtained using the larger conductance. It is also recommended that where the composition of the gases is unknown and a correction cannot therefore be made, a conductance of not less than 3 l. s^{-1} should be used.

Different workers have approached the problem of outgassing from the sample vessel in different ways. Zabel,[1] Dayton,[13] Cross,[2] Power and Robson,[7] Geller,[4] Blears[12] and Carter[10] conducted a blank run. Carter considered that since in his investigation of dry lubricants this involved finding the difference between values of the same order of magnitude, a considerable error could thus be introduced. He also expressed concern about the possibility of gas evolved from the sample being adsorbed on the walls of the apparatus.

Schram advocates the use of two similar vessels, one containing the sample and the other empty. Both are connected through conductances of equal size to the same pumping system. A diagram of this apparatus is shown in Figure 6. The outgassing rate of the sample is calculated from the difference between the pressures in the two chambers. Schram points out that a systematic error will occur due to the difference in desorption of the two vessels, and a small difference between the two conductances and a larger difference between the sensitivities of the two ionization gauges. This error can be determined by a blank run and a correction made for it in subsequent outgassing determinations. He has used conductances of 1 l. s^{-1}

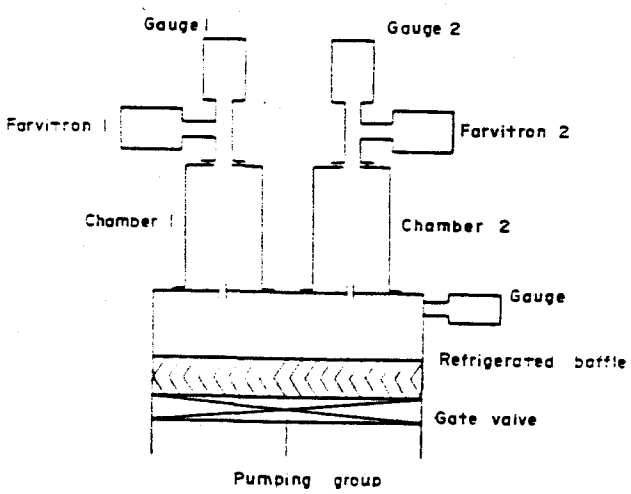

Figure 6. Apparatus with two sample chambers used by Schram.[9]

and sample areas of 1000 cm^2 to determine the outgassing rates of various metals, and also glass and elastomers. The results for the metals show a slope of 1 on a log–log plot and for the non-metals a slope of between 1.0 and 0.5.

Schittko[6] and Barton and Govier[15a] have designed their apparatus so that the sample chamber is never let up to atmospheric pressure. The sample is inserted into the chamber through a series of vacuum locks separated by valves and is pre-degassed in each successive lock. The Schittko apparatus,[16] was used to measure the outgassing rates of mainly elastomers and polymers and ceramics. Barton and Govier[15] have used their apparatus at the Culham Laboratory of the UKAEA to investigate different methods of preparation of stainless steel for vacuum use. It includes provision for baking samples and examining the evolved gases with a residual gas analyser.

Calder and Lewin,[11] Young[17] and Moraw[14] have investigated the very low outgassing of baked metals. They avoided the necessity and uncertainty of blank runs by making the sample the vessel itself and baking it *in-situ*. Their apparatuses are shown in Figures 7, 8 and 5 respectively. Calder and Lewin used an omegatron to measure the pressure on both sides of the conductance (0.1 l. s^{-1}), alternatively, by means of a system of bakeable valves. The sample surface area was 1000 cm^2. Young used a conductance of 4.4 l. s^{-1} and a sample area of 2500 cm^2. The evolved gases were examined on a separate apparatus with a monopole partial pressure gauge during a second experiment.

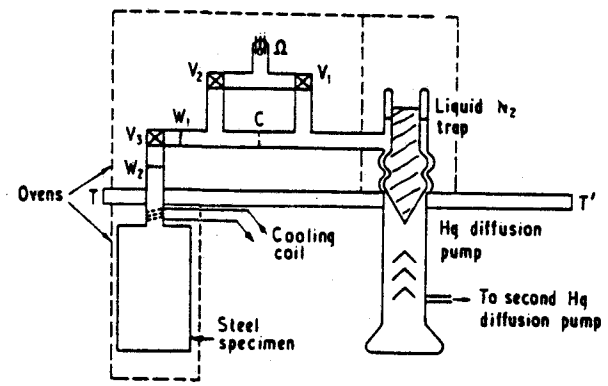

Figure 7. Apparatus where sample forms the test chamber used by Calder and Lewin.[11]

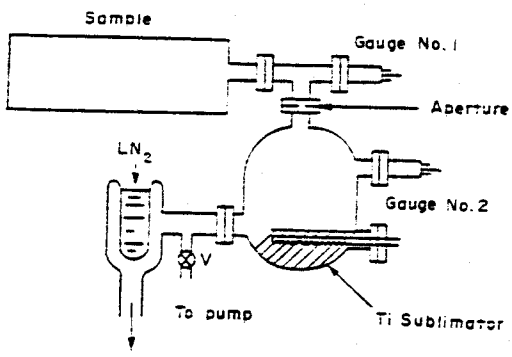

Figure 8. Apparatus used by Young.[17]

The outgassing rate for 300 series stainless steel baked for 30 h at 250°C (2–3 × 10^{-12} torr l. s^{-1} cm^{-2}) was in good agreement with that found by Calder and Lewin (3 × 10^{-12}) for stainless steel baked for 25 h at 300°C. Young also found very low outgassing rates for aluminium baked for 15 h at 250°C (4 × 10^{-13} torr l. s^{-1} cm^{-2}). Moraw has found similar outgassing rates for these metals after a 20 h bake at 100°C.

The American Vacuum Society draft standard AVS 9.1–1964 Reporting of Outgassing Data states:

'4.4.2 *Background Outgassing Rate.* In those experiments involving a sample material in a system, the background outgassing rate must be small relative to the sample outgassing rate. Information substantiating this should be supplied and may include comparative pressure–time data with the empty system and with the sample in place'.

3.2 Throughput method with variable conductance. By using a variable conductance in the throughput method in a similar way to that described by Oatley[18] for the measurement of pumping speed, it is possible to retain the accuracy of the small fixed conductance but with a much larger conductance. Thus the conditions of measurement more closely approach those of an actual vacuum system. This is the method described in Henry.[8a] Referring to Figures 9 and 10

$$\frac{1}{S} = \frac{1}{S_p} + \frac{1}{C}$$

where S is the effective pump speed at the sample vessel; C is the conductance; S_p is the speed of the pump.

Also $$Q = S.p_1 = S_p p_2$$

Then $$\frac{1}{S} = \frac{p_1}{Q}$$

and $$\frac{p_1}{Q} = \frac{1}{S_p} + \frac{1}{C}.$$

Assuming that Q and S_p are constant during the time it takes to vary the conductance (to this end a fixed conductance has to be used until the pressure has ceased to fall quickly) if C is varied, p_1 can be plotted against $1/C$ and a straight line will be obtained (Figure 10): the intercept of this line with the x-axis is equal to $-1/S_p$ and the intercept on the y axis is equal to Q/S_p. From the measurements of these two intercepts, Q may be calculated.

Henry[8b] describes a new apparatus (Figure 11) which uses this method. The variable conductance is shown in detail in

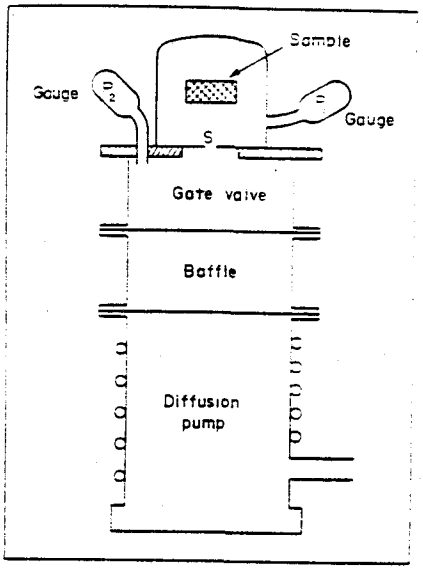

Figure 9. Apparatus with variable conductance to determine Q by Oatley method.[5]

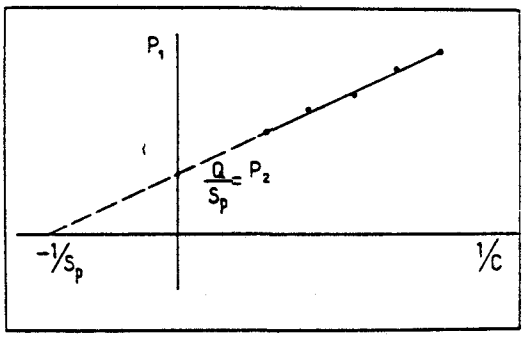

Figure 10. Plot of p_1 against $1/c$ used in Oatley method to determine Q.[5]

Figure 12. It is constructed from a variable stop designed for an aerial photography camera. The conductance can be varied between 3.5 and 173 l. s^{-1}.

3.3 Pressure-rate-of-rise method. When a vacuum system during pump-down at a constant temperature is suddenly isolated from the pumps, the pressure within the system will begin to rise. The rate of rise will be highest at the instant of isolation and will gradually decrease to zero when the outgassing rate and surface readsorption rate balance each other. The outgassing rate of the material in a system at the time of isolation will usually be proportional to this initial instantaneous rate of rise of pressure. Pump-down is then continued by opening the system to the pumps before the instantaneous outgassing rate will have changed appreciably due to readsorption of gas. This cycle is repeated at suitable intervals in order to obtain sufficient data to plot outgassing rate as a function of pumpdown time. During this cycling for some materials the effect of sorption on the sample or the system may influence the results.

$$\text{Outgassing rate} = \frac{\text{rate of pressure rise} \times \text{volume of vessel}}{\text{area of sample}}.$$

Care has to be taken that the gauge used to measure the pressure rise does not influence the result, i.e. it must be a gauge with a very low pumping speed.

Beckmann[19] has used this method to measure the outgassing rates of various rubbers. His pressure rise measurements were in the 10^{-3} torr pressure range and were made with a capacitor-diaphragm vacuum gauge (Type Atlas M M M). This gauge has a working range of 10^{-1}–10^{-4} torr with an accuracy of $\pm 1\%$, has the advantage of zero pumping speed and is independent of the nature of the gas measured. To obtain consistent results the samples measured were 'climatized' at 20°C and 60% relative humidity for 1 week before being introduced into the apparatus.

The apparatus is shown in Figure 13. The surface area of the samples was 25 cm^2 and the volume of the vessel 250 cm^3. The outgassing rate for Teflon determined by this method: 8–10 $\times$ 10^{-8} torr l. s^{-1} cm^{-2} at 9 h compares with the result obtained by Schittko[6] using the throughput method: 5 $\times$ 10^{-8} torr l. s^{-1} cm^{-2}. At 1 h, the corresponding figures are 3–8 $\times$ 10^{-7} and 2 $\times$ 10^{-7}. For silicone rubber at 1 h the corresponding figures are 4–9 $\times$ 10^{-6} and 8 $\times$ 10^{-6}. This demonstrates that for some materials the rate of rise method gives comparable results to the throughput method. The rate of rise method can be more convenient than the throughput method for materials of very high outgassing rate. Beckmann has found by this method that many polymers have outgassing rates which have a slope of -0.5 on a log K $-$log t plot.

Barton and Govier[15b] have examined the rate of rise of various evolved gases H_2, CO, H_2O and CO_2 on isolation of a stainless steel system from its pumps using a 60° sector mass spectrometer and found that the rate of rise of all these gases reduced after the first 10 s. The rate of rise of H_2O and CO_2 then became insignificant but those of H_2 and CO were about equal, at least for the next minute.

Elsey *et al*[20] studied the rate of rise of gases in an isolated stainless steel volume and also a similar titanium volume. These volumes were pumped to a high vacuum and baked for 16 h at 120°C. It was found that the only gas to continue to rise significantly in pressure for long periods was H_2. The apparatus is shown in Figure 14. The vessel A of volume 0.4 l. and internal surface area 460 cm^2 for the stainless steel vessel and 189 cm^2 for the titanium vessel was isolated for periods of up to 3 months. It was found that the rate of pressure rise of hydrogen did not vary significantly during that time even though the pressure in the vessel rose to 5 $\times$ 10^{-2} torr. To avoid interaction between the gas in the vessel and a gauge, no gauge was fitted to the vessel, which was connected to the vacuum system by a bakeable leak valve. The pumping system consisted of a liquid N_2 trapped diffusion pump charged with Convalex 10 pump oil and backed by a second diffusion pump and rotary pump. It provided an ultimate pressure of 10^{-10} torr. The connection from the leak valve led directly to the ion source of an MS10 180° mass spectrometer mounted above the pump. The effective pumping speed for hydrogen at the mass spectrometer was calculated from the dimensions of the tubing and the speed of the pump. It was approximately 20 l. s^{-1}.

The quantity of gas that had accumulated in the closed vessel was measured in the following way. The mass spectrometer was tuned to H_2 and set to an appropriate measuring range (determined by previous results). A chart recorder was started and the leak valve was quickly opened to obtain a peak reading on the chart. The leak valve once opened was left at the

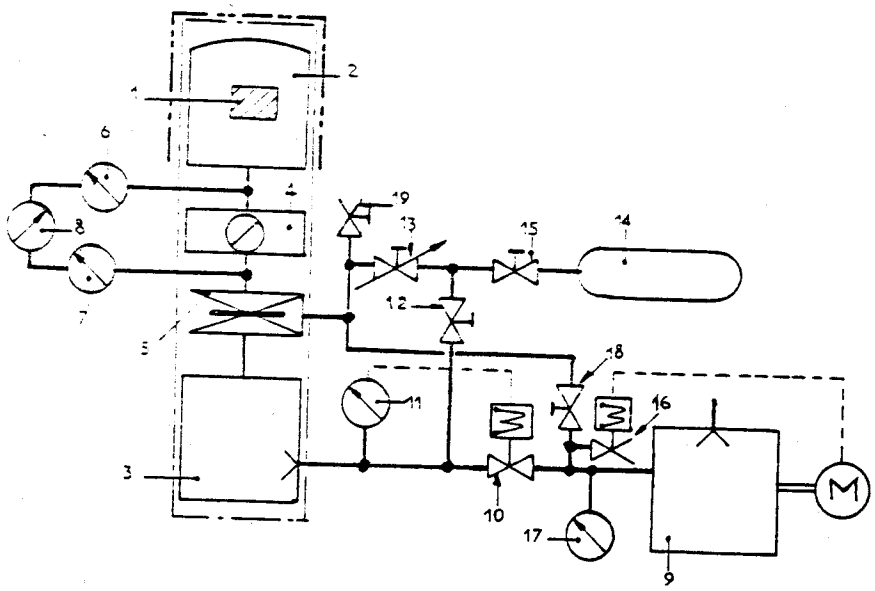

Figure 11. Apparatus with variable conductance used by Henry.[8]

same setting. The reading on the recorder then decayed exponentially. After the reading had decayed to 10% of its original reading the leak valve was closed. The peak partial pressure and the exponential decay time constant were then determined from the recording and the various parameters of the system. If G is the outgassing rate of the surfaces in the test vessel (see Figure 15):

V_2 is the volume of the test vessel;
p_2 is the pressure in the vessel;
S_2 is the pumping speed at the leak valve;
p_1 is the pressure at the mass spectrometer;
S_1 is the pumping speed at the mass spectrometer

$S_1 \gg S_2$.

If the test vessel is isolated for time t, then

$$p_2 = \frac{G.t}{V_2}. \tag{1}$$

When the leak valve is opened

$$\frac{p_1}{p_2} = \frac{S_2}{S_1}. \tag{2}$$

From (1) and (2)

$$p_1 = \frac{G.t.S_2}{V_2 S_1}.$$

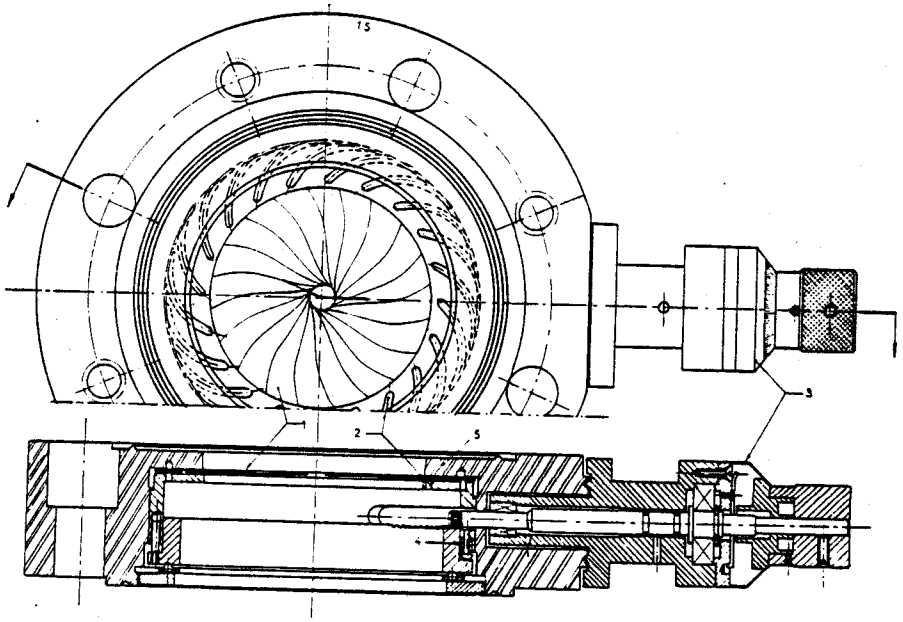

Figure 12. Variable conductance used in Henry apparatus.[8]

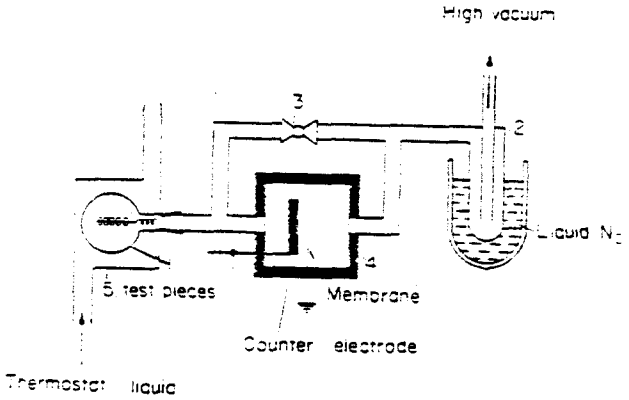

Figure 13. Rate of pressure rise apparatus used by Beckman.[19]

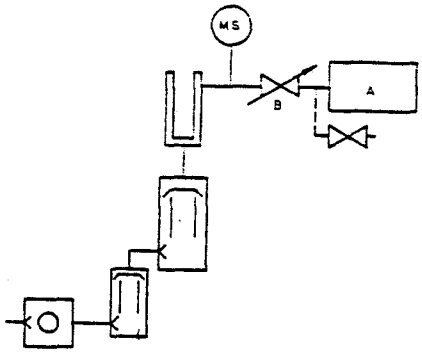

Figure 14. Apparatus to determine long term rate of pressure rise used by Elsey.

If τ is the time for p_1 to decay to $1/e$ of its original value

$$\frac{S_2}{V_2} = \frac{1}{\tau}$$

Then $$p_1 = \frac{G.t}{\tau S_1}$$

and $$G = \frac{p_1 S_1 \tau}{t}.$$

The outgassing rate for the stainless steel under these conditions was found to be 5×10^{-12} torr l. s^{-1} cm^{-2} and for titanium 3×10^{-12} torr l. s^{-1} cm^{-2}. PTFE after air baking

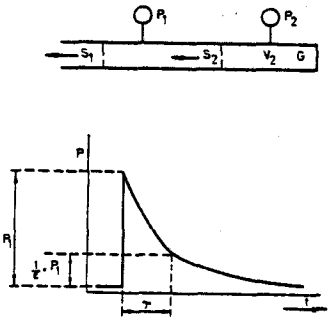

Figure 15. Recording of partial pressure on opening valve B. Used in Elsey method.

was found by the same method to have an outgassing rate of 2.5×10^{-11} torr l. s^{-1} cm^{-2}.

These tests were carried out to find suitable materials for the construction of a pressure modulated radiometer for the Nimbus F satellite. Such a radiometer is a sealed vessel of 150 cm^3 volume containing CO_2 at about 1 torr pressure. After pumping to ultra-high vacuum the vessel is filled to the required pressure with pure CO_2 and crimped off from the pump. It then is required to have a life of 2 years without significant contamination of the gas. With a measured outgassing rate of the vessel and contents of $\sim 10^{-9}$ torr l. s^{-1} it was calculated that the partial pressure of H_2 would rise to 10^{-2} torr in 2 years.

3.4 Collection method. In the collection method for determining the quantity of gas leaving a material the evolved gases are transferred by a mercury diffusion pump to a calibrated volume. The evolved gas quantity is then determined by the increased pressure in the calibrated volume at the end of an outgassing period which may vary from several minutes to many hours. The collection method for measuring outgassing has two principal disadvantages

(1) Only the total quantity of evolved gas over relatively long periods can be determined.

(2) The method is not capable of following the dynamic process.

The only mention the author has found of this method is by Henry[8b] where he uses such a collection volume for the purpose of subsequent analytical examination of the evolved gases.

3.5 Mass-loss or weight-loss method. The weight loss method has been used extensively for the measurement of the outgassing of materials and components used in space satellites. These materials include plastics, paints and rubbers and are in general too gassy to be used in high vacuum systems. The method consists of suspending the sample from a sensitive balance; the sample and the balance both being contained in a vacuum of about 10^{-5} torr. The weight of the sample is continuously recorded and the rate of weight loss can be calculated. The method is convenient for studying the effect of heat and ultra-violet light on plastics.

Podlaseck[21] has described an apparatus using an Ainsworth balance, built under a NASA contract for testing space-craft materials. The apparatus is shown in Figure 16. The samples could be heated to 230°C in the vacuum tube by radiation heating. Fulk and Horr[22] have used a similar method. The balance could measure to a precision of 0.0005 g. They have given results for many organic materials. The total weight of the sample varied from 3 to 50 g and the weight loss from 0.5 mg to 0.1 g. Their tables of results list the pumping time required to reach a constant rate of weight loss, the weight loss rate once this state has been reached and the weight loss up to the time of reaching this state.

The results do not compare well with the other methods. For example, for silicone rubber, Fulk and Horr show an outgassing rate of 3×10^{-5} g cm^{-2} h^{-1} reached after 68 h. This rate is equivalent to 10^{-5} torr l. cm^{-2} s^{-1} whereas Schittko[6] shows a rate of 8×10^{-6} torr l. cm^{-2} s^{-1} reached after 1 h.

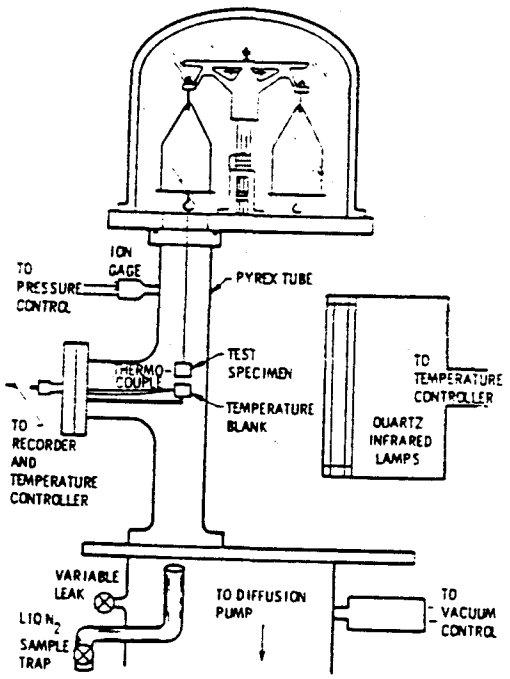

Figure 16. Apparatus used by Podlaseck[21] to determine weight loss in vacuum.

4. Outgassing rates of unbaked stainless steel after various cleaning methods

Barton and Govier[15] have investigated the effect of various cleaning methods on the outgassing rate of stainless steel. The sample tested was a cylinder of 18/9/1 stainless steel 16 cm dia and 75 cm long.

Initially the internal surface was honed and vapour degreased in trichloroethylene. It was then baked in a vacuum at 450°C to remove initial contamination. After exposing the sample to air for 24 h it was repumped for 48 h. Figure 17 shows its outgassing rate as curve (a). The outgassing rate at 48 h was 1.7×10^{-11} torr l. s^{-1} cm^{-2}. This result was used as a standard by which to judge the effect of various treatments. In order to judge the effect of vapour degreasing with trichloroethylene, the sample was removed from the apparatus and vapour degreased in a trichloroethylene vapour bath.

The sample was then re-evacuated and it produced outgassing rate curve (b) in Figure 17. It is slightly lower than curve (a), i.e. 1.5×10^{-11} torr l. s^{-1} cm^{-2}, at 48 h but it did show a

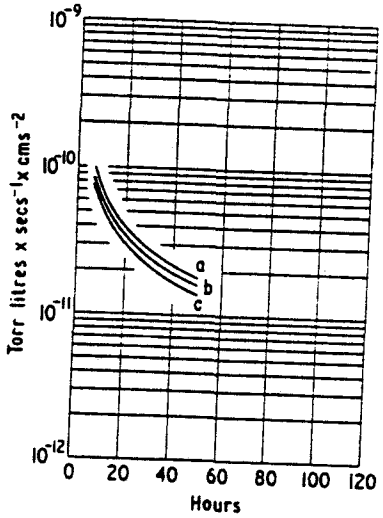

a. Honed sample following bake in vacuo at 450°C & exposed to air. (Sample 1 Exp 2)
b. Sample exposed to air & vapour degreased. (Sample 1 Exp 3)
c. Sample following smearing with cutting oil & vapour degreasing. (Sample 1 Exp 4)

Figure 17

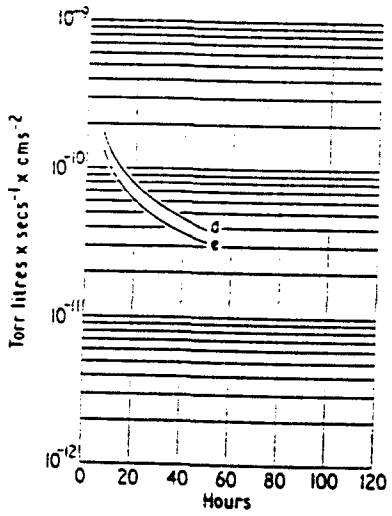

d. Sample honed & degreased (Sample 2, Exp. 5)
e. Sample machined & degreased (Sample 2, Exp. 9)

Figure 18

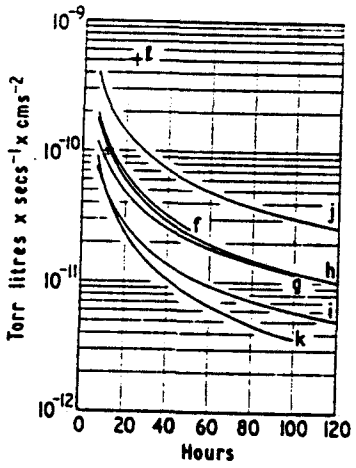

f. Sample electro polished only. (Sample 5 Exp 12)
g. Vapour degreased following Exp 12. (Sample 5 Exp 13)
h. Sample washed in demineralised water. (Sample 5 Exp 14)
i. Baked in air at 500°C following Exp 14. (Sample 5 Exp 15)
j. New sample cleaned by Diversey process. (Sample 6 Exp 17)
k. New sample machined degreased & contaminated with lard oil, then plasma cleaned. (Sample 8 Exp 23)
l. New sample contaminated with lard oil, no cleaning. (Sample 9 Exp 30)

Figure 19

Figures 17–19. Outgassing rates of 18/9/1 stainless steel after various treatments (from Barton and Govier 1970).

trace of trichloroethylene in the mass spectrometer scan. The major gases were H_2O, CO and CO_2. The sample was then removed and deliberately contaminated with machine oil. It was then vapour degreased as before and the outgassing test repeated. This time curve (c) in Figure 17 was obtained. The outgassing rate at 48 h was 1.3 × 10^{-11} torr l. s^{-1} cm^{-2}. In fact none of the curves (a), (b) or (c) was significantly different. The slight difference reflected the total pumping time of the sample. Barton and Govier concluded that vapour degreasing in trichloroethylene was completely effective. Tests were then carried out on a different sample which was honed and degreased but not vacuum baked. This followed curve (d) Figure 18 with an outgassing rate of 4 × 10^{-11} torr l. s^{-1} cm^{-2} after 48 h. This sample was then re-machined to a fine machine finish, degreased and the test repeated—curve (e) Figure 18 with a 48 h rate slightly improved at 3 × 10^{-11} l. s^{-1} cm^{-2}.

There followed tests to study the effect of (Figure 19):

Electro polishing—48 h rate 2.5 × 10^{-11} torr l. s^{-1} cm^{-2}.

Baking in air—48 h rate 1.0 × 10^{-11} torr l. s^{-1} cm^{-2}.

Diversey chemical cleaning—48 h rate 6 × 10^{-11} torr l. s^{-1} cm^{-2}

Plasma torch cleaning—48 h rate 8 × 10^{-12} torr l. s^{-1} cm^{-2}.

Vapour blasting with glass balls—48 h rate 3 × 10^{-11} torr l. s^{-1} cm^{-2}.

Except for the plasma torch cleaning none of the methods which did not involve baking at some stage produced a significant improvement. The plasma torch method was tedious for large areas but would merit further investigation. Air baking can produce lower outgassing rates if followed by a 250°C bake *in situ*. This outgassing rate of 3 × 10^{-11} torr l. s^{-1} cm^{-2} for vapour degreased unbaked stainless steel is a considerable improvement on 10 h rates of 2 × 10^{-8} torr l. s^{-1} cm^{-2} found by Blears and by Geller. However, the older work did not specify the method of cleaning the sample nor was it carried out under ultra high vacuum conditions. In some earlier work Barton and Govier[15b] showed that no improvement over standard machining methods could be obtained by machining with a clean dry tool and using no lubricants. In fact when this was done the outgassing rate obtained was a factor of three higher.

Earlier work by Roussel and Thibault[23] showed that unbaked electro-polished stainless steel reached an outgassing rate of 1 × 10^{-11} torr l. s^{-1} cm^{-2} after 50 h while Schram measured a rate of 5 × 10^{-11} for the same conditions. Amoignon and Couilland[14] have measured a 50 h outgassing rate of 2 × 10^{-11} torr l. s^{-1} cm^{-2} for stainless steel vapour blasted with glass balls.

5. The effect of different treatments in conjunction with a medium temperature vacuum bake

With a large system it is often considerably easier to bake the system to 100 or 200°C than it is to bake it to 400°C. Young[17] has investigated different treatments for 304 stainless steel. The sample tested was a cylinder of 4 mm wall thickness. It was 15 cm dia and 45 cm long.

After surface treatment the samples were baked on the outgassing measurement equipment and the outgassing rate was measured after a further 24 h of pumping at room temperature. The lowest rate recorded was 3 × 10^{-13} torr l. s^{-1} cm^{-2}. This was for stainless steel cleaned by glass bead blasting and baked in air for 61 h at 450°C followed by a 15 h vacuum bake at 250°C. To determine if the surface layer of oxide formed a barrier to the diffusion of gas from the interior of the metal, Young glass-bead blasted the surface to remove the oxide and repumped the sample with an additional 15 h vacuum bake at 280°C. The same outgassing rate was measured. It would appear that the baked stainless steel is not recontaminated easily and once it has been well degassed a low temperature bake is sufficient. Young found that electro-polished stainless steel when baked for 30 h in a vacuum at 250°C had an outgassing rate of 2 × 10^{-12} torr l. s^{-1} cm^{-2} after 24 h of room temperature pumping. The same result was found for stainless steel shot blasted with glass balls. The method of shot blasting with high velocity glass balls is useful for removing stains and oxide and leaves a matt finish. Young found no evidence to suggest that the very smooth surface produced by electro-polishing is an advantage. For comparison with high temperature baking, Young vacuum baked a sample of the same stainless steel to 450°C for 17 h. After cooling and pumping for 24 h an outgassing rate of 4 × 10^{-13} torr l. s^{-1} cm^{-2} was obtained.

Stainless steel has for many years been considered the best metal for the construction of vacuum vessels and components. In contrast, aluminium has been considered a rather poor metal for this purpose. It has a reputation as a porous gas-filled material.[25] Aluminium has a lower hydrogen solubility than other common metals, and has a low diffusion coefficient at room temperature. Aluminium is more difficult to weld than stainless steel but techniques for producing satisfactory leak tight welds are available. Vacuum cast aluminium has good properties for vacuum vessels. Also the electron storage rings at Stanford SPEAR are constructed of rectangular cross section tube extruded from aluminium. It is difficult to make bakeable all-metal leak tight seals between aluminium flanges. This problem has been solved at Stanford by explosion-bonding aluminium to stainless steel and making the flanges from this material. The aluminium part of the sandwich is welded to the aluminium tube. Young has measured an outgassing rate of 4 × 10^{-13} torr l. s^{-1} cm^{-2} for type 1100 aluminium which was cleaned with detergent, rinsed in acetone and baked for 15 h in vacuum at 250°C. At Stanford the aluminium vessels are baked in vacuum ovens before assembly and not baked *in situ*. Clean-up is achieved during operation of the electron beam.

6. Vacuum baking of stainless steel

Stainless steel contains large amounts of hydrogen. The hydrogen dissolves in the metal during manufacture. It was shown in Part I that after the initial removal of surface gas the ultimate pressure will be controlled by diffusion from the bulk. It was also shown that the rate of desorption was proportional to the initial gas concentration and to the square root of the diffusion coefficient, i.e.

$$q_t = C_0 D^{1/2} (\pi t)^{-1/2}$$

In stainless steel at room temperature, D is high enough for diffusion of hydrogen to limit the pressure attainable and yet low enough to prevent the concentration of the gas in the metal being significantly depleted in a reasonable time. D varies exponentially with temperature so to improve the vacuum either D can be lowered, e.g. drastically by immersing the metal in liquid helium[26] or the gas concentration in the metal can be

depleted more quickly by raising the metal to a high temperature.

e.g. D_{300} (H_2 stainless steel) = 3.5×10^{-8} cm^2 s^{-1}

and D_{1000} (H_2 stainless steel) = 8.7×10^{-5} cm^2 s^{-1}.

Since for onset of rapid depletion of C, $Dt/d^2 > 0.025$ a 1 h bake at 1000°C is as effective as 2500 h at 300°C. The following table[11] gives the effectiveness of intermediate temperatures, giving the theoretical time to reach an outgassing rate of 10^{-16} torr l. s^{-1} cm^{-2} for 2 mm thick stainless steel with

$C_0 = 0.3$ torr l. cm^{-3} of H_2

t (s)	D (cm^2 s^{-1})	T(°C)
1.0×10^6 (11 days)	3.5×10^{-8}	300
8.6×10^4 (24 h)	3.8×10^{-7}	420
1.1×10^4 (3 h)	3.0×10^{-6}	570
3.6×10^3 (1 h)	9.0×10^{-6}	635

The bakeout may be performed *in situ* or in a vacuum oven followed by a short low temperature bakeout *in situ*. *In situ* bakeouts at 420°C are feasible and taking permeability of atmospheric hydrogen into account a 24 h *in situ* vacuum bake should result in an outgassing rate of 4.2×10^{-17} torr l. s^{-1} cm^{-2}. Baking *in situ* to a higher temperature would not decrease the ultimate outgassing rate attainable. It would only reduce the time necessary for baking. This is due to increased permeability at higher temperatures.

Components can be baked in a vacuum furnace to temperatures of 1000°C. Providing the hydrogen partial pressure is as low as 10^{-4} torr, which is a moderate demand for a furnace, outgassing rates similar to the above can be achieved after a short *in situ* bake at 250°C to remove surface adsorbed gases. Calder and Lewin[11] investigated many different baking schedules at the CERN ISR Laboratories. Tables 1–3 show some of their results.

A specimen of U15 BM stainless steel baked for 3 h at 1000°C at a pressure of 2×10^{-6} torr was welded on to the measurement apparatus and pumped and baked for 72 h at 200°C. After cooling to 20°C an outgassing rate for hydrogen of 1.0×10^{-14} torr l. s^{-1} cm^{-2} was measured. No other gases were detected. It is believed at the CERN ISR Laboratory that baking all stainless steel components at 1000°C in a vacuum will allow the cleaning of components to be simplified to standard degreasing. Currently a furnace 3.5 m long by 1 m dia is installed. It will enable vacuum baking at 1000°C and 10^{-6} torr. It is intended to develop this technique to allow baking at 10^{-8} torr.

7. Reductions of outgassing by glow-discharge cleaning

Using a glow discharge has for many years been a technique in thin film technology for cleaning substrates. Holland[27] has given a description of the technique and its effects on glass substrates, including the improved adhesion of thin films. The use of glow discharges for cleaning vacuum vessels is relatively new. When used successfully it removes the necessity for high temperature baking.

Govier and McCracken[28] have investigated the effects of noble gas glow discharges on the outgassing properties of stainless steel. Their object was to enable a reduction of the contamination of plasmas due to the desorption of gases from the walls of their containment vessels. Their apparatus is shown in Figure 20. The vessel in which the glow discharge was carried out was a cylinder of EN58B stainless steel 15.7 cm dia and 75 cm long. It had an axial stainless steel electrode. A continuous flow method of gas inlet was used whereby the gas was let into the cylinder via a liquid nitrogen trap to remove water

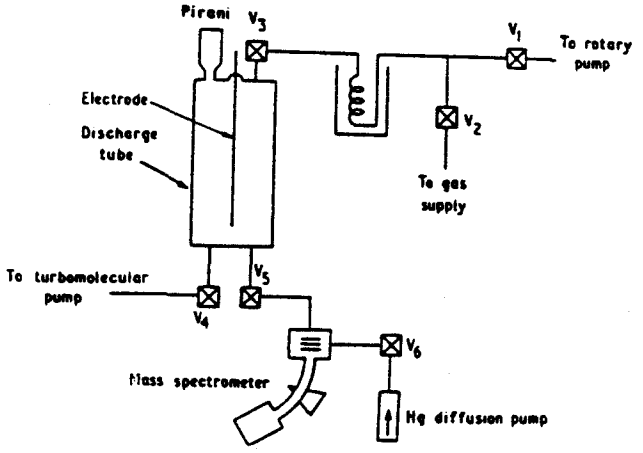

Figure 20. Apparatus for investigation of glow discharge cleaning (from Govier and McCracken[28] 1970).

Table 1. Outgassing rates of 300 series stainless steel (from Calder and Lewin[11])

Specimen A: outgassing rates (torr l. cm^{-2} s^{-1})

Specimen preparation	Measurement temperature (°C)	H_2	H_2O	CO–N_2	O_2	CO_2
Degassed several times—total of 45 h at 360°C	24	$\{1.3^{-12*}\}$ 2.6^{-12} 2.3^{-12}	—	—	—	—
	100	2.1^{-11}	—	$[4.7^{-15}]$	—	2.5^{-13}
	0	1.3^{-12}	—	—	—	—
Exposed to atmosphere for 3 h. Pumped under vacuum for 40 h	19	2.7^{-12}	6.4^{-12}	1.9^{-12}	2.2^{-12}	1.2^{-12}
Pumped under vacuum for further 4 days at room temperature	19	2.6^{-12}	1.0^{-12}	6.4^{-13}	8.4^{-14}	3.6^{-12}
Baked at 360°C for 24 h	19	9.9^{-13}	—	$[2.6^{-15}$	—	—

* The superscripts denote the power of ten by which the numbers should be multiplied.

Table 2. Outgassing rates of 300 series stainless steel (from Calder and Lewin[11])

Specimen B: outgassing rates (torr l. cm^{-2} s^{-1})

Specimen preparation	Measurement temperature (°C)	H_2	H_2O	CO–N_2	O_2	CO_2
Baked under vacuum for 25 h at 300°C	20	3.9^{-12}*	—	1.7^{-14}	—	1.9^{-14}
	20	4.5^{-12}	—	—	—	2.0^{-14}
	20	(2.6^{-12})	—	6.1^{-14}	—	1.5^{-14}
Temperature of specimen raised	40	1.3^{-11}			—	
	100	2.1^{-10}	1.0^{-13}	4.7^{-13}	1.8^{-12}	1.7^{-12}
Baked under vacuum for 25 h at 300°C	20	3.0^{-12}	—		—	1.7^{-14}
	20	3.0^{-12}				
	20	3.0^{-12}				
	20	2.8^{-12}	—	$[8.6^{-15}]$	—	1.1^{-14}
Temperature of specimen raised	35	5.6^{-12}	$[7.8^{-15}]$	(---)	—	2.5^{-14}
	53	1.6^{-11}	$[6.4^{-15}]$	(---)	—	3.3^{-14}
	75	4.4^{-11}	4.6^{-14}	—	—	5.8^{-14}
Baked under vacuum for 25 h at 300°C	20	1.5^{-12}				
	20	1.5^{-12}	(---)	(1.6^{-13})	—	(---)
	20	1.4^{-12}	—	—	—	—
Temperature of specimen raised	47	5.3^{-12}	—	$[5.2^{-15}]$	—	$[1.7^{-15}]$
	72	1.5^{-11}	—	2.8^{-14}	—	$[5.4^{-15}]$
	105	3.9^{-11}	—	6.3^{-14}	—	$[8.7^{-15}]$
	145	9.2^{-11}	3.1^{-13}	1.4^{-13}	—	1.0^{-14}
	200	2.5^{-10}	6.1^{-13}	2.6^{-13}	—	3.6^{-14}
Baked under vacuum for 25 h at 300°C	20	1.1^{-12}	—		—	—
	20	1.2^{-12}	—	$[4.3^{-15}]$	—	—

* The superscripts denote the power of ten by which the numbers should be multiplied.

Table 3. Outgassing rates of 300 series stainless steel (from Calder and Lewin[11])

Specimen C: outgassing rates (torr l. cm^{-2} s^{-1})*

Specimen preparation	Measurement temperature (°C)	H_2	H_2O	CO–N_2	O_2	CO_2
Degassed at 1000°C for 3 h in a vacuum furnace, then *in situ* bake at 360°C for 25 h	20	1.3^{-14}†	—	1.0^{-14}	—	1.9^{-15}
	20	$\{6.9^{-15}\}$	—	1.2^{-15}	—	1.9^{-15}
	20	1.3^{-14}	—	(---)	—	$[4^{-16}]$
Raise temperature of specimen	100	1.2^{-14}	—	2.1^{-14}	—	2.3^{-15}
Baked for 72 h at 200°C under vacuum	20	1.0^{-14}	—	—	—	—
Raise temperature of specimen	100	8.7^{-15}	—	(---)	—	—
	200	1.9^{-14}	—	3.1^{-14}	—	—

* Not corrected for outgassing of untreated area.
† The superscripts denote the power of ten by which the number should be multiplied.

vapour and pumped by a turbo-molecular pump. So that the cylinder had a known history it was first baked under vacuum at 450°C for 20 h and then exposed to atmosphere for 30 min. It was re-evacuated to 10^{-7} torr, the pressure of the gas was adjusted and the glow discharge struck. Voltages used varied from 200 to 600 V and were adjusted to give a current of 500 mA. Pressures varied from 0.025 to 0.1 torr. After 30 min the gas inlet valve was closed and the gas pumped away. The partial pressures of the different residual gases were then measured as a function of time.

Figure 21 shows the curves obtained. Log pressure is plotted against time (hours). Figure 21a shows the normal outgassing of the cylinder without any discharge. It shows H_2O the dominant species with CO_2 next and then equal quantities of CO and H_2. Figure 21b shows the effect of a glow discharge in 0.050 torr of helium. The most noticeable effect is that the heavier gases have nearly disappeared and helium has become the major outgassing species. Also the hydrogen outgassing rate has increased. The total outgassing rate has remained nearly constant. However the scattering effect of helium on a beam of electrons, for example, is far less than that of carbon monoxide at the same pressure. A similar result is obtained for neon Figure 21c and for argon Figure 21d.

It is noticeable from Figures 21d and 21e that the glow discharge at 0.025 torr is much more effective in removing water vapour than the discharge at 0.1 torr. The effect of pressure is explained by the greater abundance of high energy ions present in the discharge at the lower pressure. McCracken substantiated this by measuring the energy spectrum of the ions in the discharge using a retarding potential technique.

Other effects noticed were that it made no difference if the current was alternating or dc, or if the gas was static or in dynamic equilibrium with the pump. McCracken noticed that the greater the reduction of water vapour outgassing the higher the resulting hydrogen outgassing. If a glow discharge in hydrogen was used no reduction of water vapour occurred. Also when a discharge in deuterium was tried much of the H_2O was changed to D_2O. It is believed that the D_2O is produced by

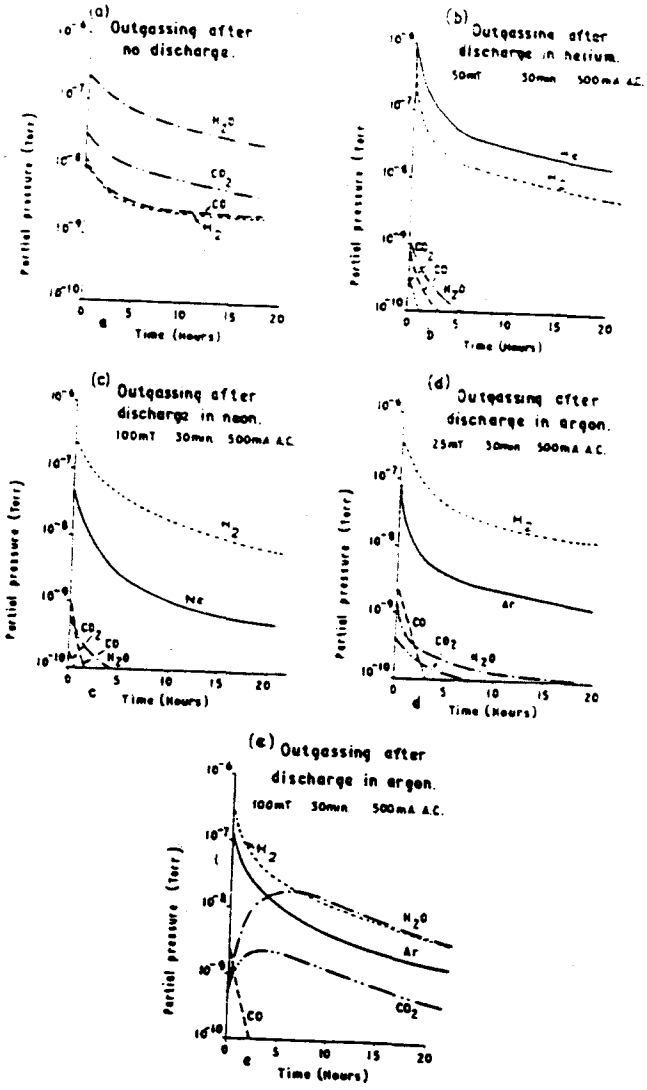

Figure 21. System partial pressures measured as a function of time immediately after discharge. Pumping speed 13 l. s^{-1} for nitrogen (from Govier and McCracken[28]).

interaction of the deterium ions and metal oxides on the surface although an exchange reaction could have occurred with H_2O molecules adsorbed on the surface or in the plasma.

The main result of the work is to show that it is feasible to use glow discharge cleaning to remove the normal residual gases from a vacuum system at the expense of replacing them with the helium and argon used for producing the discharge. These noble gases however are more readily removed with a mild bake.

The use of glow discharge cleaning in conjunction with 300°C vacuum baking has been tested at CERN for the purpose of preventing 'pressure bumps' in the ISR. Jones[29] reports the results of tests carried out in a 14 m length of a typical ISR vacuum vessel. The effect of the discharge cleaning was measured by its ability to reduce the efficiency (molecules per electron) of electron induced desorption. A probe consisting of a heated filament biased to a few hundred volts was used to give the surface of the vessel a pulse of bombarding electrons operating at a current density of 10 μA cm^{-2}. The number of molecules desorbed was determined from the resulting pressure rise and the known speed of the pumps. Because it was not possible for the discharge to spread further than 1 m from the high voltage electrode it was possible by having two probes to make a direct comparison between a treated and an untreated portion of the vacuum vessel.

The discharge of 0.5A at approximately 500 V was operated in argon at about 0.03 torr. The vessel was earthed and the high voltage electrode was powered by an ac supply. The discharge was operated intermittently during a 15 h bake at 300°C. Three 1 h periods of discharge were used separated by 3 h periods with the gas supply cut off. The first test with the electron probe was carried out 20 h after the bake-out at a pressure of 1.8 10^{-10} torr. The electron desorption efficiency of the treated portion of the vessel was an order of magnitude lower than that of the untreated portion. A further test of the condition of the surfaces was to compare the treated and untreated portions after each had been further outgassed by electron bombardment. The EID efficiency of the treated portion was further lowered by another order of magnitude while the untreated portion was only lowered by 40%. It is interesting that the low EID efficiency of the treated portion persisted even after the vessel was exposed to the atmosphere for 24 h and re-evacuated and rebaked for 12 h while that of the untreated portion returned to its pre-electron bombardment condition.

Jones advances a theory to explain the action of the glow discharge improving the surface condition of the stainless steel. He suggests that after normal vacuum bakeout the surface of the steel is coated with a thin film of graphite and it is the graphite which is the strong absorbent of gases and the source of carbon monoxide in the system. The glow discharge works by removing this coating of graphite.

This theory is supported by information published recently by Lambert and Comrie.[30] After having the misfortune of contaminating a LEED/Auger system with hydrocarbons from a component accidentally introduced in the system they found that when they attempted to produce atomically clean specimens by high temperature treatment the specimens became coated with a film of carbon, The extent of the contamination in terms of partial pressures was small: $<10^{-10}$ torr in a total pressure of 10^{-9} torr as shown by a mass spectrometer scan. A prolonged vacuum bake at 420°C failed to produce a significant reduction in the hydrocarbon background. However, a glow discharge clean in 10^{-2} torr of oxygen completely removed the hydrocarbon contamination. The discharge of 100 mA at 500 V was carried out for 10 h. Not only did the hydrocarbon background disappear but the system was restored to a fully operational condition.

8. Conclusion

It is obvious from the results of outgassing tests published by different workers (see Table 4) that very different outgassing rates have been obtained for materials apparently the same. Some of this variation can be attributed to differences in the method of measurement but it is likely that most of the variation is due to differences in the state of the samples at the start of testing. The initial state of the samples depends on manufacture, pre-treatment and storage.

The published data e.g. Tables 4 to 8 is only a small proportion of the results that have been measured. Most tests have been conducted for specific projects. The results have been used for design purposes, but have not been made available outside the organizations in which the work was carried out. From the published results generalizations can be made. It can be seen for example that

Table 4. Metals

Material	K_1 torr l. s^{-1} cm^{-2} $\times 10^{10}$	n	K_{10} torr l. s^{-1} cm^{-2} $\times 10^{10}$	n_{10}	Ref
Aluminium (fresh)	63	1.0	6.0	1.0	9
Aluminium (degassed 24 h)	41.4	3.2	3.06	0.9	9
Aluminium (3 h in air)	66.5	1.9	4.75	0.9	9
Aluminium (fresh)	62	1.0	3.25	0.9	9
Aluminium (anodised-2 μm pores)	2760	0.9	322	0.9	9
Aluminium (bright rolled)	—	—	75	1	13
Duralumin	1700	0.75	350	0.75	13
Brass (wave-guide)	4000	2.0	100	1.2	13
Copper (fresh)	400	1.0	41.5	1.0	9
Copper (mech. polished)	35	1.0	3.56	1.0	9
OFHC copper (fresh)	188	1.3	12.6	1.3	9
OFHC copper (mech. polished)	19	1.1	1.63	1.1	9
Gold (wire fresh)	1580	2.1	5.1	1	9
Mild steel	5400	1	500	1	13
Mild steel (slightly rusty)	6000	3.1	130	1	13
Mild steel (chromium plated polished)	100	1	9.0	—	13
Mild steel (aluminium spray coated)	600	0.75	100	0.75	13
Steel (chromium plated fresh)	70.5	1	5.8	1	9
Steel (chromium plated polished)	91	1	8.0	1	9
Steel (nickel plated fresh)	42.4	0.9	4.94	0.9	9
Steel (nickel plated)	27.6	1.1	2.33	1.1	9
Steel (chemically nickel plated fresh)	83	1	7.05	1	9
Steel (chemically nickel plated polished)	52.2	1	4.6	1	9
Steel (descaled)	3070	0.6	2950	0.7	9
Molybdenum	52	1.0	3.67	1	9
Stainless Steel EN58B	—	—	14	1.6	13
Stainless Steel 18/9/1 (electro polished)	—	—	2	—	15
(vapour degreased)	—	—	1	—	15
(diversey cleaned)	—	—	3	—	15
Stainless steel	1750	1.1	210	0.75	13
Stainless steel	900	0.7	200	0.75	13
Stainless steel ICN 472 (fresh)	135	0.9	14.7	0.9	9
Stainless steel ICN 472 (sanded)	82.8	1.2	10.4	0.8	9
Stainless Steel NS22S (mech. polished)	17.1	0.5	4.6	0.7	9
Stainless Steel NS22S (electro polished)	42.8	1.0	4.28	1.0	9
Stainless Steel NS22S	144	1.3	13.5	1.9	9
Zinc	2210	1.4	322	0.8	9
Titanium	113	0.6	18.4	1.1	9
Titanium	40	1.0	3.68	1	9

Table 5. Metals (vacuum baked)

Material	Treatment	K torr l. s^{-1} cm^{-2} $\times 10^{14}$	Ref
Aluminium	15 h at 250°C	40	17
Aluminium	20 h at 100°C	4	14
Copper	20 h at 100°C	110	14
U15C Stainless Steel	45 h at 360°C	260	11
U15C Stainless Steel	25 h at 300°C	450	11
U15C Stainless Steel	3 h vacuum furnace degas at 1000°C + 25 h *in situ* at 360°C	1.6	11
304 Stainless Steel (electro polished)	30 h at 250°C	300	17

metals and ceramics have lower outgassing rates than most organic materials. More general and precise data could be obtained if procedures were better standardized. Both methods of measurement and sample preparation should be compared and their relative merits determined. The main criterion should be reproducibility and relevance to large scale performance.

The factors which influence the outgassing rates of materials need further investigation. Some work on these environmental factors has already been carried out, e.g. by Santeler and by Barton and Govier, and by Young but much more is needed. In particular the most relevant factors need identifying, and the degree of environmental control required in order to achieve reproducible data needs to be ascertained. To obtain such information would be long and costly because of the time required for testing and the expense of the apparatus. Without this information standardization is impossible. In view of the importance of outgassing data to design engineers it is surprising that this subject has received relatively little attention, compared with that of the allied topics of vacuum pump or vacuum gauge designs.

Table 6. Polymers

Material	K_1 torr l. s^{-1} cm^{-2} × 10^8	α_1	K_{10} torr l. s^{-1} cm^{-2} × 10^8	α_{10}	Ref
Araldite (moulded)	116	0.8	35.2	0.8	9
Araldite D	800	0.8	220	0.78	31
Araldite D	190	0.3	125	0.5	4
Araldite F	150	0.5	73	0.5	4
Celluloid	860	0.5	430	0.5	32
Gafion (PTFE) (fresh)	16.6	0.8	3.31	0.9	9
Kel-F	4	0.57	1.7	0.53	33
Methyl methacrylate	420	0.9	140	0.57	31
Mylar (24 h at 95% RH)	230	0.75	40	—	34
Nylon	1200	0.5	600	0.5	35
Pertinax	620	0.18	290	0.5	36
Plexigias	72	0.44	27	0.44	36
Plexigias	310	0.4	180	0.4	4
Polyamid	460	0.5	230	0.5	32
Polyester-glass laminate	250	0.84	80	0.81	33
Polyethylene	23	0.5	11.5	0.5	32
Polystyrene	2000	1.6	200	1.6	33
Polystyrol	56	0.6	12	0.61	36
Polyvinylcarbazol	160	0.5	80	0.5	32
PTFE	30	0.45	15	0.56	13
PVC (24 h at 95% RH)	85	1.0	2	—	34
Teflon	6.5	0.5	2.5	0.2	36
Terephenil (fresh)	62.2	0.5	16.8	0.5	9

Table 7. Rubbers

Material	K_1 torr l. s^{-1} cm^{-2} × 10^8	α_1	K_4 torr l. s^{-1} cm^{-2} × 10^8	α_4	Ref
Butyl DR41	150	0.68	40	0.64	31
Convaseal	100	0.5	49	0.6	33
Natural crepe	730	0.7	310	0.65	31
Natural gum	120	0.5	60	0.5	33
Neoprene	3000	0.4	1800	0.4	31
Neoprene	300	0.5	145	0.5	33
Nygon	1300	0.5	650	0.6	31
Perbuman	350	0.3	220	0.5	31
Poliosocyanate	2800	0.45	1270	0.57	31
Polyurethane	50	0.5	25	0.5	32
Silicone	1800	1.0	440	1.2	32
Viton A (fresh)	114	0.8	—	—	9

Table 8. Ceramics and glasses

Material	K_1 torr l. s^{-1} cm^{-2} × 10^{10}	α_1	K_{10} torr l. s^{-1} cm^{-2} × 10^{10}	α_1	Ref
Steatite	900	1	95	1	4
Pyrophyllite	2000	1	200	1	32
Pyrex (fresh)	73.5	1.1	5.5	1.7	9
Pyrex (1 month in air)	11.6	0.9	1.6	0.7	9

Acknowledgement

The author wishes to acknowledge the assistance given by The Rutherford Laboratory in the preparation of this article.

References

[1] R M Zabel, *Rev Sci Instrum*, 4, 1933, 233.
[2] S H Cross, *Vacuum*, 10, 1960, 86.
[3] G S Grossart, *Trans 3rd Int Vac Cong*, p 89 (1965).
[4] R Geller, *Le Vide*, 13, No. 74, 1958, 71.
[5] G Mongodin, *Le Vide*, No 92, 1961.
[6] F J Schittko, *Vacuum*, 13, 1963, 525.
[7] B D Power and F C Robson, *Trans 8th AVS Vac Symp*, Vol 2, p 1175 (1961).
[8] R P Henry, (a) *Le Vide*, No 82, 1959, 226; (b) *Le Vide*, No 144, 1969, 316.
[9] A Schram, *Le Vide*, No 103, 1963, 55.
[10] G Carter, D G Armour, L de Chernatony, *Vacuum*, 20, 1970, 643.
[11] R Calder and G Lewin, *Br J appl Phys*, 18, 1967, 1459.
[12] J Blears *et al*, *Advances in Vacuum Science and Technology*, Vol 2, p 473, Pergamon Press, Oxford (1960).
[13] B B Dayton, *Trans 6th AVS Symp*, p 101 (1959).
[14] G Moraw, *Vacuum*, 24, 1974, 125.
[15] R S Barton and R P Govier, (a) *Proc 4th Int Vac Cong*, p 775 (1968); (b) *Vacuum*, 20, 1970, 1.
[16] R Jaeckel and F. J. Schittko, *Casabgabe von Werkstoffen ins Vakuum Forschungsberickte NRW*, No 369 (1957).
[17] J R Young, *J Vac Sci. Technol*, 6, 1969, 398.
[18] C W Oatley, *J appl phys*, 5, 1954, 358.
[19] W Beckmann, *Vacuum*, 13, 1963, 349.
[20] R J Elsey, P E Gear and E B Iberson, *Internal Memorandum*, Nimbus F series, Rutherford Laboratory (1972).
[21] S Podlaseck *et al*, *Trans 9th AVS Symp*, p 320 (1962).
[22] M M Fulk and K Sylhorr, *Trans 9th AVS Symp*, p 324 (1962).
[23] J Roussel and J J Thibault, *1st Int Congr of Vacuum and Space Research* (1964).
[24] J Amoignon and J P Couilland, *Le Vide*, No 141, 1969, 181.
[25] W Espe, *Materials of High Vacuum Technology*, Vol 1, p 324, Pergamon Press, New York (1966).
[26] J R J Bennett *Internal Memorandum* EPIC/MC/42, Rutherford Laboratory.
[27] L Holland, *Vacuum Deposition of Thin Films*, Chapman & Hall, London (1961).
[28] R P Govier and G M McCracken, *J Vac Sci Technol*, 7, 1970, 552.
[29] A W Jones, E Jones and E M Williams, *Vacuum*, 23, 1973, 227.
[30] R M Lambert and C M Comrie, *J Vac Sci Technol*, 11, 1974, 530.
[31] J Blears *et al*, *Trans 1st IOVST Symp* (1960).
[32] R Jaeckel and F J Schitto, *Gas Evolution from Materials in Vacuum*, West Germany Ministry Research Report.
[33] B B Dayton, *CVC Technical Report*.
[34] D J Santeler, *Trans 5th AVS Vac Symp* (1958).
[35] B D Power and D J Crawley, *Advances in Vacuum Science and Technology*, Vol 1, p 206, Pergamon Press, Oxford (1960).
[36] G. Thieme, *Vacuum*, 13, 1963, 55.

AUTHORS NOTE.

The material for these articles was originally assembled for an MSc critical survey at Sir John Cass School of Science and Technology with helpful suggestions from Dr J L Whiteman. I am indebted to many authors and also to The Chemical Society, The Institute of Physics, The Macmillan Co. Inc., The McGraw Hill Book Co., Pergamon Press, and Société Française Du Vide, for their permission to reproduce diagrams and tables from their publications.

Lansing

Glow DISCHARGE CLEANING TECHNIQUES FOR ULTRAHIGH VACUUM SYSTEMS

By Glory Anne Yango
August 23, 1985
Jet Propulsion Laboratories
Caltech SURF Project

ABSTRACT

Cleaning of the 5-kilometer, 4-foot diameter 304 L stainless steel tubes for the gravity wave detector vacuum system is discussed. A review of various ultrahigh vacuum system cleaning methods is presented, including descriptions of pretreatment, baking, pulse and glow discharge cleaning, and gettering processes. Laboratory research must be conducted before the final cleaning method for the gravity wave detector is determined, but the most efficient cleaning at a reasonable cost seems to be: 1) pretreating the tube with a known effective cleaning process like the standard Varian method or the Diversey DS-9 method 2) baking the 40-foot tube sections at high temperatures of 450° C or more before installation 3) using a low electron temperature hydrogen glow discharge in situ on the 5-kilometer tube.

1. Introduction

All matter generates a gravitational field of some kind which attracts other passing objects. Motion of matter causes these fields to vary, so that when matter undergoes irregular motion, gravitational waves are produced. These waves travel outward from the source at the speed of light; their amplitude falling as the inverse of their distance from the source.[29]

Gravitational waves alter the relative positions of particles which encounter them so that they experience motion of some degree. These waves are said to be transverse polarized since all particle motion occurs at right angles to the direction in which the wave is propagating.[29] The energy these waves carry is emitted from the source of the gravitational waves.

Scientists have been trying to detect Einstein's predicted gravitational waves. The sources of gravitational waves which have the best chance of being detected on earth are those with strong gravitational fields and high-speed motions.[29] The rapid motion of the stellar interiors during the formation of neutron stars or black holes, binary systems containing a neutron star or black hole, or a rotating neutron star slightly deformed in shape are strong emitters of gravitational waves. Gravitational wave detectors need to be built sensitive to wave amplitudes at least as small as 10^{X} if there is to be a reasonable chance of seeing gravitational waves from supernovae.[29]

Several types of instruments are being used to reach a sensitivity of detecting wave amplitudes as small as 10^{-22}: bar and crystal detectors and laser interferometers. Scientists from Caltech and MIT, in a joint project, have designed a multiple-laser interferometer to detect gravity waves. Two sites will be constructed, each consisting of an L-shaped vacuum system formed by 5-kilometer stainless steel tubes. Each vacuum system would support several laser interferometers simultaneously.

Laser interferometers use a Michelson design consisting of two freely suspended mirrors and masses and a freely suspended light splitter placed in the form of two orthogonal arms several meters in length.[29] Coherent laser light is split between the two arms at the light splitter. The light reflects off the mirrors suspended from the masses at the end of each arm back to the beam splitter and recombined and detected photoelectrically. The effect of a passing gravitational wave is to induce fractional relative displacements, of the order of the amplitude of the gravitational wave, of the two masses at the end of each arm which do not, in general, cancel.[29] A change is then observed in the intensity of the 2-beam interference pattern.

To avoid producing spurious signals, the fraction of scattered light in the vacuum system must be reduced to below 10^{-10}. The arms must also be placed in a high vacuum to avoid effects from residual gas pressure and from a refractive index

that varies with the presence of gases.[29] Large stainless steel tubes, with a diameter of four feet, surround the multiple-laser interferometer to help keep out sounds and disruptions from the outside world. The vacuum tubes must be cleaned efficiently to reduce the outgassing rate and residual gas pressure and to keep the base pressure of the vacuum system down to 10^{-8} Torr or below.

Low average pressure is the result of high pumping speed together with low outgassing rates of strongly bonded adsorbates at the surface.[9] To reduce outgassing rates, cleaning of the stainless steel tubes must be done. There are many methods of cleaning which may be used individually or in combinations on vacuum systems. Chemical or physical pretreatments, baking, pulse discharge, glow discharge, and/or gettering are effective cleaning methods depending on the material to be cleaned, the vacuum pressure desired, the outgassing rates desired, and the contaminants needed to be removed. The optimal cleaning method for the gravity wave detector must be determined by experimentation on smaller versions of the detector using cleaning procedures most suited for its parameters.

2. Wall Outgassing

Wall outgassing is a problem faced by vacuum systems with pressures of 10^{-7} Torr or below. At these low base pressures, it is impossible to maintain an atomically clean vacuum surface for more than a few seconds. The surface exposed will have a covering of many monolayers of water vapor and impurity gases. These gases will tend to desorb from the surface and diffuse from the bulk to the vacuum space, which raises the pressure of the vessel.

2.1 Impurities

The unconditioned surfaces of stainless steel represent a large source of C, O, and to a lesser extent Cl, S, and N contamination.[1] The major contaminants are carbon (61%) followed by oxygen (19%). Carbon is contained in several chemical forms, including hydrocarbons, elemental carbon, and carbon oxides. Virtually all untreated materials are covered with a 30-50 Å thick layer of common hydrocarbons, making carbon the first-order impurity problem.[1]

The passivation oxide layers comprise the first 100-200 Å of the near-surface region of stainless steel after the surface carbon has been removed.[1] Oxygen is contained in common residual gases like H_2O, CO, and CO_2 that could be adsorbed on or absorbed in the oxide layer. It may also be contained in metal oxides in the near-surface region.

The main outgassing species of unbaked surfaces is normally water vapor, with lesser quantities of carbon monoxide, carbon dioxide, and hydrogen.[4] Surface, near-surface, and bulk contamination play an important role in the impurity problems of vacuum systems. The hydrogen and contaminants must be removed in order to insure stable vacuum conditions in low base pressures. Conditioning and cleaning of the stainless steel surface is necessary to remove or reduce the amount of hydrogen and contaminants present.

2.2 Conditioning Needs

The aim of any chamber conditioning is to reduce the rate of gas desorption. The conditioning of chambers can be done during manufacturing, in the laboratory before installation, and/or in situ after installation. The conditioning techniques used on stainless steel may include use of one or more of the following procedures: 1) chemical or physical pretreatment 2) baking 3) pulse discharge cleaning 4) glow discharge cleaning and 5) wall coating or gettering.[1] Various treatments are employed to control the impurity level in various vacuum systems like tokamaks or accelerators. These include: 1) efficient and clean pumping of the vacuum vessel during baking and cleaning processes and during pump down 2) mild baking of the vacuum system and its parts to remove weakly adsorbed gas on the surface 3) specific

surface treatments of vacuum materials before assembly, and conditioning *in situ* of the inner wall by glow and/or pulsed discharges.

3. Pretreatment

Pretreatment of the stainless steel by chemical or physical processes usually occurs during manufacturing. Various stainless steel companies have "standard" methods of pretreatment.

Pretreatment processes tend to reduce gross contamination like oil and grease, as well as particulate matter. Degreasing in CCl_2H_2 or CCl_4, with ultrasonic cleaning and rinsing in demineralized water is one example of a chemical precleaning procedure normally carried out for ultrahigh vacuum systems.[4] Another example of a chemical precleaning procedure is soaking the stainless steel overnight in a 10% sodium hydroxide mixture and then rinsing and washing in a solution of Sparkleen and distilled water. After rinsing again in three changes of distilled water and once in 2-propanol, the stainless steel is air dried.[8] Some types of physical pretreatment processes include electropolishing, hydrogen firing, and mild baking.

Chemical and physical pretreatments are not enough to reduce the necessary amounts of hydrogen, carbon, and oxygen for stable, low base pressures. Effective chemical or physical

pretreatment techniques can reduce but not eliminate the hydrocarbon surface contamination, but such techniques have no effect on the passivation oxide layers.[1] Chemical cleaning, at the least, leaves a film of the final-rinse material on the surface to be cleaned. After pretreatment, the surface remains covered with carbon and oxygen. Baking, discharge cleaning, and/or gettering are techniques generally used after pretreatment to remove the contamination still present.

4. Discharge Cleaning

4.1 Principle of Operation

Discharge cleaning is a surface conditioning method used in many ultrahigh vacuum systems. The initial outgassing rates of contaminants are reduced by discharge cleaning. Therefore, the overall gas load needed to be pumped out to obtain lower base pressures is reduced. Less gas is required to be removed.

In a discharge cleaning apparatus, an electrical current is run through an anode, usually made of stainless steel and located in the vacuum system. A certain potential difference is set between the anode and the cathode. The latter is generally the stainless steel chamber. The production of electrons must be equal to or larger than the consumption of electrons in order for a self-sustained electric discharge, a necessary condition for discharge cleaning, to occur. A continuously circulating discharge gas is run through the vacuum chamber.

Figure 1[13] shows the curve of the discharge current A versus the discharge voltage V in glow discharge operation. Successful glow discharge operation occurs only in two phases where the voltage is a maximum or a minimum. These two phases are the Townsend discharge and the normal glow discharge. The transition from the Townsend phase to the normal glow discharge phase is still not understood since it is rapid and uncontrollable.[13]

Cleaning is achieved by the bombardment of the vacuum surface with energetic heavy ion projectiles or chemically active gas molecules. High energy particles impact on the surface, transferring their momentum to sputter loose contaminants. Chemically active gas particles react with contaminants, forming pumpable gases that are easily removed. Certain discharge gases can be chosen to optimize the removal of certain contaminants.

4.2 Discharge Cleaning Techniques

4.2.1 Discharge Gases

Discharge cleaning schemes can be categorized in three ways: 1) physical 2) chemical or 3) hybrid physical-chemical. If the induced effects are physical, then sputtering with an inert discharge gas will occur. If the induced effects are chemical, then desorption by an active discharge gas will occur. If the induced effects are both physical and chemical, then a

combination of sputtering and desorption occurs. Various discharge cleaning techniques used in tokamaks, accelerators, and other ultrahigh vacuum systems have used inert gases, oxygen, and/or hydrogen discharge gases.

It is found that discharges in helium, neon, and argon are all effective in reducing the outgassing of water vapor, carbon monoxide, and carbon dioxide, and that typically an ion dose of 10^4 ions/m is required for effective cleaning.[4] These heavy inert gases sputter and dislodge carbon, oxygen, and some hydrogen from the surface of the vacuum. But when the discharge cleaning is carried out with the vacuum surfaces at room temperature, the inert gas is trapped in the surface. This gas, together with hydrogen, then desorbs after the discharge cleaning. Therefore the total outgassing rate does not change by more than a factor of two or three.[4] The trapping of the inert gas in the surface of the vacuum system does not occur if the glow discharge is carried out with the surface at temperatures of 300 C or higher. Then, the total outgassing rate is reduced by many orders of magnitude.[4]

When inert gases are used in discharge cleaning in the low-velocity ion mode, water molecules are broken up, with the hydrogen being pumped out and the oxygen being deposited on the surface of the vacuum chamber. Continuous inert gas discharges result in a continuous break up of water molecules, increasing

the amount of oxygen on the surface until a monolayer is formed. At this point, oxygen begins to leave the vacuum system as oxygen gas. Inert gas discharges cannot be used to reduce the surface oxygen content below a monolayer.[11] Again, if the vacuum chamber is heated to temperatures of 300° C or higher, oxygen contamination levels can be reduced to substoichiometric levels.

Combinations of an inert gas with oxygen or hydrogen have been used as discharge gases in various cleaning techniques. It is found that a pure argon discharge reduces both the oxygen and carbon to a small fraction of a monolayer, whereas argon plus 10% oxygen removes the carbon completely but naturally leaves a significant amount of oxygen.[4] An argon and hydrogen discharge reduces carbon at a rate much lower than an argon and oxygen discharge because carbon reacts with oxygen at a higher rate than with hydrogen. Use of argon and hydrogen discharge accelerates the dissociation of oxide layers on metals, and the gas products can also be evacuated.

Oxygen discharge gas has been used in some cleaning techniques for ultrahigh vacuum systems. It is very effective in removing carbon contamination, since the chemical reaction rate of oxygen and carbon is relatively high. But if oxygen discharge is used to remove surface carbon, there is an increase in the surface oxide formation.[1] This increases oxygen contamination in the stainless steel vacuum system.

Almost all glow discharges in ultrahigh vacuum systems now use hydrogen as the discharge gas.[4] Pure hydrogen gas discharge cleaning effectively removes carbon and oxygen surface contamination without leading to other impurity problems such as inert gas outgassing or increased surface oxide formation.[1] Carbon is removed more effectively than oxygen in hydrogen discharges. Carbon reacts chemically with hydrogen to form methane, which is not normally readsorbed onto the surface of the vacuum system. Carbon is more readily removed by an oxygen or an argon and oxygen discharge, but the oxygen must still be removed, and a hydrogen discharge is much more effective in removing oxygen than an oxygen or an argon and oxygen discharge.

The most effective method for removing oxygen is a low electron temperature hydrogen gas discharge.[4] The increased rate of water formation due to low electron temperature hydrogen gas discharge leads to the removal of loosely bound oxygen. The low electron temperature discharges induce the hydrogen to chemically react with the oxygen contaminants to produce water, which is then removed from the vacuum chamber. In inert gas discharges with low or high electron temperatures, the conversion of oxygen to water does not occur because of the lack of hydrogen gas. In high electron temperature hydrogen discharges, the formation of water occurs, but because of the high electron temperature, the water molecules break up, with oxygen immediately being readsorbed onto the clean vacuum surface.

The best initial conditioning method for carbon and oxygen removal is discharge cleaning with alternating high and low electron temperature hydrogen discharges. The high electron temperature hydrogen discharges remove carbon effectively and loosen oxygen from the surface and near-surface regions of the vaccum vessel. The low electron temperature hydrogen discharges then remove the loosened oxygen from the chamber at an accelerated rate by the formation of water. Alternate high current (30 kA) and low current (4 kA) hydrogen discharge cleanings, run for 30 minutes each, are effective in removing carbon and oxygen contamination.[27]

The discharge gas chosen for a particular cleaning technique is one parameter that must be chosen according to the particular system's vacuum needs and function. Either an inert gas, hydrogen, oxygen, or a combination discharge gas and other special techniques and specific parameters need to be selected experimentally to optimize the cleaning of a specific system.

4.2.2 Pulse Discharge

Discharge cleaning techniques can also be performed in two different current patterns: 1) pulse or 2) glow. The pulse discharge cleaning uses repetitive bursts of discharge, whereas the glow discharge cleaning uses a continuous, non-interrupted generation of a glow.

Pulse discharge cleaning is mainly used in tokamaks, accelerators, and ultrahigh vacuum systems when continuous in situ discharge cleaning is applied for very long time periods with only various experimentation procedures interrupting. The method seems to require a fair amount of power to generate the discharges.

4.2.2.1 Operating Conditions

The pulse discharge cleaning usually makes use of a coil or similar anode to initiate a series of low level discharges at a high repetition rate.[1] The general principle is to subject the vacuum surface to many energetic discharges. The discharge cleaning conditions are usually a compromise between energetic discharges and fast repetition rate. The pulses can be repeated so fast as to be almost continuous.

4.2.2.2 Pulse Discharge Experiments

4.2.2.2.1 ISX-A Tokamak

Many ultrahigh vacuum systems have used the pulse discharge cleaning arrangement. One such ultrahigh vacuum system is the Impurity Study Experiment (ISX-A) tokamak.[21,23] This iron-core tokamak, in which the elliptical vacuum vessel is constructed of 304L stainless steel, has a major radius of 92 centimeters and a minor radius of 26 centimeters.

Conditioning of the ISX-A walls was continued for the first five months of its operation. Low power hydrogen discharges, pulsed at 120 Hz, were maintained in the torus for several hours. Plasma currents of approximately 200 A were obtained.

After a 62-hour exposure to pulsed hydrogen discharge cleaning, the carbon level in the stainless steel was significantly decreased; carbon reduced to concentrations of 10-20 atomic percent. Oxygen and sulfur were also reduced to concentrations of only a few atomic percent. The stainless steel oxides were not reduced noticably, except if the stainless steel surface had previously been sputtered. The oxygen concentration was reduced to concentrations less than 2 at%. Pulsed helium discharge cleaning was tried in the ISX-A, with the result that pulsed helium discharges were particularly ineffective in removing carbon.

In another set of experiments using the ISX-A tokamak,[15,16] the effects of low power discharge cleaning, with an electron temperature between 9-18 eV and a bombardment of 10^{10} -10^{11} ions/cm^3, were studied. The cleaning discharges consisted of half-millisecond long pulses applied at a rate of 120 pulses per second. Sharp voltage pulses of 20-30 volts were used to generate the low power cleaning discharges.

For 4 1/2 months, overnight discharge cleaning occurred. The base pressure reached as low as 8×10^{-8} Torr. A relatively large partial pressure of hydrogen was always present, especially after discharge cleaning. This occurred because of the decreased pumping speed of the turbomolecular pump for hydrogen and the significant hydrogen entrapment by the vacuum surface. Hydrogen was the principal residual gas, while CH_4, CO, and H_2O were the principal contaminant gases.

The carbon level, which was initially 50%, remained at a fairly high 20-30 % throughout the cleaning cycles. After a day of discharge cleaning, either carbon deposition was almost stopped or carbon deposition and removal were balanced. Carbide layers were formed on the stainless steel vacuum surface, and oxygen was effectively removed. Carbon could be reduced to substoichiometric levels.

Exposure to the hydrogen ions produced by the discharge was very important for the discharge cleaning. Discharge cleaning assisted pumping of residual gases by cleaning wall shadow regions and by keeping the wall surface clean. After discharge cleaning, water vapor, nitrogen gas, and methane decreased by ratios of 1:30, 1:10, and 1:5, respectively, while the other residual gases: hydrogen, carbon monoxide, carbon dioxide, various hydrocarbons, and argon, almost vanished.

4.2.2.2.2 MICROTOR Tokamak

The MICROTOR tokamak[11,33] was prepared by low temperature discharge cleaning applied continuously. The chamber was cleaned by audio-frequency hydrogen discharges at a frequency of 5 KHz, a current of 2 kA, a voltage of 30 V, an electron temperature of 3 eV, a pulse duration of 20 milliseconds, and a repetition rate of two bursts per second. This cleaning continued until a pressure of 4×10^{-3} Torr was reached.

When low electron temperature pulses were made, less sputtering occurred and water vapor mobility was higher. Some trapping of water vapor occurred after the discharge cleaning ended unless the vacuum walls were about 100° C or higher. Otherwise, oxygen was effectively removed from MICROTOR.

4.2.3 Glow Discharge

The glow discharge cleaning arrangement maintains a classical direct current (dc) or radiofrequency (rf) glow discharge within the vacuum vessel.[1] To ensure reasonable penetration of the discharge throughout the entire vacuum vessel, the glow discharge is usually applied using a centrally located anode, with all the remaining vessel structures electrically grounded to serve as the cathode. The vessel wall is subjected to reactive neutral and ion bombardment when the glow is applied with a discharge gas.

Cleaning up adsorbed gas is efficiently done by desorption by energetic particle bombardment. Glow discharge is more advantageous relative to other cleaning methods since it spreads out throughout the vacuum vessel so that all surfaces get a fairly uniform bombardment.

4.2.3.1 Operating Conditions

Approximately one thousand volts of direct current at one amp would be required to initiate the glow discharge process.[12] Low energy particles, with energies between one and ten electron volts, are used. The process introduces a discharge gas in the vacuum chamber at about 10^{-3} Torr. This gas is run through the vacuum chamber continuously at a low flow rate, while a voltage, usually between 100 and 400 volts, is applied across the insulated anode and the vacuum chamber walls, which are grounded as the cathode.

The pressure at which glow discharge cleaning is run has an important bearing on its effectiveness, the discharge cleaning being most effective at low pressures.[4] Lower pressures are correlated with higher energies of the ions hitting the vacuum surfaces. Total current decreases as the pressure increases, but the number of ions with higher energies decreases even more rapidly than the total current does.

Radiofrequency discharges, using radiofrequency power, are used since lower vacuum vessel pressures are needed for higher cleaning rates, and radiofrequency discharges at lower

vacuum vessel pressures tend to be also stable.[13]

Good cleaning of stainless steel vacuum surfaces can be obtained using the glow discharge process for a duration ranging from 24-120 hours. The residual gas outgassing rate determines the cleaning effectiveness. The residual gas production is found varying as 1/t versus the glow discharge time (t).[13] Most of the hydrocarbon layer on stainless steel is removed within the first two hours of glow discharge exposure.[13]

4.2.3.2 Glow Discharge Experiments

4.2.3.2.1 Govier and McCracken Study

Glow discharge cleaning in helium, neon, and argon was investigated by Govier and McCracken on gas removal from stainless steel.[5,14] A cylindrical stainless steel discharge tube 15.7 centimeters in diameter and 75 centimeters long, with an axial stainless steel electrode was used, where the tube formed a cold cathode. A discharge current of 0.5 A and an applied potential of 200-600 V were used with an alternating current discharge. The discharge gas was inert, being introduced into the vacuum chamber at a pressure of 10^{-2}-10^{-1} Torr. The flow rate was about 10^{-2}-10^{-1} Torr-liter/sec.

The vacuum tube was first baked at 450° C, then opened to the atmosphere before being glow discharged. The glow discharge reduced the high desorption rate of water vapor and carbon oxide gas after atmospheric exposure. The desorbed gas

species were removed by the continuous gas flow. A very marked reduction in the three original outgassing components (H, C, O) occurred with all three inert discharge gases used (He, Ne, Ar). There was also a considerable increase in the hydrogen outgassing rate and the appearance of the inert discharge gas in the outgassing spectrum. The outgassing rates were not very different from the outgassing rates of stainless steel without glow discharge because of the hydrogen and inert discharge gas outgassing. The total pressure in the vacuum system could have been as much as a factor of four less, though, because of the change in outgassing components. For the lighter gases, like hydrogen, the pumping speed was much higher.

Ion trapping during and after glow discharge cleaning occurred for various eventual outgassing species. The re-emission of the discharge gas occurred because of the ion trapping of the inert gas. The trapping efficiency for argon and neon was approximately 0.1 and that for helium was probably higher. During glow discharge, the concentration of the He, Ne, or Ar ions built up in the surface, to be slowly released into the vacuum vessel when it was re-evacuated. Hydrogen ions produced by the break up of water were trapped by the wall, desorbing slowly later. Oxygen ions or atoms produced by the break up of water were likely to be chemically gettered and permanently bound to the surface of the metal.

Pressure was a significant factor in obtaining effective cleaning. Water vapor desorption could be reduced to almost zero after ion bombardment if the discharge pressure was less then 2.5 x 10^{-2} Torr using argon as the feed gas, 10^{-1} Torr using neon as the feed gas, and 0.2 Torr using helium as the feed gas. The dependence of the water vapor desorption on the pressure of the glow discharge was due to the fact that the average energy of the impinging ions decreased with a rise in pressure. The higher the pressure, the lower the cleaning efficiency. Similar results were obtained with both alternating current and direct current glow discharges with the asymmetric arrangement (high cathode to anode area ratio) employed.

With a current density of 100 $\mu A/cm^2$, neon, argon, and helium, at the optimum pressure, could clean effectively in fifteen minutes. The dose of ions required was 10^{18} ions/cm^2. Runs with higher current densities, although having shorter cleaning times, could cause serious heating of the electrode and a tendency to arc. Adsorbed gases are effectively removed from vacuum surfaces by running an inert gas glow discharge, provided the vacuum surface receives enough energetic ions.

4.2.3.2.2 ASDEX Tokamak

Another vacuum system using glow discharge cleaning techniques was the ASDEX tokamak.[19] The anodes used in ASDEX were stainless steel rods 45 centimeters long and 25 millimeters in diameter. The rods were backed by a roof-shaped, stainless steel

box which is directly attached to the vacuum wall. Four of these anodes were mounted equally spaced on the outer circumference of the vacuum chamber, each being connected via 200 Ω resistors to the direct current power supply. A current density of 10 μA/cm^2 was used, with a current not above 4 A used. Hydrogen was the discharge gas.

Some residual gases present, after a week pause, after a total of eighty hours hydrogen glow discharge conditioning were CH_4, H_2O, CO_2, and CO. The water removal rate was about one monolayer per hour. The glow discharge efficiently removed the carbon contamination present in the vacuum chamber walls. For the best results in ASDEX, the glow discharge was run for a couple of hours before operation of the tokamak.

4.2.3.2.3 Poloidal Divertor Experiment Vacuum Vessel

A glow discharge technique, using hydrogen discharge gas, was developed and applied to the conditioning of the large (38 m^3) Poloidal Divertor Experiment (PDX) vacuum vessel.[1,2,17] Using a direct current, dynamically-pumped glow discharge in purified hydrogen gas, glow discharge conditioning was used in the PDX to maximize carbon and oxygen removal with a minimum of metal sputtering. The glow discharge was produced by biasing one or two internal anodes at 400 V to sustain a discharge current of 2-4 A per anode, with purified hydrogen gas at a pressure of 3×10^{-2} Torr flowing through the vacuum vessel at approximately

10 Torr-liter/sec. The anodes were made of stainless steel, each with an area of 300 cm^2. They were inserted within the vacuum vessel at midplane, where copper conductors, with a diameter of six millimeters, supported them. Each anode was connected to 0-500 V, 5 A, and a direct current power supply through a 50 Ω load resistor. The vacuum chamber was grounded.

Hydrogen gas was the discharge gas. The reactive species (H, H^+) was adsorbed and penetrated the surface layer, according to energy. Molecules formed in reactions between hydrogen ions and surface contaminants, which could be removed by either spontaneous or induced desorption. The released molecules were eventually pumped out.

Trial discharges in the PDX were initiated with N_2, O_2, Ne, H_2, and Ne/H_2 discharge gases. The discharges in H_2 or O_2 produced the most significant reaction products considered removable by the vacuum system: CH_4, CO, and C_2H_4 produced by H_2; CO and CO_2 produced by O_2. Hydrogen gas was chosen as the discharge gas because: 1) oxygen gas would have contributed to the oxygen impurity level and 2) oxygen gas was more likely to cause sputtering.

For the 120 hours of non-continuous exposure to glow discharge, residual gas pressures decreased with a roughly 1/t dependence, where t was the discharge time. Measured H_2O outgassing rates decreased during the glow discharge conditioning

period. The hydrogen gas outgassing rate was enhanced. Most of the surface hydrocarbon layer was removed before two hours of cleaning time. After glow discharge cleaning for more than two hours, a reduction in the oxygen layer appeared.

The net result after approximately a 100-hour conditioning period in the PDX was the removal of more than 100 monolayers of surface carbon and oxygen. The glow discharge cleaning even cleaned recessed areas efficiently. Base pressures reached 2-7 x 10^{-7} Torr. The effects of the glow discharge conditioning in the PDX were: 1) the efficient removal of the carbon contamination layer and 2) the hydrolysis and partial reduction of the Fe oxide layer, which suggested oxygen removal via the hydrolysis of Fe oxides.

4.2.3.2.4 Stainless Steel EN58 B Study

The effects of treating stainless steel EN58 B in glow discharges were investigated.[25] Two kinds of electrode systems were used: a planar cathode and a hollow cathode. All the experiments were done with active or inert gas continually flowing through the vacuum vessel.

Using the hollow cathode system, a stainless steel tube with a 28-millimeter diameter and a 135-millimeter length was evacuated and bombarded in argon, a mixture of 50% argon and 50% oxygen, and a mixture of 50% argon and 50% hydrogen. A voltage of 350 V and a current density of 2.3 A/m^2 were used.

Argon discharge gas mainly sputtered contaminants loose or free from the vacuum wall surface. Carbon sputtered in hollow bodies and diffusing in glow discharges was redeposited on the treated surface. Physical sputtering was also ineffective for oxygen removal because the oxygen released was also retrapped on the vacuum walls. After three hours of glow discharge treatment in argon, oxygen contamination was still present in as high concentrations as before cleaning.

When a 50% argon and 50% hydrogen mixture discharge gas was used, surface oxide reduction occurred provided that water vapor was contained in the gas mixture. An apparent rise in carbon yield was also observed because besides sputtering off carbon, reaction products between carbon and the discharge gas were formed. Therefore, the use of argon and hydrogen mixture discharges accelerated the dissociation of oxide layers on metals, and the gas products formed could be evacuated. Carbon, though, was removed from the vacuum surface at a much lower rate in argon and hydrogen than in oxygen or argon and oxygen mixtures.

For the oxygen or argon and oxygen mixture discharge gases, the bombardment of carbon by ions and neutrals in the presence of active oxygen enhanced the release of carbon oxides by implanting oxygen in the vacuum surface and sputterng the surface reaction products. In this way, carbon was removed

rapidly, being released as a gas component which was easily evacuated from the vacuum. But oxygen and hydrogen contamination still was present on the vacuum surface in large concentrations.

4.2.3.2.5

Lambert and Comrie recently had to overcome the problem of removing the last traces of hydrocarbon vapor from a stainless steel ultrahigh vacuum system which had a total pressure of approximately 10^{-9} Torr or less.[26] A stainless steel anode was placed in the center of the chamber, with all other components being connected to the chamber and grounded. 100 mA at 500 V in the presence of approximately 10^{-2} Torr of flowing oxygen discharge gas were the discharge conditions used.

All the internal surfaces were bombarded by highly reactive neutral and ionic species, while the reaction products were continuously pumped away. The discharge spread uniformly through the chamber.

The discharge was run for ten hours. After the first hour, water was present in the discharge gas, which is an expected major oxidation product of contaminant material. The low-pressure, direct current discharge in oxygen quickly removed all detectable traces of undesirable residues. In conclusion, the oxygen discharge was a simple and convenient method for removing low vapor pressure organic materials without any apparent undesirable side effects.

5. Other Cleaning Methods

5.1 Baking

The most commonly applied in situ conditioning is bakeout at temperatures between 150 and 350° C for periods ranging from a few hours to several days. Vacuum systems are baked at 200° C or 300° C to reduce thermal outgassing from the walls. Bakeout is very efficient in reducing thermal outgassing. A typical bakeout of 300° C for 24 hours reduces the desorption from stainless steel to 10^{-12} Torr-liter/sec-cm^2 or less, where approximately 99% of the remaining gas being desorbed is hydrogen diffusing from the bulk of metal to surface to vacuum.[18]

Baking does not sufficiently remove chemically bound impurities, which can outgas by electron or ion induced desorption. Baking only releases the weakly bound molecules, so that an any practical temperature, the more tightly bound molecules and atoms will remain. The desorption of adsorbed gases from the surfaces of vacuum vessels usually necessitates baking to high temperatures to produce ultrahigh vacuum, and this severely limits the materials and techniques which can be used.[14]

The removal of contaminants by baking requires high temperatures and possibly long hours. For carbon contamination, low or moderate temperature baking of the vacuum vessel has little effect on its removal because adsorbed hydrocarbons will simply dehydrogenate, with the hydrogen being pumped away, while

the carbon remains. In order to substantially reduce surface carbon, vacuum baking at temperatures sufficiently high to induce bulk diffusion is required - for stainless steel, about 700-900° C.[1] Carbon and oxygen can be dissolved in the bulk material if baking around 800-900° C is performed, but the practical difficulties arising from this technique do not normally make it beneficial when alternate methods are available.

Baking has its negative aspects which may lower cleaning effectiveness in different ultrahigh vacuum systems. Baking does not gain anything as far as the outgassing rate is concerned; it only speeds up the outgassing process, therefore decreasing the pump down time.[12] A bakeout may also bake on unknown substances which may contaminate the vacuum surface, depending on the unknown substances and the material used for the vacuum surface.

Baking effects were studied on some ultrahigh vacuum systems. In the CERN storage rings,[5,9] carbon and its compounds were the main contaminants before baking the stainless steel surfaces. Vacuum baking at 800° C was necessary to produce a surface nearly devoid of carbon and oxygen. After this baking procedure, sulfur in the stainless steel diffused to the surface, so that when the storage rings were exposed to atmosphere, the surface became oxidized. Vacuum degassing at high temperature and in situ bakeout reduced the thermo-outgassing rate of the accelerator beam tubes at Brookhaven to approximately 10^{-13} Torr-liter/sec-cm^2.

Baking effects at different temperatures were also

measured.[10] Heating stainless steel samples to 300° C produced almost no change in surface composition. Heating to 400° C and 500° C decreased the oxygen content of the surface, but the carbon concentration remained relatively static. From 600° C up to 900° C, the carbon and oxygen surface concentrations decreased, becoming very negligible at 900° C.

A bakeout of ultrahigh vacuum system chambers is very beneficial in removing weakly bound contaminants and thermal outgassing atoms and molecules. But baking large stainless steel tubes at even a low temperature such as 150° C is a very expensive process that requires an enormous power source.[12] Baking also does not reduce carbon and oxygen contaminants very efficiently unless high temperatures are used. Whereas baking in situ for very large vacuum systems is very impractical, pre-baking of the system in smaller sections is feasible, although re-contamination of the surface after exposure to atmosphere is rapid and may require another bakeout in situ to remove.

5.2 Gettering

Gettering is a cleaning method which has recently been used for ultrahigh vacuum systems. It involves chemical reactions between contaminants which outgas and a "getter substance." The getter substance binds with the outgassing impurities very strongly. This eliminates the outgassing impurities from the vacuum chamber.

Gettering could be carried out with any metal which has a high chemical reactivity as the getter substance. Gaseous

species like oxygen, carbon monoxide, and water vapor can be gettered and removed from the vacuum chamber. Molybdenum, zirconium, and iron are examples of effective getters for the common active gases. A properly cleaned, stainless steel surface is also an effective getter for oxygen.

Titanium is most commonly used as the getter substance because it is easily evaporated onto the vacuum surface and it is relatively inexpensive compared to some other getter substances.[4] Titanium reacts well especially with oxygen, forming a stable oxide with respect to reduction by hydrogen. The titanium layers also protect the underlying metal oxide layers from decomposition.

Preparation of clean surfaces for ultrahigh vacuum systems can be obtained by <u>in situ</u> evaporation of the getter substance onto the vacuum surface. A significant number of devices have employed titanium gettering of some fraction (5-60%) of the vacuum vessel surface area as a routine conditioning procedure.[1] Gettering increases the pumping speed for active gases by more than an order of magnitude over the net pumping speed provided by the vacuum system, even with just 25-40% coverage of the vacuum surface area.[1]

Titanium gettering was the principal method of wall conditioning used during the last seven weeks of ISX-A tokamak experiments.[21] The titanium was evaporated only infrequently between the tokamak discharge shots and at the end of the day's run. The initial effect of the titanium gettering was the decrease in base pressure by a factor of ten.

A titanium getter source was used in the ATC tokamak to deposit a more controllable and renewable metal surface.[4,6] The vacuum vessel consisted of stainless steel bellow surfaces. The titanium for the ATC was evaporated from a Varian Ti-ball source, which is a nearly spherical, hollow shell of titanium heated by radiation from an internal tungsten filament. The filament current could be controlled to produce sublimation rates between 0.01 and 0.5 grams per hour. The Ti-ball itself has about 50 grams of titanium to evaporate. The Ti-ball was mounted on a retractable probe so that it could be inserted in the middle of the vacuum surface when used and then withdrawn into a side-port after use. The titanium sublimed relatively uniformly in all directions from the Ti-ball, and 25% of the vacuum surface was covered. Ten monolayers of titanium were deposited in the 90-second interval between discharges.

After the getter source was turned off, the gettered surface began to pump impurity gases. The gettered surface remained active for several hours and was able to pump four Torr-liters before saturating, corresponding to about seven monolayers of hydrogen. The getterable gases included hydrogen, nitrogen, oxygen, carbon dioxide, carbon monoxide, and water. There was no significant desorption of the trapped impurities from the titanium layer.

Titanium gettering produced successful results. Reduced concentrations of impurities, particularly oxygen, which was trapped chemically in the titanium and buried under subsequently evaporated layers, were confirmed. Without gettering, the base pressure in the ATC vacuum chamber was around 2-3 x 10^{-7} Torr. With gettering, the base pressure reduced to as low as 4 x 10^{-8} Torr.

Gettering has some problems which affect the usefulness of the cleaning technique. The long-term effects are still unknown, and there is concern that titanium film may peel or flake. So far, in the ATC tokamak, the getter sources have been used for about several hundred hours over a period of six months without any difficulties. Exposing the vacuum chamber to air is also a potential difficulty. Saturation or poisoning of the titanium occurs, and fresh titanium must be sublimated onto the surface to resume effective cleaning. The ATC tokamak has been exposed to air several times without experiencing any severe difficulties or build-up of titanium. Not enough experiments have been performed with titanium gettering to elaborate on these difficulties in detail.

One of the major difficulties of gettering is the regeneration of titanium at regular intervals. There are three options for regeneration: 1) glow discharge clean the titanium sections 2) resputter another coat of titanium onto the saturated

old titanium and 3) a combination of both.[12] With all three options, the vacuum system must be shut down. New titanium can be sputtered onto the surface using titanium sublimaters, which sputter molecular titanium onto saturated old titanium through a high voltage input to a titanium ball.[12] The reconditioning can probably be done within 24 hours.

5.3 Hybrid Techniques

Combinations of individual cleaning methods can also be effective and thorough cleaning techniques. One method may remove certain impurities that another method may not. Combination techniques can also be faster and more efficient.

5.3.1 Baking/Discharge Cleaning

5.3.1.1 Baking/Discharge Cleaning Process

Baking and discharge cleaning is an effective combination that is used for cleaning many ultrahigh vacuum systems. Raising the temperature of the vacuum surface while discharge cleaning it prevents ion trapping and hydrogen sorption. Vacuum bakeout before glow discharge is also found to be more effective since most loosely bound molecules (CH_4, H_2O, N_2,...) will be removed thermally. The temperature dependence of water vapor production from stainless steel shows the advantage of discharge cleaning at moderately elevated temperatures (up to 350° C).[1] Low outgassing rates can be achieved by modest heating and glow discharge cleaning.

5.3.1.2 Baking/Discharge Cleaning Experiments

5.3.1.2.1 ASDEX Tokamak

The effects of discharge cleaning at elevated temperatures were shown on a stainless steel sample treated like the ASDEX tokamak vessel surface.[19,20] The sample was exposed to a 24-hour discharge while the vacuum vessel was heated to 120° C. The sample was completely cleaned of carbon after a 150-minute cleaning period.

An apparatus consisting of a glow discharge vessel, with an inner area of 3.0 m^2 and a volume of 0.22 m^3, which could be heated to 600° C, was used to perform experiments on glow discharge cleaning. A radiofrequency generator, with a frequency of 13.6 MHz and power less than or equal to 100 watts, was matched to a stainless steel radiofrequency coil. A direct current voltage was applied between the coil and the wall of the vessel, establishing a plasma current and converting the radiofrequency discharge into a hollow cathode glow discharge. Four parameters were tested: 1) wall temperature 2) discharge gas pressure 3) pump speed and 4) current. Emphasis was placed on deoxidation of the stainless steel via H_2O removal.

Moderate wall temperatures were much more effective than walls at room temperature for cleaning. The water vapor release was found to be negligible at room temperatures with hydrogen glow discharge. Temperatures of 100° C or above should be used.

The same degree of cleaning could be achieved in ten hours at 400° C as in about five days of continuous radiofrequency hydrogen glow discharge at 100° C. Cleaning rates were large when the wall temperature was 200° C or above, and a relatively thorough clean up of contaminants including carbon, oxygen, and hydrogen was achieved within a few hours. Large amounts of methane and carbon monoxide, equivalent to several hundreds of monolayers of carbon, were released in addition to water in the first few hours of cleaning with the wall temperature at 200° C or above. After ten hours, methane and carbon monoxide had very low vapor pressures in the vacuum system.

5.3.1.2.2 CERN Intersecting Storage Rings and Studies

Ultrahigh vacuum conditions were achieved in the stainless steel vacuum vessel of the CERN Intersecting Storage Ring through the use of argon glow discharge conditioning with baking.[2,35] The storage ring was a two-kilometer long elliptical pipe (160 x 52 millimeters), and a vacuum less than 10^{-10} Torr was achieved. Each vacuum chamber was fitted with two metal plates, about 20 centimeters long and 10 centimeters wide. The plates were used as electrodes, mounted opposite each other in the horizontal plane such that an electric field can be applied between them. One of the metal plates in each vacuum chamber was connected to the vacuum chamber and grounded. The other plate

was connected to an alternating current power supply, which could supply approximately 0.5 A while maintaining 400-500 V_{rms} between the electrode it was connected to and ground. Glow discharge with argon gas combined with bakeout as a method of cleaning was used to induce desorption by ion impact of gas adsorbed at the surface and to substitute in its place a layer of the more inert argon gas used in discharge, which would subsequently be desorbed in the course of bakeout.

Glow discharge treatment was carried out intermittently in the course of a 15-hour bakeout at 300° C, with the argon gas pressure being 3×10^{-2} Torr. The first discharge cleaning treatment occurred three hours after the vacuum system had first reached 300° C. The discharge cleaning was run for one hour. Four hours after the first discharge cleaning treatment, another discharge cleaning treatment was initiated. Three discharge cleaning treatments were run during the 15-hour bakeout. The final discharge cleaning treatment was followed by three hours of normal bakeout.

Measurements on the cleaning efficiency were carried out at different times after termination of the final bakeout. The first measurements were conducted 20 hours after bakeout, when the base pressure was 1.8×10^{-10} Torr. The value of the efficiency of desorption for the treated area was one order of magnitude lower than for untreated surfaces. The base pressure

reduced to 1 x 10^{-10} Torr during the next 100 hours, and the difference between desorption efficiencies for treated and untreated surfaces increased. After 135 hours, the sublimation pumps, which provide some gettering cleaning, were first fired and then refired at 160 and 250 hours. The base pressure decreased to 2 x 10^{-11} Torr, and the desorption efficiency for the untreated surface remained constant within $\pm$6%, whereas the desorption efficiency for the treated surface had a percentage which decreased as base pressure decreased. 40% H_2, 40% CO, 10% CH_4, and 10% H_2O were the residual gases released during argon glow discharge.

The combination cleaning method brought the pressure in the vacuum system to 10^{-10} Torr, which was further reduced after gettering via sublimation pumps. The glow discharge treatment did not influence the low pressure limit, and the argon discharge gas was efficiently removed from the vacuum chamber. With glow discharge applied, the vacuum surface retained its low desorption characteristic even after contamination with room air.

Further experiments with combination baking and glow discharge were made on sample stainless steel pipes of approximately 100 meters in length at CERN.[18] A mixture of 90% argon and 10% oxygen was the discharge gas used, run at a pressure of 2 x 10^{-3} Torr. A wire stretched through the middle of the chamber served as anode, while the vacuum chamber, kept at

300° C, was the grounded cathode. A voltage of 350 V was applied, while the ion dose was larger than 10^{18} ions/cm^2. A 300-350° C bakeout after glow discharge eliminated the argon contamination present. The glow discharge cleaning did not commence until 24 hours of baking the vacuum chamber.

The results corresponded to those obtained with the CERN Intersecting Storage Rings. 28 monolayers of carbon monoxide were removed. The desorption yield for carbon monoxide was reduced to less than 0.01, although when the vacuum chamber was subjected to a subsequent bakeout to remove residual argon, the carbon monoxide desorption yield rose slightly. Auger electron spectroscopy confirmed an important reduction of the carbon content under the influence of the glow discharge, especially if 10% oxygen was added to the argon discharge gas in CERN. Baking and argon and oxygen glow discharge effectively cleaned the pipes of their contaminants, hydrogen, and argon.

5.3.1.2.3 Colliding Beam Accelerator

The colliding beam accelerator (CBA), under construction at Brookhaven, consists of two rings having a circumference of 3.8 kilometers each.[7] Low pressures are needed for the functioning of the CBA, and a combination of baking and glow discharge were used to clean the vacuum chambers. The beam tubes are made of 304 LN stainless steel and are 8.8 centimeters in diameter and up to 5.5 meters in length. The inner surface area is 1.5 m^2.

The beam tubes were glow discharged cleaned before installation. A 0.5-millimeter diameter tungsten wire was positioned through the center of the tube to insure uniform discharge cleaning along the length of the tube. It served as the anode and the heating element during bakeout. With a 7 A current, the wire reached a temperature of approximately 1700° C and provided approximately 300 watts of radiant heat to the 5.5-meter long beam tube. A baking temperature of more than 200° C could be achieved in four hours. An isolation transformer heated the tungsten wire, while an ion pump power supply, controlled by an 8 kW Variac, supplied the direct current power required for glow discharge cleaning. Argon or a mixture of argon with 10% oxygen discharge gas was used. A voltage of 350 V and a total dosage of 2×10^{13} ions/cm^2 were the discharge parameters chosen. At a current density of 20 μA/cm^2, the temperature of the vacuum surface was around 225° C.

The beam tubes were vacuum degassed at 500° C for approximately ten hours before glow discharge cleaning began. They were then vacuum baked at temperatures of 200° C or higher for approximately sixteen hours. Glow discharge was initiated with the determined parameters as argon or argon with 10% oxygen discharge gas was run through the vacuum chamber. The first glow discharge cleaning used pure argon as the discharge gas. The second glow discharge cleaning, with an argon and 10% oxygen mixture discharge gas, used a total ion dosage of 1×10^{18} ions/cm^2 and was run after the tube was stored in atmosphere for three months.

The results of the glow discharge cleaning showed very effective carbon removal as well as the removal of other contaminants. The total amount of carbon desorbed by pure argon discharge gas was about 80 monolayers, with the discharge ion dose being 2×10^{18} ions/cm^2. The total carbon desorbed by the second glow discharge, with a dosage of 1×10^{18} ions/cm^2, was equivalent to approximately 20 monolayers of carbon monoxide, suggesting the adsorption of atmosphere carbon, during the three month storage of the tube in air, did not exceed surface saturation.

The effectiveness of carbon removal by glow discharge cleaning with an argon and 10% oxygen mixture discharge gas was larger than that of glow discharge cleaning with pure argon discharge gas. The oxygen in the mixture was almost completely consumed, especially at a high discharge current. Approximately 550 monolayers of carbon monoxide were removed using argon and 10% oxygen as the discharge gas. Surface carbon deposited or diffused out of the bulk was more easily desorbed in the presence of activated oxygen. Water vapor and hydrogen were removed more efficiently and with comparable efficiency, respectively, in glow discharge cleaning with an argon and 10% oxygen discharge gas than with pure argon as the discharge gas.

Baking and glow discharge was an effective combination cleaning method for the accelerator beam tubes. The baking reduced thermal desorption, while the glow discharge removed the more tightly bound contaminants. Carbon, water vapor, oxygen, and hydrogen were efficiently removed, and the vacuum system could be operated at a stable base pressure of 10^{-11} Torr.

5.3.2 Discharge Cleaning/Gettering

Another combination cleaning method involves combining discharge cleaning and gettering procedures. This combination cleaning procedure has been used by many of the recently-built tokamaks. Discharge cleaning effectively removes contaminants bound to the surface and near-surface region of the metal, especially carbon, some water, some hydrogen, and some oxygen. Gettering removes most of the remaining hydrogen and oxygen contaminants. Low outgassing rates and base pressures are obtained in ultrahigh vacuum systems using this combination.

Experiments were performed using the discharge cleaning and gettering combination cleaning method on the Impurity Study Experiment (ISX-A) tokamak.[16] The toroidal vacuum chamber, with a major radius of 92 centimeters and a minor radius of 26 centimeters, was made of 304 stainless steel. The titanium for the gettering was mainly deposited on the top of the vacuum vessel. The discharge cleaning used hydrogen as the discharge

gas. After 4 1/2 months of overnight discharges, titanium gettering was employed and discharge cleaning was discontinued. The titanium was sublimed during either 1-hour or 10-minute depositions between tokamak discharges.

The results proved very useful as to the cleaning effectiveness of discharge cleaning and gettering. After discharge cleaning, a base pressure of 10^{-8} Torr was established. After titanium gettering, the base pressure lowered to 10^{-9} Torr. The addition of titanium gettering to hydrogen discharge cleaning reduced the total pressure by an order of magnitude mostly because of the much higher pumping speed of the titanium surface for hydrogen. Hydrogen discharge cleaning and titanium gettering both reduced impurities like carbon and oxygen efficiently. Impurity gas levels remained more than an order of magnitude below the levels achieved without gettering.

Discharge cleaning combined with gettering is an effective cleaning method, especially when removal of carbon, hydrogen, and oxygen is the intended result. Titanium can even be sublimed using the wire representing the anode in discharge cleaning with this set up.

6. Gravity Wave Detector Cleaning

The gravity wave detector system is made up of 5-kilometer, 4-foot diameter, stainless steel tubes. These tubes will be constructed by 40-foot long tube sections. In order to reduce and stabilize the base pressure of the vacuum system to 10^{-8} Torr or below, effective cleaning of the stainless steel tubes must occur.

6.1 Impurity Problems

Stainless steel 304 L is the proposed material for the construction of the gravity wave detector vacuum chambers. Unconditioned stainless steel surfaces contain many contaminants, with carbon and oxygen being the most prominent. Major outgassing components include water vapor, carbon monoxide, carbon dioxide, and hydrogen. These residual gases and contaminants should be reduced to low concentrations to obtain the outgassing rate of 10^{-12} Torr-liter/sec-cm^2 desired for the vacuum system.

The more tightly bound contaminants, in the near-surface region, should not create serious difficulties for the gravity wave detector vacuum system because no induced desorption from ions or electrons should occur. The laser beam is made of photons which will be concentrated in the beam with as little scattering as possible. Those photons scattering towards the

vacuum surface will have long distances to travel before hitting the surface, decreasing the amount of energy they contain when hitting the surface. Therefore, induced desorption should not be a problem.

6.2 Suggested Cleaning Methods

6.2.1 Pretreatment

Various pretreatment techniques are available for stainless steel. In the Varian report, pretreatment techniques combined with baking are compared according to outgassing rates of various residual gases on 304 or 304 L stainless steel bell jars, each with a 30-inch length and an 18-inch diameter.[33]

The standard Varian cleaning treatment for 304 stainless steel consists of: 1) vapor degreasing in trichlorethylene 2) cleaning in Oakite 3) hot water rinse 4) 33% HNO_3, 33% HF, 33% H_2O bath, by volume at room temperature and 5) H_2O rinsing, dry, and bag. The stainless steel is then placed in an oven to receive a 150° C bake for 24 hours.

The results of the standard Varian cleaning treatment on the stainless steel samples are shown in Figure 2 and Figure 3. After pumping down the vacuum chamber for 33 1/3 hours, the outgassing rates of CO, CH_4, C_3H_8, and CO_2 are all below 10^{-13} Torr-liter/sec-cm^2. The outgassing rates for H_2O, H_2, N_2, and O_2 are reduced to below 10^{-11} Torr-liter/sec-cm^2. Hydrogen gas

has the highest outgassing rate of approximately 6×10^{-12} Torr-liter/sec-cm^2. It is likely that the room temperature equilibrium hydrogen outgassing rate after bakeout is the same as it was prior to bakeout because a 150° C, 24-hour bakeout is not sufficient to significantly deplete the hydrogen that is dissolved in the bulk of the stainless steel. The final outgassing rates are shown in Table 1, where the final total outgassing rate obtained is approximately 4.8×10^{-12} Torr-liter/sec-cm^2.

Another pretreatment technique involves only vapor degreasing the sample in trichlorethylene after it has been assembled. The sample is then placed in an oven to receive a 150° C bake for 24 hours.

The results are shown in Figure 4 and Figure 5. Outgassing rates for CO, CH_4, C_3H_8, and CO_2, after pumping down about 33 1/3 hours, are reduced to below 10^{-13} Torr-liter/sec-cm^2. Outgassing rates for H_2O, H_2, N_2, and O_2 are reduced to below 10^{-11} Torr-liter/sec-cm^2. Again, hydrogen gas has the highest outgassing rate of approximately 3×10^{-12} Torr-liter/sec-cm^2. This is probably because a 150° C bake for 24 hours does not sufficiently reduce the bulk hydrogen. Initially, before pump down, most outgassing rates are higher for the standard Varian cleaning sample than for the only-degreased sample. Before bakeout started, most outgassing rates are higher for the only-

degreased sample than for the standard Varian cleaning sample because of slower pump down rates. After bakeout, both samples have essentially the same room temperature outgassing rates.

The third pretreatment technique tested involves treating the stainless steel sample with the Diversey DS-9 process without the additional bakeout. The results are shown in Figure 6. The outgassing rates obtained after approximately 46 hours of pump down are below 10^{-10} Torr-liter/sec-cm^2. Water vapor has the highest outgassing rate of 7×10^{-11} Torr-liter/sec-cm^2. The measured outgassing rates are, in nearly all cases, higher than those obtained in comparable situations from samples cleaned by the standard Varian cleaning treatment. The net result is a higher total outgassing rate for the DS-9 treated sample than for the standard Varian cleaning treated sample.

Pretreatment of the stainless steel vacuum tubes before installation for the gravity wave detector is necessary and worthwhile. Surface contaminants and outgassing components can be reduced considerably. After pretreatment, baking before installation at higher temperatures, like 300° C or more, seems to be beneficial in sufficiently removing the bulk hydrogen and reducing the outgassing rates of most of the prominent outgassing components.

6.2.2 Major Cleaning

The major cleaning of the gravity wave detector system can be done either before installation or *in situ*. Because the gravity wave tubes are very large, the easiest and probably the most cost effective method is to clean each tube in 40-foot sections before installation. Then, the surfaces to be cleaned are smaller and cleaning equipment can be used again for each section. An *in situ* cleaning technique must be devised to remove the contaminants which enter the tube during installation and in case the vacuum, in the future, needs to be brought up to atmosphere.

6.2.2.1 Baking

One of the necessary cleaning techniques is baking. Baking the stainless steel tube is necessary to sufficiently remove the bulk hydrogen and, if glow discharge cleaning is also used, to prevent readsorption of desorbed contaminants and adsorption of the discharge gas. The baking can be done before and after glow discharge cleaning or during glow discharge cleaning. Just baking the gravity wave vacuum tubes requires high temperatures for a reasonable length of time. But an *in situ* bakeout must be done after installation and after each time the vacuum system is brought up to atmosphere, and this is very costly. Even a low temperature bake at 100-150° C of the 5-kilometer, 4-foot diameter tube requires a large amount of power.[12] *In situ* baking is very costly and inconvenient.

6.2.2.2 Inert Glow Discharge

Glow discharge cleaning is also an effective cleaning technique when combined with baking. Both Dr. Chou and Dr. Dylla recommend inert gas discharge cleaning with baking.[30,31,32] Inert glow discharge cleaning without baking does not remove the bulk hydrogen or prevent adsorption of the inert discharge gas.

Figures 7-11[14] show the results of discharge cleaning with inert gases on cylindrical stainless steel discharge tubes 15.7 centimeters in diameter and 75 centimeters in length. These experiments were performed by Govier and McCracken, with a glow discharge run through an axial stainless steel electrode.[14] The discharge tube was first baked under vacuum to 450° C for 20 hours, then exposed to atmosphere for 30 minutes before being re-evacuated.

Twenty hours after glow discharge cleaning for approximately 30 minutes with helium, neon, and argon, the outgassing rates of water vapor, carbon dioxide, and carbon monoxide reduced significantly. Hydrogen and the inert gas, though, had high partial pressures and outgassing rates. From Table 2,[14] the outgassing rates did not reduce after inert glow discharge cleaning alone. But even before inert glow discharge cleaning, the 450° C bakeout for 20 hours only brought the outgassing rate down to approximately 10^{-10} Torr-liter/sec-cm^2.

Inert glow discharge cleaning must be combined with a bakeout before and after or during the discharge cleaning period. For the gravity wave vacuum tubes, both Dr. Chou and Dr. Dylla recommend before installation baking and inert glow discharge cleaning of the 40-foot sections.[30,31,32]

6.2.2.3 Recommendations

6.2.2.3.1 Dr. T. S. Chou

Dr. Chou recommends a method similar to that used on the ISABELLE accelerator at Brookhaven.[30,31] A vacuum firing at high temperatures (800-950^{0} C) is done before glow discharge. A 90% argon and 10% oxygen discharge gas is then run, using a 20-30 μm tungsten wire run along the center of the tube. The amount of current used is about 10 $\mu A/cm^2$ with an anode-cathode potential of 350 V. The bombardment rate is 10^{18} ions/cm^2, with the discharge gas pumped into the system at a pressure between 2-5 x 10^{-2} Torr.

Dr. Chou recommends that the glow discharging is done on the 40-foot tube sections one at a time, with the tube sections separated from each other by rubber seals. After all the 40-foot tube sections are cleaned, an automatic welding machine is used to weld each section together. Throughout the welding process, low-pressure argon gas is run through the 40-foot tube sections, and, after the system is assembled as a whole, the entire tube is flushed with argon to remove contaminants which enter the vacuum tube during the welding process.

6.2.2.3.2 Dr. H. F. Dylla

Dr. Dylla also suggests an extensive cleaning method using a combination of baking and inert glow discharge cleaning.[32] He suggests a high temperature (450° C) bakeout, for a time length determined by the thickness of the metal, followed by a glow discharge for each 40-foot tube section. This is one of the most cost effective methods for baking and glow discharging the vacuum tube.

The glow discharge is run with a current density of 1-5 $\mu A/cm^2$, with the voltage determined by the discharge (up to 600 V). The discharge gas is either a mixture of helium and oxygen to eliminate most of the carbon contamination or hydrogen to eliminate most of the water vapor contamination. A wire running through the center of the tube is the positive anode, while the stainless steel tube is the negatively grounded cathode. When the system is fully assembled into the 5-kilometer tubes, warm nitrogen gas is run through the tubes at a few hundred milliTorrs to obtain the final pressure desired.

If cleaning is still necessary after the assembly and sealing of the 5-kilometer tubes, an <u>in situ</u> glow discharge could be run using a 95% helium and 5% oxygen mixture discharge gas. Hopefully, though, the treatment of baking and glow discharge cleaning of the 40-foot sections will be sufficient to remove most of the contaminants likely to naturally outgas. Dr. Dylla

says that it would be most cost effective if an in situ glow discharge is not necessary. Then only a direct current power supply for the glow discharge and baking equipment needed for baking a 40-foot tube section to 450° C is required.

6.2.2.3.3 CERN accelerators

Another combination baking and inert glow discharge cleaning method that may be effective in cleaning the gravity wave detector system is the method used on the CERN accelerators.[3,18] Table 3[18] shows the results of the CO desorption yield in stainless steel after a pretreatment cleaning, a 24-hour bakeout at 300° C, glow discharge cleaning, and another bakeout for 24 hours at 300° C.

The glow dicharge gas is a mixture of 90% argon and 10% oxygen run at a pressure of 2×10^{-2} Torr. A voltage of 350 V is applied to a wire stretched in the middle of the chamber, which is kept at a temperature of 300° C. The ion dose is 10^{18} ions/cm^2.

Carbon monoxide is monitored as it is the major outgassing component left after the 24-hour bakeout at 300° C before glow discharge treatment. The outgassing of hydrogen gas and methane is minimal after baking and very low after glow discharge cleaning. The carbon monoxide desorption yield is still high after baking but is reduced to at least a factor of 100 less. The argon gas is effectively removed by the subsequent bakeout.

6.2.2.3.4 Optimal Method suggestion

Instead of inert discharge gas, hydrogen gas can also be used as a discharge gas in these methods. Hydrogen has a lower removal rate of carbon, but oxygen is completely removed by water formation. Hydrogen glow discharge with low temperature electrons may even be a feasible in situ glow discharge method.

An optimal method of cleaning that might be more cost effective than just baking the tube sections at high temperatures and then baking the 5-kilometer tube in situ at low temperatures (which is necessary to remove the hydrogen and contaminants which enter the tube during installation and when the tube is brought up to atmosphere) is to bake the 40-foot tube sections at high temperatures to bring the outgassing rate down to 10^{-11} to 10^{-12} Torr-liter/sec-cm^2, and then assemble the 5-kilometer tube, running a hydrogen glow discharge in situ. The hydrogen glow discharge can be run with low temperature electrons at 350 V with a current density of 5-10 $\mu A/cm^2$. Anode rings can be used, since a central wire interferes with the laser interferometer. The rings can be positioned at regular intervals (maybe 100-200 meters apart).

The tube will be cleaned of the surface contaminants present from installation, and after glow discharge cleaning, a stainless steel vacuum tube, brought up to atmosphere, only recontaminates at the surface level. Therefore, the vacuum system can be brought up to atmosphere and easily re-cleaned by a short hydrogen glow discharge when pumped down again.

6.3 Experimentation

Experimentation is very important for determining the optimal method of cleaning the gravity wave detector vacuum system at the least cost. Both Dr. Dylla and Dr. Taylor stress the need for experiments on smaller prototypes of the gravity wave detector.[12,32] Dr. Dylla recommends that at least a year of laboratory research be done before deciding on the optimal cleaning method.[32] All methods should be tried, with results compared side-by-side. Combinations of pretreatment (Varian, Diversey DS-9, etc...), baking, and/or glow discharge cleaning (inert or hydrogen) should be experimented upon, as well as extensive cleaning before installation or <u>in situ</u>. Only by experimentation will the most beneficial cleaning method for the gravity wave detector system be determined.

7. <u>Conclusion</u>

In order for the gravity wave detector to be able to detect gravity waves with amplitudes as small as 10^{-22}, the multi-laser interferometer must be stored in a vacuum system with a base pressure at least as low as 10^{-8} Torr. The vacuum system is made out of two 304 L stainless steel tubes, each with a length of 5 kilometers and a diameter of 4 feet.

Untreated 304 L stainless steel contains many impurities, including carbon, oxygen, and hydrogen. When the pressure is as low as 10^{-8} Torr inside of the stainless steel tube, these impurities start to desorb from the surface into the

vacuum space. This desorption raises the vacuum pressure. In order to obtain a stable vacuum pressure of 10^{-8} Torr, these impurities must be removed by cleaning the stainless steel tubes.

Cleaning processes for ultrahigh vacuum systems include pretreatment, baking, discharge cleaning, and/or gettering. The gravity wave detector vacuum system needs a thorough cleaning of thermal outgassing components as well as surface cleaning of strongly bound molecules. Extensive cleaning of the 40-foot tube sections before construction of the 5-kilometer tubes is the most cost efficient plan. An in situ cleaning method must be devised, though, to remove the surface contaminants present in the vacuum system after installation and after each time the vacuum system is brought up to atmosphere and then re-evacuated.

The most recommended method of cleaning the vacuum tube is a combination of baking at high temperatures and glow discharge cleaning with either inert gas or hydrogen gas. The 40-foot tube sections are first pretreated with a known effective chemical/physical process, like the standard Varian cleaning process or the Diversey DS-9 process. They are then baked at temperatures above 450° C at a time length determined by the thickness of the metal and the amount of bulk hydrogen removed. An inert glow discharge with argon/oxygen or helium/oxygen discharge gas can be run during the bakeout of the 40-foot tube sections, thereby making sure that the inert discharge gas is removed from the vacuum system. This extensive cleaning method

is cost efficient as it only uses equipment necessary for baking and glow discharge cleaning 40-foot tube sections, not a 5-kilometer tube.

Instead of glow discharge cleaning during the bakeout, an *in situ* low electron temperature hydrogen glow discharge can be run using anode rings placed 100-200 meters apart or a distance determined by experimentation. This will provide the *in situ* method necessary for after installation cleaning and for cleaning each time the vacuum system is brought up to atmosphere and then re-evacuated.

Experimentation on prototypes is very necessary for determining the efficient and cost effective cleaning method for the gravity wave detector system. The most efficient parameters, such as temperature of bake, discharge gas, set up, etc... can be determined by comparisons of data in the laboratory. Time, money, and effort need to be spent on laboratory research work for the most reliable cleaning of the gravity wave detector.

LIST OF TABLES

AND

FIGURES

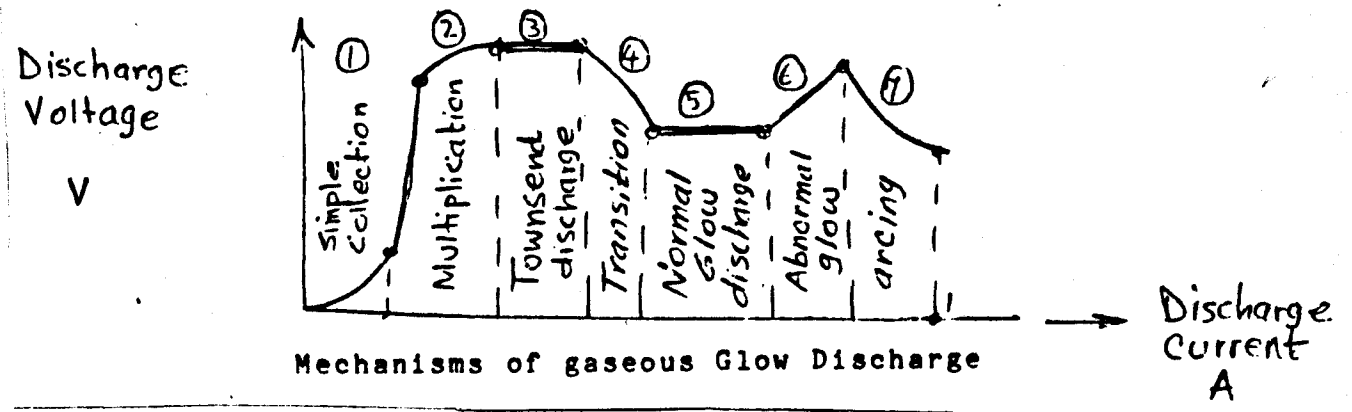

Mechanisms of gaseous Glow Discharge

FIGURE 1

NORMAL AND TOWNSEND DISCHARGE HAVE STABLE GLOW

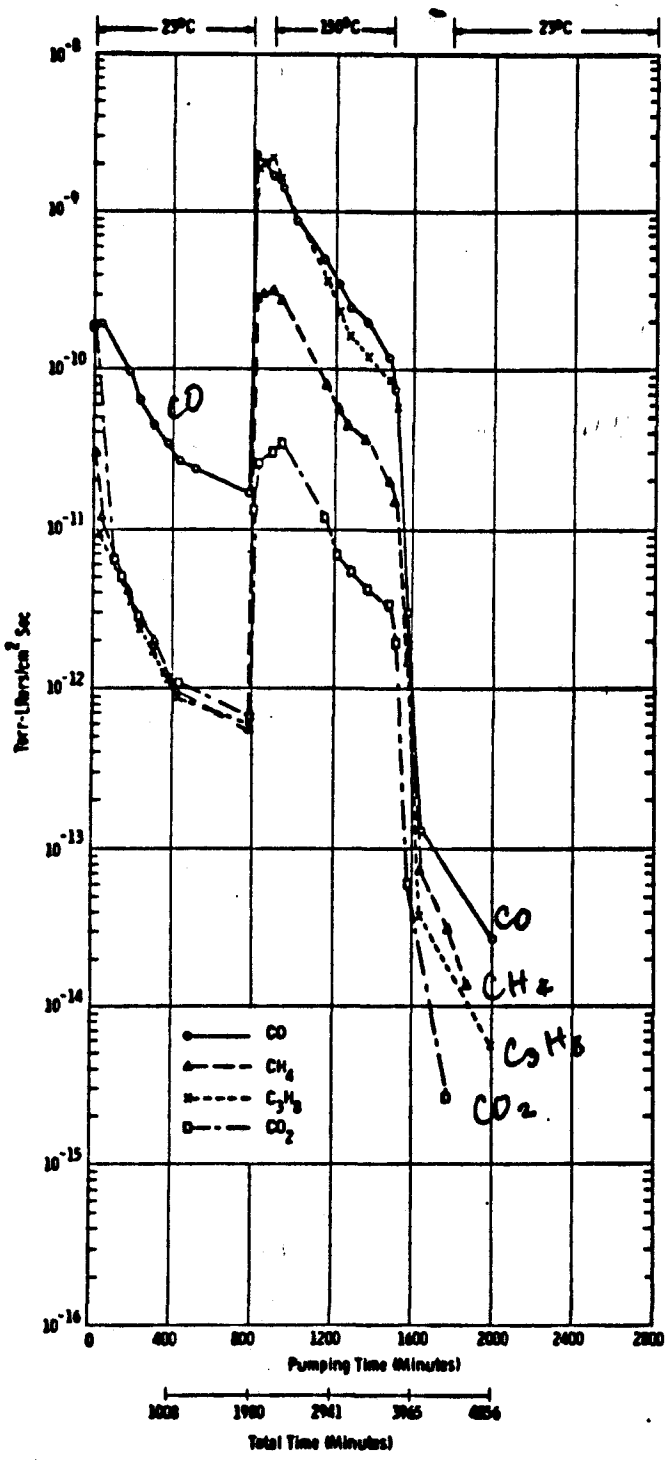

Outgassing Rates for CO, CH_4, C_3H_8, CO_2 from Sample with 33% HF Cleaning

FIGURE 2 VARIAN REPORT

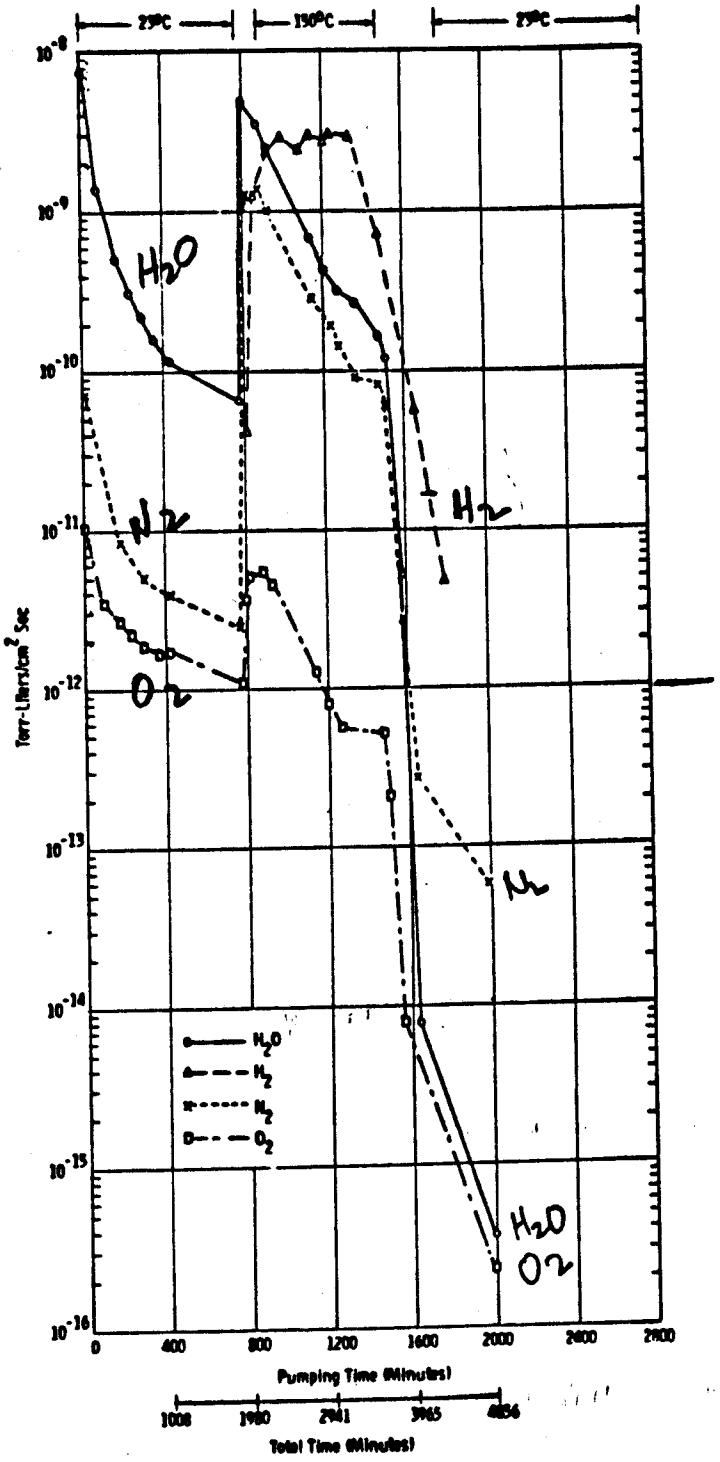

Outgassing Rates for H_2O, H_2, N_2, O_2 from Sample with 33% HF Cleaning

FIGURE 3 VARIAN REPORT

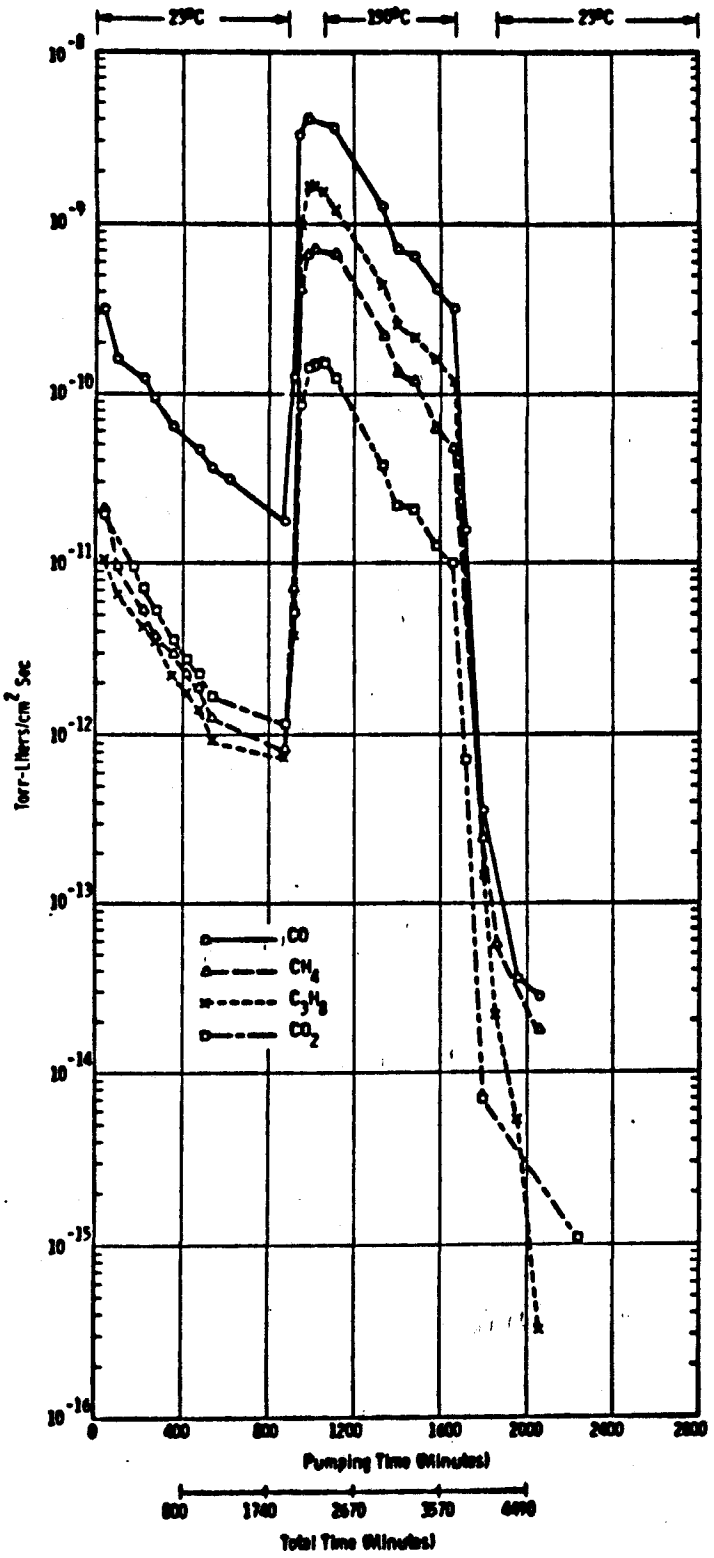

Outgassing Rates for CO, CH_4, C_3H_8, CO_2 from Sample with Only-Degreasing

FIGURE 4 VARIAN REPORT

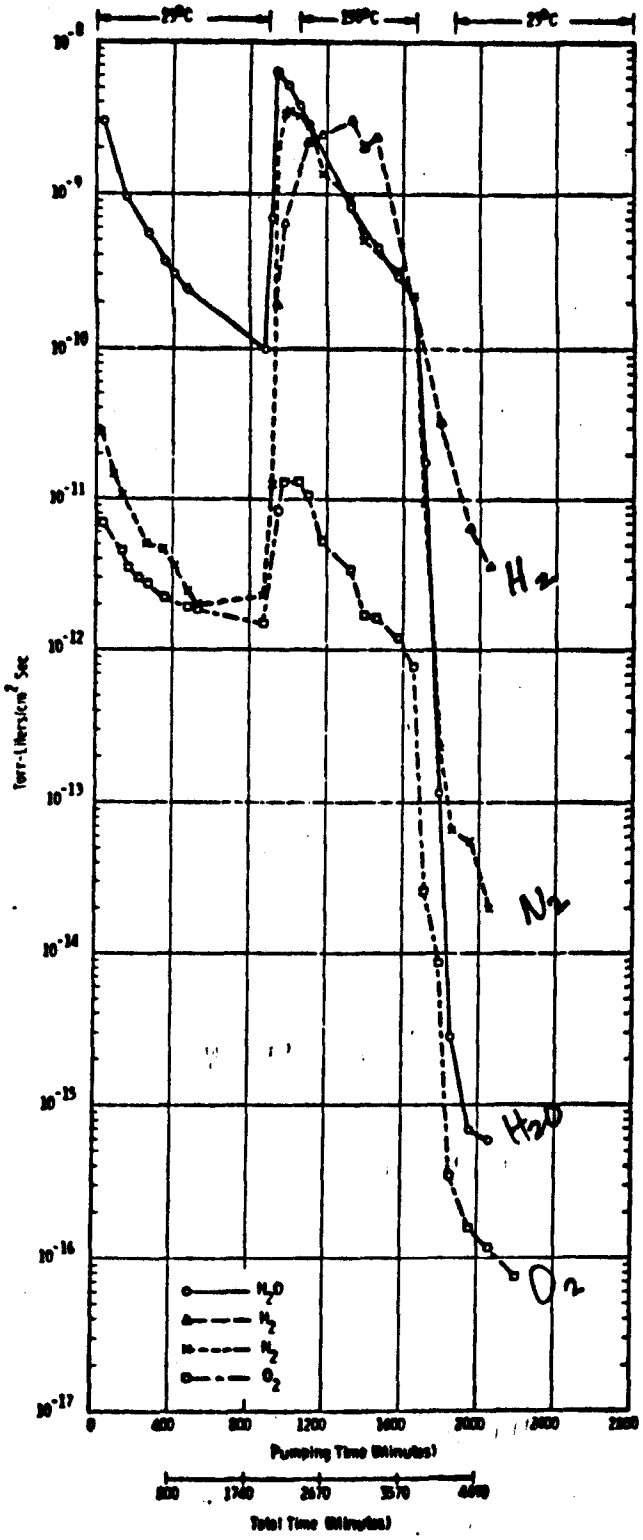

Outgassing Rates for H_2O, H_2, N_2, O_2 from Sample with Only-Degreasing

FIGURE 5

VARIAN REPORT

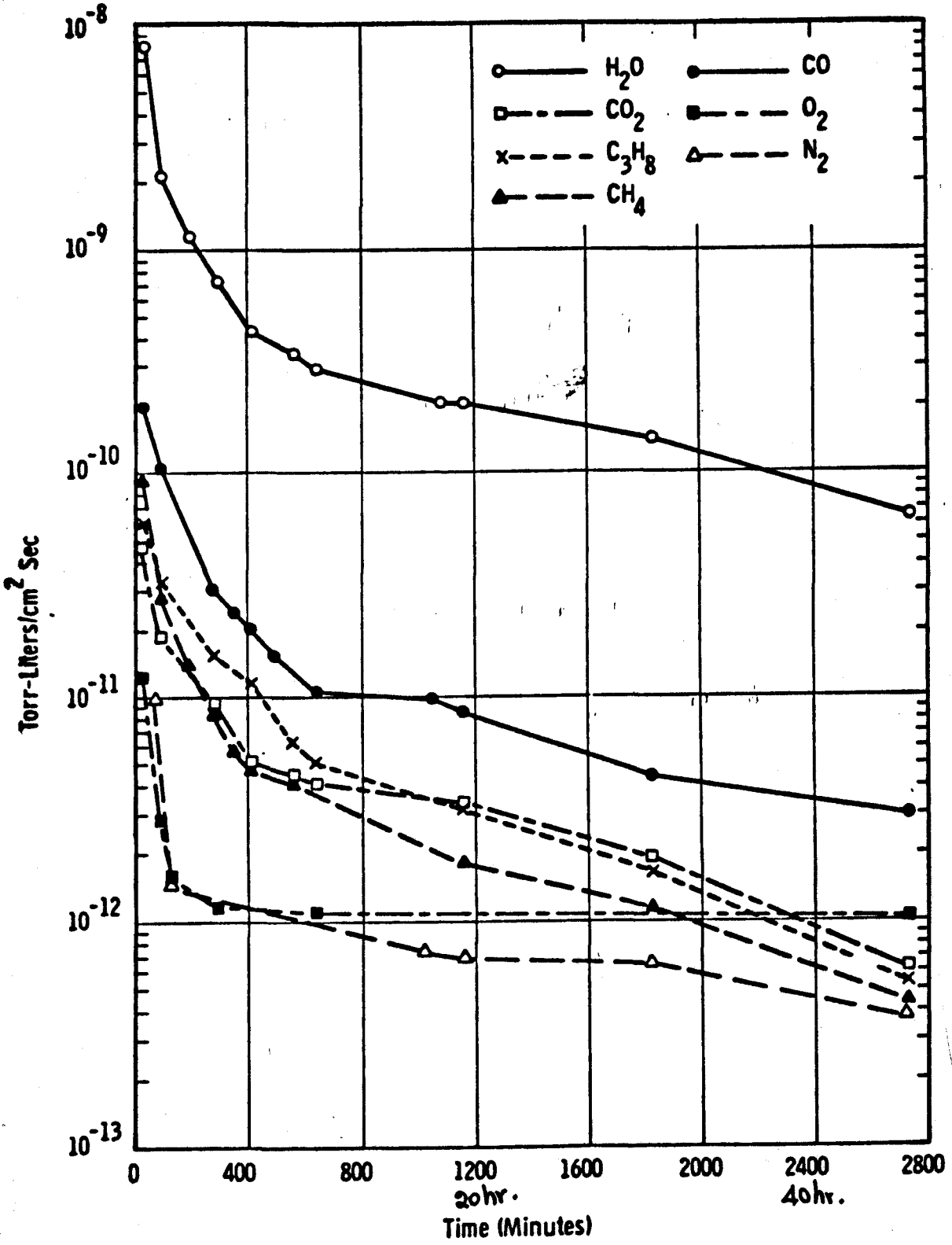

Outgassing Rates for Sample Cleaned by Diversey DS-9 Cleaning

FIGURE 6

VARIAN REPORT

NO BAKEOUT NEEDED

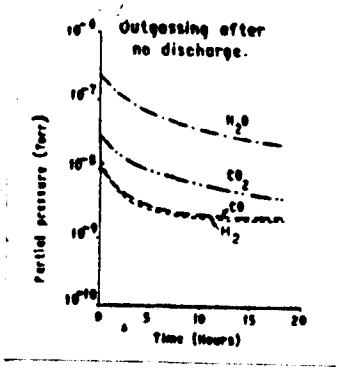

FIGURE 7

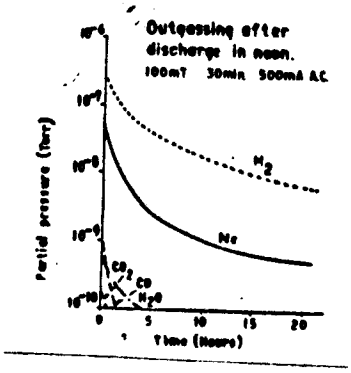

FIGURE 8

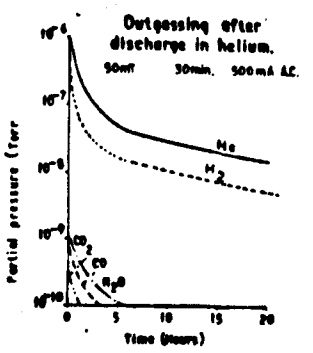

FIGURE 9

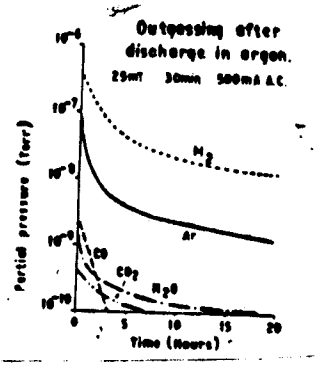

FIGURE 10

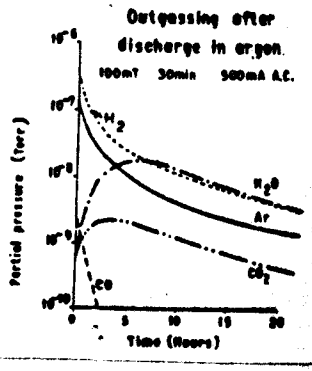

FIGURE 11

SYSTEM PARTIAL PRESSURES MEASURED AS A FUNCTION OF TIME IMMEDIATELY AFTER DISCHARGE CLEANING.

GOVIER AND McCRACKEN REPORT

AT ~100 MINUTES INTO THE PUMPDOWNS:

Outgassing Rates

Gas	With 33% HF Cleaning (Torr-liter/sec-cm²)
H_2O	1.4×10^{-9}
CO	1.8×10^{-10}
CO_2	1.0×10^{-11}
O_2	3.5×10^{-12}
CH_4	1.1×10^{-11}
C_3H_8	8.7×10^{-12}

TABLE 1

VARIAN REPORT

TABLE Outgassing rate of different gas species 20 h after discharge cleaning (10^{-10} Torr liter sec^{-1} cm^{-2}).

	No discharge	He discharge	Ne discharge	Ar discharge
Rare gas	...	1.4	0.02	0.03
H_2O	0.87	...	...	...
CO_2	0.09	...	...	...
CO	0.06	...	...	...
H_2	0.25	0.6	0.83	1.5
Total	1.3	2.0	0.9	1.5
Total pressure (10^{-8} Torr)	3.1	2.3	0.8	1.4

TABLE 2

GOVIER AND McCRACKEN REPORT

CO Desorption Yield (η_{CO}) in molecules/ion from three different materials after a sequence of treatments

After :	stainless steel	pure aluminium	titanium alloy
cleaning	10	8.5	9
bakeout 24 h 300°C	1.8	1.2	1.8
discharge 10^{18} ions/cm^2	<0.01	< 0.01	< 0.01
bakeout 24 h 300°C	0.15	0.05	0.12
air 12 h 1 bar	5	5.5	4
bakeout 24 h 300°C	0.9	0.4	0.7

TABLE 3

CERN ACCELERATORS

REFERENCES

1. Dylla, H. F., "A Review of the Wall Problem and Conditioning Techniques for Tokamaks," Journal of Nuclear Materials, Vol. 93 & 94, North-Holland Publishing Company, c 1980, pp. 61-74.

2. Dylla, H. F., Cohen, S. A., Rossnagel, S. M., McCracken, G. M., Staib, Ph., "Glow Discharge Conditioning of the PDX Vacuum Vessel," 26th National Symposium of the American Vacuum Society, New York, c 1979.

3. Jones, A. W., Jones, E., and Williams, E. M., "Investigation by Techniques of Electron Stimulated Desorption of the Merits of Glow Discharge Cleaning of the Surfaces of Vacuum Chambers at the CERN Intersecting Storage Rings," Vacuum, Vol. 23, Pergamon Press, Great Britain, c 1973, pp. 227-230.

4. McCracken, G. M. and Stott, P. E., "Plasma-Surface Interactions in Tokamaks," Nuclear Fusion, Vol. 19, c 1979, pp. 889-972.

5. Holland, L., "Treating and Passivating Vacuum Systems and Components in Cold Cathode Discharges," Vacuum, Vol. 26, Pergamon Press, Great Britain, c 1976, pp. 97-103.

6. Stott, P. E., Daughney, C. C., and Ellis, R. A. Jr., "Control of Re-cycling and Impurities in the ATC Tokamak By Means of Gettered Surfaces," Nuclear Fusion, Vol. 15, c 1975, pp. 431-439.

7. Hseuh, H. C., Chou, T. S., and Christianson, C. A., "Glow Discharge Cleaning of Stainless Steel Accelerator Beam Tubes," Journal of Vacuum Science Technology, Vol. 3, American Vacuum Society, c 1985, pp. 518-522.

8. Weston, James P. and Balwanz, William W., "Surface Cleaning by Glow Discharge in a High-Volume Gas Flow," Naval Research Laboratory, Washington D. C., c 1976, pp. 1-55.

9. Chou, T. S. and Hseuh, H. C., "D. C. Glow Discharge Cleaning For Accelerator," Proceedings: Tenth International Symposium on Discharges and Electrical Insulation in Vacuum, South Carolina, c 1982, pp. 1-4.

10. Mathewson, A. and Achard, Marie-Helene, "The Temperature Dependence of the Surface Composition and Electron and Ion Induced Gas Desorption Coefficients of Inconel 718 and 316 L + N Stainless Steel," Proceedings 7th International Vacuum Congress and 3rd International Conference Solid Surfaces, Vol. 2, Vienna, c 1977, pp. 1217-1220.

11. Oren, L. and Taylor, R. J., "Trapping and Removal of Oxygen in Tokamaks," Nuclear Fusion, Vol. 17, c 1977, pp. 1143-1151.

12. Killian, David, "Discussion with Dr. R. J. Taylor," Interoffice Memorandum, J. P. L., Pasadena, c 1985, pp.1-3.

13. Lansing,F. L., "Glow Discharge Cleaning for GWO," Interoffice Memorandum, J. P. L., Pasadena, c 1985, pp. 1-10.

14. Govier, R. P. and McCracken, G. M., "Gas Discharge Cleaning of Vacuum Surfaces," Journal of Vacuum Science and Technology, Vol. 7, c 1970, pp. 552-556.

15. Clausing, R. E. et al., "Wall Conditioning by Low Power Discharge in the ISX-A Tokamak," Journal of Vacuum Science Technology, Vol. 16, American Vacuum Society, c 1979, pp. 918-923.

16. Simpkins, J. E., Colchin, R. J., and Overbey, D. R., "Residual Gas Analysis in the ISX-A Tokamak," Journal of Vacuum Science Technology, Vol. 16, American Vacuum Society, c 1979, pp. 763-765.

17. Staib, Ph., Dylla, H. F., and Rossnagel, S. M., "X-ray Photoelectron Spectroscopy (XPS) Studies of Oxygen and Carbon Bonding to Tokamak Walls," Journal of Vacuum Science Technology, Vol. 17, American Vacuum Society, c 1980, pp. 291-293.

18. Fischer, E., "Ultrahigh Vacuum Technology for Storage Rings," IEEE Transactions on Nuclear Science, Vol. NS-24, No. 3, Geneva, c 1977, pp. 1227-1232.

19. Paschenrieder, W., Staudenmaier, G., and Staib, P., "Conditioning of ASDEX By Glow Discharge," Journal of Nuclear Materials, Vol. 93 & 94, North-Holland Publishing Company, c 1980, pp. 322-329.

20. Winter, J. et al., "On the Cleaning of First Wall Materials By Glow Discharges in Hydrogen," Journal of Nuclear Materials, Vol. 93 & 94, North-Holland Publishing Company, c 1980, pp. 812-819.

21. Colchin, R. J. et al., "Plasma-Wall Impurity Experiments in ISX-A," Journal of Nuclear Materials, Vol. 76 & 77, North-Holland Publishing Company, c 1978, pp. 405-411.

22. Taylor, R. J., "Surface Interactions and Conditioning Techniques in Tokamaks," Journal of Nuclear Materials, Vol. 76 & 77, North-Holland Publishing Company, c 1978, pp. 41-43.

23. Emerson, L. C., Clausing, R. E., and Heatherly, L., "Surface Impurities Studies During the Start-Up and Early Operations of ISX-A Using a Surface Analysis Station With Sample Transfer," Journal of Nuclear Materials, Vol. 76 & 77, North-Holland Publishing Company, c 1978, pp. 472-476.

24. TFR Group, "Surface Conditioning and Mass Spectroscopy in the TFR-600 Tokamak," Journal of Nuclear Materials, Vol. 76 & 77, North-Holland Publishing Company, c 1978, pp. 587-592.

25. Holland, L. and Rizk, A. S., "The Effects of Treating Plane and Hollow Components of Stainless Steel and Inconel in Glow Discharges," Journal of Nuclear Materials, Vol. 76 & 77, North-Holland Publishing Company, c 1978, pp. 605-607.

26. Clausing, R. E. et al., "Surface Impurities and Clean-Up Techniques in ORMAK," Journal of Nuclear Materials, Vol. 63, North-Holland Publishing Company, c 1976, pp. 495-500.

27. TFR Group, "Recycling and Particle Confinement Characteristics in TFR 600," Journal of Nuclear Materials, Vol. 93 & 94, North-Holland Publishing Company, c 1980, pp. 272-281.

28. Lambert, R. M. and Comrie, C. M., "A Convenient Electrical Discharge Method for Eliminating Hydrocarbon Contamination From Stainless Steel UHV Systems," Journal of Vacuum Science Technology, Vol. 11, American Vacuum Society, c 1974, pp. 530-531.

29. Shapiro, Stuart L, Stark, Richard F., and Teukolsky, Saul A., "The Search for Gravitational Waves," American Scientist, Vol. 73, c 1985, pp. 248-257.

30. Ghosh, Supriya, "Discussion with Dr. T. S. Chou," Interoffice Memorandum, J. P. L., c 1985, pp. 1-3.

31. Ghosh, Supriya, "Discussion with Dr. H. J. Halama," Interoffice Memorandum, J. P. L., c 1985, pp. 1-3.

32. Yango, GloryAnne, "Discussion with Dr. H. F. Dylla," Interoffice Memorandum, J. P. L., c 1985, pp. 1-4.

33. Strausser, Yale, "Review of Outgassing Results," Varian Associates, California, c 1969, pp. 1-69.

BATCH START

STAPLE
OR
DIVIDER

ALTERNATE CONFIGURATION

COSTING AND SCHEDULING DATA

GWO - LENGTH, DIAMETER & CHAMBER VARIABLE ESTIMATED COSTS 6/21/85
CHERRYFIELD, MAINE - VACUUM (3000) AND FACILITIES (5000) SUBSYS

1984 DOLLARS, 4/24/85 FUNC BLK DIAG EST COSTS, WITHOUT GA&P

INCLUDES: 5/8/85 FUNCTIONAL REQUIREMENTS COST ESTIMATE

EXCLUDES: COSTS FOR GA&P AND TO CENTERLINE OF CONSTRUCTION

		$ M				
LENGTH	TUBE DIA	3 CHMBR	5 CHMBR	8 CHMBR	11 CHMBR	13 CHMBR
2.5 KM	36"	19.65	20.94	22.63	24.09	25.10
	42"	20.23	21.52	23.21	24.67	25.68
	48"	20.80	22.09	23.78	25.24	26.25
3.0 KM	36"	22.06	23.35	25.04	26.50	27.51
	42"	22.75	24.04	25.73	27.19	28.20
	48"	23.44	24.73	26.42	27.88	28.89
3.5 KM	36"	24.47	25.76	27.45	28.91	29.92
	42"	25.28	26.57	28.26	29.72	30.73
	48"	26.08	27.37	29.06	30.52	31.53
4.0 KM	36"	26.88	28.17	29.86	31.32	32.33
	42"	27.80	29.09	30.78	32.24	33.25
	48"	28.72	30.01	31.70	33.16	34.17
4.5 KM	36"	29.29	30.58	32.27	33.73	34.74
	42"	30.32	31.61	33.30	34.76	35.77
	48"	31.36	32.65	34.34	35.80	36.81
5.0 KM	36"	31.70	32.99	34.68	36.14	37.15
	42"	32.85	34.14	35.83	37.29	38.30
	48"	34.00	35.29	36.98	38.44	39.45

NOTE: LENGTH INCREMENTS INCLUDE: PIPE/SUPP/PUMPS/BAKE/ST DEV/HSG/PWR
TUBE DIA INCREMENTS INCLUDE: PIPE/PUMPS (10'DIA CULV NO CHG)
CHAMBER INCREMENTS INCLUDE: CHMB/SUPP/BLDG/PIPE/FLG/PUMPS
ADD 25% FOR GA&P
ADD 25% FOR 1988 CENTERLINE OF CONSTRUCTION COST (6%/YR)

GWO - LENGTH, DIAMETER & CHAMBER VARIABLE ESTIMATED COSTS 6/21/85
CHERRYFIELD, MAINE - VACUUM (3000) AND FACILITIES (5000) SUBSYS

(2 OF 3)

1984 DOLLARS, 4/24/85 FUNCTIONAL BLOCK DIAGRAM EST COSTS

INCLUDES: 25% GA&P AND 5/8/85 FUNCTIONAL REQUIREMENTS COST ESTIMATE

EXCLUDES: COSTS TO CENTERLINE OF CONSTRUCTION

		$ M				
LENGTH	TUBE DIA	3 CHMBR	5 CHMBR	8 CHMBR	11 CHMBR	13 CHMBR
2.5 KM	36"	24.56	26.18	28.29	30.11	31.38
	42"	25.29	26.90	29.01	30.84	32.10
	48"	26.00	27.61	29.73	31.55	32.81
3.0 KM	36"	27.58	29.19	31.30	33.13	34.39
	42"	28.44	30.05	32.16	33.99	35.25
	48"	29.30	30.91	33.03	34.85	36.11
3.5 KM	36"	30.59	32.20	34.31	36.14	37.40
	42"	31.60	33.21	35.33	37.15	38.41
	48"	32.60	34.21	36.33	38.15	39.41
4.0 KM	36"	33.60	35.21	37.33	39.15	40.41
	42"	34.75	36.36	38.48	40.30	41.56
	48"	35.90	37.51	39.63	41.45	42.71
4.5 KM	36"	36.61	38.23	40.34	42.16	43.43
	42"	37.90	39.51	41.63	43.45	44.71
	48"	39.20	40.81	42.93	44.75	46.01
5.0 KM	36"	39.63	41.24	43.35	45.18	46.44
	42"	41.06	42.68	44.79	46.61	47.88
	48"	42.50	44.11	46.23	48.05	49.31

NOTE: LENGTH INCREMENTS INCLUDE: PIPE/SUPP/PUMPS/BAKE/ST DEV/HSG/PWR
TUBE DIA INCREMENTS INCLUDE: PIPE/PUMPS (10'DIA CULV NO CHG)
CHAMBER INCREMENTS INCLUDE: CHMB/SUPP/BLDG/PIPE/FLG/PUMPS
ADD 25% FOR 1988 CENTERLINE OF CONSTRUCTION COST (6%/YR)

GWO - LENGTH, DIAMETER & CHAMBER VARIABLE ESTIMATED COSTS 6/21/85
CHERRYFIELD, MAINE - VACUUM (3000) AND FACILITIES (5000) SUBSYS

(3 OF 3)

1984 DOLLARS, 4/24/85 FUNCTIONAL BLOCK DIAGRAM EST COSTS

INCLUDES: 5/8/85 FUNCTIONAL REQUIREMENTS COST ESTIMATE
25% GA&P
25% TO 1988 CENTERLINE OF CONST COSTS (6%/YR)

		$ M				
LENGTH	TUBE DIA	3 CHMBR	5 CHMBR	8 CHMBR	11 CHMBR	13 CHMBR
2.5 KM	36"	30.70	32.72	35.36	37.64	39.22
	42"	31.61	33.63	36.27	38.55	40.13
	48"	32.50	34.52	37.16	39.44	41.02
3.0 KM	36"	34.47	36.48	39.13	41.41	42.98
	42"	35.55	37.56	40.20	42.48	44.06
	48"	36.63	38.64	41.28	43.56	45.14
3.5 KM	36"	38.23	40.25	42.89	45.17	46.75
	42"	39.50	41.52	44.16	46.44	48.02
	48"	40.75	42.77	45.41	47.69	49.27
4.0 KM	36"	42.00	44.02	46.66	48.94	50.52
	42"	43.44	45.45	48.09	50.38	51.95
	48"	44.88	46.89	49.53	51.81	53.39
4.5 KM	36"	45.77	47.78	50.42	52.70	54.28
	42"	47.38	49.39	52.03	54.31	55.89
	48"	49.00	51.02	53.66	55.94	57.52
5.0 KM	36"	49.53	51.55	54.19	56.47	58.05
	42"	51.33	53.34	55.98	58.27	59.84
	48"	53.13	55.14	57.78	60.06	61.64

NOTE: LENGTH INCREMENTS INCLUDE: PIPE/SUPP/PUMPS/BAKE/ST DEV/HSG/PWR
TUBE DIA INCREMENTS INCLUDE: PIPE/PUMPS (10'DIA CULV NO CHG)
CHAMBER INCREMENTS INCLUDE: CHMB/SUPP/BLDG/PIPE/FLG/PUMPS/BAKE

JET PROPULSION LABORATORY March 6, 1985

GRAVITY WAVE OBSERVATORY PROTECTIVE HOUSING COSTS (APPROX)
1984 DOLLARS/INSTALLED/INCL 25 PERCENT G & A AND PROFIT

HOUSING ELEMENT	$/FOOT	$K/FAC
A. Multiplate culvert/11'x 7'/12 ga	250	8200
B. Round corr culvert/12'dia/10 ga	227	7446
C. Round corr culvert/12'dia/12 ga	182	5956
D. Round corr culvert/10'dia/10 ga	159	5215
E. Round corr culvert/10'dia/12 ga	135	4428
F. Prefab building/9'w x 8'h	100	3280
G. Dome corr 8'dia + 4'sides/10 ga	131	4297
H. Half round corr culv/8'dia/12 ga	71	2329
FOUNDATION/FOOTINGS		
J. Slab and walls/10'w x 5'h	156	5116
K. Runners/slab 11'w x 2'deep	70	2296
L. Runners/spreaders 11'w x 2'deep	40	1312
EXCAVATION/BACKFILL/BERM (ASSUMES FLAT SITE-NO CUT/FILL/DRAINAGE)		
M. Buried 12'dia culvert	100	3280
N. Buried 10'dia culvert or 11'x 7'multi	75	2460
P. Semi-buried 10'w x 4'deep	12	393
Q. Above ground prep for runners	30	984
R. Above ground prep for piers	15	492
S. Berm over 4'h x 8'w housing	27	885
T. Berm over 9'h x 8'w housing	84	2745
U. Berm over vacuum tube	82+	2689+

PROTECTIVE HOUSING COSTS (cont)

INSULATION	$/FOOT	$K/FAC
V. Foamglas 2" + jacket x 4'dia (9.50/sq ft)	127	4165
W. R19 8'x 9'x 8'x 4" (1.00/sq ft)	25	820
X. R19 4'rad x 180 deg (1.00/sq ft)	13	426

PUMP/EQUIPMENT ENCLOSURE		
Y. Eq encl/Access (50.00/sq ft x 60 sq ft x 60)	8	240
Z. Eq encl (20.00/sq ft x 36 sq ft x 80)	2	66

COMBINATION EXAMPLES (STRUCTURE ONLY-NO HVAC/LTG/ELEC/BAKE)		
1. Multiplate/buried (A,N,Y)	333	10922
2. Round 12'culvert/buried (C,M,Y)	290	9512
3. Round 10'culvert/buried (D,N,Y)	242	7938
4. Prefab building/above (F,K,Q,W)	225	7380
5. Prefab building/above (F,L,Q,W)	195	6396
6. Dome 8'+ 4'sides/above (G,L,Q,W,Z)	231	7577
7. Dome 8'+ 4'sides/buried (1.5xG,R,P,X,Z)	239	7839
8. Half round 8'/semi-above (H,J,P,Q,X,Z)	284	9315
9. Two half rounds 8'/buried (H,H,3xP,Z)	180	5904
10.No housing no insulation/above (P,Z)	17	558
11.Runners only/above (L,Q,Z) (add to later)	72	2361
12.Insulation only/above (P,V,Z)	144	4723

NOV 26, 1986

SEQUENCE OF CONSTRUCTION AND PROCUREMENT FOR BURIED LIGO

VACUUM & FACILITY SUBSYSTEMS CONSTRUCTION/INSTALLATION

SEQ:	WBS #	STEP DESCRIPTION	(PRECEEDING STEP REQD)
1.	5010	CONSTRUCTION SURVEY	(-)
2.		PRELIMINARY ACCESS ROADS-SITE	(1)
3.	5065	POWER SOURCE TO SUBSTATION (34.5KV LINE)	(2)
4.	5061-5061C	UTIL SUBSTAT XFMR 34.5KV/4160V/MTR/SW GEAR	(2)
5.	5012	WATER SUPPLY-SITE	(1)
6.	5051A	DE-WATER/EXCAVATION/CUT/TRENCH-TUNNEL	(2)
7.	5051D	DRAINAGE STRUCTURES-TUNNEL	(6)
8.	5051E	EROSION CONTROL-TUNNEL	(6)
9.	5062A	POWER OVERHEAD LINE (4160V) 8 KM	(6)
10.	5062B	TRANSFORMERS, 4160/480V, 250 KVA	(6)
11.	5051B	PREPARE TUNNEL BASE	(7)
12.	5021A	EXCAVATION/GRADING-CENTRAL STATION BLDG	(11)
13.	5031A	EXCAVATION/GRADING-MID STATION BLDG	(11)
14.	5041A	EXCAVATION/GRADING-END STATION BLDG	(11)
15.	5701A	EXCAVATION/GRADING-SUPPORT BLDG	(2)
16.	3041	CHAMBR FNDN/PIERS-CENT/MID/END STATNS	(12,13,14)
17.	5021B	FLOOR SLAB/RETAINING WALLS-CENT STATN BLDG	(16)
18.	5031B	FLOOR SLAB/RETAINING WALLS-MID STATION BLDG	(16)
19.	5041B	FLOOR SLAB/RETAINING WALLS-END STATION BLDG	(16)
20.	5702	FLOOR SLAB-SUPPORT BLDG	(15)
21.	5022-5022D	STRUCT FRMNG/SIDING/INTERIOR/INSUL/ROOF-CENT	(17)
22.	5032-5032D	STRUCT FRMNG/SIDING/INTERIOR/INSUL/ROOF-MID	(18)
23.	5042-5042D	STRUCT FRMNG/SIDING/INTERIOR/INSUL/ROOF-END	(19)
24.	5730	BRIDGE CRANE 20 TON-CENTRAL STATION BLDG	(21)
25.	5830	BRIDGE CRANE 15 TON-MID STATION BLDG	(22)
26.	5930	BRIDGE CRANE 15 TON-END STATION BLDG	(23)
27.	5703-5703D	STRUCT FRMNG/SIDING/INTERIOR/INSUL/ROOF-SUPP	(20)
28.	5063-5064	POWER DIST-CENT/MID/END/SUPP BLDGS	(21,22,23,27)
29.	5028	LIGHTING/UTILITY RECEPTACLES-CENT BLDG	(28)
30.	5038	LIGHTING/UTILITY RECEPTACLES-MID BLDG	(28)
31.	5048	LIGHTING/UTILITY RECEPTACLES-END BLDG	(28)
32.	5709	LIGHTING/UTILITY RECEPTACLES-SUPPORT BLDG	(28)
33.	5054-5054E	INSTALL TUNNEL SECTIONS/CART TRACK/EQ ENCL	(11)
34.	3062-3062E	SUPPORT FOUNDATIONS-PIPE	(33)
35.	3061-3061D	SUPPORTS/ANCHORS-PIPE	(34)
36.	5062C-5062E	PNL/XFMR 480/120-208V/CABL/TRAY-PIPE	(35)
37.	5053F-5053I	LADDER/DECK/POWER/LIGHTING/WINCH-EQ ENCL	(36)
38.	5056	LIGHTING/UTILITY RECEPTACLES-TUNNEL	(36)
39.	5059	VENTILATION SYSTEM-TUNNEL	(36)
40.	5051C	FILL/BACKFILL-TUNNEL	(35)
41.	5013-5013D	ACCESS ROAD SURFACE	(40)

VACUUM & FACILITY SUBSYSTEMS CONSTRUCTION/INSTALLATION (CONT)

SEQ:	WBS #	STEP DESCRIPTION	(PRECEEDING STEP REQD)
42.	5015	FIRE PROTECTION (CENTRAL AREA)	(2)
43.	5029-5029J	HVAC-CENTRAL STATION BLDG	(28)
44.	5039-5039J	HVAC-MID STATION BLDG	(28)
45.	5049-5049J	HVAC-END STATION BLDG	(28)
46.	5710-5710J	HVAC-SUPPORT BLDG	(28)
47.	3051F	INSTALL/FIELD WELD-EXP JNT/PIPE	(35)
48.	3052	INSTALL EXP JOINTS	(47)
49.	3053	INSTALL ISOLATION VALVES	(48)
50.	3071-3071F	VACUUM PUMPS-PIPE	(49)
51.		CLEAN/TEST-PIPE	(47)
52.	3045	AUXILLIARY JACKS-CHAMBERS	(24,25,26)
53.	3044	TRAVEL STOPS-CHAMBERS	(52)
54.	3043	AIR MOUNT-CHAMBERS	(53)
55.	3042	SUPPORT FRAME-CHAMBER	(54)
56.	3011-3013E	VACUUM CHAMBERS-CENTRAL STATION BLDG	(55)
57.	3021-3021E	VACUUM CHAMBER-MID STATION BLDG	(55)
58.	3031-3031E	VACUUM CHAMBER-END STATION BLDG	(55)
59.	3014-3014J	VACUUM PUMPS-CENTRAL STATION BLDG	(56)
60.	3022-3022J	VACUUM PUMPS-MID STATION BLDG	(57)
61.	3032-3032J	VACUUM PUMPS-END STATION BLDG	(58)
62.	3076-3076C	NITROGEN SUPPLY	(39)
63.	3077-3077C	DIAGNOSTIC EQUIPMENT	(39)
64.	5090	HOUSEKEEPING ASSEMBLY	(39)
65.	5100	INTERCOM ASSEMBLY	(39)
66.	5120	SECURITY ASSEMBLY	(39)
67.	5130	SEISMIC MONITORING ASSEMBLY	(39)
68.	57,58,5931	FIRE DETECTION/SUPPRESSION	(39)
69.	5023-5027E	PARTNS/RSD FLRS/ACOUS ISOL/DRAINS/SANI-CENT	(59)
70.	5033-5037E	PARTNS/RSD FLRS/ACOUS ISOL/DRAINS/SANI-MID	(60)
71.	5043-5047E	PARTNS/RSD FLRS/ACOUS ISOL/DRAINS/SANI-END	(61)
72.	5704-5708E	PARTNS/FLOORS/ACOUS ISOL/DRAINS/SANI-SUPP	(32)
73.	3080-3088	VACUUM BAKEOUT POWER DIST-PIPE	(51)
74.	3088-3089A	VACUUM BAKEOUT/MOBILE GEN/FUEL-PIPE	(73)
75.	3090-3092	CHAMBER BAKEOUT COVERS	(59,60,61)
76.	5014-5014A	SECURITY, FENCING/GATES	(21,22,23,27)
77.	5070-5081	LASER COOLING	(12)
78.	5150-5152	EMERGENCY/BACKUP EQUIPMENT	(72)
79.		SITE CLEANUP	(78)
80.	5111-5112	FURNISHINGS, SHOP EQ/OFFICE EQ	(72)
81.	5140	TRANSPORTATION VEHICLES	(2)

VACUUM & FACILITY SUBSYSTEMS PROCUREMENT LEAD TIME

	WBS #	STEP	COMPONENT DESCRIPTION	LEAD TIME
A.	3051A-E	(47)	PIPE-ON SITE ROLL FORM MACHINE	24 MO
			304L MILL RUN/DELIVERY	12 MO
			ROLL FORM PIPE SECTIONS	2 MO
				NET 26 MO
B.	3053A-B	(49)	ISOLATION VALVES	18 MO
C.	5730	(24)		
	5830	(25)		
	5930	(26)	BRIDGE CRANES	18 MO
D.	3014A-J	(59)		
	3022A-J	(60)		
	3032A-J	(61)	VAC PUMPS	12 MO
E.	3011A-E	(56)		
	3022A-E	(57)		
	3032A-E	(58)	VAC CHAMBERS	12 MO
F.	3052A-C	(48)	EXP JOINTS	12 MO
G.	5052A-5053C	(33)	TUNNEL-ON SITE ROLL FORM MACHINE	6 MO
			10-12 GA STEEL DELIVERY	3 MO
			ROLL FORM TUNNEL SECTIONS	3 MO
				NET 9 MO
H.	3076A-C	(62)	NITROGEN SUPPLY EQ	9 MO
I.	5065	(3)	POWER SOURCE TO SUBSTATION	9 MO
J.	5061A-C	(4)	POWER SUB STATION	8 MO
K.	5070-5081	(77)	LASER COOLING EQ	8 MO
L.	5043A-E	(54)	AIR MOUNTS	8 MO
M.	5029A-J	(43)		
	5039A-J	(44)		
	5049A-J	(45)		
	5710A-J	(46)	HVAC EQ	8 MO
N.	5022-5022D	(21)		
	5032-5032D	(22)		
	5042-5042D	(23)		
	5703-5703D	(27)	PREFAB BLDGS	6 MO

VACUUM & FACILITY SUBSYSTEMS PROCUREMENT LEAD TIME (CONT)

	WBS #	STEP	COMPONENT DESCRIPTION	LEAD TIME
O.	3077A-C	(63)	DIAGNOSTIC EQ	6 MO
P.	5090	(64)	HSE KEEPING EQ	6 MO
Q.	5100	(64)	INTERCOM	6 MO
R.	5120	(66)	SECURITY	6 MO
S.	5130	(67)	SEISMIC	6 MO
T.	5731	(68)		
	5831	(68)		
	5931	(68)	FIRE DETECTION EQ	6 MO
U.	5111-5112	(80)	FURNISHING/SHOP EQ	4 MO
V.	5114A-B	(81)	VEHICLES	3 MO